GEOSCIENCE AUSTRALIA RECORD 2003/19

PETROLEUM GEOLOGY OF THE BASS BASIN – INTERPRETATION REPORT

An Output of the Western Tasmanian Regional Minerals Program

Jane E. Blevin (Compiler)
Geoscience Australia
Petroleum and Marine Division

WITH CONTRIBUTIONS BY

Jane E. Blevin, Chris J. Boreham and Kathe R. Trigg, Geoscience Australia

Aaron Cummings, Ric Daniel, John Kaldi, Simon Lang, Nick Lemon, Rob Root and Peter Tingate, National Centre for Petroleum Geology and Geophysics, University of Adelaide

Alan D. Partridge, Biostrata Pty Ltd.

Canberra Australia 2003

Geoscience Australia

Chief Executive Officer: Neil Williams

Department of Industry, Tourism & Resources

Minister for Industry, Tourism & Resources: The Hon Ian Macfarlane MP
Parliamentary Secretary: The Hon Warren Entsch MP
Secretary: Mark Patterson

ISSN: 1448-2177
ISBN: 0 642 46777 3

Bibliographic references:

Blevin, J. (Compiler), 2003. Petroleum Geology of the Bass Basin – Interpretation Report, An Output of the Western Tasmanian Regional Minerals Program. Geoscience Australia, Record 2003/19.

Boreham, C., 2003. Petroleum geochemistry of source rocks, oils and gases. In: Blevin, J. (Compiler), Petroleum Geology of the Bass Basin – Interpretation Report, An Output of the Western Tasmanian Regional Minerals Program, Geoscience Australia, Record 2003/19.

Geoscience Australia Website: www.ga.gov.au

TABLE OF CONTENTS

APPENDICES - VOLUME II (CD-ROM ONLY)

APPENDIX A. List of petroleum exploration wells in the Bass Basin (Jane Blevin, Geoscience Australia)

APPENDIX B: List of horizons interpreted in the Bass Basin wells (Jane Blevin, Geoscience Australia)

APPENDIX C. Biostratigraphy Reports (Alan Partridge, Biostrata Pty Ltd.)

- **C1.** Palynological analysis of Eocene interval 1380 to 2036 m in Cormorant-1, Bass Basin
- **C2.** Palynological review of Upper Cretaceous units in Durroon-1, Bass Basin
- **C3.** Palynological analysis of Eocene interval 1390 to 2036 m in King-1, Bass Basin
- **C4.** Quantitative palynological analysis of Paleocene to Middle Eocene interval Konkon-1, Bass Basin
- **C5.** Quantitative palynological analysis of eleven cuttings samples from 2266 to 3115 m in Koorkah-1, Bass Basin
- **C6.** Quantitative palynological analysis of Eastern View and Demons Bluff Groups in Poonboon-1, Bass Basin
- **C7.** Palynological analysis of Oligocene sandstones in Squid-1, Bass Basin
- **C8.** Bass Basin palynological project, unravelling a Late Cretaceous to Eocene geological history of large palaeolakes, coastal lagoons and marine bays

APPENDIX D. List of core and cuttings from the Bass Basin analysed for organic geochemistry (Chris Boreham, Geoscience Australia)

APPENDIX E. Vitrinite-inertinite reflectance and fluorescence (VRF™ or VIRF) results for Cormorant-1 and Pelican-5 (Jane Newman, Newman Pty Ltd.)

APPENDIX F. Palynology of coals and claystones from Cormorant-1 and Pelican-5 used for oil-source correlations (Mike Macphail, Australian National University)

APPENDIX G. List of oil and gases in the Bass Basin analysed for this study (Chris Boreham, Geoscience Australia)

APPENDIX H. Small Angle Neutron Scattering (SANS) study on low-ash coals from Cormorant-1 and Pelican-5 (Andrzej Radlinski, Alan Hinde and Chris Boreham, Geoscience Australia)

APPENDIX I. Organic petrology of selected samples from the Bass Basin (Alan Cook, Keiraville Konsultants Pty Ltd.)

APPENDIX J. Uncorrected bottom hole temperature data for Bass Basin wells (Aaron Cummings and Peter Tingate, National Centre for Petroleum Geology and Geophysics)

APPENDIX K. Kinetic modelling of Pelican-5 (Aaron Cummings, National Centre for Petroleum Geology and Geophysics)

APPENDIX L. Mercury injection capillary pressure test results and analytical equipment (Ric Daniel and John Kaldi, National Centre for Petroleum Geology and Geophysics)

APPENDIX M. Core photos of selected wells in the Bass Basin (Simon Lang and Rob Root, National Centre for Petroleum Geology and Geophysics)

EXECUTIVE SUMMARY

The Bass Basin is a moderately explored Cretaceous to Cainozoic intracratonic rift basin on Australia's southeastern margin, underlying the shallow seabed between Tasmania and the Victorian mainland (Bass Strait; Figure 1). The basin contains proven commercial reserves of gas and condensate that are soon to be developed (Yolla gas field, Origin Energy Resources Ltd-operated BassGas Project). Other discoveries in the basin include the White Ibis and Pelican gas fields. To date, the 32 wells drilled have targeted Upper Cretaceous to Middle Eocene reservoirs within fault blocks and anticlinal structures. The targeted succession comprises interbedded fluvio-deltaic and lacustrine sandstones, siltstones and shales. The principal source rocks in the Bass Basin are interbedded coals (ranging from 5 to 25 m thick) and lacustrine shales of early Palaeogene age. Geochemical analyses show these source rocks have generated liquid and gaseous hydrocarbons, with the coals being the dominant source for the liquids (Boreham et al., 2003).

As part of the Commonwealth-funded *Western Tasmanian Regional Minerals Program*, Mineral Resources Tasmania (MRT) initiated a collaborative study of the Bass Basin, in partnership with Geoscience Australia (GA) and the National Centre for Petroleum Geology and Geophysics (NCPGG). Commercial inputs into the project were sought from Biostrata Pty Ltd, SRK Consulting, Fugro MCS and CSIRO. The aim of this work was to enhance the petroleum prospectivity of the northern and western regions of offshore Tasmania through an improved understanding of basin geology, an analysis of petroleum systems elements (source rocks, reservoirs and seals), and enhanced access to basic datasets critical to the exploration industry.

This Record presents the results of the geological, geochemical and biostratigrahic studies. Additional reports and data covering other objectives of the Western Tasmanian Regional Minerals Program (WTRMP) are outlined in Table A1. The key findings of the WTRMP Bass Basin study include:

Petroleum Geochemistry and Geohistory Modelling

- The Bass Basin is prospective for oil and gas generation in areas where adequate quantities of coaly source rocks of early Palaeogene age are buried to depths of approximately 2450 m (onset of oil generation) to 3200 m (2700 to 3200 m onset of oil expulsion/primary migration). The main gas window lies at approximately 3650 m in the Pelican Trough.
- Geochemical analyses have yielded strong evidence that Paleocene to Early Eocene coals have sourced the oil and gas at the Yolla, Pelican and Cormorant accumulations.
- The pattern of hydrocarbon charge indicates generation in the main troughs with migration to structures within the depocentre and along the flanks. Oil migration was followed by gas charge, which has displaced some accumulations. A later phase of oil and water migration below the "Demons Bluff" regional seal during the late Palaeogene to early Neogene is suggested.
- A broad decrease in geothermal gradient occurs from the northwest of the basin towards the southeast.

- The main source rocks linked to hydrocarbon accumulations within the basin entered the oil generation window just prior to and following the deposition of the "Demons Bluff" regional seal.

Geology and Petroleum Systems

- Identification of six Basin Phases and related megasequences/supersequences that correlate to three periods of extension, a rift-transition phase, and two subsidence phases. The complex nature of facies relationships across the basin is attributed to the (mostly) terrestrial setting of the basin until the Middle Eocene, multiple phases of extension, strong compartmentalisation of the basin due to underlying basement fabric, and differential subsidence during extension and early subsidence phases. The "Eastern View Coal Measures" (or "Eastern View Group") has been subdivided into three megasequences (Durroon, Bass and Aroo megasequences). A further three component sequences have been recognised within the Bass Megasequence (Furneaux, Tilana and Narimba sequences). Basin boundaries have also been redefined using seismic and potential field datasets.
- A well audit has identified four main areas of exploration risk (Trigg et al., 2003): a) invalid tests due to artefacts or poor data quality; b) trap integrity and seal risk; c) reservoir quality; and, d) lack of adequate hydrocarbon charge.
- Results of MICP analyses of selected potential seal facies indicate that the average column height of oil is 605 m (density 0.735g/cc) and the average column height of gas is 262 m (density 0.1 g/cc). Facies of lower shoreface, fluvial overbank and lagoonal mudstones show the highest seal capacity. The single sample of the regional sealing facies "Demons Bluff" mudstone showed poor seal capacity.
- A sequence of diagenetic events has been integrated from a range of studies. The lack of marine influence is the key difference between reservoirs of the Bass and Gippsland basins. Early cementation is beneficial in that intergranular porosity is preserved during loading and compaction. Dissolution of the carbonate cement at a later stage results in effective secondary intergranular porosity and permeability. Porosity and permeability is overestimated in some samples due to micro-intragranular porosity in clays.
- Facies analyses indicate the highest ranking reservoir facies are coarse-grained sandstones within fluvial channels, with secondary ranking facies of coarse-grained lacustrine shoreface and foreshore sandstones.
- Biostratigraphic studies have identified lacustrine cycles during the Late Cretaceous to Middle Eocene (Partridge, 2002; Appendix C). Integration with geological data indicate these lakes developed during times of increased accommodation.
- The "Demons Bluff" regional seal was deposited in bay and shallow marine environments during a regional transgressive event. Intraformational seals with potentially high sealing capabilities include mudstones within the *L. balmei* to *N. asperus* zones.
- Optimum play conditions exist within coarse-grained fluvial channel belt sandstones or lacustrine shoreline and deltaic facies sealed by lacustrine deposits within the *L. balmei* zone (Tilana and lower Narimba sequences). Higher risk plays occur within fine-grained lacustrine or coastal lagoon shoreface facies, or in compositionally immature coarse-grained alluvial fan and proximal facies.

Other related outputs from the Western Tasmanian Regional Mineral Program include:

- Well audit report of petroleum exploration wells in the Bass Basin (CD-ROM, Geoscience Australia Record 2003/11).
- Reprocessed seismic data from Surveys T69A and T70A along western Tasmania (Sorell Basin), available in SEG-Y format, with navigation and velocity data included (CD-ROM, Geoscience Australia Record 2003/6).
- Regional potential field study of the Bass Basin, commissioned by Geoscience Australia in support of the WTRMP (CD-ROM, Geoscience Australia Record 2003/4).
- Compilation and review of biostratigraphic data from the Bass Basin (CD-ROM, Geoscience Australia Record 2003/7).
- Basic geological data compilation from the Bass Basin (including bathymetry, gravity and magnetic images; and Excel format downloads of open-file biostratigraphy, porosity/permeability, geochemistry and checkshot data) (CD-ROM, Geoscience Australia Record 2003/17).
- Bass Basin GIS Project (CD-ROM, Geoscience Australia Record 2003/18).

For further information on the Western Tasmanian Regional Mineral Program, Petroleum Program Outputs, please contact Carol Bacon, Managing Geologist, Mineral Resources Tasmania, (03) 6233-8326.

1. INTRODUCTION

J. Blevin, Geoscience Australia

1.1 REGIONAL SETTING AND AIMS OF THE BASS BASIN STUDY

The Bass Basin is a moderately explored Cretaceous to Cainozoic intracratonic rift basin on Australia's southeastern margin (Figure 1.1). The basin contains proven commercial reserves of gas and condensate that are soon to be developed (Yolla gas field, Origin Energy Resources Ltd-operated BassGas Project). Other discoveries in the basin include the White Ibis and Pelican gas fields. To date, the 32 exploration wells have targeted Upper Cretaceous to Middle Eocene reservoirs within fault blocks and anticlinal structures. The targeted succession comprises interbedded fluvio-deltaic and lacustrine sandstones, siltstones and shales. The principal source rocks in the Bass Basin are interbedded coals (ranging from 5 to 25 m thick) and lacustrine shales of Palaeogene age. Geochemical analyses show these source rocks have generated liquid and gaseous hydrocarbons, with the coals being the dominant source for the liquids (Boreham et al., 2003). Volcanic rocks are common throughout the basin as sills and flows, often associated with large rift faults and accommodation zones. Petroleum exploration of the Bass Basin began in 1965. Of the 32 wells drilled, only four contain commercial to sub-economic accumulations. A review of exploration wells has identified four main areas of risk (Trigg et al., 2003): a) invalid tests due to artefacts or poor data quality; b) trap integrity and seal risk; c) reservoir quality; and, d) lack of adequate hydrocarbon charge.

Under the auspices of the Commonwealth-funded Western Tasmanian Regional Minerals Program (WTRMP; Section 1.2), Mineral Resource Tasmania sponsored and coordinated a study of the Bass Basin. Modules of the work program were undertaken at Geoscience Australia (seismic and well log interpretation, basin mapping, petroleum geochemistry), the National Centre for Petroleum Geology and Geophysics (geohistory modelling, reservoir, seal and facies analyses), and through a commercial contract with Biostrata Pty Ltd (biostratigraphic analyses). Most of the results of the Bass Basin study are presented in this Record. Other products associated with the Bass Basin and the WTRMP are shown in Table 1.1.

Collectively, the study aimed to address the following objectives:

- improving prospectivity and reduce exploration risk though a better understanding of basin forming processes, particularly those relating to hydrocarbon generation and entrapment; and,
- upgrading the quality and access to exploration data (including seismic reprocessing programs, biostratigraphic and geochemical databases).

1.2 WESTERN TASMANIAN REGIONAL MINERALS PROGRAM

In 1998, the Commonwealth Government of Australia established the Regional Minerals Program to encourage a coordinated regional approach to minerals development (Woodward-Clyde, 1999). The Western Tasmanian Regional Minerals Program (WTRMP) forms part of this program and is a tripartite agreement

between the Commonwealth and Tasmanian Governments and the Minerals Industry. The program covers the areas of western and northern Tasmania as far east as the River Tamar, including the offshore Bass and Sorell basins (Figure 1.2). The WTRMP is coordinated by Mineral Resources Tasmania (MRT) in conjunction with a Management Committee consisting of representatives from the Minerals Industry in Tasmania, MRT and the Commonwealth Department of Industry, Tourism and Resources.

The aims of the WTRMP include addressing the uncertainty over the pricing and forms of available energy – issues which are critical to the expansion of existing facilities and the development of new projects that will further utilise the wealth of northwestern Tasmania. In September 2000, as part of this initiative, MRT sought external consultation to scope projects that could assist in the implementation of recommendations contained in the Final Regional Development Plan (http://www.mrt.tas.gov.au). The result was a series of proposed studies aimed at enhancing prospectivity and encouraging exploration in the northwest Tasmania offshore region (Fardon, 2000). These studies included the following topics: 1) sequence stratigraphy of the Bass Basin; 2) the effects of volcanics and coals on seismic data; 3) biostratigraphic review of the Bass Basin; 4) thermal maturation modelling of the Bass and Sorell basins; 5) study of reservoir quality in the Bass Basin; 6) reprocessing of seismic data in the Sorell Basin; and, 7) updated palaeogeographic maps of the Bass Basin (Fardon, 2000). In addition, the recommendations recognised the importance of ready access to basic geological datasets to explorers in the region.

In early 2001, MRT established a collaborative project to address the recommendations of Fardon (2000). The collaborative partners included MRT, Geoscience Australia (GA), and the National Centre for Petroleum Geology and Geophysics (NCPGG). Services were also sought through commercial contracts with Biostrata Pty. Ltd., SRK Consulting and Fugro Multi Client Services (formerly Seismic Australia). The results of this work are now available as a series of reports and basic data downloads (Table 1.1). This Geoscience Record addresses the research topics 1 to 5, and 7, as outlined by Fardon (2000). Reprocessed seismic data (Fardon, 2000; research topic 6) is now available as Geoscience Australia Record 2003/6 (Fleming and Blevin, 2003). For further information on this or other WTRMP products, please contact Mineral Resources Tasmania, or the Sales Centre, Geoscience Australia (http://www.ga.gov.au).

Table 1.1 List of products produced as part of the Western Tasmanian Regional Minerals Program. These products are available through Mineral Resources Tasmania, or the Sales Centre, Geoscience Australia (02 6249-9519). These products are available at the cost of transfer.

Product Format	Title	Publication Number
CD-ROM, Hardcopy	Petroleum geology of the Bass Basin – interpretation report	Geoscience Australia Record 2003/19
CD-ROM	Regional potential field interpretation report, Bass Basin	Geoscience Australia Record 2003/4
CD-ROM	Western Tasmania regional seismic data, selected reprocessed lines from seismic surveys T69A and T70A	Geoscience Australia Record 2003/6
CD-ROM	Review and compilation of open file micropalaeontology and palynology data from offshore Tasmania	Geoscience Australia Record 2003/7
CD-ROM	An audit of petroleum exploration wells in the Bass Basin, 1965-1999	Geoscience Australia Record 2003/11
CD-ROM	Bass Basin, basic data compilation (including bathymetry, gravity and magnetic images; biostratigraphy, porosity, permeability, geochemistry, checkshot, deviation and seismic navigation data)	Geoscience Australia Record 2003/17
CD-ROM	Bass Basin GIS Project	Geoscience Australia Record 2003/18

Figure 1.1 Location map of the Bass Basin and adjacent region, southeastern Australia. The basin outline, permits, well and field locations, including the 2002 (black) and 2003 (red) Acreage Release areas, are also shown.

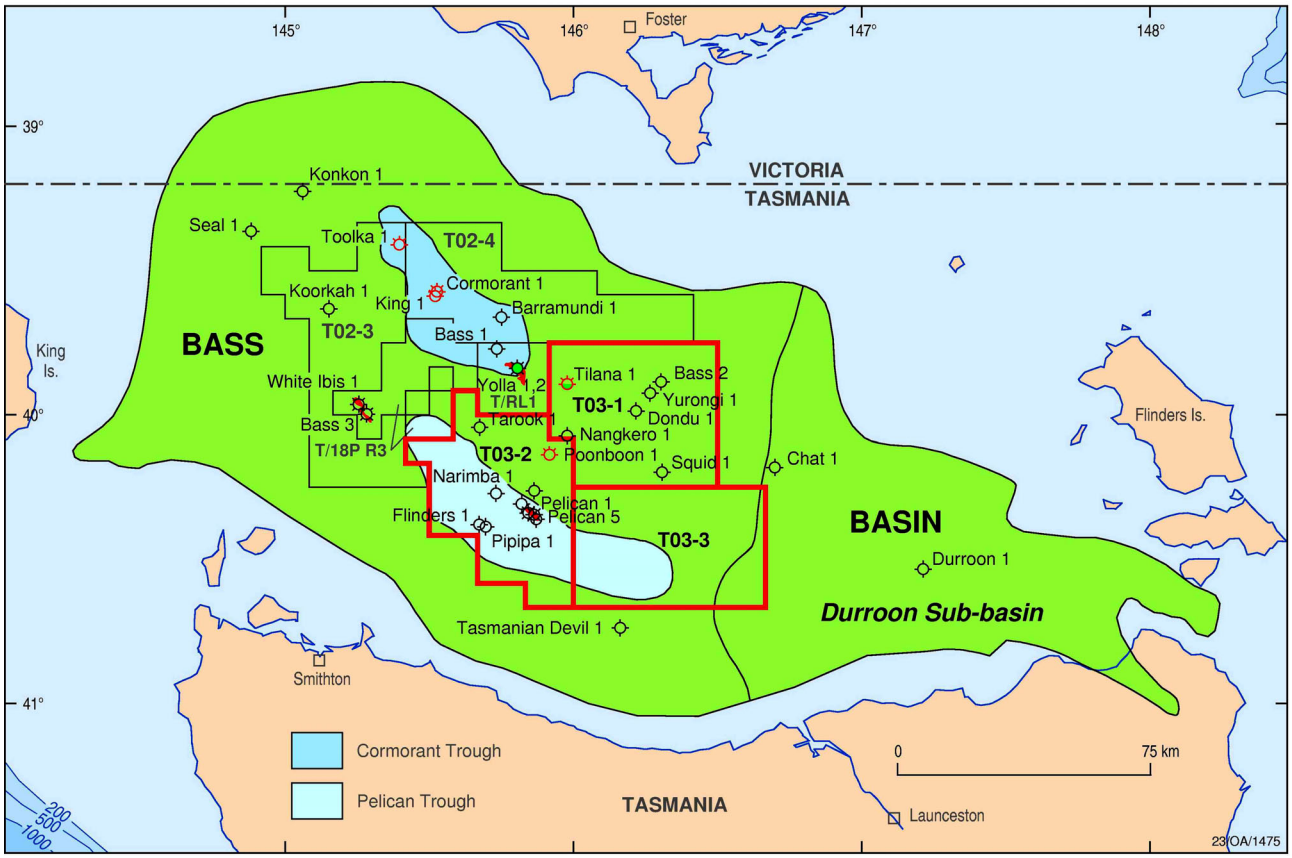

2. EXPLORATION HISTORY

J. Blevin and K. Trigg, Geoscience Australia

The Bass Basin is a moderately explored basin with 32 wells drilled since 1965 (Figure 2.1). The basin has a drilling density of approximately one well per 1,320 km^2. Similar to other basins along the Australia's southern margin, exploration has occurred in phases. Two areas in the western Bass Basin were gazetted as part of the 2002 Release of Offshore Petroleum Exploration Areas, and a further three were released in 2003 offshore acreage release round (Figure 2.1). There is one current permit, T/18P (R3), operated by Origin Energy Resources Limited, and one retention lease, T/RL1, also held by Origin Energy Resources Limited.

2.1 HYDROCARBON ACCUMULATIONS AND PETROLEUM SYSTEMS

The hydrocarbons discovered to date on the southern margin of Australia have been assigned to the Austral Petroleum Supersystem based on the age of their source rocks and common tectonic history (Austral A3; Edwards et al., 1999). In the Bass Basin, exploration drilling has confirmed hydrocarbon accumulations at Yolla, Pelican, White Ibis and Cormorant, reservoired in sands of Paleocene to Eocene age (*L. balmei* to *M. diversus* zones). At present, only the accumulation at Yolla is being considered for commercialisation ($400M Origin Energy-operated BassGas Project; The Australian Financial Review, 2002). The project will produce natural gas and liquids from the Yolla field that will be piped under Bass Strait and processed in a new plant to be built near Lang Lang, southeastern Victoria (Wood, 2003). The project is expected to come on-line in the third quarter of 2004 (Wood, 2003).

The Bass Basin oils and gases have a terrestrial source affinity and are geochemically similar to the Gippsland Basin oils (Summons, 1996). The Yolla-1 oil is a medium-gravity (46° API) crude with a correspondingly high wax content, whereas the Cormorant-1 oil is a heavy crude (21° API) as a result of biodegradation (Edwards et al., 1999). Geochemical analyses of the hydrocarbons indicate an input of predominantly land-plant material to the source kerogens, and there is no evidence of marine organic matter (Edwards et al., 1999).

Previous authors (e.g., Nicholas et al., 1981; Miyazaki, 1995) have suggested that liquid hydrocarbons were generated from disseminated organic matter within carbonaceous claystones, while gases were sourced mainly from coaly facies. However, recent oil-to-source correlations undertaken as part of this study (Chapter 5; Boreham et al., 2003) have shown that the oils were sourced from Tertiary coals, particularly those concentrated within the Middle to Early Eocene succession. Oils in the basin are a single oil population (Yolla and Pelican accumulations), while in-reservoir biodegradation of the Cormorant oil has resulted in its statistical classification as a separate oil family (Chapter 5; Boreham et al., 2003). Recent fluid inclusions studies (Kempton et al., 2002) have identified palaeo-oil zones at Yolla-1 and Cormorant-1, along with suspected zones at King-1 and Pelican-5. In addition, several potential palaeo-hydrocarbon zones were

identified at Yurongi-1, Chat-1, Seal-1, Tilana-1 and Squid-1. These zones are characterised by aqueous inclusions containing small amounts of oil (Kempton et al., 2002). Overall, the pattern of hydrocarbon distribution in the basin shows that hydrocarbon generation has occurred in the Cormorant, Yolla and Pelican troughs with migration into structures within those depocentres and on the adjacent flanks.

2.2 PREVIOUS EXPLORATION

Commercial exploration of the Bass Basin began in the early 1960s with permits awarded to Hematite Petroleum Pty Ltd (BHP) and Esso Exploration and Production Australia Ltd (Esso) (Robinson, 1974; Smith, 1986). Bass-1, the first well in the basin, was drilled by Esso in 1965. Esso's subsequent exploration program included 15 wells drilled over the ensuing nine year period from 1966 to 1974. During this exploration phase, gas and condensate accumulations were discovered at Pelican-1 and Pelican-2, while numerous gas shows were recorded at Bass-3, Pelican-3, Poonboon-1, Toolka-1, and Aroo-1. Several thin pay zones were encountered within the Eastern View Group at Cormorant-1, including a 2 m oil column, and 2 m and 3 m gas and condensate columns (Ozimic et al., 1986). Hematite Petroleum Pty Ltd drilled a further four wells between 1974 and 1978, however no further hydrocarbon discoveries were made. The stratigraphic terms in the following exploration review reflect the nomenclature used at the time of drilling (Figure 2.2).

Yolla-1, drilled in 1985 by Amoco Australia Petroleum Company, was sited as a crestal test of the Eastern View Group within a four-way dip and fault-closed structure. Light oil and associated gas shows were recorded in sands at the "Top Eastern View Group". Wireline pressure tests (RFTs) and logs indicated the presence of at least three separate gas columns within sandstones of the Eastern View Group. Final log analysis indicates that Yolla-1 encountered approximately 30 m of net gas pay over a 278 m interval (Lennon et al., 1999). In addition, the well penetrated a gross hydrocarbon column of 31 m (wet gas cap of 20.4 m overlying a 10.6 m oil leg). The stacked hydrocarbon accumulations within the Eastern View Group at Yolla are sealed by relatively thick and laterally continuous intraformational shales that were deposited in a lacustrine environment (Lennon et al., 1999).

In 1998, Boral Energy Resources Ltd and partners drilled two wells in the central Bass Basin – Yolla-2 and White Ibis-1. Both wells encountered gas columns in the Paleocene to Lower Eocene succession, with liquids-rich gas recovered from reservoirs in wireline tests (Lennon et al., 1999). Yolla-2 was an appraisal well that confirmed a resource of between 450 to 600 billion cubic feet of liquids-rich gas and 70 million barrels of oil in place (OIP). The White Ibis-1 well, located in exploration permit T/18P, was a crestal test over a large basement high updip of Bass-3. Formation pressure data suggests the presence of a thin oil rim, with the well encountering a gas accumulation estimated at 85 BCF of oil and gas in place (OGIP).

Barramundi-1, drilled by GLOBEX Far East in 1999, is the most recent well in the Bass Basin. The well tested a faulted rollover structure with closure at the top of the Eocene succession. A large AVO anomaly corresponding to interpreted thick sands was interpreted (pre-drill) as evidence of a valid hydrocarbon accumulation (Crist et al., 2001). No commercial quantities of hydrocarbons were encountered during drilling

at Barramundi-1. Failure of the well was attributed to breaching of the trap during Miocene inversion which resulted in faulting and fracturing of the overlying Demons Bluff regional seal.

2.3 EXPLORATION RISKS

As part of the Western Tasmanian Regional Minerals Program (WTRMP), Geoscience Australia undertook an audit of all 32 wells drilled in the basin since 1965. The well audit is available as a separate report (Trigg, et al., 2003; Trigg and Blevin, 2003) through Mineral Resources Tasmania or Geoscience Australia (see Table 1.1). Details of the wells drilled in the Bass Basin from 1965 to 1999 are summarised in Table 2.1.

The outcome of the well audit showed four main areas of exploration risk (Trigg et al., 2003; Trigg and Blevin, 2003): a) invalid tests due to artefacts or poor data quality; b) trap integrity and seal risk; c) reservoir quality; and, d) lack of hydrocarbon charge. Work undertaken as part of the WTRMP study aimed to provide a better understanding of these factors to reduce the perception of risk (Chapters 3 to 10).

2.4 2002 ACREAGE RELEASE AREAS

Areas T02-3 and 4 are located in western Bass Strait, north of Tasmania and east of King Island (Figure 2.1). They comprise 40 and 38 graticular blocks, respectively. The release areas cover approximately 2680 (T02-3) and 2550 km^2 (T02-4), for a total area of approximately 5230 km^2. Water depths across both areas are less than 75 metres. The release areas are adjacent to current exploration permit T/18P (R3) operated by Origin Energy Resources Limited, and retention lease T/RL1, also held by Origin Energy Resources.

The 2002 Release Areas (T02-3 and T02-4) are located in the western part of the Bass Basin. Area T02-3 includes the Koorkah-1 and Toolka-1A wells, while Area T02-4 includes the King-1, Cormorant-1 and Barramundi-1 wells. A number of exploration wells with strong hydrocarbon shows surround the current release areas (Table 2.1), including the Yolla gas field located south of T02-4. Play types in the 2002 Release Areas are likely to be related to reactivated rift structures such as inversion anticlines and faulted controlled traps, with primary targets within the Eastern View Group.

Area T02-3

Koorkah-1 targeted Upper Cretaceous to Lower Eocene sandstones of the Eastern View Group. Post-drill interpretations show that the primary objective sandstones had low porosity and permeability due to diagenetic processes. Sediments at Koorkah-1 were thermally immature to marginally mature and deemed to be gas-prone. Traces of free oil evident from 2,400 m to TD were apparently derived from a deeper mature source rock that was relatively rich in resinite.

Toolka-1A was drilled in 1974 to evaluate the stratigraphic equivalents of the Middle Eocene hydrocarbon-bearing sands encountered nearby at Cormorant-1. The discontinuous nature of these sands resulted in only minor oil and gas shows being recorded. The anticlinal structure drilled at Toolka-1A was deemed to be a valid test, with the failure of the well attributed to lean source rocks and lack of reservoir sands.

A 'flat spot anomaly' has been identified on intersecting seismic lines in the western part of Area T02-3 (Das and Lemon, 2000a). This anomaly has the seismic characteristics of a gas-liquid contact, with a two-way time structure map showing that its occurrence coincides with an elongate, northeast/southwest-trending faulted anticline at the Eastern View Group stratigraphic level (Das and Lemon, 2000a). The anomaly covers approximately 40 km^2 and has a maximum structural relief of about 40 milliseconds two-way time. More detailed amplitude-versus-offset (AVO) analysis is needed to fully understand the nature of these seismic features, and to assess their validity as indicators of in-place hydrocarbon accumulations.

Area T02-4

Drilled in the central Bass Basin during 1970, Cormorant-1 encountered significant oil, gas and condensate shows within the Eastern View Group (Figure 2.3). The Cormorant structure is a large, northwest-southeast trending anticline that formed as a result of Miocene compression. Several pay zones were encountered within the Eastern View Group, including a 2 m oil column, and 2 m and 3 m gas and condensate columns. The lack of an economic accumulation at Cormorant-1 was attributed to ineffective seal and late development of the trapping structure.

King-1 was drilled in 1992 as a follow-up to Cormorant-1. The well targeted basal Eocene fluvial sands (*N. asperus* spore/pollen zone) of the Eastern View Group in a crestal position on the previously defined Cormorant anticlinal structure. Although the target sands were water saturated at King-1, they displayed excellent reservoir characteristics (porosities of 20 to 30% and permeabilities of 0.7 mD to 1D). The King-1 structure was found to be valid, and potential source rocks were assessed as mature, with encouraging hydrocarbon shows. Possible reasons for failure include poor migration pathways into the structure from mature Paleocene source rocks and possible fault breaching of the Demons Bluff top seal.

2.5 2003 ACREAGE RELEASE AREAS

Areas T03-1, -2 and -3 are located in the Bass Strait region, north of Tasmania and west of Flinders Island (Figure 1). Each release area consists of 40 graticular blocks, covering areas of approximately 2670 km^2 (T03-1), 2665 km^2 (T03-2), and 2660 km^2 (T03-3). Water depths across the areas are less than 75 metres. The release areas are adjacent to current exploration permit T/18P (R3) operated by Origin Energy Resources Limited, and retention lease T/RL1, also held by Origin Energy Resources.

The 2003 Release Areas are located in the central part of the Bass Basin. Area T03-2 overlies the Pelican gas field, which was discovered by Esso in 1970. A number of exploration wells with strong hydrocarbon shows surround the current release areas, including the Yolla field located to the west of T03-1. Play types in the area include rotated fault blocks with drape closure (Figure 2.4), and anticlinal structures that formed in shallower strata during Miocene compression. A host of stratigraphic plays also exist, but these are unlikely to be primary targets. Descriptions of the structures and drilling results from exploration wells in the 2003 Release Areas are presented in Table 2.1 – these include: Area T03-1/Tilana-1, Nangkero-1, Bass-2,

Yurongi-1, Dondu-1 and Squid-1; and, Area T03-2/Tarook-1, Poonboon-1, Narimba-1, Flinders-1, Pipipa-1, and Pelican-1 to -5 wells (including the Pelican gas field). No wells have been drilled in T03-3.

Table 2.1 Drilling results and hydrocarbon occurrences in the Bass Basin.

Well Name, Operator and Year	Play Type and Target Horizon(s)	Results	Comments
Aroo-1 Hematite Petroleum 1974	Drape over basement high; Paleocene to Early Eocene sands	P&A Fluorescence, minor gas shows	Structural interpretation inaccurate due to the presence of volcanic rocks near target horizons.
Barramundi-1 Globex Far East 1999	Faulted rollover; Paleocene to Early Eocene sands	P&A CO^2 shows	Failure due to breach of regional seal.
Bass-1 Esso E & P Australia 1965	Carbonate reef complex	P&A No shows	Pre-drill interpreted reef structure was invalid. Intersected volcanic section of pyroclastic material.
Bass-2 Esso E & P Australia 1966	Anticlinal structure; Early Eocene sands	P&A No shows	No seal facies; igneous intrusion near TD.
Bass-3 Esso E & P Australia 1966	Anticlinal structure over basement fault block; Mid-Eocene sands	P&A Minor gas	Minor gas shows between 2054.05 to 2055.57 m. Deeper section was water wet. Later drilling of White Ibis-1 in 1998 showed that Bass-3 was not optimally located over the structure.
Chat-1 Bridge Oil Ltd 1986	Faulted dependent closure; Eocene and younger	P&A No shows	Lack of hydrocarbon charge; volcanics intersected near TD.
Cormorant-1 Esso E & P Australia 1970	Anticlinal structure; Paleocene to Early Eocene sands	P&A Minor gas and oil legs	Several pay zones encountered within the Eastern View Group, including a 2 m oil column, and 2 m and 3 m gas and condensate columns. Failure caused by ineffective seal due to late stage reactivation of trap.
Dondu-1 Esso E & P Australia 1973	Anticlinal structure; Paleocene to Early Eocene sands	P&A No shows	Dispersed minor gas shows associated with coals. Good reservoir quality sands above 2743 m.
Durroon-1 Esso E & P Australia 1972	Fault block with updip closure; Early Cretaceous	P&A No shows	No structural closure, lack of seal facies, variable porosity and permeability
Flinders-1 SAGASCO Resources 1992	Fault block; Early Eocene sands	P&A No shows	Water saturated; igneous intrusion near primary objective.
King-1 SAGASCO Resources 1992	Anticlinal structure; Paleocene to Early Eocene sands	P&A Fluorescence, gas shows, trace oil	Water saturated reservoir.
Konkon-1 Esso E & P Australia 1973	Four-way dip closed structure; Paleocene to Early Eocene sands	P&A No shows	Lack of reservoir and regional seal units.
Koorkah-1 Amoco Australia Exploration 1985	Anticlinal structure; Paleocene to Early Eocene sands	P&A No shows	Poor reservoir quality, possible lack of hydrocarbon charge.
Nangkero-1 Hematite Petroleum 1974	Fault block with overlying drape closure; Early to Middle Eocene sands	P&A No shows	Good reservoir and seal rocks encountered.
Narimba-1 Esso E & P Australia 1973	Anticlinal structure; Early Eocene	P&A No shows	Lack of hydrocarbon charge.

Pelican-1 Esso E & P Australia 1970	Anticlinal structure; Maastrichtian to Early Paleocene sands	P&A Gas and condensate discovery	Non-commercial accumulation with 12 gas/condensate-bearing sands between 2471 and 3162 m KB.
Pelican-2 Esso E & P Australia 1970	Anticlinal structure; Maastrichtian to Early Paleocene sands	P&A Gas and condensate	Appraisal well of gas/condensate discovery at Pelican-1. 16 gas/ condensate-bearing sands between 2272 and 3066 m KB.
Pelican-3 Esso E & P Australia 1972	Fault block; Late Paleocene sands	P&A Minor gas shows, weak fluorescence	Hydrocarbon-bearing sands encountered at Pelican-1 and -2 (Lower *M. diversus*) were absent at Pelican-3.
Pelican-4 Hematite Petroleum 1979	Anticlinal structure; Maastrichtian to Early Paleocene sands	P&A Gas and condensate shows	Further appraisal of gas/condensate-bearing sands at Pelican-1 and -2. Also aimed to test flow characteristics of reservoirs – however sands were too tight to conduct production tests. Three main gas/condensate-bearing intervals encountered, with minor gas and fluorescence recorded in thinner beds.
Pelican-5 Amoco Australia Exploration 1985	Faulted anticlinal structure; Maastrichtian to Early Eocene sands	P&A Gas and condensate flows (DST)	Further testing of Pelican structure. Six DSTs with 2 flows. Log evaluation indicates moveable hydrocarbons at various levels from 2750 to 4050 m KB. Low permeability reservoirs encountered.
Pipipa-1 Hematite Petroleum 1982	Faulted anticlinal structure; Early Eocene sands	P&A Trace gas, weak fluorescence	Good reservoir and seal rocks encountered. Water saturated.
Poonboon-1 Esso E & P Australia 1972	Anticlinal structure, drape over fault block; Late Paleocene to Eocene sands	P&A No shows	Good reservoir and seal rocks encountered. Water saturated. Minor gas kicks associated with coals.
Seal-1 Bridge Oil Ltd 1986	Anticlinal structure; Paleocene to Early Eocene sands	P&A No shows	Lack of hydrocarbon charge (access to mature source rocks).
Squid-1 Weaver Gas & Oil Corporation Australia 1984	Faulted anticlinal structure and overlying Oligocene sand lens; Late Cretaceous to Eocene sands	P&A No shows	Minor gas kicks associated with coals.
Tarook-1 Esso E & P Australia 1972	Low relief anticlinal structure; Early to Middle Eocene sands	P&A No shows	Good reservoir and seal rocks encountered.
Tasmanian Devil-1 Weaver Gas & Oil Corporation Australia 1984	Tilted fault block; Eocene and older sands	P&A No shows	Strata penetrated was significantly different to pre-drill prediction.
Tilana-1 Amoco Australia Exploration 1985	Anticlinal structure; Late Cretaceous to Eocene sands	P&A Minor oil and gas shows	Fluorescence recorded over intervals 3081 to 3096, 3260 and 3573 m KB. Overmature sediments may be due to local intrusions. Target sands had low permeability and porosity.
Toolka-1 Esso E & P Australia 1974	Anticlinal structure; Paleocene to Early Eocene sands	P&A Gas shows, Minor oil	Discontinuous reservoir sands.
White Ibis-1 Boral Energy Resources 1998	Anticlinal structure; Paleocene to Early Eocene sands	P&A Gas discovery	Suspended gas discovery.
Yolla-1 Amoco Australia Exploration 1985	Faulted basement high with dip and fault closure; Paleocene to Early Eocene sands	Suspended Condensate, gas and oil discovery	Production due to come on-line in 2004 (Origin Energy operated BassGas Project).

Yolla-2 Premier Oil Australasia 1998	Appraisal well of Yolla-1 downdip along anticline	P&A Gas shows	Successful in evaluating the Yolla accumulation.
Yurongi-1 Esso E & P Australia 1973	Anticlinal structure; Late Paleocene to Eocene sands	P&A No shows	Good reservoir and seal rocks encountered.

Figure 2.1 Location map of the Bass Basin and adjacent region, southeastern Australia. The basin outline, permits, well and field locations, including the 2002 (black) and 2003 (red) Acreage Release areas, are also shown.

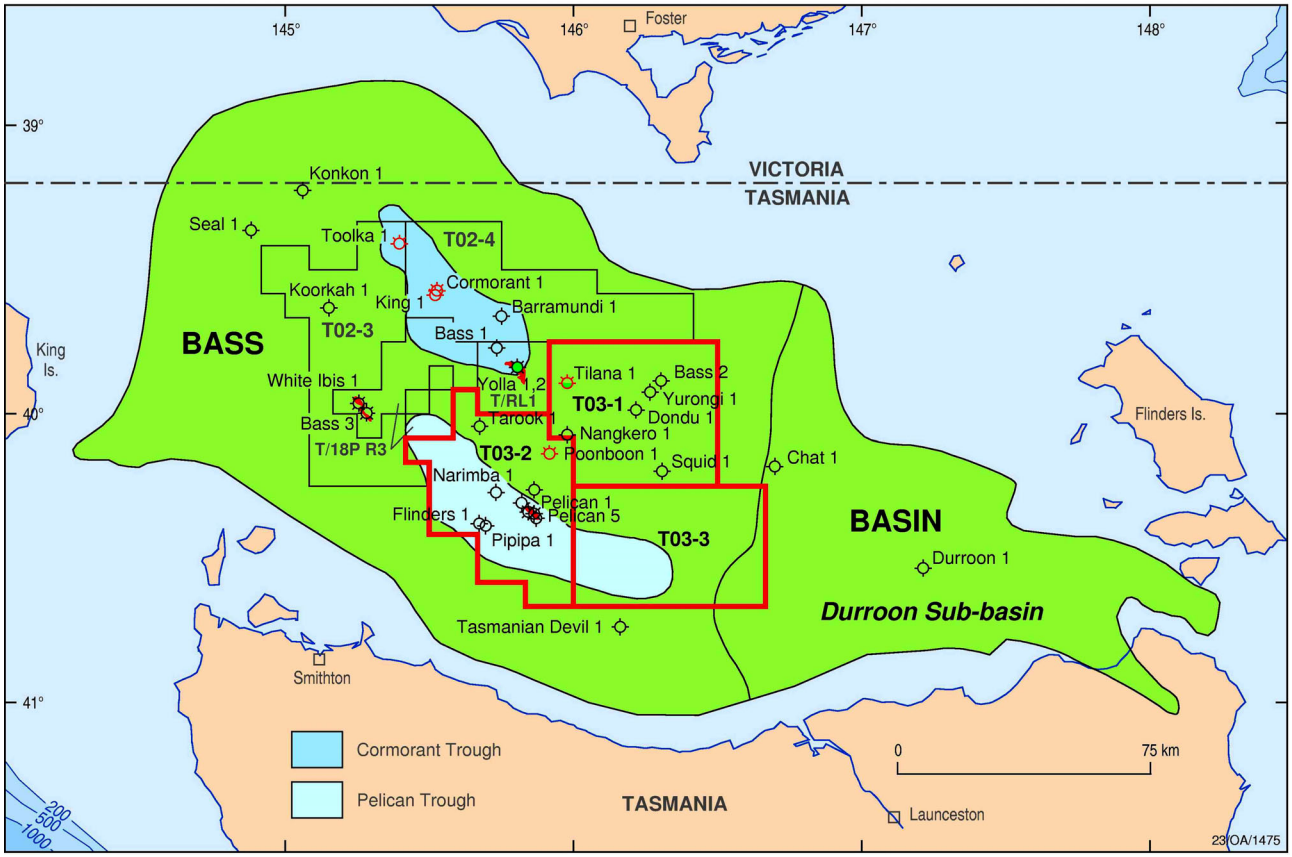

Figure 2.2 Generalised stratigraphy of the Bass Basin (after Lennon et al., 1999), including hydrocarbon accumulations and shows.

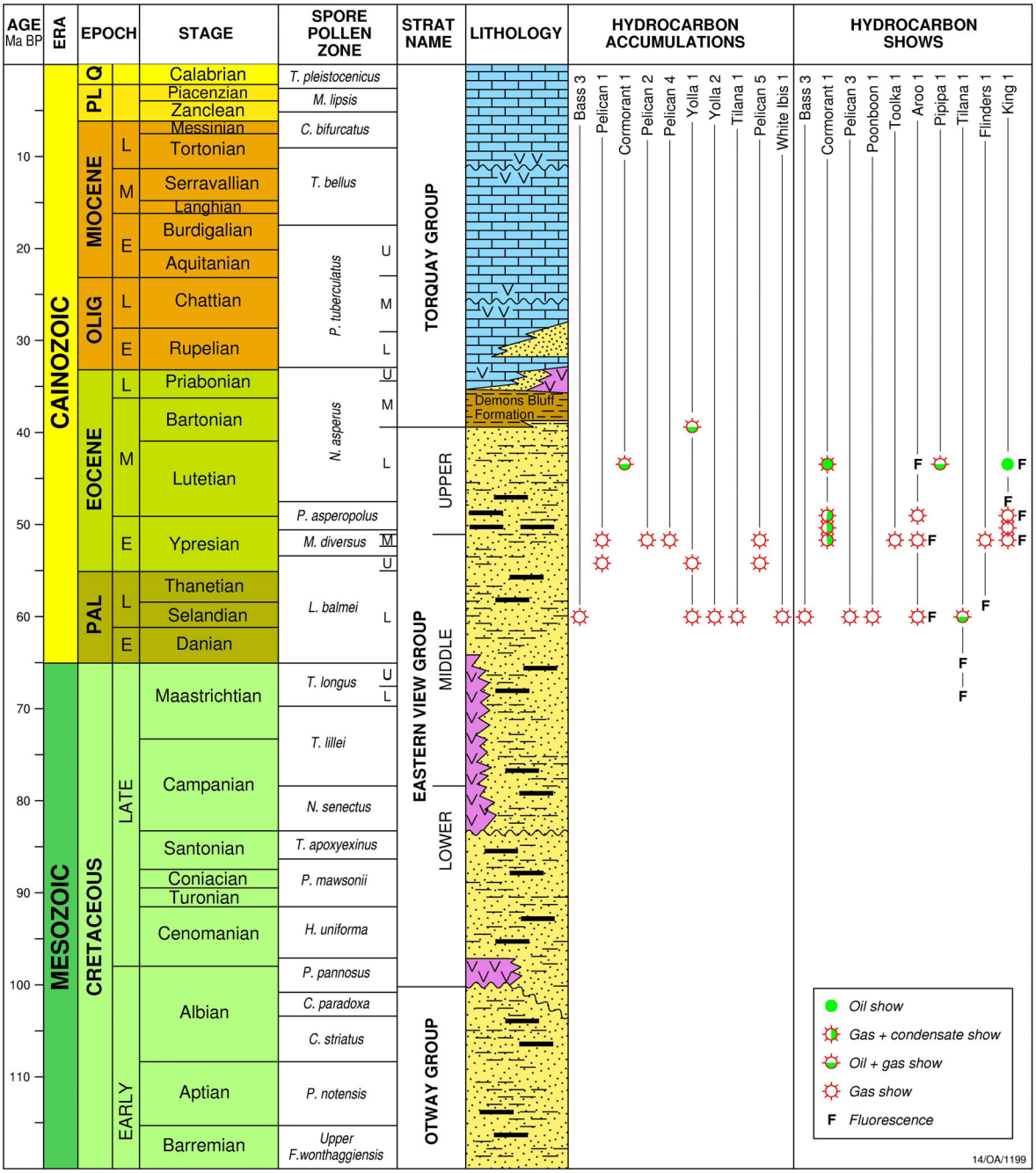

Figure 2.3 Seismic line across the Cormorant Anticline in the northwestern Bass Basin. The anticline formed as a result of Miocene compression. Cormorant-1 was drilled into a minor crestal collapse graben, and encountered several pay zones within the Eastern View Group, including a 2 m oil column, and 2 m and 3 m gas and condensate columns. The well also intersected several volcanic horizons (Late Oligocene, 0.68 ms TWT; sill at 1.99 ms TWT). This seismic image is used with the permission of Fugro MCS.

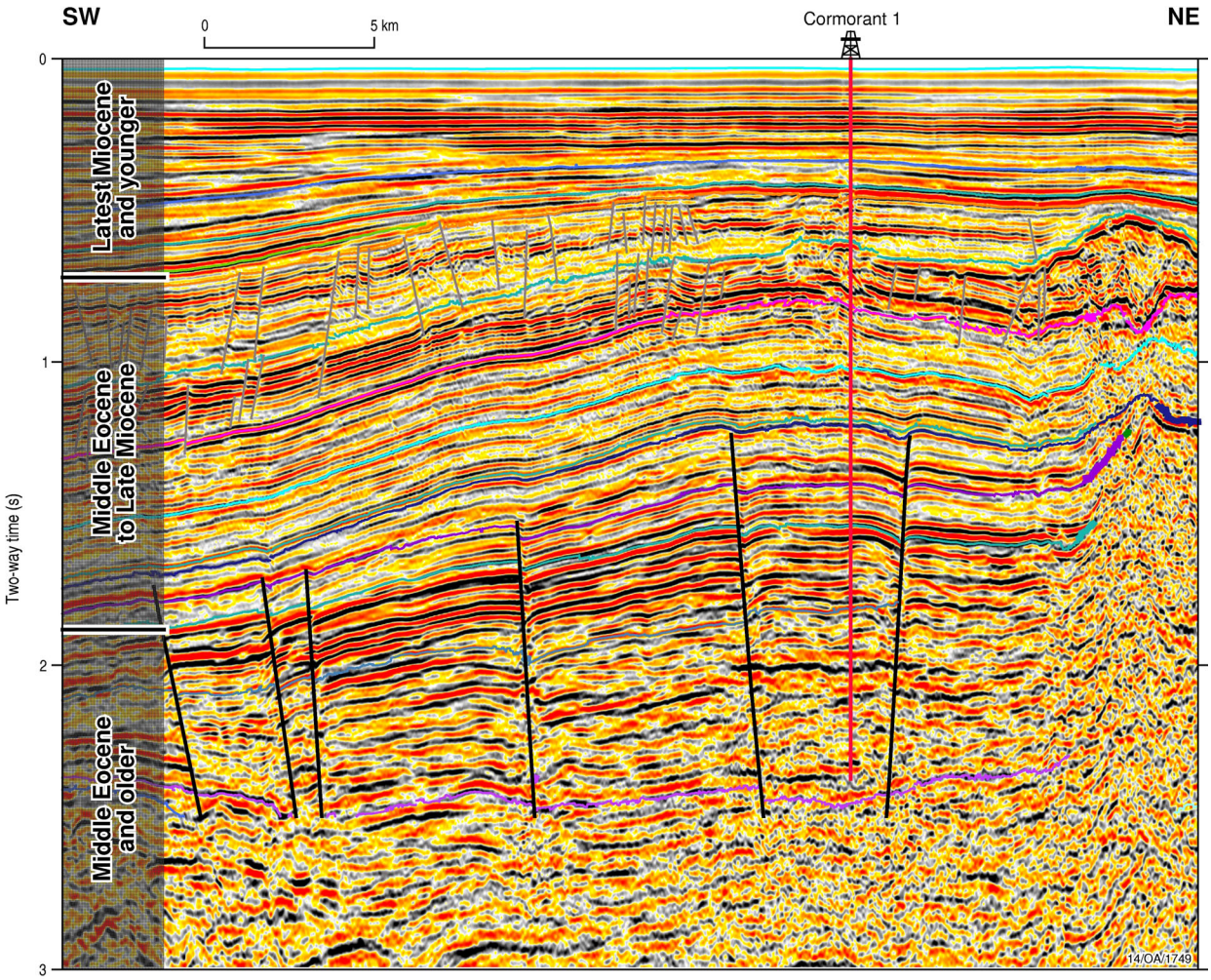

Figure 2.4 Seismic line across the Pelican Trough in Release Area T03-2. Exploration well Pelican-5 was drilled into a crestal collapse structure within the handing well, and is projected for correlation purposes. This seismic image is used with the permission of Fugro MCS.

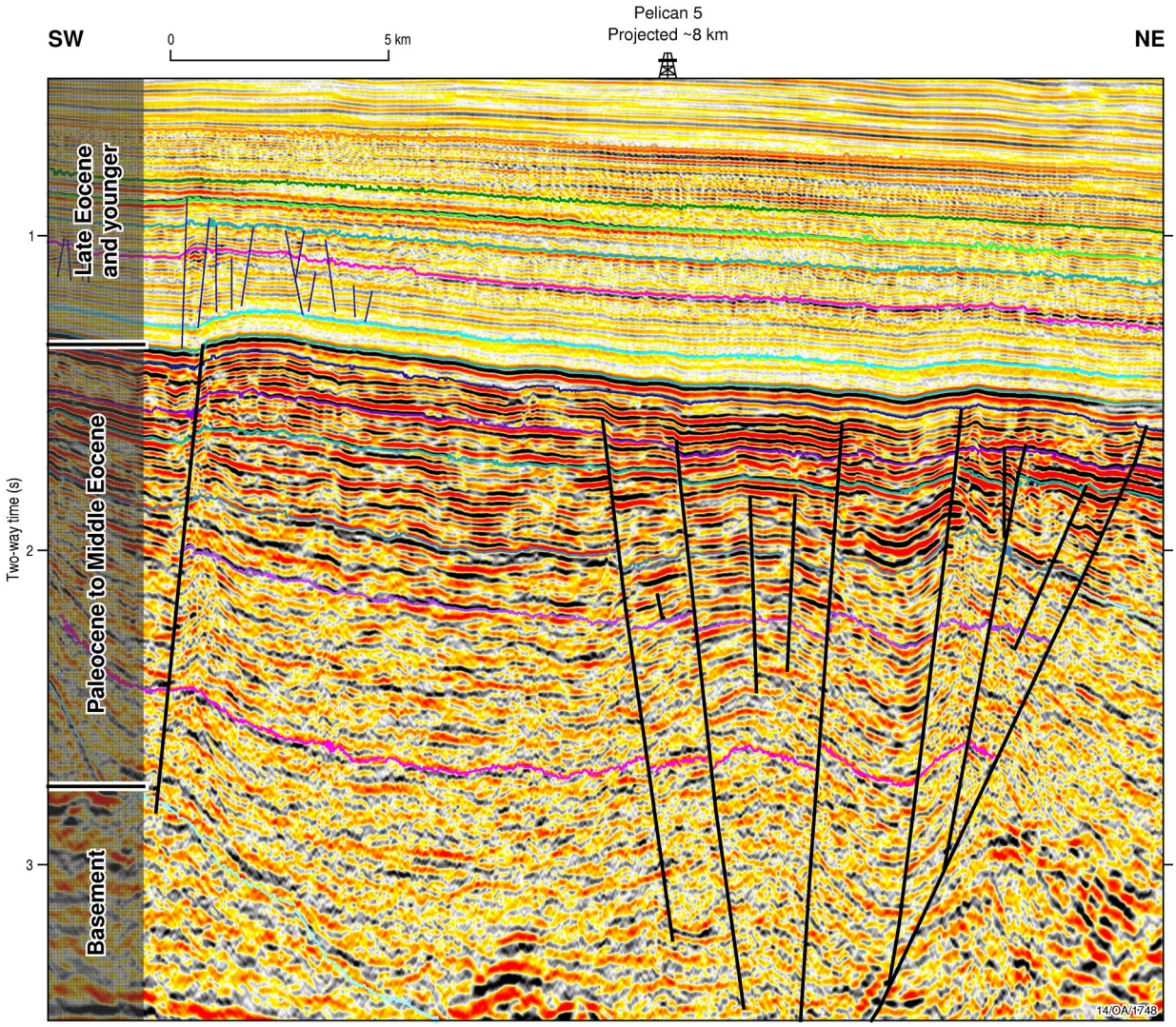

3. TECTONIC EVOLUTION

J. Blevin, Geoscience Australia

3.1 KEY POINTS

- The formation of the Mesozoic Bass Basin was strongly controlled by the fabric of Proterozoic and Palaeozoic basement terranes that underlie the basin. In the western Bass Basin, basement rocks are Proterozoic fold belt metasediments, while in the east, the basin is underlain by metasediments and granitic intrusions of the Palaeozoic Lachlan Fold Belt.
- The Bass Basin is dissected by a north-to-northeast-trending accommodation structure – the Chat Accommodation Zone. A change in rift polarity is observed across this zone. The Chat-1 well was drilled near this accommodation zone and intersected dolerites at total depth.
- The formation of the Chat Accommodation Zone was probably controlled by an underlying terrane boundary within basement, possibly the boundary between the Proterozoic and Palaeozoic fold belts. The zone sub-divides the Bass Basin into the Durroon Sub-basin (east) and the Cape Wickham Sub-basin (west).
- The Mesozoic Bass Basin formed through multiple periods of upper crustal extension associated with three main regional events: a) rifting in the Southern Margin Rift System (Stagg et al., 1990) to the west; b) rifting associated with the formation of the Tasman Basin to the east; and, c) prolonged separation, fragmentation and clearance between the Australian and Antarctic plates along the western margin of Tasmania.
- The amount and rate of subsidence varied across the basin, particularly between the Cape Wickham and Durroon sub-basins. Structural elements within the Cape Wickham Sub-basin also experienced different subsidence histories.
- Three phases of extension are recognised based on seismic mapping and well log interpretations. It is likely that the latest stage of extension was the result of far-field stresses and was oblique in orientation. The late Early Eocene to Middle Eocene was a time of rift-transition, when it appears that the effects of intra-plate stresses progressively waned from east to west, as Antarctica moved further south relative to the west Tasmanian margin.
- Most of the coaly source rocks now typed to liquid hydrocarbon generation (Chapter 5; Boreham et al., 2003) were deposited during the period of late Early Eocene to Middle Eocene rift-transition.
- A combination of factors including multiple rift events, a complex basement fabric, differential subsidence, and deposition within a terrestrial landlocked basin (until the Middle Eocene) has resulted in complex facies relationships across the basin.

3.2 BASIN STRUCTURE AND REGIONAL TECTONIC SETTING

The Bass Basin is a northwest-trending, intracratonic rift basin that underlies the Bass Strait region between northern Tasmania and southern Victoria (Figure 3.1). The basin covers an area of approximately 42,000 km^2, and is separated from the Otway Basin to the west and northwest by the King Island High, and from

the Gippsland Basin to the northeast by Flinders Island and the Bassian Rise. The orientation of rift-related extensional stresses in the Bass Basin has been proposed as north-northeast, resulting in a series of west to northwest-striking basement-controlled normal faults offset along strike by northeast-trending accommodation zones (Etheridge et al., 1985; Young et al., 1991; Gunn et al., 1996; Lennon et al., 1999). In the Otway Basin, Hill et al. (1994) suggest that Early Cretaceous extension may have been broadly north-south across an area with pre-existing northeast and northwest basement fabrics. The Bass Basin is characterised by a half-graben structural style, with tilted Palaeozoic and Proterozoic basement blocks showing large scale offset along northeast and southwest dipping normal faults. Fault throws are in the order of 3 to 5 km, with the total sedimentary succession (syn-rift and post-rift) reaching thicknesses of 8 to 10.5 km (Williamson et al., 1987). The deepest depocentres in the basin have been informally named the Cormorant, Yolla, and Pelican troughs (Lennon et al., 1999). The structural style of the eastern Bass Basin differs significantly, and this eastern region has been referred to as the Durroon Basin or Sub-basin (Baillie and Pickering, 1991; Das and Lemon, 2000b).

The rifted margins of eastern and southern Australia formed during multiple periods of extension associated with the fragmentation and dispersal of Gondwana in the Late Jurassic to early Palaeogene (Veevers and Ettreim, 1988; Veevers et al., 1991). Along with the flanking Otway, Gippsland and Sorell basins, the Bass Basin was initiated in the Late Jurassic to Early Cretaceous (Tithonian-Barremian) as part of the Southern Rift System (SRS; Stagg et al., 1990; Willcox and Stagg, 1990; Etheridge et al., 1985). This major rift system extended from Broken Ridge in the west, to the South Tasman Rise in the east. Extension during the Jurassic and Early Cretaceous resulted in the formation of a series of west-northwesterly trending continental rift basins along the southern margin of Australia and a series of north-northwest trending transtensional basins along the western margin of Tasmania. The amount of upper crustal extension varied between basins of the SRS, with relatively thick, early syn-rift sediments of Late Jurassic to earliest Cretaceous age preserved in half-graben systems in the Bight Basin (Eyre, inner Recherche, eastern Ceduna and Duntroon sub-basins; Totterdell et al., in press) and western onshore Otway and Gippsland basins. There is presently no direct evidence of Jurassic age sediments in the Bass Basin, although the prolific extrusion of dolerites across central Tasmania is thought to mark the onset of rifting. Other research has suggested the onset of rifting in the Bass Basin may have occurred as late as Early Cretaceous along with extensive associated volcanism (Gleadow and Duddy, 1980).

This phase of upper crustal extension preceded the eventual breakup between the Australian and Antarctic plates off the Bight Basin in the latest Santonian to earliest Campanian (83 Ma; Sayers et al., 2001). In the eastern Otway-Sorell basins region, oceanic crust was probably not generated until the Eocene (Moore et al., 1992; Norvick and Smith, 2001). The onset of regional thermal subsidence has been inferred as diachronous (Mutter et al., 1985; Moore et al., 1992), progressing east from the Bight Basin and eventually jumping south along the Tasman Fracture Zone, leaving Tasmania attached to the Australian craton (Hill et al., 1994). After separation, the transform margin along the Tasman Fracture Zone underwent severe shear deformation as the Antarctic plate moved southward relative to the Australian plate. This deformation

continued to affect the southernmost part of the South Tasman Rise until the Early Miocene (chron 6B, 23 Ma) when the Southeast Indian Ridge axis cleared from the western edge of the South Tasman Rise (Royer and Rollet, 1997). These far-field stresses related to prolonged separation of the continents continued to affect existing structures in the Bass Basin until the latest Eocene, coincident with the opening of the Southern Gateway (Exon et al., 2001).

In the incipient southern Tasman Basin to the east of the Bass Basin, seafloor spreading began at about 83 Ma (earliest Campanian, chron 33), approximately coeval with southern margin breakup, in a west-southwest direction (Hayes and Ringis 1973; Weissel and Hayes 1977; Shaw 1978). Extension preceding Tasman breakup began approximately 10 m.y. earlier in the Turonian (Symonds et al., 1996), resulting in deposition of the Turonian to Santonian age Emperor and Golden Beach megasequences in the Gippsland Basin (Norvick and Smith, 2001), and similar age syn-rift megasequences in the Durroon Sub-basin (Baillie and Pickering 1991; Blevin, 2001; Cummings et al., 2002). Royer and Rollet (1997) identified the oldest magnetic anomaly (chron 34) in the Tasman Basin just north of the East Tasman Plateau, indicating that spreading may have commenced slightly earlier in the southernmost Lord Howe Rise. Although extension progressed to breakup and seafloor spreading in Southern Ocean and Tasman basins, the Bass Basin and the adjacent Torquay Sub-basin remained 'failed rift' basins where breakup did not occur.

3.3 REDEFINITION OF BASIN BOUNDARIES AND BASIN NOMENCLATURE

The boundaries of the Bass Basin have been remapped using seismic and potential field data to more accurately reflect the distribution of the main depocentres (Figures 3.1 and 3.2). This outline is defined by a series of northwest-trending basin edge faults and depositional hinges. Latest Miocene to Recent highstand sediments extend beyond this boundary onto shallow basement, but are not considered highly prospective for petroleum exploration.

In the southwest, the basin margin is a northeast-dipping flexural ramp that forms the hanging wall to a northwest-striking normal fault near the Bass-3 and White Ibis-1 wells (Figure 3.3). Although seismic data is limited, there is some indication (at the end of lines) that small half graben also occur to the east of King Island (Figure 3.3). However, given the size and shallow nature of these features, it is unlikely that they are prospective for petroleum exploration. These half graben show some similarity to the King Island Sub-basin of the Sorell Basin, where Clam-1 was drilled.

The northwestern edge of the Bass Basin is difficult to define in both location and nature due to the presence of thick volcanics that degrade data quality (Figures 3.2 and 3.4). The prominence of volcanic material at or near the seabed masks seismic penetration below 200 m depth. Potential field datasets are similarly affected and cannot be reliably used to determine the extent of the basin. However, based on the presence of a large inversion structure over which Cormorant-1 and King-1 were drilled, it is likely that this margin is formed by a steeply dipping, northwest-striking normal fault that dips to the southwest.

The prominent effects of volcanism appear to lessen east of the Yolla-1 and Tilana-1 wells. From Yurongi-1 to just west of Chat-1, the basin margin is defined by a east – west striking normal fault, although there is significant lateral offset on this fault segment. A prominent change in the polarity of the rift basin occurs just north of Chat-1. Here, the basin margin changes from a faulted edge (as seen near Yurongi-1) to a southwesterly-dipping ramp margin. This accommodation zone can be mapped southward across the basin to west of the Tasmanian Devil-1 well (Figure 3.2), where a similar change in basin polarity is observed. The west-southwesterly extent of the basin is defined by onshore mapping and outcrop (Moore et al., 1984). The onshore extension of the Bass Basin has been called the Boobyalla Sub-basin (Moore et al., 1984), however this area is now considered the easternmost part of the Durroon Sub-basin. The most southerly boundary of the Durroon Sub-basin is a northeast-dipping normal fault. Seismic mapping has now shown that significant inversion occurred along this margin in the Cenomanian and Late Miocene.

The accommodation zone defined here by the change in rift polarity marks the boundary between the "western" and "eastern" depocentres of the Bass Basin. The eastern depocentre was previously named the Durroon Basin (Baillie and Pickering, 1991). This name was later modified to the Durroon Sub-basin, in recognition of the similar structural history between the two depocentres, suggesting that a separate basin status (or hierarchy) was not warranted. That view is supported by the mapping undertaken during this study. The new name "Cape Wickham Sub-basin" is proposed to described the western depocentres of the Bass Basin. Cape Wickham occurs on the northernmost tip of King Island; it lies in Tasmanian waters, and marks the most westerly extent of the Bass Basin (Figure 3.1). The boundary between the Durroon and Cape Wickham sub-basins is recognised as a structural accommodation zone marked by a change in rift polarity.

3.4 BASIN STRUCTURAL ELEMENTS

The Bass Basin has been described as a system of multiple northwest-trending, inter-linked half graben (Etheridge et al, 1985; Gunn et al., 1996; Lennon et al., 1999). The integration of basement geology and mapping of the depocentres has helped to clarify the nature of structural elements within the basin. Lennon et al. (1999) defined the Cormorant, Yolla and Pelican troughs as the deepest depocentres within the Bass Basin (Figure 3.2). Two adjacent areas where sediments were significantly thinner were called the Tertiary platforms (Lennon et al., 1999). Some modification has been made to the Lennon et al. (1999) definition of structural elements – mainly, in the Pelican Trough, the Tertiary Platform area near Yurongi-1 and Dondu-1, and the introduction of the White Ibis Trough (Figure 3.2). In addition, the accommodation zone that sub-divides the basin into the Cape Wickham and Durroon sub-basins is recognised as a fundamental structural and depositional hinge that controlled sedimentation from the Late Cretaceous onwards.

The Pelican Trough is defined by a west – northwest-striking normal fault that dips to the southwest. Pelican-1, -2, -3 and -5 and Narimba-1 were drilled on a crestal collapse structure that formed in syn-tectonic sediments deposited over the hanging wall (Figure 3.5). The Pelican Trough dies-out along strike towards the White Ibis-1 and Bass-3 wells. The eastern end of the Pelican Trough also dies-out along strike,

although the bounding fault is eventually truncated by the accommodation zone between the Durroon and Cape Wickham sub-basins. The new name "White Ibis Trough" is proposed for the half graben that lies northeast of the White Ibis-1 and Bass-3 wells. This is consistent with other nomenclature proposed for the basin (Lennon et al., 1999) which uses the names of wells that either intersect the type sections within the trough (e.g., Pelican and Cormorant wells), or are positioned near basement structures that define the trough (e.g., Yolla and White Ibis wells).

The separation of the Cormorant and Yolla troughs as shown by Lennon et al. (1999) recognises the offset along strike and possible change in polarity of the rift faults in this area. The structural complexity in this part of the Mesozoic basin suggests that it is located over a major boundary between basement terranes. East of Yolla-1, the strike of basement faults within the central basin switch from a north-northwest to northwest orientation. The area defined by these northwest trending faults and the accommodation zone to the east has been termed the Tertiary Platform by Lennon et al. (1999). This term "Tertiary Platform" suggests potentially low prospectivity due to a lack of thick Palaeogene sediments (i.e., potential source rocks). However, mapping undertaken during this study suggests that basement beneath the Tertiary Platform can be mapped considerably deeper than proposed by Lennon et al. (1999). It is clear from seismic data and the stacking patterns interpreted from well logs at Yurongi-1, Dondu-1 and Tilana-1 that subsidence (or accommodation) was much slower in this part of the basin, particularly during the Paleocene and Early Eocene. However, a thick Late Cretaceous to earliest Palaeogene section can be interpreted to lie above basement. There is no suggestion of inversion or uplift to account for the thinner Cainozoic section, and it is interpreted that this area is underlain by a stable basement block that was not affected by upper crustal deformation during the early Palaeogene.

The location of the accommodation zone that separates the Durroon and Cape Wickham sub-basins was also strongly influenced by underlying basement fabric. As the Chat-1 well was drilled within this zone (Figure 3.6), the name Chat Accommodation Zone (CAZ) is proposed for the structure. An interpretation of basement from potential field data was commissioned by Geoscience Australia during the early stages of the Bass Basin study. The results (Teasdale et al., 2001, 2003) indicate that the Mesozoic basin geometry was strongly controlled by the proposed Moyston-Tamar Fault Zone, a northwest-trending basement fracture system (Figure 3.7). However, seismic mapping that followed the Teasdale et al. (2001, 2003) study shows that there are probably multiple splays off the fracture zone, some of which may trend northwest. In particular, the change in rift polarity that is observed along the northern basin margin could be due to a splay off the fracture zone, or alternatively, a boundary between accreted terranes within the Lachlan Fold Belt. Two parallel northeast-trending seismic lines from either side of the CAZ show the change in rift polarity (Figures 3.8 and 3.9).

East of the Chat Accommodation Zone, the Durroon Sub-basin has a distinctly different structural style to the western part of the Bass Basin (Baillie and Pickering, 1991). Here, the half-graben structures are narrower and more intensely faulted (Figure 3.10). The underlying basement fabric was also likely to have influenced

the geometry of the rift structures. While the Cape Wickham Sub-basin overlies Proterozoic fold belt metasediments, the Durroon Sub-basin overlies sediments and intruded granites of the Palaeozoic Lachlan Fold Belt. It is also apparent from potential field and other evidence that the Early-Middle Jurassic dolerites that cover much of central Tasmania also extend to areas under the Cretaceous Durroon Sub-basin. The dolerite intersected at total depth in Chat-1 has been submitted for isotope dating by the argon/argon technique, however results were unavailable at the time of publication.

3.5 BASIN EVOLUTION

Due to its regional tectonic setting between two major rift systems, the Bass Basin was affected by multiple episodes of upper crustal extension and compression, driven by both inter- and intra-plate stresses. Structural development was further influenced after breakup along the central Southern Margin by the prolonged fragmentation and clearance of Antarctica along western Tasmania. The fact that the Bass Basin is underlain by basement of differing fabric has also influenced the different structural styles observed within the overlying Mesozoic rift basin. Stresses across the basin are likely to have been partioned by the Chat Accommodation Zone, which is clearly a basement-controlled feature. Basement character also played a role in the different post-rift subsidence histories observed between the Cape Wickham and Durroon sub-basins. On its margins, the Bass Basin is flanked by basement buttresses forming the King Island High to the west-northwest, and the Bassian Rise to the northeast. These features acted to focus and partition Cretaceous and Cainozoic compressional stress along the northern, eastern and western margins of the Bass Basin.

From the integration of well logs and regional seismic mapping, at least three broad phases of upper crustal extension, spanning the Early Cretaceous to the Early Eocene, can be recognised in the Bass Basin (Figure 3.11). These basin phases are correlated to megasequences or supersequences (first and second-order cycles of deposition; Chapter 4). The first phase of rifting occurred during the ?Barremian to earliest Cenomanian (Otway Rift Phase), as part of a broader phase of extension that affected the eastern part of the southern margin (Otway-Sorell region). The second phase of rifting during the Turonian to Campanian was associated with extensional stresses that preceded Tasman Basin breakup (Durroon Rift Phase). Although mapping of the deeper syn-tectonic section in the western Bass Basin is difficult (due to depth of burial), the early Otway Rift Phase appears to have affected most of the Bass Basin, while the effects of the Tasman rift phase are more pronounced in the Durroon and central Cape Wickham sub-basins. The Durroon Sub-basin ceased to be tectonically active in the mid-Campanian, with sediments from the Late Cretaceous until the Miocene deposited under conditions of post-rift thermal subsidence. The third phase of extension focused on the central and western regions of the Bass Basin, particularly structures within the Pelican and Cormorant troughs (Bass Rift Phase; Smit, 1988). This final phase of upper crustal extension may have been related to propagated far-field, intra-plate stresses associated with the prolonged clearance of the Antarctic and Australian plates, and therefore was probably highly oblique to the existing rift-bounding faults. This phase of extension resulted in successive reactivation of existing Lower Cretaceous half-graben structures during the Campanian to Late Maastrichtian, the Late Maastrichtian to Early Paleocene, and again during the Late Paleocene to Early Eocene.

Seismic and well log interpretations have shown that each of the structural elements of the Bass Basin is different in its evolution. During the early phases of extension when the rate of tectonic-driven subsidence was high, sedimentation in the evolving depocentres was probably more uniform, although somewhat geographically focused within the axis of the depocentre. As tectonic subsidence slowed and became more focused in the central and western parts of the basin, sedimentation patterns began to diverge. Tectonic processes ceased to affect the Durroon Sub-basin from the late Campanian onward. In the central Bass Basin, many faults were active until the Late Paleocene, while in the western part of the basin faulting continued until the Middle Eocene. It is during this period of basin evolution (Campanian to Middle Eocene) that sediments show the greatest diversity in facies type, depositional environment and thickness. The stratigraphy of the Bass Basin is presented in Chapter 4.

Early Cretaceous Extension – Rift Phase 1: Otway Rift Phase

Durroon-1 is the only well in the Bass Basin to intersect sediments of Early Cretaceous age (Figure 3.10). Correlation between the well and seismic data is difficult because of the steep dip of the beds intersected. The well is also located over a basement block where the onlapping beds have thinned, and some erosion related to footwall uplift has occurred. Durroon-1 intersected two syn-tectonic sequences – an Early Cretaceous (Aptian to Albian) succession (Otway Megasequence) and a mid-to-Late Cretaceous succession (Turonian to mid-Campanian, Durroon Megasequence – see below). The Otway Megasequence syn-rift succession overlies basement, and is itself the pre-rift section to the later Turonian to mid-Campanian syn-rift succession (Durroon Megasequence; Figures 3.10 and 3.12). Sediments of the Early Cretaceous rift phase (Durroon-1) are distinctly similar in their lithic and volcanogenic character to equivalent age sediments in the Otway Basin (Eumeralla Formation). However, in the Otway Basin, the Eumeralla Formation has been identified as a largely post-rift succession ("Otway Syn-rift/Post-rift Megasequence 3"; Norvick and Smith, 2001). In some instances, the Otway Megasequence in the Durroon Sub-basin appears as a relatively flat-lying succession overlying Palaeozoic basement (i.e., no apparent evidence of syn-tectonic deposition). However, structural restorations of the Otway Megasequence by Cummings et al. (2002; personal communication, 2003) have shown its deposition to be fault-controlled.

Mapping of the syn-rift sediments of the Otway Phase beyond the Durroon Sub-basin is problematic. This is mainly due to an increased depth of burial (poor imaging) and lack of penetration in the Cape Wickham Sub-basin. The patchy distribution of the Otway Phase syn-tectonic sediments suggest that the effects of extension across the broader Bass Basin were limited and probably resulted in formation of isolated shallow half graben. Only during the subsequent phase of extension (Durroon Phase) did the fault segments propagate and link to form more continuous rift features. Interpretation of the Durroon-1 succession indicates the dominance of sand-rich fluvial systems with a significant input of volcanic sediment during this period of basin evolution (Chapter 4).

Turonian to mid-Campanian Extension – Rift Phase 2: Durroon Rift Phase

The Turonian to mid-Campanian Durroon Rift Phase is related to upper crustal extension that preceded breakup and spreading in the Tasman Basin to the east. Although extension probably affected most of the Bass Basin, the effect is most clearly observed in the Durroon Sub-basin. The Durroon Rift Phase is also poorly documented through drilling, although Durroon-1 does provide clear evidence to date this phase of basin development (Figure 3.10 and 3.12). Seismic correlation away from the Durroon-1 well provides more extensive evidence of this syn-rift package, and suggests episodic pulses of fault movement punctuated by short intervening periods of erosion (Figure 3.13). Although several syn-rift wedges are observed on seismic data around the Durroon-1 well, only the "top of Durroon Megasequence" can be correlated westward beyond the Chat Accommodation Zone. New biostratigraphic analyses undertaken as part of this study (Partridge 2002; Appendix C) provide evidence of lacustrine environments within the developing basin (Chapter 4). It is proposed that during deformation, fault segments and associated half graben that were initiated during the previous Otway Phase propagated to form a system of interlinked rift depocentres. Correlation with the Durroon-1 well indicates that extension ceased between 75 and 78 Ma following breakup in the Tasman Basin during the latest Santonian to early Campanian. At the end of the Durroon Rift Phase, the Durroon Sub-basin underwent an extended phase of slow post-rift subsidence.

Late Cretaceous to Early Palaeogene Extension – Rift Phase 3: Bass Rift Phase

While extension in the Durroon Sub-basin ceased in the mid-Campanian, extension continued to episodically affect the central and western parts of the Bass Basin. This coincided with continuing tectonic activity in parts of the Otway Basin and across much of the Sorell Basin along western Tasmania. The age of breakup off the Otway Basin has been suggested as Maastrichtian, although the oldest seafloor lineaments are only Early-Middle Eocene in age (Norvick and Smith, 2001). Final separation and clearance between the Antarctic and Australian plates did not occur until the Late Eocene, signaled by the subsequent opening of the Southern Gateway at around 33 Ma (Exon et al., 2001).

The integration of seismic and well log interpretations clearly shows that the Bass Rift Phase encompasses a series of "pulses" of far-field, upper crustal extension (growth faults). This is probably because the Bass Basin failed to breakup at the end of the Otway and Durroon rift phases, and the locus of extensional stresses associated with fragmentation of the Otway-Sorell-South Tasman Rise region moved progressively further away from the Bass Basin with time. This is reflected in the waning magnitude of each successive event (or "pulse") in Rift Phase 3. In addition, far-field tectonic stresses probably became more oblique through time, such that by the end of Rift Phase 3, only select faults of particular orientations were affected. These events have been consolidated into a single rift/basin phase (and corresponding megasequence) in recognition that they affected only the Cape Wickham Sub-basin (i.e., not the Durroon Sub-basin), and collectively equate to the recognised timeframe of a tectonic cycle (i.e., 20 Ma yrs). The localised nature of these events (and accommodation) has meant that sediments deposited during the Bass Rift Phase vary widely in facies type, environment and thickness. Partridge (2002, Appendix C) has recognised the

widespread development of lacustrine environments across the northern and central Cape Wickham Sub-basin during this time (Chapter 4).

Three unconformity-bounded sequences related to episodes of growth faulting are recognised within the Bass Rift – the Furneaux Sequence (mid-Campanian to late Maastrichtian), Tilana Sequence (late Maastrichtian to mid-Late Paleocene), and Narimba Sequence (mid-Late Paleocene to late Early Eocene). The Furneaux Sequence uses the nomenclature of Maung et al. (1993) who subdivided the Eastern View Coals Measures into two broad lithostratigraphic units based on the abundance of coal. Evidence of the Furneaux rift episode is derived mainly from seismic mapping between the Durroon and Cape Wickham sub-basins. Sediments from only the uppermost part of the Furneaux Sequence have been penetrated by drilling in the western Bass Basin (Lower and Upper *F. longus zones*; Koorkah-1, Poonboon-1, and Tilana-1). Here, the syn-rift nature of the Furneaux Sequence is apparent on seismic data. By contrast, in the Pelican Trough (Pelican-5), later faulting has obscured the syn-rift nature of the sequence (Figure 3.5).

The overlying Tilana Sequence correlates to a basinward thickening wedge of sediment of latest Maastrichtian to Late Paleocene age. Unlike the underlying Furneaux Sequence, the Tilana Sequence does not consistently display stratal geometries indicative of strong syn-tectonic growth (Figure 3.14). However, much of this sequence is heavily affected by (post-depositional) igneous intrusions. The emplaced volcanic material and associated fluids have laterally invaded porous or fractured strata of a coaly/sandy nature. The intrusions mask the original stratal geometry of the sequence on seismic data, resulting in chaotic, high-amplitude and low-frequency reflections throughout the affected succession. Faults controlling deposition of the Tilana Sequence appear to be reactivated older faults of the underlying Cretaceous rift. Towards the upper part of the Tilana Sequence as growth fault-related movement slowed, accommodation was probably heavily influenced by sediment loading and compaction which continued until the latest Paleocene.

The upper part of the Bass Rift Phase (Narimba episode) is more confidently documented by both drilling and seismic correlation. This episode of faulting was probably largely oblique and driven by far-field stresses. Only some faults bounding the Pelican, Yolla and Cormorant troughs were most affected, with growth accommodated by reactivation of the underlying Cretaceous rift faults. The Narimba-1 well intersected over 900 m of latest Paleocene to Early Eocene syn-tectonic sediments in the Pelican Trough. In areas unaffected by reactivation (Poonboon-1, Dondu-1), this succession is less than 150 m thick. The Narimba rift phase was probably oblique in orientation to existing structures, and resulted in the selected reactivation of the early rift faults depending on their orientation. The key period of fault movement, constrained by well and seismic correlations, occurred from the latest Late Paleocene (intra-Upper *L. balmei* zone) until the late Early Eocene (base Upper *M. diversus* zone). The "expanded" syn-tectonic section has also been intersected at Cormorant-1 and in the western Cape Wickham Sub-basin (Koorkah-1, Toolka-1A and Konkon-1).

Early to Middle Eocene Post-Rift Sag – Subsidence Phase 1: Aroo Sequence

From the late Early Eocene until the Middle Eocene (Upper *M. diversus* to intra-Lower *N. asperus* zones) basin-scale tectonic activity waned, marking the transition from rift to post-rift conditions. Many faults within the basin succession terminate at or near the "Base Upper *M. diversus*" or "Base *P. asperopolus*" horizons on seismic data. However, it is clear from well log and seismic correlations that there was not a synchronous end to tectonic activity, thus the nature of this basin phase differs slightly across the basin. In parts of the basin that were not affected by the preceding Narimba rift phase (Poonboon-1, Dondu-1), the transition to post-rift conditions may have begun earlier (possibly Late Paleocene). The deposition of coaly facies increased from the latest Paleocene to Middle Eocene in response to a reduction in the rate of accommodation (the transition from rift to post-rift subsidence). The concentration of coals within this megasequence is clearly observed on seismic data (high amplitude, low frequency). Minor contractional events recorded during this phase are important in the formation of hydrocarbon traps.

Post-Rift Sag – Subsidence Phase 2: Demons Bluff Supersequence

The base of Subsidence Phase 2 in the western Bass Basin is correlated in wells to an unconformity within the Lower *N. asperus* spore/pollen zone. Seismically, this megasequence shows extensive development of fluvial channels and lateral variations in the seismic reflection character within the lower section, grading upward to more uniform bedding and thin progradational units along the basin margin. Biostratigraphic evidence indicates the occurrence of widespread shallow lacustrine environments (Partridge, 2002; Appendix C). Subsidence Phase 2 also coincides with the slow onset of a post-rift transgression that began with fluctuations in base level before any marine influence commenced in the basin. There are multiple localised unconformities within this megasequence, reflecting the low gradient within the former basin depocentres. Widespread marine flooding of the basin occurred during the late Middle Eocene with the deposition of the "Demons Bluff" shale facies (formerly the "Eocene Shale"). Shallow bay to open marine conditions continued until the time of a sea level fall in the mid-Oligocene.

Post-Rift Sage – Subsidence Phase 3: Torquay Supersequence

A sea-level fall in the mid-Oligocene (approximately at the Early/Late Oligocene boundary) resulted in the formation of a regional unconformity across the Bass Basin. This unconformity correlates to the most continuous seismic horizon observed within the basin. By this time, any relicts of the underlying basin topography were buried beneath the fine-grained sediments of the Demons Bluff Supersequence, and the basin was flat and featureless. A rise in eustatic sea level resulted in flooding of the basin in the Late Oligocene and the onset of deposition of fine-grained shallow marine clastic sediment (siltstone and marl). Increasingly open marine conditions developed in the Middle Miocene signaled by the deposition of bioclastic carbonates.

Polygonal faulting is widespread throughout the basin (Das, 2001), but generally only affects fine-grained sediments of Late Oligocene to Early Miocene age (Figure 3.15). From the Miocene to Pliocene, the Australian craton was placed into compression following arc collision 3500 km to the north. The long-distance transmission of these compressional stresses through the lithosphere (Hill et al., 1995) resulted in

multiple periods of Neogene (mid-Miocene) contraction in southeastern Australia (Etheridge et al., 1985; Young et al., 1991; Hill et al., 1995). The western and northwestern margins of the Bass Basin were affected by these contractional events, with large-scale anticlines formed within the syn- and post-rift successions from Miocene through Pliocene time. Several of these structures have been targeted for drilling (e.g., Cormorant-1; Figure 3.15). Similar stresses in the Gippsland Basin resulted in the formation of an en-echelon series of northeast-soutwest trending anticlinal structures on east-west striking Early Cretaceous normal faults (Young et al., 1991). Etheridge et al. (1985) proposed that Neogene inversion occurred along inferred northeast-southwest trending transfer faults throughout the Bass Strait region, rather than by inversion of extensional faults. The Bass Basin and adjacent areas of mainland Tasmania and Victoria have been affected by multiple periods of volcanic activity during the post-rift phases of basin evolution. Offshore, these events are marked by the widespread emplacement of intrusive and extrusive rocks, particularly in the southern and western parts of the basin in association with large-scale faults and accommodation zones (Figures 3.4 and 3.15).

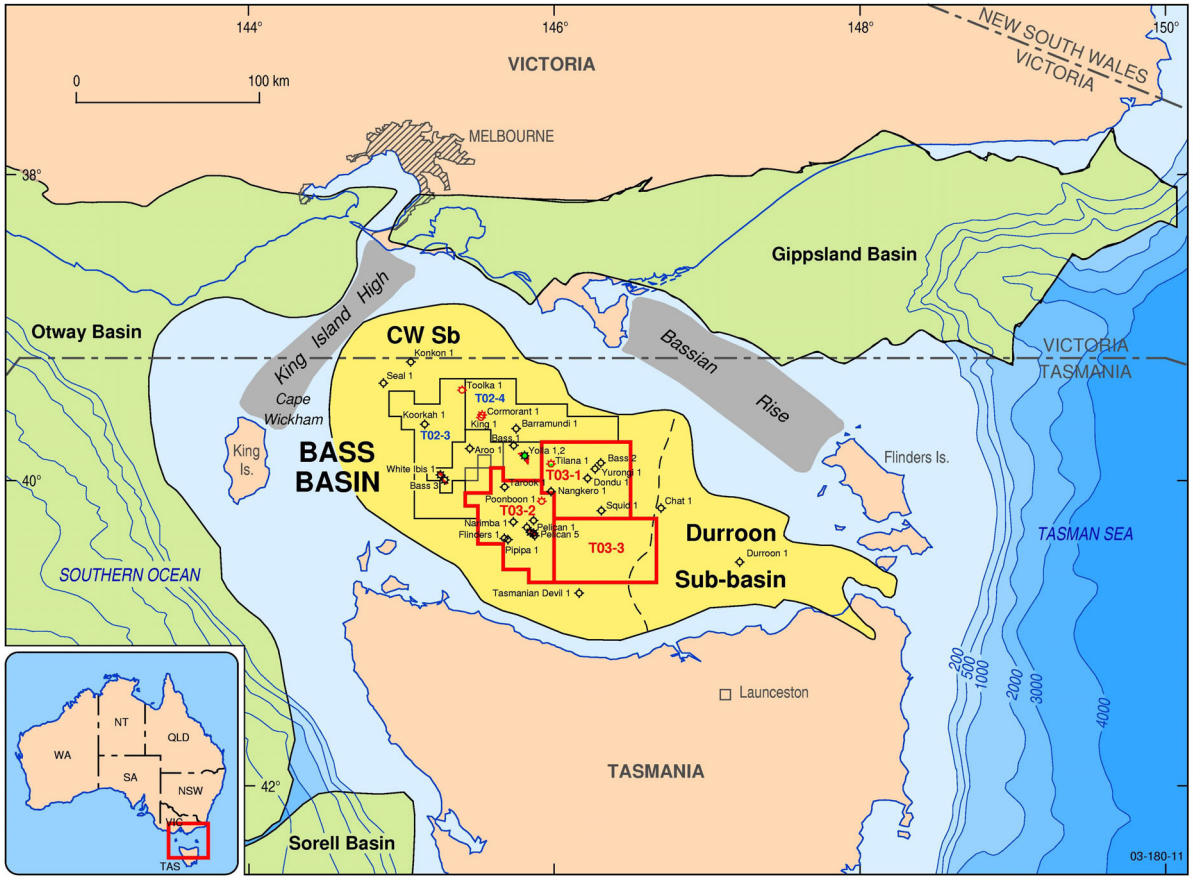

Figure 3.1 Regional map showing the location of the Bass Basin, Bassian Rise, King Island High and surrounding basins (Gippsland, Otway and Sorell basins). The location of Bass Basin wells, fields and the 2003 and 2002 Offshore Acreage Release areas are also shown. Note the location of Cape Wickham on the northeastern tip of King Island, the Cape Wickham Sub-basin (CW Sb; western Bass Basin) and the Durroon Sub-basin (eastern Bass Basin).

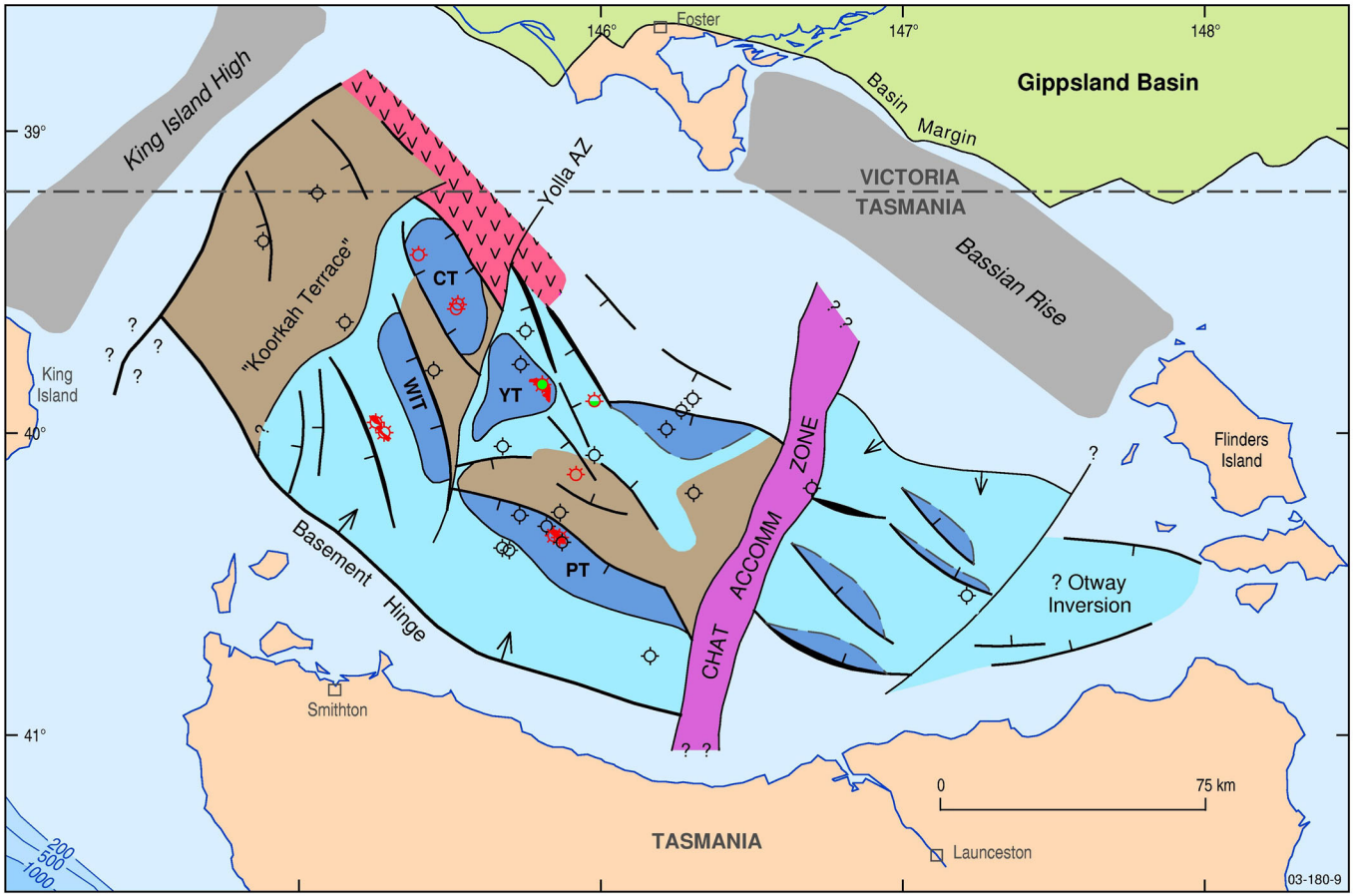

Figure 3.2 Regional map showing the location of tectonic elements and generalised basement fault trends in the Bass Basin. The location of the main Cretaceous half graben in the Cape Wickham Sub-basin are shown by the Cormorant (CT), Yolla (YT), White Ibis (WIT) and Pelican troughs (PT). The Chat Accommodation Zone (CAZ) marks the boundary between the Cape Wickham and Durroon sub-basins. Note the change in overall rift polarity across the CAZ. Early Cretaceous depocentres in the Durroon Sub-basin are generalised (see Baillie and Pickering, 1991 for detailed fault trends). Informal names used here include the Koorkah Terrace and Yolla Accommodation Zone (YAZ).

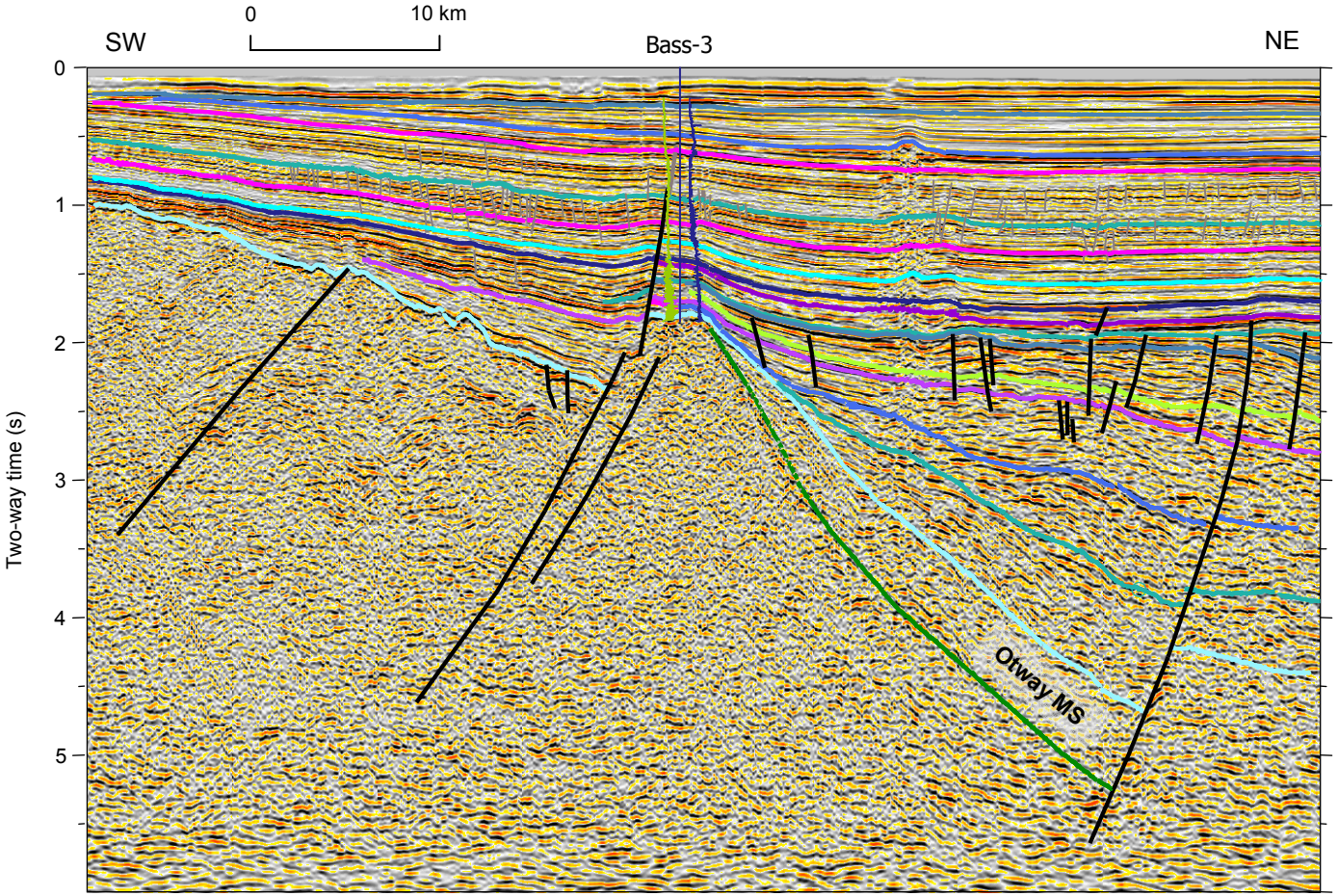

Figure 3.3 Geoscience Australia seismic line in the western Bass Basin showing the hinged nature of the southern basin boundary. Note the location of the Bass-3 well situated at the crest of a basement fault block (footwall), and the thickening of mid-Cretaceous to Early Eocene sediments (towards the northeast). The Otway Megasequence has been interpreted below the "Base-2" horizon (light blue). Also note the volcanic intrusion northeast of the Bass-3 well extending into Late Miocene and younger sediments. The seismic image used in this figure is published with the permission of Fugro MCS.

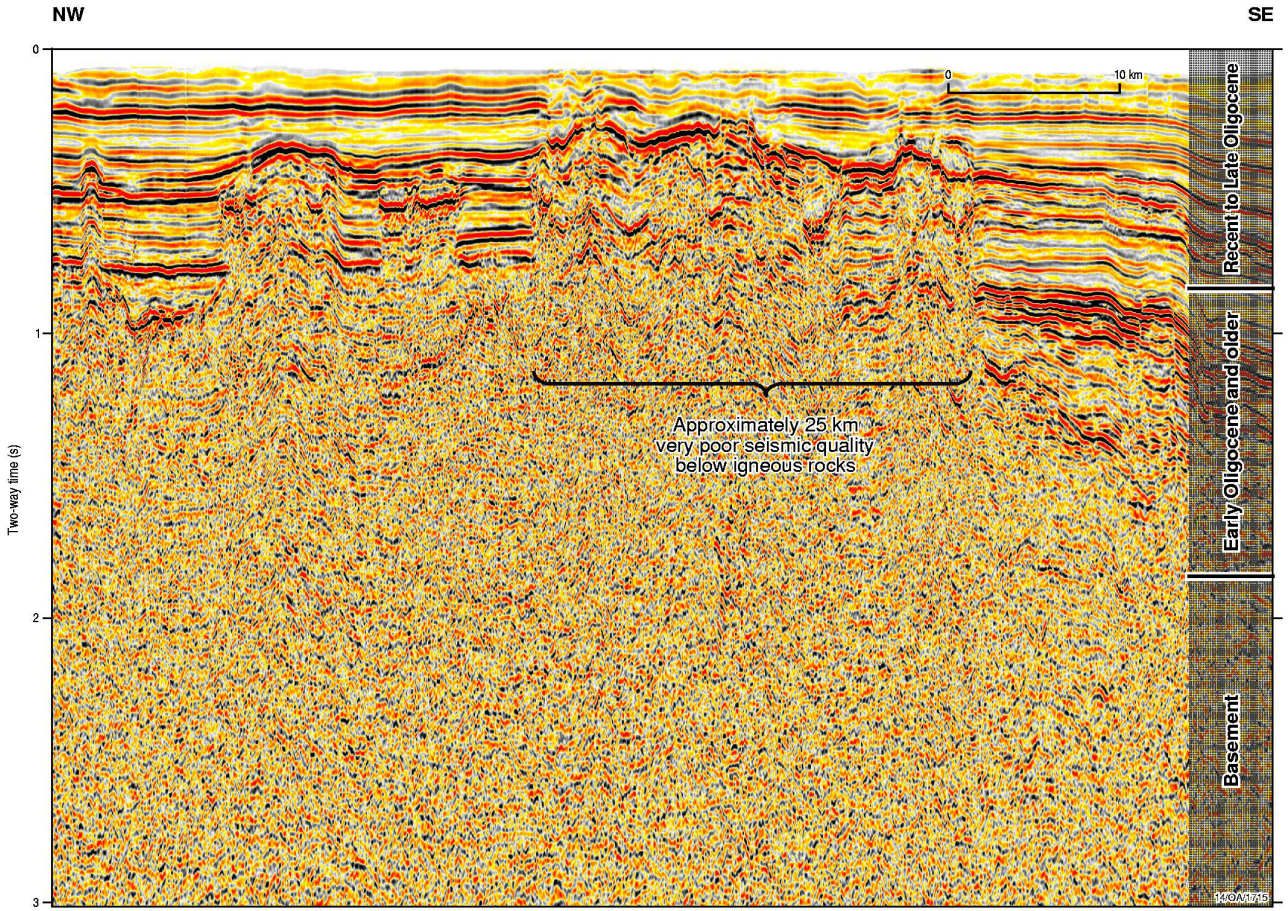

Figure 3.4 Geoscience Australia seismic line in the Bass Basin showing the occurrence of volcanic intrusions and extrusions into Late Oligocene and younger sediments along the northwestern basin boundary. The volcanics obscure the faulted nature of the margin and the overall thickness of the underlying succession. This seismic image is published with the permission of Fugro MCS.

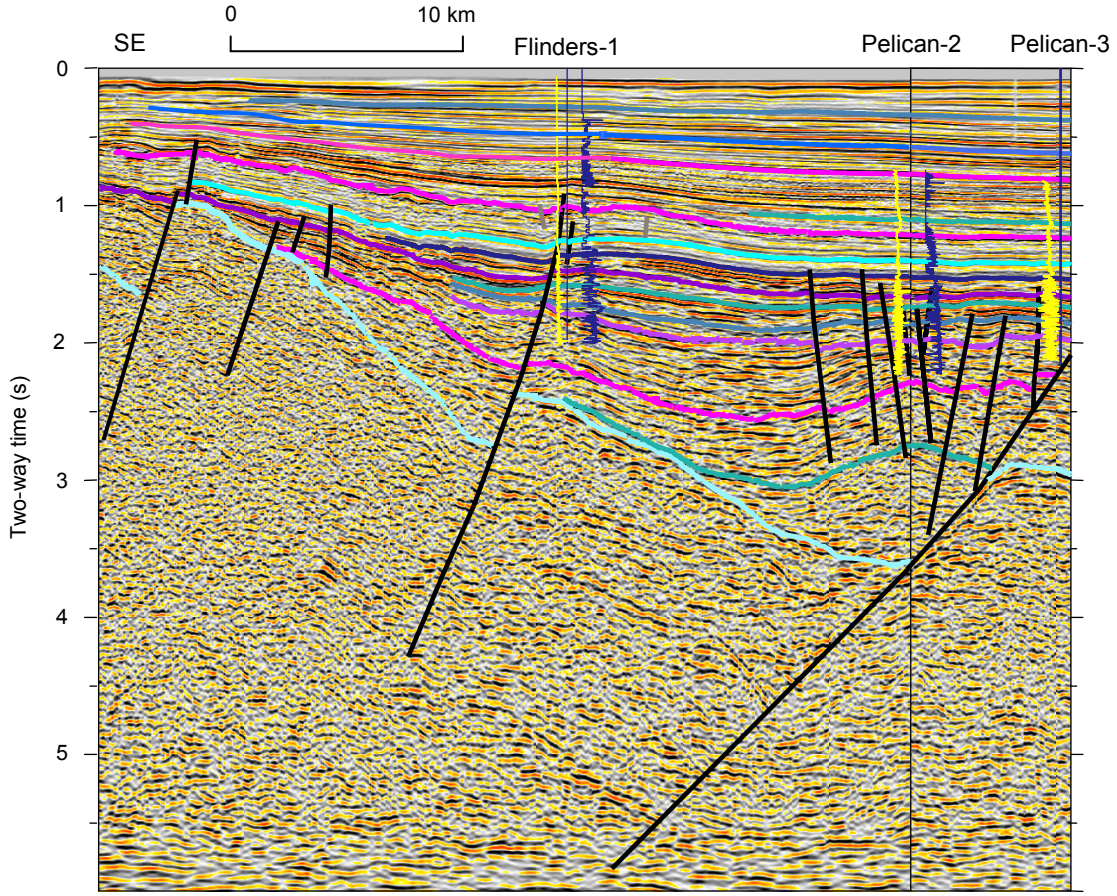

Figure 3.5 Geoscience Australia seismic line across the Pelican Trough in the southern-central Bass Basin. The section shows the location of the Pelican-2, -3 and Flinders-1 wells. The Pelican wells drilled into a crestal collapse structure within the hanging wall of the Pelican Trough, while Flinders-1 is located updip over a footwall block. Structural closure at the Flinders-1 well extends well into the Late Miocene section (pink horizon at approximately 0.65 s TWT), while trap formation in the Pelican Trough mainly occurred during the Eocene. See Figure 2.4 for a more detailed section across the Pelican Trough. This seismic image is published with the permission of Fugro MCS.

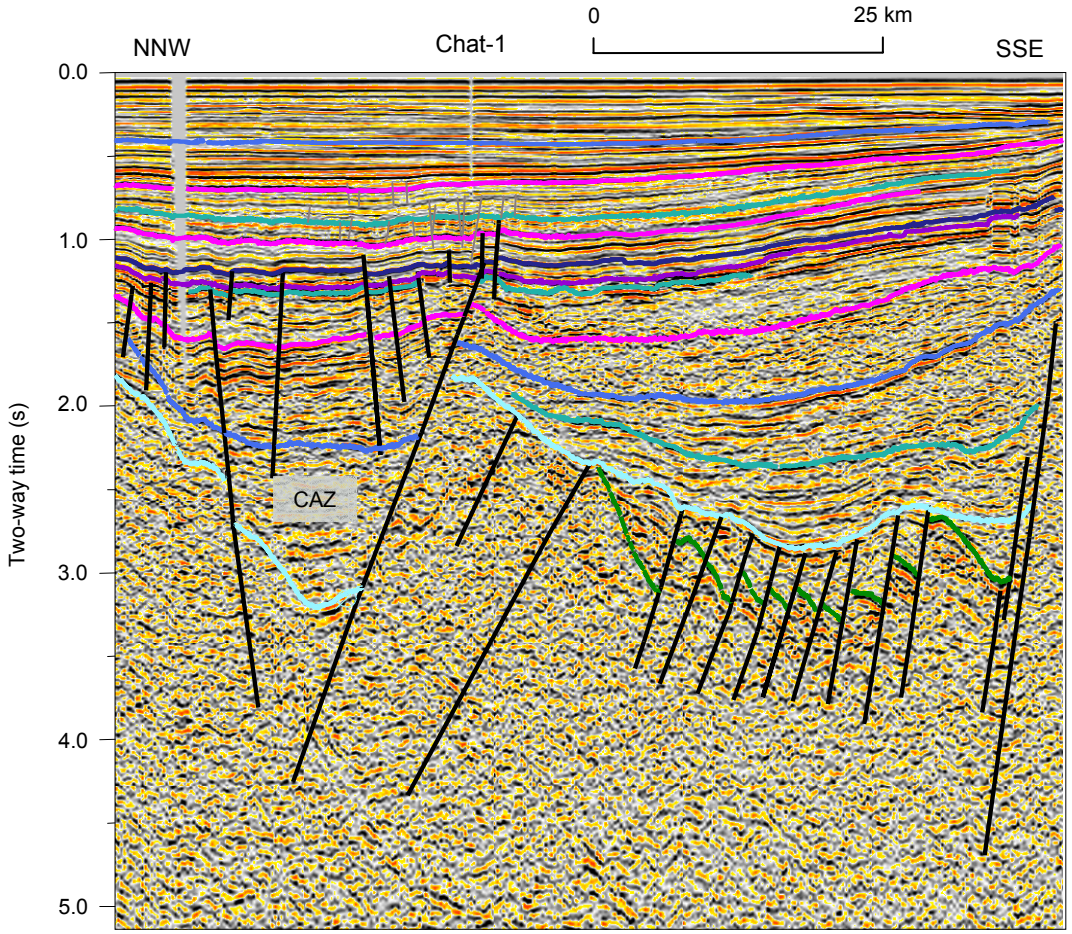

Figure 3.6 Geoscience Australia seismic line across the Chat Accommodation Zone (CAZ). Chat-1 was drilled in the Durroon Sub-basin over an uplifted basement block near the CAZ. The well intersected Cainozoic to Upper Cretaceous sediments before reaching total depth in a dolerite of interpreted mid-Jurassic age. Note the thickening of Palaeogene and younger sediments from east (Durroon Sub-basin) to west (Cape Wickham Sub-basin). This seismic image is published with the permission of Fugro MCS.

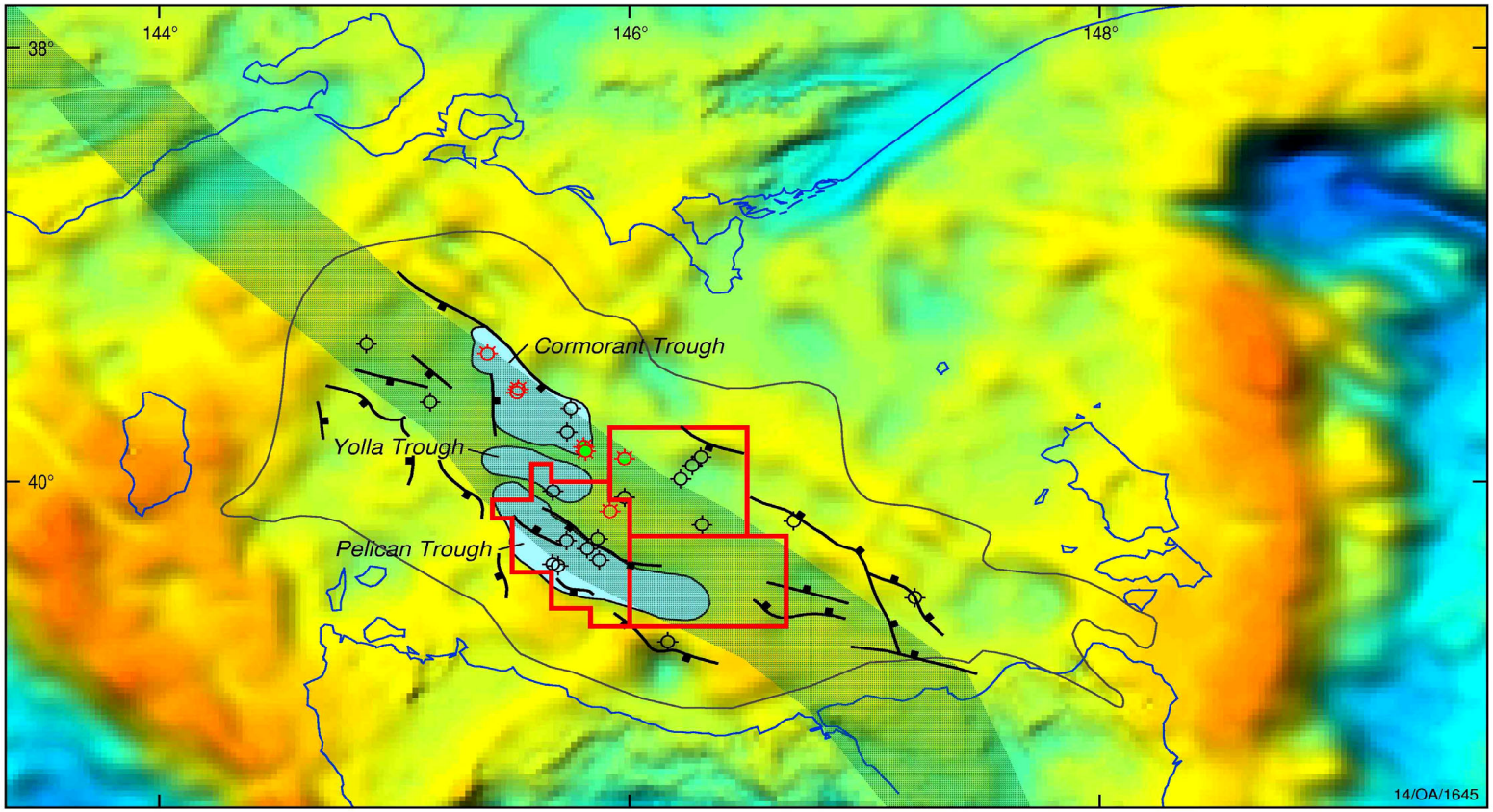

Figure 3.7 Free-air gravity map of the Bass Basin showing the approximate location of a basement fracture zone (shaded area) interpreted to underlie the Bass Basin (Teasdale et al., 2001, 2003). The major bounding faults and depocentres of the Bass Basin are after Lennon et al. (1999). Exploration wells and the 2003 Acreage Release Areas are also shown.

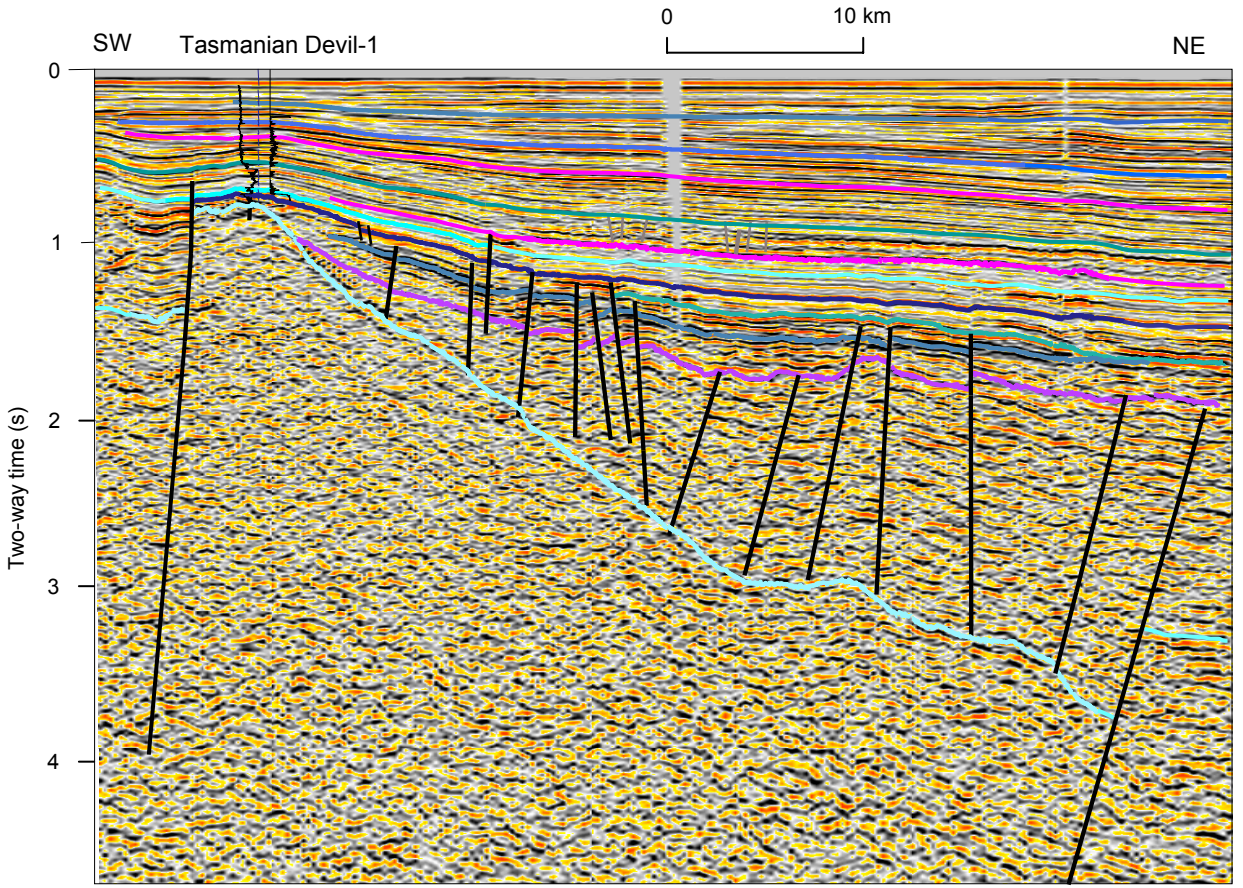

Figure 3.8 Geoscience Australia seismic line across the southern margin of the Bass Basin. The section has been highly decimated to show the nature of major northwest-striking normal faults that dip to the southwest (towards northern Tasmania). This line lies to the west of the Chat Accommodation Zone (CAZ) in the Cape Wickham Sub-basin (near the Pelican Trough). This seismic image is published with the permission of Fugro MCS.

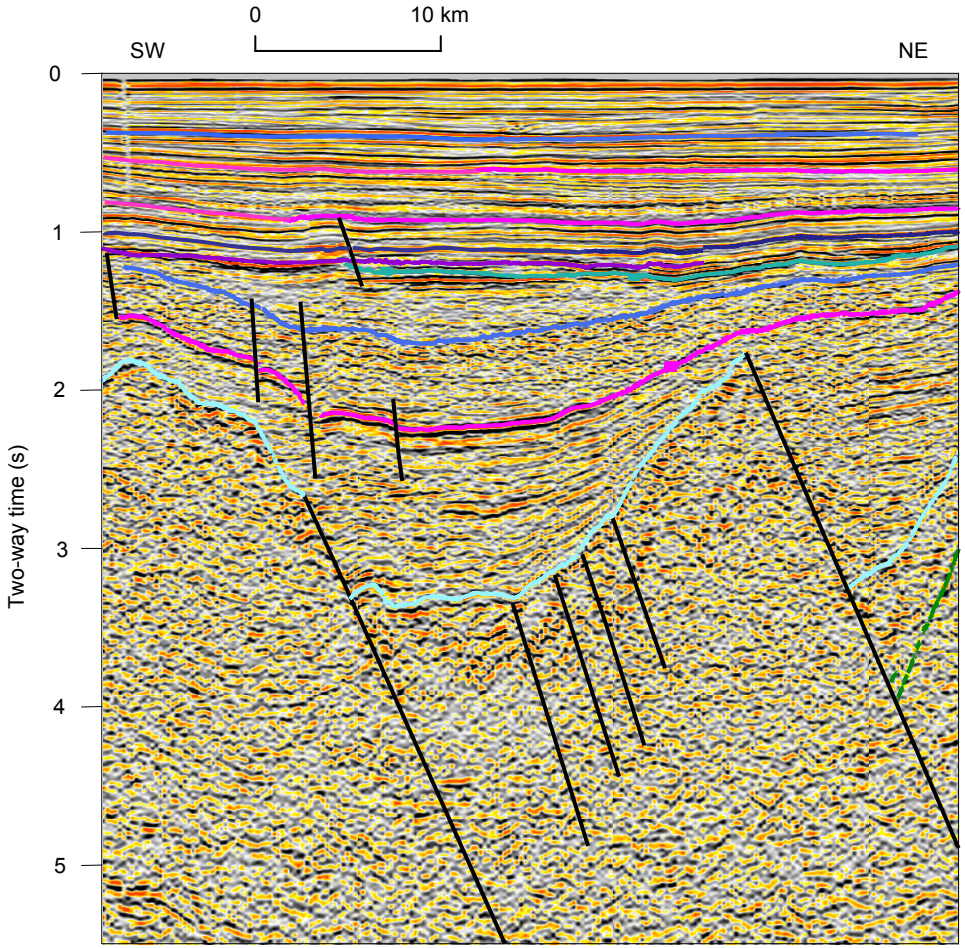

Figure 3.9 Geoscience Australia seismic line across the southeastern margin of the Bass Basin. The section has been highly decimated to show the nature of basin margin and major northwest-striking normal faults that dip to the northeast (towards Flinders Island and the Bassian Rise). This line lies to the east of the Chat Accommodation Zone (CAZ) in the Durroon Sub-basin. This seismic image is published with the permission of Fugro MCS.

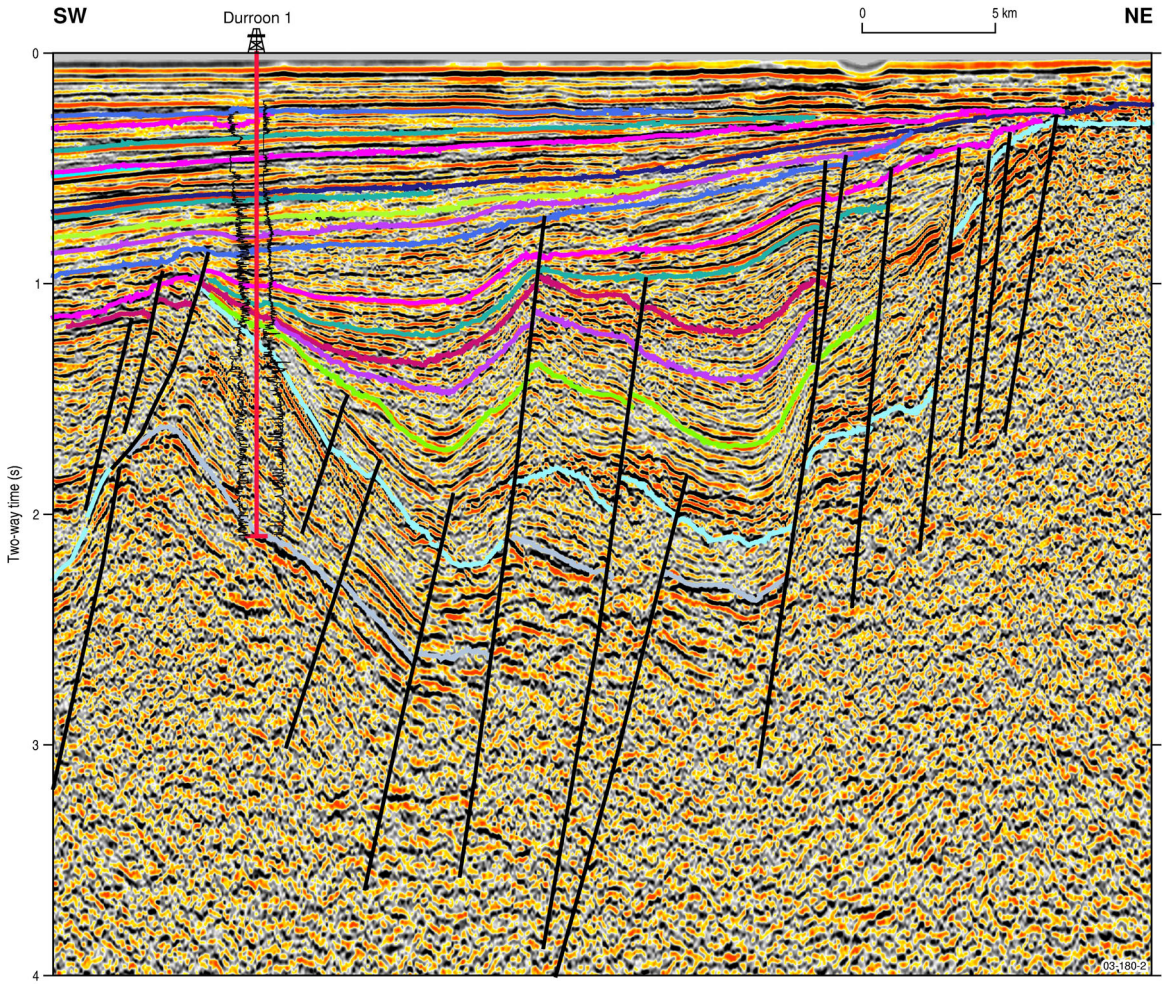

Figure 3.10 Geoscience Australia seismic line across the Durroon Sub-basin showing the structural style of the depocentre and the location of the Durroon-1 well over a faulted footwall block. The well penetrated two syn-tectonic successions of Early Cretaceous (Otway Megasequence) and Late Cretaceous (Durroon Megasequence) age. An interpretation of this line is shown in Figure 3.12. This seismic image is published with the permission of Fugro MCS.

Figure 3.11 Stratigraphic correlation chart for the Bass Basin showing the relationship between lithostratigraphy, sequence stratigraphy, basin phases, events and horizons mapped. The basin phases are shown in detail for the Cape Wickham (CW) and Durroon (Durr) sub-basins. The timescale is from Young and Laurie (1996), with modifications to spore/pollen zones from Partridge (2001).

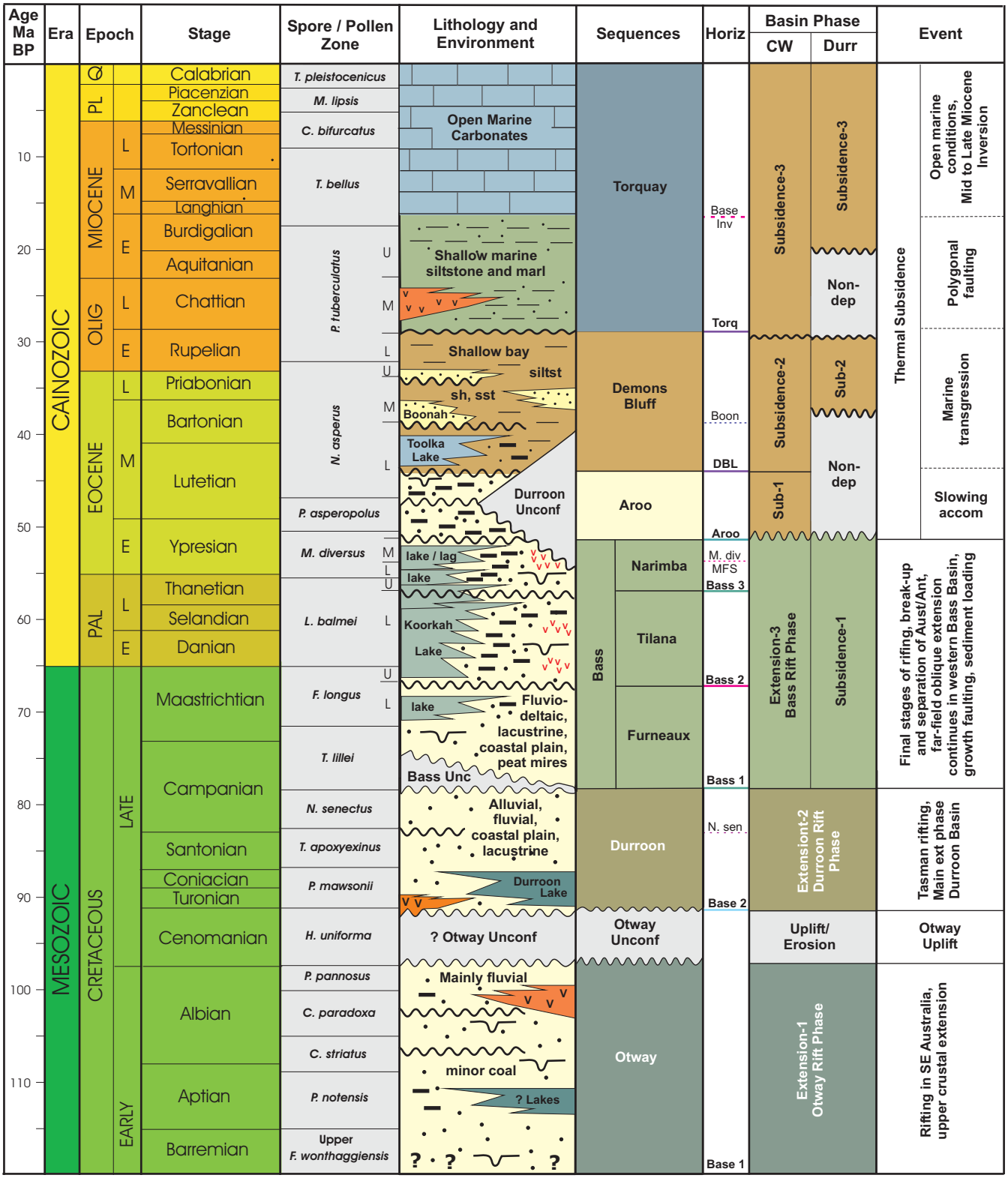

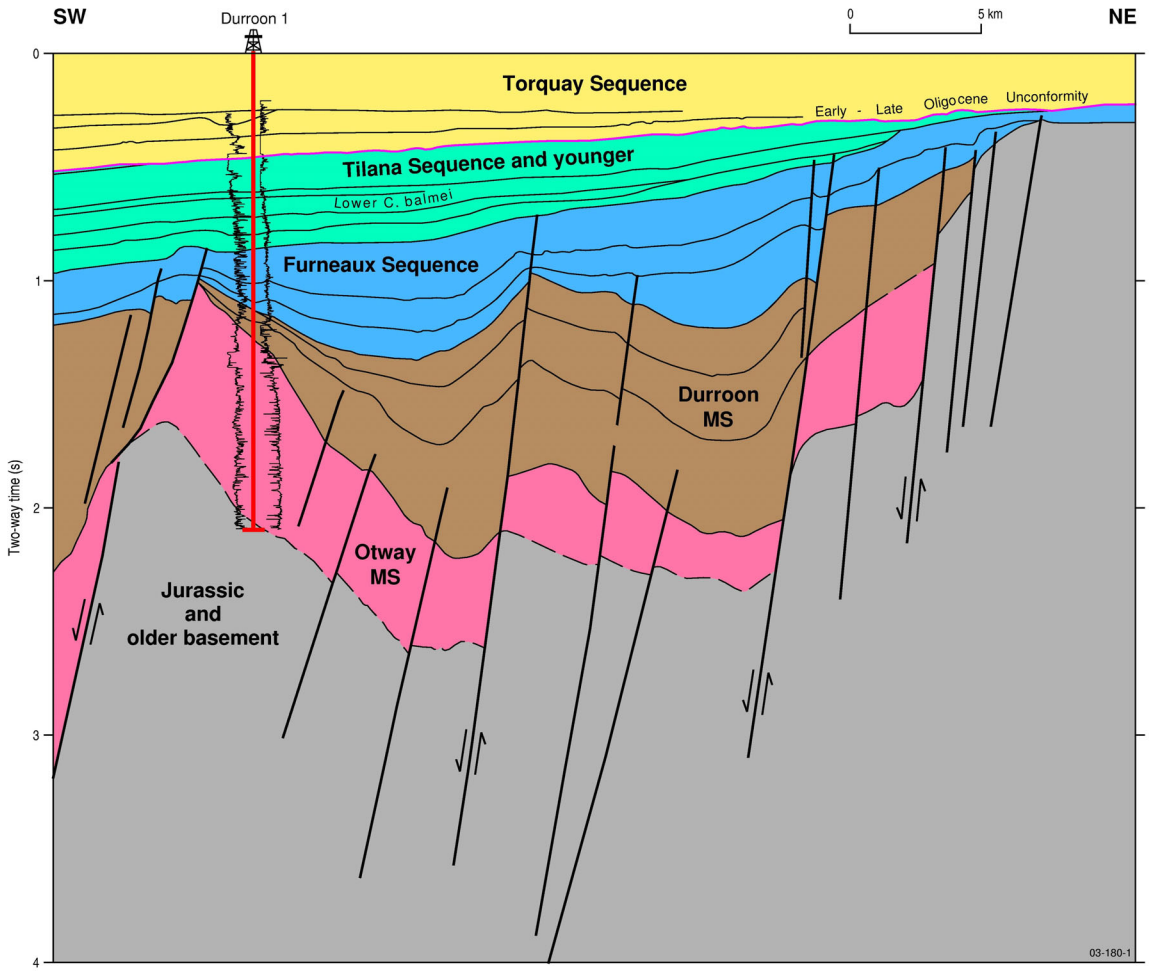

Figure 3.12 A geoseismic section across across the Durroon Sub-basin (see Figure 3.10) showing the structural style of the depocentre and the location of the Durroon-1 well over a faulted footwall block. The well penetrated two syn-tectonic successions of Early Cretaceous (Otway Megasequence) and Late Cretaceous (Durroon Megasequence) age.

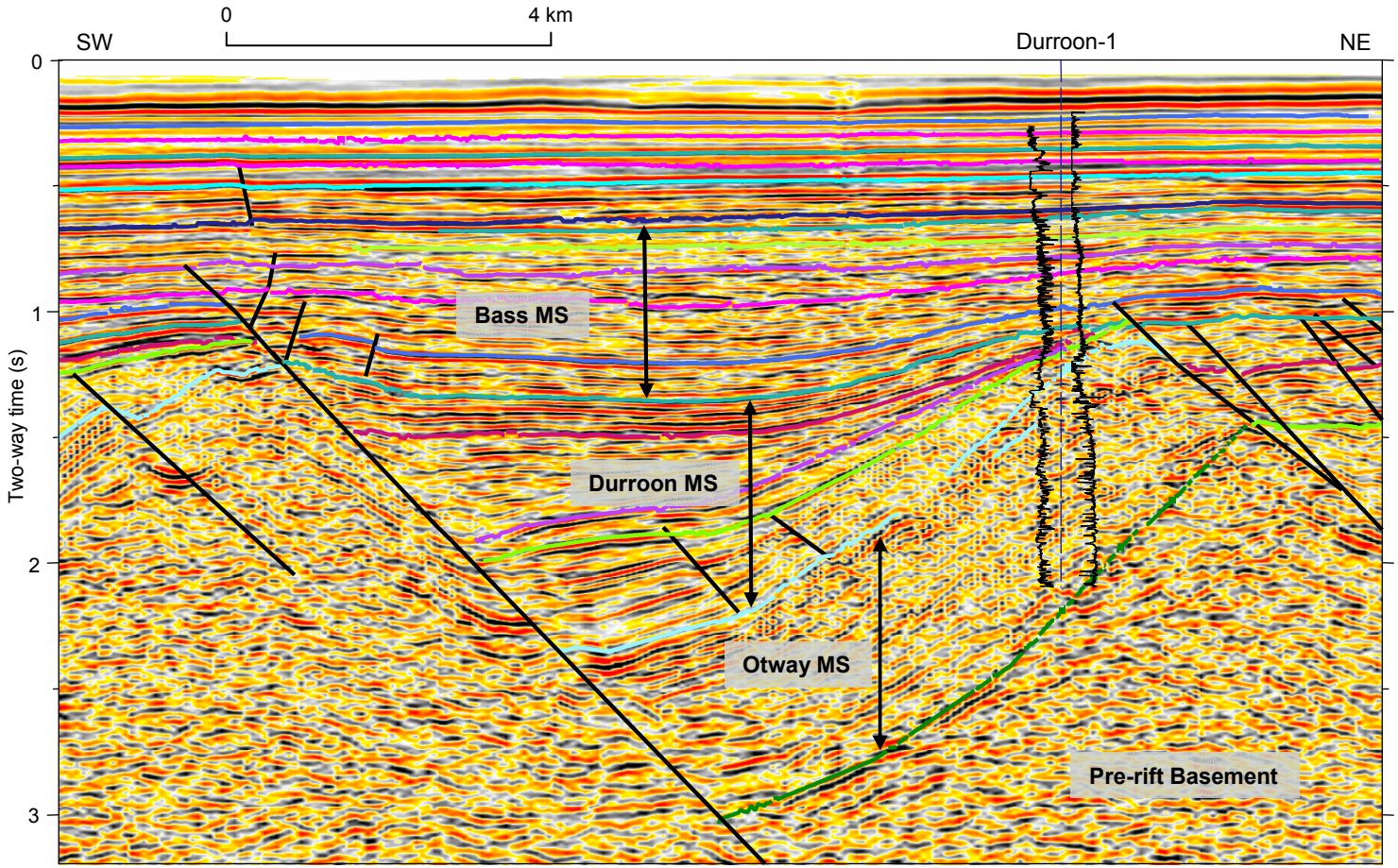

Figure 3.13 Geoscience Australia seismic line across part of the Durroon Sub-basin. This section shows in more detail the syn-tectonic successions intersected at the Durroon-1 well: the Early Cretaceous Otway Megasequence (Rift Phase 1) and the overlying early Late Cretaceous Durroon Megasequence (Rift Phase 2). In the Durroon Sub-basin, the Late Cretaceous Bass Megasequence is largely a sag-related succession deposited during post-rift subsidence. This seismic image is published with the permission of Fugro MCS.

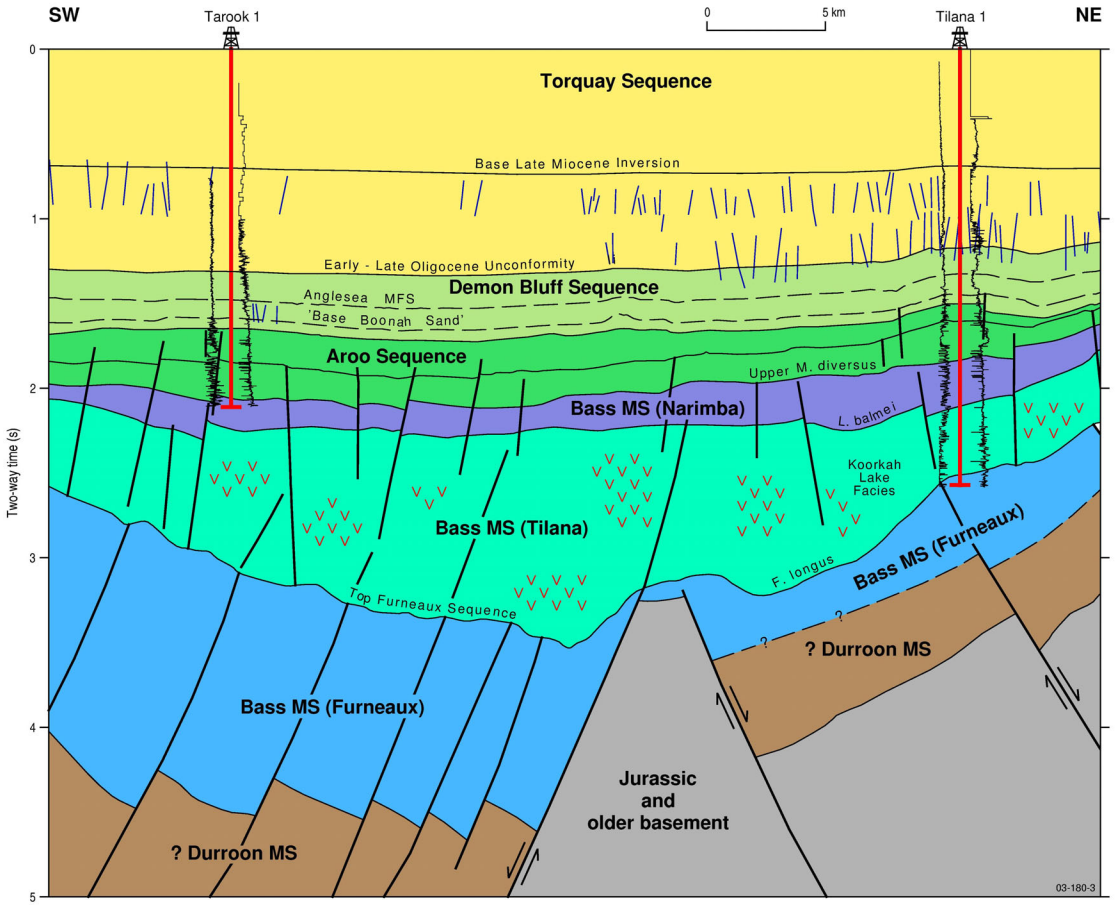

Figure 3.14 Diagrammatic cross-section across the central Bass Basin showing the syntectonic nature of the Durroon and Bass sequences (Furneaux, Tilana and Narimba sequences), and the overlying post-rift successions of Aroo, Demons Bluff and Torquay sequences. The stratal geometry and faults controlling the deposition of the Tilana Sequence are obscured due to the prolific intrusion of volcanics into the succession. The Narimba Sequence shows only minimal growth on this section.

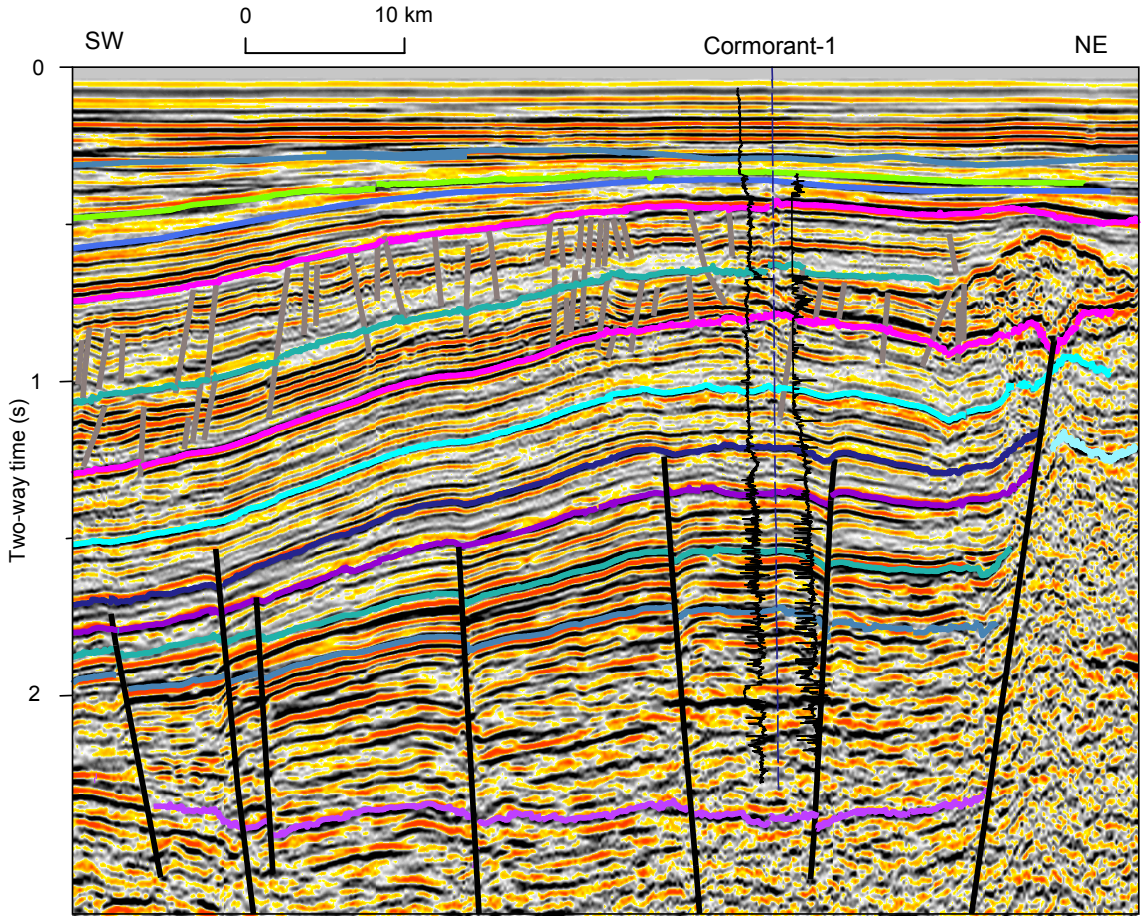

Figure 3.15 Geoscience Australia seismic line across the Cormorant Anticline. The anticline is an inversion structure that formed against the northwestern margin of the basin. The syn-inversion succession at Cormorant-1 has been dated as late Middle Miocene and younger. Cormorant-1 well drilled a minor graben within the crestal collapse structure, and intersected minor oil and gas legs in the Palaeogene succession. High-amplitude, cross-cutting volcanic intrusions seen near 2.00 s TWT were intersected by the well. In addition, a large volcanic mound is observed to the north of Cormorant-1. The mound overlies the mid-Oligocene unconformity and maybe associated with basinward polygonal faulting. This seismic image is published with the permission of Fugro MCS.

4. ACCOMMODATION CYCLES AND SEQUENCE STRATIGRAPHY

J. Blevin and K. Trigg, Geoscience Australia
S. Lang, National Centre for Petroleum Geology and Geophysics
A. Partridge, Biostrata Pty Ltd.

4.1 KEY POINTS

- The integration of biostratigraphy, sequence and seismic stratigraphy to identify accommodation cycles and related environments has resulted in a sub-division of the Bass Basin stratigraphic succession. Six depositional sequences – mainly megasequences and supersequences – are recognised and correlated to phases of tectonic activity and eustatic fluctuation.
- Three megasequences are related to phases of rift-related extension. Evidence of the initial rift phase (Otway Megasequence) is only clearly observed in the Durroon Sub-basin and in the southwestern Cape Wickham Sub-basin (near Bass-3/White Ibis-1 wells).
- The second rift phase (Durroon Megasequence) is pervasive throughout the Bass Basin, although a full succession of this megasequence was only penetrated in the Durroon Sub-basin.
- The third-rift phase (Bass Megasequence) is also pervasive throughout the basin, but appeared to affect only particular depocentres such as the Pelican, Cormorant and Yolla troughs. Here, expanded syn-tectonic growth sections have been intersected (Narimba-1). There is wide variation in facies type, environment and thickness of the Bass Megasequence due to differential rates of subsidence. Three component sequences have been recognised with the Bass Megasequence (Furneaux, Tilana and Narimba sequences). Each sequence correlates to discrete periods of increased accommodation.
- The shift from rift-to-post-rift conditions (Subsidence Phase 1 – Aroo Megasequence) was signaled by waning subsidence rates and an increasing brackish influence. A wide variation in facies types, environments and thicknesses is also observed within this megasequence. The frequency and thickness of coals began to increase during the deposition of this megasequence, lasting from Early Eocene until the mid-Middle Eocene. A slow down in subsidence rates allowed the aggradation of coaly facies and indicates there was a balance between accommodation, sediment supply and peat production.
- The most important megasequences for petroleum generation and trapping are the Bass and Aroo megasequences. Accommodation has controlled the stacking of oil-prone coaly facies, while the increasing marine influence has provided an early cement to fluvial and deltaic sandstone reservoirs. Optimal conditions for seal deposition occurred during lacustrine cycles in the Late Cretaceous to Early Eocene, and the mid-Eocene.

4.2 METHODS AND TIMESCALES

A dataset of geophysical well logs, biostratigraphic and seismic data was interpreted and integrated using principles of seismic and sequence stratigraphy to define a broad-scale basin framework. Petrophysical logs

from 29 of the 32 wells in the Bass Basin were interpreted and correlated via synthetic seismograms (generated using Geoquest software) to a 4,000+ km regional seismic grid (Fig. 4.1). The grid included reprocessed industry data (licensed through Fugro MCS) and reprocessed deep seismic data acquired by Geoscience Australia during 1990-92 (Geoscience Australia Surveys 40, 82 and 90). Seismic images used as figures in this report are published with the permission of Fugro MCS.

A modified version of the Geoscience Australia (formerly AGSO) Phanerozoic Timescale and Biozonation Chart (Young and Laurie, 1996) was used as the reference timescale for this study (Figures 4.2a and 4.2b). The Mesozoic portion of the biozonation scheme is based on Helby et al. (1987), with modifications to age boundaries provided by subsequent radiometric analyses. Further modifications to the timescale were made to incorporate changes to biozonations boundaries as published by Partridge (2001). These changes affected biozones within the Albian to Late Paleocene age range. The present study incorporates the new biostratigraphic work commissioned by Geoscience Australia, on behalf of Mineral Resources Tasmania under the funding auspices of the Western Tasmanian Regional Minerals Program. The work was undertaken by Dr. Alan Partridge, Biostrata Pty Ltd on selected well intervals to address specific scientific questions relating to depositional environment (including processing for microplankton and other evidence indicative of marine influence) and evidence of cyclicity. In addition, the sampling program targeted gaps in the drilled section at key wells. Overall, intervals within seven wells were studied (Cormorant-1, King-1, Konkon-1, Koorkah-1, Poonboon-1, Squid-1 and Durroon-1) – the full reports of these analyses are included as Appendices C1 to C8 of this Record (which includes a Summary Report). A new stratigraphic chart for the Bass Basin proposed by Partridge (2002) summarises this work (Figure 4.3).

4.3 SEQUENCES MAPPED AND NOMENCLATURE

A total of 15 seismic horizons were mapped throughout the seismic grid (Appendix B). These horizons include megasequence and sequence boundaries, as well as multiple marker horizons within sequences. Consistent with a sequence stratigraphic approach, the *bases of sequences* were mapped throughout the seismic grid. Most horizons mapped correlate to unconformities within the stratigraphic succession, although in some instances (particularly in the uppermost Torquay marine succession) some horizons mark lithologic changes such as marl-to-carbonate facies. The approach used in this study aimed to understand the tectonostratigraphic nature of the basin succession, and to overcome difficulties often experienced in regional lithostratigraphic correlations in a terrestrial basin system. Further descriptions of facies and palaeo-environmental interpretations of selected intervals are presented in Chapter 9 and Appendix C.

There are several published nomenclature schemes for the Bass Basin stratigraphic succession (Robinson, 1974; Smith, 1986; Williamson et al., 1987; Maung, et al., 1993; Hill et al., 1995; Lennon et al., 1999). Most vary in their sub-division and use of the terms "Eastern View Coal Measures" (Lennon et al., 1999) and "Eastern View Group" (Smith, 1986; Maung et al., 1993). The most recent scheme (Lennon et al., 1999; Figure 4.2b) divided the entire Bass Basin stratigraphic succession into three broad lithostratigraphic units -

the Torquay Group, the Eastern View Coal Measures (includes Upper, Middle and Lower sub-divisions) and the Otway Group (Figure 4.3).

An aim of this study has been to subdivide the stratigraphic succession into tectonically-controlled cycles of deposition (megasequences) and, in particular, to recognise depostional cycles within the "Eastern View Group". Adopting existing names (such as the "Eastern View Coal Measures") into a new sequence stratigraphic framework is useful, particularly where there is some correlation between lithostratigraphy and the new sequences identified. However, in the case of the Bass Basin, many of the names in use were drawn from type sections in other basins (e.g., the Eastern View Coals Measures was identified in the Torquay Basin – Raggatt and Crespin, 1952, 1955; then applied to the Bass Basin – Brown, 1976). To avoid confusion, new names have been adopted for sequences where type sections have been identified.

4.4 ACCOMMODATION CYCLES

The Bass Basin contains sediments ranging in age from Early Cretaceous to Recent. Jurassic dolerites, Palaeozoic and older sediments are present within the pre-rift basement blocks that floor the Mesozoic basin. The Bass Basin formed as an intra-cratonic rift basin within the shallow basement ridge system that underlies the present-day Bass Strait. As continental breakup and seafloor spreading bypassed this region, the Bass Basin did not progress to become a passive margin basin, as occurred in the flanking Otway, Sorell and Gippsland basins. From the Early Cretaceous to Middle Eocene, much of Bass Basin sedimentary succession was deposited in terrestrial to marginal marine environments. Sediments eroded from the basin flanks and adjacent highlands were deposited in fluvial and lacustrine environments in the developing rift basin as part of an internal drainage system. Widespread marine flooding of the basin did not occur until the late Middle Eocene, with deepening marine environments dominating from the Late Miocene onwards.

The regional tectonic setting of the Bass Basin between two major rift systems (Southern Rift System and Tasman Basin) has meant that the basin was subjected to complex inter- and intra-plate stresses and multiple periods of upper crustal extension prior to seafloor spreading in the adjacent basins. The basin was particularly influenced by the prolonged process of separation that occurred between Australia and Antarctica during the Paleocene to Late Eocene. It is also suggested that a fundamental basement boundary underlies the Bass Basin (Chapter 3). This boundary may have acted to partition stresses and further influence the nature of tectonically-driven accommodation cycles. Although the present-day geometry of the Bass Basin appears to have evolved as a series of linked, relatively simple half graben, regional chronostratigraphic correlations now show that cycles and rates of accommodation varied between individual depocentres. This scenario, together with the difficulty in correlating terrestrial facies of limited lateral extent, has meant that lithology-based correlations are difficult. In addition, the lack of significant time gaps in the stratigraphic succession suggests that deposition across the basin has been more-or-less continuous, particularly from the Late Cretaceous onward. The overall succession is riddled with multiple third- and four-order unconformities, often of local extent.

Six regional-scale basin phases and associated megasequences and sequences have been identified (Chapter 3). Factors that controlled the complex facies relationships observed in the basin have been discussed in Chapter 3. Three megasequences are related to phases of extension. Evidence of the initial rift phase (Otway Megasequence) is only clearly observed in the Durroon Sub-basin and in the southwestern Cape Wickham Sub-basin (near Bass-3 and White Ibis-1). The second rift phase (Durroon Megasequence) is pervasive throughout the Bass Basin, although the full succession of sediments of this megasequence was only penetrated in the Durroon Sub-basin. The third-rift phase (Bass Megasequence) is also pervasive throughout the basin, but appeared to affect only particular depocentres where expanded syn-tectonic growth sections have been intersected (Narimba-1). There are wide variations in facies type, environment and thickness of the Bass Megasequence due to differential rates of subsidence. The rift-to-post-rift phase of basin evolution (Subsidence Phase 1 – Aroo Sequence) signaled a shift to waning subsidence rates and increasing brackish influence. Wide variations in facies types, environments and thicknesses are also observed within this sequence. The Demons Bluff and Torquay sequences were deposited during subsequent periods of post-rift thermal subsidence (Subsidence Phases-2 and -3). Multiple episodes of margin uplift, inversion and volcanic intrusion/extrusion affected the basin during the deposition of the Subsidence Phase-3 sequence. These effects are often localised and they have not been identified as separate basin phases. Presented below is a summary of the megasequences/sequences and accommodation cycles determined from this study.

4.5 OTWAY MEGASEQUENCE

Durroon-1 was the only well in the Bass Basin to intersect Early Cretaceous sediments of the Otway Megasequence (Baillie and Pickering, 1991; Figures 4.4 and 4.5; Table 4.1). Durroon-1 intersected two syn-tectonic sequences – an Early Cretaceous, 1452 m thick succession of Aptian to late Albian age sediments (Otway Megasequence), overlain by a 374 m thick syn-rift succession of Turonian to Mid-Campanian age (Durroon Megasequence – see below). These sequences are separated by a 36 m thick basaltic unit. The Early Cretaceous (Otway Megasequence) syn-rift succession overlies basement, and is itself the pre-rift to the later Turonian to mid-Campanian syn-rift succession (Figure 4.4; Durroon Megasequence). The Otway Megasequence is the chronostratigraphic equivalent of the post-rift Eumeralla Formation in the Otway Basin, and the post-rift Upper Strzelecki Group in the Gippsland Basin, as defined by Norvick and Smith (2001). The age and stratal geometries of the early Otway Megasequence suggest that it was deposited during a period of slow subsidence within a low relief trough, possibly during the initiation of the rift basin, but prior to the onset of rapid upper crustal extension. Strong truncation at the "top" of the Otway Megasequence is observed on footwall fault blocks (Baillie and Pickering, 1991), suggesting that a moderate amount of uplift occurred during fault movement prior to deposition of the overlying Durroon Megasequence.

The Otway Megasequence consists of a stacked succession of blocky, fluvial channel sands with thin, coaly overbank-floodplain shales (Figure 4.5). These sediments bear a strong lithological similarity to the Eumeralla Formation in the Otway Basin. Overall, organic-rich facies are typically thin, although the frequency of coals increases in uppermost 650 m of the sequence. Potential sealing facies are limited to thin

(<10 m thick) intraformational shales interbedded with the coals. A single core of lithic sandstone had a measured porosity of 6 to 10%, and permeability of 0.07 to 0.74 md (Core Laboratories Inc., 1985).

Table 4.1 Otway Megasequence (Rift Phase 1)

Age:	Aptian to latest Albian (?possibly Barremian – inferred)
Top:	Late Albian, *P. pannosus* (Otway Unconformity)
Base:	Aptian, *C. hughesii* (approximate *P. notensis* equivalent)
Type Section:	Durroon-1
Formation Equivalent:	Otway Group Equivalent (Lennon et al., 1999)
Dominant Lithology:	Sandstones with volcanogenic clastics and minor coal
Environment:	Fluvio-deltaic
Unconformities:	Multiple (Intra-*C. striatus*, Intra-*C. paradoxa*)
Sequence Character:	Aggradational stacked channel sands, multiple (6) transgressive-regressive cycles
Aerial Extent:	Limited to early trough/s and half graben in the Durroon Sub-basin. May lie deeply buried in similar structures in the Cape Wickham Sub-basin.
Play Elements:	Probably variable prospectivity; mostly lean source rocks, although some intervals with higher source potential (98 to 112 Ma; Chapter 5); moderate reservoir quality, only minor intraformational sealing facies

4.6 DURROON MEGASEQUENCE

Durroon-1 was the only well in the Bass Basin to intersect a complete stratigraphic succession of early Late Cretaceous age of the Durroon Megasequence (Figures 4.4 and 4.5; Table 4.2). Chat-1, Koorkah-1 and Pelican-5 penetrated strata of similar mid-Campanian age (*T. lillei* spore/pollen zone), but recent work by Partridge (2002) has shown the zone at Koorkah-1 to be younger (i.e., *F. longus* in age and thus not part of the Durroon Megasequence). Elsewhere in the basin, this sequence is imaged on seismic data where it lies deep within the depocentres. Only two wells have tested plays within the Durroon Megasequence (Durroon-1 and Chat-1).

In the Durroon-1 well, the megasequence consists of approximately 36 m of basalt, overlain by 374 m of shale, siltstone and sandstone of Turonian to mid-Campanian age. Informally, Baillie (cited by Partridge, 2002) proposed the following lithostratigraphic subdivision of the Durroon Megasequence: "Furneaux Group" (1544 - 1646 m), "Durroon Formation" (1370 - 1544 m), and the "Boobyalla Formation" (1235 - 1370 m). The Durroon Formation was later formally proposed by Smith (1986) for the shaley section lying between 1374 and 1545 m. Recent biostratigraphic work by Partridge (2002; Appendix C) on the Durroon Formation suggests deposition in a distal, probably deep, freshwater lacustrine environment (Figure 4.6). These facies contain a moderate to high abundance of non-marine microplankton and abundant *Dilwynites* and *Araucariacites* pollen. The Durroon Formation is the chronostratigraphic equivalent of the youngest part of

the Kipper Shale in the Gippsland Basin. Deposition in a lacustrine environment is consistent with the tectonostratigraphic interpretation of these facies as tectonically-controlled rift lakes. Partridge (2002; Figure 4.6; Appendix C) has not identified Santonian (*T. apoxyexinus* spore/pollen zone) sediments in the Durroon-1 well. However, sediments of this age have been interpreted on seismic data, with absence at the well due to stratigraphic pinchout (onlap) onto steeply dipping footwall blocks.

In contrast to the underlying Otway Megasequence, the Durroon Megasequence shows strong syn-tectonic growth of strata against the bounding normal faults (Figure 4.4). This indicates that the main phase of rift-related accommodation occurred during a relatively short-lived period of upper crustal extension lasting from the Turonian to mid-Campanian, associated with rifting in the Tasman Basin to the east. In the Gippsland Basin, this event is recorded by the syn-rift Emperor and rift-transition Golden Beach megasequences (Norvick and Smith, 2001). Due to depth of burial and its association with volcanic material in the western Bass Basin, only the "top" of the sequence can be confidently picked on seismic data.

Table 4.2 Durroon Megasequence (Rift Phase 2)

Age:	Turonian to mid-Campanian
Top:	Mid-Campanian, intra- *T. lillei* spore/pollen zone
Base:	Early Turonian, *P. mawsonii* spore/pollen zone (zone not present in well succession, but inferred from seismic interpretations); overlies the Otway Unconformity
Type Section:	Durroon-1
Formation Equivalent:	Lower Eastern View Coal Measures/Durroon Formation (Lennon et al., 1999)
Dominant Lithology:	Basal volcanic rocks, overlain by sandstones that grade upward to shales and siltstones
Environment:	Fluvio-deltaic to lacustrine, syn-rift lakes and associated marginal environments
Unconformities:	Multiple minor unconformities, probably related to high-order changes in the rate of accommodation or sediment supply; intra-*T. apoxyexinus*; intra-*N. senectus* zones
Sequence Character:	Basal channel sandstones (blocky), maximum flooding surface with lacustrine shales overlain by lacustrine deltaic sands
Aerial Extent:	Widespread across the half graben of the Durroon Sub-basin (seismically mapped, although difficult well tie due to steepness of dipping beds). Probably lies deeply buried in the Cape Wickham Sub-basin, but difficult to map.
Play Elements:	Low source potential (Chapter 5), although only one well has fully tested the sequence to determine source potential; moderate to poor reservoir quality, possible lacustrine sealing facies to alluvial and lacustrine deltaic sands

4.7 BASS MEGASEQUENCE

The mid-Campanian to late Early Eocene Bass Megasequence (Tables 4.3, 4.4 and 4.5) has been subdivided into three second- or third-order sequences based on the recognition of significant bounding unconformities

and intervals of syn-tectonic growth: **Furneaux** (mid-Campanian to latest Maastrichtian), **Tilana** (latest Maastrichtian to late Late Paleocene) and **Narimba Sequences** (latest Paleocene to late Early Eocene). The megasequence and its sequence components can be difficult to map seismically across the basin due to significant lateral changes in facies, seismic character and overall unit thickness (300 to >2500 m). During this period of basin evolution, region-scale tectonic processes were waning and the locus of accommodation shifted between different structural elements within the basin. Pelican-5 is the only well to penetrate all three sequences (Figure 4.7). Unfortunately, intense faulting within the Pelican Trough has meant that it is difficult to confidently map the sequence boundaries beyond this structure (Figure 4.8). Other wells with significant sections are Narimba-1, Poonboon-1, Tilana-1, Aroo-1, and Koorkah-1. The Bass Megasequence is roughly correlative to the "Middle Eastern View Coal Measures" of Lennon et al. (1999; Figure 4.2b), although subdivisions within the unit have not been previously documented.

The Furneaux Sequence encompasses the mid-Campanian (intra-*T. lillei* zone) to latest Maastrichtian (Near base Upper *F. longus* zone; Table 4.3) succession. The sequence is well imaged on seismic data in the central and western basin, around the Poonboon-1, Tilana-1 and Tarook-1, and Koorkah-1 and Toolka-1A wells (Figure 4.9). The upper sequence boundary was penetrated at Koorkah-1 (2955 m) and Pelican-5 (3695 m), but lies below TD in the other wells. Seismic interpretation suggests that the Furneaux Sequence was deposited as a syn-rift succession as a result of reactivation of older Early Cretaceous extensional faults (Figure 4.9). The sequence is heavily intruded by volcanic material and associated fluids (Tilana-1; Figure 4.10), and has undergone mild inversion during the latest Cretaceous. The Furneaux Sequence is the chronostratigraphic equivalent of the upper part of the syn-rift Sherbrook Group in the Otway Basin (Norvick and Smith, 2001). Where penetrated, the sequence ranges from interbedded fluvio-deltaic sandstones and freshwater lacustrine shales (Koorkah-1), to fluvio-deltaic sandstones and thin interbedded overbank or delta plain shales and coals (Pelican-5). The upper sequence boundary is marked by an angular unconformity, and is approximately coeval with Maastrichtian breakup in the flanking Otway Basin.

Table 4.3 Bass Megasequence: Furneaux Sequence (Rift Phase 3)

Age:	Mid-Campanian to Late Maastrichtian
Top:	mid-Late Maastrichtian, near base of Upper *F. longus* spore/pollen zone
Base:	Mid-Campanian, lower intra-*T. lillei* zone (only intersected in a few wells; some confusion on *T. lillei* picks in wells drilled during the 1980s – Koorkah-1).
Type Section:	Koorkah-1, Pelican-5
Formation Equivalent:	Part of the Middle Eastern View Coal Measures (Lennon et al., 1999)
Dominant Lithology:	Interbedded sandstone, siltstone and shale, with lacustrine shale and minor coal
Environment:	Fluvio-deltaic with minor freshwater lacustrine influence
Unconformities:	Minor within Lower *F. longus* spore/pollen zone
Sequence Character:	Overall transgressive – regressive cycle with multiple higher-order cycles within

Aerial Extent:	Across most of the Bass Basin, deeply buried except along the basin margins
Play Elements:	Transgressive-regressive cycles provide good stacking of reservoir and seal facies

The Tilana Sequence encompasses the latest Maastrichtian (near base Upper *F. longus* zone) to latest Paleocene (near base Upper *L. balmei* zone) succession. Seismic correlations suggest that deposition of the Tilana Sequence was controlled by a combination of reactivation of underlying Early Cretaceous faults, tectonic subsidence, sediment loading and compaction (Figure 4.9). Some areas of the basin appear to have been unaffected by increased subsidence during this time (Poonboon-1) suggesting that rates of accommodation varied significantly between the different rift segments. This variation in accommodation is clearly shown in the thickness and range of facies types deposited.

Biostratigraphic work undertaken by Partridge (2002) for the WTRMP focused on the evaluation of Late Cretaceous to Eocene facies in Koorkah-1, Poonboon-1 and Konkon-1 (Appendices C4, C5 and C6). These analyses show the occurrence of lagoonal, freshwater and brackish lacustrine environments across the Bass Basin from the latest Maastrichtian to late Early Eocene (Figures 4.11 and 4.12). The "Lower Koorkah" lake cycle (base Upper *F. longus* to base Upper *L. balmei* zones) generally correlates with the Tilana Sequence, while the "Upper Koorkah" lake cycle (Upper *L. balmei* to base Upper *M. diversus* zones) correlates with the overlying Narimba Sequence (Figures 4.9 and 4.11). Koorkah-1, Tilana-1 and Aroo-1 are type sections of these facies. The wells show basal fluvial channels sandstones overlain by thick (100+ m), freshwater lacustrine shales, grading upward to progradational lacustrine deltaic and shoreface sandstones capped by thin coal beds (Figure 4.11). Unfortunately, no cores were available to determine seal capacity of the lacustrine shales (MICP analysis; Chapter 7), but the thickness and widespread nature of these facies suggest good sealing capability. Geochemical analysis show moderate source potential (Chapter 5).

The Koorkah Lake facies are best developed in areas where fault-controlled subsidence rates were moderate to high (4.13). In contrast to the strongly aggradational and progradational nature of the Koorkah Lake facies, deltaic-to-lower coastal plain facies characterise areas like the "Tertiary Platform" (Lennon et al., 1999), where only minimal subsidence occurred. Here, the equivalent age facies are thinly bedded successions of fluvio-deltaic sandstones, floodplain shales and peat mire coals (Figure 4.14; Poonboon-1). Significantly, the geochemical characterisation of interbedded coals and shales undertaken for this project (Chapter 5) identified two instances of hydrogen-rich coals. The oldest occurrence was noted at Poonboon-1 (3042 m), and suggests that while lakes occupied the deeper areas of the basin, oil-prone coals were forming on the fringing floodplains and peat mires. This scenario is depicted in a palaeogeographic map of the Bass Basin (Figure 4.15), and potentially upgrades the prospectivity of the margins where subsidence rates were low and potential oil-prone coals accumulated.

Similar to the underlying Furneaux Sequence, the Tilana Sequence is also associated with extensive volcanic activity (probably both syn- and post-depositional; Figure 4.9). Selected intervals within the thick succession of "volcanic rock" penetrated at Tilana-1 have been re-examined in thin section. This has shown that some

of the rocks are highly fractured, lithic sandstones cemented by basaltic material (A. Lambeck, T. Dance, Geoscience Australia, personal communication, 2003). This intrusion of volcanic material into the sandstones is thought to reflect the initial high porosity. While this process has destroyed porosity and permeability, the sills could act as effective seals. Similarly, where unaffected by volcanic intrusions, the lacustrine deltaic sandstones should have good reservoir qualities (Koorkah-1).

Table 4.4 Bass Megasequence: Tilana Sequence (Rift Phase 3)

Age:	Latest Maastrichtian to latest Paleocene
Top:	Late Paleocene, near base of Upper *L. balmei* spore/pollen zone
Base:	Late Maastrichtian, near base Upper *F. longus* spore/pollen zone
Type Section:	Koorkah-1, Tilana-1, Aroo-1
Formation Equivalent:	Part of the Middle Eastern View Coal Measures (Lennon et al., 1999)
Dominant Lithology:	Fluvio-deltaic sandstones, floodplain shales and coals. Lacustrine shale with interbedded lacustrine deltaic sandstones and minor coal.
Environment:	Fluvio-deltaic, floodplain and freshwater lacustrine
Unconformities:	Minor unconformity within Lower *L. balmei* spore/pollen zone
Sequence Character:	Overall transgressive – regressive cycle with multiple higher-order cycles within
Aerial Extent:	Across most of the Cape Wickham Sub-basin, thinning in the Durroon Sub-basin
Other:	Transgressive-regressive lacustrine cycles provide good stacking of reservoir and seal facies; associated coals fringing the lakes provide source rocks (Poonboon-1).

The latest Late Paleocene to late Early Eocene Narimba Sequence is the youngest sequence within the Bass Megasequence. The Narimba Sequence was deposited across most of the Bass Basin as a result of the reactivation of select Early Cretaceous rift faults. Seismic interpretations show that significant growth occurred in the Pelican, Yolla and Cormorant troughs (Smit, 1988; Lennon et al., 1999) over the interval defined by "base Upper *L. balmei* " to "base Upper *M. diversus* ". A similarly thick section is encountered at Squid-1 just west of the accommodation zone. As tectonic stresses during this period were largely oblique and far-field, much of the basin was unaffected by significant fault movement (thinner sections were penetrated at Poonboon-1, Nangkero-1, Dondu-1 and Yurongi-1). As a result, the Narimba Sequence shows the broadest range in lithology and facies types, environments and thickness across the Cape Wickham Sub-basin.

Narimba-1 is the type section for the syn-tectonic facies of the Narimba Sequence (Figure 4.16). The well penetrated an 800+ m thick succession of aggradational fluvio-deltaic to floodplain sandstones, shales and thin coals beds. A combination of high rates of accommodation and a steady supply of sandy sediment feeding down the flanks of the rift from northern Tasmania account for the unusually high rate of sedimentation in the Pelican Trough. Similarly high accommodation rates existed in the Cormorant and Yolla troughs. At Poonboon-1, where subsidence rates were lower, equivalent age facies consists of <400 m of

thinly bedded shale, sandstone and coal deposited in lacustrine, lower delta plain and peat mire environments (Figure 4.14). Biostratigraphic analysis (Partridge, 2002) indicate the onset of brackish influence in these wells within the lowermost part of the Upper *L. balmei* succession. The Narimba Sequence is equivalent to the "Upper Koorkah" lake facies identified by Partridge (2002) in Koorkah-1.

While the facies and thicknesses of the Narimba Sequence vary widely, there is one distinct event that can be correlated in almost every well in the basin - a maximum flooding surface (MFS) within the Lower *M. diversus* succession (Figure 4.17). At Poonboon-1, this flooding surface marks the turnaround from transgressive (fining-upward and retrogradational cycles) to regressive facies (largely progradational cycles) within the Narimba Sequence. In this example, coals are rarer in the lower transgressive succession, but became increasingly more frequent and thicker in the regressive succession (Poonboon-1, Dondu-1). This pattern of facies stacking also has direct significant for petroleum exploration. A transgressive shale from 2342.0 m (Upper *L. balmei* zone) at Dondu-1 yielded the highest measured seal capacity of the 15 samples analysed for this study (1395 m/ maximum oil column height, 567 m/maximum gas column height; Chapter 7). In Pelican-5, coals sampled just above the MFS (2800 m) were determined to be hydrogen-rich (HI = 406.5 mg hydrocarbons/gTOC) and have a higher sulphur content (2.46%), while shales within at the MFS could be characterised as "oil shales" (Chapter 6; Boreham et al., 2003).

In the westernmost part of the Bass Basin, Lower Cretaceous rifts also underwent reactivation and moderate extension during deposition of the Narimba Succession. Toolka-1A is located within a shallow half graben and penetrated the entire syn-tectonic succession (Figure 4.13). This well recorded an "intermediate example" between the higher (Narimba-1) and lower (Poonboon-1) rates of accommodation observed across the basin. Both the "Upper Koorkah" and "Lower Koorkah" lake facies are recognised in the well. The "Lower Koorkah" succession (Tilana Sequence) at Toolka-1A is a 418 m thick (2264 - 2682 m), monotonous shale deposited in a moderately deep rift lake environment. The overlying "Upper Koorkah" lake facies (1917 - 2264 m) indicate a shallower lake setting, with prograding lacustrine-deltaic sandstones capped by moderately thick coals (2 to 8 m thick). The upward increase in coals is clearly evident on seismic data.

Table 4.5 Bass Megasequence: Narimba Sequence (Rift Phase 3)

Age:	Late Paleocene to mid-Early Eocene
Top:	mid-Early Eocene, base of Upper *M. diversus* spore/pollen zone
Base:	Late Paleocene, near base Upper *L. balmei* spore/pollen zone
Type Sections:	Localised syn-tectonic facies usually occur over the interval defined by intra-Lower *L. balmei* to base Upper *M. diversus* zones. The expanded section is related to reactivation of selected growth faults within the Pelican, Yolla and Cormorant troughs. In areas unaffected by fault movement, slower rates of subsidence prevailed. Narimba-1: Lower *L. balmei* to base Upper *M. diversus* zones – expanded terrestrial fluvial section due to growth faulting

	Nangkero-1: *L. balmei* to base *M. diversus* zones – terrestrial fluvial 'condensed section' due to slow subsidence
Formation Equivalent:	Uppermost part of the Middle Eastern View Coal Measures (Lennon et al., 1999)
Dominant Lithology:	Narimba-1: sandstones, shales with thin coals at the top of progradational units Nangkero-1: thinly bedded sandstones, shales and coal Koorkah-1: lacustrine mudstone with shoreface and prograding deltaic sandstones and minor coal
Environment:	Narimba-1: fluvio-deltaic to delta-plain with only minor lacustrine influence Nangkero-1: mostly fluvial-deltaic Koorkah-1 and Aroo-1: freshwater to brackish lacustrine or lagoonal
Unconformities and other markers:	Intra-Lower *M. diversus* "maximum flooding surface" (in many wells, signaling maximum accommodation or rise in base level)
Sequence character:	Variable with environment; aggradational to progradational
Aerial extent:	Across most of the Bass Basin but variable thickness (<100 to 900+ m)
Play elements:	Lacustrine mudstones are excellent intraformational seals; Lacustrine progradational and shoreface sands have variable reservoir quality; Hydrogen-rich coals deposited during transgressive cycle (Poonboon-1) possible with lacustrine association.

4.8 AROO SEQUENCE

The late Early Eocene to early Middle Eocene Aroo Sequence (base Upper *M. diversus* to Intra-Lower *N. asperus* zones; Table 4.6) marks the period when large-scale tectonic activity had ceased across most the Bass Basin (Subsidence Phase 1). Many faults that experienced significant movement throughout the evolution of the basin terminated at either the 'Base Upper *M. diversus*" or "Base *P. asperopolus*" horizons. The shift from rift-to-post-rift conditions was signaled by waning subsidence rates and an increasing brackish influence. The frequency and thickness of coals began to increase during the deposition of this sequence, beginning in late Early Eocene and lasting until the mid-Middle Eocene. A slow down in subsidence rates was accompanied by the proliferation of peat mires in broad floodplain environments and along the fringing margins of localised, shallow lakes. The aggradation of coaly facies indicates there was a balance between accommodation, sediment supply and peat production. The lower sequence boundary at Nangkero-1 and Dondu-1 (base Upper *M. diversus* zone) is marked by distinctively thick coals that are 10 and 25 m thick, respectively.

In the Cormorant and Yolla troughs, sedimentation rates were marginally higher during this period. This was probably due to a combination of factors, most likely higher compaction rates (within the underlying syn-tectonic succession) and the fact that these structures were the locus of recent tectonic activity. At Cormorant-1 and Yolla-1, the lower boundary of the Aroo Sequence is difficult to recognize, suggesting that accommodation rates varied only slightly across this boundary. However, as noted elsewhere in basin, the

frequency and thickness of coals increases within the Aroo Sequence in the Cormorant and Yolla troughs, occurring mainly as thin coals that cap short-cycles of coarsening-upward progradation. Palynological evidence suggest the existence of lagoonal to restricted marine conditions in the Cormorant Trough (Partridge, 2002; Appendix C). In contrast, mainly fluvial conditions persisted in the Pelican Trough and along southern margin of the Bass Basin. Here, sand-dominated fluvial systems migrated from northern Tasmania across the low relief flank of basin depocentre. Coals are present in this succession, but thinner and less frequent in the Pelican Trough.

There are a number of significant surfaces within the Aroo Sequence, including a lower-order unconformity in the latest Early Eocene (near the "base of *P. asperopolus*" zone; 2297 m at Pelican-5), and a regional flooding surface in the early Middle Eocene (near the boundary between the *P. asperopolus* to Lower *N. asperus* zones). The flooding surface coincides with a change from coastal plain and deltaic environments, to lagoonal-brackish conditions, as recorded by palynological evidence in Cormorant-1 (Partridge, 2002; Appendix C).

Table 4.6 Aroo Megasequence (Subsidence Phase 1)

Age:	late Early Eocene to mid-Middle Eocene
Top:	Middle Eocene, intra-Lower *N. asperus* spore/pollen zone
Base:	Early Eocene, base Upper *M. diversus* spore/pollen zone
Type Section:	Cormorant-1, Tarook-1, Bass-1, Pelican-3, Yurongi-1, Dondu-1, Chat-1
Formation Equivalent:	Upper Eastern View Coal Measures (Lennon et al., 1999)
Dominant Lithology:	Cormorant-1: mainly siltstone/shale with thin interbeds of sand and coal Pelican-5: stacked channel sandstones with shale and thin coal Yurongi-1, Dondu-1: thick sandstones and coal
Environment:	Fluvio-deltaic, shallow lacustrine and lagoonal-to-restricted marine surrounded by peat mires (central and western basin). Fluvial environments dominated in the southern basin.
Unconformities and other markers:	Latest Early Eocene unconformity (base *P. asperopolus* zone), followed by flooding surface in the early Middle Eocene (boundary between *P. asperopolus* and *N. asperus* zones).
Sequence Character:	Trend from sand-rich to coal-rich is observed in correlation of wells from east to west. This reflects localised continued subsidence in the palaeo-depocentres such as the Cormorant and Yolla troughs, while fluvial systems continued to dominate in the southern part of the basin. Cormorant and Yolla troughs: Aggradation to progradational cycles capped by thin coals (lacustrine delta and shoreface sands).
Aerial Extent:	Widespread across the Bass Basin, but variable in thickness and facies type.
Play Elements:	Excellent source potential in coals, good reservoirs in fluvial sands.

4.9 DEMONS BLUFF SEQUENCE (SUBSIDENCE PHASE 2)

The Middle Eocene to Early Oligocene Demons Bluff Sequence is an overall transgressive-regressive succession that was deposited during a later stage of thermal subsidence (Table 4.7; Subsidence Phase 2). The Demons Bluff Sequence contains formation-based units such as the "Boonah Sand", Anglesea Formation and the regional sealing facies of the "Demons Bluff Formation", that have been described by previous workers (Figure 4.3). The base of the sequence (intra-Lower *N. asperus* zone) is clearly defined by thick channels sands at wells such as Pelican-3 (2048 m) and Narimba-1 (2048 m) on the margins the Pelican Trough. In the central and northern Bass Basin, the boundary is also well defined by thick sandstone units as seen at Poonboon-1 (2169 m), Aroo-1 (2255 m), Yurongi-1 (1490 m) and Dondu-1 (1889 m). Similar to the underlying Aroo Sequence, the basal boundary of the Demons Bluff Sequence is difficult to distinguish in the Cormorant and Yolla troughs, as well as in the western basin near Koorkah-1 and Toolka-1A. In these areas, it is suggested that the boundary is marked by a "correlative conformity" where deposition continued more-or-less uninterrupted due to locally higher rates of subsidence. Regional mapping on seismic data suggests that by the Middle Eocene, the depocentres of the former rift basin were buried and most of the rift-related topographic was obscured. The flanks of the basin were emergent and fluvial systems continued to feed sediment into low-lying areas. The former basin was relatively flat and featureless, except for subtle topographic lows which formed locally over areas of most recent tectonic activity (Cormorant and Yolla troughs; westernmost Bass Basin).

It was during this period in the Middle Eocene (Lower *N. asperus* zone), that Toolka Lake formed in the western Bass Basin (Partridge, 2002; Appendix C). Unlike the Upper Cretaceous to Paleocene Koorkah Lake, which was deeper and primarily confined to fault-controlled topographic lows, Toolka Lake covered a much wider area and was probably shallower (Figure 4.13). Recent palynological work has shown that Toolka Lake had a brackish influence (Figure 4.18; Cormorant-1; Partridge, 2002; Appendix C). Well log correlations suggest that the aerial extend of Toolka Lake expanded and contracted through time, with two lacustrine cycles recognised. The Toolka Lake succession has a distinctive stratal character on seismic data (Figure 4.19). Figure 4.20 depicts the palaeogeographic setting of the basin during the time of the Toolka Lake cycles. At times of maximum extent, the lake covered the deepest part of the western and central Bass Basin, with a proposed marine influence from the west/northwest (Partridge, 2002; Appendix C). Lacustrine shales and thin lacustrine deltaic and shoreface sands are recognised in wells such as Toolka-1A, Cormorant-1 and Koorkah-1. Fringing peat mires, lower delta plain, and fluvial-to-upper delta plain environments dominated the central and western parts of the basin (Figure 4.20).

In the late Middle Eocene (base Middle *N. asperus* zone), a fall in base-level resulted the demise of Lake Toolka and incision of the fluvial systems across the former lake. The fluvial sandstones that mark this boundary are known as the "Boonah Sand" (Figures 4.2a and 4.3). While this unit varies significantly in thickness, it is present across most of the Bass Basin and is the uppermost reservoir within the basin succession ("top reservoir"). The upper boundary of the "Boonah Sand" is a maximum flooding surface (MFS) that correlates to the base of the "Anglesea Formation", a shallow bay siltstone/shale facies. The

"Anglesea MFS" (intra-Middle *N. asperus* zone) is very distinct in wells in the central and southern Bass Basin, such as Pelican-5 (1749 m; Figure 4.7) and Dondu-1 (1622 m). However, mapping of this surface across the basin shows that the relationship between the "Boonah Sand" and the "Anglesea MFS" is more complex than a single, base wide flooding event. Several minor flooding surfaces can be identified below the "Anglesea MFS" that is so clearly seen in wells within the central and southern parts of the basin. This is useful in understanding the progradational nature of some of the underlying "Boonah Sand" facies. From the late Middle Eocene until the mid-Oligocene, the basin was under deepening marine influence. During this time, up to 350 m of siltstones and shales were deposited - including the regional sealing facies of the "Demons Bluff Formation".

Table 4.7 Demons Bluff Sequence (Subsidence Phase 2)

Age:	Middle Eocene to mid-Oligocene
Top:	Boundary between Early and Late Oligocene, I1/I2 planktic foraminifera zone
Base:	Middle Eocene, intra-Lower *N. asperus* spore/pollen zone
Type Section:	Pelican-3, Narimba-1, Konkon-1, Poonboon-1, Yurongi-1, Cormorant-1
Formation Equivalent:	Demons Bluff Formation and lower Torquay Group (Lennon et al., 1999)
Dominant Lithology:	channel and progradational sandstones, marine shales
Environment:	Lowstand fluvio-deltaic and shallow lacustrine systems (Toolka Lake) surrounded by peat mires, grading upward to shallow marine environments
Unconformities and other markers:	Base Middle *N. asperus* zone unconformity ("Base Boonah Sand"); intra-Middle *N. asperus* zone maximum flooding surface ("Anglesea MFS").
Sequence Character:	Overall transgressive-regressive cycle. Mostly aggradational with some progradation.
Aerial Extent:	Widespread across the Bass Basin, deposition in the Durroon Sub-basin recommenced after extended hiatus
Play Elements:	Good reservoir in fluvial sands and high potential for lacustrine shale sealing facies; regional sealing unit of the "Demons Bluff" shale.

4.10 TORQUAY SEQUENCE

An unconformity at the Early/Late Oligocene boundary is recorded in all wells throughout the Bass Basin. On seismic data, this unconformity correlates to the most regionally extensive surface (strong peak) that can be mapped confidently across the entire basin. The spatial extent and prominence of this surface suggest that it is related to a major fall in sea level (mid-Oligocene). By this time, any relicts of the underlying deep basin topography had been buried beneath the fine-grained sediments of the Demons Bluff Sequence, and the former basin depocentre was virtually flat and featureless. This scenario is supported by "flattened" seismic sections that show minimal palaeotopography in the basin at this time. Deposition of the Torquay Sequence (Table 4.8) commenced after a rise in eustatic sea level flooded the basin during the Late Oligocene,

bringing the onset of fine-grained shallow marine clastic sedimentation (siltstones and marls). Increasingly open marine conditions developed in the Middle Miocene, signaled by the deposition of bioclastic carbonates.

Precise dating of the Torquay Sequence is somewhat problematic due to a lack of biostratigraphic analyses (primarily planktonic foraminifera), as well as inconsistencies within the available data. The inconsistency within the dataset appears to be related to different authors and vintages of analyses. Overall, the best age control for the Torquay Sequence comes from Narimba-1 and the Pelican wells, while the foraminifera zones identified at Koorkah-1 are inconsistent and considered less reliable. The youngest sediments dated within the basin were recorded in Bass-3 (at 450 m) as latest Middle Miocene in age (planktonic foraminifera Zone C). Subsea coring by Blom and Alsop (1988) has shown a relatively thick succession (>36 m) of Late Pleistocene to Holocene sediments in Bass Strait.

Four prominent seismic horizons within the Torquay Sequence succession can be mapped regionally (listed from oldest to youngest): Base Torquay, Torquay-1, Torquay-2 and Torquay-3. Each horizon is correlated in wells to either higher-order sequence boundaries within the Torquay Sequence, or late-stage structural movements. Polygonal faulting is widespread throughout the basin (Das, 2001; Figure 4.21), but generally only affected ultrafine-grained sediments of Late Oligocene to Early Miocene age. Within the main basinal area, two sets of layer-bounded polygonal faults are recognised: Polygonal Fault Set-1 is bounded by horizons Base Torquay and Torquay-1, while Polygonal Fault Set-2 is bounded by surfaces within the Torquay-1 succession (mapped locally as Torquay-1A/base and Torquay-1C/top). The occurrence of polygonal faults is strongly facies controlled, thus variations to the distinct layer-bound fault sets are observed near the basin margins where lateral lithological changes occur. In the main basin, the thickness of the unfaulted sedimentary succession between the two polygonal-fault sets varies widely. Where this unit is in excess of 150 m thick, a strong separation of the polygonal fault sets is observed. In instances where the intervening unit is thinner, the two fault-sets are often linked, with some faults from the lowermost set propagating upward. The occurrence of polygonal faulting is often recognisable by the 'noisy' nature of the sonic logs over affected intervals.

Polygonal faults are believed to be formed through the process of syneresis (Cartwright and Dewhurst, 1998), and thus not necessarily related to regional tectonic events. In the Bass Basin, there appears to be some temporal coincidence between the formation of polygonal faults and the emplacement of volcanic material (Figure 4.21). For example, near Cormorant-1 a prominent volcanic mound is observed on seismic data to intrude and overlie the Base Torquay horizon. Sediments of the Torquay-1 succession onlap the margins of the mound, suggesting that emplacement of these volcanic rocks occurred during early Late Oligocene to latest Early Miocene – approximately coeval with the formation of faults within Polygonal Fault Set-1. While volcanic emplacement may have locally influenced some faults (perhaps through proximal heating), the ubiquitous nature of the polygonal faults across the basin suggest their formation was largely unrelated.

Multiple periods of Cainozoic contraction have been recognised in the Bass Basin (Young et al., 1991; Hill et al., 1994; Hill et al., 1995). These contractional events formed large scale anticlines within the syn- and post-rift successions. Sediments in the western and northwestern parts of the basin were most affected by these events. Middle to Late Miocene inversion of the Paleocene to Early Miocene succession at Cormorant-1 resulted in the largest single post-rift structure in the basin – the Cormorant Anticline (Figures 2.3 and 4.21). Cormorant-1 and King-1 tested the trapping capability of this structure, with multiple oil shows recorded during drilling through the inverted section. Recent work undertaken by Geoscience Australia and CSIRO (Kempton et al., 2002), has revealed a palaeo-oil zone near 2800 m depth in Cormorant-1 (Lower *M. diversus* zone), suggesting the Miocene inversion event breached an existing oil accumulation. More subtle structures resulting from Miocene contraction occur along the northern margin of the basin, extending as far east as Dondu-1. The onset of contraction in the Bass Basin can be constrained at the Cormorant-1 and Konkon-1 wells where the syn-inversion succession is penetrated. At Cormorant-1, movement began during the early-Middle to mid-Middle Miocene (Torquay-2, planktonic foraminifera zones E1/D2), and probably ended during the Late Miocene. The precise end of contractional deformation is uncertain due to lack of age dating in Cormorant-1, although regional correlations of the Torquay-4 horizon (top of syn-inversion succession) to Bass-3 show this horizon to be younger than latest Middle Miocene.

Along the southern margin of the Bass Basin, inversion structures within the basinal succession (similar to the Cormorant Anticline) are generally absent. However, mapping of sedimentary packages around Bass-3 suggests that from the early Middle Miocene onward contractional stresses resulted in basement uplift at the margins of the basin (see Figure 3.3). The difference in strain between the northern and southern Bass Basin probably reflects the geometry of the basement fault – the Cormorant Anticline occurs in the hanging wall of a steeply-dipping normal fault, while the southern edge of the basin is a flexural ramp margin.

To the west, in the Torquay Sub-basin of the Otway Basin, contraction that began in the Middle Miocene continued through the Pliocene and persisted into Recent times. In the Bass Basin, the area to west of Konkon-1 and Seal-1 also shows evidence of a similar post-Miocene inversion history. The basement ridge that separates the Torquay Sub-basin from the Bass Basin is known as the King Island High. This feature is a high-standing basement block, although it was likely to have been a less prominent feature in pre-Middle Miocene times. That is, the Miocene and younger inversion has enhanced the magnitude of the structure and possibly masked a inter-basinal link between the Torquay Sub-basin and the western Bass Basin in pre-Miocene times. Partridge (2002, Appendix C) suggests that the marine flooding of the Bass Basin during the Cainozoic occurred via a passage to the west. This scenario has also been suggested by Maung et al. (1999), with "flattened" seismic sections (along strike of the King Island High) supporting this hypothesis.

Table 4.8 Torquay Sequence (Subsidence Phase 3)

Top:	Holocene (seabed)
Base:	Boundary between Early and Late Oligocene, I1/I2 planktic foraminifera zone
Type Section:	Tarook-1, Aroo-1, Cormorant-1, Narimba-1 and the Pelican wells

Formation Equivalent:	Torquay Group (Lennon et al., 1999)
Dominant Lithology:	Late Oligocene to mid-Miocene succession consists of argillaceous sediments (shale, marl, siltstone, up to 650 m thick); late-Middle Miocene and younger sediments are mostly calcarenites (860 m thick)
Environment:	Shallow marine shelf later deepening to open marine
Unconformities:	Tectonic inversion from the mid-Middle Miocene to the early Late Miocene resulted in sub-aerial exposure of areas adjacent to the basin margins (Cormorant-1)
Sequence Character:	Overall transgressive – regressive cycle with multiple higher-order cycles
Aerial Extent:	Across the basin, thicker in Cape Wickham Sub-basin, thinner in Durroon Sub-basin
Play Elements:	Regional loading facies for source rocks of the upper Bass and Aroo megasequences

4.11 NATURE AND DISTRIBUTION OF IGNEOUS ROCKS

A. Cummings, National Centre for Petroleum Geology and Geophysics

J. Blevin, Geoscience Australia

The Bass Basin and adjacent areas of mainland Tasmania and Victoria have been affected by multiple periods of volcanic activity during the several phases of basin evolution. Offshore, these events are marked by the widespread emplacement of intrusive and extrusive rocks, particularly in the southern and western parts of the basin in association with large-scale faults and accommodation zones. Intrusive and extrusive igneous rocks ranging from Early Cretaceous to Late Miocene age occur throughout the Bass Basin.

Early Cretaceous Volcanoclastic Sediments (Otway Megasequence)

The Aptian-Albian Otway Megasequence, as intersected at Durroon-1, consists of volcanolithic sandstone and slightly carbonaceous siltstone interbedded with rare conglomerate and thin coal seams (Williamson et al., 1985). This unit bears close lithological similarities to the Otway Group and Upper Strzelecki Group of the Otway and Gippsland basins, respectively. The volcanoclastic material is thought to have derived principally from ignimbritic volcanoes situated along the Lord Howe Rise (Bryan et al., 1997). Input of volcanic sediment into the Bass Strait region from mid-Barremian to Albian time was so great that the volume of continentally derived sediment appears to have been as low as 25% (Norvick and Smith, 2001).

Middle Cretaceous Volcanics (Otway and Durroon megasequences)

The Durroon-1 well intersected a 100+ m thick succession of highly altered amygdaloidal olivine basalt, interbedded with clastic sediment. This volcanic succession overlies the Barremian to Albian Otway Megasequence, and is directly overlain by the Cenomanian to Campanian Durroon Megasequence. The volcanics can be observed on seismic data across much of the Durroon Sub-basin, often in the form of flows, mounds, and cones situated in close proximity to major faults (Edgerley and Taylor, 1990). A lack of well

control and poor seismic resolution at depth has meant that the extent of these mid-Cretaceous volcanic rocks is poorly constrained west of the Durroon Sub-basin. Mid-Cretaceous volcanism appears to have been related to upper crustal extension associated with the onset of rifting in the Tasman Basin. Basaltic flows intersected at Durroon-1 represent a number of episodes of volcanism, separated by the deposition of clastic sediment derived from the uplifted half-graben shoulders and margins of the basin.

Late Cretaceous to Paleocene Volcanics (Bass Megasequence)

Campanian to Paleocene volcanic rocks have been intersected at Aroo-1, Bass-2, Chat-1, Tilana-1, Yolla-1 and Yolla-2. The distribution of these wells suggests that volcanism during this period was confined to central and northeastern regions of the Bass Basin. However, the full extent of volcanism cannot be precisely determined, as many wells were not drilled deep enough to penetrate the full succession (Baillie, 1993). Late Cretaceous to Paleocene volcanics are difficult to define on seismic data as reflections are typically parallel to the overlying coals in the Bass Megasequence.

A new petrographic examination of well intervals that intersected volcanic rocks has recently been undertaken (T. Dance and A. Lambeck, pers. comm., 2003). Some of these samples show that "volcanic" intervals, as described in well completion reports, are not wholly volcanic in origin. Instead, the rocks consist of medium-to-coarse grained quartzose sandstones that were subsequently intruded by volcanic fluids. These hot fluids have altered the quartz grains and, upon cooling, have acted to cement the rock. This evidence, together with other geophysical evidence from seismic data, suggest that intrusive magmas and associated fluids were emplaced upward into the stratigraphic succession, and then often migrated laterally along porous or fractured strata (primarily sandstones and coals). This could explain the close association and the apparent interbedded nature of the volcanic, sandstone and coaly strata. Occurrences of sills, such as that intersected at Cormorant-1 (2413 to 2469 m), show a slight discordance to the regional strata and increased amplitudes on seismic data (see Figure 2.3). Coal beds and volcanic intrusions/extrusions often show a similar high-amplitude seismic character that decreases in "brightness" laterally along the bed.

Other Upper Cretaceous to Paleocene volcanic suites are composed largely of fine grained amygdaloidal basaltic flows, some displaying weathered tops, interbedded with minor sandstone, siltstone and shale units. Samples collected from drilling indicate the volcanics have undergone varying degrees of alteration, possibly due to prolonged exposure between flows. Petrographic analyses of the volcanic units suggest that the composition of the mafic flows ranges from alkali olivine basalt, to basanite and picrite. Volcanic units of this age have proved difficult to date using conventional geochronology, as alteration has significantly reduced the effectiveness of K/Ar dating. However, palynofloras from within the volcanic suite place the volcanics within the age range of late Cretaceous to Paleocene (~ 55-75 Ma) (Baillie, 1993).

Oligocene to Miocene Volcanics (Torquay Megasequence)

Oligocene to Miocene volcanics are widespread throughout the central and northeastern regions of the Bass Basin (Figure 4.21). Both intrusive bodies and extrusive volcanics are observed on seismic data. Late

Oligocene to Miocene compressional events led to the strike-slip reactivation of a number of pre-existing structures throughout the Bass Basin (Smit, 1988). Large basement-involved faults with significant displacement appear to have been preferentially reactivated. Strike-slip movement along these structures resulted in the development of north-south oriented zones of pop-up and pull-apart flower structures (Smit, 1988). During the Early Miocene, extensive volcanism occurred in the western half of the basin and multiple volcanic complexes of this age are clearly recognisable on seismic data. Intrusions of this age appear to be related to the distribution of the reactivated structures, where faults acted as feeder conduits for the extrusion of volcanic material (Lennon et al., 1999).

Miocene volcanic sequences were intersected at Bass-1, Tilana-1 and Yolla-1. Volcanic mounds and cones are observed on seismic data within the central and northwestern regions of the basin. Evidence from Bass Basin seismic data, and analogue studies of volcanics of similar composition within western Victoria, suggest the main eruption centres were probably scoria cones located along active faults that acted as feeder conduits (Faustmann, 1995). Volcanic facies intersected by wells within the Bass Basin include olivine basalt flows and highly weathered pyroclastics. This indicates a combination of magmatic and phreatomagmatic volcanism was active during this period. The marine setting of the basin during Cainozoic volcanic episodes would have provided an abundance of water to react with the rising magma, enhancing the likelihood of explosive volcanism (Faustmann, 1995). The variation observed in seismic velocities within the Miocene volcanics may be related to facies changes within the volcanic pile (Faustmann, 1995). This variation poses a significant complication for the correction of seismic pull-up and push-down for depth conversion and the accurate interpretation of exploration targets beneath the volcanic units and intrusive bodies (Taylor, 2001).

Miocene intrusive bodies have been encountered at Cormorant-1, Flinders-1, Koorkah-1, Seal-1, Squid-1, Tilana-1, Toolka-1A and Yolla-1. Intrusive bodies are common in the Bass and Aroo megasequences, varying in thickness from a few meters to over 150 m (Tilana-1). Intrusives appear on seismic sections as prominent reflections, often terminating at major faults. Petrographic analysis of Miocene sills show that composition of the mafic intrusions varies from dolerite at Flinders-1, Seal-1, Yolla-1 and Koorkah-1, to olivine gabbro and syenite at Cormorant-1, and alkali olivine basalt at Squid-1.

Cainozoic volcanism within the Bass Basin appears to be both temporally and spatially extensive. The presence of multiple periods of volcanism of a similar mafic composition over such a significant period of time suggests that the source of volcanism may be hotspot related. Tertiary mafic intrusions (alkali basalts) from King Island appear to be enriched in TiO_2 and contain a comparatively small Zr/Nb ratio. This composition indicates a strong affinity to "oceanic intraplate basalts" such as those from Hawaii (Streit, 1994). Primitive mantle normalised abundance patterns for incompatible and insoluble elements from King Island Cainozoic mafic intrusions also suggest a similar affinity to a plume-related source. The relationship of plume related volcanism to regionally elevated geotherms is discussed further in Chapter 6.

Figure 4.1 Location map of seismic lines interpreted for the Bass Basin study. These seismic lines include reprocessed data from Geoscience Australia Surveys 40, 82 and 90 (blue), and selected reprocessed industry lines (yellow) licensed through Fugro MCS. The total grid coverage is approximately 4,000 line kms.

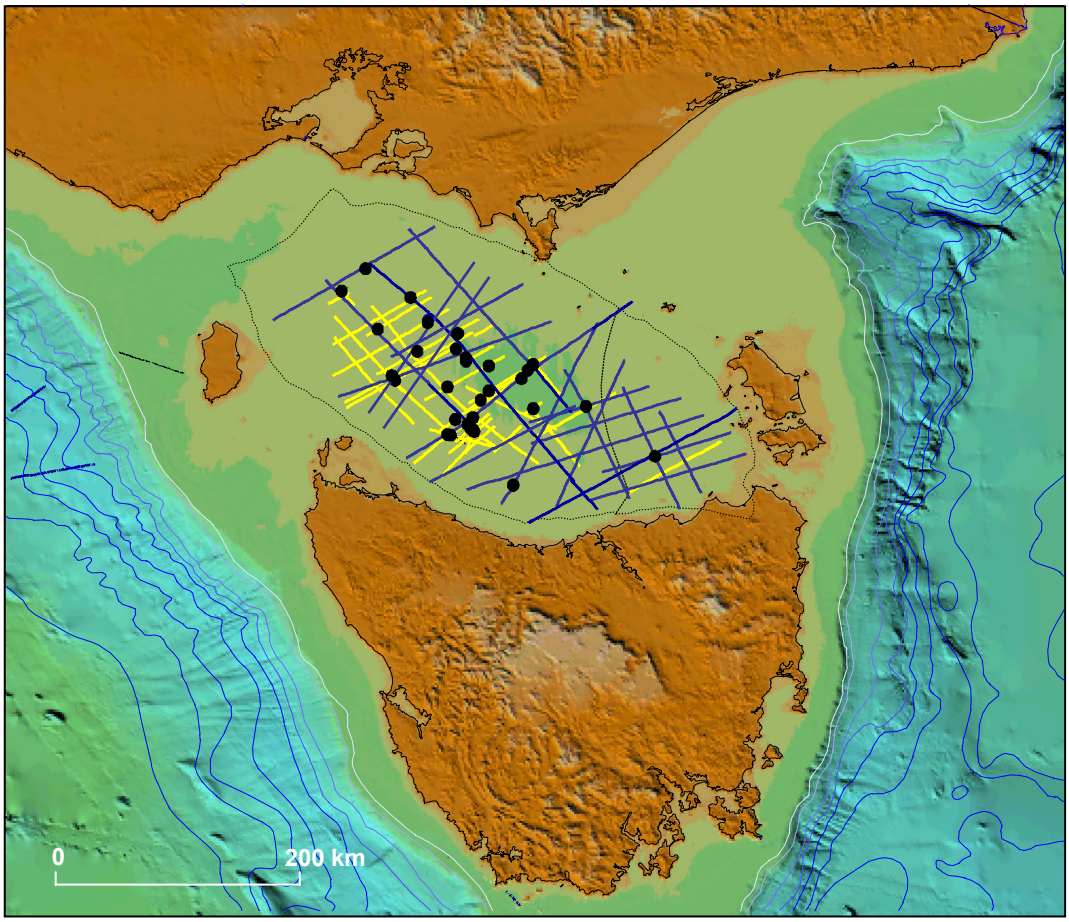

Figure 4.2a Stratigraphic correlation chart for the Bass Basin showing the relationship between age, lithostratigraphy, sequence stratigraphy, basin phases, tectonic events and horizons mapped. The basin phases are shown in detail for the Cape Wickham (CW) and Durroon (Durr) sub-basins. The time scale is from Young and Laurie (1996), with modifications to spore/pollen zones from Partridge (2001).

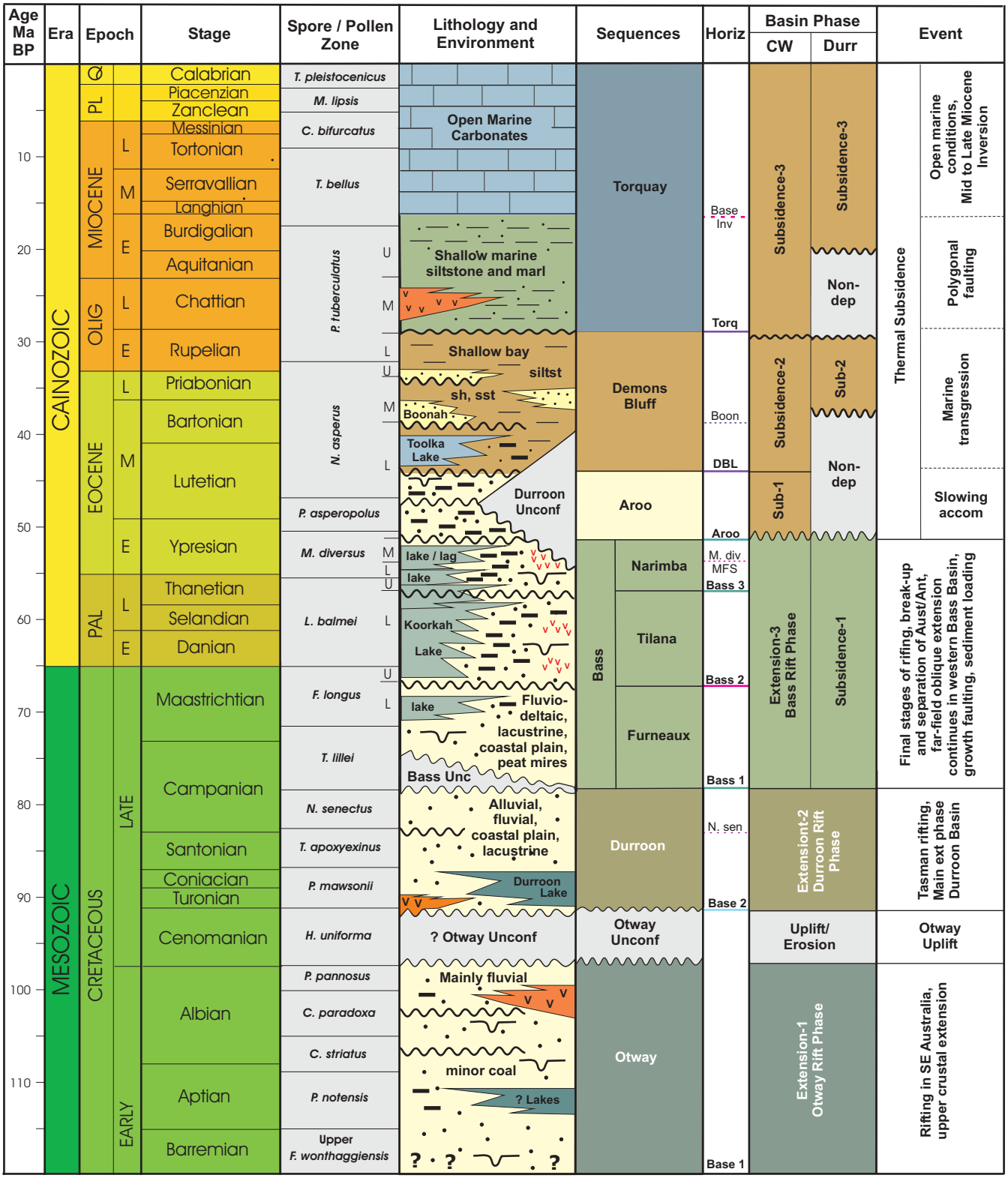

Figure 4.2b Stratigraphic correlation chart for the Bass Basin showing the relationship between the stratigraphic nomenclature scheme of Lennon et al. (1999) and the framework proposed in this report. The time scale is from Young and Laurie (1996), with modifications to spore/pollen zones from Partridge (2001).

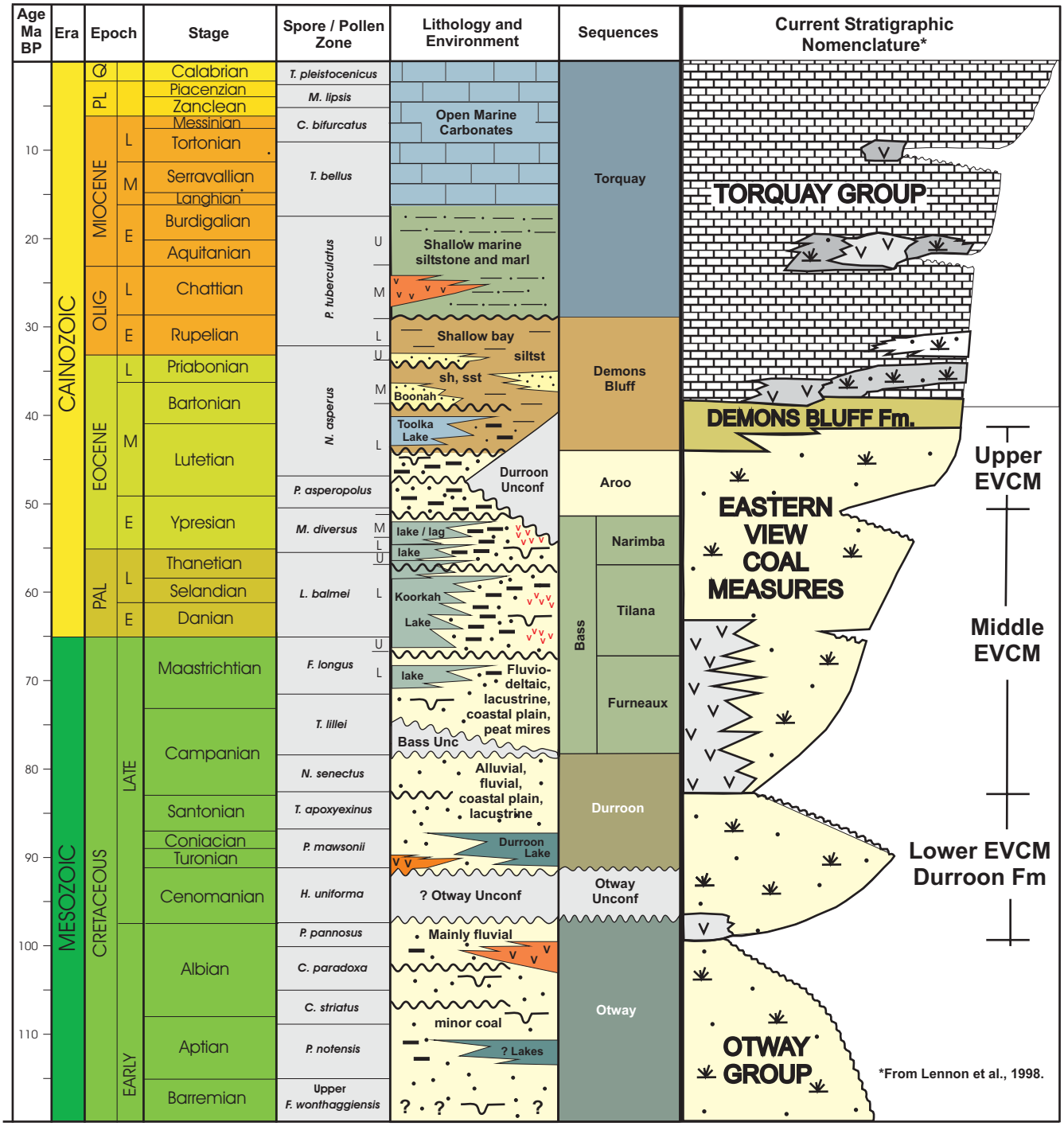

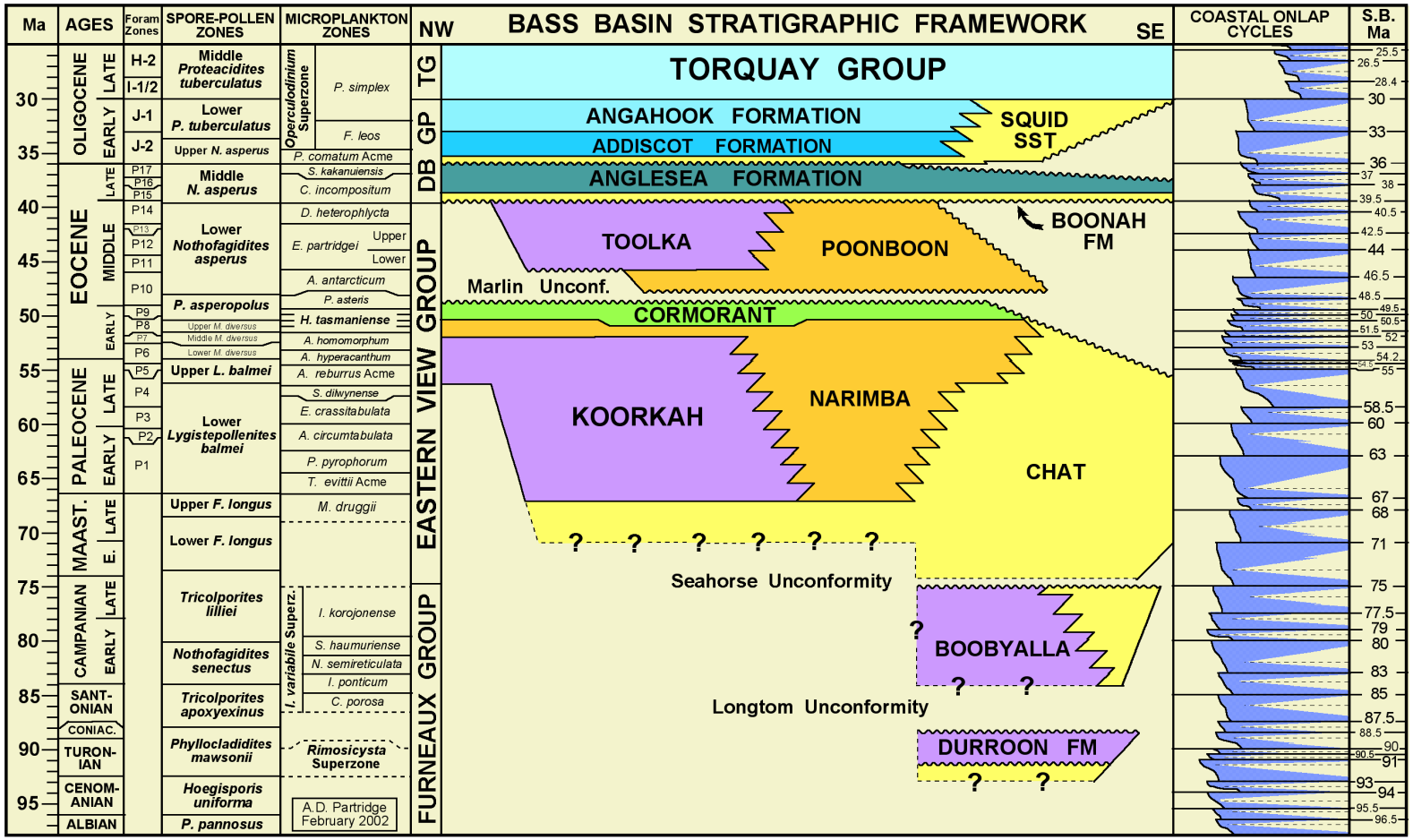

Figure 4.3 Proposed stratigraphic framework for the Bass Basin based on the biostratigraphic analysis and log correlations of Partridge (2002; Appendix C). The palynological zones and correlation to timescale of Haq et al. (1988) is adapted from Partridge (1999). Informal group names used include the Furneaux Group, Eastern View Group, Demons Bluff Group (DB GP) and the Torquay Group (TG). This framework was modified to produced the correlation charts as shown in Figures 4.2a and 4.2b.

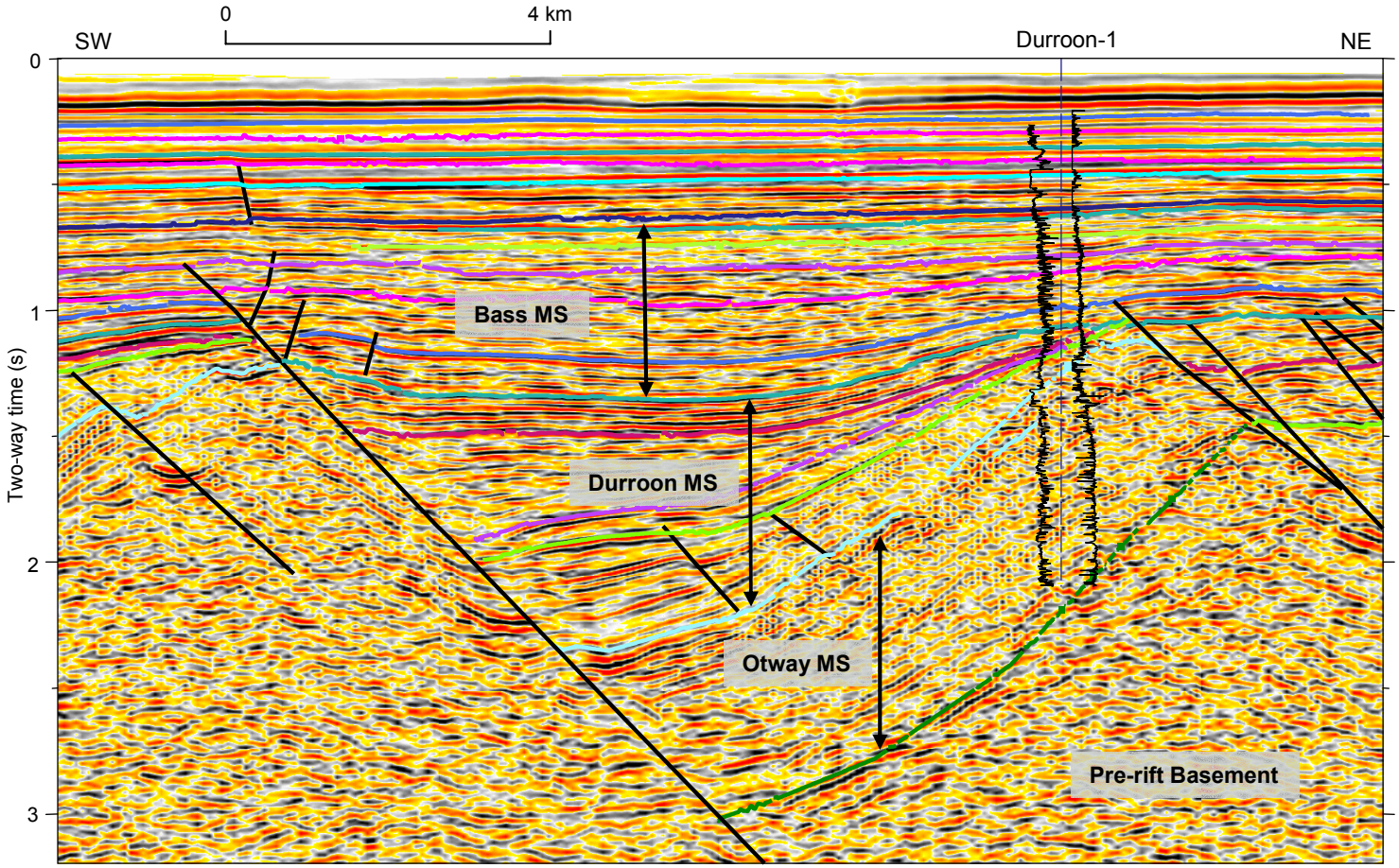

Figure 4.4 Geoscience Australia seismic line across part of the Durroon Sub-basin. This section shows in more detail the syn-tectonic successions intersected at the Durroon-1 well: the Early Cretaceous Otway Megasequence (Rift Phase 1) and the overlying early Late Cretaceous Durroon Megasequence (Rift Phase 2). In the Durroon Sub-basin, the Late Cretaceous Bass Megasequence is largely a sag-related succession deposited during post-rift subsidence. This seismic image is published with the permission of Fugro MCS.

Figure 4.5 Well logs (gamma and sonic) for the Durroon-1 well in the Durroon Sub-basin. The well intersected two syn-rift successions - the Early Cretaceous Otway Megasequence, and the Late Cretaceous Durroon Megasequence. Ages and interpreted sequences, as well as minor unconfomrities within the Otway Megasequence, are shown.

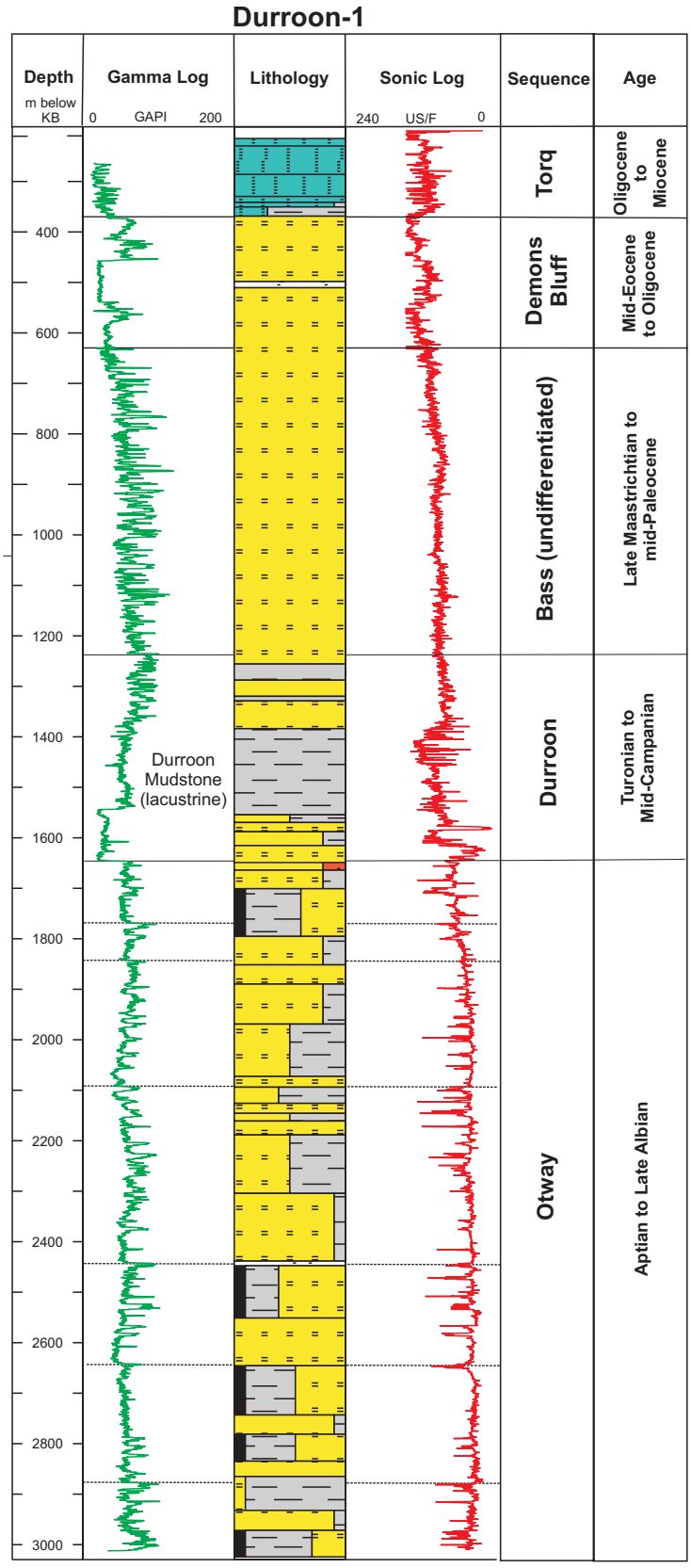

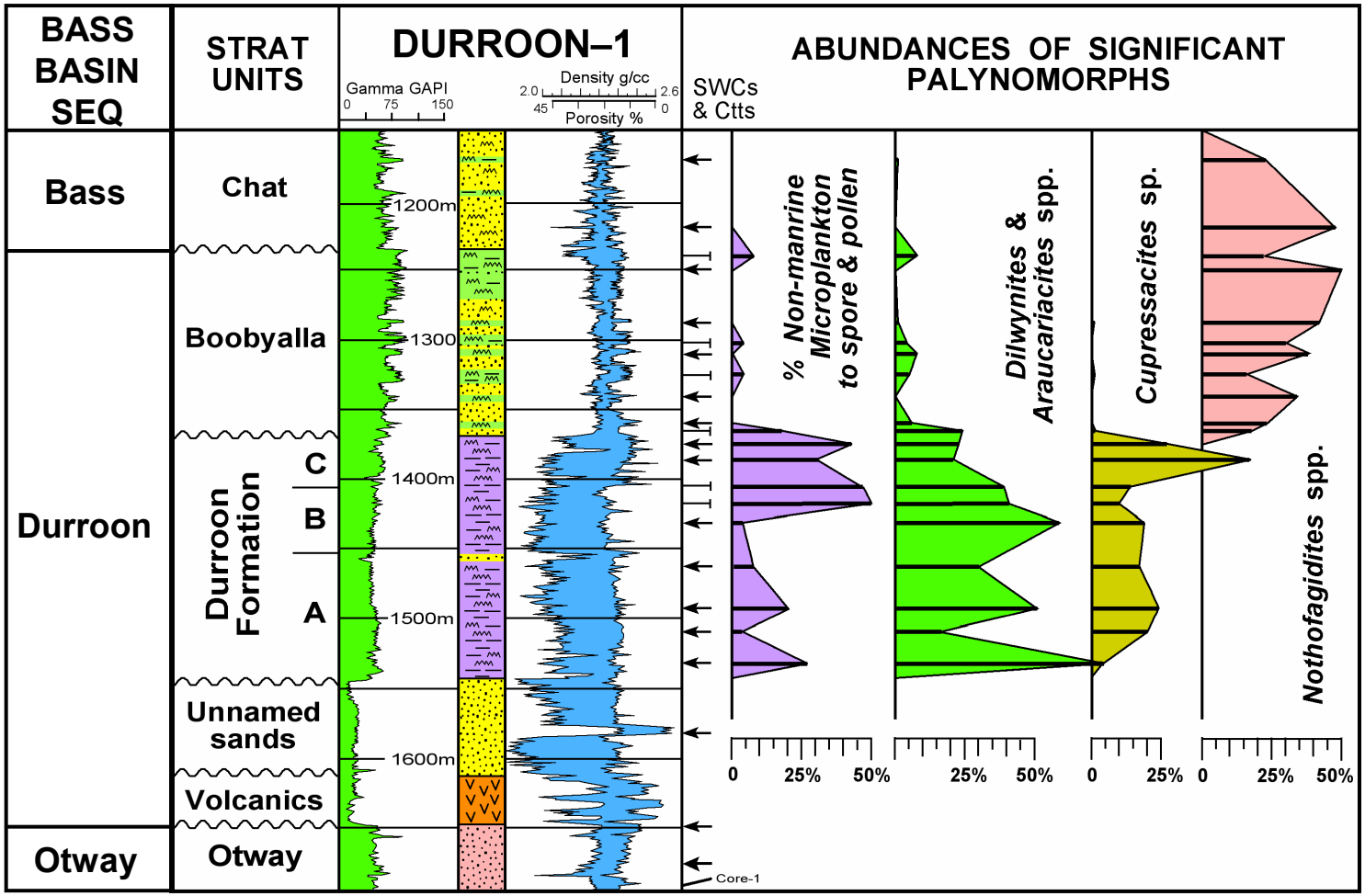

Figure 4.6 Well logs and abundances of significant palynomorphs for samples from Durroon-1 over the interval (1140 to 1670 m; Partridge, 2002). Lithostratigraphic units refer to terms used in Figure 4.3, while sequence names relate to nomenclature proposed in Figure 4.2.

Figure 4.7 Well logs (gamma and sonic) for the Pelican-5 well in the Pelican Trough. The well intersected a complete succession of the Bass Megasequence (Furneaux, Tilana and Narimba sequences). Note the occurrence of a hydrogen-rich coal at 2792 m, above the Intra-Lower M. diversus MFS at 2808 m.

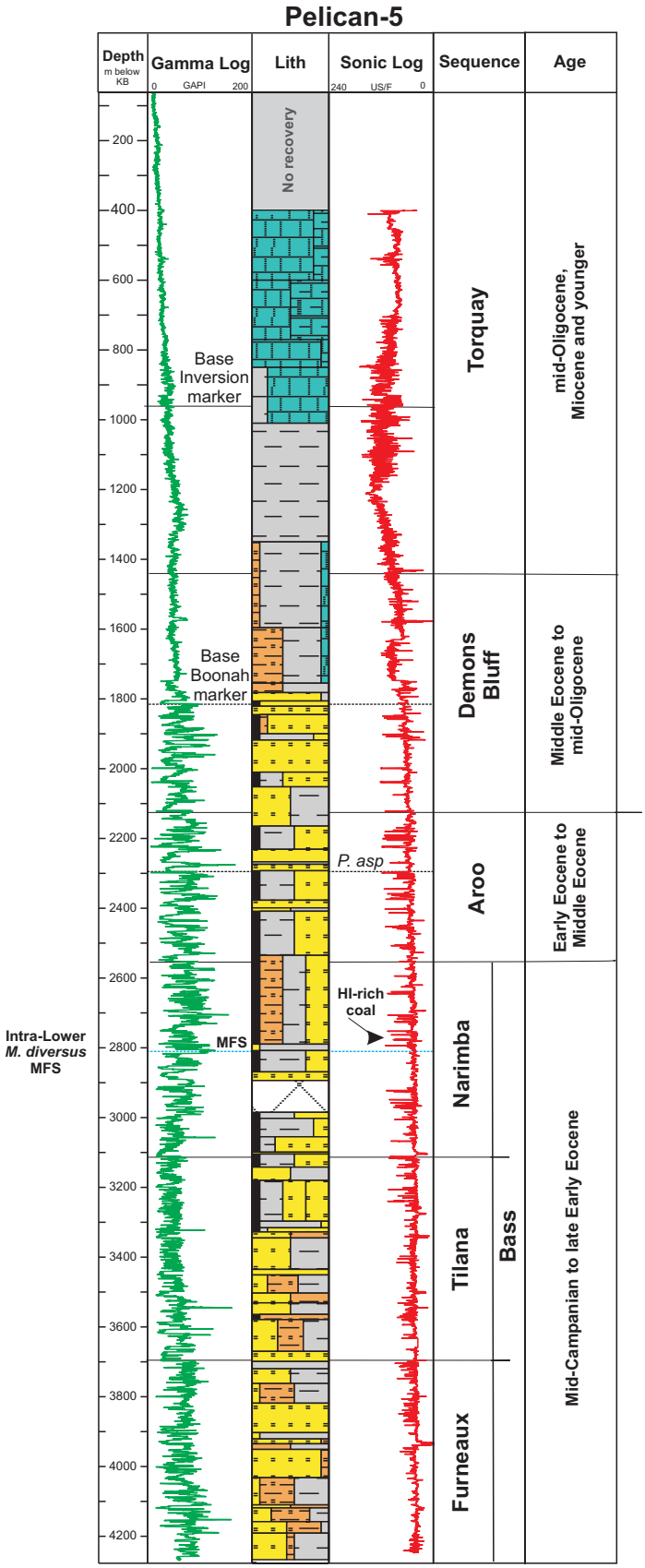

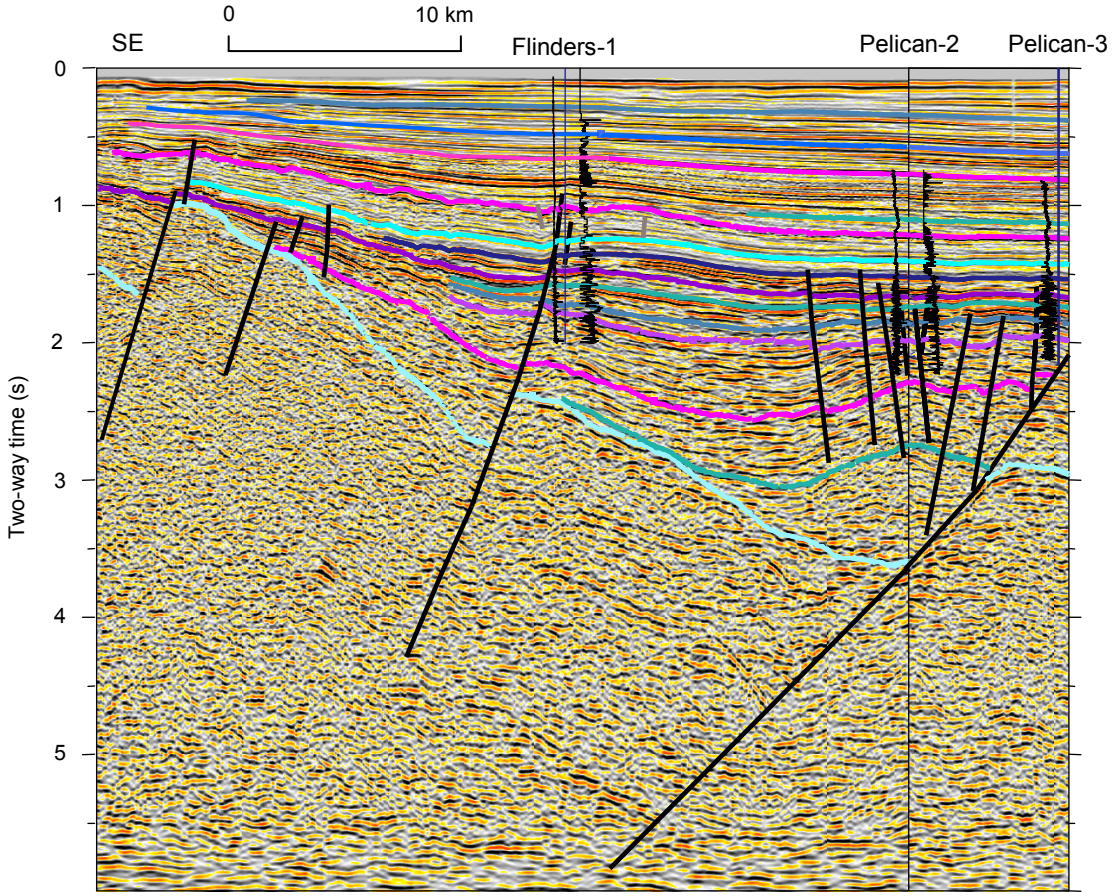

Figure 4.8 Geoscience Australia seismic line across the Pelican Trough in the central Bass Basin. The Pelican wells were drilled into a crestal collapse structure within the hanging wall of the Pelican Trough. Deformation of the deeper sedimentary succession has meant that it is difficult to confidently correlate horizons within the Bass Megasequence away from the Pelican Trough. This seismic image is published with the permission of Fugro MCS.

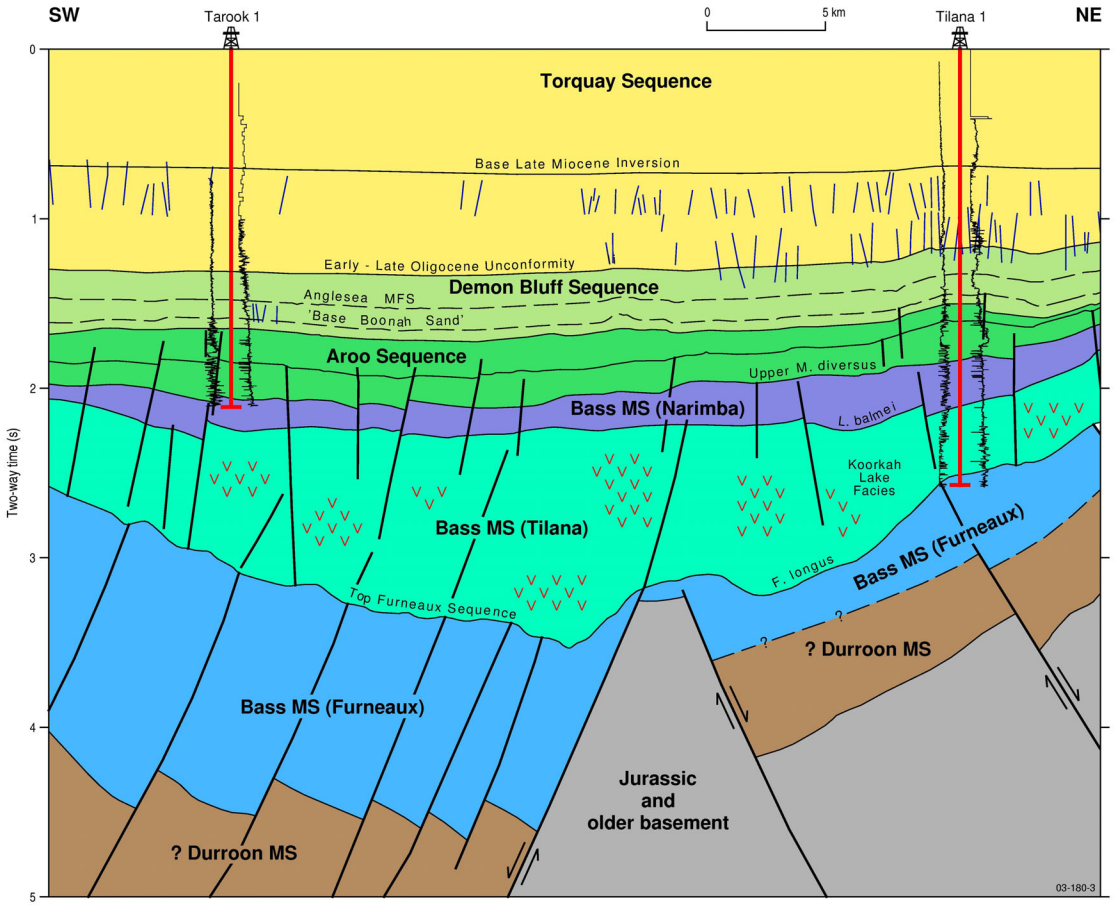

Figure 4.9 Diagrammatic cross-section across the central Bass Basin showing the syn-tectonic nature of the Durroon and Bass sequences (Furneaux, Tilana and Narimba sequences), and the overlying post-rift successions of Aroo, Demons Bluff and Torquay sequences. The stratal geometry and faults controlling the deposition of the Tilana Sequence are obscured due to the prolific intrusion of volcanics into the succession. The Narimba Sequence shows only minimal growth on this section.

Figure 4.10 Well logs (gamma and sonic) for the Tilana-1 well in the central Bass Basin. The well intersected multiple intervals of intrusive and extrusive volcanic rocks. The thick basaltic succession below 3100 m consists of basaltic flows and Paleocene sandstones cemented by intruded volcanic fluids.

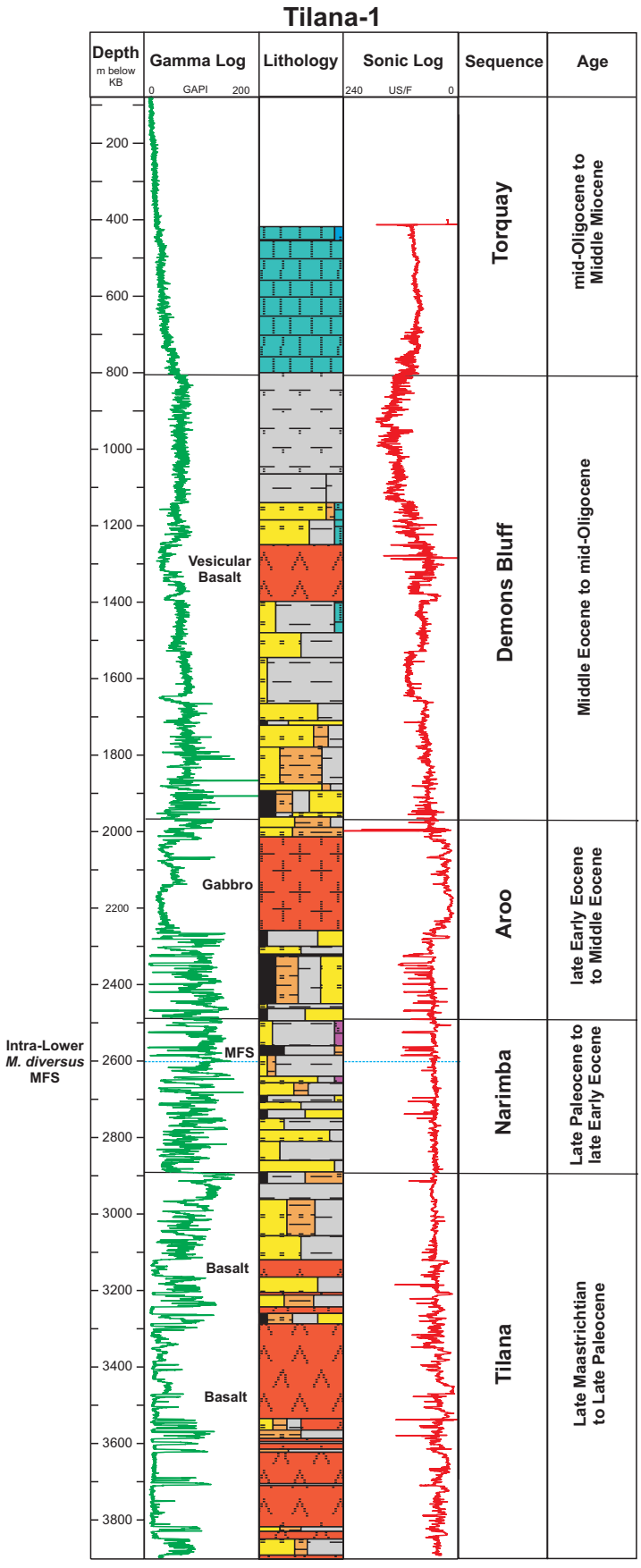

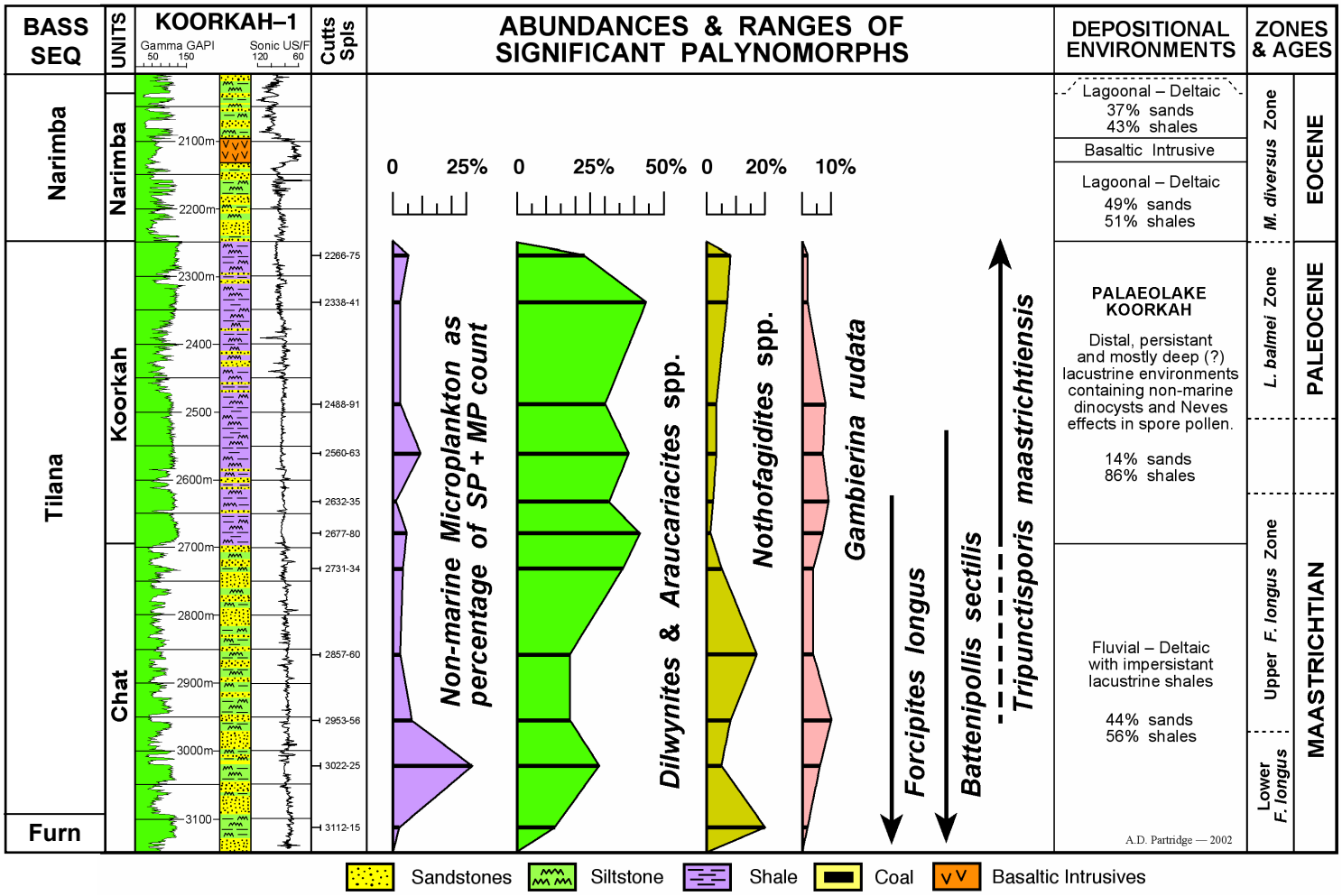

Figure 4.11 Well logs, abundances and ranges of significant palynomorphs for Maastrichtian to Paleocene samples from Koorkah-1 over the interval (2030 to 3140 m; Partridge, 2002). Lithostratigraphic units refer to terms used in Figure 4.3, while sequence names relate to nomenclature proposed in Figure 4.2.

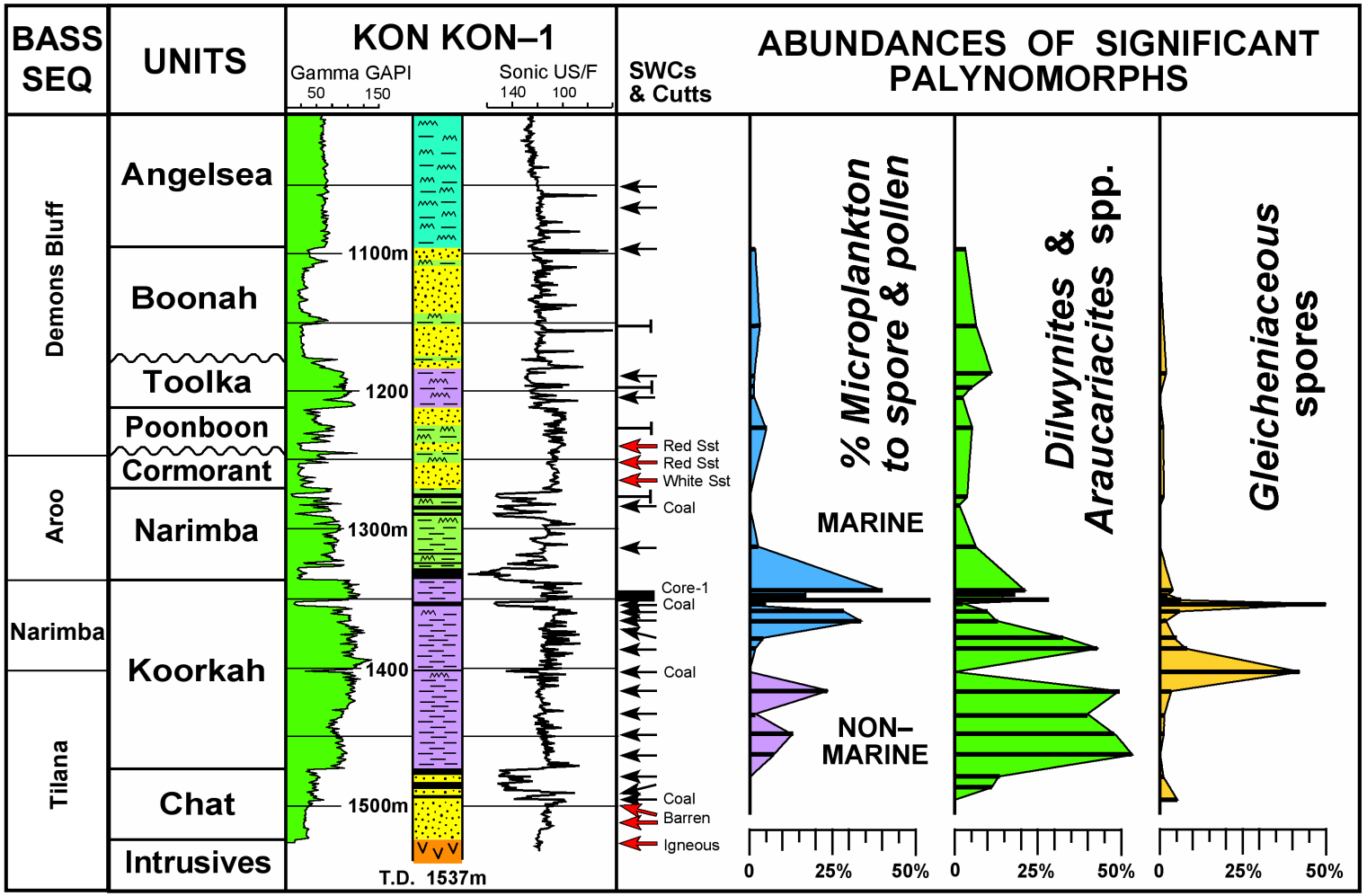

Figure 4.12 Well logs, abundances and ranges of significant palynomorphs for Paleocene to Eocene samples from Konkon-1 over the interval (1000 to 1537 m; Partridge, 2002). Lithostratigraphic units refer to terms used in Figure 4.3, while sequence names relate to nomenclature proposed in Figure 4.2.

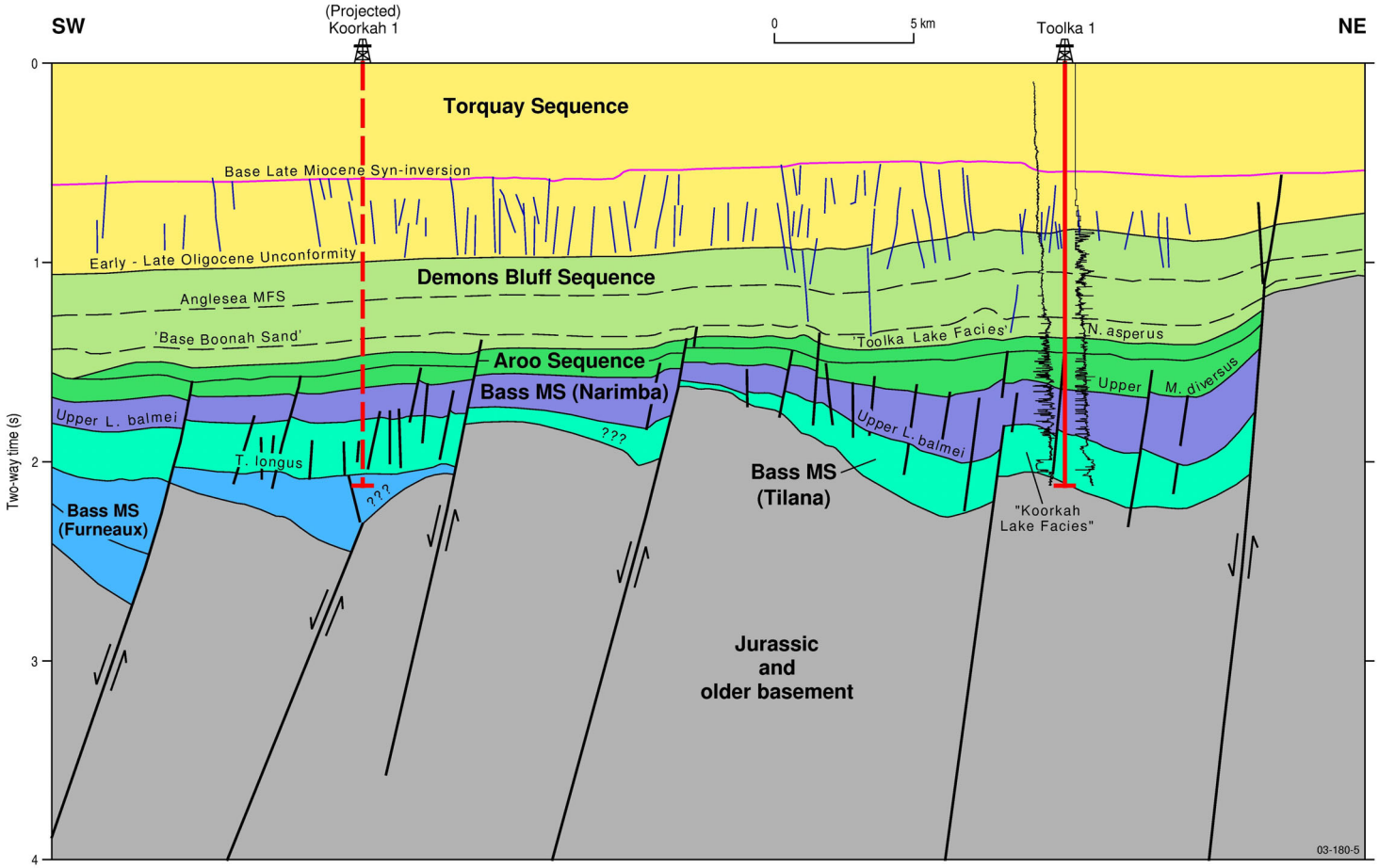

Figure 4.13 Diagrammatic cross-section across the western Bass Basin (near the Toolka-1A and Koorkah-1 wells) showing the syn-tectonic nature of the Bass Megasequence. Growth faulting during the Late Cretaceous to Late Paleocene controlled the development of localised depocentres where deepwater lakes formed (Koorkah Lake). By contrast, the development of Toolka Lake was less influenced by tectonic processes, with the resulting lake being shallower and more widespread than the earlier Koorkah Lake.

Figure 4.14 Well logs (gamma and sonic) for the Poonboon-1 well in the central Bass Basin. The well intersected a lower delta plain to lacustrine succession of Paleocene to Eocene age (Koorkah Lake equivalent facies). The Narimba Sequence is approximately 400 m thick, while in the Pelican Trough this syn-tectonic succession reaches thicknesses of up to 1200 m.

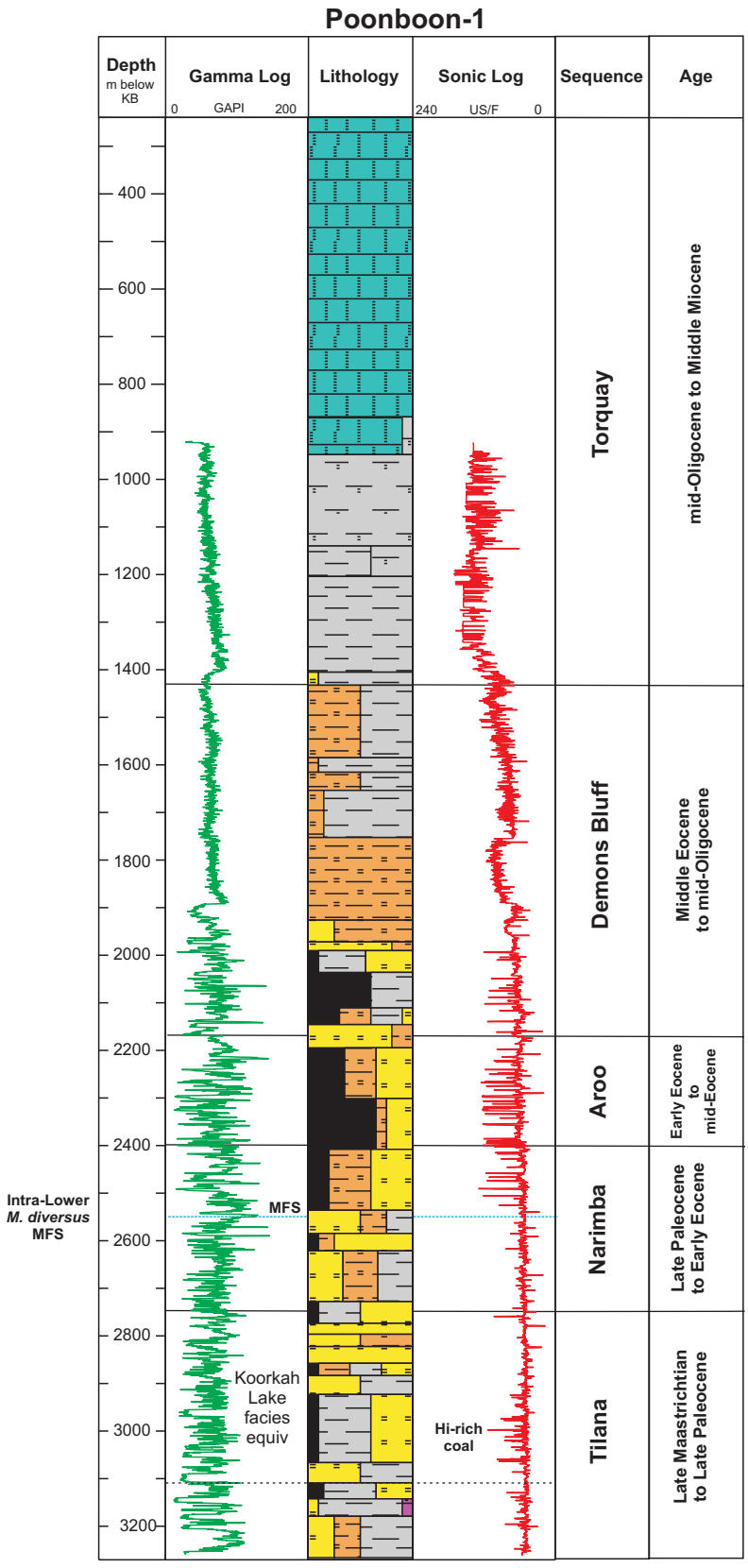

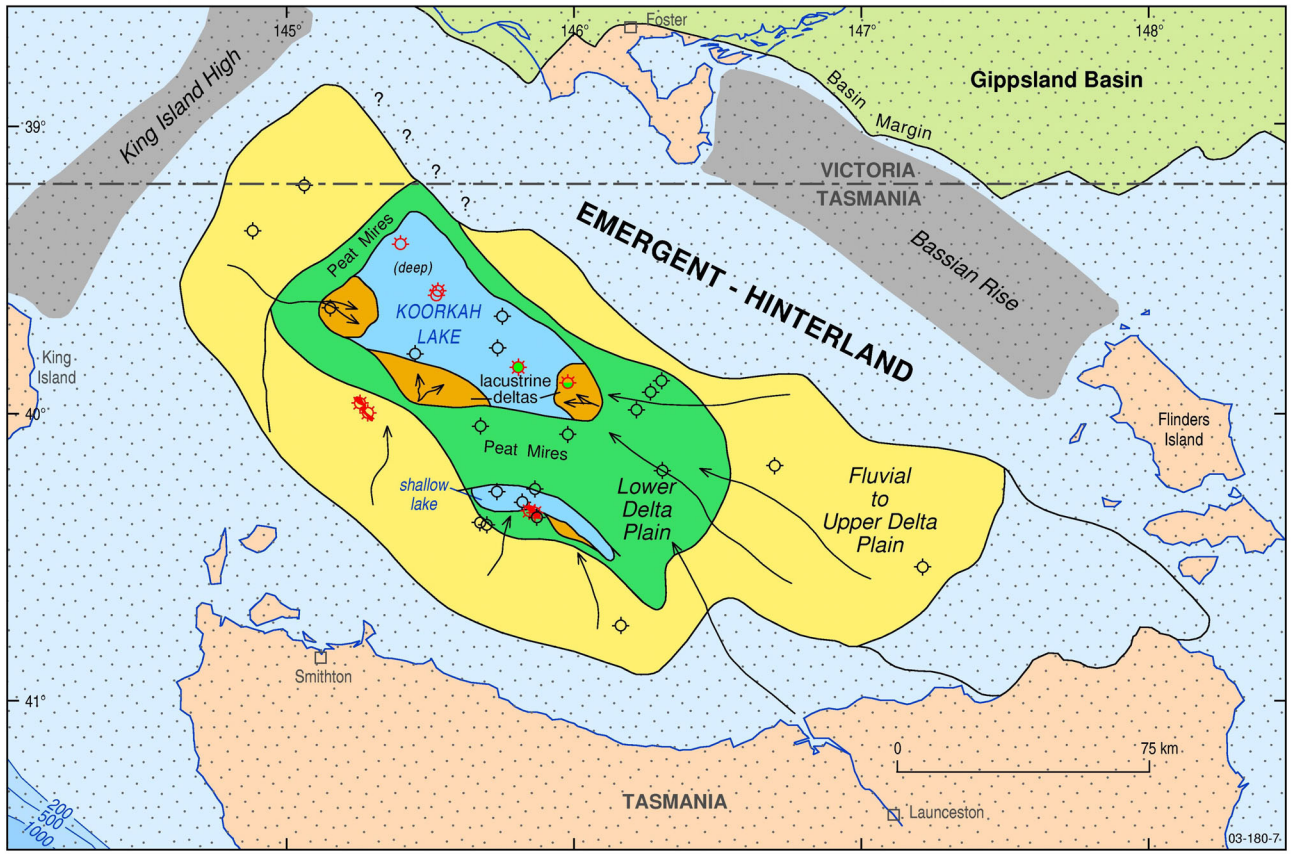

Figure 4.15 Generalised palaeogeographic map showing the maximum extent of Lake Koorkah (Partridge, 2002; Tilana and Narimba sequences). During the lake highstand, deepwater lacustrine shales and lacustrine shoreface/deltaic sands were deposited in mainly faulted-controlled depocentres, while peat mires fringed the margins of the lakes. Hydrogen-rich coals of this age were detected at Poonboon-1 (Chapter 5). The lakes were absent in the Durroon Sub-basin, where mainly fluvial environments dominated during the Late Cretaceous to the early Palaeogene.

Figure 4.16 Well logs (gamma and sonic) for the Narimba-1 in the Pelican Trough. The well intersected an expanded (syn-tectonic) section of the Narimba Sequence (base Upper L. Balmei to base Upper M. diversus zones).

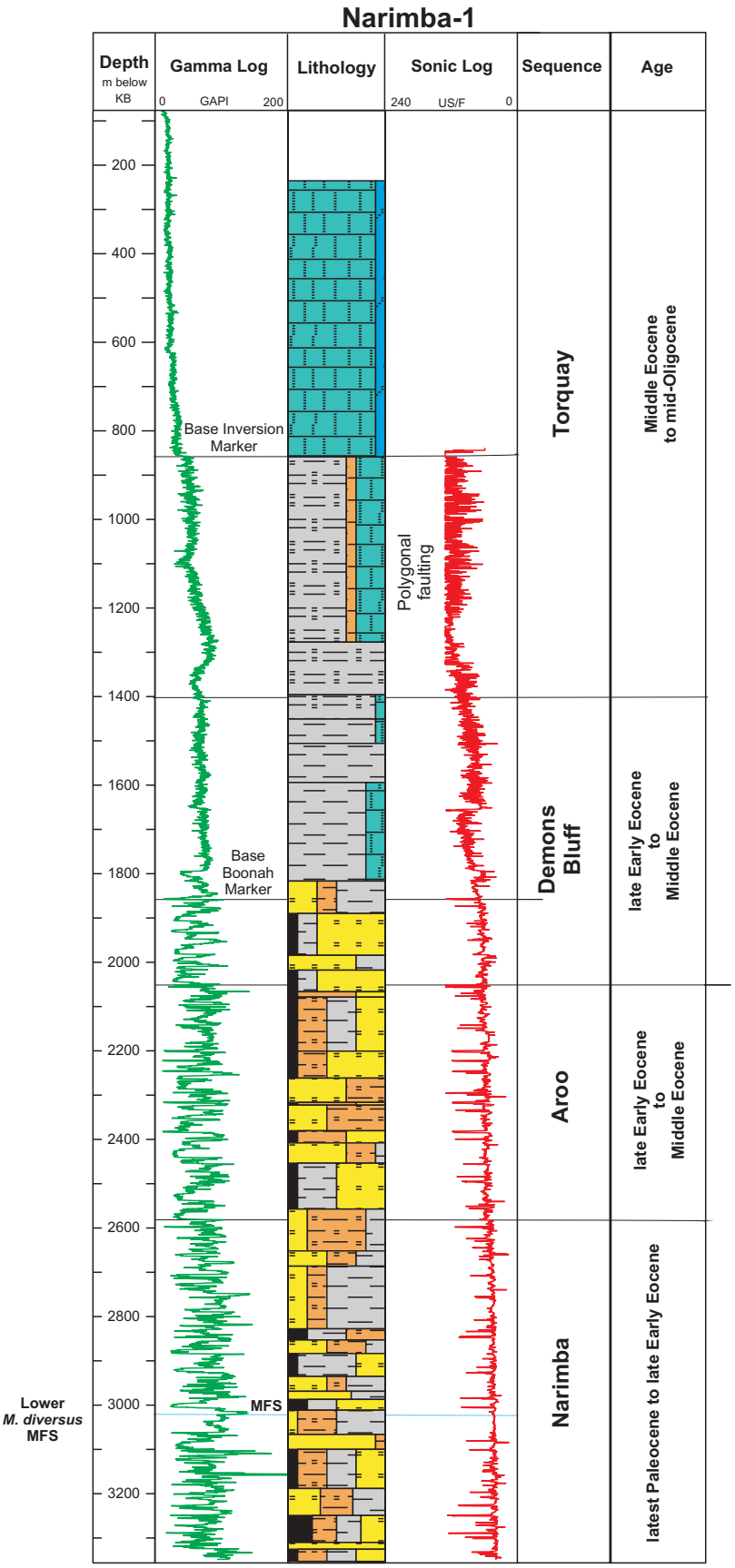

Figure 4.17 Well logs (gamma) for the Poonboon-1 and Nangkero-1 wells in the central Bass Basin showing the correlation of multiple flooding surfaces in the Early Eocene to Late Oligocene succession. MICP analyses indicate that the shales near the Lower M. diversus MFS have a the high seal capacity (1400 m; Chapter 7) of the 15 samples analysed. Shales of the Demons Bluff FS are the regional sealing facies for the Bass Basin succession.

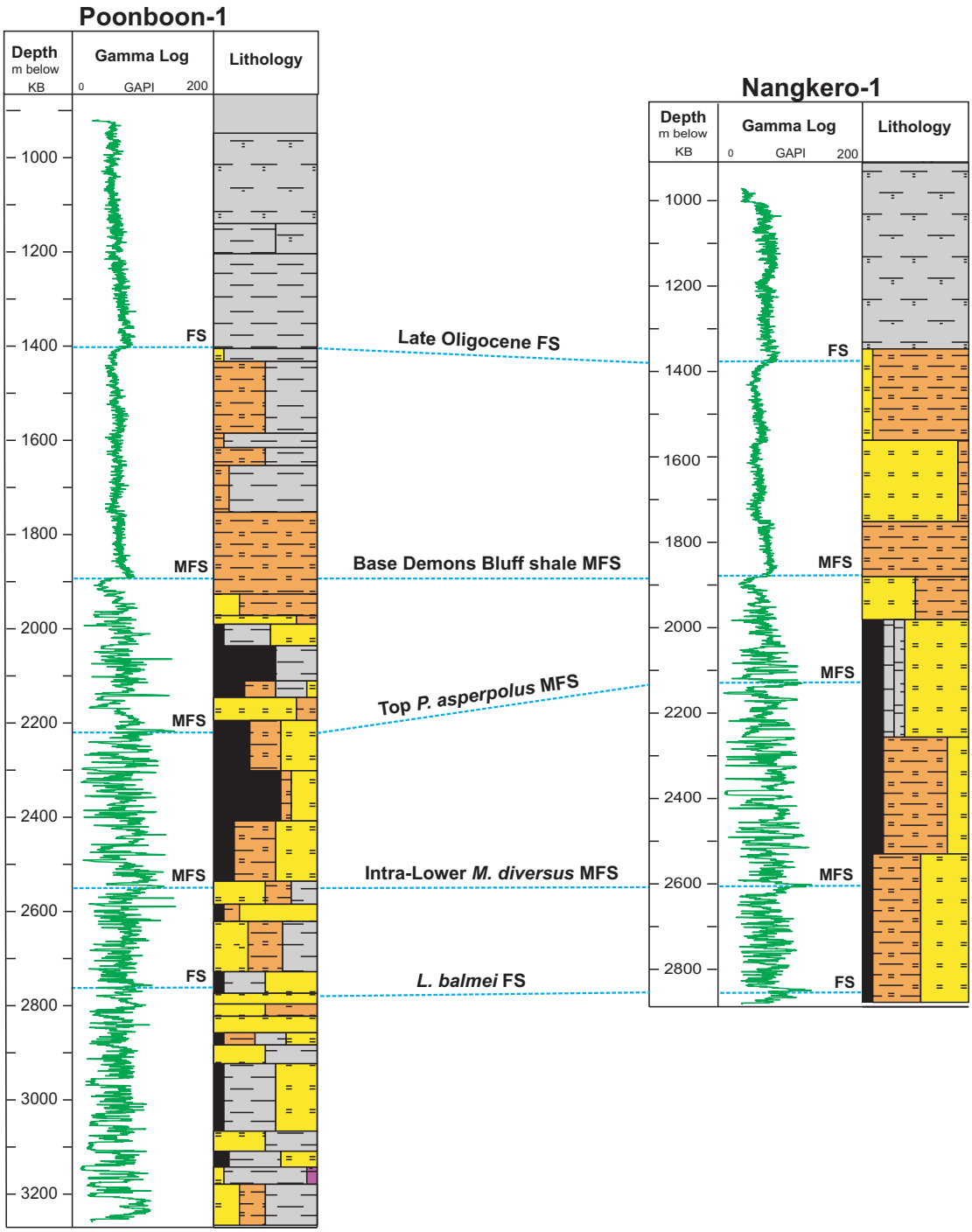

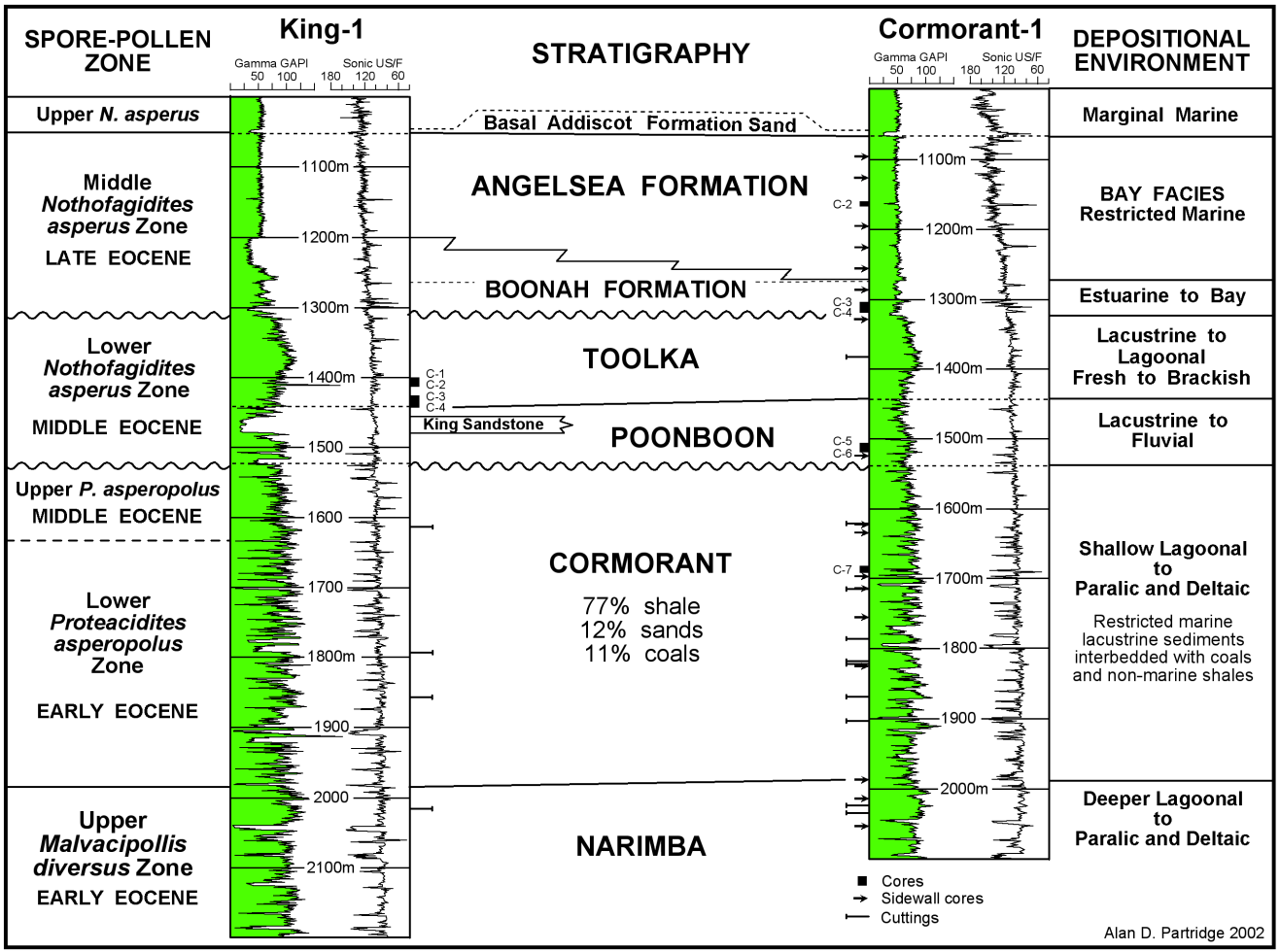

Figure 4.18 Palynological and log correlation between King-1 and Cormorant-1 **(**Partridge, 2002), showing the occurrence of lacustrine, shallow lagoonal and paralic/deltic environments during the Eocene in the northwestern Bass Basin. Lithostratigraphic units refer to terms used in Figure 4.3.

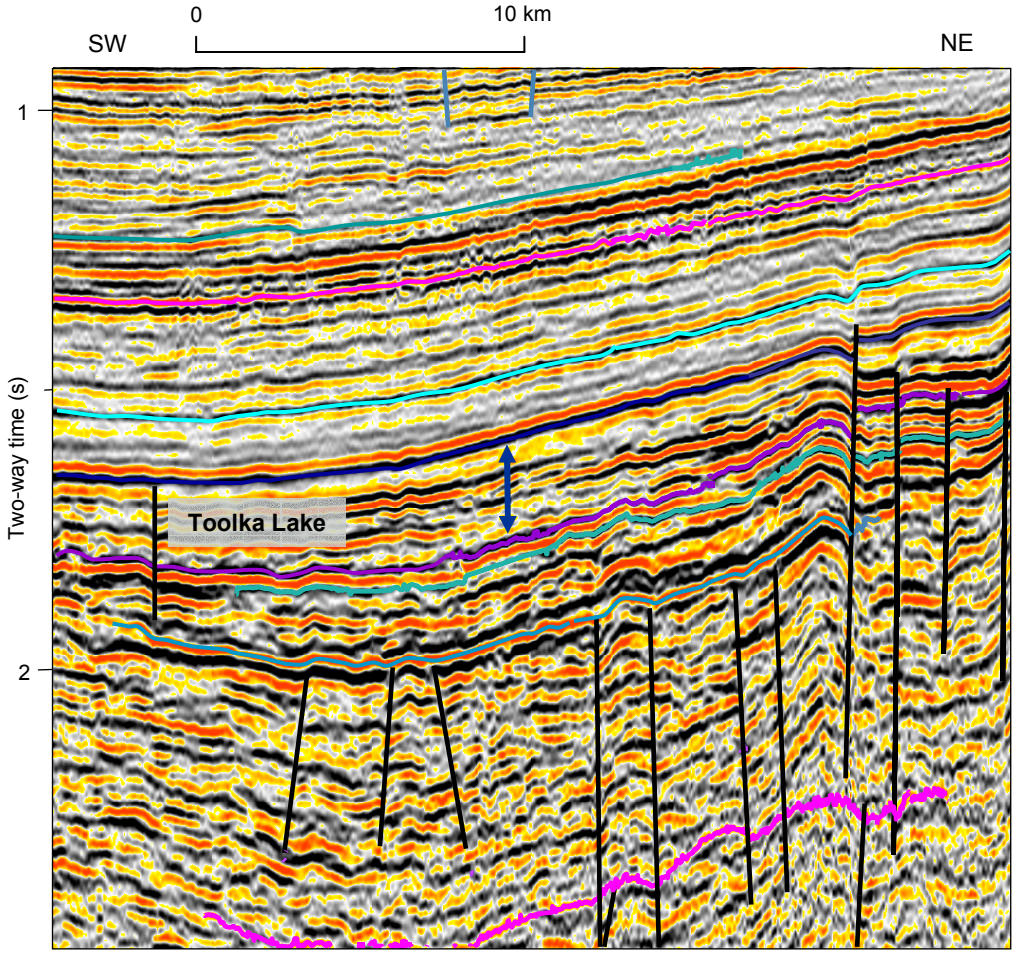

Figure 4.19 Geoscience Australia seismic line across the central Bass Basin showing the geometry and stratal character of the Toolka Lake succession. The dark blue horizon marks the "Base of the Boonah Sand". This figure is published with the permission of Fugro MCS.

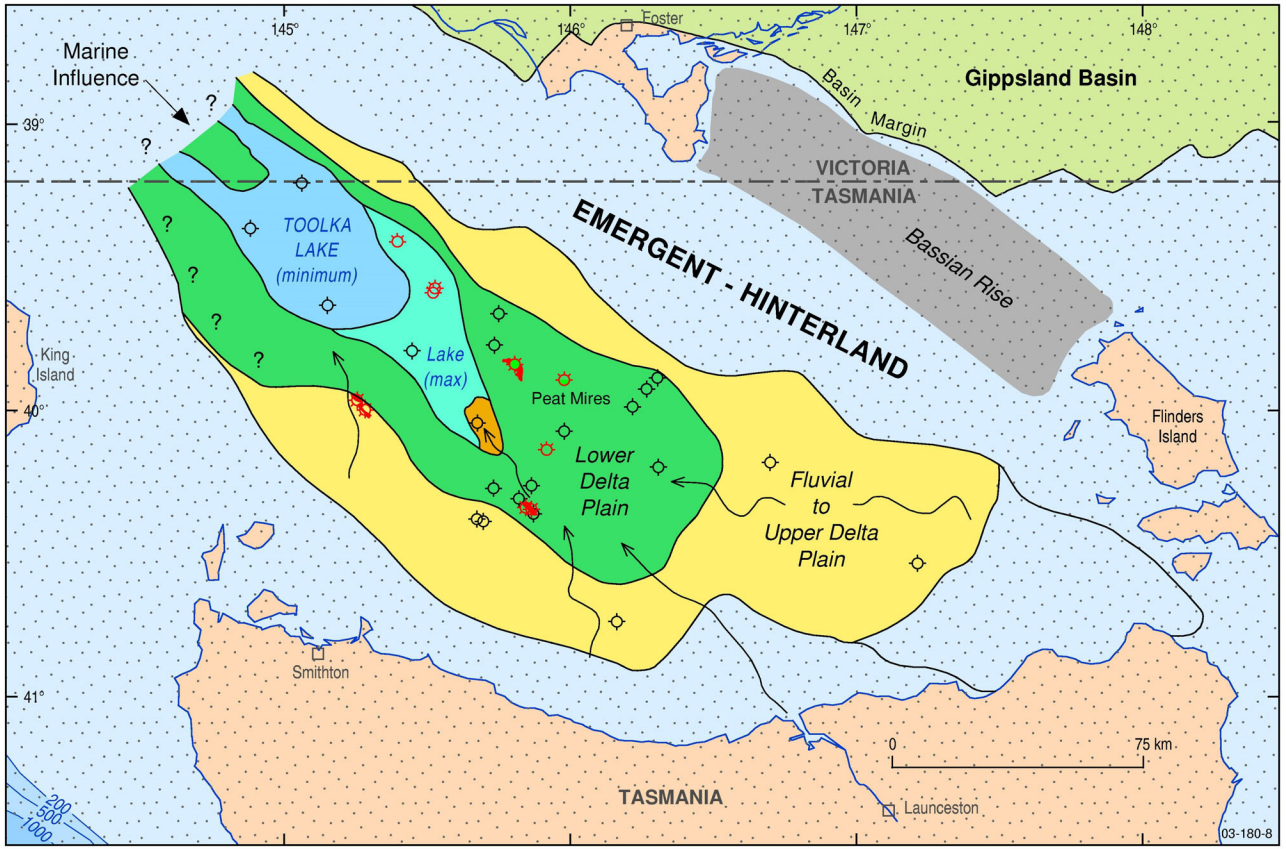

Figure 4.20 Generalised palaeogeographic map showing the minimum and maximum extents of Lake Toolka (Partridge, 2002; Aroo Sequence; Lower to Middle *N. asperus*). During the Middle Eocene lake highstand, shallow water lacustrine shales and lacustrine shoreface/deltaic sands were deposited in broad, low-relief depocentres while peat mires fringed the margins of the lakes. A lagoonal influence was detected in areas to the northwest. The lakes were absent in the Durroon Sub-basin, where mainly fluvial environments dominated from the Late Cretaceous to early Palaeogene.

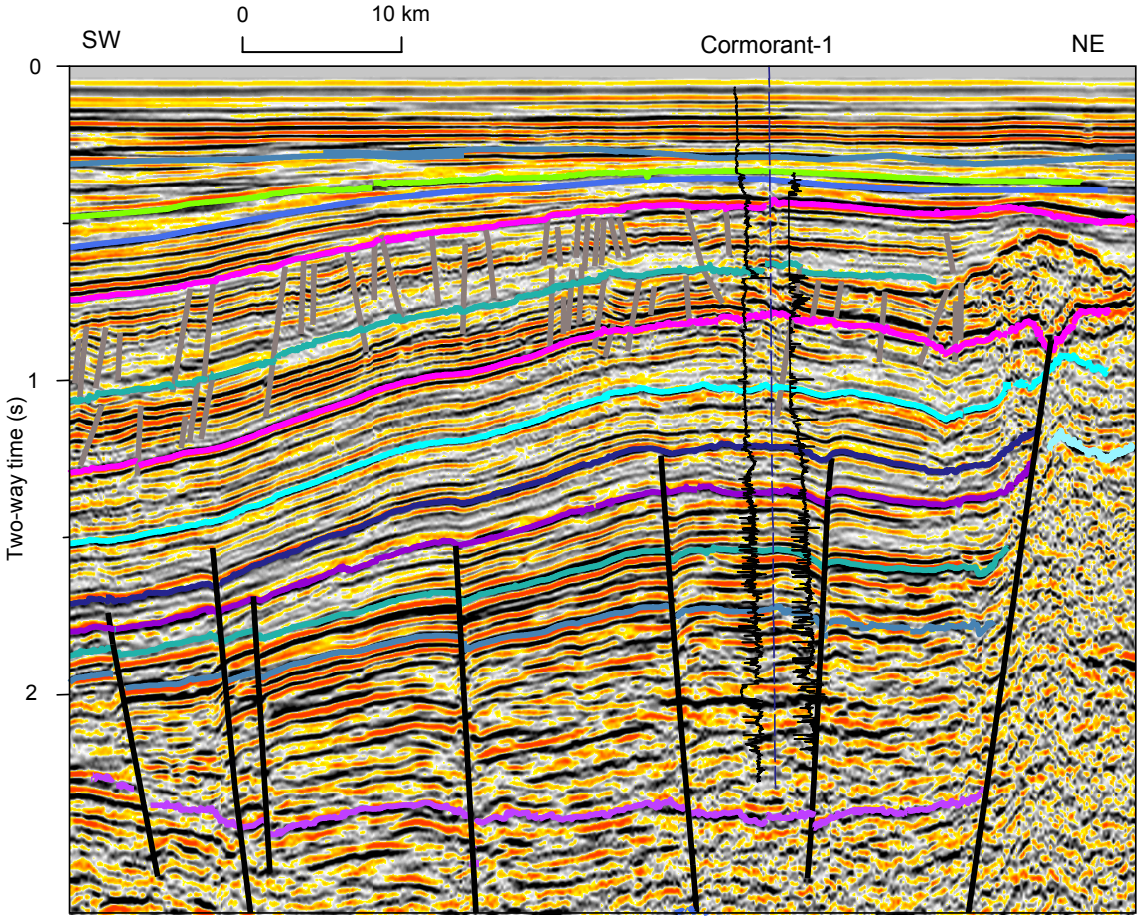

Figure 4.21 Geoscience Australia seismic line across the Cormorant Anticline. The anticline is an inversion structure that formed against the fault bounding the northwestern margin of the basin. The syn-inversion succession at Cormorant-1 has been dated as late Middle Miocene and younger. High-amplitude, cross-cutting volcanic intrusions seen near 2.00 s TWT were intersected by the well. In addition, a large volcanic mound is observed to the north of Cormorant-1. The mound overlies the mid-Oligocene unconformity and maybe associated with basinward polygonal faulting within the Late Oligocene to Late Miocene strata. This seismic image is published with the permission of Fugro MCS.

5. PETROLEUM GEOCHEMISTRY OF SOURCE ROCKS, OILS AND GASES

C. Boreham, Geoscience Australia

5.1 KEY POINTS

- Potential oil-prone source rocks in the Bass Basin are Palaeogene coals, mainly concentrated in the Early to Middle Eocene succession, with Hydrogen Indices (HI) up to 500 mg hydrocarbons/gTOC, while associated disseminated organic matter in claystones is mainly gas prone.
- Maturity is sufficient for oil and gas generation, with vitrinite reflectance (VR) up to 1.8% at the base of Pelican-5. Igneous intrusions, mainly within Paleocene, Oligocene and Miocene sediments, produced localised elevated maturity up to 5% VR.
- Key events in the process of petroleum generation and migration from effective source rocks are:
  - onset of oil generation occurred at a VR of 0.65% (2450 m in Pelican-5)
  - onset of expulsion (primary migration) occurred at a VR of 0.75% (2700 to 3200 m in Bass Basin; 2850 m in Pelican-5)
  - main oil window occurred between VR of 0.75% and 0.95% (2850 to 3300 m in Pelican-5)
  - main gas window occurred at VR>1.2% (>3650 m in Pelican-5).
- Coals and claystones show a range in laboratory-generated chemical kinetic properties, which when applied to the geological timeframe, translates to an approximate 500 m range in the onset of primary migration.
- Oils in the Bass Basin are a single oil population sourced mainly from Early Eocene to Paleocene coals. Biodegradation of the Cormorant oil results in a statistically separate oil family compared to the Pelican and Yolla crudes.
- Much better oil-to-source correlations are found between the oils and the coals, than the claystones.
- Gases in the Bass Basin are wet and high in CO_2 content. The CO_2 is sourced from igneous intrusions.
- Gaseous hydrocarbons have a similar source to oils, but are generated over a wider maturity range. White Ibis-1 gas is of higher maturity than Yolla-2 gas.

5.2 INTRODUCTION

Situated in offshore southeastern Australia, the Bass Basin is a minor terrestrial oil and gas province. It lies to the southwest of the Gippsland Basin, which is Australia's premier petroleum province. Oil and gas in the Gippsland Basin are sourced from terrestrial organic matter (Moore et al., 1992, Boreham et al., 2001). The oil in the Bass Basin is typically paraffinic with oil in shallower reservoirs undergoing significant alteration by biodegradation (Edwards et al., 1999). Biomarker and carbon isotopic data (Edwards et al., 1999), and the lack of a significant potential marine source rock over most of the basin (Miyazaki, 1995) indicate that the oil is sourced primarily from terrestrial organic matter within the Late Cretaceous to Eocene Bass, Aroo and lower Demons Bluff sequences (Eastern View Group). Miyazaki (1995) suggested that disseminated organic

matter within the carbonaceous claystones are the main effective source rocks for oil, while gas is the primary expulsion product from the associated coals. The latter is based on the concept that oil initially generated from the coal over a maturity range of 0.6 to 1.4% vitrinite reflectance (VR) would remain 'absorbed' within the organic matrix. Subsequent expulsion of gas from the coal would only have occurred at higher maturities when oil-to-gas cracking became significant (Miyazaki, 1995).

In the Bass Basin, there is a critical need for more detailed information on the spatial variations in petroleum potential, gas:condensate ratios (GCR), gas:oil ratios (GOR) and maturation characteristics within organic-rich rocks to help identify the potential source(s) for the oil and gas. Previous interpretations of vitrinite reflectance profiles and bulk geochemical parameters, such as Rock-Eval and extractable organic matter (bitumen) content, were undertaken at a regional scale within the Bass Basin (Miyazaki, 1995). This approach did not allow for stratigraphic variations in source rock characteristics to be fully addressed.

5.3 AIMS, SAMPLES AND METHODS

The geochemistry program undertaken as part of the WTRMP aimed to address fundamental questions related to hydrocarbon generation in the Bass Basin, in particular:

- are some coals and claystones more oil-prone than others, and if so, is it possible to predict their distribution?
- what are the respective contributions of coals and associated carbonaceous lithologies to oil and gas generation and expulsion?
- is there evidence that oil is expelled from coal?
- can gas-oil-source correlations be established in the basin?
- are there variations in chemical kinetics for kerogen degradation that would cause source rocks to mature (i.e., generate and expel hydrocarbons) at different temperatures, and can the distribution of these rocks be predicted?

ORGCHEM, Geoscience Australia's Oracle-based organic geochemistry database (http://www.ga.gov.au), was the source for the bulk Rock Eval and vitrinite reflectance data interpreted for this study, while top and base ages (Ma) over the depth interval of the sample were estimated using STRATDAT (Geoscience Australia's Oracle-based biostratigraphy database). This data was complied from well completion reports submitted under the *Petroleum Submerged Lands Act (PSLA) 1967,* and destructive analysis reports submitted to Geoscience Australia by external agencies following analyses of sediments sampled at Geoscience Australia's Core and Cuttings Repository (Canberra).

Additional cores and cuttings were sampled as part of this study and are listed in Appendix D. Coals with a low percentage of ash (<20 % ash) were separated from other lithologies using a heavy liquid of density 1.5 (Sykes, 2001). Standard coal analyses were undertaken by CRL Energy Ltd, Lower Hutt, and ACIRL Ltd, Sydney, following international and in-house standard procedures. These analyses included: proximate

analysis (moisture, ash and volatile matter), elemental analysis (C, H, N), total sulphur, forms of sulphur (sulphate, pyritic and organic) and calorific value. This suite of analyses allows determination of both coal type (on a chemical basis) and rank, while sulphur contents provide a record of the degree of marine influence within the coal-forming environment. Rock Eval and total organic carbon (TOC) were determined using a Rock Eval 6 instrument. Bulk chemical kinetic parameters were calculated from the Rockin™ software by processing Rock Eval S2-rate data collected at 1, 2, 5, 10 and 15^{o}C/min to give a discrete distribution of activation energy (Ea) and a single frequency factor (Arrhenius constant, A). Additionally, gas-to-oil ratios were applied to each individual Ea using the stepwise-pyrolysis gas chromatography mass spectrometry method described in Boreham et al. (1999).

Vitrinite-inertinite reflectance and fluorescence (VRF™ or VIRF) measurements on Cormorant-1 and Pelican-5 (Appendix E) were performed using the procedures described in Newman (1997) and Newman et al. (2000). Quantitative grain fluorescence (QGF) and grains-with-oil-inclusions (GOI™) analyses were determined using the procedures of Liu et al. (2001) and Eadington et al. (1996), respectively. Palynological analysis using procedures described in Boreham et al. (2002) was undertaken on a representative split of the sample used for geochemistry (Appendix F). In all cases, pollen spores and other acid-resistant plant microfossils were extracted using the same standard oxidation and filtration techniques designed to eliminate fines with maximum diameters of less than 5 μm.

Natural gases were obtained for Yolla-1 and While Ibis-1, and oil samples were collected from Cormorant-1, Yolla-1 and Pelican-1 and -2 (Appendix G). Molecular and carbon isotopic compositions of individual gaseous components were compiled from public domain sources such as open-file well completion and literature reports (Geoscience Australia's ORGCHEM database) together with new analyses undertaken by Geoscience Australia's Isotope and Organic Geochemistry Laboratory using analytical procedures described in Boreham and de Boer (1998). All carbon isotope values are reported in the δ^{13}C notation:

$$\delta = \frac{R_{sample} - R_{standard}}{R_{standard}} \times 1000 \left({}^{o}/_{oo} \right)$$

where the standard is PDB limestone with $R_{standard} = {}^{13}C/{}^{12}C = 0.011237$.

All the isotope analyses were run in duplicate with a reproducibility of ± 0.3 ‰. Errors on the molecular composition of the hydrocarbon components analysed by gas chromatography-thermal conductivity detector are of the order of ± 0.05 %.

Gas chromatography-mass spectrometry of the saturated hydrocarbons from oils and source rock extracts using selected ion monitoring (GCMS-SIR) and compound specific carbon isotopic analysis of the *n*-alkanes (isolated from 5Å molecular sieve adducts) by gas chromatography-combustion-isotope ratio mass spectrometry (GC-C-IRMS) were conducted according to Boreham and Summons (1999).

5.4 SOURCE ROCK GEOCHEMISTRY

Geochemical data (Rock Eval, TOC and vitrinite reflectance) are available for 28 exploration wells in the Bass Basin (includes all wells except Barramundi-1, King-1, White Ibis-1 and Yolla-2). These data were partitioned into the following age intervals in order to reflect recognised subdivisions within the stratigraphic succession (Chapter 4):

- >73 Ma (Campanian and older);
- 73-65 Ma (Maastrichtian);
- 65-53 Ma (Paleocene to earliest Eocene, *L. balmei* zone);
- 53-50.5 Ma (Early Eocene, *M. diversus* zone);
- 50.5-47.5 Ma (late Early Eocene to Middle Eocene, *P. asperopolus* zone);
- 47.5-38 Ma (Middle Eocene, Lower *N. asperus* zone);
- 38-35 Ma (Middle to Late Eocene, Middle *N. asperus* Zone; and,
- <35 Ma (latest Eocene and younger, Upper *N. asperus* and younger zones).

Source Richness and Quality

Figure 5.1 shows the plot of TOC versus age for 28 wells in the Bass Basin. Figures 5.2 to 5.9 show these samples subdivided into the specific age intervals. Figure 5.1 shows that the coals (TOC>40%) are clearly concentrated within specific time intervals. The Upper Cretaceous to Eocene succession is the dominant coal-bearing section, while intervals within the Early Eocene to early Middle Eocene section (Upper *L. balmei* to *P. asperopolus* zone) have the greatest concentration of coal (Figures 5.1, 5.5 and 5.6; Bass-1, Cormorant-1, Dondu-1 Konkon-1, Nangkero-1, Narimba-1, Pelican-2, -4, -5, Poonboon-1, Squid-1, Tarook-1, Toolka-1A, Yolla-1 and Yurongi-1). Minor coal occurrences are seen within the Albian (Figure 5.2; Durroon-1), Paleocene (Figure 5.4; Chat-1, Nangkero-1, Narimba-1, Pelican-2, -5 and Poonboon-1), and Middle Eocene sections (Figure 5.7; Bass-1, -3, Cormorant-1, Dondu-1, Flinders-1, Pelican-2, -4, -5, Poonboon-1, Toolka-1A and Yurongi-1), and in the Middle Miocene marine succession (Figure 5.9; Pipipa-1).

Using a TOC value of 2% as the lower limit for an effective source rock containing disseminated organic matter, it is clear that the Cenomanian to Campanian succession has limited source potential (Figure 5.1b; 98-73 Ma). Such an extended period of poor quality source rock development did not occur again until the Oligocene to Middle Miocene (Figure 5.1b; 35-15 Ma). Although potential source rocks exist with sufficient disseminated organic matter (TOC>2%) at other time periods (Figure 5.1), the critical issue is source quality. This is addressed here using a plot of S2 verses TOC (Figures 5.2 to 5.9), where the slope of a line projected from the sample values to the origin (zero TOC and zero S2) is a measure of the Hydrogen Index (HI). For samples with low TOC (<3%), projection to non-zero TOC can be used to account for the mineral matrix effect, which would otherwise lead to a suppressed HI owing to forced projection through zero TOC (Boreham et al., 2002).

Using HI (mg hydrocarbons/gTOC) ranges of >300, 200-300, 100-200 and <100 to indicate oil potential, gas with minor oil potential, gas (wet) potential, and minor gas to no source potential, respectively, the following summations can be made for each time interval:

>73 Ma (Campanian and older)

- Generally poor source potential, except for some good to excellent oil potential in organic-rich sediments from the Aptian-Albian (average HI=300) in Durroon-1 (Figure 5.2);

73-65 Ma (Maastrichtian)

- Good to excellent oil potential in organic-rich Maastrichtian sediments in Chat-1 (average HI=370), and isolated samples from Bass-3 and Pelican-5. All other samples with TOC>2% show, at best, gas potential (Figure 5.3);

65-53 Ma (*L. balmei* zone)

- The Paleocene to earliest Eocene succession has a good representation in the overall dataset with 21 of the 28 wells having analytical data. The coal at 2678 m in Poonboon-1 shows the greatest oil potential with an HI of approximately 500. Oil potential of coaly clastic rocks (TOC>10%, Figure 5.4a) is shown at Nangkero-1 (average HI=400) and at Pelican-5 (average HI=320), while similar organic-rich sediments at Nangkero-1 (average HI=235) show limited oil potential. All other wells have no oil potential. Sediments with TOC <10% (Figure 5.4b), display reduced oil potential with the bulk of the data having HI<300. The exceptions are Bass-2 (1500 m) and in Pelican-5.

53-50.5 Ma (*M. diversus* zone)

- The majority of the wells (23) have analytical data over the Early Eocene interval indicative of a high oil potential. Several wells contain coaly sediments with HI>300 (Figure 5.5a; Chat-1, Cormorant-1, Nangkero-1, Pelican-2, -4, -5, Poonboon-1, Tilana-1, Toolka-1A and Yurongi-1), while maximum HI's of 519 and 482 occur in Pelican-4 and Poonboon-1 at 2701 m and 2430 m, respectively. The carbonaceous clastic rocks (TOC<10 %; Figure 5.5b) have lower hydrocarbon potential with only samples from Pelican-5, Squid-1 (2645 m) and Yolla-1 (2300 m) showing significant liquids potential.

50.5-47.5 Ma (*P. asperopolus* zone)

- Source rocks in the late Early Eocene to early Middle Eocene interval are geochemically similar to the Early Eocene rocks. Twenty-two wells have geochemical data (Figure 5.6), and at least half show major oil potential in the coaly sediments with HI>300 (Figure 5.6a; Bass-1, -2, Cormorant-1, Nangkero-1, Narimba-1, Pelican-2, -4, -5, Tarook-1 and Yolla-1). Only the Pelican-5 well shows major oil potential in organically-lean rocks with TOC<10 % (Figure 5.6b).

47.5-38 Ma (Lower *N. asperus*)

- The Middle Eocene interval is represented in 21 wells with oil-prone source quality (HI>300) occurring in the coaly sediments from approximately half of the wells (Figure 5.7a; Aroo-1, Bass-1, -2, -3, Cormorant-1, Pelican-2, -4, -5, Poonboon-1 and Yurongi-1). Samples from Bass-3 (1787 m) and Pelican-4 (1890 m) have the greatest oil potential, with HI>450 (Figure 5.7a). A poorer source quality is evident for sediments with TOC<10 % with only those from Bass-1 and Pelican-5 at 1952.3 m and 2063 m, respectively, having oil potential (Figure 5.7b).

38-35 Ma (Middle *N. asperus* zone)

- The mainly Late Eocene interval, encompassing the shaley regional sealing facies of the Demons Bluff Sequence ("Eocene Shale"), shows no oil potential in any of the 17 wells intersected (Figure 5.8). In rocks with adequate organic richness to be considered potential source rocks (TOC>2%), only minor gas potential is evident (Figure 5.8; Squid-1 at 1840 m, Yolla-1 at 1765 m)

<35 Ma (Upper *N. asperus* zone and younger)

- The latest Late Eocene and younger age interval is sampled in 12 wells. However, only two organic-rich samples have hydrocarbon potential. Bass-1 at 631 m (HI=178) and Pipipa-1 at 599 m (HI=117) show wet gas and minor gas potential, respectively.

Source Maturity

In the Bass Basin there is a large database of vitrinite reflectance measurements available in the public domain that has been compiled in GA's ORGCHEM database. However, it is well documented that vitrinite reflectance can vary widely depending on the laboratory and analyst. It can also suffer from vitrinite suppression, especially when the vitrinite maceral is strongly associated with hydrogen-rich exinite maceral. The question of reliability of vitrinite reflectance data in the Bass Basin was addressed by new vitrinite reflectance measurements using only normal vitrinite identified using a vitrinite-inertinite reflectance and fluorescence (VRF™) approach (Figure 5.10; Newman, 1997; Newman et al., 2000). Cormorant-1 and Pelican-5 were chosen for analysis as they are in different depocentres and both cover a wide maturity range to total depth. Both wells are currently at their maximum depth of burial. The VRF data show that coal and associated disseminated organic matter in claystones have the same VR, indicating that reflectance measurements are independent of mineral content (Appendix E). Furthermore, the new VR data are comparable with the existing VR data (Figure 5.11), suggesting that existing data can be used with a high degree of confidence.

Figures 5.12 and 5.13 show vitrinite reflectance plotted against depth and age for 28 wells in the Bass Basin. Vitrinite reflectance measurements range from 0.3 to 4.9%, indicating a range from immature to highly overmature sediments within the low metamorphic grade. Intervals with high to extremely high maturity zones (VR>1.5 %) are not necessarily the deepest samples analysed in the wells (except at Pelican-5), suggesting an external, localised heating has supplemented the geothermal gradient. This profile is consistent with the observed influence of igneous intrusions in sediments lying between 1500 and 2500 m depths (Figure 5.12), with ages ranging from Paleocene to Late Miocene (Figure 5.13). In Pelican-5, there is

a smooth increase in vitrinite reflectance with depth, with a maximum VR=1.77 % recorded at the base of the well (Figure 5.11).

Based on a vitrinite reflectance of 0.75% as the threshold for primary migration from the source rock (see below), only Aroo-1, Cormorant-1, Durroon-1, Flinders-1, Koorkah-1, Narimba-1, Pelican-1, -5, Tilana-1 and Yolla-1 have reached that critical maturity. This occurs between 2700 and 3200 m within Eocene or older sediments, while the end of the main phase of oil expulsion (0.95% VR) occurs between 3200 and 3500 m (Figure 5.13).

5.5 PETROLEUM GENERATION AND EXPULSION

The key maturity horizons in the pathway of kerogen transformation to petroleum are: a) the onset of oil generation; b) the onset of expulsion from the source rock (primary migration or critical moment in the petroleum system); c) the oil window; and, d) the onset of gas generation and expulsion. The latter is problematic as gas is generated throughout the oil window over which there is a transition from wet to dry gas in the overmature region. Here, field data using the estimated maturities of the reservoired fluids, analysis of the residual petroleum potential of source rocks (Rock Eval), and the change in pore space geometry and fluid composition (Small Angle Neutron Scattering, SANS; Appendix H) allow a good estimation of these key horizons.

Figure 5.14 shows the depth plot of Hydrogen Index (HI) and Bitumen Index (BI) for low-ash coals in the Pelican-5 well, which was chosen as its shows the greatest maturity range (excluding igneous intrusions) from immature to overmature. The coals form a rather homogeneous set dominated mainly by gymnosperm remains (Appendix F). For HI, a measure of the residual petroleum potential, there is an 'evolution' from fairly constant HI=250 (minor oil potential) in coals shallower than 2450 m, to a rapid increase in HI, which maximises at 440 (major oil potential), at 2850 m. This is followed by an initially sharp decrease in HI and continual decay. Similar trends have recently been documented in New Zealand coals of similar age (Sykes, 2001). Like the New Zealand trends, the Bass Basin trends are interpreted to indicate the onset of oil generation at 2450 m and the onset of expulsion at 2850 m, corresponding to VR of 0.65% and 0.75%, respectively, using the best-fit curve for the VR profile in Figure 5.11.

The main oil window is defined from 0.75% to 0.95% VR (2850 to 3300 m in Pelican-5; Figure 5.11) using methylphenanthrene-based (MPI) chemical maturity parameters for the Pelican and Yolla oils (Table 5.1). The response of BI (residual free hydrocarbons in the coal) is slightly different to HI with a rapid increase up to the onset of expulsion (2850 m) maximising to a constant value to 3650 m (1.2% VR), followed by a steady decrease. The constantly high value in BI represents a steady-state maintenance of maximum oil saturation, while decreasing BI below 3650 m corresponds either to a more efficient expulsion of residual liquids due to a higher gas:oil ratio for the primary generated hydrocarbons or the beginning of oil-to-gas cracking, or a combination of both. Support for the above comes from a SANS analysis on the low-ash coals

in Pelican-5 (Figure 5.15; Appendix H). Filling of pore space with oil is evident between 2400 m to 2800 m where the scattering intensity is at its minimum and remains constant due to constant oil saturation.

5.6 KINETICS OF PETROLEUM GENERATION

Oil and gas generation from organic matter in source rocks is a kinetic process controlled by the time-temperature history. Individual source rocks have their own specific chemical kinetics, which can be determined in the laboratory and applied to the geological timeframe (Boreham et al., 1999; see Chapter 6). Plotted here (Figure 5.16) is the proportion of organic matter transformed versus temperature for a simple linear temperature increase of 1^{o}C/Ma for representative coals (claystones also plot with the range of the coals) in the Bass Basin, together with a calculated vitrinite reflectance (Burnham and Sweeney, 1989). A VR of 0.75% (onset of expulsion) correlates to a transformation ratio (TR) between 0.2 to 0.3 for the range of kinetic parameters for the immature coals (Figure 5.16), whereas by the end of the main phase of oil generation between 50% and 65% of the reactive kerogen has been transformed to oil and gas with a fairly constant gas:oil ratio 0f 0.2.

5.7 OIL GEOCHEMISTRY

Oil-Oil Correlation

To clarify the intra-basinal relationships between the Bass Basin oils and inter-basinal relationships with other oils in the region (Gippsland and Otway basins), a multivariant statistical analysis was employed involving a wide range of GC, GCMS and carbon isotope parameters (Table 5.2). Such an approach has previously been shown to group together chemically-related populations and families of oils that also have geological significance (AGSO and GeoMark Research, 1996; Boreham and Summons, 1999; Boreham et al., 2002, Geoscience Australia and GeoMark Research, 2002). Using the parameters in Table 5.2 and unpublished data (Geoscience Australia and GeoMark Research, 2002), hierarchical cluster analysis (Einsight^{TM} software) was used to generate the dendrograms displayed in Figure 5.17.

Confidence in the statistical approach is supported by the oil population associations (Figure 5.17) following those previously identified within the Austral Petroleum Supersystem for oils from the Otway and Bass basins (Edwards et al., 1999). Furthermore, the set of geochemical variables clusters in geochemically recognisable groups (Figure 5.17), reflecting primary source and depositional environment controls. Thus, the land plant inputs are directly associated with higher %29 sterane, and the Pr/Ph and oleanane contents with stronger bacterial reworking (C31 hopane content). The %27, %28, 29/H, 28/H are associated with minor algal and marine influences, the tricyclic and tetracyclic parameters reflect the changing bacterial communities, while the carbon isotopes, the main distinguishing feature between Bass Basin oils and the other oils, are a fundamental control reflecting inputs from different plant communities.

Oils from the Gippsland Basin separate into two main populations, indicating different generation and preservation histories (Geoscience Australia and GeoMark Research, 2002), while the three main oil populations observed in the Otway Basin (Figure 5.17) reflect multiple source rock organic facies of Late

Jurassic to Early Cretaceous age (Edwards et al., 1999; Geoscience Australia and GeoMark Research, 2002). Furthermore, there is only a weak association between oils from the different basins, suggesting a difference in the nature of terrestrial organic facies between (and also within) the basins.

The Bass Basin oil population (A3 petroleum system of Edwards et al., 1999) shows two families of oils, one family represented by the Pelican and Yolla oils, and the other by the Cormorant oil (Figure 5.17). However, it is suggested that the Cormorant-1 oil was generated from the same source rock facies as the other Bass Basin oils and that in-reservoir alteration has perturbed various geochemical parameters (Edwards et al., 1999). Biodegradation has resulted in depletion in the carbon isotopes due to removal of all *n*-alkanes and various aromatic hydrocarbons, lower Pr/Ph as a result of preferential removal of pristane, selective removal of the higher molecular weight homologues in the tricyclics, and the loss of lower molecular weight hopanes and steranes. The source rock facies for the Bass Basin oils appears to be uniform considering the closer associations shown between Yolla and Pelican oils than between oils from the same well (Figure 5.17). These subtle differences most likely reflect slight maturity differences and alteration effects associated with migration fractionation (Boreham and Summons, 1999)

Oil-Source Correlation

In order to establish inter-relationships between the Bass Basin oils and potential source rocks, a multivariant statistical analysis (Einsight™ software) was employed using biomarker ratios based on diterpane, triterpane, hopane and sterane contents in the saturated hydrocarbon fractions (Table 5.2). Good reproducibility of the analytical protocol is indicated by the close correlation between repeat analyses for the Gippsland basin oils from Halibut-A1 and West Seahorse-1 (Figure 5.18).

The potential source rocks analysed include coals and claystones from Cormorant-1 and Pelican-5, while the oils were from Cormorant-1, Pelican-1, -2 and Yolla-1. Good correlation (correlation coefficient >0.6) with Pelican and Yolla crudes is only seen for coals from Pelican-5 at depths >3000 m. This is consistent with the depth range of the oil window in Pelican-5 (Figure 5.14). A slightly weaker correlation is obtained between Cormorant-1 crude and coals from both Pelcian-5 (2791 m) and Cormorant-1 (2758 and 2941 m). However, biodegradation of the Cormorant-1 crude may have masked a closer correlation. The correlation between the coals and different depocentres in the Bass Basin suggests that there is a wide distribution of a rather uniform source rock facies. Claystones in Cormorant-1 and Pelican-5 do not show any correlation with the oils. Thus, this is the first demonstration of a good oil-source correlation involving Australian coal as the source rock for oil (Boreham and Powell, 1994; Powell and Boreham, 1994).

5.8 GAS GEOCHEMISTRY

Molecular and Carbon Isotopic Composition

For the wet gases from the Bass Basin, the relative proportions of methane (C_1) to wet gas (C_2-C_5 hydrocarbons), represented by the ratio % C_1/C_1-C_5 in Figure 5.19, shows an average of 85.6% for White

Ibis-1 and 87% for Yolla-2. Thus, the Bass Basin gases have a similar wet gas content to average Gippsland Basin gases (85%), while gases from the Otway Basin are, on average (93%), drier (Boreham et al., 2001).

The range in carbon isotopic composition of the individual gaseous hydrocarbons in 'unaltered' natural gases from Australian sedimentary basin is shown in Figure 5.20 (Boreham et al., 2001). The wide carbon isotopic range, 16‰ for methane reducing to 8‰ for *n*-pentane (Figure 5.20), is very significant and enables deconvolution of inter-related factors and processes that can control the carbon isotopic composition in gases. Natural gases that fall outside the normal carbon isotopic range for their respective individual basins (Figure 5.20) have been influenced by very high maturities, have multiple sources or have undergone secondary alteration within the reservoir (Boreham et al., 2001).

The similar carbon isotopic composition and relatively limited isotopic range (<2‰) for gases from the Bass and Gippsland basins (Figure 5.20) suggests that gases in each basin were generated from similar organic facies or from multiple sources that are isotopically similar. The wider isotopic range in gases from the Otway Basin shows that gases were generated from multiple source rock horizons that are isotopically distinct (Figure 5.20; Boreham et al., 2001)

Source and Maturity of Gases

Source and maturity are the primary control on hydrocarbon composition and carbon isotopes, which are at times difficult to deconvolute (Boreham et al., 2001). The approximately linear relationship between the carbon isotopic composition of the individual linear gaseous hydrocarbons and the reciprocal of the carbon number (Figure 5.21; natural gas plot of Chung et al., 1988), is further evidence of a single source input to the Bass Basin gases.

The maturity influence on carbon isotopic composition has a theoretical basis wherein the carbon isotopic difference between individual gas components decreases with increasing maturity (James, 1983, 1990). Thus, by plotting the carbon isotopic differences, source controls are effectively eliminated or considerably reduced (James, 1983, 1990). Such an approach is shown in Figure 5.22, which plots the isotopic differences between methane and ethane against propane and ethane, together with their theoretical maturity relationship developed by James (1983). Using this approach, maturities with vitrinite reflectance >1.5% are required for the effective source rocks for gas reservoired at White Ibis-1 and Yolla-2 wells (Figure 5.22). Similar high maturities are predicted for natural gases in the adjacent Gippsland and Otway basins. However, for terrestrial organic matter sources, the approach in Figure 5.22 can overestimate gas maturities (James, 1990), albeit to different extents depending on organic facies, which currently cannot be effectively quantified (Boreham et al., 2001). Nevertheless, gas maturity is generally higher than maturity of accompanying liquid hydrocarbons (Moore et al., 1992; Edwards et al., 1999; Geoscience Australia and GeoMark Research, 2002) indicating that gas and oil were generated at different times from the same source rocks.

Of the non-hydrocarbon gases in the Bass Basin, nitrogen contents are low (max. 2 mole%) while hydrogen is found at trace levels (0.04 mole%) and helium is below the detection limit (Table 5.3). Carbon dioxide is the most abundant with a very high 20 mole% in Yolla-2 (Table 5.3), although much higher CO_2 contents occur in the Gippsland (54 mole% at Gunter-1) and Otway (99 mole% at Caroline-1) basins (Boreham et al., 2001). An appreciation of the origin of CO_2 can be demonstrated using the relationship between molecular and carbon isotopic compositions (Figure 5.23). The Bass Basin gases plot within the band between -3 and -10‰ and are considered to be derived from an inorganic igneous and/or mantle source (Smith and Pallasser, 1996; Boreham et al., 2001). The pervasive magmatic intrusions within the Bass Basin are undoubtedly the source of the CO_2 gas.

Gas and Oil Correlation

The combination of carbon isotopic compositions of the gaseous hydrocarbons and the *n*-alkanes of oil has proven to be most effective in gas-oil correlation studies (Boreham et al., 2001). Figure 5.24 shows the C_1-C_{30} extended *n*-alkane carbon isotopic profile for gases and oils in the Bass Basin, together with representative gas-oil pairs from the Gippsland Basin. The similar range in $\delta^{13}C$ (< 2‰ for C_{7+} *n*-alkanes of the same carbon number) for the White Ibis-1 and Yolla-1 oils suggests an origin from very similar source rock facies. The consistent depletion in ^{13}C (isotopically light) in the C_{7+} *n*-alkanes for the shallower oil from Yolla-1 (1830 m) is consistent with reservoir spill-fill with an earlier generated, lower maturity liquid. However, the stacked liquids at Yolla-1 have similar maturities based on chemical maturity parameters (Table 5.1) despite vertical separation of 1000 m. Alternatively, this could indicate multiple sourcing from slightly different terrestrial source facies. Compared to the Gippsland Basin hydrocarbons, the Bass Basin C_{2+} *n*-alkanes are consistently 1 to 2 ‰ depleted in ^{13}C (Figure 5.24).

In order to understand the relationship of the gas to the oil, use is made of the position and shape of the extended *n*-alkane carbon isotope profile. A relatively 'smooth' continuum in the carbon isotopic data from the linear C_4-C_5 wet gas components through to the low molecular weight (< C_9) *n*-alkanes in the oil, as is the case for the Yolla-2 gas/Yolla-1 oil pair, indicates that the gas and the liquid hydrocarbons are genetically related, most likely generated from the same source. Maturity estimates indicate that the gas was generated at a slightly higher maturity compared to the oil. Obviously, this maturity difference is relatively isotopically insensitive and does not result in carbon isotopic discrimination in the low molecular weight hydrocarbons. On the other hand, the increase in ^{13}C content (isotopically heavy) for the wet gas components in White Ibis-1 is, most likely, a result of a much higher maturity source rock at the time of primary gas expulsion than in the case of the Yolla-2 gases.

5.9 CONCLUSIONS

- Coals and associated organic matter in claystones (TOC>2%) show good to excellent source rock richness; coal facies dominate in the Early Eocene to early Middle Eocene (Upper *L. balmei* to *P. asperopolus* zone).

- Coals show good source quality for oil with HIs up to 500 mg hydrocarbons/gTOC, while claystones are mainly gas-prone.
- Campanian and older sediments generally have very low source potential, except for some good to excellent oil potential in organic-rich sediments from the Aptian-Albian (average HI=300) in Durroon-1.
- Maastrichtian sediments showing good to excellent oil potential occur in organic-rich facies in Chat-1 and isolated samples from Bass-3 and Pelican-5. All other samples with TOC>2% show some gas potential.
- Paleocene (65-53 Ma; *L. balmei* zone) sediments show oil potential (HI>300) in coals from Poonboon-1, Nangkero-1, Pelican-5 while those from Nangkero-1 have wet gas potential. Only claystones in Bass-2 and Pelican-5 show oil potential (TOC<10%).
- Early Eocene (53-50.5 Ma; *M. diversus* zone) coals consistently show the highest oil potential in Chat-1, Cormorant-1, Nangkero-1, Pelican-2, -4, -5, Poonboon-1, Tilana-1, Toolka-1A and Yurongi-1. The carbonaceous clastic rocks have lower hydrocarbon potential (TOC<10%), with only samples from Pelican-5, Squid-1 and Yolla-1 showing major liquids potential.
- Latest Early Eocene to early Middle Eocene (50.5-47.5 Ma; *P. asperopolus* zone) coals show oil potential in Bass-1, -2, Cormorant-1, Nangkero-1, Narimba-1, Pelican-2, -4, -5, Tarook-1 and Yolla-1. Only the Pelican-5 well shows major oil potential in the organically-leaner rocks with TOC<10%.
- Middle Eocene (47.5-38 Ma; Lower to Middle *N. asperus* zone) coals are oil-prone at Aroo-1, Bass-1-, -2, -3, Cormorant-1, Pelican-2, -4, -5, Poonboon-1 and Yurongi-1. A poorer source quality is evident for sediments with TOC<10%, with only those from Bass-1 and Pelican-5 having oil potential.
- The mainly Late Eocene (38-35 Ma; nominally marine "Demons Bluff shale") sediments have no oil potential and only minor gas potential at Squid-1.
- The latest Late Eocene and younger (<35 Ma; Upper *N. asperus* zone and younger) sediments contain no oil-prone organic matter, although there is limited wet gas and minor gas potential at Bass-1 and Pipipa-1.
- Vitrinite reflectance data indicate that potential source rocks have attained maturities sufficient for oil and gas generation with highest VR values of 1.8% at the base of Pelican-5 attained through burial. Igneous intrusions in Paleocene, Oligocene and younger sediments have elevated localised VR values up to 5.0%.
- Key 'thresholds' in petroleum generation and expulsion were defined in Pelican-5, using a combination of SANS, Rock Eval and chemical maturity parameters for the Bass Basin oils: onset of oil generation, onset of oil expulsion (primary migration), and onset of gas generation occurs at 2450 m, 2850 m and 3650 m, respectively. This corresponds to vitrinite reflectance thresholds of 0.65%, 0.75% and 1.2%, respectively. The main oil window is defined between 0.75% and 0.95% VR (2850 to 3300 m in Pelican-5) based on oil maturity.
- Laboratory-generated chemical kinetic parameters for Paleocene to Eocene coals have identified end-member labile and resistant organic facies. Extrapolation to the geological timeframe results in an approximately 500 m depth range for primary migration, depending on the choice of kinetic parameters. Furthermore, approximately 20-30% of the organic matter needs to be transformed to petroleum before an oil-wet pore space is capable of supporting primary migration from coal.

- Oil-oil correlation in the Bass, Gippsland and Otway basins using GC, isotopes and biomarkers has shown:
  - A single Bass Basin oil population (the Cormorant-1 oil was affected by biodegradation);
  - A uniform terrestrial source rock facies for Bass oils;
  - Distinct oil families for each of the different basins in the Bass Strait region;
- Oil-source correlations using biomarkers (diterpanes, triterpanes, hopanes and steranes) between Bass Basin oils and coals and claystones from Cormorant-1 and Pelican-5 have shown:
  - A good oil-to-source correlation was obtained between oils and coals, but claystones do not show as strong a link.
  - Coals below 2750 and 3000 m (Early Eocene to Paleocene) in Cormorant-1 and Pelican-5, respectively, can be correlated with Bass Basin oils. This is in agreement with depth (and maturity) intervals defined for expulsion from effective source rocks.
- Gas composition and carbon isotopic comparisons between gases and liquids has shown:
  - A high CO_2 content in Bass Basin gases that is derived from inorganic (igneous) sources.
  - Bass Basin gases (and oils) are isotopically light (depleted in ^{13}C) compared to Gippsland Basin hydrocarbons.
  - Yolla gases are associated with Yolla oils, and both were generated from the same source and at similar maturities.
  - White Ibis gases were generated at a higher maturity than Yolla gases.

Table 5.1 Chemical maturity parameters for oils from the Bass Basin.

Well	Pelican-1	Pelican-2	Cormorant-1	Yolla-1	Yolla-1
Geoscience Australia No.	2001950	2001951	10037	10036	10035
DNR-1	8.61	7.89	0.36	0.77	10.00
TNR-1	1.18	0.86	0.36	0.82	1.29
TNR-2	0.77	0.46	0.54	0.47	0.73
TeNR	0.77	0.45	0.51	0.48	0.68
MPI -1	0.80	0.55	0.31	0.76	0.84
Rc-1	0.88	0.73	0.58	0.86	0.90

DNR-1 = 26-+27-)/15-dimethylnaphthalene
TNR-1 = 236-/(146- + 135-)trimethylnaphthalene
TNR-2 = 136-/(136- + 125-)trimethylnaphthalene
TeNR = 1367-/(1367- + 1256)tetramethylnaphthalene
MPI-1 = 1.5*(3- + 2-)methylphenenatrene/(phenanthrene*rf+ (9- + 1-)methylphenenthrene) where rf = 0.83 (response factor relative to methylphenanthrenes in GCMS)
Rc-1 =0.6*MPI + 0.4 (Radke and Welte 1983)

Table 5.2 OilMod™ parameters based on GC, carbon isotopes and biomarkers collected on oils and potential source rocks.

GA No.	Well	Top, metres	Type	19T/23T	24T/23T	Tet/23T	29H/30H	OL/30H	31R/30H	%27	%28	%29	kaur/phyll	ipim/phyll	19-ipim/ipim	labd/phyll	fich/phyll	bery/phyll
10037	Cormorant-1	1500	FIT 6	15.30	1.61	10.59	0.64	0.03	0.54	6.6	26.8	66.6	0.15	1.69	1.05	0.21	0.54	0.90
19999150	Pelican-1	3161.4		4.66	0.52	1.87	0.69	0.11	0.19	17.4	30.0	52.6	0.11	0.64	1.72	0.32	0.22	0.91
19999151	Pelican-2	2879.5	FIT 1	8.40	0.51	6.26	0.62	0.04	0.24	16.1	25.9	58.0	0.12	1.02	0.97	0.44	0.32	1.04
10036	Yolla-1	1830	DST 2	0.98	0.31	3.62	0.71	0.03	0.43	10.3	30.4	59.3	0.15	1.59	0.21	0.19	0.24	1.22
10035	Yolla-1	2824	DST 1	0.22	0.47	1.80	0.55	0.04	0.19	13.1	31.5	55.4	0.11	0.89	0.20	0.24	0.25	1.08
20010071	Cormorant-1	2340.9	coal (cutt)	8.25	0.53	3.90	0.96	0.03	0.45	13.5	28.6	57.9	0.20	0.77	3.64	0.11	0.68	0.90
20010072	Cormorant-1	2758.5	coal (cutt)	15.12	0.30	15.75	0.56	0.02	0.17	7.7	26.0	66.3	0.13	0.33	2.34	0.07	0.26	0.24
20010073	Cormorant-1	2990.1	clyst (cutt)	2.28	0.38	1.97	0.77	0.03	0.39	25.2	22.6	52.2	0.18	0.42	2.53	0.20	0.44	0.94
20010374	Cormorant-1	2941.4	coal (cutt)	10.17	0.40	12.98	0.53	0.02	0.13	11.7	28.0	60.2	0.10	0.52	1.46	0.08	0.23	0.31
20010380	Pelican-5	2592	coal (cutt)	4.67	0.93	5.39	1.09	0.01	0.54	11.6	34.7	53.8	0.41	1.60	1.01	0.24	0.49	2.05
20010051	Pelican-5	2640	clyst (cutt)	7.37	0.73	5.06	1.67	0.01	0.69	7.7	26.5	65.8	0.22	0.93	0.86	0.13	0.25	0.43
20010052	Pelican-5	2791.9	coal (core)	16.31	1.88	37.52	0.79	0.01	0.38	10.0	22.5	67.5	0.14	0.99	0.80	0.07	0.28	0.22
20010053	Pelican-5	2792.1	clyst (core)	4.72	0.30	8.03	0.70	0.02	0.26	22.1	22.6	55.2	0.18	0.63	1.03	0.15	0.43	0.50
20010054	Pelican-5	3015	clyst (cutt)	2.28	0.12	4.90	0.74	0.02	0.28	20.2	27.5	52.3	0.17	5.20	0.18	0.39	0.25	0.48
20010384	Pelican-5	3063	coal (cutt)	4.47	0.40	5.92	0.63	0.02	0.23	12.4	30.9	56.7	0.14	1.52	0.90	0.28	0.25	0.59
20010385	Pelican-5	3162	coal (cutt)	9.06	0.43	14.46	0.58	0.04	0.30	11.1	25.9	63.0	0.17	2.03	0.59	0.29	0.27	1.96
20010055	Pelican-5	3399	clyst (cutt)	1.66	0.44	2.07	0.60	0.02	0.34	18.3	29.7	52.0	0.23	3.87	0.46	0.38	0.29	1.10

19T/23T = ratio of C19 tricyclic to C23 tricyclic
24T/23T = ratio of C24 tricyclic to C23 tricyclic
Tet/23T = ratio of C24 tetracyclic to C23 tricyclic
29H/30H = ratio of C29 abhopane to C30 abhopane
Ol/30H = ratio of oleanane to C30 abhopane
31R/30H = ratio of C31 abhopane 22R to C30 abhopane
%27 = percentage of C27 abb 20S to sum C27, C28, C29 abb 20S steranes
%28 = percentage of C28 abb 20S to sum C27, C28, C29 abb 20S steranes
%29 = percentage of C29 abb 20S to sum C27, C28, C29 abb 20S steranes
kaur/phyll = a-kaurane/b-phyllocladane
ipim/phyll - *iso*-pimarane/b-phyllocladane
19-ipim/ipim - 19-nor-pimarane/*iso*-pimarane
labd/phyll - b-labdane/b-phyllocladane
fich/phyll = fichtilite/b-phyllocladane
bery/phyll = beryene/b-phyllocladane

Table 5.3 Molecular and carbon isotopic composition of gases from the Bass Basin.

Well Name	White Ibis -1	White Ibis -1	Yolla -2	Yolla -2
Geoscience Australia No.	**20009241**	**20009247**	**20009248**	**20009250**
Sample Depth - Top (m)	2015.2	2048.5	2802.0	2815.0
Molecular composition (mole %)				
CH4	72.33	78.57	72.07	20.42
C2	5.96	6.05	6.52	17.46
C3	3.61	2.34	2.55	6.95
i-C4	1.63	0.70	0.39	1.24
C4	1.38	0.76	0.63	2.09
i-C5	0.97	0.36	0.17	0.54
C5	0.69	0.21	0.17	0.66
C6+	3.30	0.56	0.49	1.18
CO2	8.16	8.13	16.72	48.50
N2	1.97	2.32	0.30	0.92
Carbon isotopic composition ($^{o}/_{oo}$ PDB)				
CH4	-37.20	-37.02	-36.85	-36.86
C2	-27.21	-27.03	-29.16	-29.03
C3	-26.73	-26.27	-27.95	-27.86
i-C4	-27.71	-26.99	-28.17	-28.03
C4	-26.13	-25.70	-27.20	-27.02
i-C5	-26.34	-25.47	-27.19	-27.11
C5	-25.98	-25.17	-26.75	-26.74
CO2	-4.36	-4.83	-5.40	-6.86

Figure 5.1 Age (Ma) plot of total organic matter (S2-TOC) for a) all data, and b) sediments with TOC<10%.

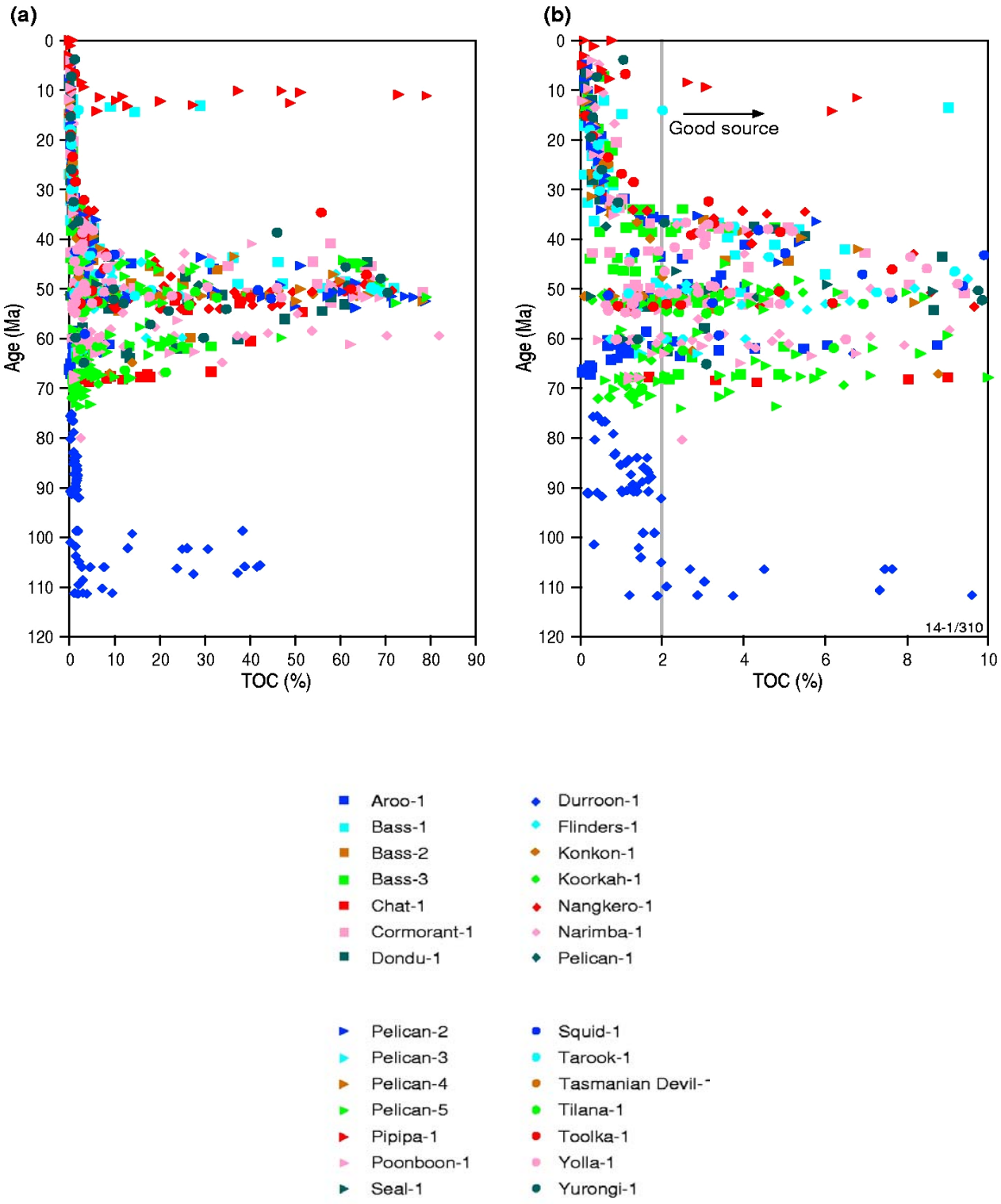

Figure 5.2 Specific age interval (>73 Ma)—S2-TOC plot for a) all data, and b) sediments with TOC<10%.

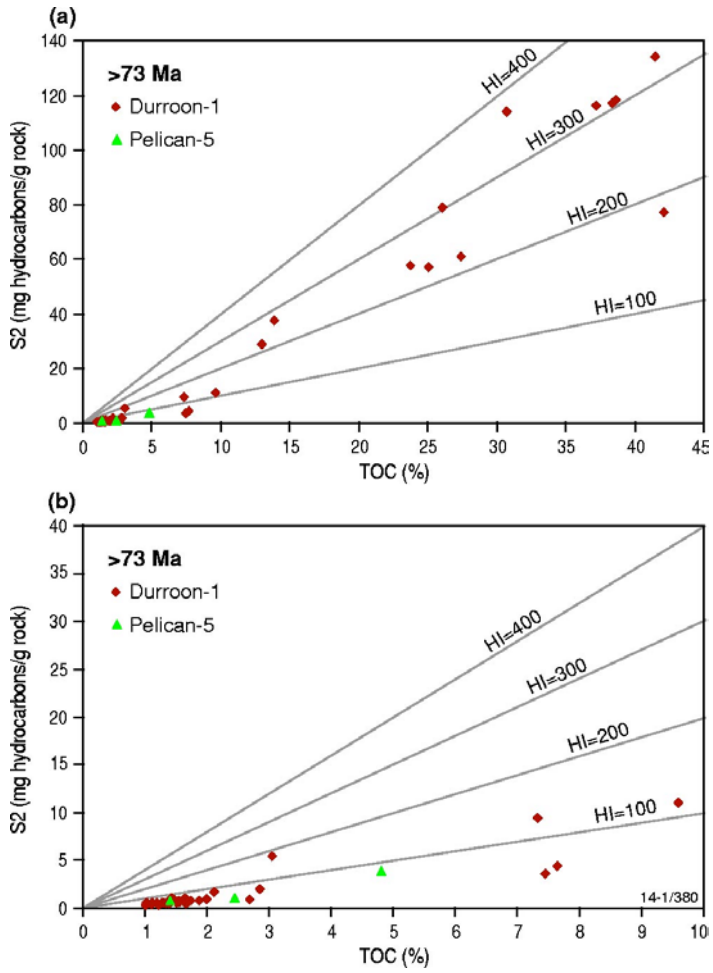

Figure 5.3 Specific age interval (73-65 Ma)—S2-TOC plot for a) all data, and b) sediments with TOC<10%.

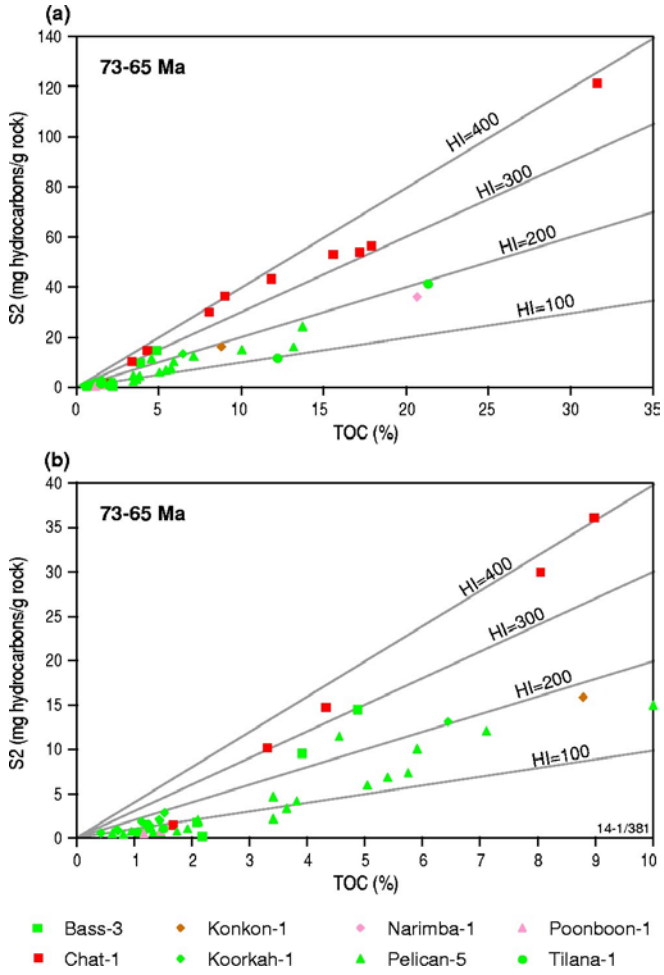

Figure 5.4 Specific age interval (65-53 Ma)—S2-TOC plot for a) all data, and b) sediments with TOC<10%.

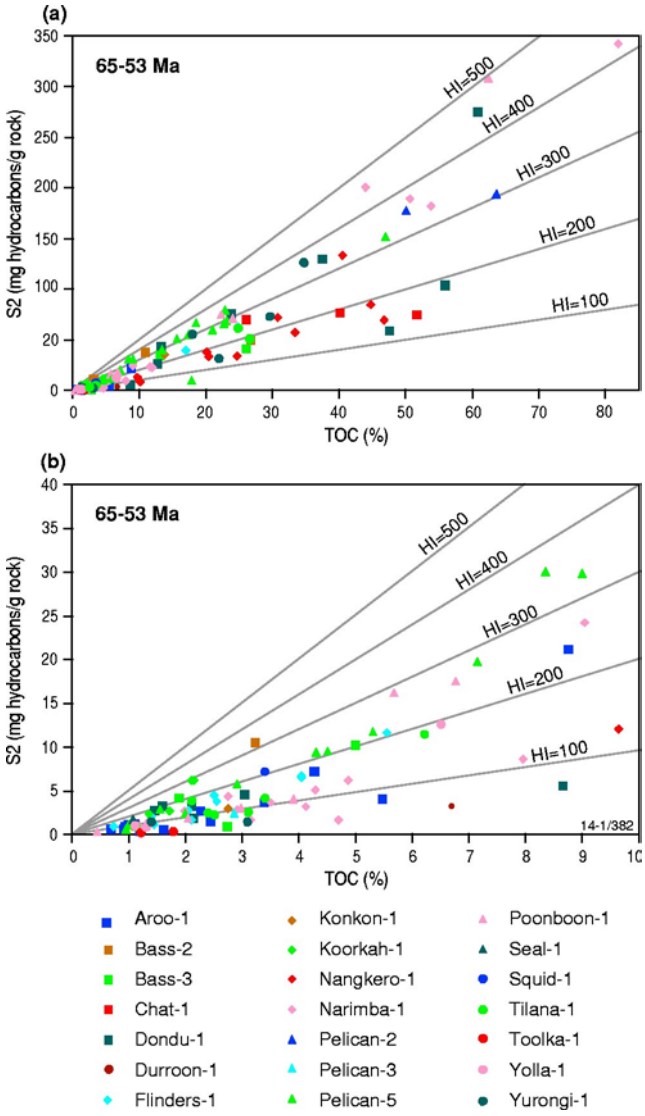

Figure 5.5 Specific age interval (53-50.5 Ma)—S2-TOC plot for a) all data, and b) sediments with TOC<10%.

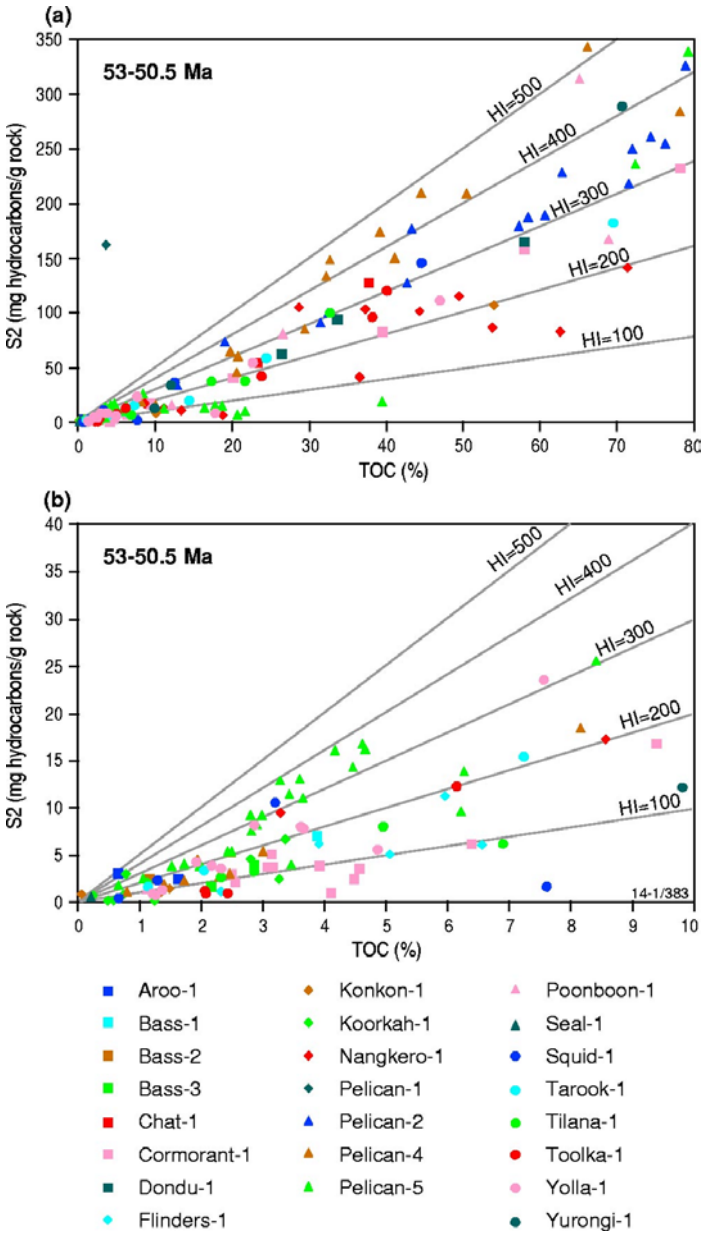

Figure 5.6 Specific age interval (50.5-47.5 Ma)—S2-TOC plot for a) all data, and b) sediments with TOC<10%.

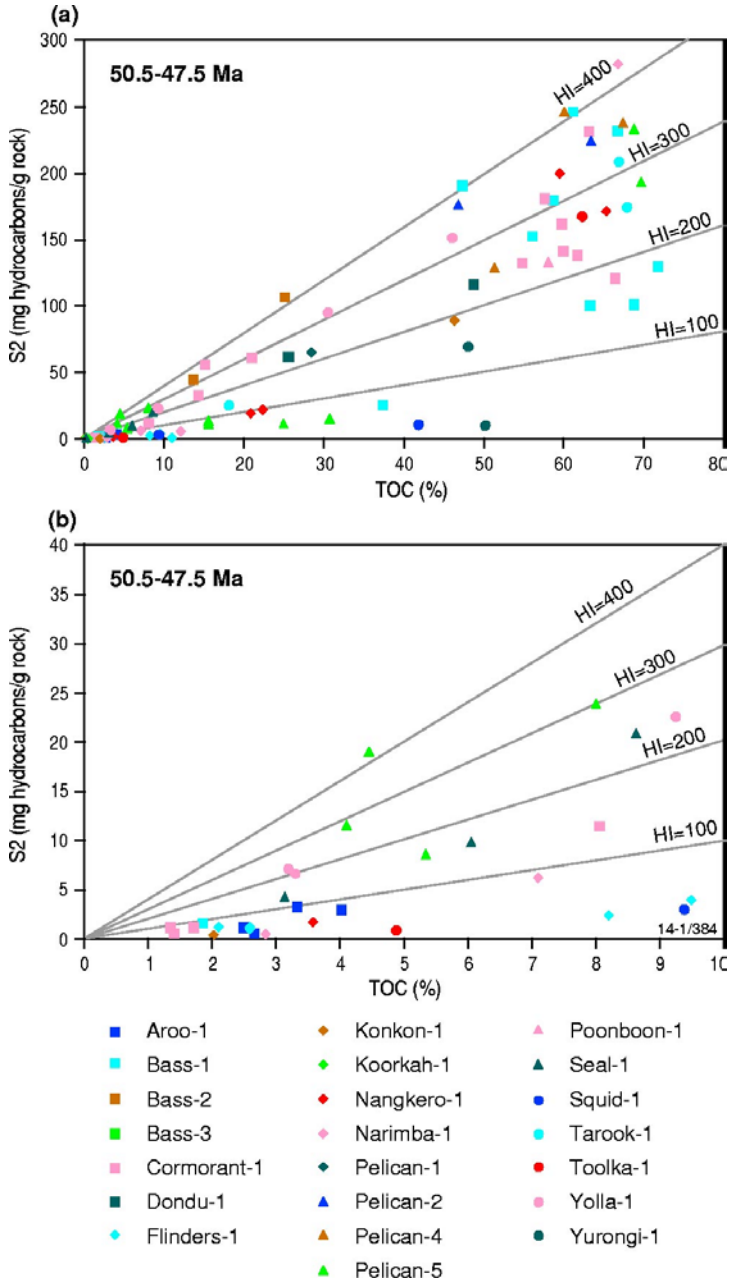

Figure 5.7 Specific age interval (47.5-38 Ma)—S2-TOC plot for a) all data, and b) sediments with TOC<10%.

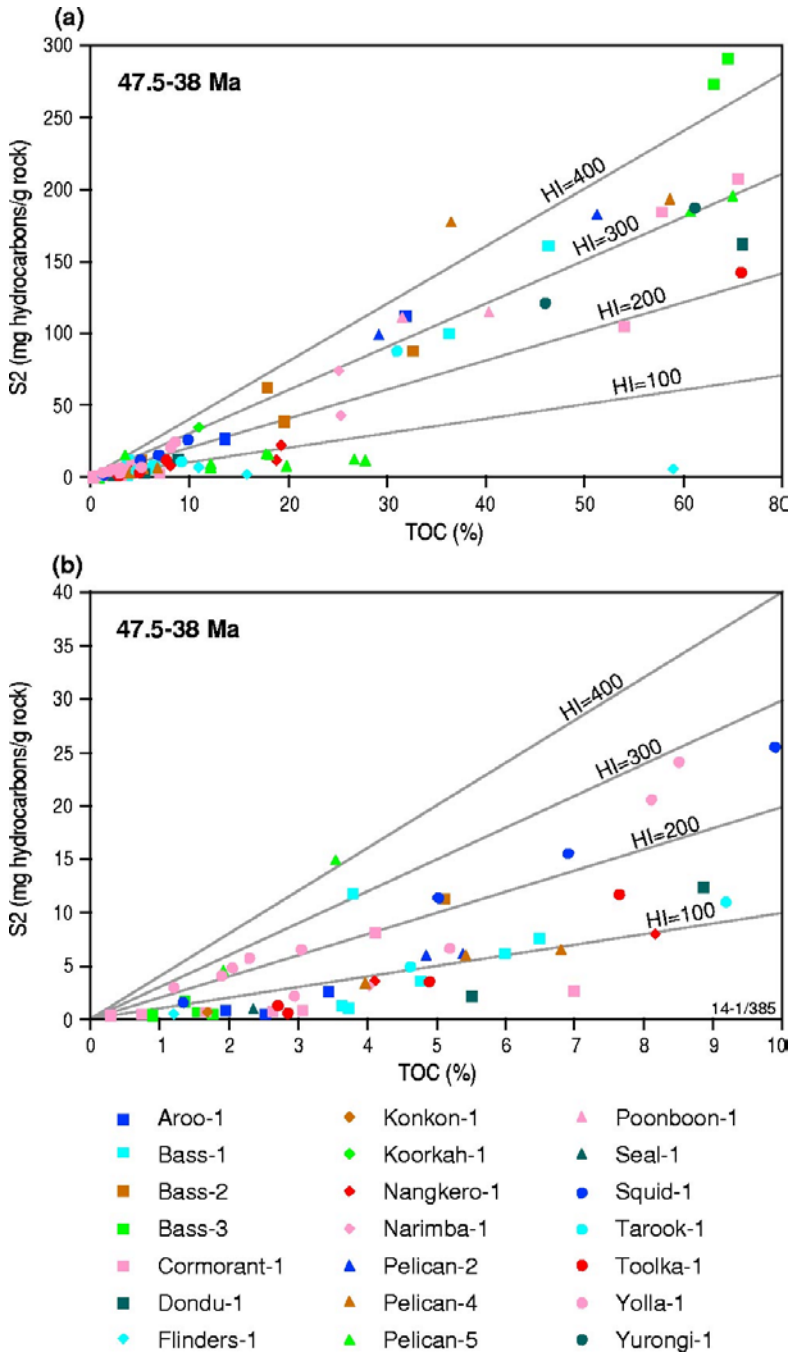

Figure 5.8 Specific age interval (38-35 Ma)—S2-TOC plot for data.

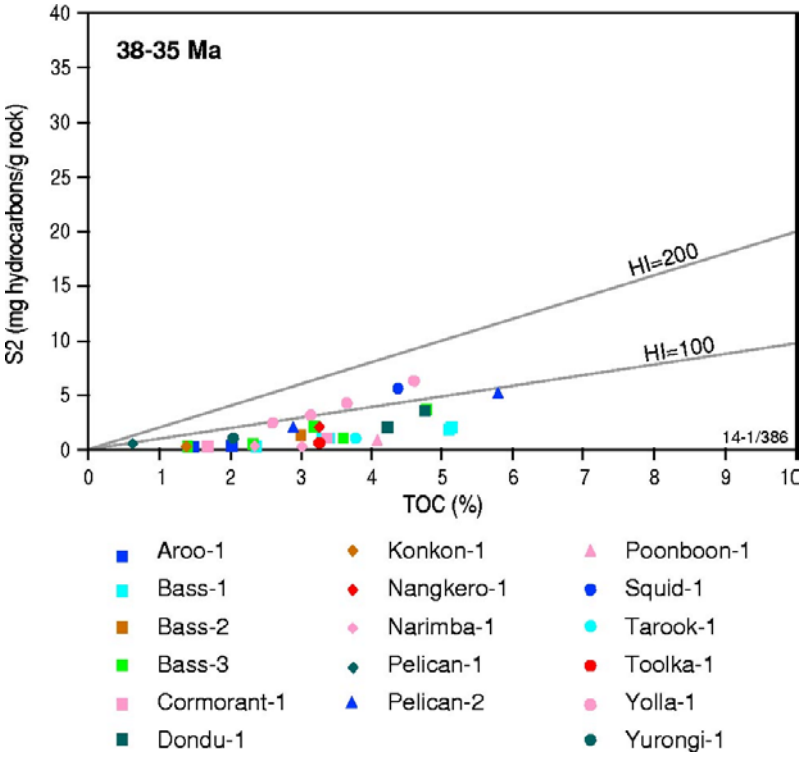

Figure 5.9 Specific age interval (<35 Ma)—S2-TOC plot for a) all data, and b) sediments with TOC<10%.

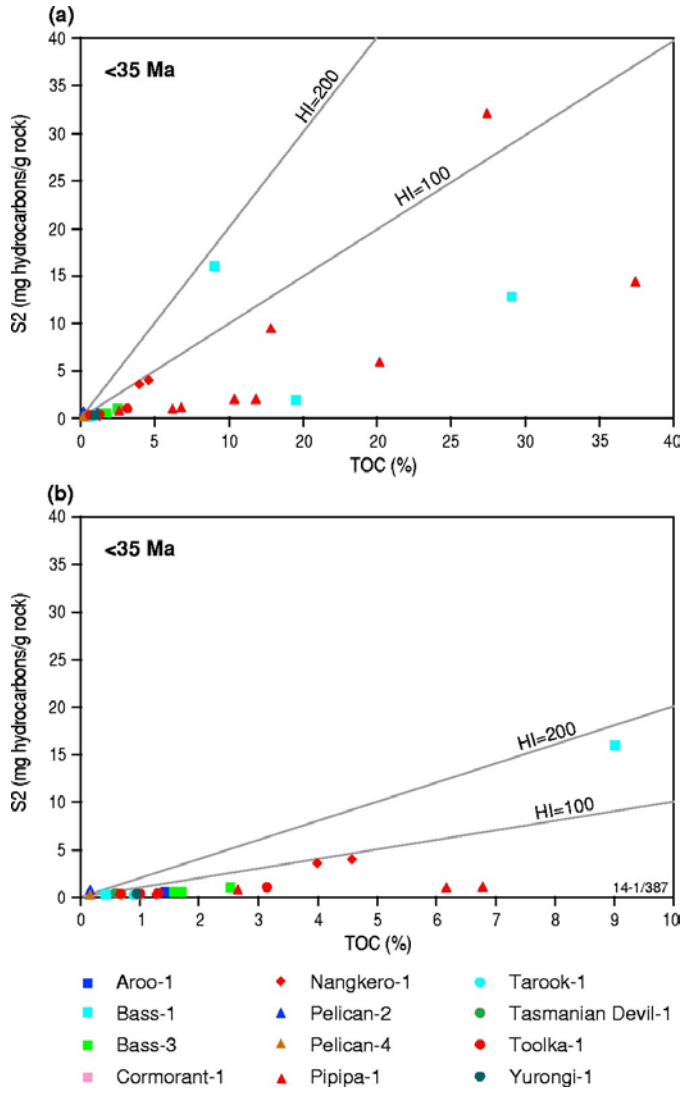

Figure 5.10 VIRF measurements on Pelican-5 sediment showing the identification of perhydrous vitrinite, normal vitrinite and inertinite.

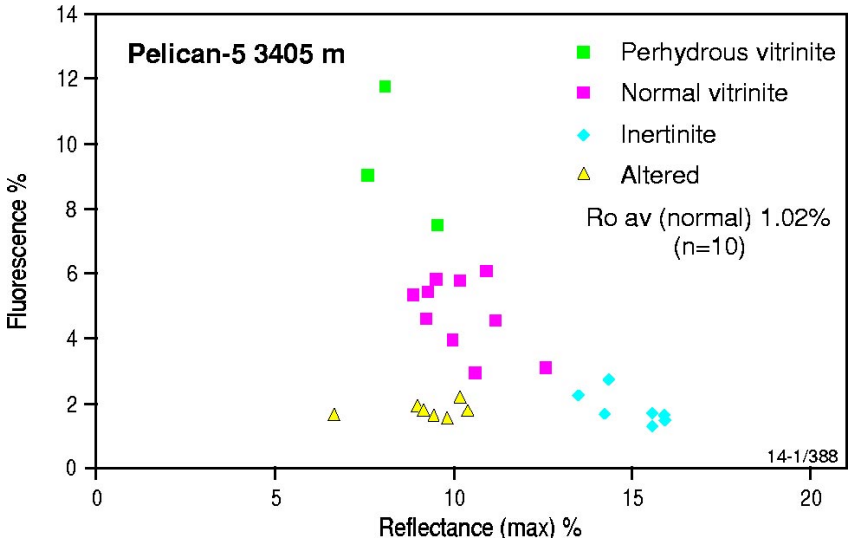

Figure 5.11 Plot of vitrinite reflectance versus depth for sediments from Cormorant-1 and Pelican-5.

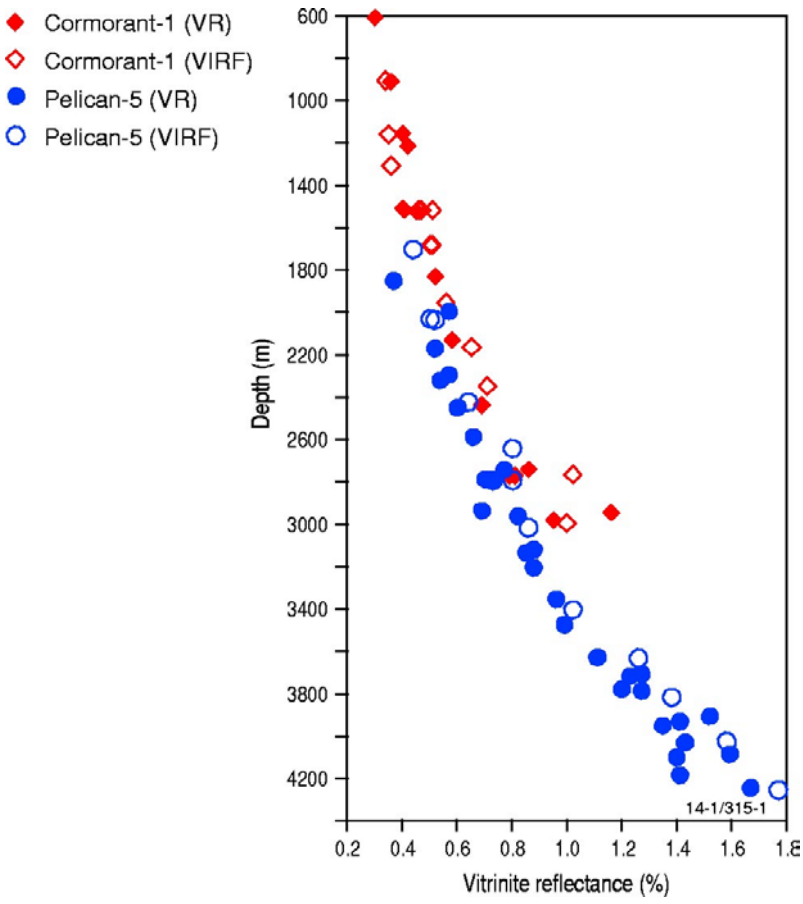

Figure 5.12 Plot of vitrinite reflectance versus age for wells in the Bass Basin.

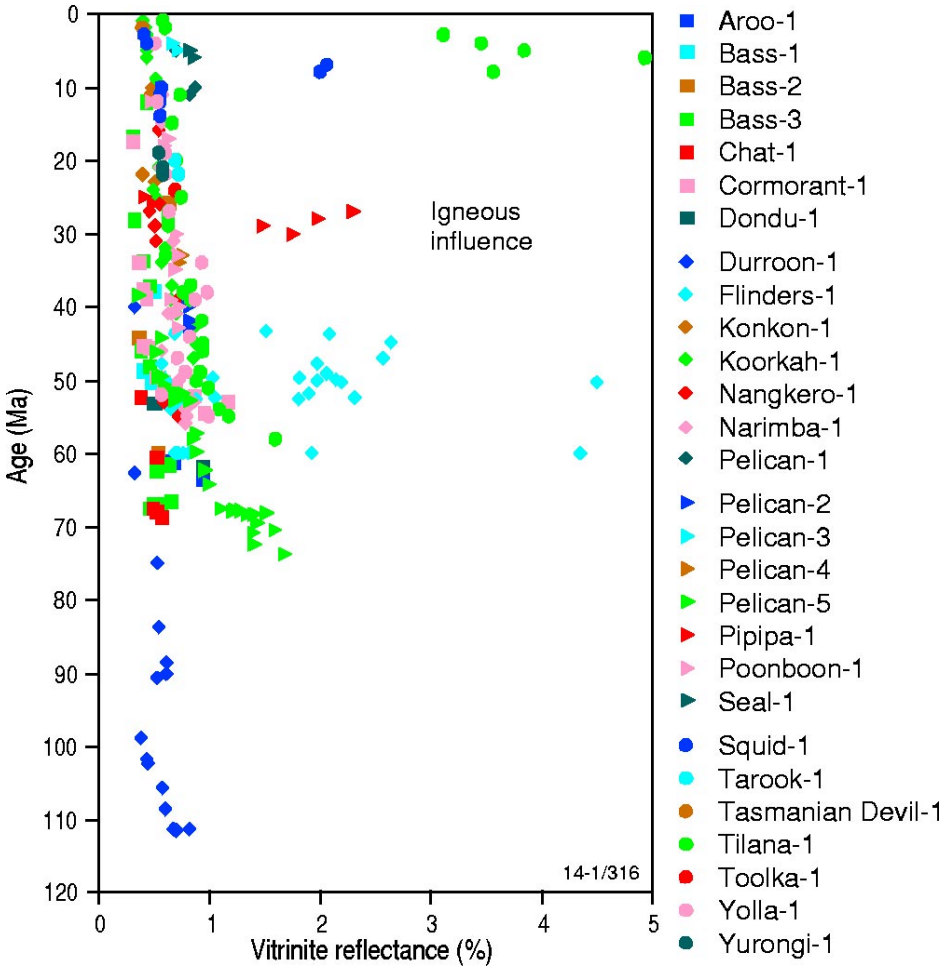

Figure 5.13 Plot of vitrinite reflectance versus depth for wells in the Bass Basin.

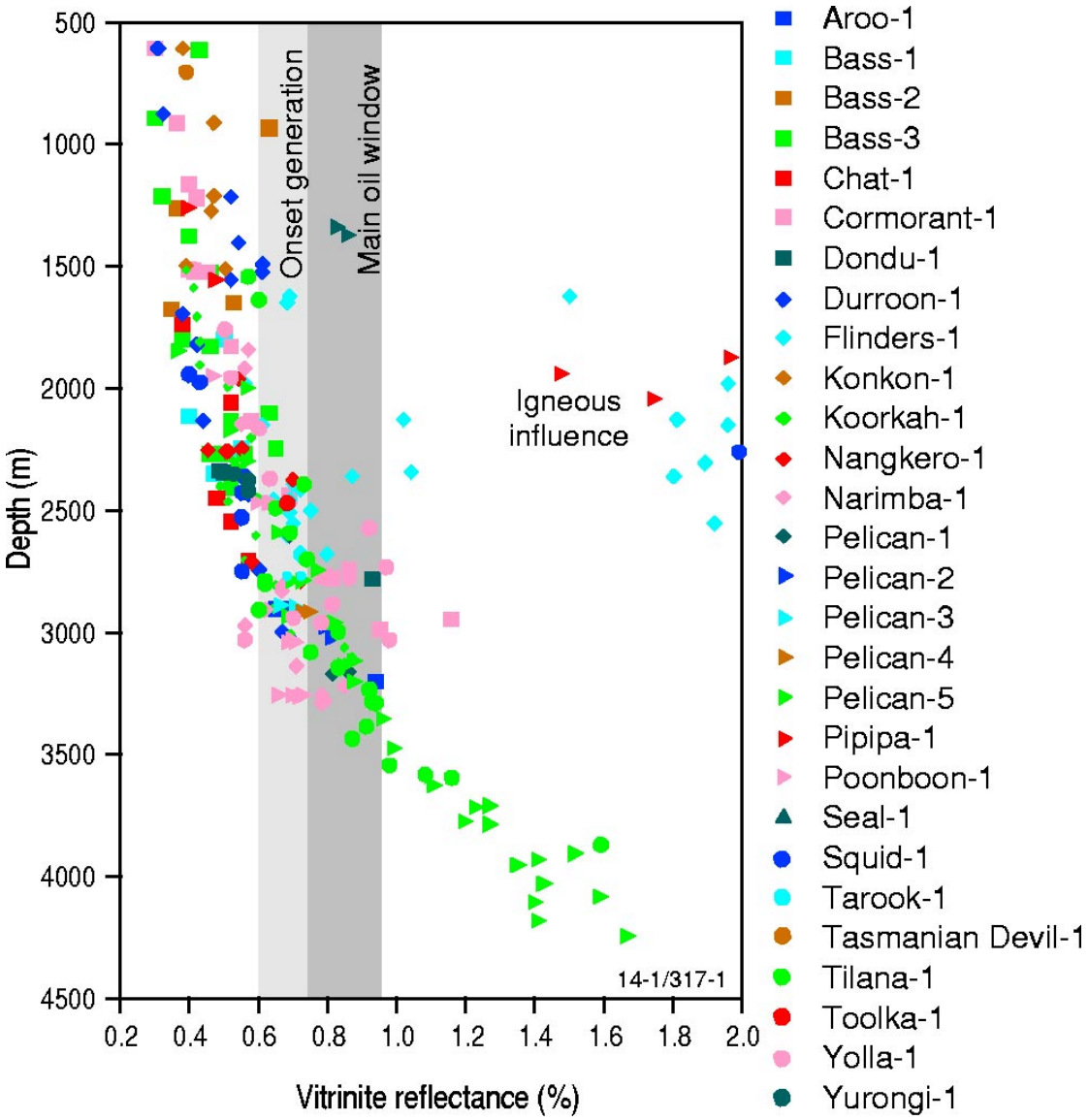

Figure 5.14 Depth plot of Hydrogen Index (HI) and Bitumen Index (BI) for low-ash coals in Pelican-5.

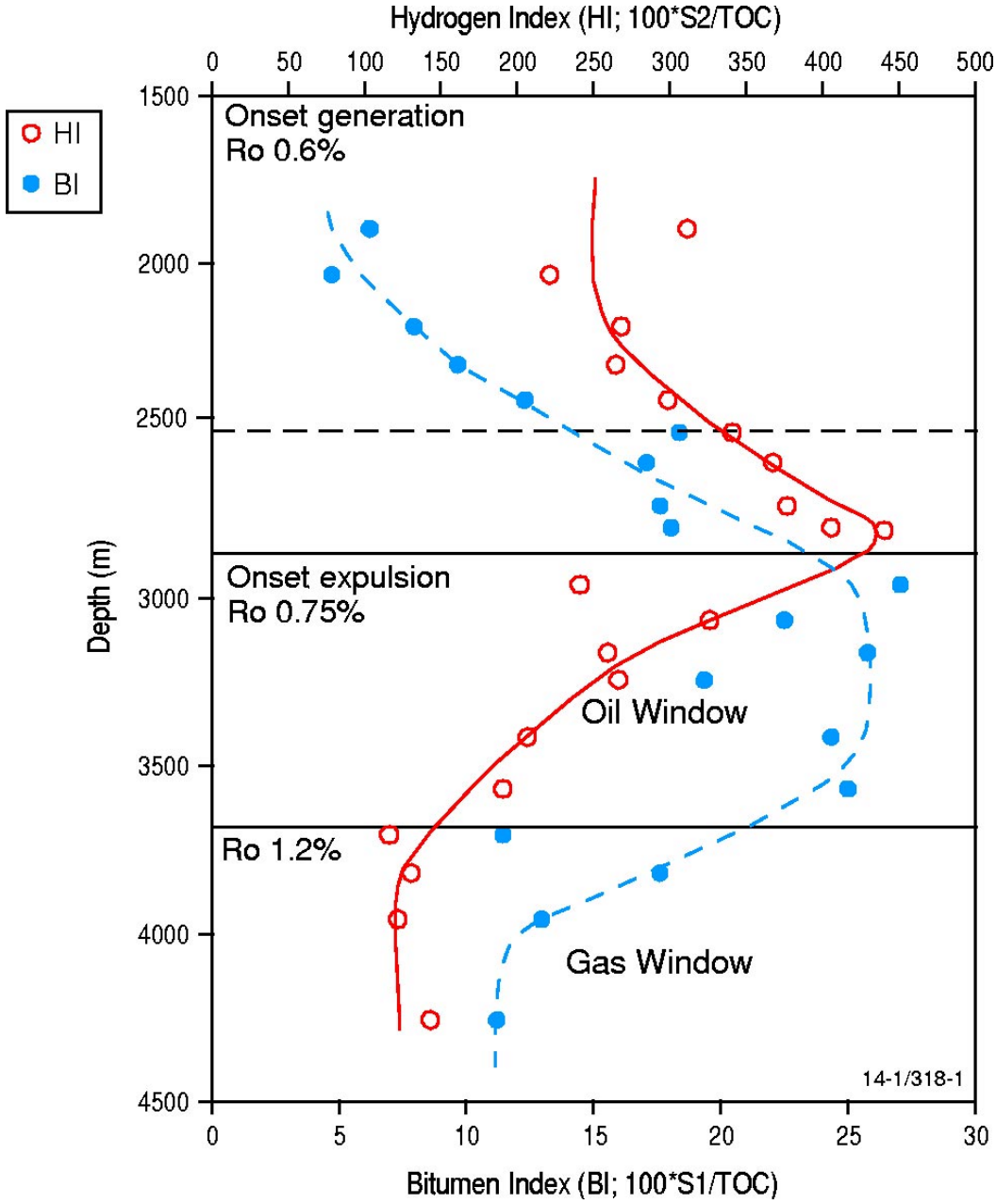

Figure 5.15 Small Angle Neutron Scattering (SANS) results for coals from Pelican-5 showing (a) the calculated pore number density (proportional to the pore size distribution) for three micropore sizes (100Å = 0.01 μm). Note the marked decrease of the pore number density within the depth range 2400 to 2600 m, and (b) the variation of the scattering intensity with depth for mean micropore size 0.025 μm ± 50%.

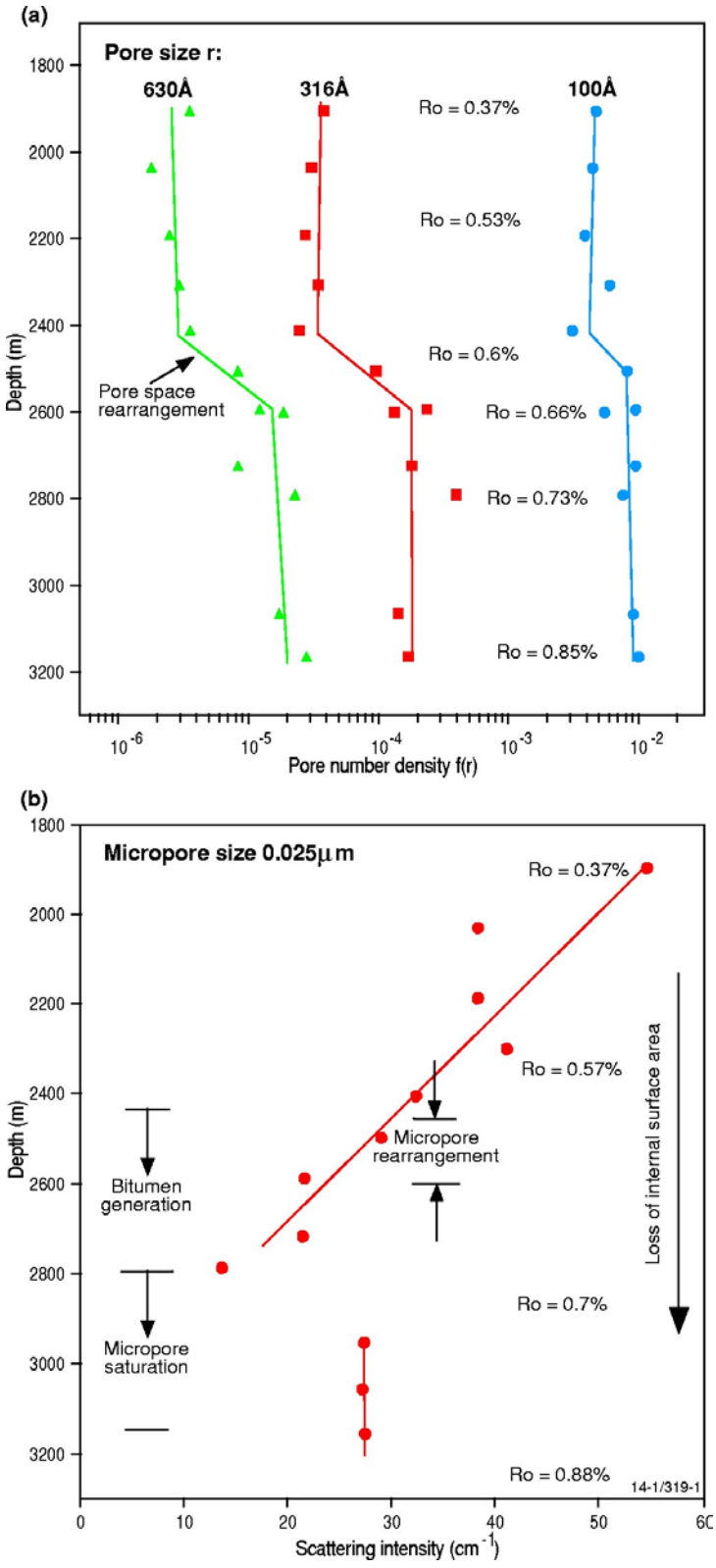

Figure 5.16 Plot of temperature (°C) versus kerogen transformation ratio (TR) and calculated vitrinite reflectance (VR) for a heating rate of 1 °C/Ma.

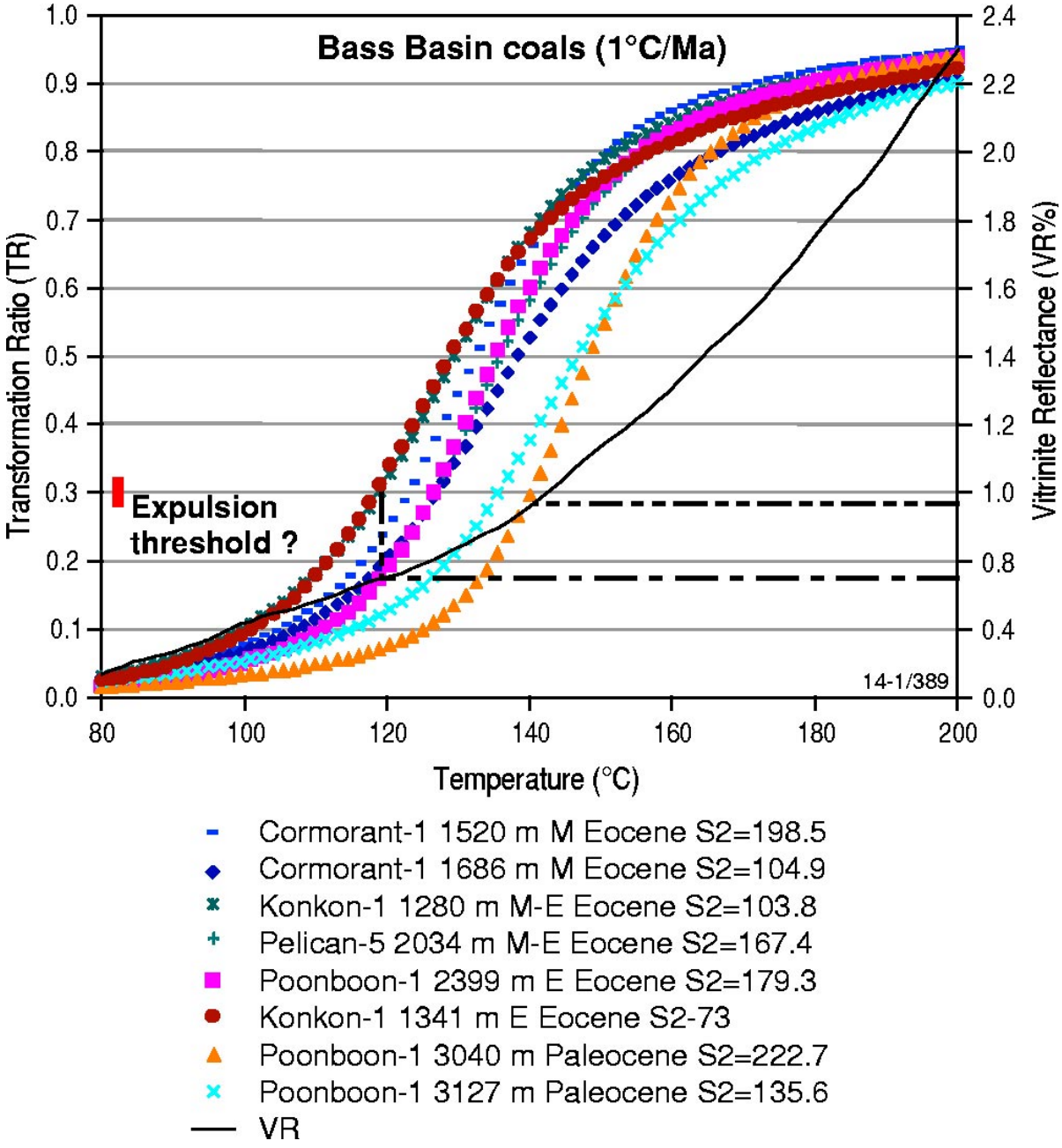

Figure 5.17 Dendrograms resulting from hierarchical cluster analysis using samples and the variables in Table 5.1. Oils from the Bass Basin include those from Cormorant-1, Pelican-1 and –2, and Yolla-1, oils from the Gippsland Basin are represented by Bream, Cobia, Dolphin, Fortescue, Halibut, Kingfish, Kipper, Luderick, Mackeral, Marlin, Perch, Snapper, Sunfish, Tarwhine, Tuna and Wirrah (Geoscience Australia and GeoMark Research, 2002), while oils from the Otway Basin include Haselgrove, Haselgrove South, Katnook, Killanoola, Lindon, Nunga Mia, Port Campbell, Redman, Sawpit, Windermere, Wynn (Edwards et al., 1999; Geoscience Australia and GeoMark Research, 2002). Note: A = Austral Petroleum Supersystem; A1, A2, A3 petroleum systems; A1- F2 freshwater lacustrine facies; A1- F3 = fluvio-lacustrine facies.

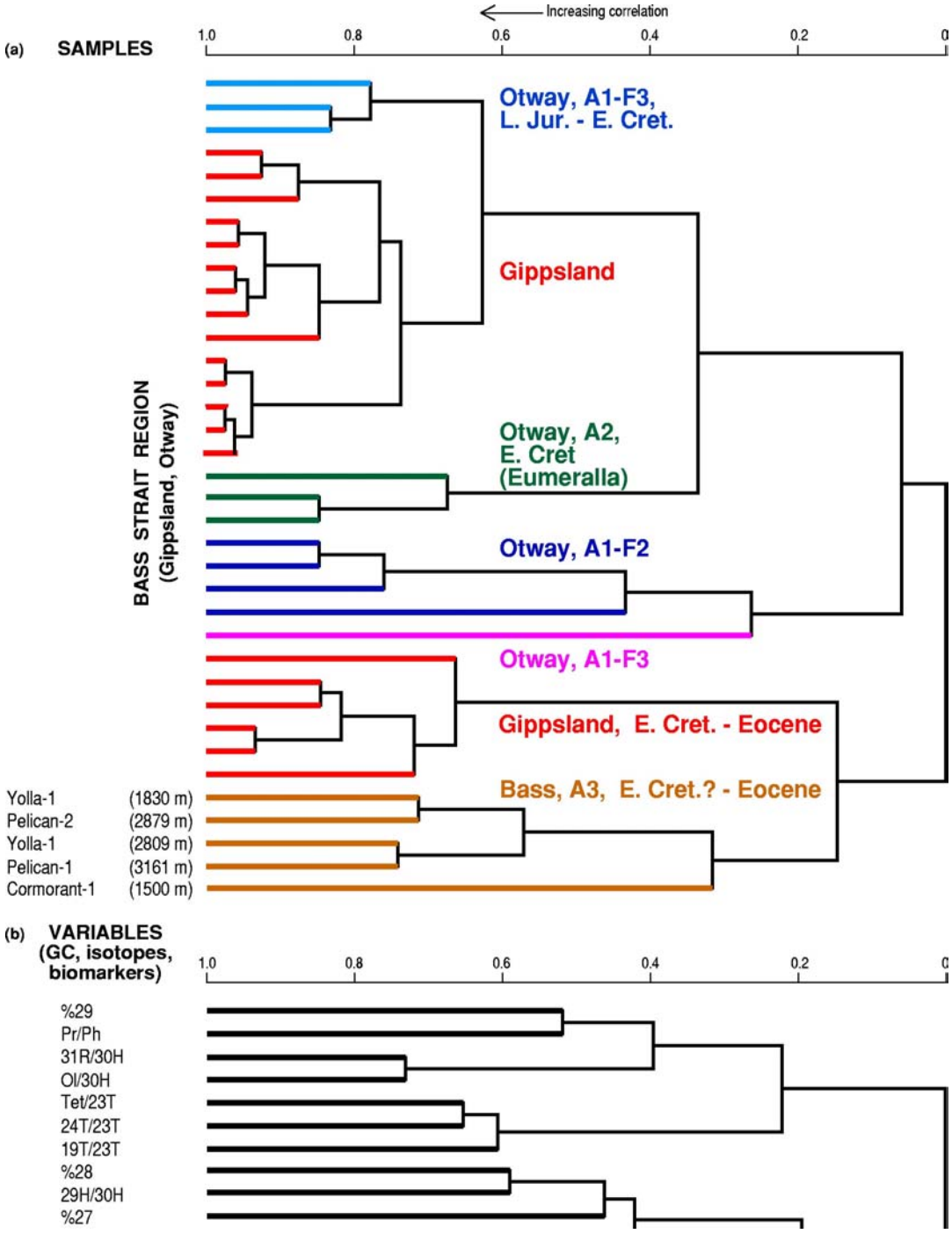

Figure 5.18 Dendrograms resulting from hierarchical cluster analysis using the samples and variables in Table 5.1. The potential source rocks are coals and claystones from Cormorant-1 and Pelican-5. Oils from the Bass Basin include those from Cormorant-1, Pelican 1 and –2, and Yolla-1, while oils from the Gippsland Basin are representative of the compositional extremes seen in Gippsland crudes (Geoscience Australia and GeoMark Research, 2002).

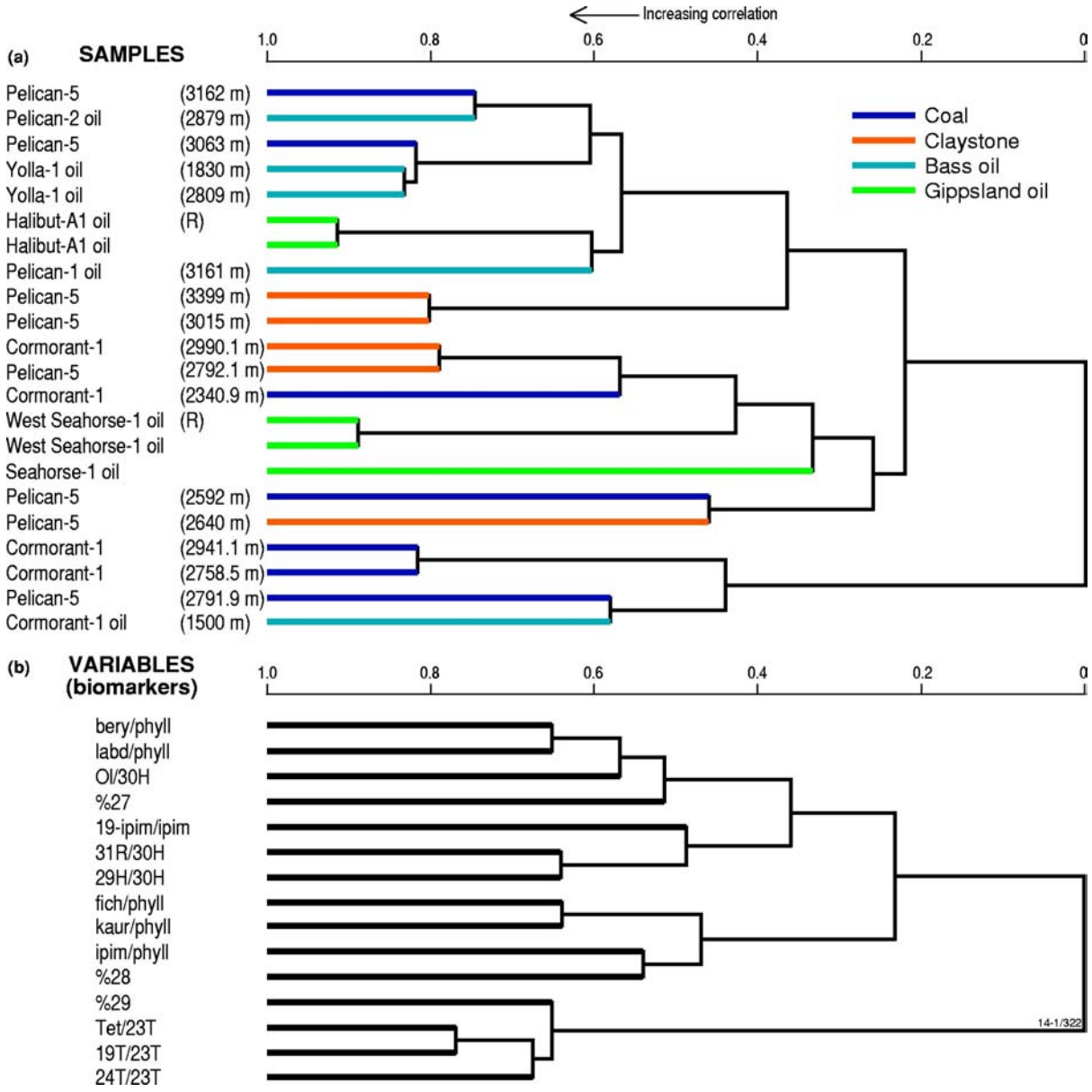

Figure 5.19 Hydrocarbon composition of Bass Basin natural gases expressed as a plot of percentage methane%/(methane% + ethane% + propane% + *iso*- & *n*-butane% + *iso* & *n*-pentane%) versus ethane%/propane% (100 * $\%C_1/\%C_1\text{-}C_5$ vs $\%C_2/\%C_3$). Also plotted are the compositions of gases from the adjacent Gippsland, Otway and other Australian sedimentary basins (Boreham et al., 2001).

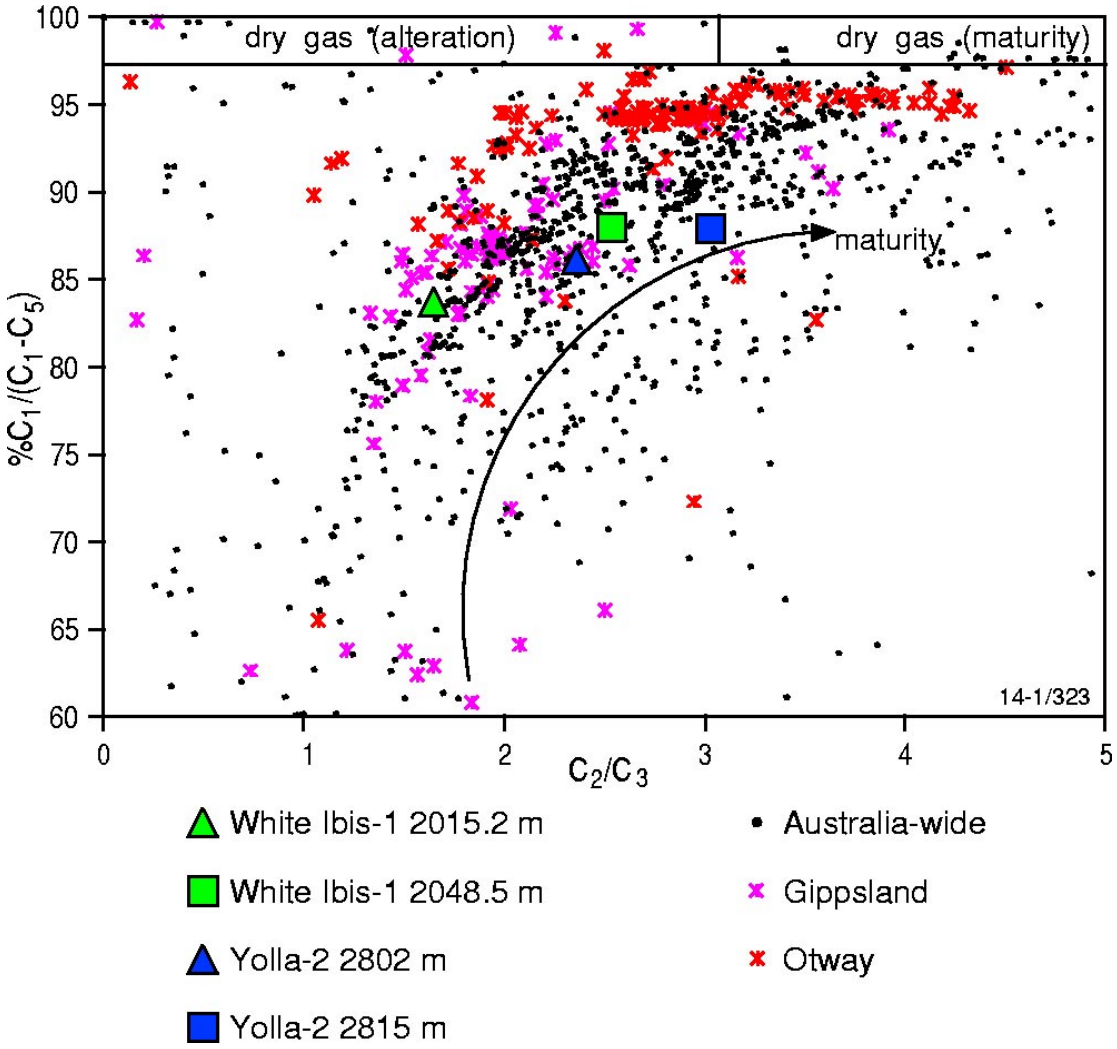

Figure 5.20 Plot of carbon isotopic composition of individual C_1-C_5 gaseous hydrocarbons from the Bass Basin. Also plotted are the carbon isotopic range for unaltered natural gases from Gippsland, Otway and other Australian sedimentary basins (Boreham et al., 2001).

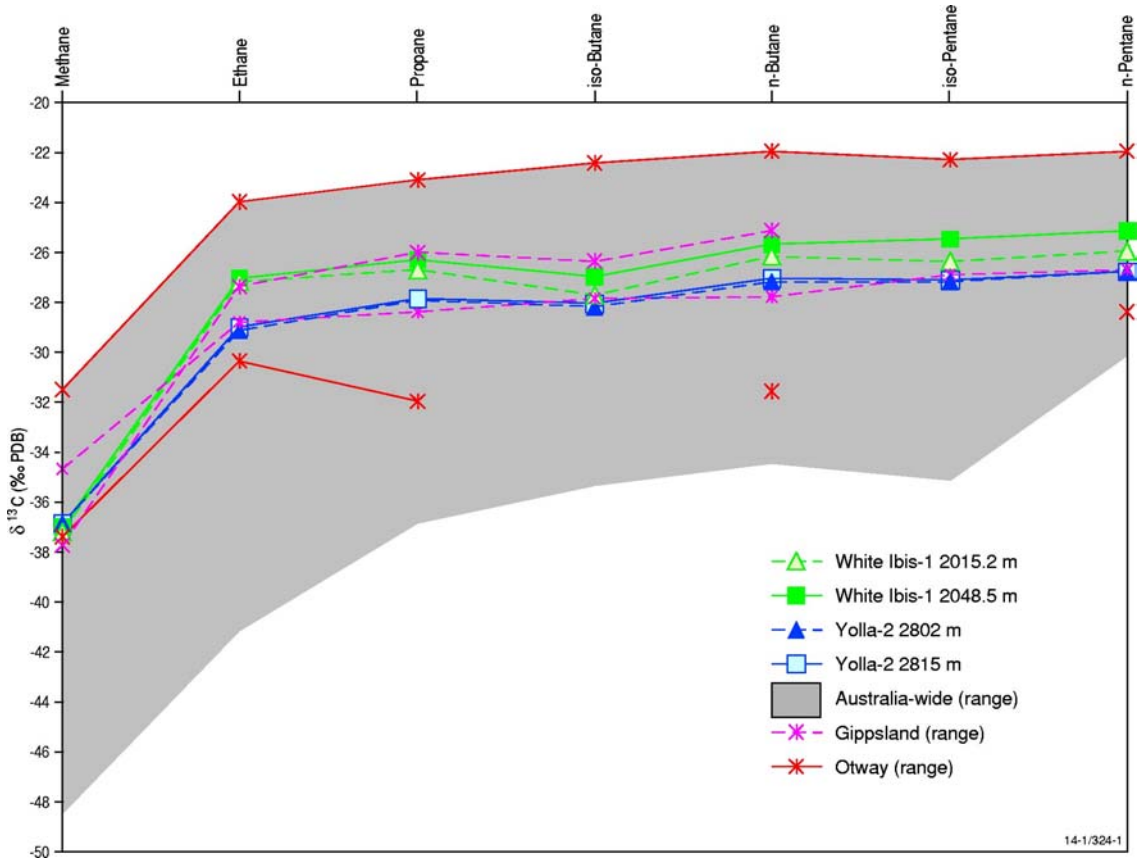

Figure 5.21 Natural gas plot (Chung *et al.*, 1988) for natural gases from the Bass Basin.

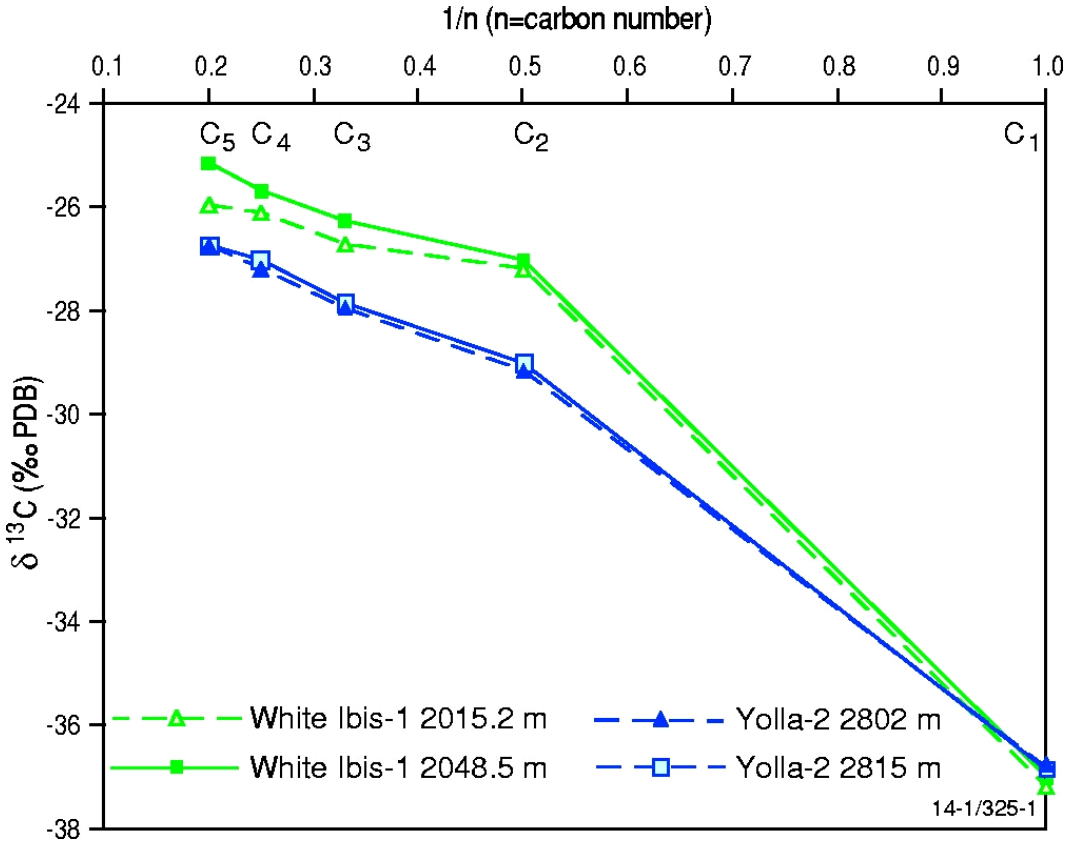

Figure 5.22 Plot of carbon isotopic difference between $\delta^{13}C_{methane}$ and $\delta^{13}C_{ethane}$ versus the carbon isotopic difference between $\delta^{13}C_{ethane}$ and $\delta^{13}C_{propane}$ for natural gases from the Bass Basin. Also plotted are the isotopic differences of gases from Gippsland, Otway and other Australian sedimentary basins (Boreham et al., 2001). Note the predicted evolution of carbon isotopic difference with maturity (numbers refer to Ro %) according to James (1990).

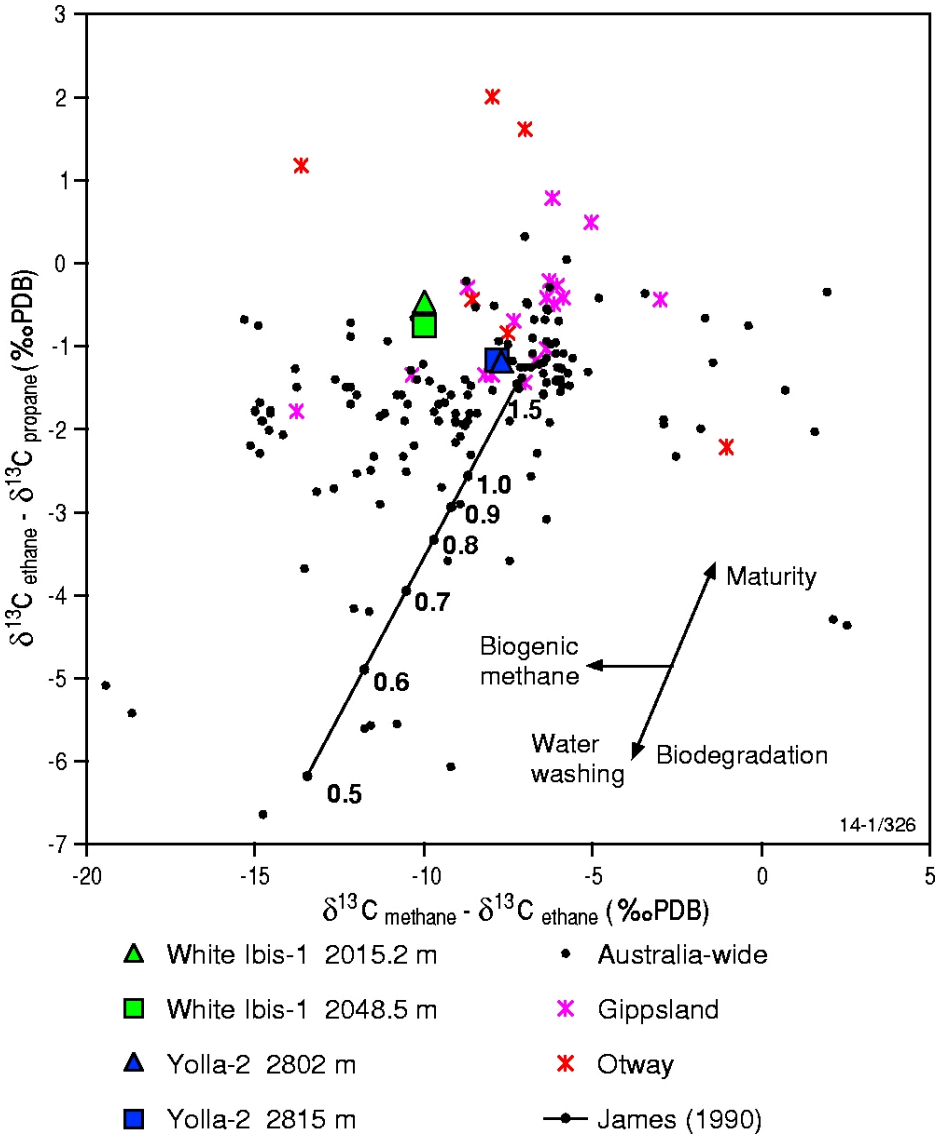

Figure 5.23 Plot of carbon isotopic composition of CO_2 versus molecular percentage of CO_2 for natural gases from the Bass Basin. Also plotted are the corresponding data for gases from Gippsland, Otway and other Australian sedimentary basins (Boreham et al., 2001). Note that the grey-fill depicts the isotopic range of an inorganic source.

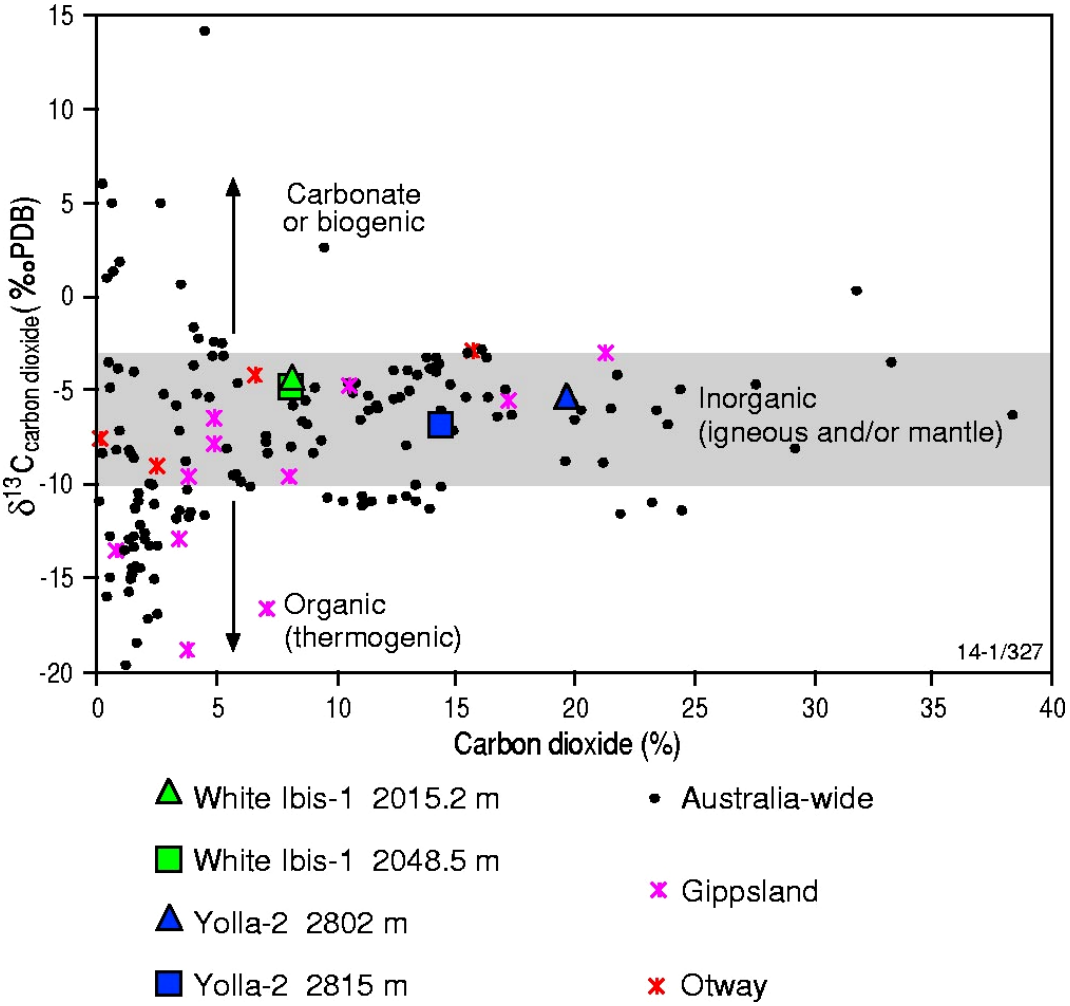

Figure 5.24 Carbon isotopic composition of individual C_1-C_{30} *n*-alkanes for gases and oils from the Bass Basin. Also plotted are representative gases and oils from the Gippsland Basin (Boreham et al., 2001).

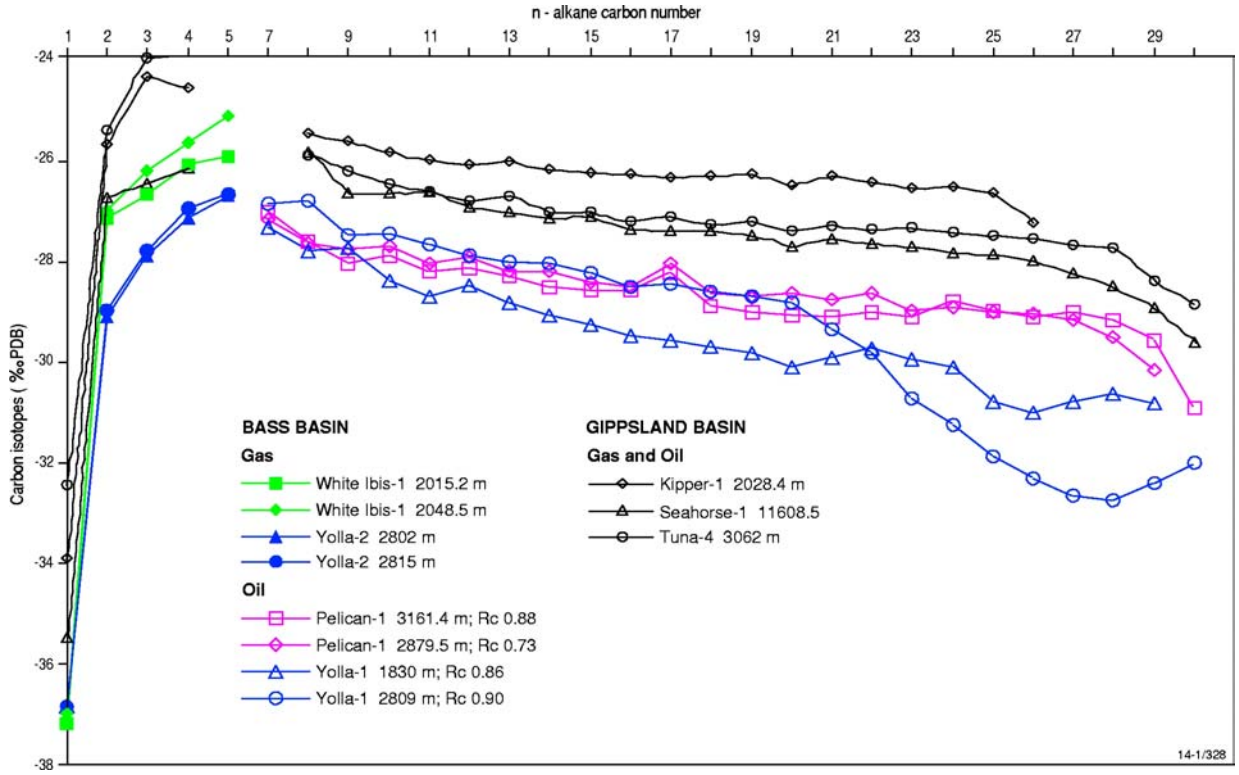

6. GEOHISTORY AND MATURITY MODELLING

A. Cummings and P. Tingate, National Centre for Petroleum Geology and Geophysics

6.1 KEY POINTS

- Geothermal gradients within the Bass Basin vary from 3.3°C/100m in the Pelican Trough, to up to 6.5°C/100m at Konkon-1. A broad decrease in geothermal gradient occurs from the northwest of the basin towards the southeast. A similar pattern is reflected in calculated heatflow values.
- 'Default Thermal History' (DTH) models of 13 wells from the Bass Basin indicate that the Late Cretaceous to Recent section is experiencing maximum temperatures today. The majority of wells show a strong correlation between measured and predicted VR profiles.
- DTH models of Koorkah-1, Chat-1, and Durroon-1 display elevated calculated VR profiles with respect to measured VR values, indicating they may have been subjected to a recent heating event (< 2 Ma).
- Burial geohistory diagrams of the wells studied indicate a consistent rate of subsidence and sedimentation from the Late Cretaceous to the present, reflecting the post-rift depositional setting.
- The defined source rocks linked to hydrocarbon accumulations within the Bass Basin (Paleocene to Early Eocene coals) entered the oil generation window just prior to and following deposition of the Demons Bluff shale, and after the major trap forming structural events of the Late Cretaceous and Early Eocene. Paleocene to Early Eocene units continued to pass into the oil expulsion window during and after Miocene structural reactivation events.
- The base of the Pelican-5 well (~ 67 Ma, Maastrichtian) entered the main gas generation window (1.15 – 2.6 %Ro) around the start of the Miocene (~23 Ma). Paleocene to Early Eocene source rock intervals have not entered the main gas generation window. However, deeper undrilled sediments of the Durroon Megasequence (Tasman Rift Phase) may have entered the main gas generation window as early as the Paleocene.

6.2 INTRODUCTION

Successful drilling within the Bass Basin has shown that effective petroleum systems have been active within the region. Geochemical analyses of oils indicate they were sourced predominantly from Paleocene to Early Eocene coals, while gaseous hydrocarbons show a similar source to oils but were generated over a wider maturity range (Chapter 5; Boreham et al., 2003). The aim of this study was to examine thermal and maturation history throughout the Bass Basin in order to constrain the timing of hydrocarbon generation and expulsion. This study draws from the preliminary results of a broader PhD project on the Bass Basin (A. Cummings, in prep.). Key questions that need to be addressed in order to better understand petroleum migration within the Bass Basin include:

- What are the present day thermal conditions within the basin?

- What can we tell of past thermal conditions through the use of palaeothermometers?
- What is the timing of hydrocarbon generation and expulsion from the defined source rock units relative to deposition of the regional seal; and,
- How has Cainozoic structural reactivation within the region affected the distribution of hydrocarbons?
-

This chapter presents the results of 1-D thermal maturation modelling of thirteen key wells and four synthetic well sections throughout the Bass Basin. Modelling was carried out using the 1-D basin modelling software package BasinMod^{TM} (Version 4.2, Platte River Associates). The thirteen wells were modelled using a "Default Thermal History" (DTH) based on the preserved stratigraphy and constant temperature conditions through time (based on present). Using the calculated maturity profiles for the 13 wells, the distribution and timing of hydrocarbon generation throughout the basin was examined. Four pseudowell sections were constructed from detailed seismic mapping of key basin depocentres. The pseudowells were used to examine the subsidence and maturation history through deeper, undrilled sections within the Bass Basin. An investigation of palaeoheatflow was undertaken in the Durroon-1 well, the results of which were applied to the pseudowell sections. Maturity windows and kinetic parameters used were those defined specifically for the Bass Basin by Geoscience Australia (Chapter 5; Boreham et al., 2003).

6.3 PREVIOUS STUDIES

Detailed investigation into the burial and thermal geohistory of the Bass Basin was first undertaken in the early 1980s with the advent of basin modelling computer software (Deighton, 1981; Nicholas et al., 1981; Middleton, 1982). Deighton (1981) noted that prime exploration targets for mature source rock units were Early Eocene and older sequences of the Eastern View Coal Measures (EVCM). It was also shown that many wells drilled within the basin terminated above or just within the predicted maturity zone. Etheridge et al. (1984, 1985) analysed a synthetic well section through the central region of the basin (close to Bass-1), concluding that late Cretaceous and Paleocene source rocks became mature for oil (VR = 0.6%) towards the end of the Oligocene. Williamson and Pigram (1986) completed thermal maturity analysis on 16 wells throughout the Bass Basin and proposed that the Upper Cretaceous EVCM has been mature since Late Eocene times (40 Ma), after the major period of structural activity within the basin had ceased. Russell and Baillie (1989) presented a detailed analysis of present-day thermal conditions, testing the use of vitrinite reflectance as an absolute palaeogeothermometer. They concluded that many of the well sections within the basin have undergone significant cooling of the sedimentary sequence below maximum palaeotemperature (between 40 and 80^{o}C). A review of petroleum prospectivity within the Bass Basin (Miyazaki, 1993) provides an excellent compilation and overview of open file data acquired up until the early 1990s. SAGASCO (Knowles et al., 1994) undertook detailed thermal maturity modelling of Flinders-1, Pelican-5 and a synthetic well within the Pelican Trough. They also investigated the effects of localised Tertiary igneous activity on the vitrinite reflectance profile shown in the Flinders-1 well.

6.4 DATABASE AND METHODS

Data used in this report were compiled from various open file sources. Data for geohistory input, including stratigraphic and lithological information, bottom hole temperature (BHT) and drill stem test (DST) temperature data, measured vitrinite reflectance and other thermal history parameters were collected from open file well completion reports (WCRs), and government reports. Detailed stratigraphic and structural mapping of open file seismic data was incorporated into the study, to constrain the position of unconformities within the Tertiary sequence and to estimate the thickness of eroded sections. Localised source rock kinetic and maturity data, defined specifically for this study of the Bass Basin, was provided by Geoscience Australia (Chapter 5; Boreham et al., 2003). The zone of initial oil generation was taken as 0.65 to 0.75 % Ro, oil expulsion 0.75 to 1.2 % Ro and main gas generation 1.2 to 2.6 % Ro.

Vitrinite reflectance data were compiled for 28 wells throughout the Bass Basin. In addition, a further 27 samples from 11 wells (core and cuttings) were collected from Geoscience Australia's core and cuttings repository and submitted for vitrinite reflectance analysis by Keiraville Konsultants Pty Ltd (Appendix I; Cook, 2002). Sampling was targeted where coal and shale sequences were indicated on geophysical logs and where previous sampling for vitrinite reflectance was lacking. Apatite fission track analysis (AFTA) data the Durroon-1 well (Duddy 1992) was used to investigate palaeoheatflow.

Measured downhole temperatures provide valuable data for the estimation of present-day temperature profiles within wells. An accurate estimation of *in situ* formation temperature is essential for rigorous thermal history calibration and maturity modelling (Waples, 1998). Due to the cooling effects of mud circulation while drilling, log derived temperatures must always be corrected (increased) to approximate true formation temperatures. Unfortunately, within the Bass Basin the quality of subsurface temperature data is highly variable and in many cases bottom hole temperature (BHT) data have not been recorded in sufficient detail for thorough analysis (BHT uncorrected data, Appendix J). Russell and Baillie (1989) undertook a detailed investigation into the correction of BHT data from Bass Basin wells using a number of published techniques. BHTs were re-corrected as part of this study using a recent correction technique (Waples and Ramly, 2001).

The technique described by Waples and Ramly (2001) incorporates a statistically derived empirical correction for single BHT measurements and Horner plot corrected measurements based on subsurface temperature data from the Malay Basin. Where sufficient information was available, including time since circulation data (TSC) and mud circulation times, BHT data from Bass Basin wells were corrected using standard Horner plots (Horner Corrected BHT) and then further corrected using the Waples and Ramly (2001) method. Where mud circulation times were not available, Horner plots were constructed for each well using assumed mud circulation times of 1, 2, 3 and 4 hours. The four corrected temperatures were then averaged (Averaged Horner Corrected BHT). This averaged Horner corrected temperature was then further corrected using the Waples and Ramly (2001) method. For older wells where multiple temperature readings at the same depth were not recorded (e.g. Bass-1, -2, and -3), single BHT data points were corrected using the Waples and Ramly (2001) method (Single Corrected BHT). The temperature correction methods outlined

above have been successful in correcting BHTs to approximate measured DST temperatures throughout the basin (Figure 6.1, Table 6.1).

Estimates of present day seafloor temperatures were calculated based on a present average ocean surface temperature of 15°C that is reduced by 4°C/100m through the water column (Waples et al., 1992). Using this method, it appears that water-sediment interface temperatures vary between 11.6°C (~85m water depth) and 12.6°C (~60m water depth) throughout the basin. Due to the minor variation, an average sea-bottom temperature of 12°C was used for all wells modelled. For modelling, it was assumed that the palaeosurface temperature had remained constant at the estimated present day temperature.

Vitrinite reflectance data are typically presented as either mean random reflectance or mean maximum reflectance. For the purpose of general modelling, both types of reflectance values can be used (Kaiko, 1988; Sweeney and Burnham, 1990). Vitrinite reflectance data from some wells could not be identified as being either mean random or mean maximum reflectance data, as there was insufficient accompanying information. Therefore, the available vitrinite reflectance data was entered as it was reported, without any distinction being made between the two forms of vitrinite reflectance measurements. Kinetic modeling of Pelican-5 well is shown in Appendix K.

One-dimensional thermal maturation modelling of wells within the Bass Basin was carried out using BasinMod™ (Version 4.2, Platte River Associates, Inc) to constrain the timing of hydrocarbon generation and migration. Vitrinite reflectance values were calculated using the Lawrence Livermore National Laboratories (LLNL) kinetics option. Defined stratigraphic units within wells were expressed as a combination of eight pure lithologies, whereby lithology mixes were based on data from cuttings descriptions, composite well logs and log interpretation. BasinMod™ default values were used as inputs for initial porosity, density, grain size, matrix thermal conductivity and matrix thermal capacity. Porosity-depth relationships were modelled using the Middleton (1982) compaction option. Palaeo-water depths used were those outlined by Deighton (1981) or were estimated using foraminiferal data compiled from well completion reports.

6.5 GEOTHERMAL GRADIENTS AND HEATFLOW

The regional variation of geothermal gradients calculated from corrected BHT data is shown in Figure 6.2. Geothermal gradients vary from 3.3°C/100 m at Pelican-2 and Pelican-3, up to 6.5°C/100 m at Konkon-1, with a mean basin gradient of 4.7°C/100 m. A broad decrease in geothermal gradient is observed from the northwestern sector of the basin toward the Durroon Sub-basin. Gradients appear elevated on structural highs and are reduced along the central axis of the basin where the post-rift sequence is thickest.

Heatflow values were calculated at each well location, based on preserved stratigraphy and present-day temperature conditions (Table 1). Simple steady state conduction was assumed where heatflow (Q), is a product of thermal conductivity (k) and geothermal gradient (dT/DZ)(Gretener, 1982).

$$Q = K \times dT/dZ$$

Figure 6.3 shows the areal distribution of calculated heatflow values throughout the basin. It shows a similar trend to the gradient map, where heatflow decreases towards the southeast and along the central axis of the basin.

6.6 THERMAL MODELLING

Thermal modelling was undertaken using the method outlined by Waples et al. (1996), and Duddy and Erout (2001). In order to investigate possible differences in thermal history across the basin, thirteen wells were modelled (Figures 6.4 and 6.5) assuming simple progressive burial through time, non-deposition at all time breaks in stratigraphy and a constant heatflow through time (based upon current temperature conditions). This simple model, termed a 'default thermal history' (DTH), forms a basis from which more detailed investigations into past temperature conditions can be assessed.

Vitrinite reflectance profiles were calculated (Maturity VR LLNL) using a default thermal history scenario and the Falvey and Middleton (1982) compaction option. Calculated VR profiles were then compared to the measured vitrinite reflectance data from each well (Figure 6.5). Comparison of measured and calculated data highlights three situations within DTH models of Bass Basin wells:

- Calculated VR < measured VR
- Calculated VR = measured VR
- Calculated VR > measured VR

It is necessary to investigate the reasons why some data are in accordance with present day thermal conditions and others are not (Figure 6.5).

Where calculated VR < measured VR

A number of wells, including Seal-1, Toolka-1A, Yolla-1, Tilana-1, Nangkero-1, Flinders-1, and Durroon-1, contain intervals where measured VR values are higher than the calculated VR profile. Elevated VR values in Seal-1, Yolla-1, Tilana-1, and Flinders-1 are in close proximity to Miocene igneous intrusions (Figure 6.5) that occur sporadically through the Cainozoic succession in the Bass Basin. Measured VR samples lying proximal to intrusive bodies appear to approach a background reflectance profile, where calculated VR is approximately equal to the measured values.

Elevated VR measurements from samples in both Toolka-1A and Nangkero-1 do not appear to be associated with localised igneous activity. Recent petrographic analysis of cuttings samples from both wells indicates that 'frypanning effects' are a common feature in coal samples collected from cuttings. This may explain the anomalously high VR values observed within these wells (Cook, 2002). "Frypanning" is the term given to a process where cuttings samples are heated during the initial drying process to excessive temperatures

whereby the organic matter oxidises. Rims and cracks within the coal grains display a higher reflectance when they have been affected by frypanning. Conversely, the cores of affected grains often show lower VR values, possibly due to migration of tars into the coals. This makes it difficult to determine the original reflectance of the vitrinite. Cook (2002) observed frypanning within cuttings samples from Aroo-1, Nangkero-1, Tarook-1, and Toolka-1A. Thus, care should be taken when using VR data derived from these four wells, and other wells within the Bass Basin where less detailed petrographic analysis has been undertaken.

The elevation of VR measurements from the Durroon Mudstone (Chapter 4) within the Durroon-1 well do not appear to be related to either localised igneous intrusions, or the effects of frypanning (Figure 6.5). Duddy (1992) indicated that elevated measured VR values observed in samples from the Durroon Mudstone are high due to the effects of oxidation. The VR values estimated from Thermal Alteration Index (TAI) data from the same level appear to be far lower and are in accordance with other samples from the well.

Where calculated VR = measured VR

When a measured VR value is equal to the calculated value predicted from a default thermal history model, it indicates that the sample has not been exposed to palaeotemperatures higher than present temperatures since deposition (Duddy and Erout, 2001). Following the technique proposed by Kaiko (1998), a well was considered to be currently experiencing maximum temperature if the calculated VR profile could be made to correspond to the measured VR profile by adjusting the BHT by no more than ±10 % of the initial corrected BHT value. This allows for any divergence in maturity estimates that may occur from the use of corrected BHT's, and also accounts for possible variation between plotting measured random reflectance and measured maximum reflectance (Ro_{Max} = 1.066 x Ro_{Random}; Ting, 1978; Kaiko, 1998).

Calculated Ro profiles within Seal-1, Cormorant-1, Bass-3, Aroo-1, Yolla-1, Tilana-1, Nangkero-1, Flinders-1, and Pelican-5 appear to approximate measured VR profiles (Figure 6.5). This indicates that stratigraphic sections intersected by these wells are currently experiencing maximum temperature, apart from localised departures associated with intrusions. Any thermal variation due to uplift and erosion that may have occurred in the past has been overprinted by present-day thermal conditions. In this situation, additional thermal history data (e.g., Apatite Fission Track Analysis/AFTA, VR, biomarkers) from these well locations cannot reveal further details to constrain the background thermal history (Duddy and Erout, 2001).

Where calculated VR > measured VR

Koorkah-1, Chat-1 and Durroon-1 all contain measured VR values that are lower than what is predicted from their respective default thermal history models (Figure 6.5). If we assume that both measured VR data and subsurface temperature data are correct, present thermal conditions within these wells may be the result of a relatively recent heating event. Such a thermal increase would need to have occurred after 2 Ma to prevent measured VR reaching equilibrium with present day conditions (Kaiko, 1998).

Another explanation may be that present day temperature conditions have been overestimated through the overcorrection of BHT data. In addition, measured VR values may underestimate the true maturity for reasons including the presence of caved material within cuttings samples, misidentification of true in-situ vitrinite, or the suppression of reflectance in certain organic macerals (Duddy and Erout, 2001). Recent VRF studies however, indicate that VR suppression within the basin appears to be limited (Boreham et al., 2003; Chapter 5). The corrected BHT data and measured VR data at Koorkah-1 and Chat-1 are considered to be accurate, suggesting that a recent heating event is likely.

Irrespective of the reasons for the elevated calculated VR profiles within Koorkah-1, Chat-1 and Durroon-1 (based upon DTH models), the rocks intersected by these wells appear to be experiencing maximum temperature conditions today.

6.7 RESULTS FROM DEFAULT THERMAL HISTORY MODELS

DTH models of the 13 wells studied indicate the Late Cretaceous to Recent section within the Bass Basin has not been exposed to palaeotemperatures any higher than the present temperatures since deposition (excluding the effects of localised igneous activity). The majority of wells show a strong correlation between measured and calculated VR profiles, indicating they are at maximum temperature (Figure 6.5). DTH models for Koorkah-1, Chat-1, and Durroon-1 display elevated calculated maturity profiles with respect to measured values, indicating they may have been subjected to a recent heating event (< 2 Ma). All three wells are located towards the margins of the basin (Figure 6.4).

Maps were constructed showing the areal distribution of VR across the basin, based upon calculated VR profiles from DTH models (Figures 6.6 to 6.12). As the maps were constructed from calculated VR profiles (to investigate regional background VR trends), the localised effects of igneous intrusions on VR have been ignored. However, the effects of localised igneous activity should be considered when undertaking smaller scale investigations of hydrocarbon generation and expulsion, as intrusive bodies are common within Cainozoic succession.

The distribution of calculated VR across the Bass Basin highlights the following points (Figures 6.6 to 6.12):

- Depth to the oil generation window (0.65% Ro) varies between ~1.6 and 2.4 km below seafloor. The top of the defined oil window is deepest in the central region of the basin, and shallowest towards the northwest, where geothermal gradients are highest (Figure 6.6). The average depth to the oil generation window within the basin is 2.0 km below seafloor.
- Depth to the onset of oil expulsion (0.75% Ro) varies between ~2.3 and 3.0 km below seafloor, and is deepest in the central part of the basin, shallowing towards the northwest (Figure 6.7). The average depth to the oil expulsion window within the basin is 2.6 km below seafloor.
- Average VR across the Bass Basin at 2000 m is approximately 0.57%, varying between 0.48 and 0.65% (Figure 6.8). VR shows a broad increase towards the west of the basin where Seal-1, Bass-3, Yolla-1 and Flinders-1 have entered the oil generation window at this depth.

- Average VR across the Bass Basin at 2500 m is approximately 0.70%, varying between 0.62% and 0.78% (Figure 6.9). All lithologies at 2500 m across the basin appear to have entered the defined oil generation window. However, a few wells, including Seal-1, Bass-3, and Yolla-1, are greater than 0.75% Ro implying that they are within the oil expulsion window (>0.75% Ro).
- The Middle to Late Eocene succession (Middle *N. asperus* zone; top of the "Eastern View Group" and base of the regional sealing unit, the Demons Bluff Formation) has a basin-wide average VR of 0.43%. Ranging between 0.3% and 0.56%, sediments of late Middle Eocene age and younger are immature for oil generation across the basin (Figure 6.10).
- The top of the Bass Megasequence (base Upper *M. diversus*; top of the "Middle Eastern View Group") has an average VR across the basin of 0.59%, just below the defined oil generation window of 0.6 %. VR at this level varies between ~ 0.3% to 0.69%. Figure 6.11a shows that the top of the Bass Megasequence ("Middle Eastern View Group") has entered the oil generation window in a north-south oriented zone, directly overlying the Cormorant, Yolla and Pelican Troughs, within the central axis of the basin.
- The top of the Paleocene (top Lower *L. balmei;* top of the Tilana Sequence) has an average VR across the basin of 0.71%, within the defined oil generation window. VR at the top Paleocene level varies between ~ 0.3% and 0.95%. Figure 6.12a shows that the top of the Paleocene has entered the oil generation window within the central region of the basin. Within the central axis of the basin, the top Paleocene level has entered the defined oil expulsion window (> 0.75%Ro).

6.8 PALAEOHEATFLOW MODELLING OF THE DURROON-1 WELL

A DTH model for Durroon-1 has been presented (Figure 6.5) using present day temperature conditions defined by a corrected BHT of 114^{o}C at 3021.5 m (all depths measured below KB), a geothermal gradient of 34.7^{o}C/km, and a heat flow value of 73.1 mW/m^{2}. Durroon-1 is the only well within the Bass Basin to intersect both the Early Cretaceous Otway Megasequence and the Late Cretaceous Durroon Megasequence (Chapter 4). As such, modelling Durroon-1 provides an opportunity to investigate palaeoheatflow throughout the major rifting events that influenced basin development.

While BHT, TAI, VR and AFTA data are available for the well, data quality is highly variable and is consistent with a number of thermal history scenarios. Despite the issues relating to data quality, a number of "end-member" scenarios can be defined, whereby further palaeothermal indicator analysis (VR or AFTA) by future workers may provide further clarification.

Duddy (1992) outlined a comprehensive assessment of thermal history data from the Durroon-1 well, including AFTA data for three samples from the depths 1696 m (L4-116), 2560 m (L4-117), and 3023 m (L4-118) within the Otway Megasequence. Duddy (1992) emphasised that the results of the AFTA data were tentative, as compositional kinetic factors were not fully taken into account, coupled with uncertainties in the estimation of subsurface temperatures. Important aspects of the Durroon-1 thermal history are given below:

- The maximum present temperature defined by the AFTA sample at 3023 m is 90°C (Duddy 1992), suggesting that the present day heat flow value estimated from a corrected BHT value of 114.25°C at 3023 m (used for DTH model), is too high or has risen to that level within the last 2 Ma.
- AFTA age data from the deepest sample (3023 m) suggests that the sample had experienced palaeotemperatures after deposition that were sufficient to totally, or near totally, erase fission tracks in all apatites (Duddy, 1992). A minimum temperature of at least 120°C would be required to do this (as compared to a revised present temperature of 90°C or 114°C at 3023 m) (Figure 6.6).
- There is some evidence from the AFTA data that cooling from maximum palaeotemperature occurred between ~90 and 100 Ma, following early Cretaceous deposition of the Otway Megasequence and the outpouring of mid-Cretaceous basalt (Duddy, 1992) (Figure 6.6). The timing of cooling is consistent with the onset of significant structural extension across the region, related to the initial phase of Tasman rifting (Cummings et al., 2002). Seismic mapping indicates that approximately 300 m of erosion took place at the well location during this period.
- VR data are variable throughout the well section (Figures 6.5 and 6.6), providing equivocal palaeotemperature information. The predicted VR profile from the DTH model overestimates most measured values throughout the Early Cretaceous section, however it significantly underestimates values measured in the "Durroon Mudstone". As mentioned above, these samples are considered to be elevated due to the effects of oxidation (Duddy, 1992).

Two palaeoheatflow models were implemented to analyse the Durroon-1 data (Figure 6.13). Palaeoheatflow models were modified from a regional model outlined by Duddy and Erout (2001), and modelled to fit measured AFTA and VR data from Durroon-1. Heatflow prior to the Tasman rifting event was estimated at approximately 90 mW/m^2 and was elevated to 120 mW/m^2 with the onset of Tasman Rifting around 95 Ma. Heatflow then declined until approximately 65 Ma where it remained constant through to present day (~ 73 mW/m^2). The second palaeoheatflow model involves a reduction in heat flow to approximately 57 mW/m^2 at 65 Ma through to 2 Ma, when heat flow increased rapidly to the present temperature conditions of 73 mW/m^2. Palaeoheatflow model 1 (Figure 6.13) shows a similar calculated VR profile to the DTH (Figure 6.5). The calculated VR profile defined by palaeoheatflow model 2 (Figure 6.13) involving a recent heating event, shows a greater correlation with measured VR samples.

In summary, thermal history models based on the current AFTA and VR data from the Durroon-1 well are equivocal. VR data are consistent with a maximum temperature at present day (DTH model), whereas the thermal history indicated by AFTA data implies a cooling of 10 to 35°C in the mid-Cretaceous (Duddy, 1992). To constrain the thermal history of Durroon-1, a more extensive suit of VR data must be collected and new AFTA samples must be examined using more recent compositional kinetic parameters. Unfortunately, additional VR sampling from the Durroon-1 well could not be incorporated into this study due to a lack of available samples.

6.9 SUBSIDENCE MODELLING

Burial geohistory diagrams were constructed for the 13 wells modelled within the Bass Basin, using the Middleton (1982) decompaction option, palaeo-water depths derived from palaeontological data and uplift amounts estimated from seismic mapping (Figures 6.14a to 6.14d). All wells within the Bass Basin, apart from Durroon-1, were drilled wholly within the Campanian to Recent succession. As such, subsidence curves for most wells within the Bass Basin display a consistent rate of subsidence and sedimentation from the Late Cretaceous to the present, reflecting their post-rift depositional setting.

An increase in the rate of burial is observed from the Early to Middle Eocene within most subsidence models across the basin (Figure 6.15). While sediment accumulation within the basin was largely controlled by regional post-rift thermal subsidence processes from the Campanian onwards, subsidence along the central axis of the basin appears to be related to intermittent periods of sinistral transtension associated with the continued separation of Australia from Antarctica along the "Tasman-Antarctic Shear" to the west of Tasmania (Cummings et al., 2002; Hill et al., 2001). Deposition of the potentially oil-prone Middle to Early Eocene coaly source rocks correlates with the enhanced rate of subsidence within central regions of the basin during this period of structural reactivation.

The onset of fast sea-floor spreading in the Southern Ocean, coupled with the collision of the northern edge of the Australian Plate with Southeast Asia led to compression across many regions of Australia during the mid-to-Late Cainozoic (Smit, 1988; Etheridge et al., 1991). Within the Bass Basin, Late Oligocene to Miocene compression led to the strike-slip reactivation of a number of pre-existing structures. Structural inversion was restricted to the northern margin of the basin and was particularly focused within the Cormorant Trough (Figure 6.16).

Four pseudowells were constructed to investigate subsidence within the major long-lived basin depocentres (Figures 6.16 and 6.17). Three pseudowells were constructed within the three major troughs along the central axis of the basin, the Cormorant, Yolla and Pelican troughs (Figure 6.4). The Cormorant Trough and Pelican Trough models were extended at depth from the Cormorant-1 and Pelican-5 wells respectively (Figure 6.16). A pseudowell was also constructed through the deepest section of the "Boobyalla Half-graben" (Baillie and Pickering, 1991), situated within the Durroon Sub-basin (Figure 6.17).

Subsidence patterns within the Cormorant, Yolla and Pelican troughs show an enhanced rate of subsidence from the Cenomanian to the Campanian (Figures 6.16 and 6.17). The increased accommodation rate during this period is due to basin-wide extension associated with the Tasman rifting event (Cummings et al., 2002). An increase in the rate of accommodation is also evident from the Paleocene to the Early-Middle Eocene. Increased subsidence is considered to be the result of transtensional reactivation of earlier rift structures within the central axis of the Bass Basin. The subsidence curve for the "Boobyalla Half-graben" highlights the impact of Tasman Rifting on development of accommodation space within the southeastern region of the basin (Figure 6.17). In general, the development of accommodation space within the central axis of the Bass

Basin appears to have been largely controlled by post-rift thermal sag process, whereas towards the southeast (Durroon Sub-basin), the dominant influence was Late Cretaceous rift-related subsidence.

6.10 TIMING OF HYDROCARBON GENERATION AND EXPULSION

The timing of hydrocarbon generation and expulsion within the Bass Basin has been investigated through the use of the DTH models from thirteen wells (Figure 6.15). Through the use of the maturation history diagrams, maps were constructed displaying the regional variation of VR for key periods of development within the basin. Boreham et al. (2003; Chapter 5) showed that the dominant oil-prone source rocks found within the Bass Basin are the Palaeogene coals, in particular, those found within Middle to Early Eocene sequences across the basin. To investigate the basin-wide maturation history of this source rich sequence, regional VR distribution maps were constructed for the top of the Middle *M. diversus* zone (top of the Narimba Sequence, "Middle Eastern View Group"; Figure 6.11) and the top of the Lower *L. balmei* zone (top of the Tilana Sequence, Figure 6.12). Where appropriate, areal VR distribution maps for these horizons have been reconstructed to the time when the regional sealing unit was deposited (~34 Ma) and the period when Cainozoic structural reactivation was greatest (~15 Ma, Middle Miocene).

Thermal-maturity plots based on the DTH models indicate that the base of the Eocene sequence (top Lower *L. balmei*, top of Tilana Sequence) was largely immature for oil generation during deposition of the "Demons Bluff" regional sealing unit around 34 Ma (Figures 6.12c). However, this horizon does appear to have entered the oil generation window (> 0.6% Ro) within the centre of the Cormorant Trough and in the vicinity of Tilana-1. By 15 Ma, the base of the Eocene succession had entered the oil generation window along the central axis of the basin, in the Cormorant, Yolla and Pelican troughs (Figure 6.12b). In addition, the deepest regions of the Pelican and Cormorant troughs appear to have entered the oil expulsion window (> 0.75% Ro). Today the base of the Eocene succession lies within the oil generation window across a significant proportion of the basin (Figure 6.12a). Oil expulsion from the base of the Eocene succession appears to have been restricted to a central north-south zone along the axis of the basin, within the Cormorant, Yolla and Pelican troughs.

Prior to 15 Ma, the top of the Middle *M. diversus* zone (top of the Bass Megasequence, top Middle Eastern View Group) had not entered the oil generation window (> 0.6% Ro) (Figure 6.11b). However, the top of the Middle *M. diversus* zone appears to have entered the oil generation window in the central part of the basin within recent times (Figure 6.11a).

Source rock intervals defined for each well by Boreham et al. (2003; Chapter 5) appear to have entered the oil generation window within the central axis of the basin. Maturity models for wells within the central part of the Bass Basin indicate that the Paleocene succession entered the oil generation window following deposition of the "Demons Bluff" regional sealing unit (~ 36 to 40 Ma). Therefore, the source rocks linked to major oil accumulations within the basin appear to have entered the oil generation window following

deposition of regional sealing units, and after the major trap forming structural events of the Late Cretaceous and Early Eocene.

To investigate the timing of hydrocarbon generation and expulsion from deeper undrilled sequences within the basin, maturation histories were defined for the four pseudowell sections modelled (Figures 6.16 and 6.17). A palaeoheatflow model defined for the Durroon-1 well (Model 1) was applied to all four models, incorporating a rapid increase in heatflow during the deposition of Cenomanian to Campanian units, followed by constant heatflow (present levels) from ~ 65 Ma to the present (Figure 6.13).

Within the Cormorant, Yolla and Pelican troughs, the Otway Megasequence appears to have passed through the oil and gas generation windows during the Late Cretaceous deposition of the overlying Durroon Megasequence (Tasman Rift Phase; "Lower Eastern View Group") (Figures 6.16 and 6.17). The Cenomanian to Campanian Durroon Megasequence passed into the oil generation window soon after deposition. It passed completely into the gas generation window by the Eocene within the Cormorant Trough, but maintained a longer residence time within the oil generation and expulsion windows (until the Miocene) within the Yolla and Pelican troughs.

Within the Durroon Sub-basin, the Otway Megasequence passed into the oil and gas generation window during the rapid deposition of overlying Durroon Megasequence (Tasman Rift Phase) (Figure 6.17). Following this high heatflow event, the Otway and Durroon megasequences appear to have failed to reach adequate temperatures to restart hydrocarbon generation (Figure 6.17).

6.11 CONCLUSIONS

- Geothermal gradients within the Bass Basin vary from 3.3^{o}C/100m in the Pelican Trough, up to 6.5^{o}C/100m at Konkon-1. A broad decrease in geothermal gradient occurs from the northwest of the basin towards the southeast. A similar pattern is reflected in calculated heatflow values.
- 'Default Thermal History' (DTH) models of 13 wells from the Bass Basin indicate that the Late Cretaceous to Recent succession is experiencing maximum temperatures today. The majority of wells show a strong correlation between measured and predicted VR profiles.
- DTH models of Koorkah-1, Chat-1, and Durroon-1 display elevated calculated VR profiles with respect to measured VR values, indicating they may have been subjected to a recent heating event (< 2 Ma).
- Igneous intrusions within the Cainozoic succession produced localised elevated maturity above regional profiles defined by calculated VR profiles. Future work involving smaller scale investigations of hydrocarbon generation should consider the impact of igneous activity on hydrocarbon generation within the basin.
- The distribution of VR across the Bass Basin, based on calculated VR profiles (DTH models, ignoring localised igneous events) highlights the following:
    - Depth to the oil generation window (0.65% Ro) varies between ~1.6 and 2.4 km below seafloor. The average depth to the oil generation window across the basin is 2.0 km below seafloor.

- Depth to the oil expulsion window (0.75% Ro) varies between ~2.3 and 3.0 km below seafloor. The average depth to the oil expulsion window across the basin is 2.6 km below seafloor.
- The base of the "Demons Bluff" regional sealing facies is immature for oil generation across the basin, with an average calculated VR of 0.43%.
- The top of the Middle *M. diversus* zone (top of the Narimba Sequence, top "Middle Eastern View Group") has an average VR across the basin of 0.59%. The top of this zone has entered the oil generation window in a north-south oriented region, directly overlying the Cormorant, Yolla, and Pelican troughs.
- The top of the Lower *L. balmei* zone (top Paleocene) has an average VR across the basin of 0.71%, within the defined oil generation window. The top of the Paleocene sequence has entered the oil generation window within the central area of the basin, and the oil expulsion window along a north-south oriented central axis of the basin.

- Thermal history models based on current AFTA and VR data from the Durroon-1 well are equivocal. VR data are consistent with a maximum temperature at present day (DTH model), whereas the thermal history indicated by AFTA data implies a cooling of 10 to 35^{o}C in the mid-Cretaceous (Duddy, 1992). To constrain palaeoheatflow from the Durroon-1 well, a more extensive suite of VR data and revised AFTA analysis is required.
- Burial geohistory diagrams of the wells studied indicate a consistent rate of subsidence and sedimentation from the Late Cretaceous to the Recent, reflecting the post-rift depositional setting.
- The timing of hydrocarbon generation and expulsion within the Bass Basin, as defined by the DTH models from thirteen wells across the basin indicates:
  - The base of the source-rich (oil-prone) Early Eocene coal sequences entered the oil generation window (> 0.65% Ro) after deposition of the "Demons Bluff" regional sealing facies (~ 34 Ma).
  - By the Middle Miocene (~ 15 Ma), significant structural reactivation was occurring. The base of the Eocene succession entered the oil generation window along the central axis of the basin during the Middle Miocene, while in the deepest regions of the Cormorant, Yolla and Pelican Troughs, sediments entered the oil expulsion window (> 0.75% Ro).
  - Prior to 15 Ma, the top of the Middle *M. diversus* succession (top of the Narimba Sequence, "top Middle Eastern View Group") had not entered the oil generation window. However, today the top of the Middle *M. diversus* succession appears to have entered the oil generation window in the central part of the basin.
- The defined source rocks linked to hydrocarbon accumulations within the Bass Basin (Early Eocene to Paleocene coals) entered the oil generation window just prior to and following deposition of the regional sealing units, and after the major trap forming structural events of the Late Cretaceous and Early Eocene. These units continued to pass into the oil expulsion window during and after Miocene structural reactivation events within the basin.
- Pseudowell reconstructions and a defined palaeoheatflow model (Model 1, Figure 6.13) indicate that the Otway Megasequence passed through the oil and gas generation windows in deeper parts of the

Bass Basin (Cormorant, Yolla, and Pelican troughs) during the Late Cretaceous, prior to deposition of the regional sealing units.

- The largely undrilled Durroon Megasequence (Tasman Rift Phase, "Lower Eastern View Group") appears to have entered the oil generation window soon after deposition. The sequence passed completely into the gas generation window by the Eocene within the Cormorant Trough, but maintained a longer residence time within the oil generation/expulsion windows (to the Miocene) within the Yolla and Pelican troughs (based on defined palaeoheatflow, Model 1, Figure 6.13).

Table 6.1 Bass Basin Bottom Hole Temperature (BHT) summary

	KB	Water Depth	Total Depth (KB)	BHT Depth	Highest	Horner Corr.	Waples & Ramly (2001)	Geothermal Gradient
Well Name	**m**	**m**	**m**	**m**	**BHT °C**	**BHT °C**	**Corr. BHT**	**°C/100m**
Aroo-1	9.8	76.2	3652.11	3652.10	138.89	145	-	3.73
Bass-1	9.4	80.8	2349.40	2349.40	96.70	-	138.72	5.61
Bass-2	9.4	85.3	1800.45	1800.45	72.20	-	101.3	5.24
Bass-3	9.4	61.6	2433.80	2433.83	97.80	-	140.05	5.42
Chat-1	25.3	81.4	3107.00	3107.00	104.40	110.24	125.02	3.77
Cormorant-1	30.5	73.2	3000.80	3000.76	114.40	124.16	138.76	4.38
Dondu-1	9.8	79.5	2927.00	2926.99	126.70	146.26	162.03	5.29
Durroon-1	9.8	68.6	3024.23	3021.50	91.11	-	114.25	3.47
Flinders-1	22.3	69.3	2718.80	2718.80	126.10	132.18	146.56	5.12
King-1	22	72.8	2225.00	2122.00	102.20	108.34	112.01	4.93
Konkon-1	9.8	70.1	1537.10	1537.11	69.90	-	107.13	6.53
Koorkah-1	22.5	67.6	3146.20	3146.15	131.70	140.86	148.33	4.46
Nangkero-1	9.8	69.8	2877.30	2877.31	97.80	102.49	114.88	3.68
Narimba-1	9.8	77.1	3353.70	3353.71	138.90	147.3	177.23	5.06
Pelican-1	30.48	76.5	3178.50	-	-	-	-	?
Pelican-2	30.5	77.7	3068.10	3068.12	92.20	93.31	110.66	3.33
Pelican-3	9.8	80.2	2905.00	2799.00	95.60	105.85	102	3.32
Pelican-4	25	77.4	3050.70	3050.74	115.60	148.07	171.25	5.40
Pelican-5	22.3	77.4	4267.00	4267.20	177.80	179.33	179.09	4.01
Pipipa-1	21	73	2115.00	2115.01	86.10	96.26	107.79	4.74
Poonboon-1	9.8	78.9	3258.30	3258.31	120.00	124.15	145.49	4.21
Seal-1	25.3	64.6	1669.00	1669.00	74.40	83.49	98.95	5.51
Squid-1	22.3	80.5		-	-	-	-	?
Tarook-1	9.8	79.6	2773.70	2773.68	94.40	118.07	150.38	5.16
Tas Devil-1	21.9	73.8		-	-	-	-	?
Tilana-1	22.3	82	3900.20	3900.22	115.60	120.79	138.68	3.34
Toolka-1A	9.8	78.6	2714.90	2714.85	106.70	108.87	119.05	4.08
White Ibis-1				-	-	-	-	-
Yolla-1	11	79.5	3347.00	3347.01	143.30	157.51	173.69	4.97
Yolla-2				-	-	-	-	-
Yurongi-1	9.8	81.7	3438.40	2438.40	105.60	113.13	124.96	4.81

Single Corrected BHT

Averaged Horner Corrected BHT

Horner Corrected BHT

Figure 6.1 Plot of measured (uncorrected) and corrected temperatures with depth in Pelican-5 and Yolla-1. Bottom Hole Temperatures (BHT) were corrected by the methods established by Waples and Ramly (2001). Note that corrected BHT values are consistent with the temperature profile of the DST data.

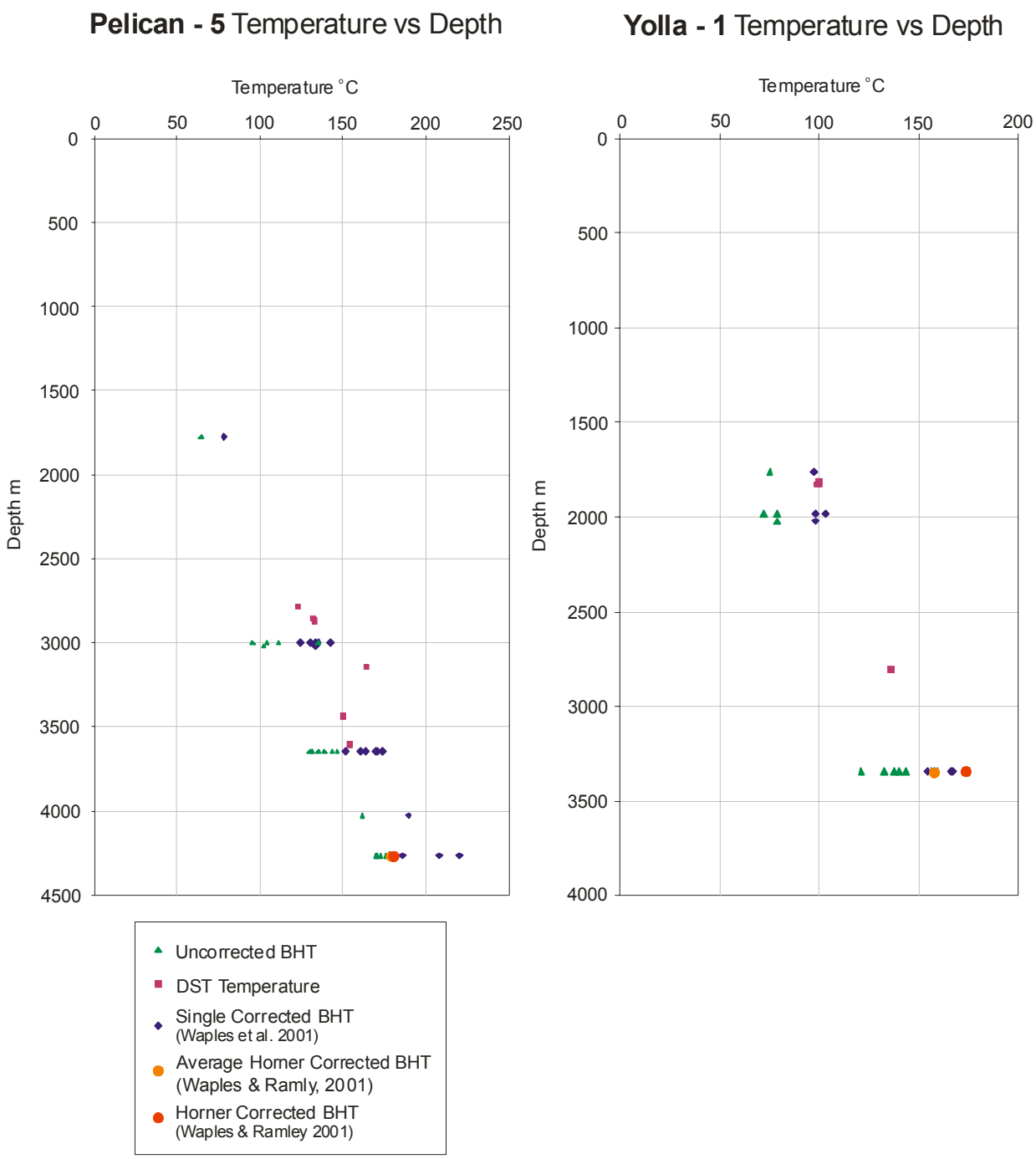

Figure 6.2 Areal distribution of geothermal gradients (coloured circles), generalised structure (modified from Lennon et al., 1999) and basement (Teasdale et al., 2001).

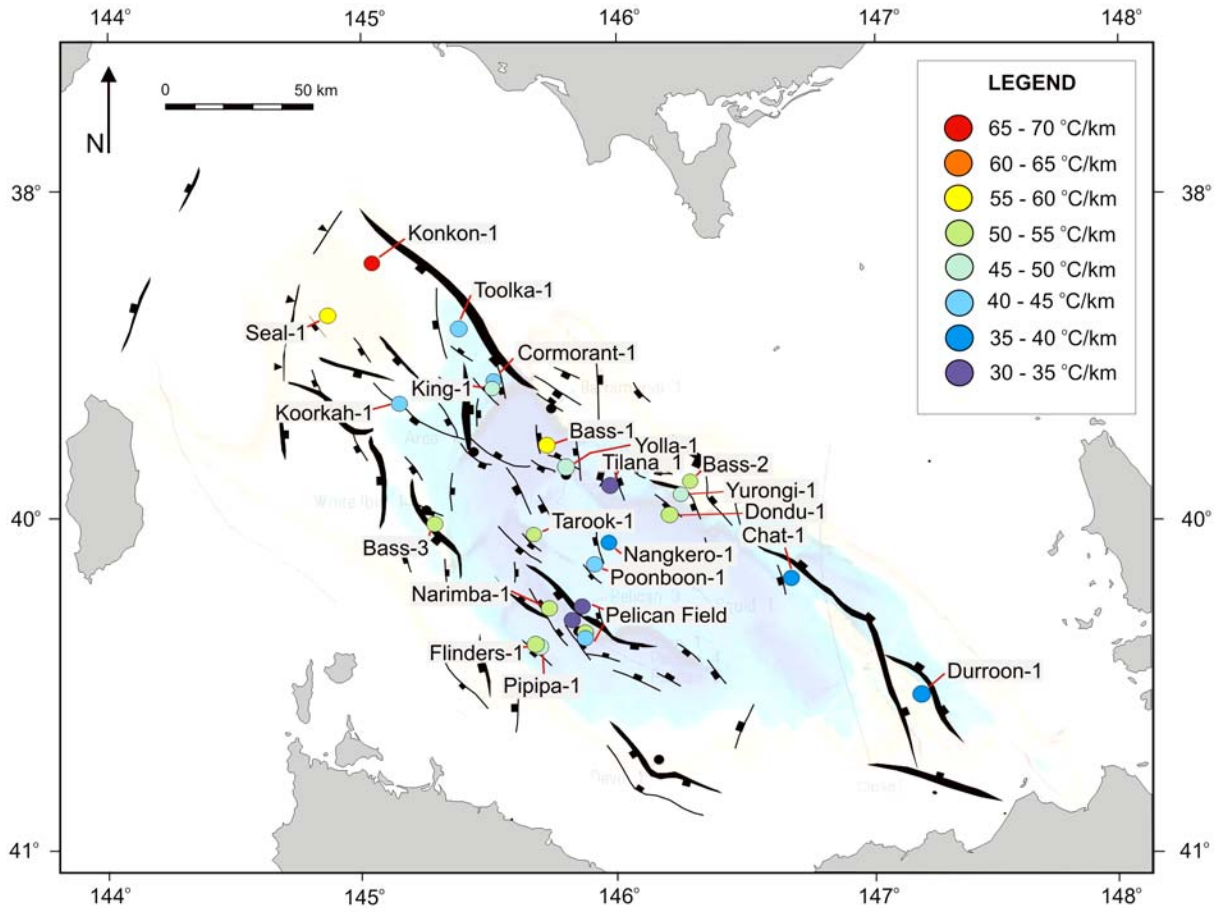

Figure 6.3 Areal distribution of heatflow values (coloured circles). Generalised structure map modified from Lennon et al. (1999) and Teasdale et al. (2001).

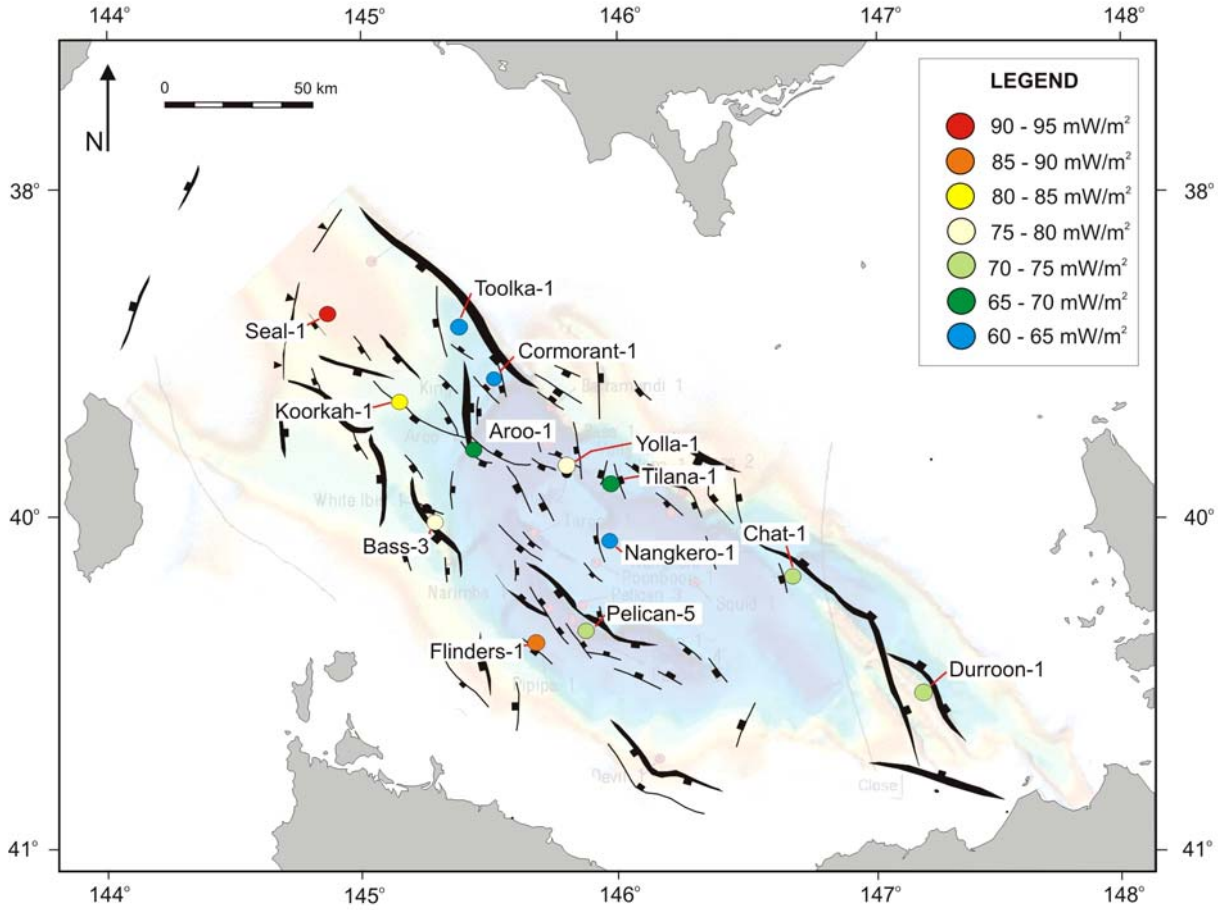

Figure 6.4 Location of wells and pseudowells studied (map modified from Lennon et al., 1999).

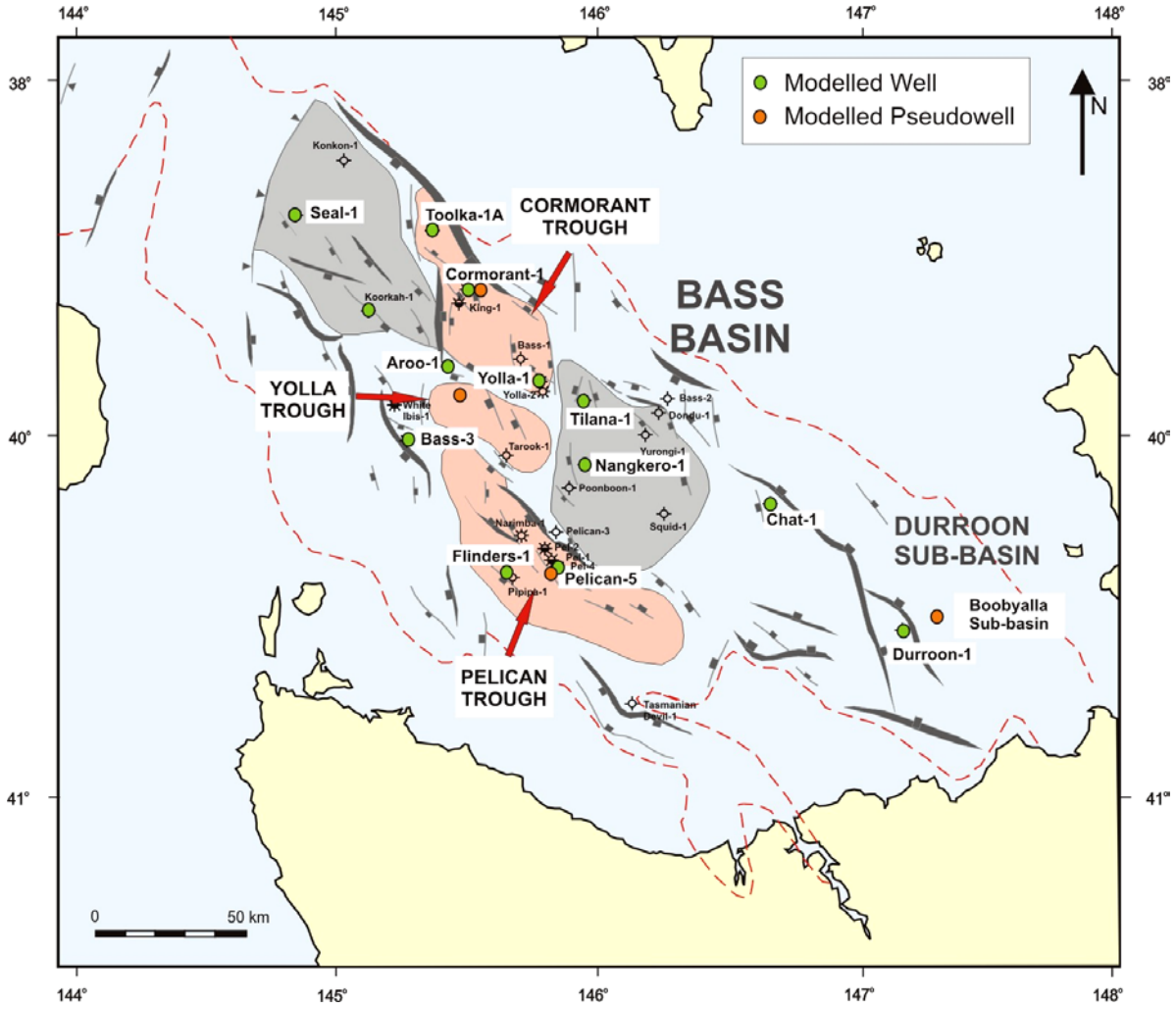

Figure 6.5a Maturity depth plots for Default Thermal History (DTH) models (constant heatflow through time).

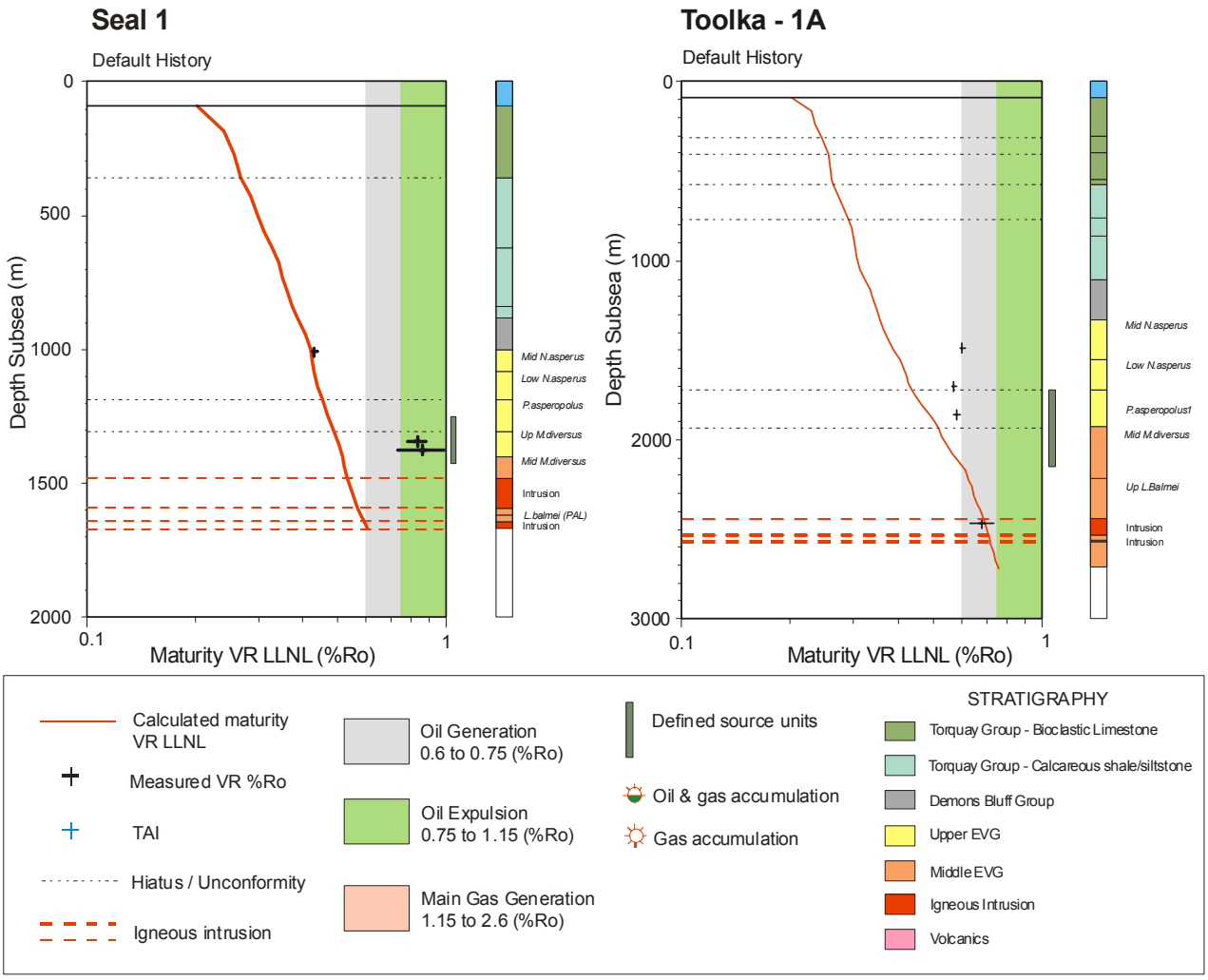

Figure 6.5b Maturity depth plots for Default Thermal History (DTH) models (constant heatflow through time).

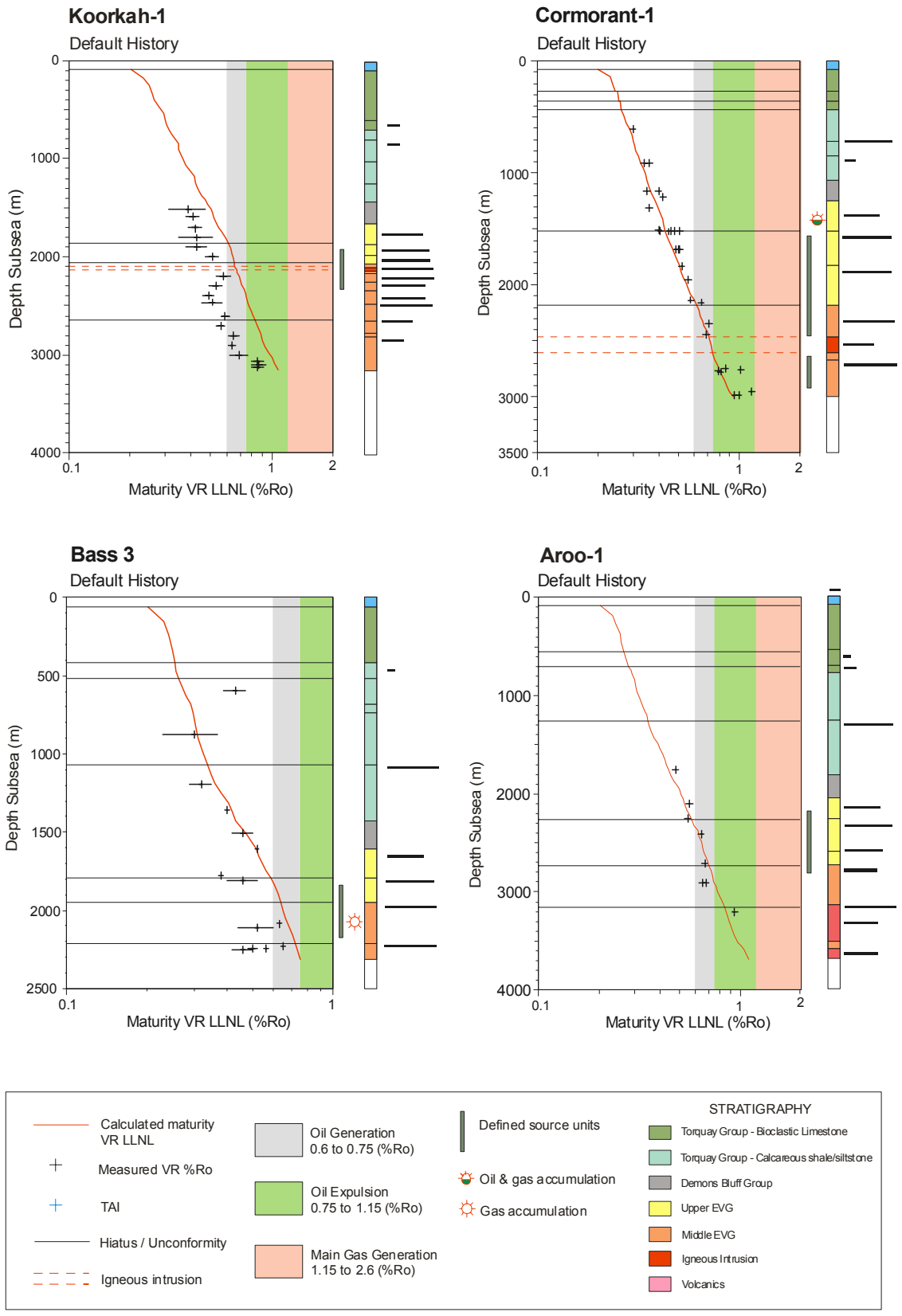

Figure 6.5c Maturity depth plots for Default Thermal History (DTH) models (constant heatflow through time).

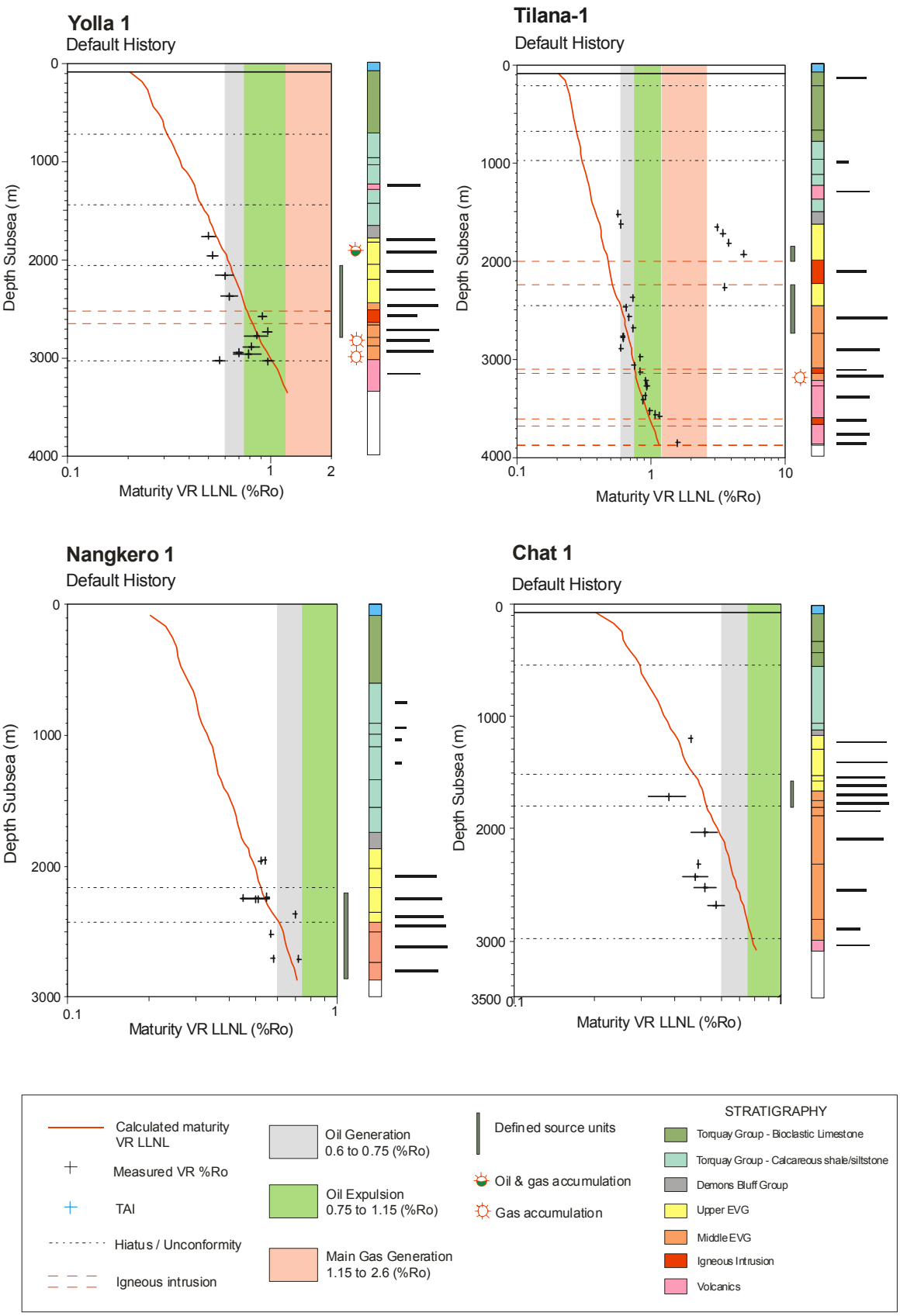

Figure 6.5d Maturity depth plots for Default Thermal History (DTH) models (constant heatflow through time).

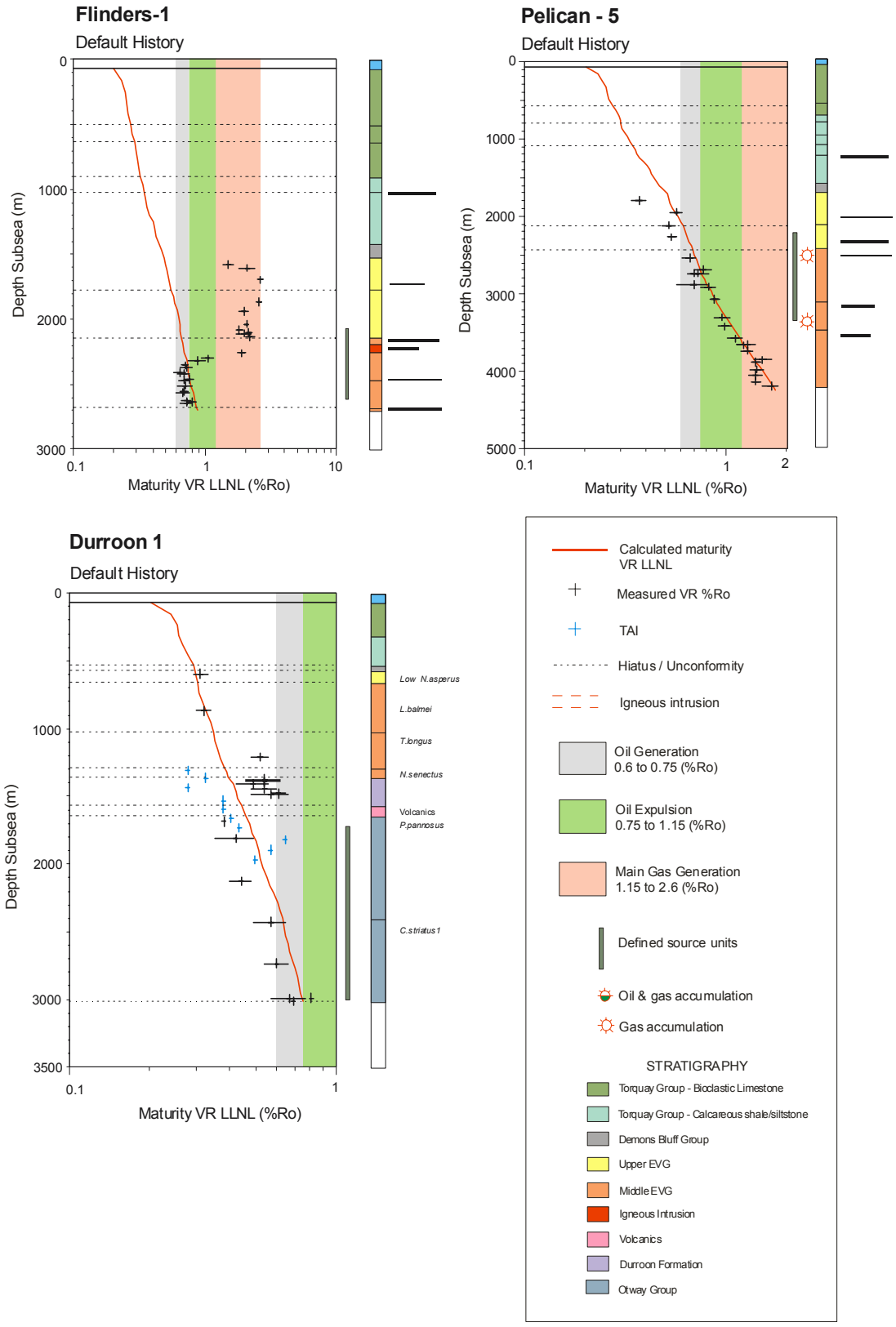

Figure 6.6 Depth at metres below seafloor (mbsf) to the 0.6% Ro isoreflectance surface (map modified from Lennon et al., 1999).

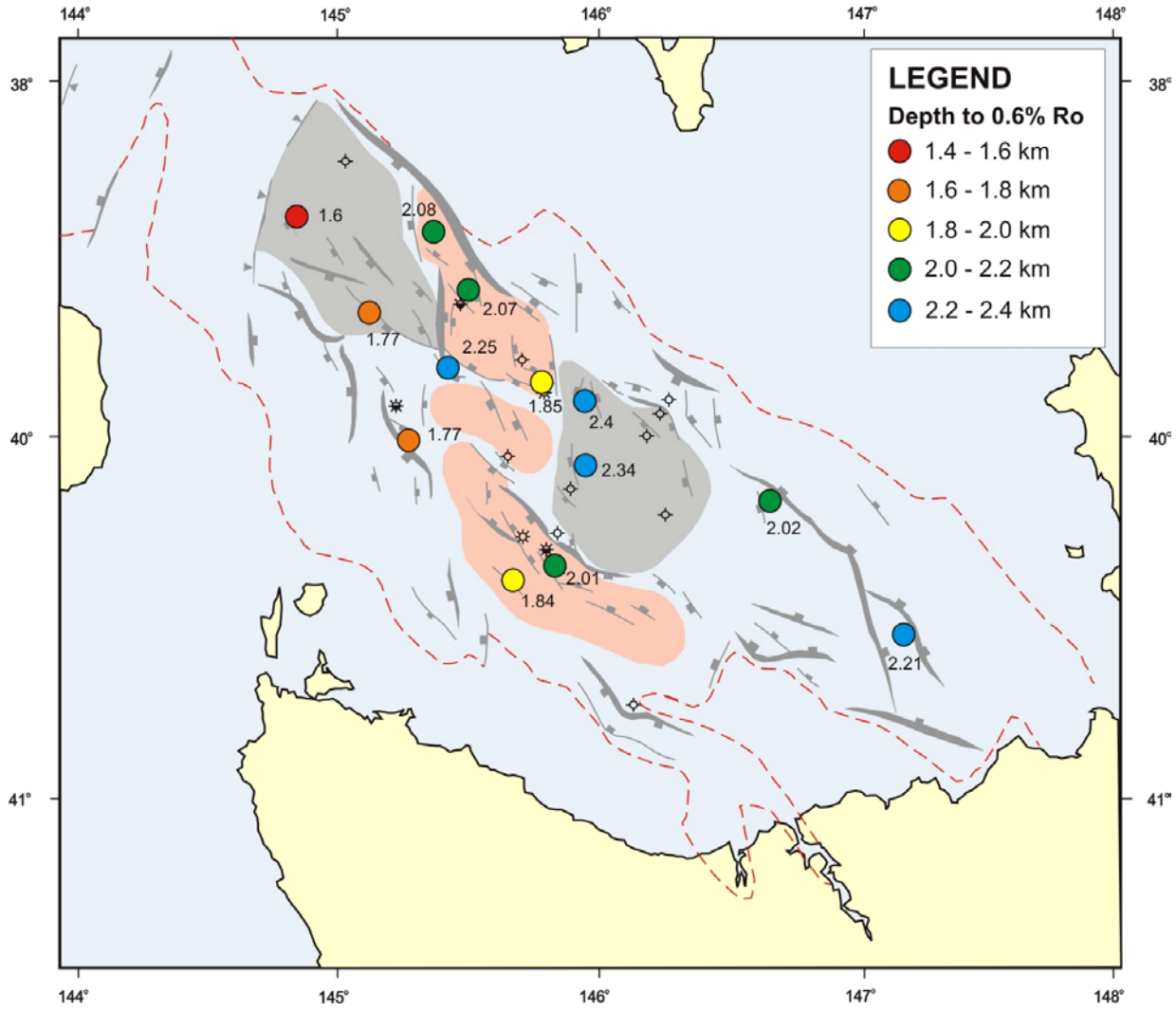

Figure 6.7 Depth (mbsf) to the 0.75% Ro isoreflectance surface (map modified from Lennon et al., 1999).

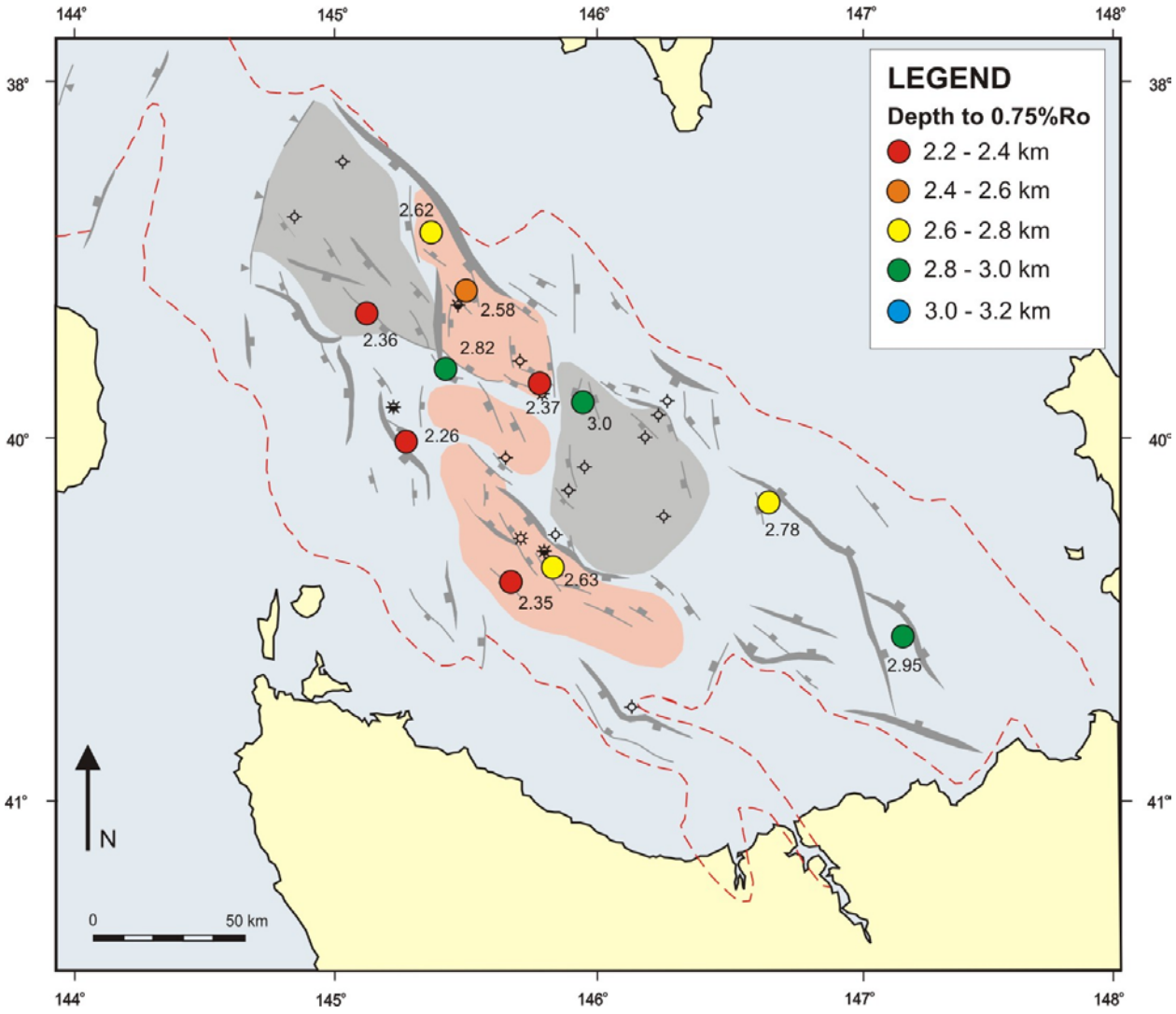

Figure 6.8 Areal variation in calculated maturity at 2000 mbsf (map modified from Lennon et al., 1999).

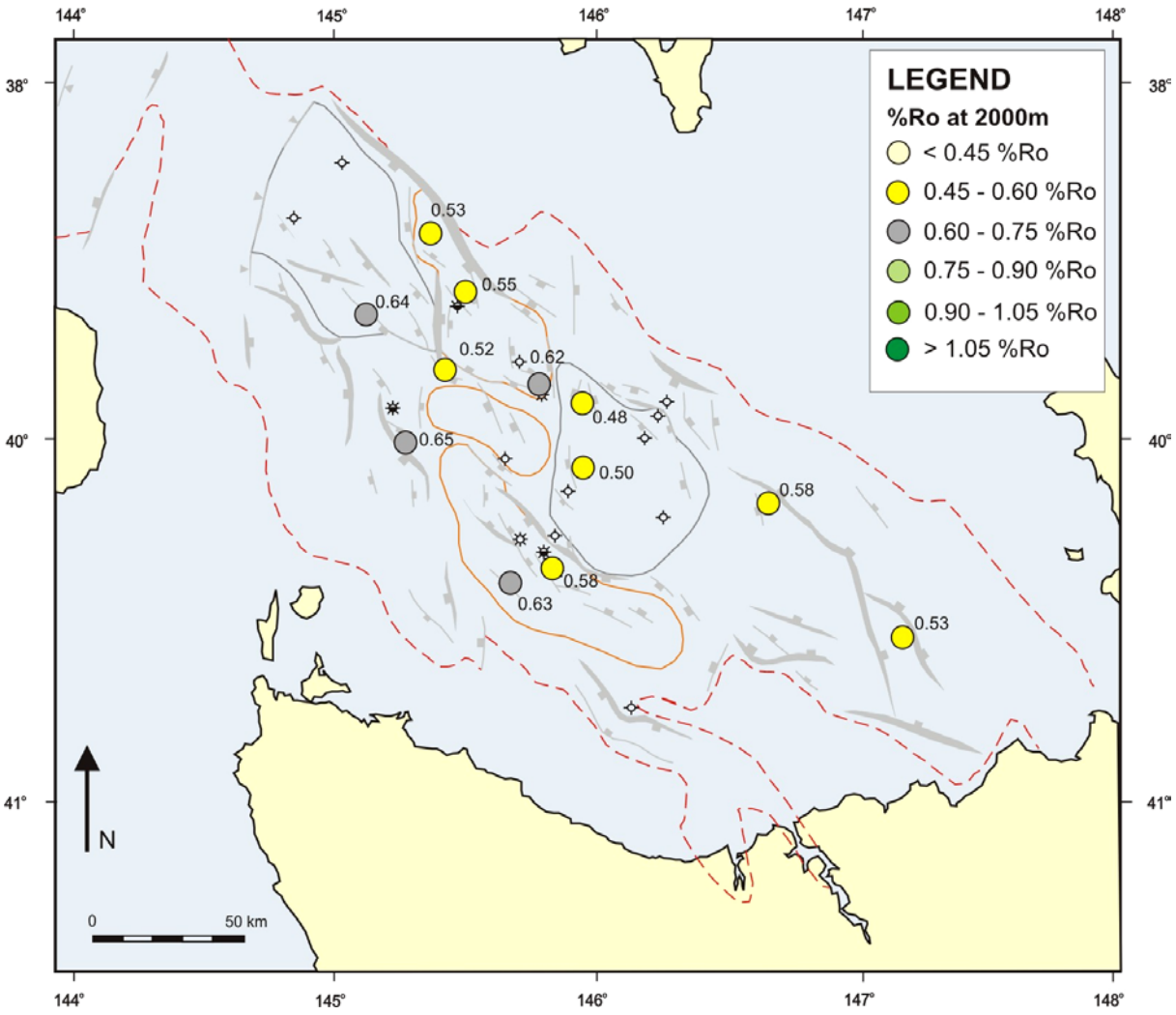

Figure 6.9 Areal variation in calculated maturity at 2500 mbsf (map modified from Lennon et al., 1999).

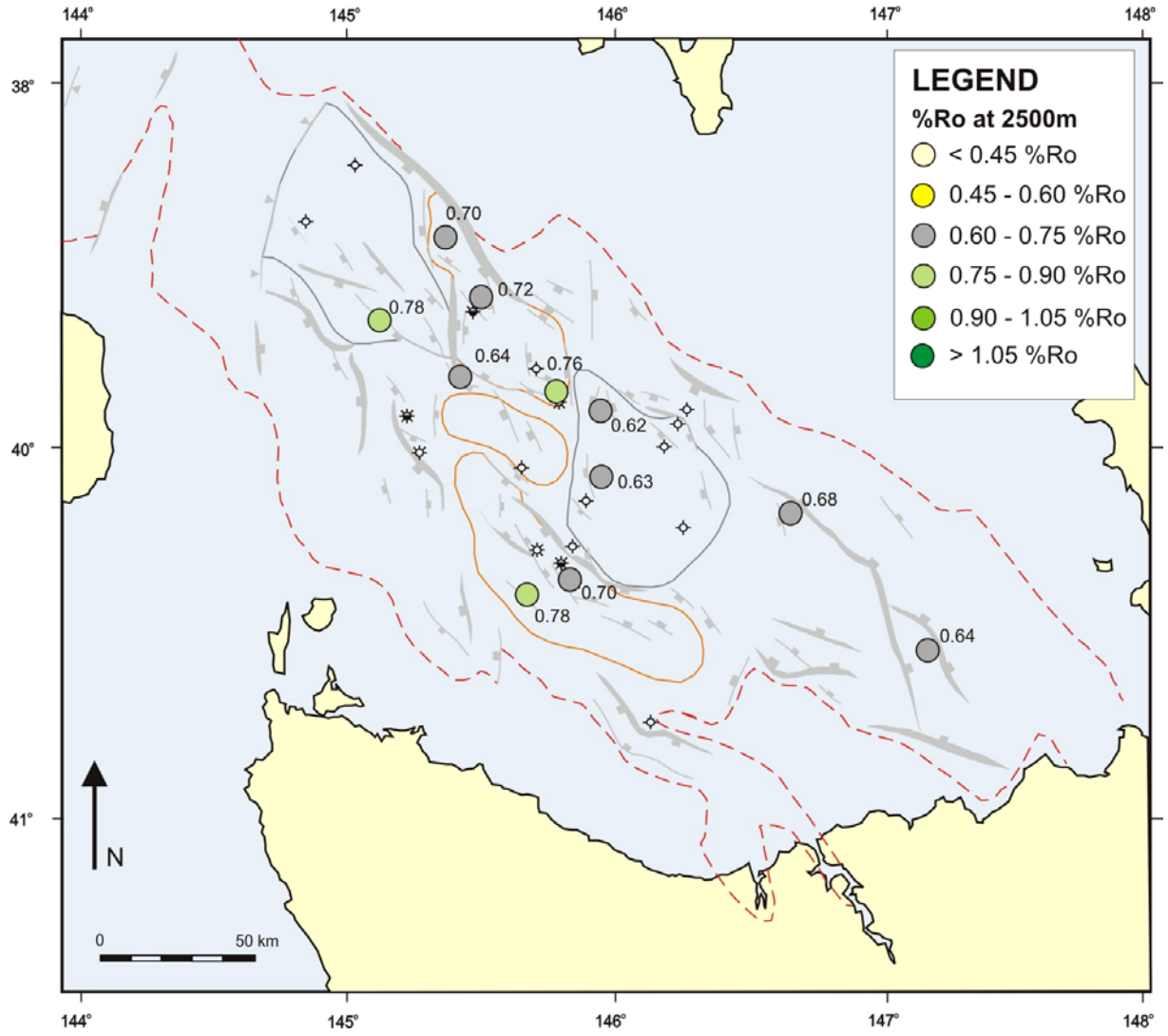

Figure 6.10 Areal variation in calculated maturity at the top of the Middle Eocene (top of the EVG; map modified from Lennon et al., 1999).

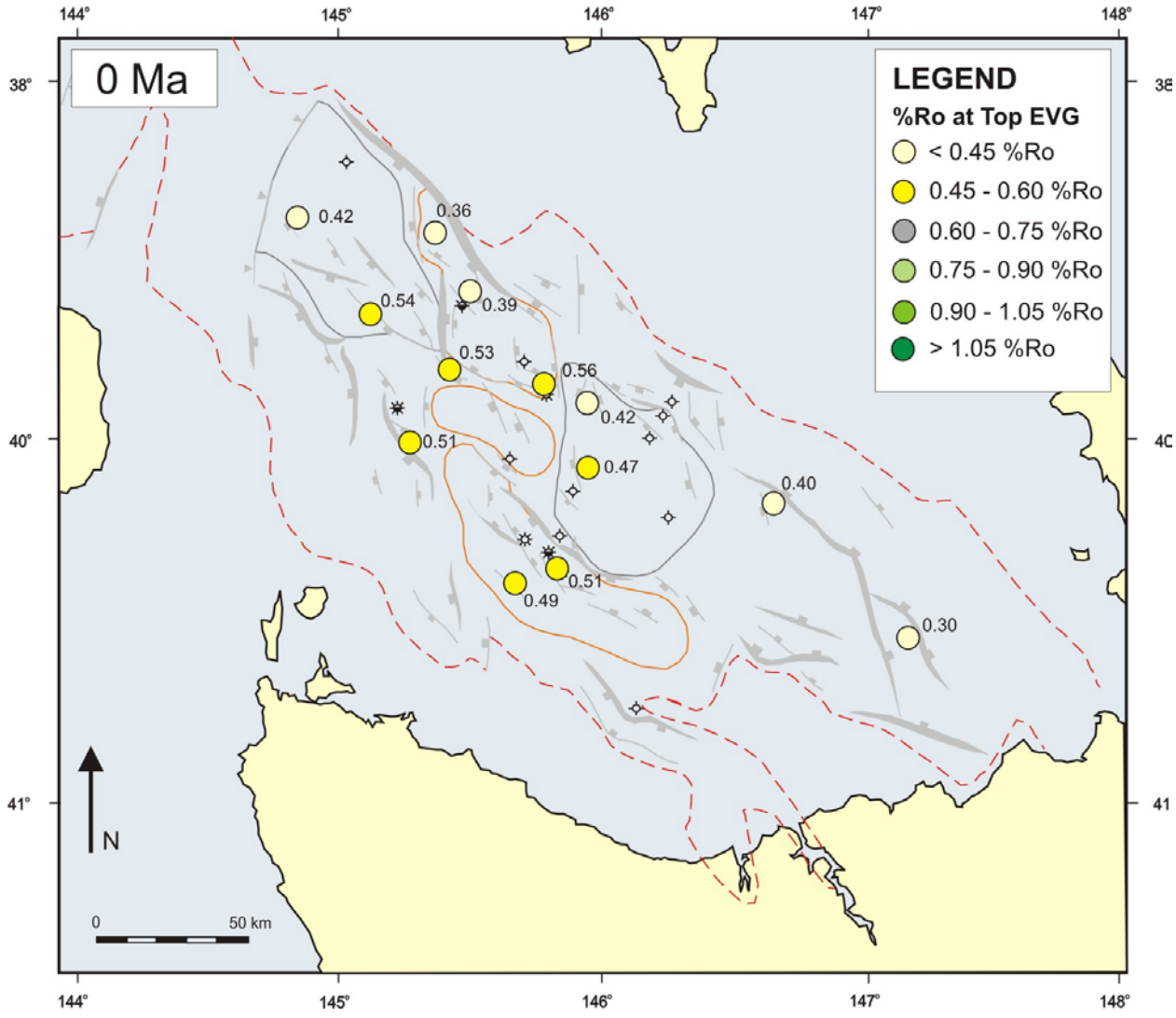

Figure 6.11a Areal variation in calculated maturity at the top Narimba Sequence (top of Middle EVG; top Middle *M. diversus* zone; map modified from Lennon et al., 1999).

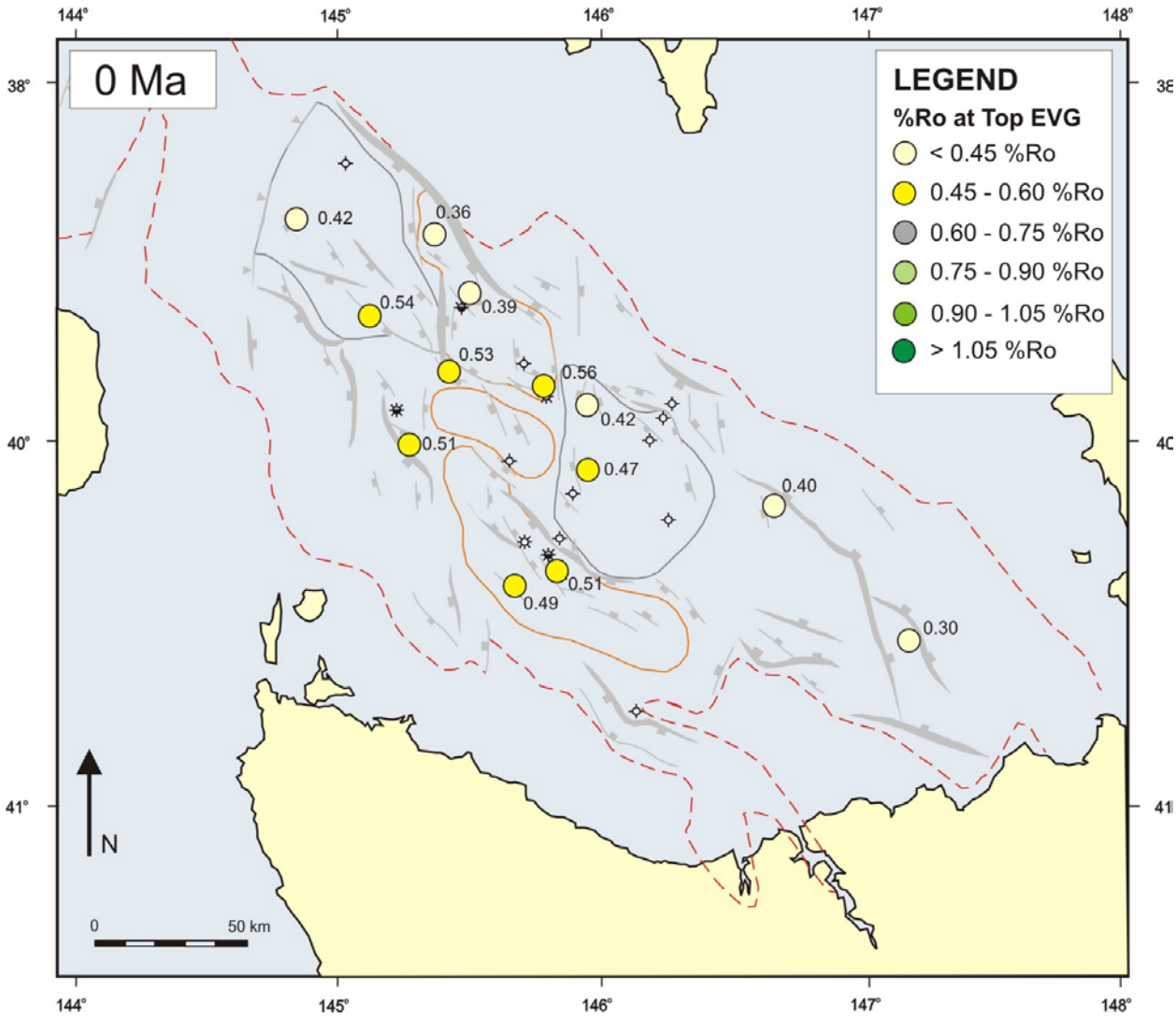

Figure 6.11b Areal variation in calculated maturity at the top of the Narimba Sequence at 15 Ma (top Middle EVG; top Middle *M. diversus* zone; map modified from Lennon et al., 1999).

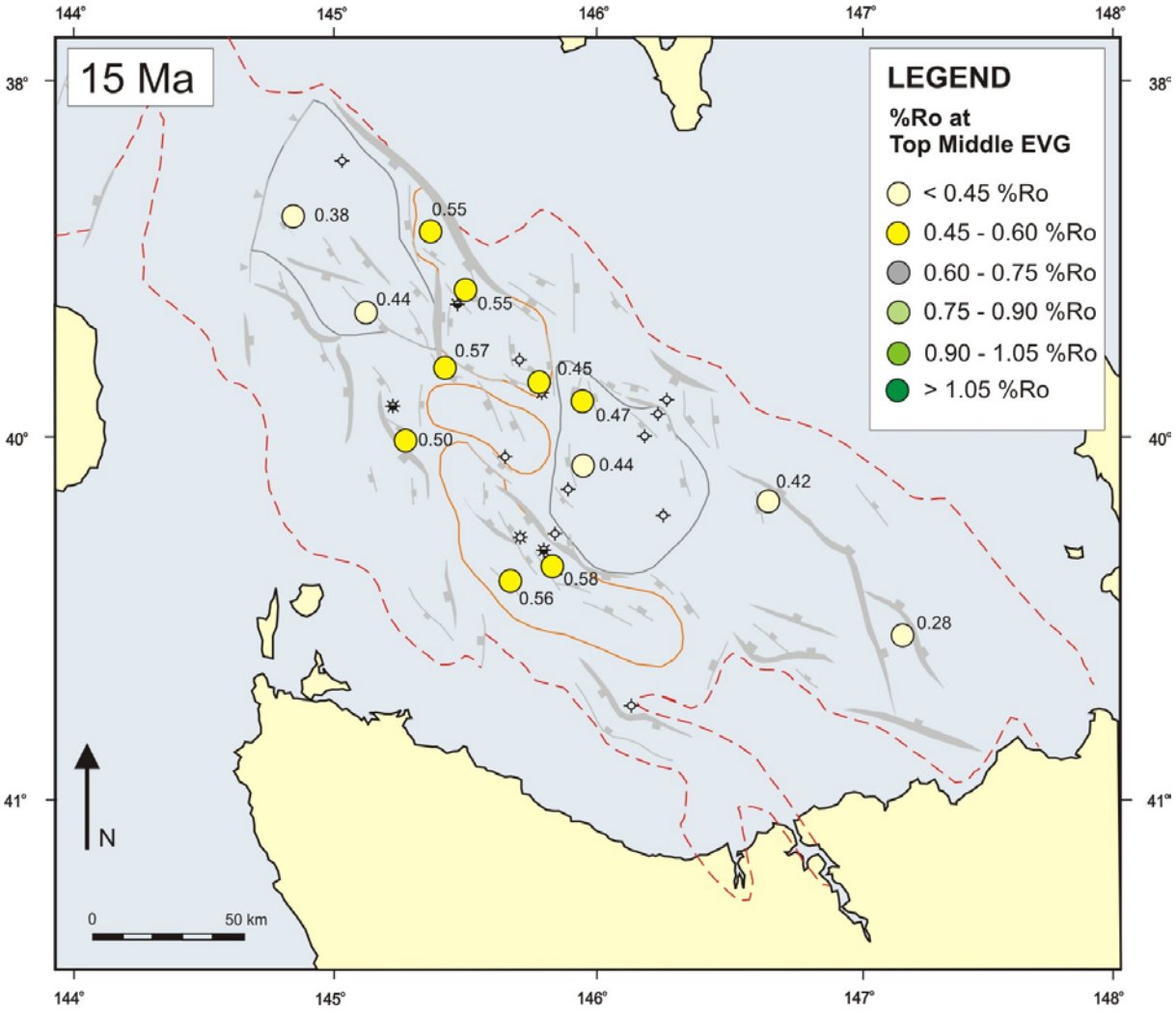

Figure 6.12a Areal variation in calculated maturity at the top Paleocene (top Lower *L. balmei* zone; map modified from Lennon et al., 1999).

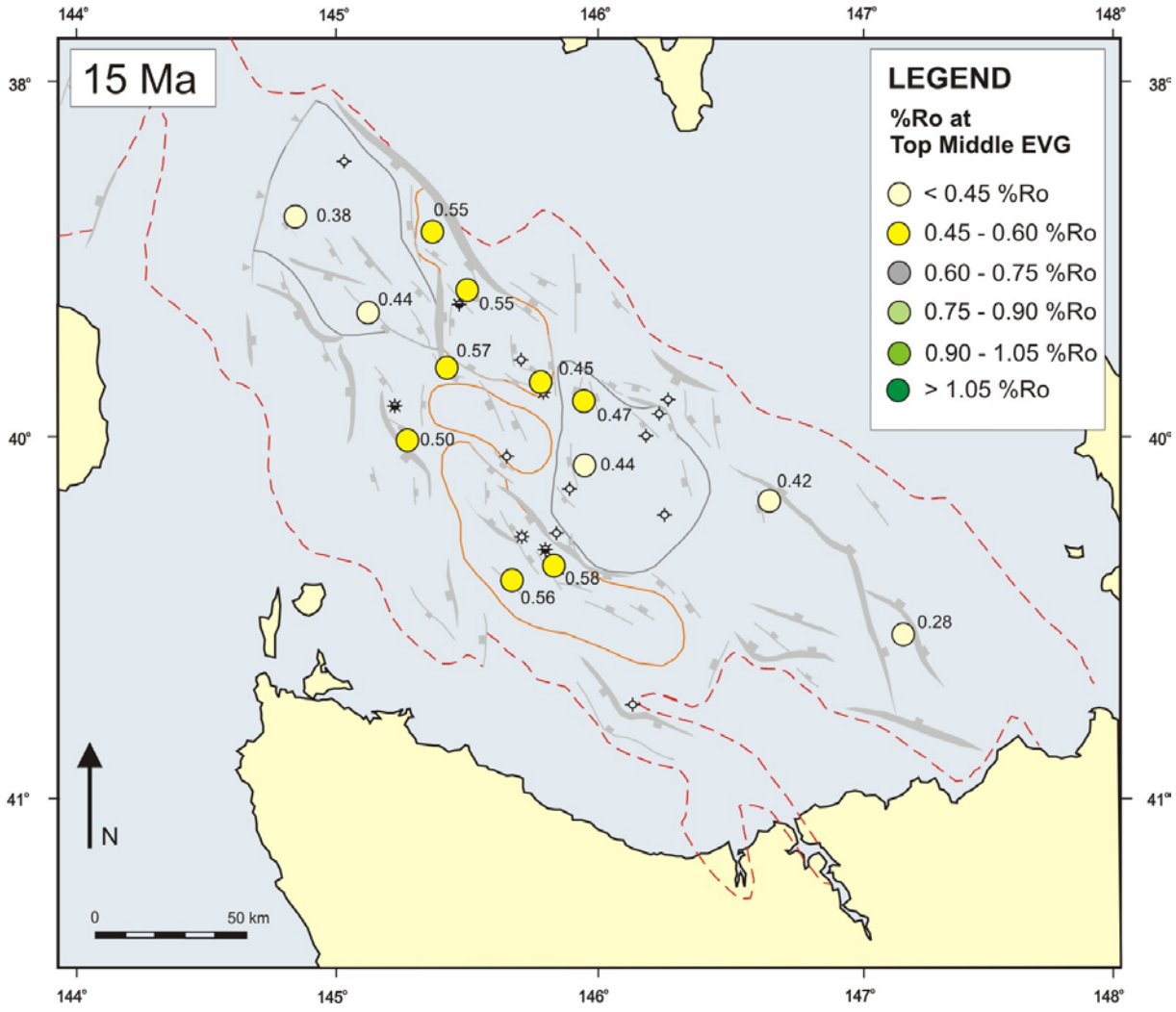

Figure 6.12b Areal variation in calculated maturity at the top of the Narimba Sequence at 15 Ma (Middle EVG; top of Middle *M. diversus* zone; map modified after Lennon et al., 1999).

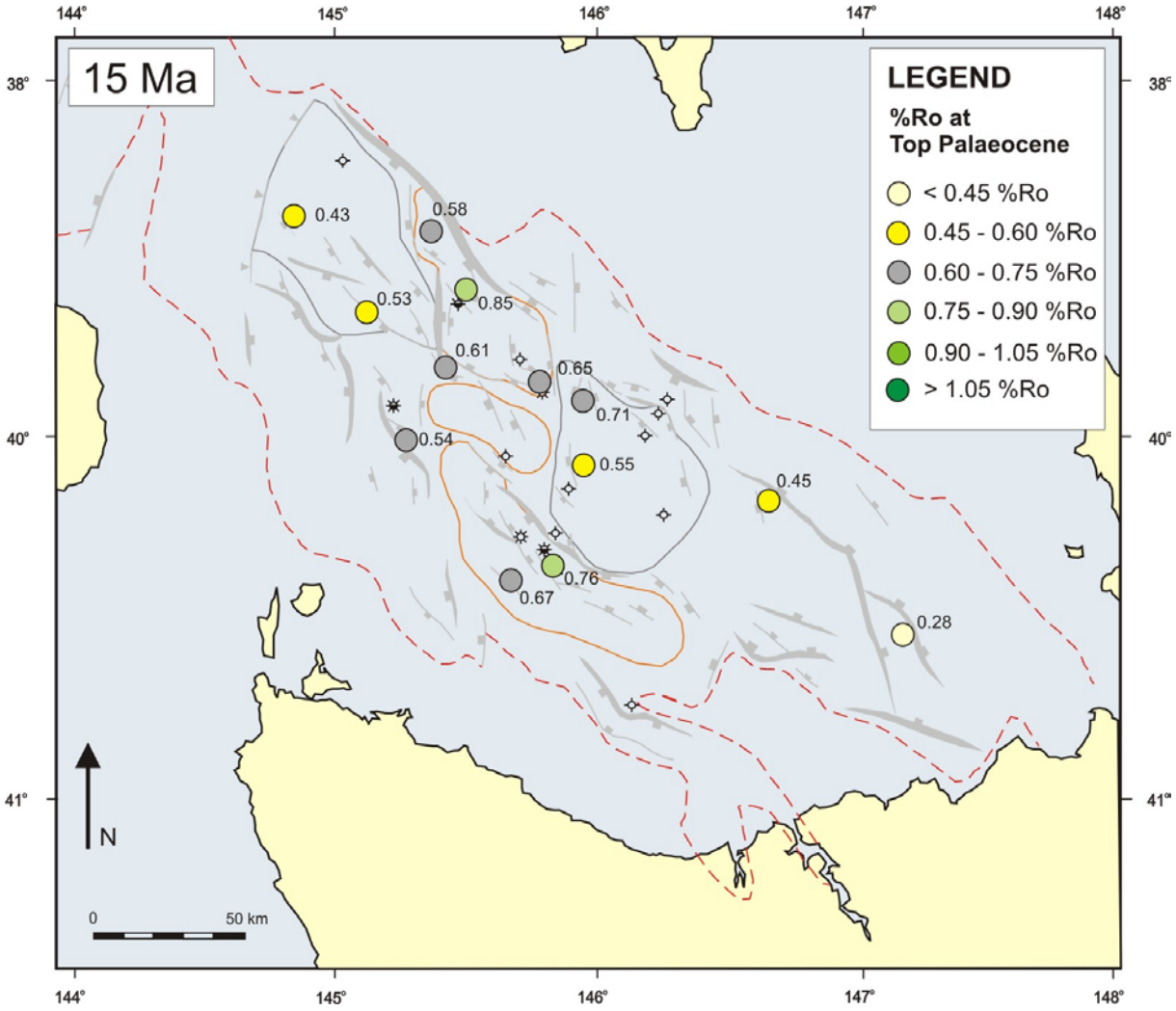

Figure 6.12c Areal variation in calculated maturity at the Narimba Sequence at 34 Ma (top Middle EVG; top of Middle *M. diversus* zone; map modified after Lennon et al., 1999).

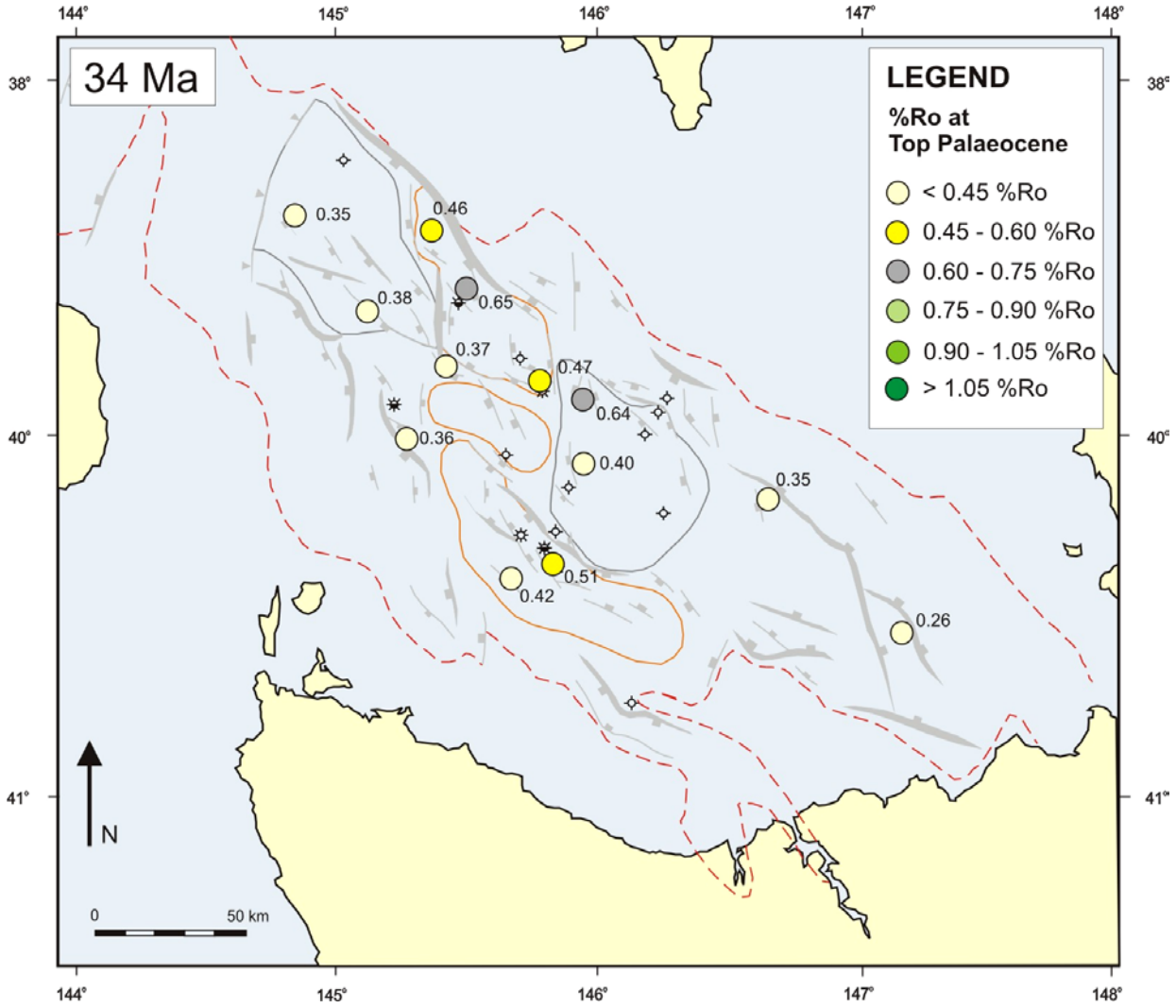

Figure 6.13 a) Palaeo-heatflow models derived from regional tectonic model. Model 1 shows a rapid increase in heatflow due to the Durroon Rift Phase (Tasman Rifting), followed by constant heatflow from the Paleocene onwards. Model 2 includes lower heatflow from the Paleocene and a late-stage heating event. b) Temperature through time with AFTA thermal history solution for sample L4-118 (3023 m) from Durroon-1. c) Maturity depth plots for palaeo-heatflow Models 1 and 2.

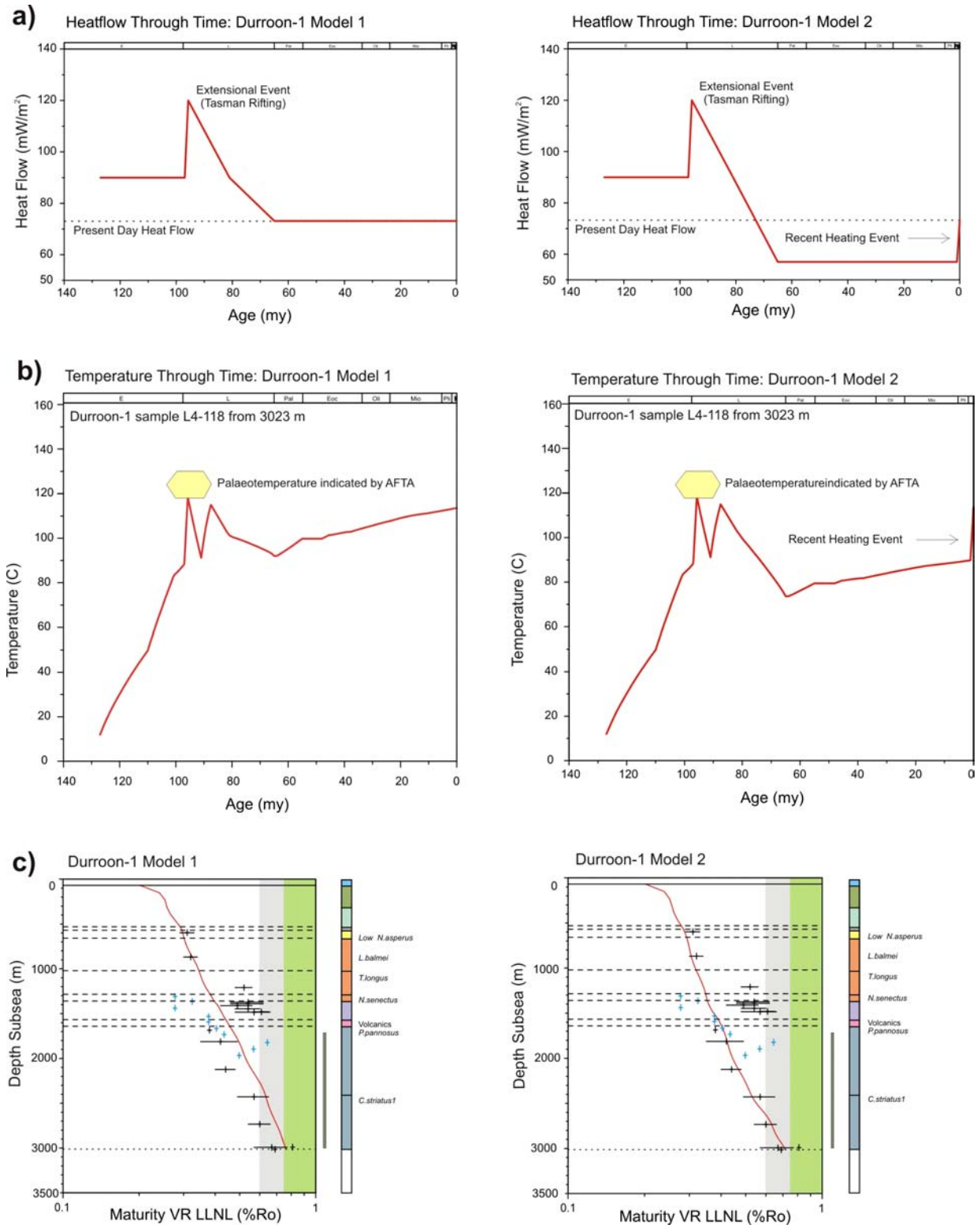

Figure 6.14a Default burial history and maturity models for wells studied, derived from the preserved stratigraphy. Amounts of uplift were estimated from seismic mapping.

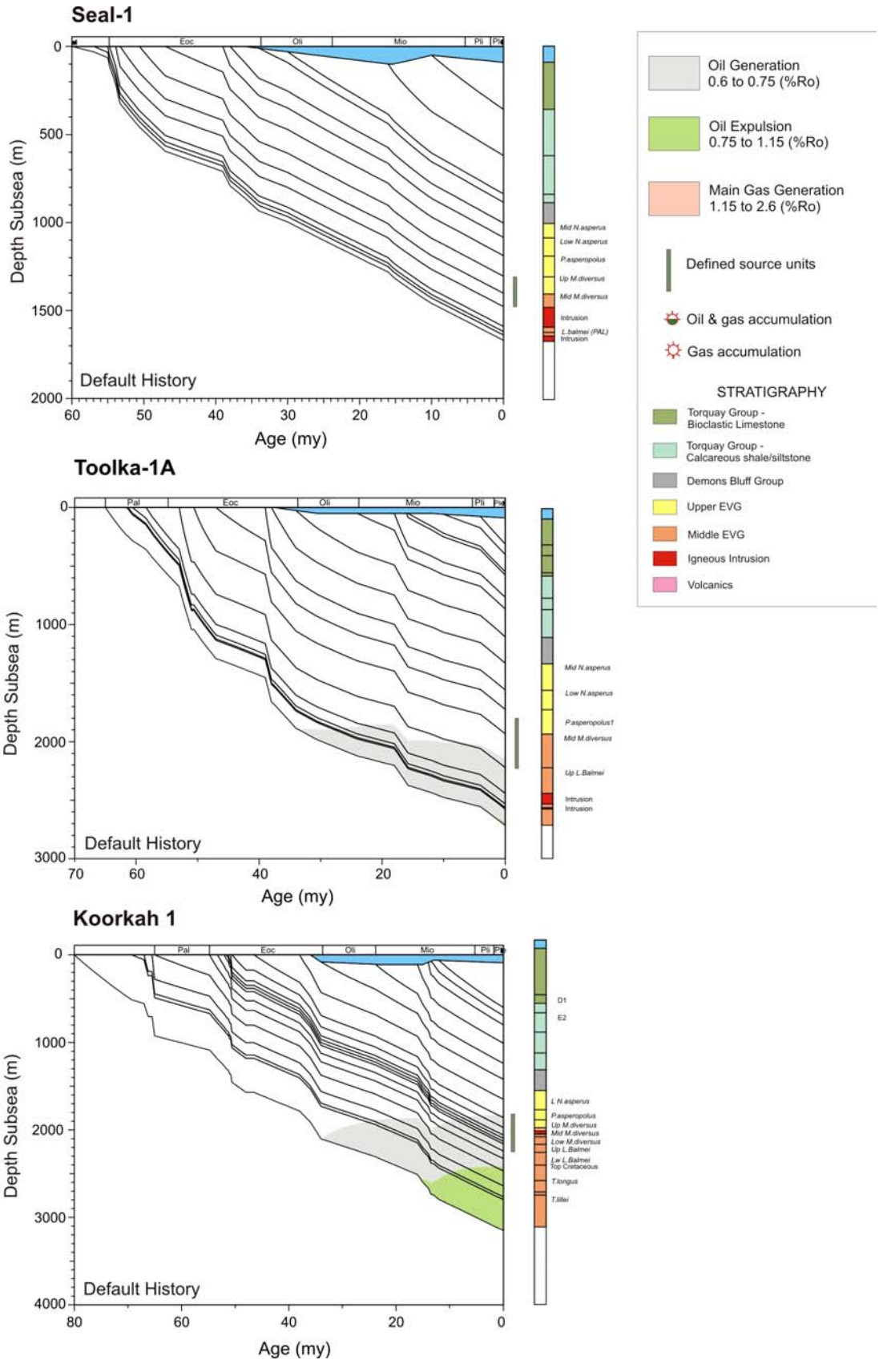

Figure 6.14b Default burial history and maturity models for wells studied, derived from the preserved stratigraphy. Amounts of uplift were estimated from seismic mapping.

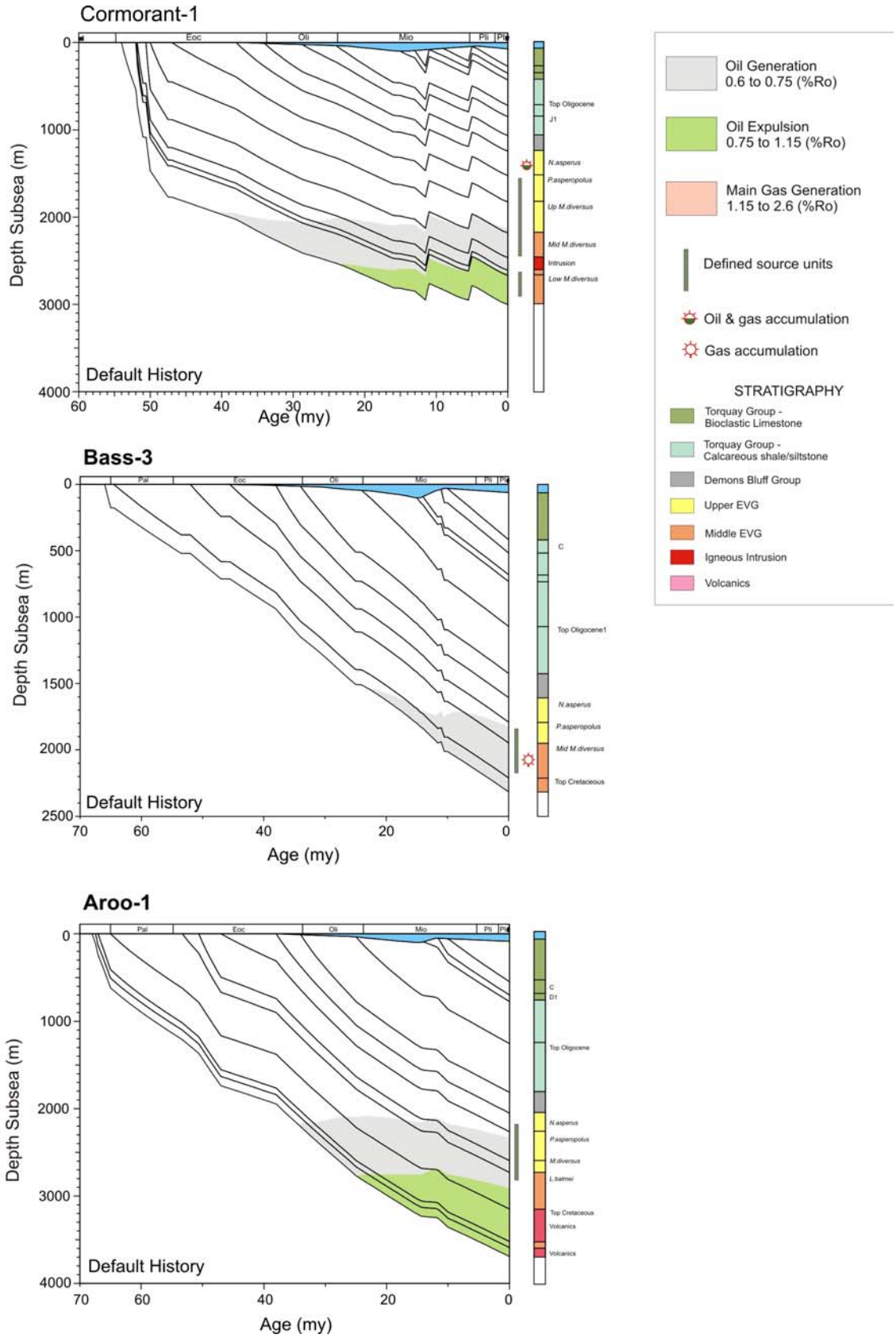

Figure 6.14c Default burial history and maturity models for wells studied, derived from the preserved stratigraphy. Amounts of uplift were estimated from seismic mapping.

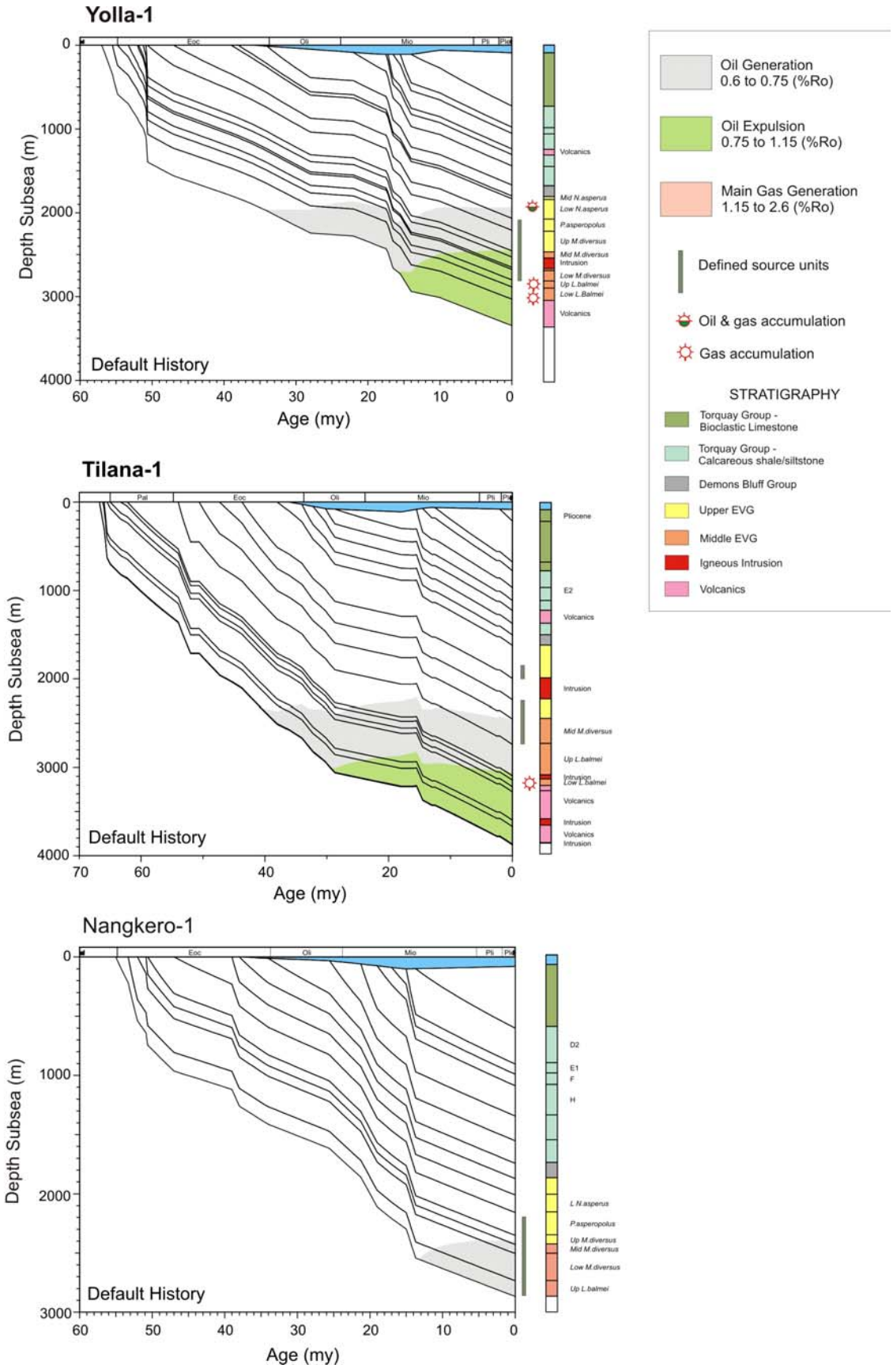

Figure 6.14d Default burial history and maturity models for wells studied, derived from the preserved stratigraphy. Amounts of uplift were estimated from seismic mapping.

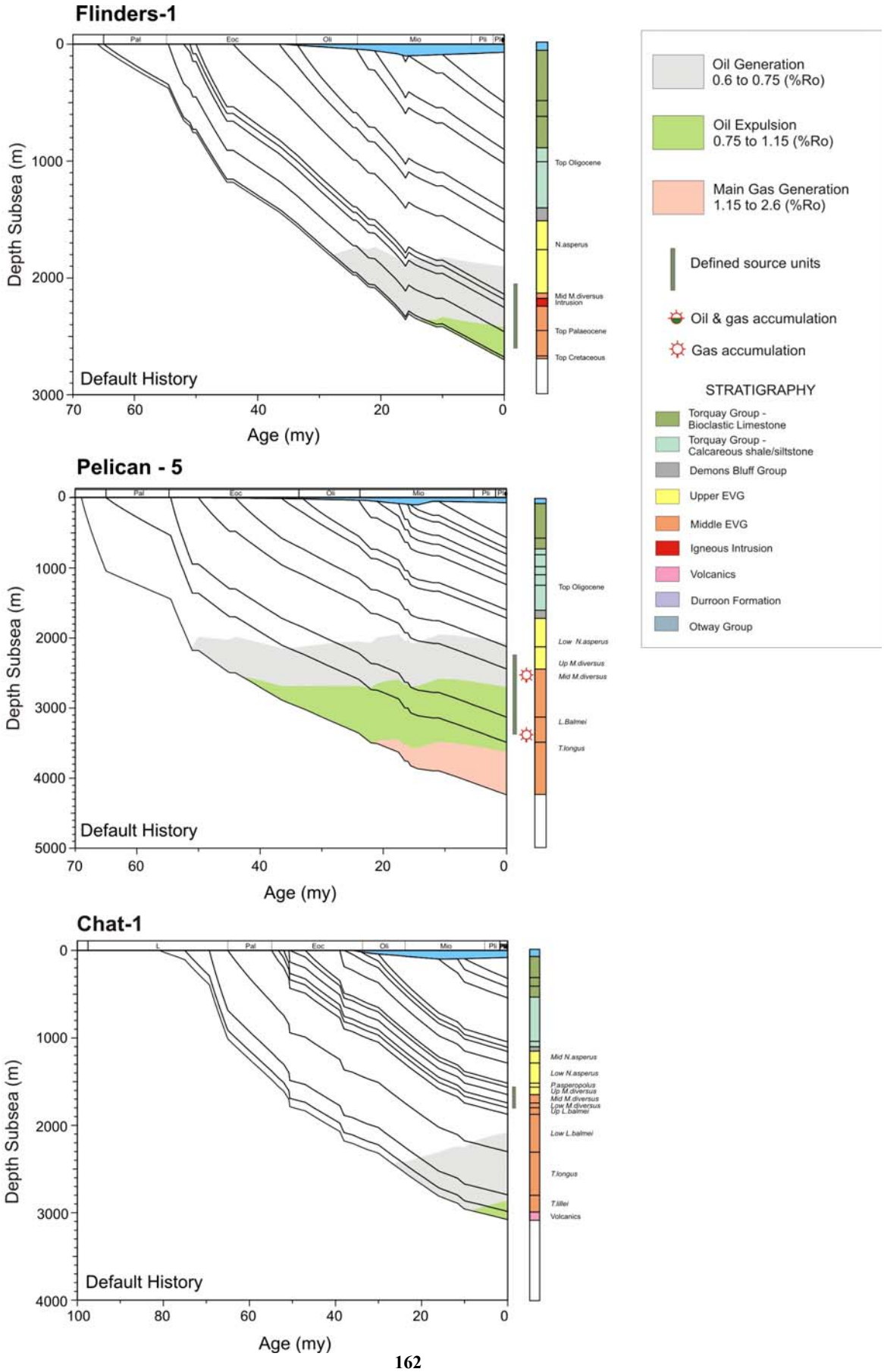

Figure 6.15 A) Subsidence and maturity curve based on Default Thermal History (DTH) for Durroon-1. B) Subsidence and maturity curve based on palaeo-heatflow Model 1 (see Figure 6.6). C) Subsidence and maturity curve based on palaeo-heatflow Model 2 (see Figure 6.6). The amount of mid-Cretaceous uplift was estimated from seismic mapping.

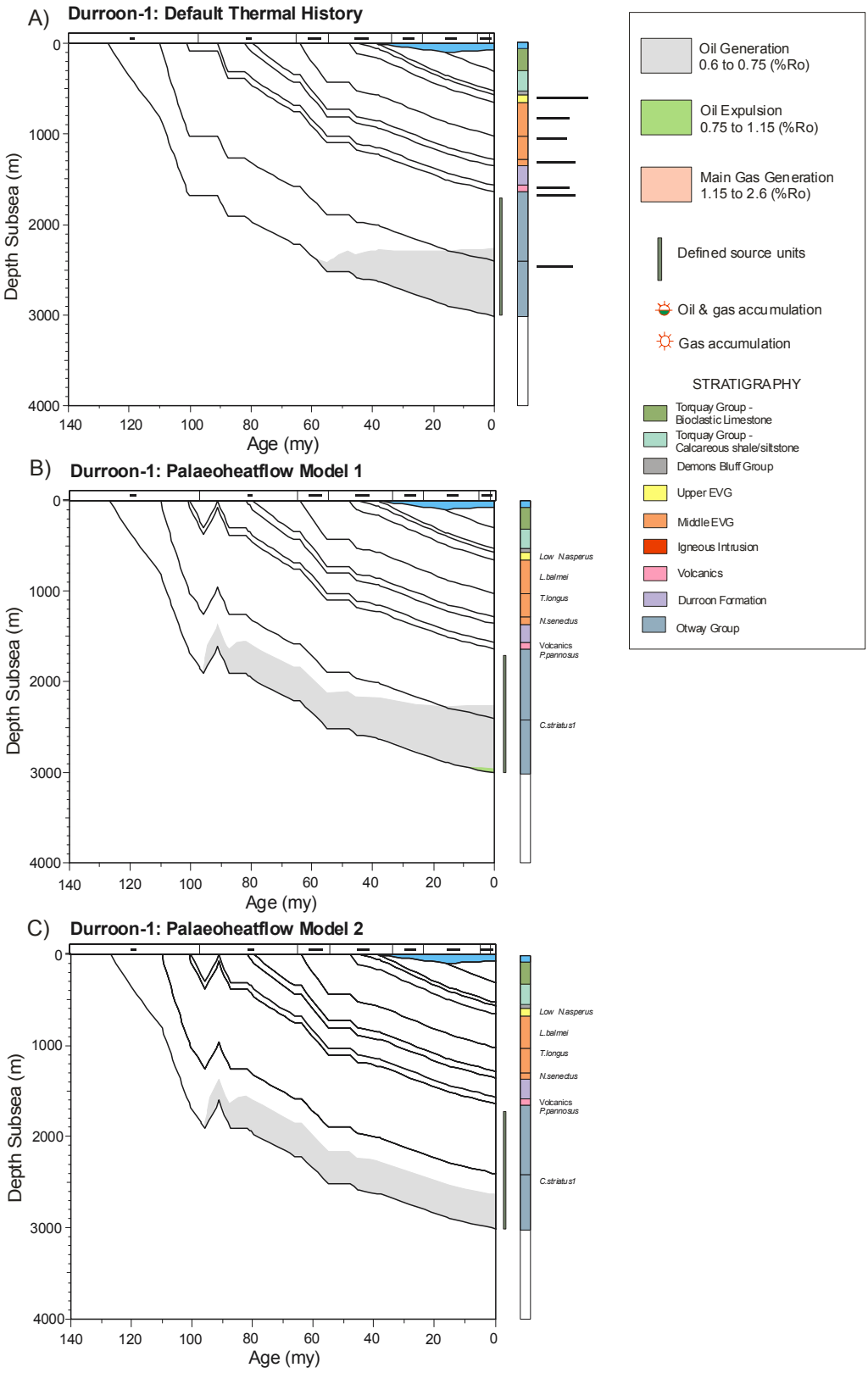

Figure 6.16 Subsidence and maturity curves for pseudowells in the Cormorant and Pelican troughs (extended at depth below Cormorant-1 and Pelican-5 wells with seismic control). Palaeo-heatflow defined from Durroon-1 Model 1 (see Figure 6.6). See Figure 6.4 for pseudowell locations.

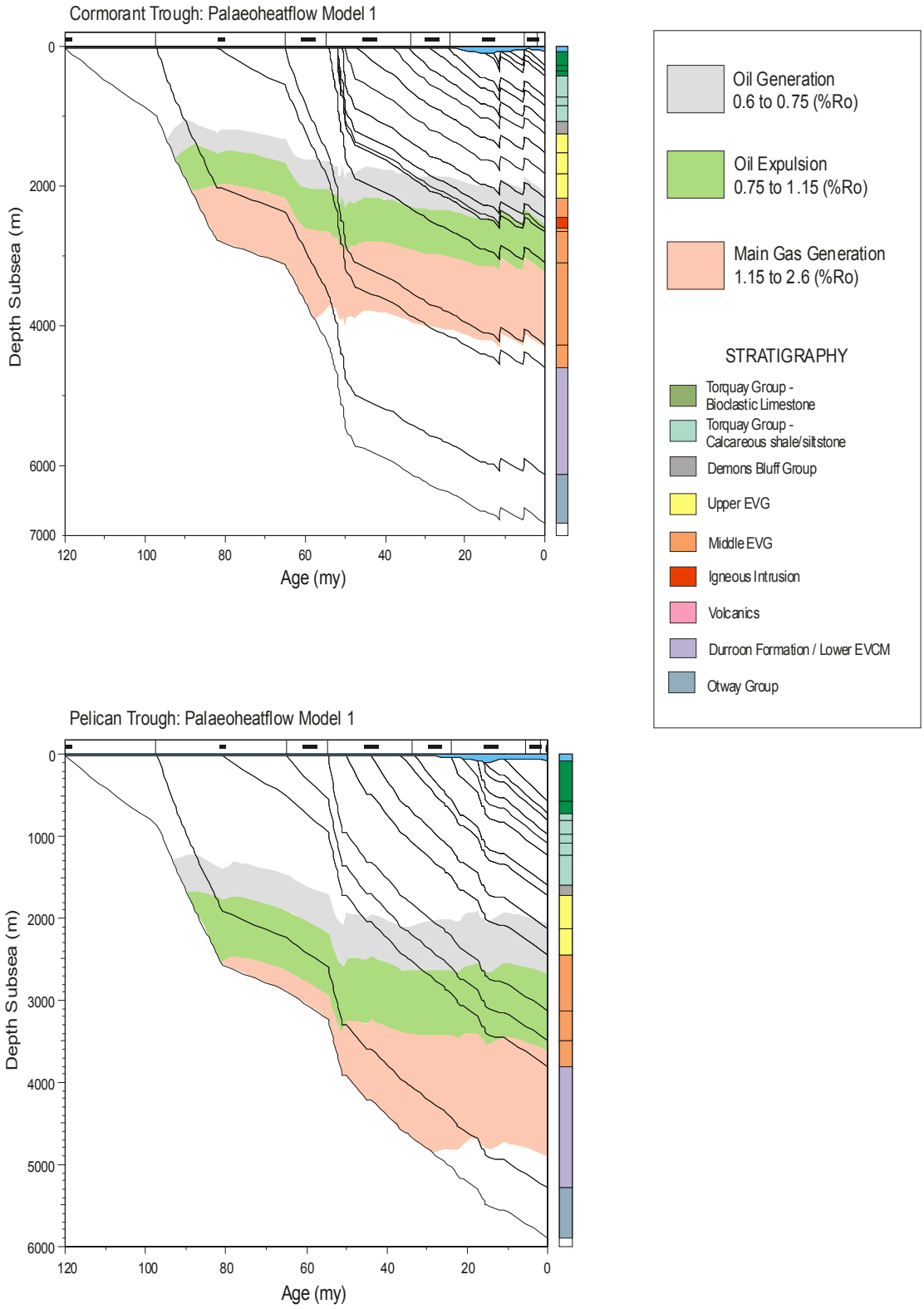

Figure 6.17 Subsidence and maturity curves for Yolla Trough and Durroon Sub-basin pseudowells (defined from seismic mapping). Palaeo-heatflow defined from Durroon-1 Model 1 (see Figure 6.6). See Figure 6.4 for pseudowell locations.

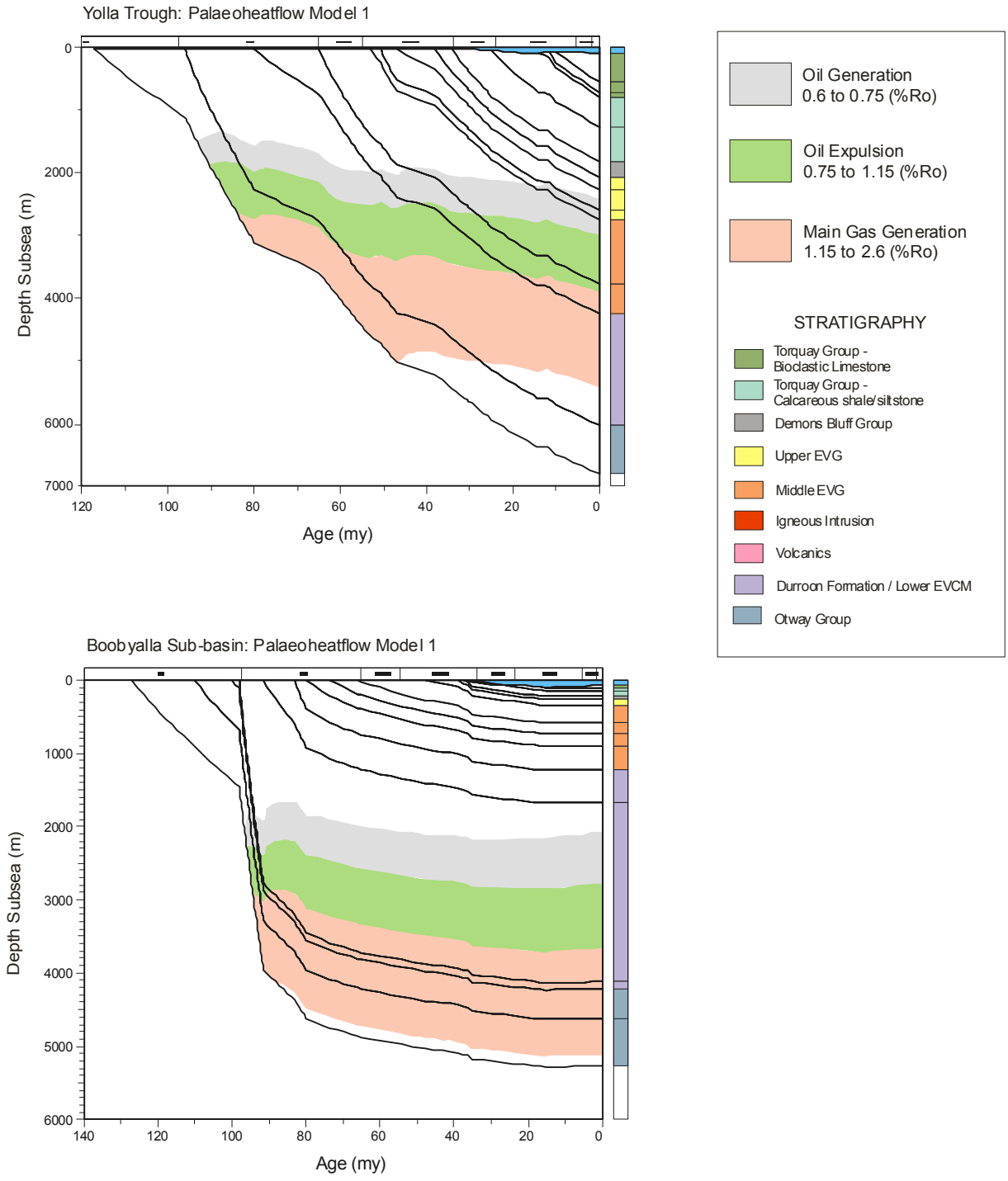

7. HYDROCARBON SEAL EVALUATION

R. Daniel, J. Kaldi and R. Root, National Centre for Petroleum Geology and Geophysics

7.1 KEY POINTS

The National Centre for Petroleum Geology and Geophysics (NCPGG) conducted a study to determine the seal capacity of 15 samples from eight wells in the Bass Basin, offshore Tasmania. The aim of the study was to assess the sealing capacity of the selected mudstones and siltstones by Mercury Injection Capillary Pressure (MICP) Porosimetry. The samples were taken from cores of potential sealing facies that ranged in age from Late Cretaceous to Late Eocene. Samples were collected as part of the facies analyses phase of the Bass Basin study (see Chapter 9 and Appendix M for core descriptions and environmental interpretations). Sensitivities to variations in contact angle, IFT and subsurface fluid density were included in the analysis. Capillary pressure results were used to determine seal capacities (hydrocarbon height retention), as well as pore-throat size distributions and height above free water (HAFWL) versus water saturation (Sw). Hydrocarbon column heights for oil and gas were calculated for each sample. A cross plot of depositional environments (Chapter 9) and seal capacities with varying sensitivities indicates that environments containing facies with significant sealing capacity are: a) lower and upper shoreface; b) interdistributary bays; c) lagoons; and d) stacked crevasse channels.

The sensitivities, in turn, were averaged for each sample for both oil and gas hydrocarbons. An average sealing capacity of all samples, based on the sensitivities for both oil and gas, were also plotted (Appendix L). The average column height of oil above freewater level for all samples is 605 metres (density 0.735g/cc) and a column height of 262 metres for gas (density 0.1 g/cc). The highest oil column (>1400 m) is supported by muds from the lower shoreface in Dondu-1 (2342 m). Lagoonal muds from Cormorant-1 (1999 m) will support an ~1140m column of oil, while the abandoned fluvial channel fills from Durroon-1 (3021 m) and Tilana-1 (2800 m) support >700m oil column. Coastal plain, fluvial overbank and back barrier berm deposits are the least significant sealing lithologies in this study, supporting <200 m oil columns. Details on the operation and quality control of the porosimeter, as well as a complete set of analytical results, are included in Appendix L.

Table 7.1 Samples from Bass Basin wells analysed by MICP.

Well Name	Depth, metres	Sample type	Rock type
Bass-2	1164	Core	Carbonaceous laminated siltstone/mudstone
Bass-2	1262	Core	Carbonaceous laminated siltstone
Cormorant-1	1999	Core	Laminated mudstone
Cormorant-1	2231	Core	Very-fine grained sandstone/siltstone

Dondu-1	2342	Core	Carbonaceous mudstone/siltstone
Durroon-1	3021	Core	Mudstone, very-fine grained sandstone
Pelican-5	2863	Core	Siltstone/sandstone
Pelican-5	2890	Core	Laminated siltstone
Poonboon-1	2474	Core	Carbonaceous laminated siltstone
Poonboon-1	2689	Core	Very-fine grained sandstone
Poonboon-1	3035	Core	Siltstone
Poonboon-1	3259	Core	Mudstone
Tilana-1	1667	Core	Carbonaceous siltstone, very-fine grained sandstone
Tilana-1	2800	Core	Carbonaceous mudstone
Yolla-2	3039	Core	Siltstone, very-fine grained sandstone

7.2 METHODOLOGY

Capillary Pressure

The samples were analysed using the Mercury Injection Capillary Pressure (MICP) techniques described in Appendix L. MICP involves forcing a non-wetting fluid (mercury) into the pore system of a cleaned and dried core sample. The mercury displaces the wetting phase (air) that initially saturated the pores within the rock. Surface forces oppose the entrance of the mercury and pressure must be exerted to enable the mercury to enter the pores and thereby displace the air (Purcell, 1949). The smaller the pore throats, the greater the pressure required for the mercury to enter the rock. Mercury saturation is commonly plotted as a function of mercury injection pressure.

Capillary pressure can be expressed as the relationship:

1. $Pc = 2\sigma \cos \theta / r$

Where: Pc = Capillary Pressure (psi)
σ = interfacial tension (dynes/cm)
θ = contact angle (degrees)
r = radius of capillary (microns)

MICP plots of sidewall cores and cuttings samples are presented in the first two graphs in each set of analyses (Appendix L). These display the data in a lognormal format from 0 – 60,000 psi against volume of mercury injected into the sample (the lognormal format is useful for differentiating data points in the low-pressure regime when analysing reservoir lithologies). The second graph displays plots of pressure against volume of mercury injected as a percentage (this is used for calculating the water saturation graphs) (Appendix L).

Using the following data for the air mercury system from Vavra et al. (1992), capillary pressure data were converted to effective pore throat size:

Air/mercury contact angle (θa/m) = 140°, and
interfacial tension (σa/m) = 480 dynes/cm.
σ(a/m) cos θ(a/m)= 370
1 cm = 10,000 µm, (microns)
1 psi = 69035 dynes/cm2

Solving for r in equation (1) results in the following relationship of capillary pressure to pore throat size:

1 psi = (approx.) 100 microns
10 psi = (approx.) 10 microns
100 psi = (approx.) 1 micron
1000 psi = (approx.) 0.1 micron

The cumulative pore-throat size distributions for the samples are presented in the third figure of the sample analysis set as lognormal size distribution (Appendix L).

7.3 WATER SATURATION

While MICP studies done solely for the purpose of determining pore throat radius and pore throat size distribution are valuable, there is even greater benefit in using these analyses to relate the rock types to saturations as a function of height above the FWL. The mercury/air capillary pressure system is used to replicate static distribution of hydrocarbons in the subsurface. The initial pressure at which the mercury first displaces the air is referred to as "displacement pressure" (Pd). In the subsurface, buoyancy pressure drives hydrocarbon (the non-wetting phase) movement and forces it into the pore throats of a rock, displacing water (the wetting phase). Buoyancy is simply the density difference between hydrocarbon and brine multiplied by the column height and a constant (k) gravitational factor, which is 0.433. The greater the column thickness, the greater the buoyancy pressure driving the hydrocarbon.

Pd in the reservoir system is the pressure at which hydrocarbon first entered the pore system by displacing the water. Different rocks with different pore throat sizes will have different displacement pressures and different saturations as a function of height (h) above the free water level (FWL). Thus, in any given reservoir section, the lowest indication of live (vs residual) hydrocarbon in a particular rock type approximates the displacement pressure (Pd) for that rock. The Pd can thus be considered as the hydrocarbon – water contact *for that particular rock type*. It should be remembered that a reservoir may have several hydrocarbon water contacts (as a function of pore properties controlled by rock type), but will have only one FWL. It is therefore of significance to determine the FWL.

In order to do this, capillary pressure data must first be converted to height above free water level information by using the equation:

2. $P_{cb/o} = h(\rho b - \rho o) \times 0.433$

   Where: $P_{cb/o}$ = Capillary Pressure (psi) reservoir brine/oil system

   h = height (in ft.)

   ρb = brine density (gm/cc)

   ρo = oil density (gm/cc)

In order to use the capillary pressure relationships to interpret real subsurface data in such a way, the data must first be converted from the air/mercury system used in the laboratory to the hydrocarbon/brine system in the reservoir. Laboratory analyses of fluid samples from well completion reports indicate the following reservoir fluid parameters for the wells:

Gas Density - 0.1 gm/cc

Oil Density – 0.735 to 0.797 gm/cc

Brine Density – 1.01- 1.05 gm/cc

No measurements for Contact Angle and Interfacial Tensions were available, so based on existing data from other samples in the region the following values were considered reasonable:

System	Contact angle (θ)	Interfacial tension (σ)
Brine/oil	5	15 dynes/cm
Brine/gas	0°	30 dynes/cm
Air/mercury	140°	485 dynes/cm

Once the capillary pressure values have been converted to h (height in feet), a plot of height versus mercury (non-wetting phase) saturations can be constructed. However, conversion of mercury (non-wetting phase) to hydrocarbon (non-wetting phase) will now result in a height versus hydrocarbon saturation plot. Since water (wetting phase) saturation is more commonly used in the oil and gas industry, the non-wetting phase

saturation needs to be converted to water (wetting-phase) saturation (Schowalter, 1979). This is done using the simple conversion:

3. Sw = 1 - Snw

   Where: Sw = wetting phase (water) saturation

   Snw = non-wetting phase (hydrocarbon) saturation

   Combining equations 2 and 3 results in a plot of height (above FWL)

   versus water saturation.

Saturation height functions were calculated using input parameters of the brine and hydrocarbon densities indicated in well completion reports. The conversion was run using a brine density value (1.01 gm/cc) and the oil density (0.735 to 0.797 gm/cc), and the Sw versus height functions were plotted on the fourth and fifth graph (linear and semi log formats, respectively) for each sample analysis (Appendix L). The height versus water saturation curves for each well were also plotted on a single graph for comparison, both in linear and semi-log plot (Appendix L).

7.4 INTERPRETATION OF SEAL CAPACITY

Table 7.1 presents a summary of average (oil and gas) heights determined for each of the 14 samples analysed. A summary of the water saturation curves for the samples from the Bass Basin is presented in Appendix L as a series of composite coloured graphs of normal (linear) and lognormal parameters. The average hydrocarbon height and displacement pressure is highlighted on each graph (Appendix L). The lognormal graphs are more definitive as a result of larger scale values in the lower height range. Sensitivities used for the study were determined from Bass Basin well completion reports, corroborated with data from adjacent areas.

The threshold or displacement pressure in the samples from the Bass Basin averages 5760 psia at 605 metres above free water level before it leaks off. This means that the sealing lithology will support a 605 metre column of oil with a density of ~ 0.735 gm/cc (or a 262 metre column of gas with a density of 0.1 gm/cc)

The results and interpretation of the analyses on sediments from the these wells (Table 7.1) can be viewed in terms of minimum hydrocarbon heights that can be supported by the sealing lithologies. The seal lithological samples were derived from a variety of depositional environments (Chapter 9), including: shelf, lower shoreface, foreshore-upper shoreface, back barrier lagoon/lake, lacustrine/marine shelf, back barrier berm, coastal plain, interdistributary bay/lake, interdistributary swamp/marsh, fluvial channel, fluvial overbank, stacked crevasse channel, fluvial overbank, and crevasse splays/channels.

Plots of length versus width and area versus thickness of ancient and modern analogues of seal depositional environments (mudstone and siltstone lithologies) are presented in Figure 7.1. These diagrams highlight the spatial extent of the various depositional environments attributed to the potential sealing lithologies analysed in this study. Significant seal depositional environments determined from this study are lower shoreface (muds), lagoons (silty muds) and abandoned channel fill (silty muds). Based on modern and ancient analogues, the areal distributions of these environments are estimated at >1,000 km^2, 10-1000 km^2 and 1 km^2, with thicknesses of 1-30 m, 1-50 m and 5-10 m, respectively (Figure 7.1).

Table 7.1 Average hydrocarbon (oil and gas) heights for 15 samples from the Bass Basin.

Sample, Depth and Environment	OIL WCR Data	OIL 46API, 1.01 brine	OIL 57API, 1.01 brine	OIL 61API, 1.01 brine	OIL 49API (av), 1.05 brine	Average Oil Height (m)	GAS 0.1g/c 15/0	GAS 0.1g/c 30/0	Average Gas Height (m)
Bass-2 1164.5 m Shelf	389	474	389	367	379	400	111	223	167
Bass-2 1261 m Coastal plain	160	169	142	135	154	152	44	88	66
Cormorant 1 1999.3 m Lagoon	1157	1344	1103	1040	1075	1144	316	631	474
Cormorant-1 2231.6 m Interdistributary bay	806	936	768	725	749	797	220	440	330
Dondu-1 2342 m Lower shoreface	1515	1609	1320	1246	1287	1395	378	756	567
Durroon-1 3021.9 Stacked crevasse channel	1073	1139	935	882	911	988	268	535	402
Pelican-5 2863.8 m Interdistributary bay	723	759	645	614	750	698	209	417	313
Pelican-5 2890.8 m Upper shoreface	882	927	788	750	916	853	255	509	382
Poonboon-1 2474 m Fluvial overbank	193	201	177	170	266	201	68	135	102
Poonboon-1 2689 m Back barrier berm	99	103	91	87	136	103	35	69	52
Poonboon-1 3035 m Interdistributary swamp	387	401	354	341	532	403	135	271	203
Poonboon-1 3259.8 Lacustrine	545	565	499	481	749	568	191	381	286
Tilana-1 1667 m	4	5	4	4	5	4	1	3	2
Tilana-1 2800 m Fluvial channel	947	998	838	795	911	898	259	518	389
Yolla-2 3039.5 m Fluvial overbank	578	406	474	447	462	473	136	271	204
Average	631	669	568	539	619	605	175	350	262

Figure 7.1 Plots showing the relationships between a) thickness and areal extent, and b) length and width for seal depositional environments (based on analogue data).

a.

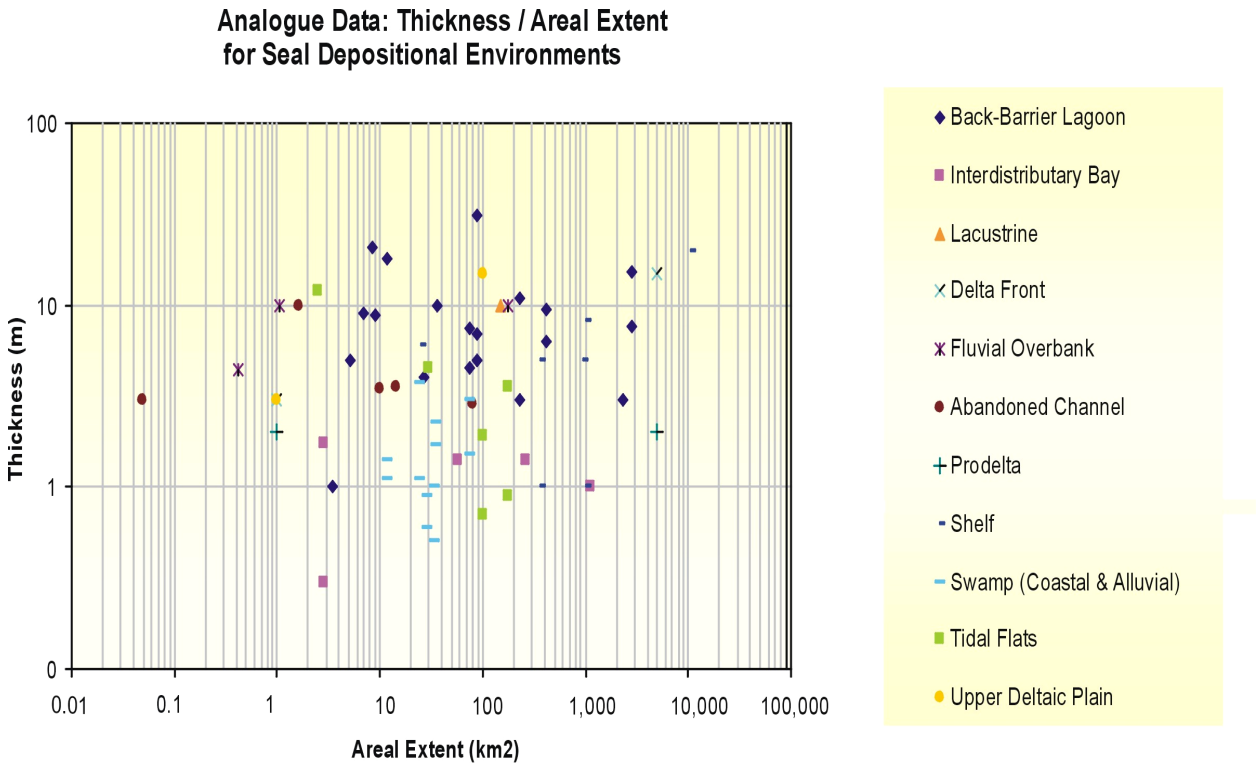

b.

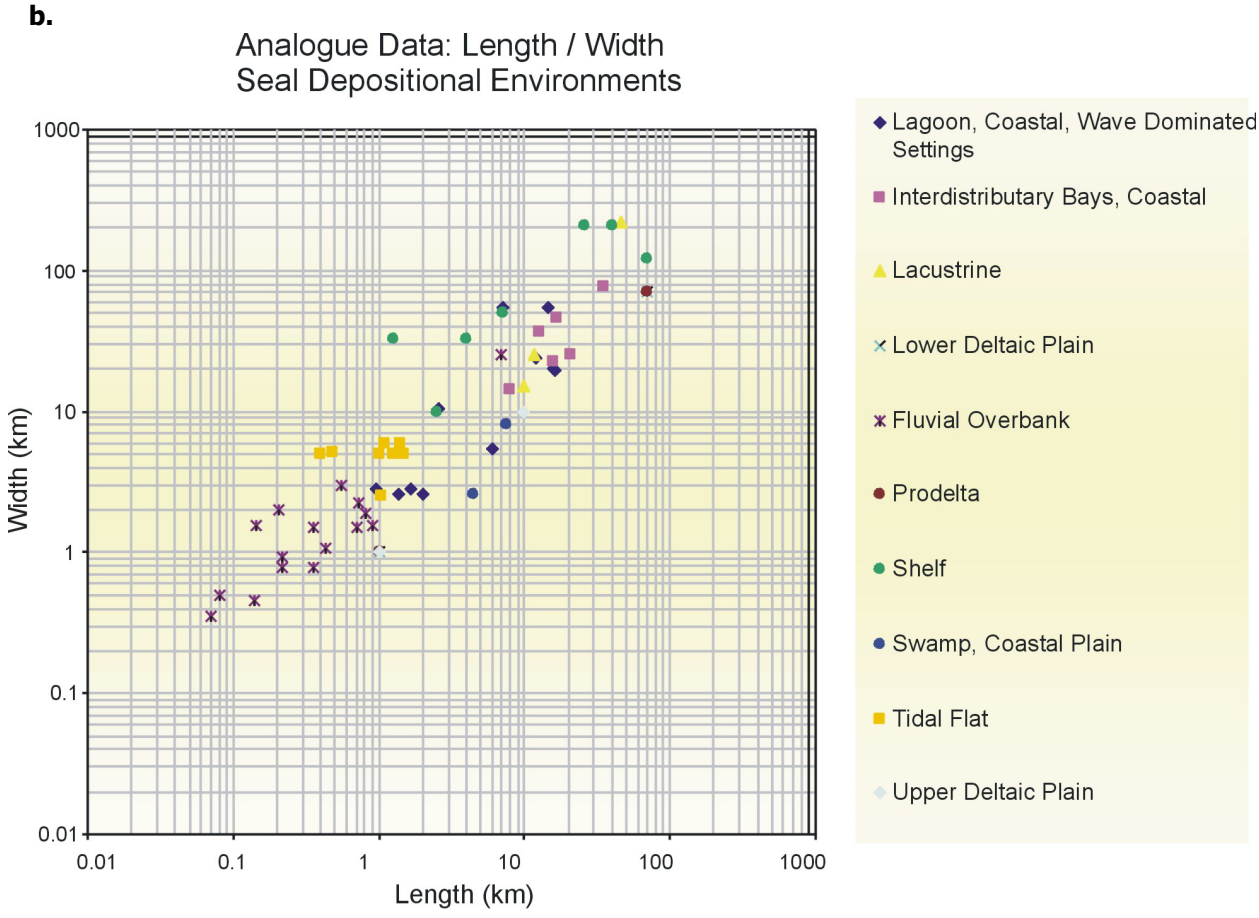

8. DIAGENESIS OF HYDROCARBON RESERVOIRS

N. Lemon*, National Centre for Petroleum Geology and Geophysics

**Present address: Santos Ltd, Santos House, 91 King William Street, Adelaide SA 5000*

8.1 KEY POINTS

- The lack of marine influence is one of the main differences between the reservoirs of the Bass and Gippsland basins. The Gippsland reservoirs are commonly clean, coarse, well sorted marine shoreline sands, while many of the Bass Basin reservoirs are silty, fluvial channels sands and lacustrine delta sands. The better reservoir sands in the Bass Basin are those where some marine influence is apparent.
- Cross plots of porosity against permeability, grainsize and various petrographic parameters show a series of cut off values below which good reservoir quality is unlikely. Permeability becomes negligible below 12% plug porosity. Observable thin section porosity is zero below 12% plug porosity. The cause of this discrepancy is due to the amount of microporosity within the abundant tightly-packed kaolin. Permeability drops below effective values in sandstones of smaller than medium grain size.
- A sequence of diagenetic events determined by previous authors has been updated. Early siderite cementation and compaction were accompanied by the first stage of quartz cementation. Dolomite cementation followed in parts of the succession where carbonate was available. Dolomite was subsequently replaced by ankerite in the deeper parts of the section. Dissolution porosity is the main form of porosity seen at depth.
- Cathodoluminescence reveals that the quartz cementation history was long and complex. A major pulse of quartz cementation took place after some dissolution of carbonate. It was accompanied by extensive alteration of feldspars to kaolinite and precipitation of kaolinite in adjacent pores. A late dissolution phase removed more dolomite, ankerite and siderite to create some porosity, but also allowed late compaction to reduce those pore spaces. Later illite formation diminished some permeability, but this was primarily a function of temperature and the depth of burial.
- Maps of heat flow determined from corrected bottom hole temperatures show considerable variation across the basin. This is particularly evident in the areas known to have been the focus of later volcanic activity. Steep lateral temperature gradients are apparent across the Pelican Field and several diagenetic events, such as the onset of illite formation, occur at shallower depths where the heat flow was raised.
- Reservoir quality in the Bass Basin is a function of the maturity of the original sediment, grain size, the degree of marine influence, depth of burial, heat flow and level within the stratigraphic succession. Silt-free sediments were more likely to develop and retain high quality reservoir properties. Only sandstones of medium grain size or larger were likely to retain effective reservoir quality. Marine influence during sedimentation removed silt and provided some carbonate that acted

as an early cement until removed by later dissolution processes. Raised temperatures facilitated the growth of illite which damaged permeability. All the favourable factors for high quality reservoir development were combined in the upper parts of the "Eastern View Group" (Aroo Megasequence), which fortuitously underlies the regional sealing facies of the "Demons Bluff shale".

8.2 DATASET AND PREVIOUS WORK

Sandstones of the Upper Cretaceous to Middle Eocene age 'Eastern View Group' (EVG) are the main hydrocarbon-bearing reservoirs in the Bass Basin. Previous studies of the diagenetic history of these intervals have been summarised from published material (Baillie et al., 1991; Cubitt, 1992; Meszoly et al., 1986; Zampatti, 1991), and supplemented with new evidence and interpretations to formulate the diagenetic history of the basin. This new evidence draws heavily on understanding key mineral relationships in thin section utilising transmitted light microscopy and cathodoluminescence microscopy (CL). Scanning Electron Microscope (SEM) micrographs and X-ray Diffraction (XRD) scans of all samples were also available through previous research projects undertaken at the National Centre for Petroleum Geology and Geophysics (NCPGG), University of Adelaide (Zampatti, 1991; Cubitt, 1992).

In addition, Baillie and Bacon (1989) presented results of a systematic study of depositional environments and reservoir quality of the Eastern View Group based on cores from exploration wells in the Bass Basin. This systematic approach was subsequently applied to additional wells in the basin (Baillie et al., 1991), and used by Zampatti (1991) and Cubitt (1992) in research projects at the NCPGG. Collectively, these reports provide consistent coverage of most core material available until the end of 1992, and form the basis for this report.

8.3 STRATIGRAPHY AND DEPOSITIONAL HISTORY

Coals of the Eastern View Group (also know as the "Eastern View Coal Measures"; EVCM) were deposited across the Bass Basin area (Figure 8.1). This succession shows indications of subaqueous sedimentation in the northwestern part of the basin. Sedimentation in this region was probably largely lacustrine with periods of marine influence occurring from late Middle Eocene onwards. Marine dinoflagellates are rarely observed in sediments of the EVG. Sandstone-capped, coarsening-upwards profiles overlying flaser bedded muddy sandstones, as seen in the Dondu-1 core (Figure 8.2; Baillie et al., 1991) are attributed to lake shoreline deposition.

Baillie et al. (1991) followed the informal subdivision of the failed rift part of the succession suggested by Robinson (1974), Smith (1986) and Williamson et al. (1987). They subdivided the Eastern View Group into a lower section of Late Cretaceous to Middle Eocene age comprising interbedded mudstone, sandstone, minor coal and volcanics, and an upper mainly Eocene interval, sandier and more coal-rich than below. Lennon et al. (1999) identify lower, middle and upper subdivisions, with a Cenomanian to Coniacian interval below a thick interval of volcanics in the middle EVG. These authors also use the "Eastern View Coal Measures" (EVCM) terminology rather than the "Eastern View Group" determination.

Coal percentage maps for time slices identified on palynological data were presented by Baillie and Bacon (1989) and Baillie et al. (1991). These show the coals were very patchy during the Cretaceous, but spread across the basin from the south during the Early Eocene, before contracting to the southern end of the basin by the Late Eocene. Baillie et al. (1991) used the nature of the coals and their contacts with the underlying rocks to suggest that the peat swamps were located on upper and lower delta plains marginal to large lakes.

8.4 DIAGENETIC HISTORY

A series of alteration, cementation, dissolution and compaction events have overprinted the sediments of the Eastern View Group in the Bass Basin (Table 8.1; Figure 8.3). Of these event, the precipitation and subsequent dissolution of dolomite, the formation of kaolinite and late compaction were the key modifiers of reservoir quality in the EVG. The events described here are similar to those described from the Permian coal measures succession in the Cooper Basin of South Australia and Queensland (Schulz-Rojahn and Phillips, 1989; Rezaee et al., 1997). The reducing conditions induced by the abundant organic matter, together with organic acids and generation of carbon dioxide formed during maturation of the abundant kerogen, were major controlling influences in both cases. The difference in the Bass Basin was the marginal marine influence that added additional carbonate to the succession.

A key factor in the diagenetic history observed by Cubitt (1992) was that the best reservoir characteristics in the EVG were in the Paleocene (lower *L. balmei* zone) sands of the "Middle EVG" (Lennon et al., 1999). Figure 8.1 shows the stratigraphic distribution of hydrocarbon recovered in the Bass Basin. Although the major reserves are in the upper part of the EVG, there are a number of occurrences in the Paleocene section, trapped by intraformational seals of the EVG. Cubitt (1992) reported porosities of 10-15% in places at this stratigraphic level. Whether those porosities were a function of the depth of burial, the temperature reached, or the nature of the sediments was not determined.

The study by Baillie et al. (1991) concentrated on the Lower EVG, as earlier work had suggested that sediments of the Upper EVG were thermally immature and that the muddy succession inhibited vertical migration of hydrocarbons. A purely statistical look at the reservoir quality in the Paleocene interval of the EVG is summarised by a series of cross plots produced by Baillie et al. (1991) from data relating specifically to Pelican-1 and Tilana-1 (Figure 8.4).

A plot of plug porosity against plug permeability shows a relatively tight "straight line relationship", and that permeability drops below 1 millidarcy (mD) at around 12% porosity. This drop in permeability is due to the abundance of kaolinite. Kaolinite booklets fill much of the primary pore space and replace feldspar grains. While the microporosity between the booklets is registered during routine core analysis on plugs, the kaolinite virtually blocks flow through the rock. Sandstones with less than 1 mD are unlikely to be effective reservoirs. A plot of thin section porosity against plug porosity (Figure 8.4) confirms the microscopic nature

of the porosity. Micropores are not easily recorded during examination of a thin section under transmitted light. The cross plot shows thin section porosity is negligible when plug porosity is still around 11-12%.

The plot of plug permeability against grainsize shows that the reservoir becomes ineffective (below 1 mD) when the grain size drops below medium sand sized. This appears to correspond with a drop in porosity as illite increases, but this is not a direct relationship. There is more total illite in the finer grained samples, present in the silty, muddy matrix. The porosity drop is a function of compaction facilitated by the clays and attendant organic matter, not by the precipitation of an illite cement. Similarly, the plot of plug permeability against thin section illite is a *de facto* representation of a grain size effect.

Each of the events listed in Table 8.1 and its likely distribution and influence in the basin is discussed with reference to the figures in the following section. The figures are a pictorial representation of the diagenetic events. Thin sections were chosen to show the biggest range of diagenetic events and to provide a direct comparison between similar environments of deposition (Figure 8.3).

Siderite Micrite

The earliest cementation event in the EVG is the precipitation of micritic siderite. Fine, golden crystals of micritic siderite rim the quartz and feldspar framework grains (Figure 8.5). Siderite ($FeCO_3$) contains ferrous iron (2^+ oxidation state) that requires reducing conditions to precipitate. Figure 8.5 shows the occurrence of abundant siderite within a siltstone layer and abundant organic matter associated with the finer sediment fractions. Figure 8.6, images collected only 0.5 mm from the edge of the lamina depicted in Figure 8.5, shows less siderite around the framework grains. The amount of siderite shown in Figure 8.7, two millimetres from the silty layer, is further from the silt fraction and associated organic matter. The micritic siderite is corrosive and etches the silicate framework grains.

Siderite Spar and Microspar

The micritic siderite provides a focal point for the precipitation of later siderite, which became coarser grained and less coloured (clearer) as the diagenetic history progressed. Microspar siderite grows on the micrite, eventually progressing to sparry siderite where porosity permits. In some cases, microspar siderite grows within altered and deformed grains. Figure 8.8 shows microspar siderite within a deformed muscovite flake. The lack of alignment of the siderite crystals suggests that they formed after the compactional deformation of the muscovite. The sparry types of siderite formed over an extended period of the diagenetic history of the EVG. The siderite deeply etched the quartz and feldspar grains to produce a distinctive scalloped edge to the grains.

Early Compaction

The silty layers within the EVG provide evidence of the earliest compaction event. Figure 8.9 shows stylolites that developed around organic matter. This relationship indicates that the organic matter and clays, which resided together within the sediment, catalysed the dissolution of silicate minerals. The organic matter was

insoluble, and therefore became concentrated along the dissolution seams. The clusters of siderite micrite are globular and do not appear to have been effected by compaction. The lack of compaction could indicate that either the early cement supported the rock against compaction, or that micritic cementation postdated compaction. While there is no clear evidence in the samples investigated, although other studies of coaly fluvial sediments indicate that siderite tends to form at or near the surface within the soil profile, usually before the rock has been buried or compacted.

Feldspar Dissolution

Cubitt (1992) and Baillie et al. (1991) described feldspar dissolution as a significant diagenetic process within the EVG sediments. While dissolution has occurred, it appears to be far less important than feldspar alteration in the modification of EVG reservoirs. The emplacement of dolomite cement etched silicate grains and had a particularly strong effect the feldspars grains (Figures 8.10 and 8.11). The subsequent dissolution of the carbonate phase created secondary porosity in the then skeletal feldspar grains. Feldspar dissolution is also implied by the relationships observed in Figure 8.12. For siderite spar to occur as a substrate below kaolinite indicates that the altered feldspar (in a composite granitic grain with quartz) must first have been dissolved.

Dolomite Cement

Some shallower samples from the EVG show complete cementation by dolomite. Meszoly et al. (1986) described these shallow carbonate cements as the "Bass Type", as distinct from the "Pelican Type", where dolomite was dissolved and kaolin precipitated in deeper parts of the basin. Figure 8.7 shows the that porosity which remained after early siderite cementation was later occluded by brightly luminescing dolomite. The bright colours under CL imply that the dolomite has a low iron content with respect to trace amounts of manganese which excite the CL response. The lack of colour banding in the dolomite (Figure 8.10) implies that the dolomite may have recrystallised. Faint banding in other samples (Figure 8.11) suggests that growth banding is present, although the distinction between early and later dolomite cements is minimal. The banding is of the order expected, with the brightest cement (lowest iron) rimming the substrate grains, and the slightly darker (a trace more iron) filling the remaining porosity. Dolomite cement is reported by Meszoly et al. (1986) and Cubitt (1992) as being more common in the coarser grained sandstones. This is not surprising, as the finer grain sizes may well have had pores occluded by siderite micrite or by early compaction induced by clays and organic matter. The emplacement of dolomite cement has deeply etched the framework silicate grains, quartz and particularly feldspar.

Ankerite Cement

Baillie et al. (1991) did not report dolomite in the samples they studied. Their work concentrated on samples from farther down in the EVG succession, and this may well be the reason for not recording dolomite. Ankerite, the ferroan form of dolomite, often forms after dolomite, at a greater depth or higher temperature. Increased temperature and depth of burial facilitate the dewatering of mudstones which released iron into the groundwater. The iron was then available for inclusion in the crystal structure of carbonates that form at

those levels. The high iron content of ankerite suppresses the CL response, so that these crystals appear black (Figure 8.13).

Previous studies of the diagenesis in the Bass Basin have reported strong evidence of dolomite dissolution. Figure 8.13 shows the ragged edges of dolomite crystals where secondary pores have been created prior to the emplacement of kaolinite cement. Many of the framework quartz grains at depth in the EVG show irregular edges from dissolution of carbonate. Figure 8.14 shows a good example of the scalloped edges produced when carbonate, which had previously etched the grains, is removed. If the dissolution were the result of aggressive formation waters, then all surfaces in the rock would have been attacked. The current evidence suggests that deep etching is sporadic with some grains untouched (Figure 8.14).

Quartz Cement

Cathodoluminescence (CL) is the key tool in understanding quartz cementation, with Figure 8.14 providing an excellent example of its use. The framework quartz grains are divided by colour. Those with a blue tint are, in this case, of igneous origin and show limited internal strain. Grains with a red and brown tint are of metamorphic origin and show a higher level of internal strain. These grains show only a thin overgrowth rim or a drusy surface, if present at all. The high level of strain means that the quartz is more susceptible to dissolution. The igneous grains, however, have a thick coating of overgrowth cement.

Early compaction has cracked some of the grains and the first phase of quartz cementation has healed these fractures. This is often a two-way relationship, as the compaction which cracked the grains also produced some of the silica that healed the fractures through pressure solution at the grain to grain contacts. Subtle banding is seen in the thick quartz cements. Figure 8.14 shows traces of kaolinite cement, all of which postdate the quartz cement and some of which filled the etched holes left by removal of a patchy carbonate cement. Despite the relationships observed in Figure 8.14, most of the quartz cement seen in samples from the EVG is intergrown with kaolinite booklets (Figure 8.15). Kaolinite, which responds with a bright mid-blue colour under CL, shows a jagged contact with all the dark purplish quartz overgrowths on the framework grains. The intergrowth of the two minerals indicates they were co-genetic. The most common reaction that produces both kaolinite and quartz at the same time is the alteration of feldspar. This can occur either under the influence of carboxylic acids produced during the maturation of kerogen, or under the influence of an excess of carbon dioxide, also probably a product of kerogen maturation.

Kaolinite Cement

As described previously, kaolinite formed at the same time as the majority of the quartz cement in the EVG. Patches of densely packed kaolinite booklets match the size and shape of framework grains (Figure 8.16). These are interpreted to be altered feldspar grains. Where these patches opened to original primary pores, more kaolin has grown, although these areas show some slightly different characteristics, such as larger booklet size or less dense packing. The kaolinite formed by alteration of the feldspars postdates the formation of micritic siderite, some sparry siderite, some quartz cement and feldspar dissolution. Pore-filling

kaolinite postdates dolomite dissolution, postdates most alteration kaolin and is co-genetic with the majority of each quartz overgrowth. Figure 8.17 shows several of the relationships of large patches of kaolin with quartz overgrowths and with dolomite and its dissolution.

The formation of kaolinite from the alteration or dissolution of feldspar has been frequently reported in the literature, often in the context of the development of secondary porosity (e.g., Siebert et al. 1984). Surdam et al. (1984) proposed a series of reaction pathways dependent on the balance of carboxylic acids and carbonic acid, i.e., the concentration of carbon dioxide. There was most likely a plentiful supply of carboxylic acids as a result of the kerogen maturation in the EVG, such that early feldspar alteration was likely to follow that process. Surdam et al. (1986) suggested that the result would be dissolution of feldspar. As alkalinity increased and carbon dioxide remained in the system, aluminium ions would be immobilised and the products of the feldspar reaction (kaolin) would remain in the rock. At high concentrations of carbon dioxide, feldspars would alter without the need for carboxylic acids.

Rock Fragmentation Alteration

Few of the rock fragments in the framework grain suite have retained their original mineralogy. Most fragments are now a mixture of kaolinite and illite. Figure 8.18b shows the characteristic speckled nature of this clays mixture under crossed polarised light. Once the rock fragments have been altered, they become soft and ductile. In this state they are easily compacted to block pore throats, and in many cases, completely block all porosity and impede permeability (Figure 8.18). This stage of compaction probably occurred progressively as the grains were altered. It is expected that the alteration of rock fragments was coincident with the alteration of feldspars, as kaolin is the main product in both instances.

Siderite Dissolution

Siderite dissolution is difficult to prove as there are no rocks that show dissolution with all siderite removed. However, circumstantial evidence shows porosity at depths well below that where primary pores are expected to be closed. These pores are often an amalgam of smaller pores that are the size and shape of areas/grains of micritic siderite and sparry siderite. Some dolomite and ankerite may have remained at these depths, but most of the dolomite was dissolved by the time pore-filling kaolinite was emplaced. Siderite is present in the tight areas depicted in Figures 8.18 and 8.19, but is absent from the open pores in those images. Siderite dissolution is brought about by low pH conditions, such as induced by an increase in carbon dioxide or carboxylic acids.

Late Compaction

Evidence that a late compaction phase postdated thick quartz cementation is shown in Figures 8.19 and 8.20. In Figure 8.19, a quartz grain with an overgrowth has a concavo-convex contact with another grain with its own overgrowth. The occurrence of overgrowth within the concave area is evidence of late compaction. Similarly, in Figure 8.20, a partly altered muscovite grain is wrapped around a quartz grain with a distinct overgrowth. The overgrowth is not complete along that contact as the softer grain probably

prevented growth along the contact margin. Compaction after the quartz overgrowth has resulted in the soft grain being wrapped around parts of the quartz grain.

The driving mechanism for late compaction appears to have been the dissolution of siderite and other carbonate phases that persisted in the rock to that stage. Dissolution was a significant event in that it created secondary pores at a depth where primary porosity is usually absent. The development of secondary pores was patchy and related to the amount of carbonate that was present. Similarly, the amount of late compaction was patchy and it destroyed most of the secondary pores. Effective secondary porosity is therefore a result of the percentage of pores created and the amount that were subsequently destroyed by compaction.

Late carbonate dissolution and compaction appear to be depth related, and the best examples are observed in the Pelican field. Heat flow and temperature contours are very tight in this area, with high temperatures and rapid lateral changes induced by igneous intrusives. The high temperatures may have played a part in carbonate dissolution by driving the maturation of kerogen to produce carbon dioxide. Alternatively, the intrusions themselves could have been responsible for dissolution through degassing and release of carbon dioxide into formation waters. Carbon dioxide released by the degassing of volcanics has been reported by Lennon et al. (1999). Carbon dioxide acts to facilitate the dissolution of carbonate cements, and could have been a key mechanism that brought about late compaction and the development of secondary porosity.

Illite Growth

This study did not recognise the late development of pore-lining and pore-bridging fibrous illite because the samples were not analysed under the Scanning Electron Microscope (SEM). However, previous studies that used the SEM (Baillie et al. 1991; Cubitt, 1992) proved conclusively the occurrence of late illite formation. Illite was observed within the pores and as small fibres attached to kaolin booklets (Baillie, et al., 1991). In these instances, illite fibres are likely to have significantly reduced permeability, even if their effect on porosity reduction was minimal.

8.5 THERMAL SETTING

Many of the diagenetic processes identified by previous authors and in this report are directly or indirectly dependent on elevated temperatures. Heat flow in the Bass Basin has been locally influenced by the occurrence of volcanic and intrusive rocks and by subsequent tectonic episodes. Downthrown extensional blocks and later uplift during inversion have also created rapid lateral changes in temperature. Figure 8.21 plots the distribution of heat flux through the basin as measured by an assessment of the bottom hole temperatures. There is a strong gradient from high temperatures in the southern basin, to lower temperatures along the northeast margin of the basin. A perturbation in this trend occurs in the vicinity of Dondu-1, Yolla-1 and Bass-2, and appears to be related to the localised occurrence of volcanic rocks (Lennon et al., 1999).

Wells that intersect intrusive sills, such as Yolla-1 and Koorkah-1 (Cubitt, 1992), show an increase in vitrinite reflectance profiles for up to 150 m on either side of the intrusion. Other local perturbations could be related to intrusions and volcanics rocks that occur nearby, but are not necessarily intersected by wells (Figure 8.21). A map of the temperature variations at 1000 m below sea level (Figure 8.22), shows the combined influence of structural movements, differences in thermal conductivity and possibly local intrusions. There is a very steep temperature gradient across the Pelican field, although this trend may be partly due to data distribution.

The raised temperatures localised over the Pelican field have meant that several of the diagenetic effects described in this report occur at shallower depths than elsewhere in the basin. Enhancement of reservoir qualities through dissolution of carbonate phases, especially siderite, occurs higher in the section (Cubitt, 1992). As previously mentioned, carbonate dissolution is brought about by the acidic conditions associated with raised carbon dioxide levels, either by maturation of kerogen or by degassing of nearby volcanics and intrusives. However, not all the events are positive in terms of reservoir quality. Through the transformation of smectite and potash alteration of kaolinite, illite growth is facilitated by high temperatures. Illite is particularly damaging to permeability as the fibrous growths of this mineral fringe the grains and bridge across pore throats. There is a balance between the creation of pore space through dissolution and the destruction of permeability through illite growth, as both are related to increased temperatures.

Figure 8.23 shows the temperature distribution across the basin at a particular choronostratigraphic interval (*P. asperopolus* zone). The *P. asperopolus* zone lies just above the top of the upper *L. balmei* zone, the stratigraphic level where many of the hydrocarbons are reservoired (Figure 8.1). High temperatures and a horizontal temperature gradient are evident over the Pelican field, as well as in the subsea depth map (Figures 8.22 and 8.23). While this may have degraded reservoir conditions in the Pelican field, several hydrocarbon shows were detected at this chronostratigraphic level in Poonboon-1, Bass-3 and Yolla-1, all of which are currently at lower temperatures. Clearly, temperature alone has not controlled reservoir quality.

8.6 SUMMARY

The Bass Basin has been a focus for hydrocarbon exploration since the discovery of giant oil and gas fields in the adjacent Gippsland Basin. Exploration success, however, has been more elusive in the Bass Basin despite a number of tantalising shows and smaller fields. These discoveries have been reservoired in the Upper Cretaceous to Eocene Eastern View Group (EVG) succession. The most promising hydrocarbon occurrences are concentrated in sandstones of *N. asperus* and Upper *L. balmei* age.

One of the main differences between the reservoirs of the Bass and Gippsland basins is the lack of marine influence. The Gippsland Basin reservoirs are commonly clean, coarse, well-sorted marine shoreline sands, while many of the Bass Basin reservoirs are silty, fluvial channels sands and lacustrine deltaic sands. The better reservoir sands in the Bass Basin are those where some marine influence is apparent.

Cross plots of porosity against permeability, grainsize and various petrographic parameters show a series of cut off values below which good reservoir quality is unlikely. Permeability becomes negligible below 12% plug porosity. Similarly, observable thin section porosity is zero below 12% plug porosity. The reason for these observations is the amount of microporosity preserved within abundant tightly-packed kaolin. Permeability drops below effective values in sandstones with grain sizes smaller than medium.

The sequence of diagenetic events has largely been determined by previous authors (Baillie, et al., 1991; Cubitt, 1992; Meszoly et al., 1986; Zampatti, 1991), however changes in their order have been highlighted by this study. Early siderite cementation and compaction were accompanied by the first stage of quartz cementation. Dolomite cementation followed in parts of the basin where carbonate was available. Dolomite was subsequently replaced by ankerite in the deeper parts of the stratigraphic succession. All authors report the dissolution of dolomite and ankerite. Dissolution porosity is the main type of porosity observed at depth. Cathodoluminescence studies have revealed that the quartz cementation process was both long and complex. A major phase of quartz cementation occurred after some dissolution of carbonate. It was accompanied by extensive alteration of feldspars to kaolinite and the precipitation of kaolinite in adjacent pore spaces. A late dissolution phase further removed dolomite, ankerite and siderite. This late dissolution phase resulted in some increase in porosity, but also allowed a reduction in pore space due to late compaction. There was some late illite formation which diminishes permeability, but this process appears to have been a function of temperature and depth of burial.

Maps of heat flow (determined from corrected bottom hole temperatures) show considerable variation across the basin. This variation is evident in areas affected by volcanic activity. Steep lateral temperature gradients are apparent across the Pelican field, and several diagenetic processed, such as the onset of illite formation, occurred at shallower depths where the localised heat flow was raised. It is likely that other variations in the heat flow gradient also occur due to igneous activity, however data density is insufficient to clearly define this trend.

Reservoir quality in the Bass Basin is a function of the maturity of the original sediment, the grainsize, the degree of marine influence in the sediment, the depth of burial and the heat flow, and stratigraphic level. Present-day good quality reservoirs were originally free of silt. Only sandstones of medium grain size or larger are likely to have retained effective reservoir quality to the present day. Marine influence during deposition acted to remove silt from the sediment, and provide carbonate to act as an early cement that could subsequently be removed through dissolution. Raised temperatures that facilitated the growth of illite has damaged permeability. The best conditions for reservoir development and preservation occurred in sediments of the "Upper EVG", just below the regional sealing facies of the "Demons Bluff" shale.

Table 8.1 Stratigraphic column for the Bass Basin, including information on hydrocarbon accumulations and shows. A reference column from Lennon et al. (1999) is also shown.

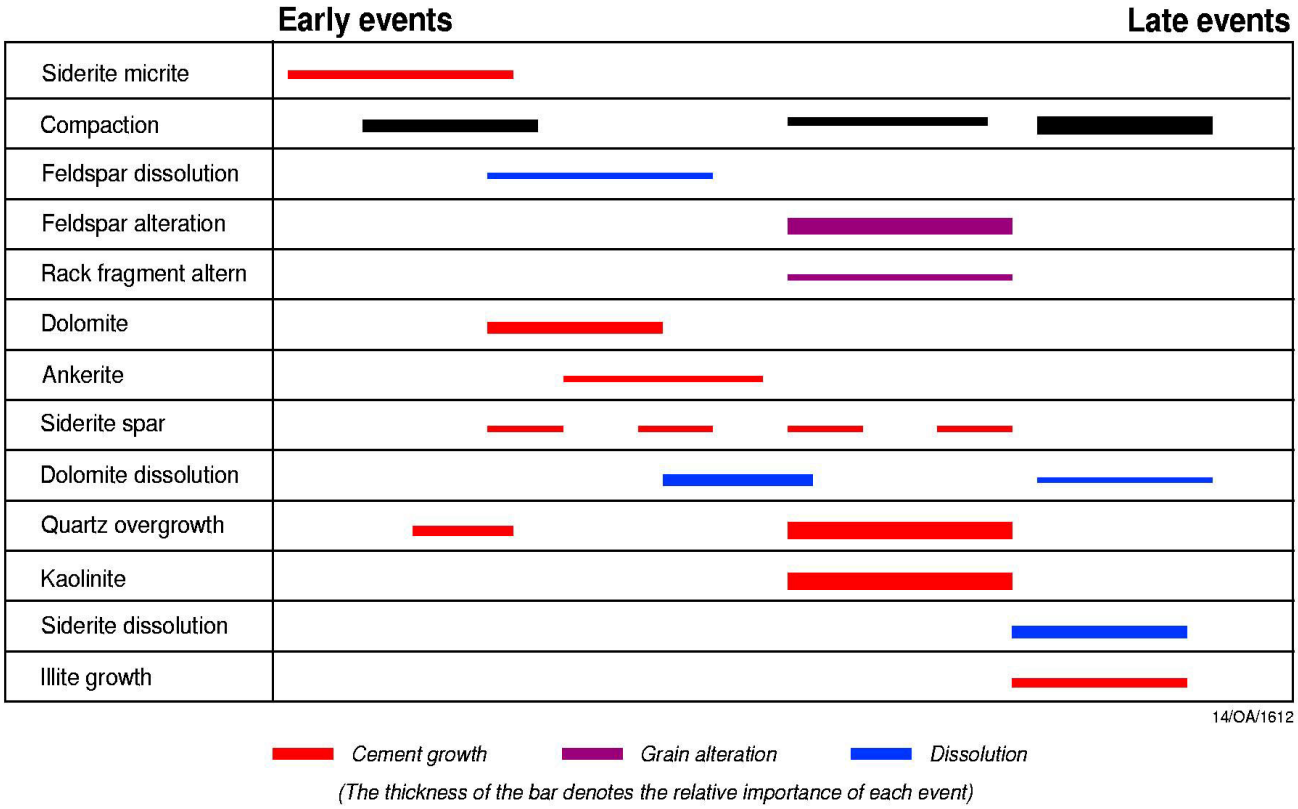

Figure 8.1 Stratigraphic chart for the Bass Basin using the nomenclature scheme of Lennon et al. (1999). The distribution of hydrocarbon accumulations and shows are indicated.

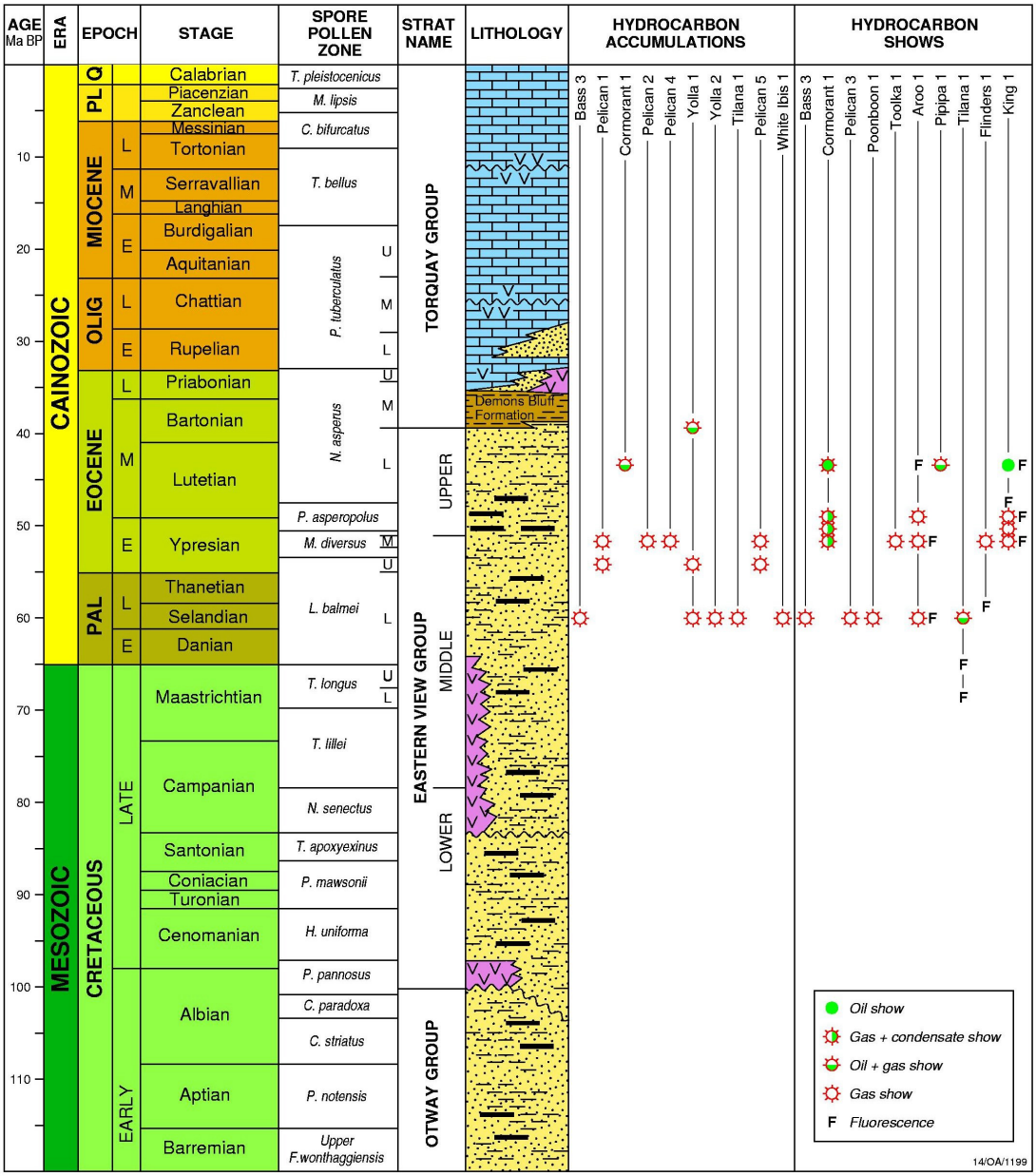

Figure 8.2 The core intervals logged by Baillie et al. (1991). The coarsening-upwards cycle in Dondu-1 is interpreted as a lake shoreline deposit. Coal-topped fining-upward intervals, such as Pelican-1 (Core 4), are interpreted as meandering fluvial systems. Flaser bedded units are probably lacustrine, while the core at Poonboon-1 probably represents deposition of stacked fluvial channels.

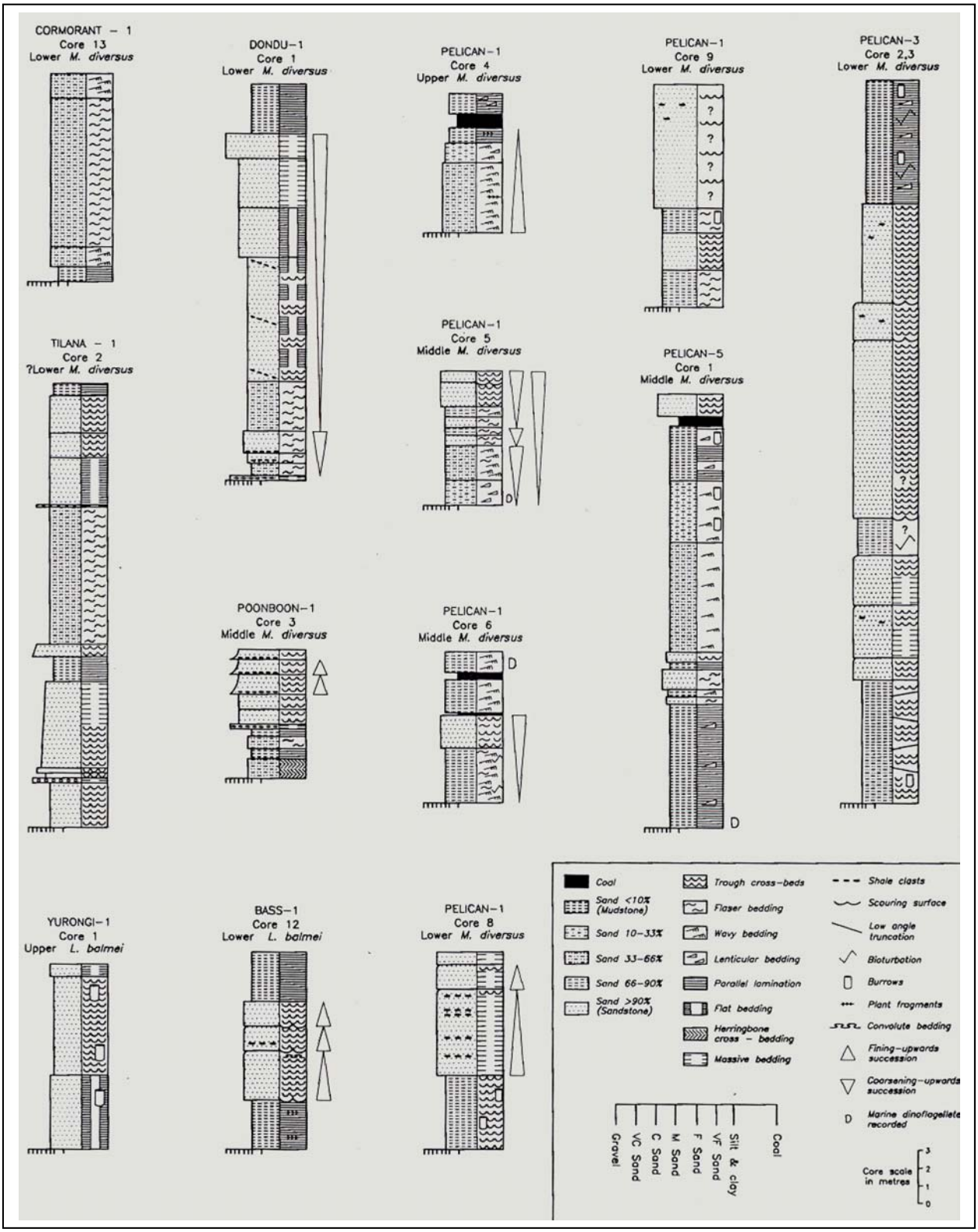

Figure 8.3 Scans of **t**hin sections to illustrate the nature of diagenetic events in the Bass Basin. Sediments in Bass-1 shows weak bioturbation, while Bass-2 is a bedded conglomerate. Dondu-1 has silty-to-very fine-grained sand interbedded with coarse to very coarse sand. The two mud rip-up conglomerates were chosen to show different diagenetic effects at different locations within the same environment of deposition. The deep Cormorant-1 sample shows ripple cross lamination.

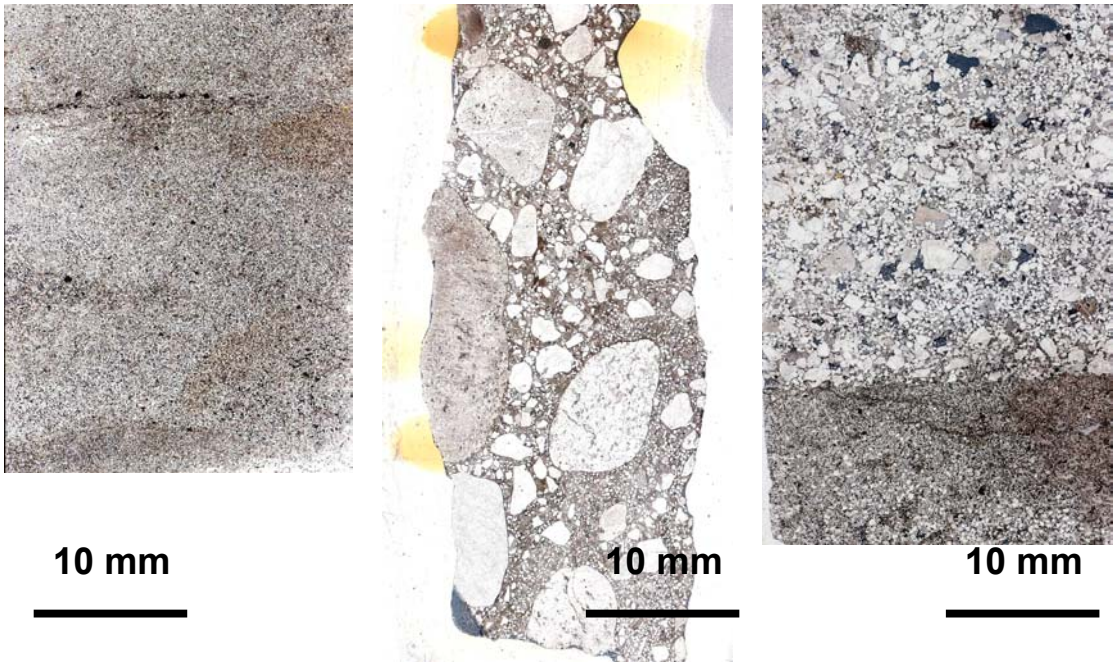

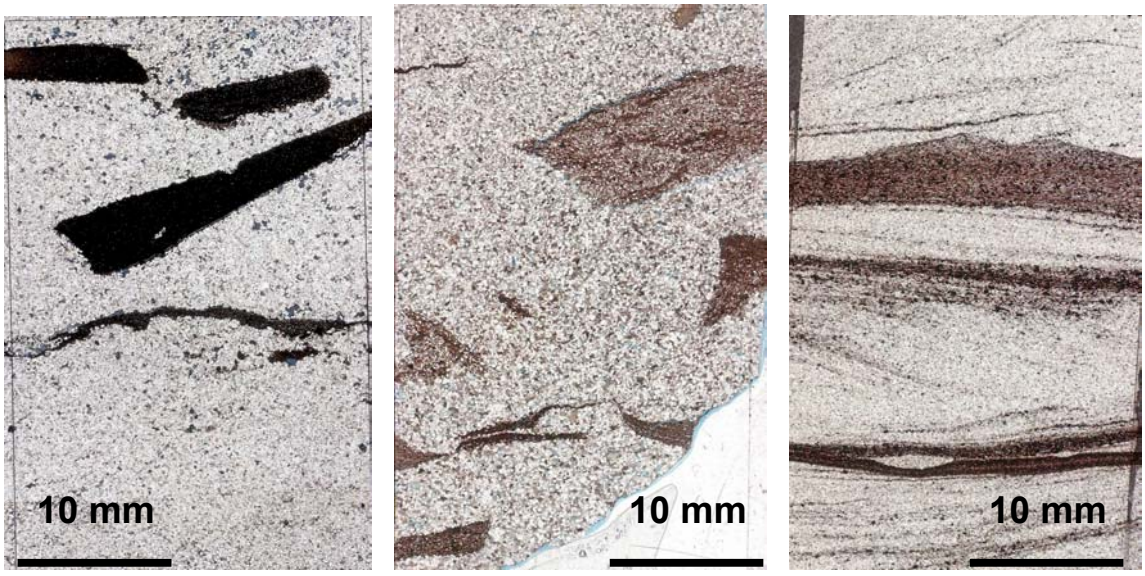

Figure 8.4 Core plug and petrographic data from Pelican-1 and Tilana-1 (from Baillie et al., 1991).

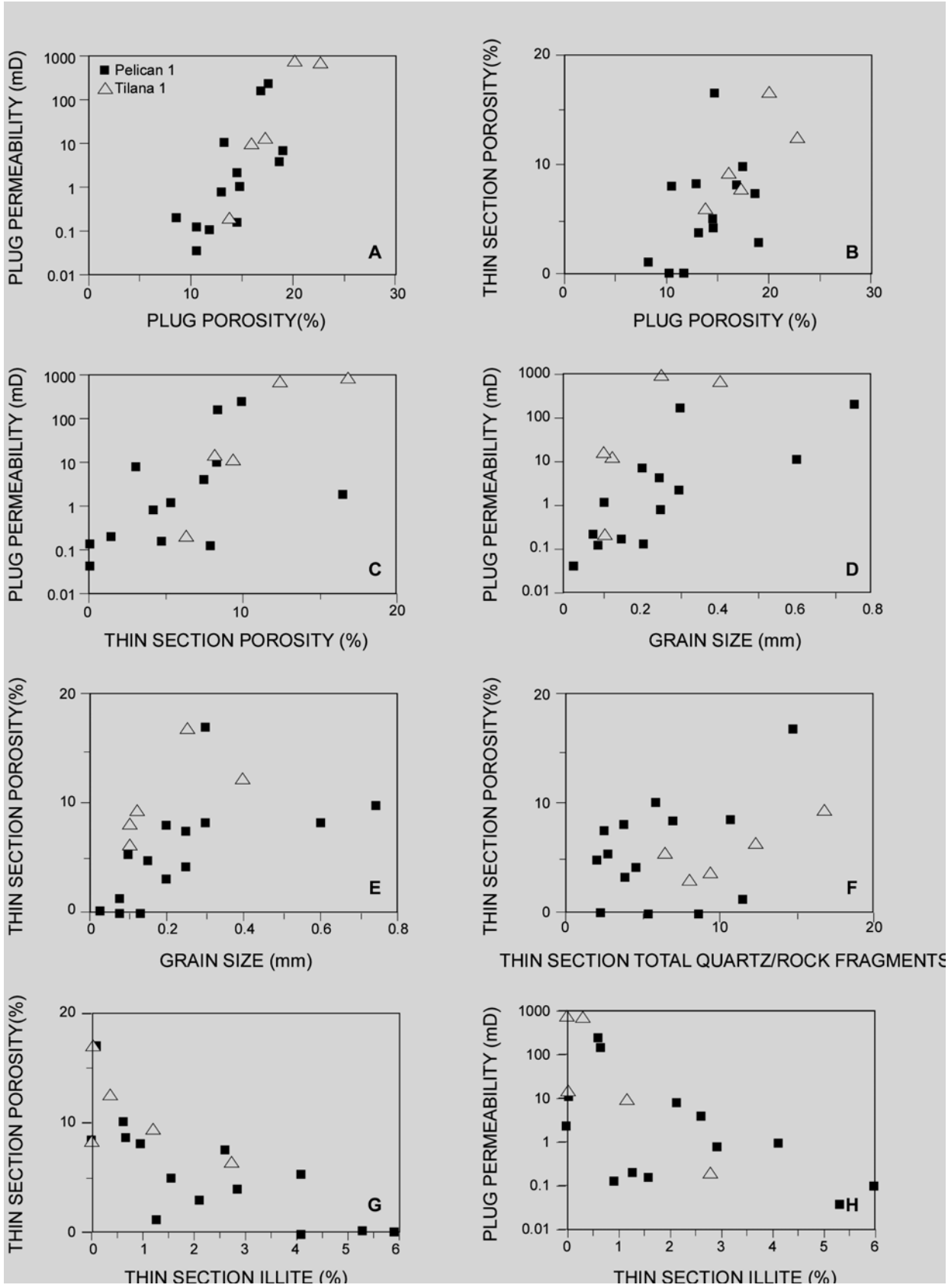

Figure 8.5 Cormorant-1, 2773 m. Photomicrographs of a ripple cross-laminated, interbedded carbonaceous siltstone and very fine sandstone. The images show abundant micritic to microspar siderite, the first cementation stage. The reducing conditions associated with the organic matter allow the siderite to grow. Stylolites are common with dissolution encouraged by the organic matter and clay. Other compaction indicators are the deformed muscovite flakes and complete lack of porosity.

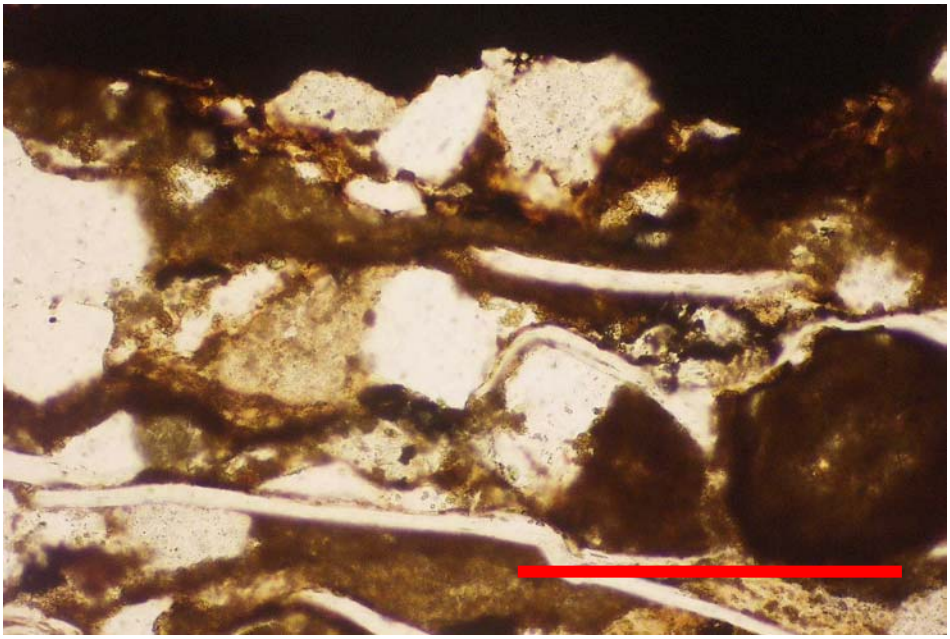

Figure 8.5a Plane polarised light (Scale bar 0.2mm)

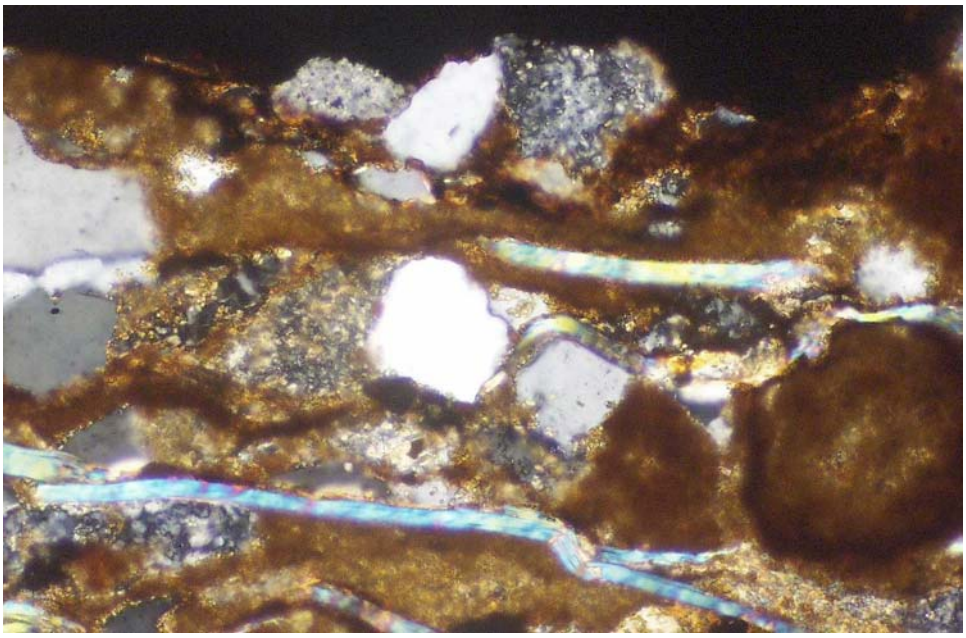

Figure 8.5b Crossed polars

Figure 8.6 Cormorant-1, 2773 m. Photomicrographs of a ripple cross-laminated, interbedded carbonaceous siltstone and very fine sandstone. 0.5 mm from a carbonaceous silt layer siderite is present, rimming the framework grains, but there is far less than in the silt band. The cross-polar image shows siderite as bright golden brown microspar (yellow circle) in contact with the allogenic quartz. Feldspars are completely altered to dense masses of kaolin (green circle).

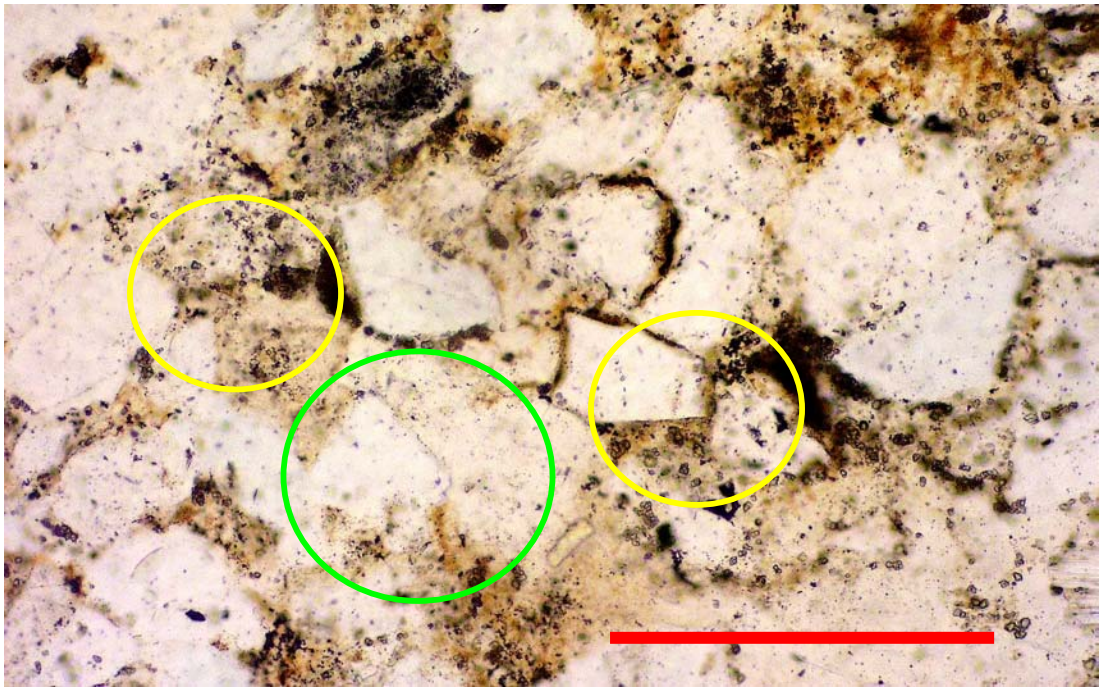

Figure 8.6a Plane polarised light (Scale bar 0.2 mm)

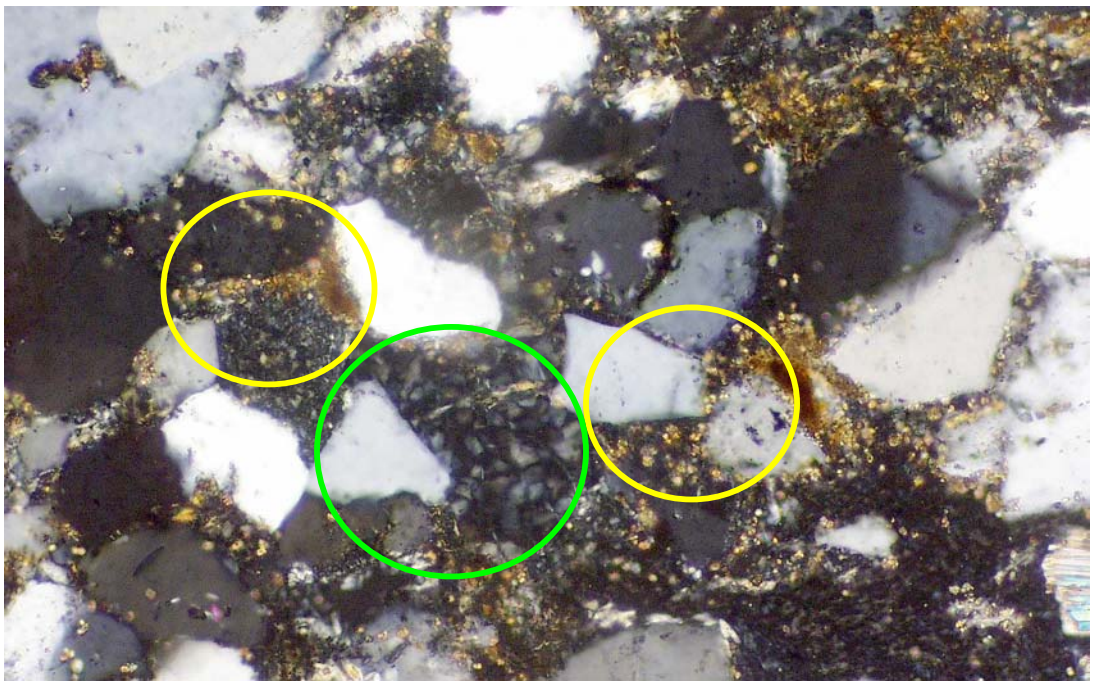

Figure 8.6b Crossed polars

Figure 8.7 Cormorant-1, 2773 m. Photomicrographs of a ripple cross-laminated, interbedded carbonaceous siltstone and very fine sandstnoe. Two millimetres from the nearest siltstone band, the amount of early siderite is minimal. This indicates that the reducing conditions associated with organic matter are essential in the precipitation of this cement phase. Feldspars are completed altered to areas of dense kaolin booklets (yellow circle) and rock fragments are altered to a mix of kaolin and illite (green circle).

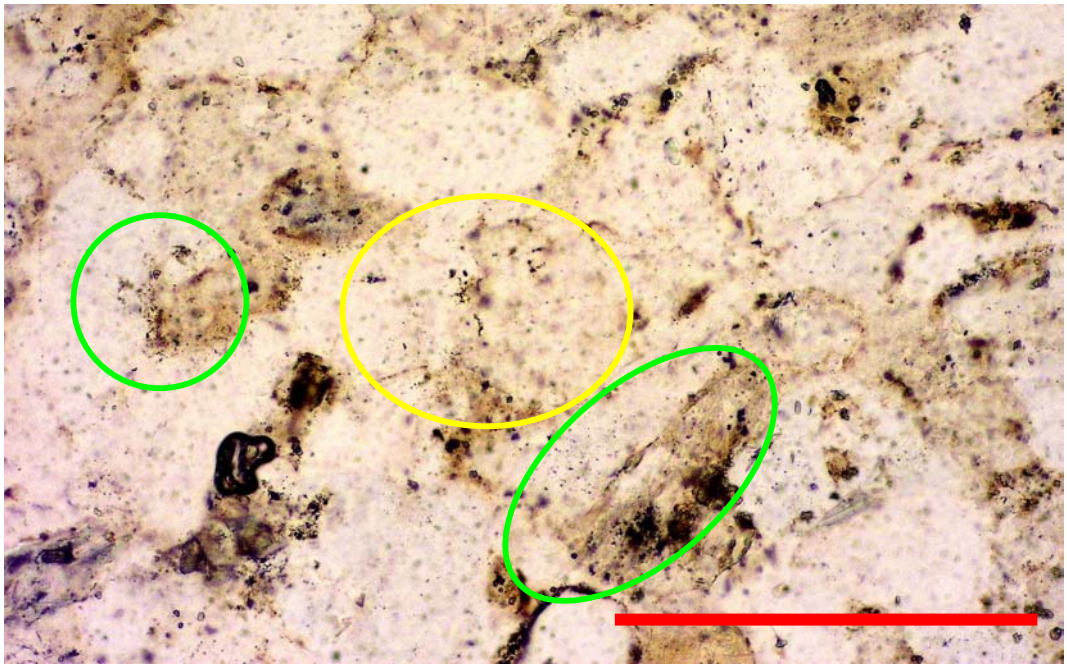

Figure 8.7a Plane polarised light (Scale bar 0.2 mm)

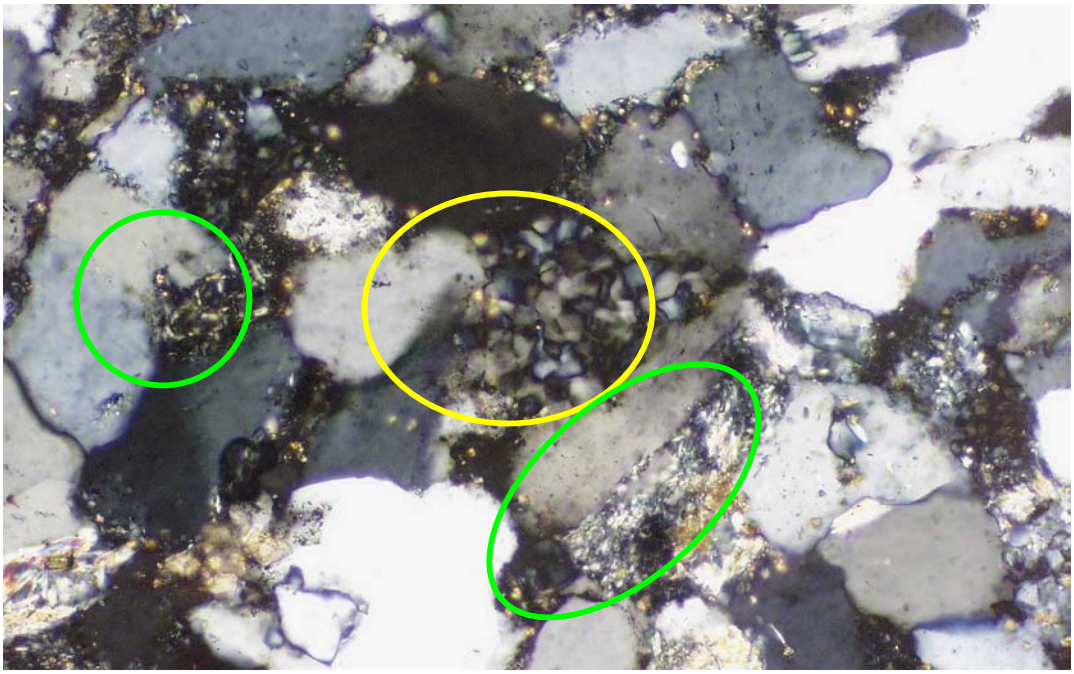

Figure 8.7b Crossed polars

Figure 8.8 Pelican-1, 2896.15 m. Mud rip-up clast conglomerate in medium to coarse sandstone. Microspar siderite growing within a deformed muscovite flake. The siderite post-dates compactional deformation.

Figure 8.8a Plane polarised light (Scale bar 0.2 mm)

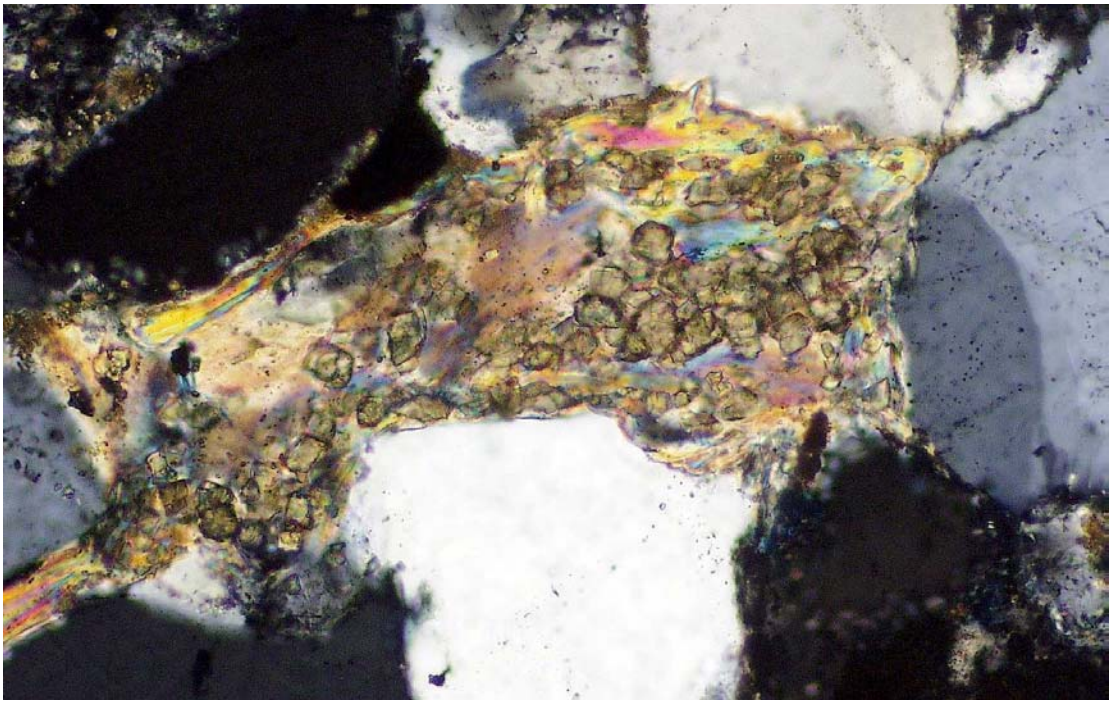

Figure 8.8b Crossed polars

Figure 8.9 Cormorant-1, 2773 m. Photomicrograph of ripple cross laminated, interbedded carbonaceous siltstone and very fine-grained sandstone. Detail in a silty layer shows the abundance of micritic and microspar siderite in association with organic matter. The siderite can form in clumps which replace the allogenic component of the rock (red circle) or scattered through the sample as a cement phase. The dark organic matter focuses dissolution of the silicate minerals, eventually forming stylolites (green circle). Muscovite flakes are deformed by compaction, sometimes altering to coarse-grained hydromuscovite or kaolin (yellow circle). The feature at centre left is an air bubble, an artifact of thin section preparation.

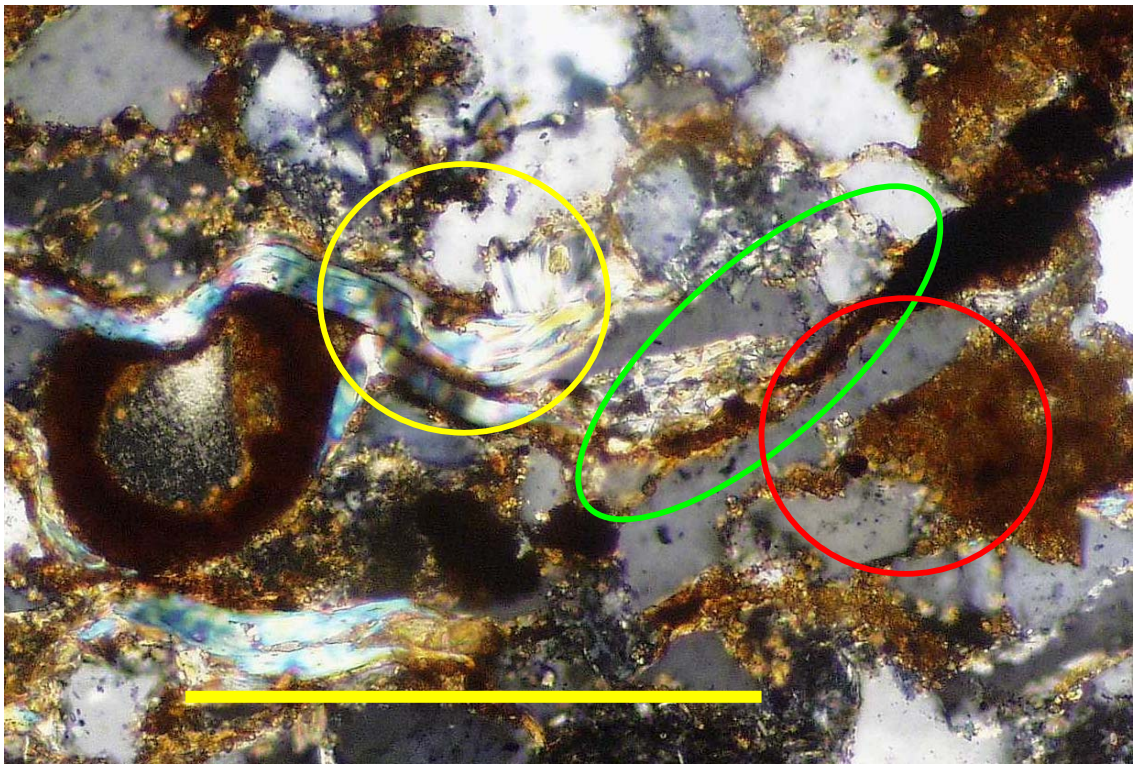

Figure 8.9 Crossed polars (Scale bar 0.2 mm)

Figure 8.10 Bass-2, 1441.26 m. Photomicrographs of a thin conglomerate layer within a sandy siltstone with mud rip-up clasts, possible floodplain deposits. Extensive low-Fe dolomite cement fills the porosity and etches quartz grains and their siderite rims (green circle) and dissolves feldspar grains (bright pale blue under CL). The dolomite appears to have been recrystallised as there is no obvious internal banding.

Figure 8.10a Plane polarised light (Scale bar 0.5 mm)

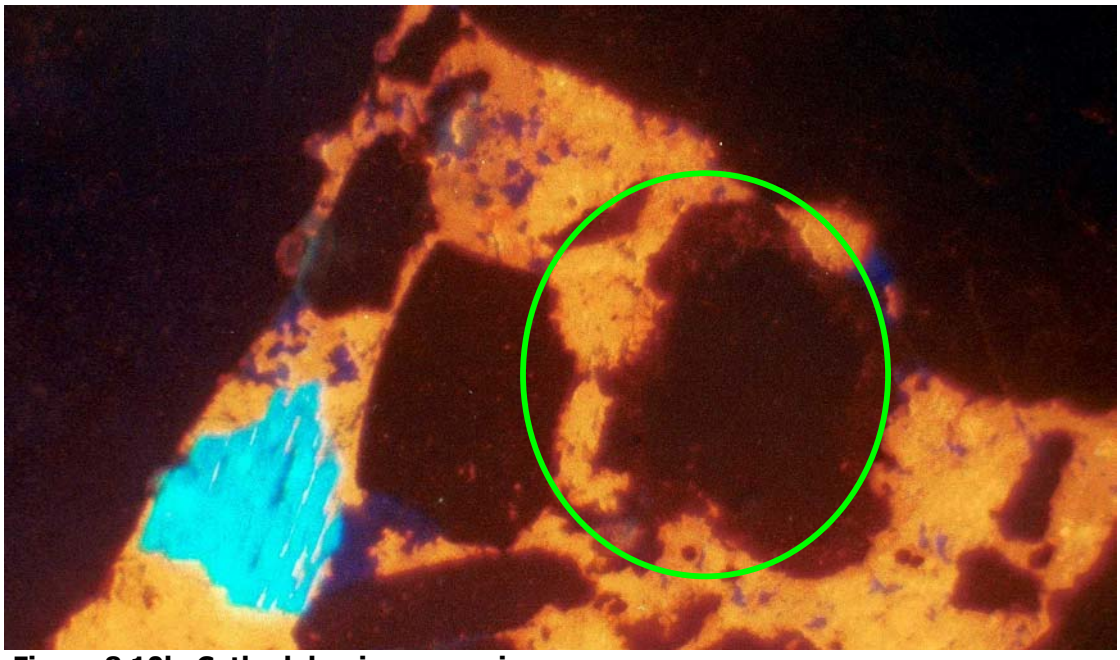

Figure 8.10b Cathodoluminescence image

Figure 8.11 Bass-2, 1441.26 m. Photomicrographs of a thin conglomerate layer within a sandy siltstone with mud rip-up clasts, possible floodplain deposits. Low-Fe dolomite completely fills pore space and dissolves a feldspar grain. Faint CL banding suggests a bright dolomite phase rimming the grains followed by a darker, pore-filling phase (green circle).

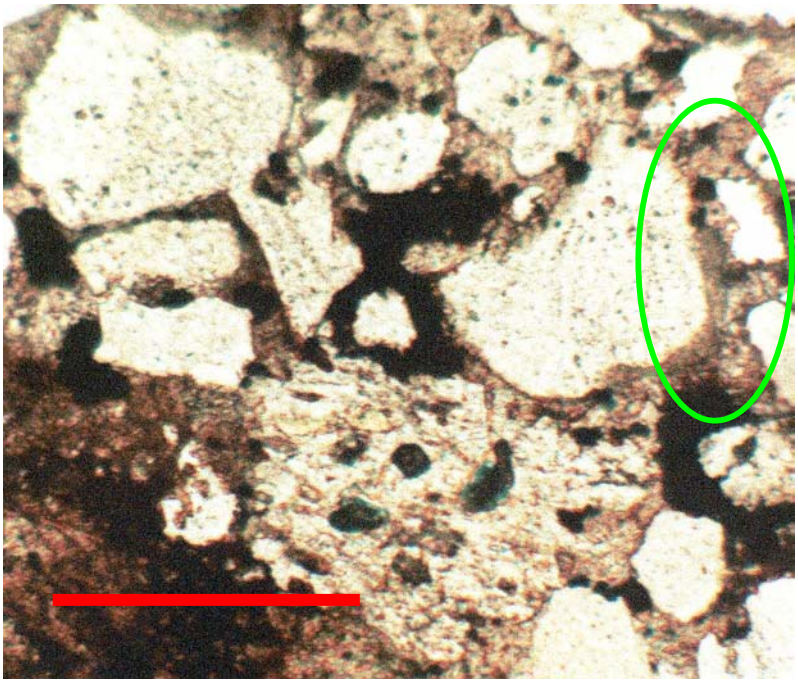

Figure 8.11a Plane polarised light (Scale bar 0.5mm)

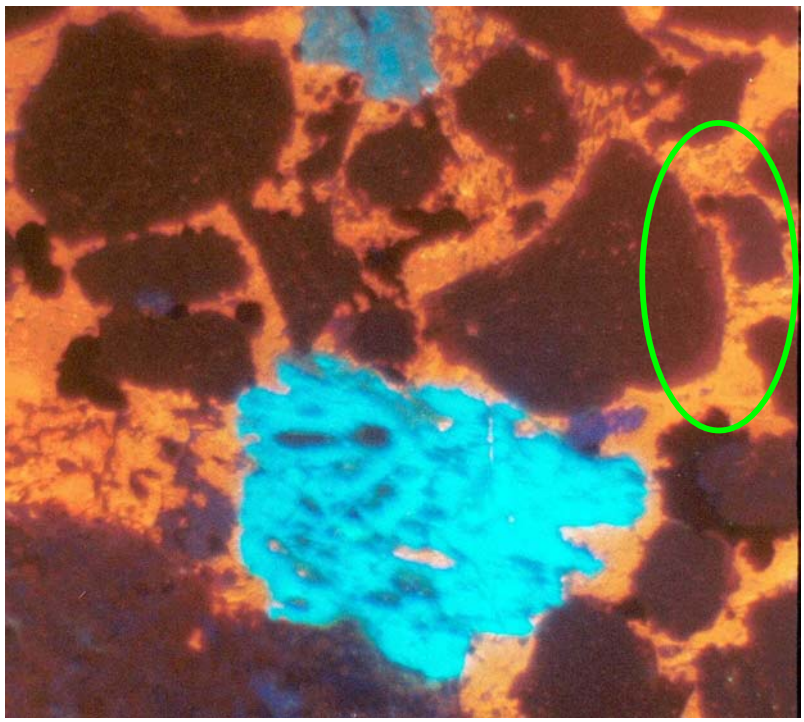

Figure 8.11b Cathodoluminescence image

Figure 8.12 Bass-1, 2108.54 m. Photomicrographs of siderite spare rhombs (dark in CL, yellow circle) grow on the edge of siderite micrite (dark in plane light) which cements and etches quartz silt. A composite granitic grain which was largely feldspar, has altered to a dense mass of kaolin (bright blue in CL). There was some feldspar dissolution prior to alteration to allow siderite cement against the odd-shaped quartz grain within the composite grain. Loose-packed kaolin grows away from the altered feldspar in pores among the framework grains.

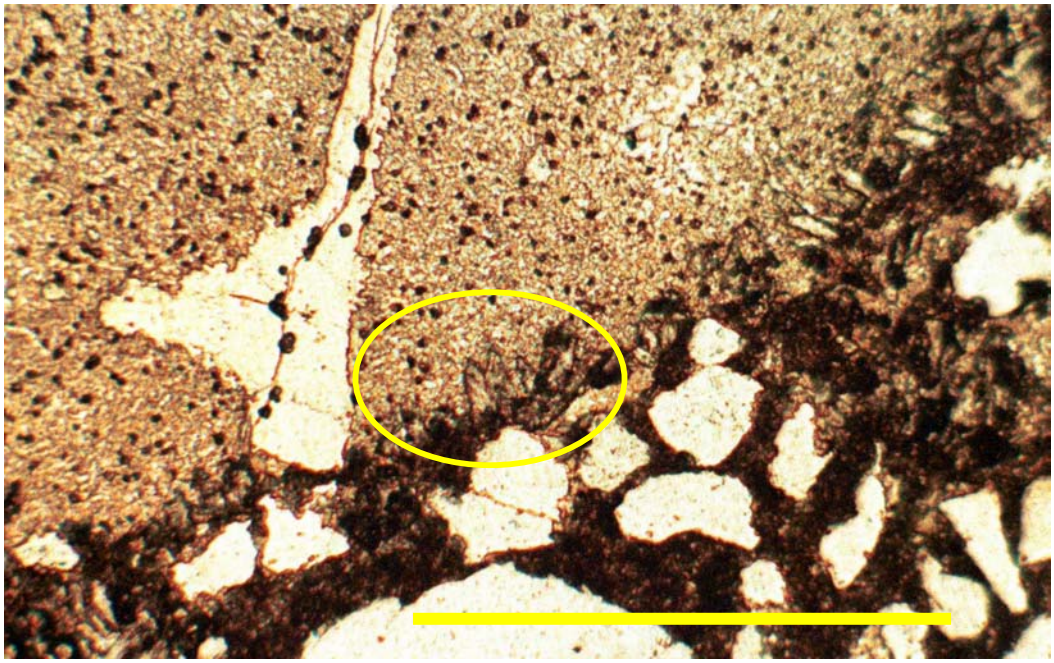

Figure 8.12a Plane polarised light (Scale bar 0.5 mm)

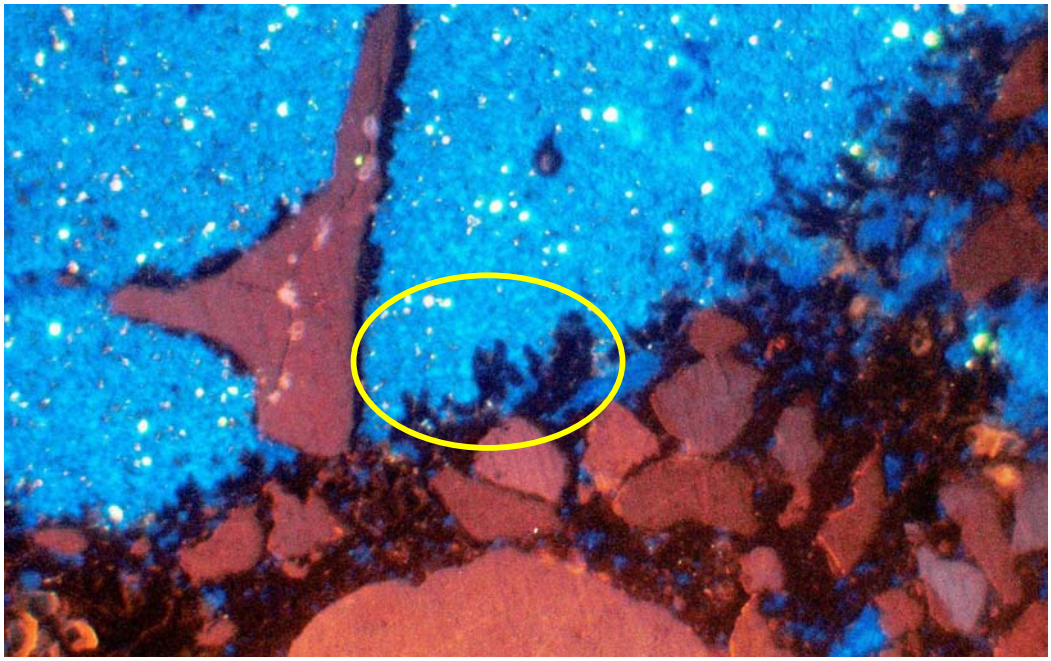

Figure 8.12b Cathodoluminescence image

Figure 8.13 Bass-2, 1441.26 m. Photomicrograph of a thin conglomerate layer within a sandy siltstone with mud rip-up clasts, possible flood plain deposits. Brightly luminescent dolomite partly fills porosity between quartz grains. There is extensive dissolution of dolomite (red circles) before the precipitation of kaolinite (speckled blue). Ankerite, or possible siderite rhombs (yellow circle) are clear under CL but the pitted surface of the slide make them hard to see in plain light.

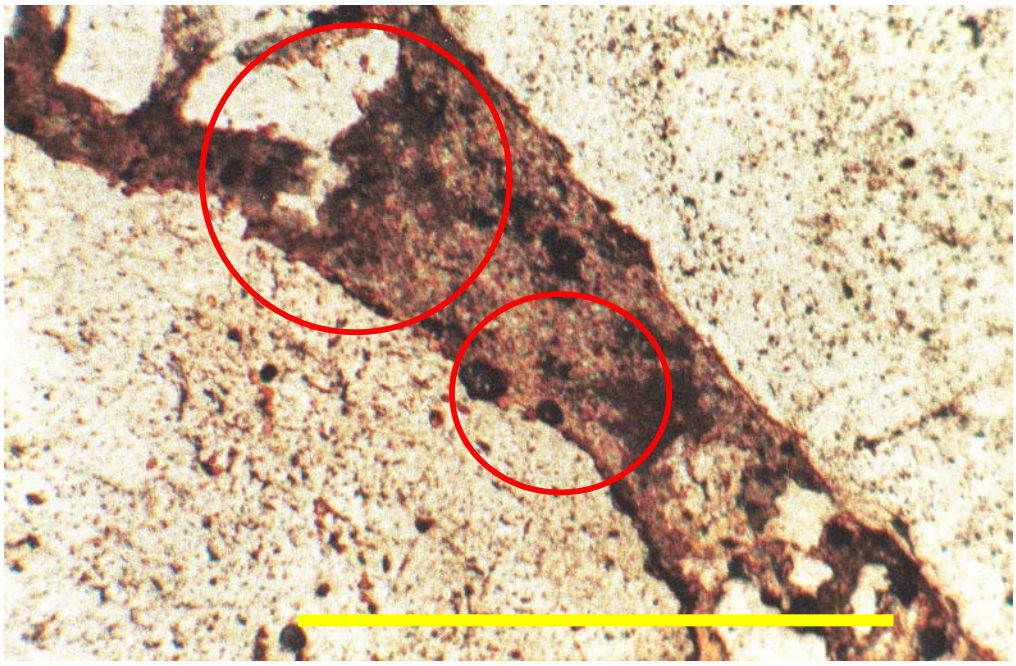

Figure 8.13a Plane polarised light (Scale bar 0.5 mm)

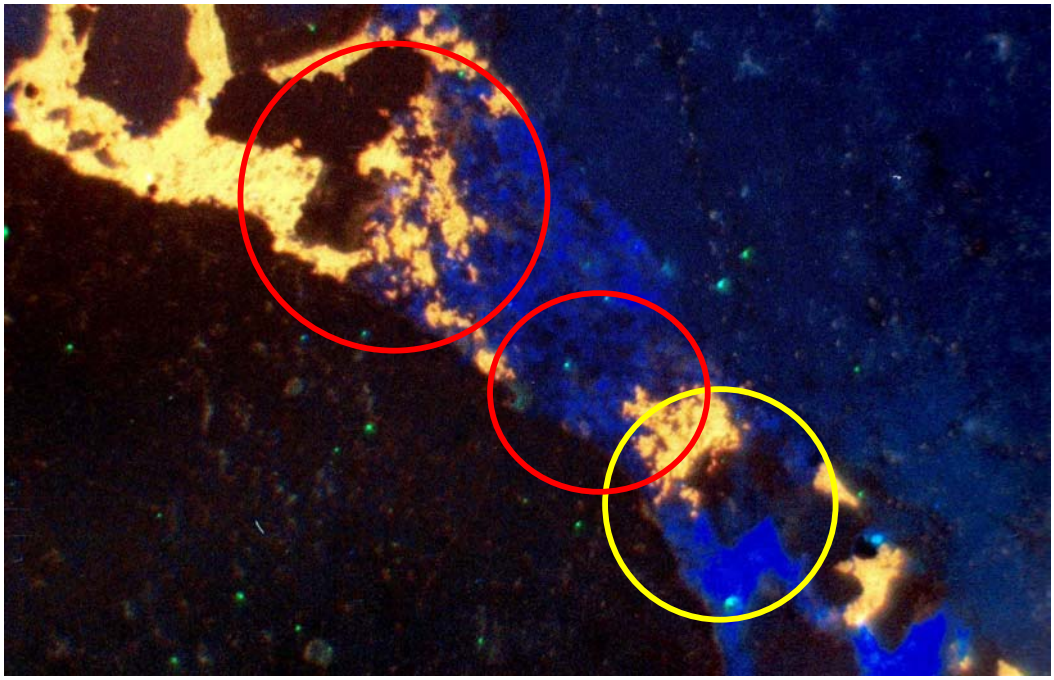

Figure 8.13b Cathodoluminescence image

Figure 8.14 Pelican-1, 2606.6 m. Photomicrographs of a fine sandstone with flaser bedding and trough cross bedding. These two images illustrate several points in the history of quartz diagenesis. The blue grain was fractured by early compaction then healed with quartz cement (pale brown in CL). The same cement rims most framework grains. Metamorphic quartz (reddish grains) has no overgrowth or only a thin rim. Most quartz rims have been subjected to local dissolution, probably by carbonate grains, which have been subsequently dissolved to give irregular outlines to the grains. The orange colours in plain light are burn marks in araldite resin from prolonged CL exposure.

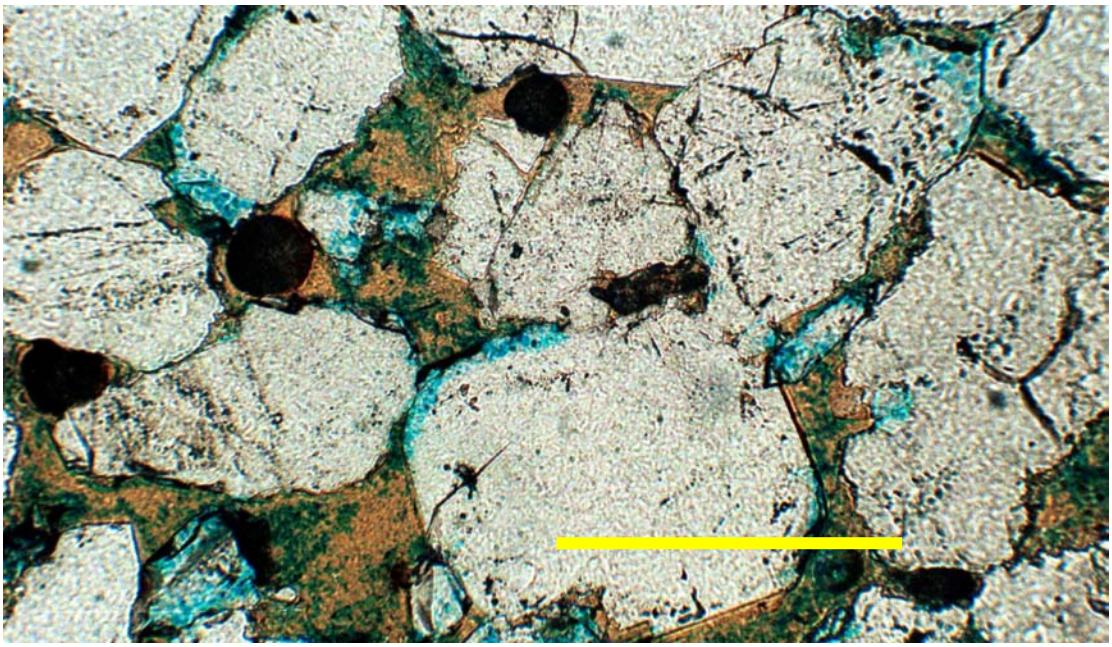

Figure 8.14a Plane polarised light (Scale bar 0.2 mm)

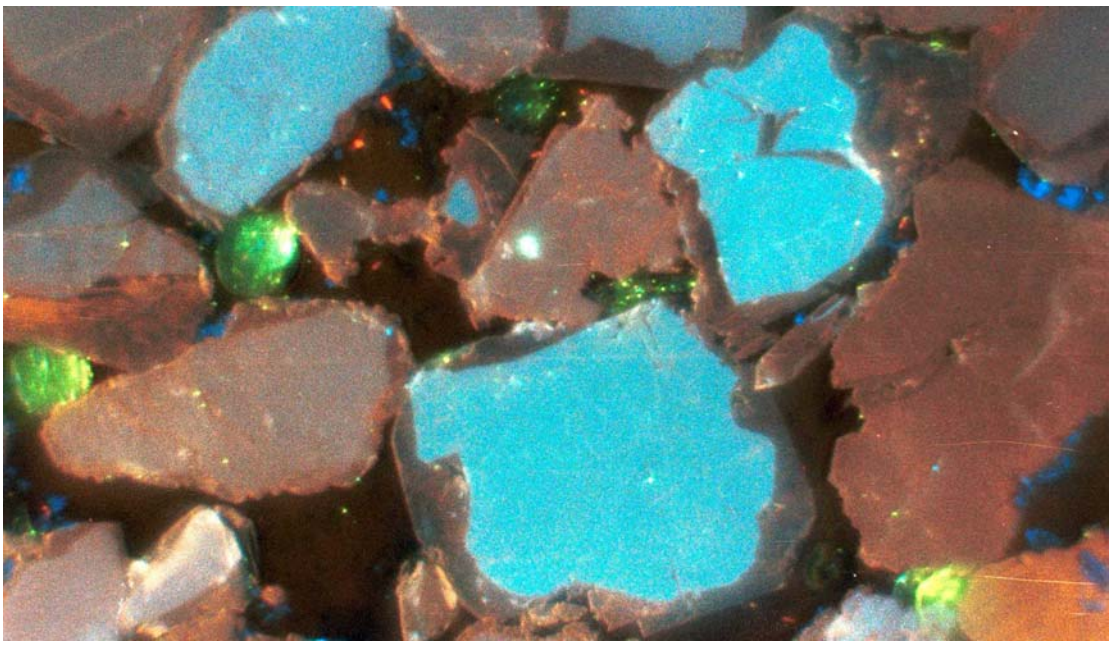

Figure 8.14b Cathodoluminescence image

Figure 8.15 Dondu-1, 2349 m. Photomicrographs of a coarse to very coarse-grained sand that appears to be a channel sandstone as the interval above is a lacustrine shoreline unit. Quartz cement fringes the framework quartz grains (pale purple in CL). Masses of kaolin (bright blue in CL) fill the pores. The jagged contact between the quartz cement and kaolin is a function of intergrowth of the two cements, indicating they are co-genetic. The fact that these two minerals grow together indicates a common origin, probably from the alteration and dissolution of feldspar. The mid-blue patches of kaolin under CL (circle) are the areas mixed with organic matter, possible recrystallised matrix.

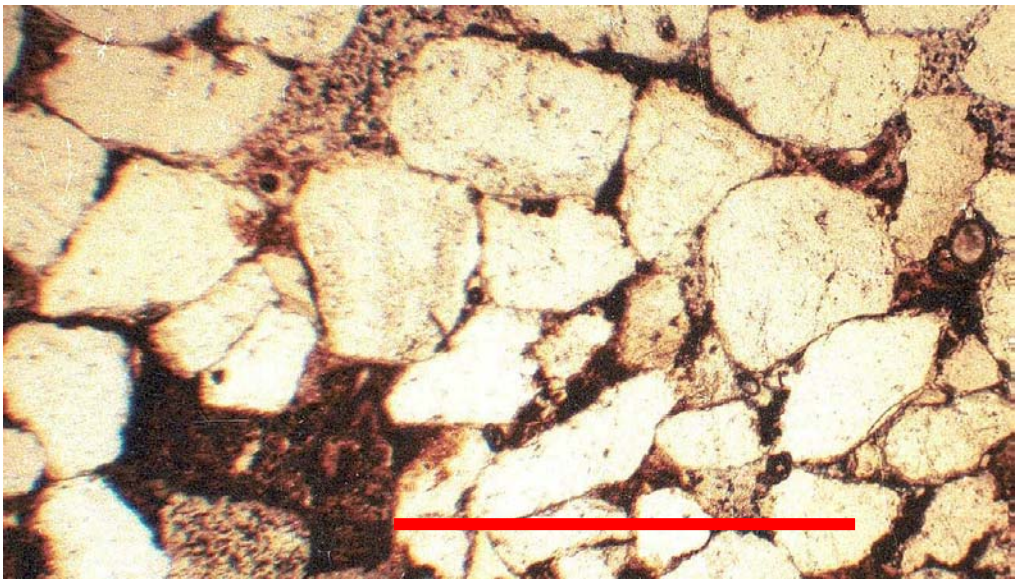

Figure 8.15a Plane polarised light (scale bar 0.5 mm)

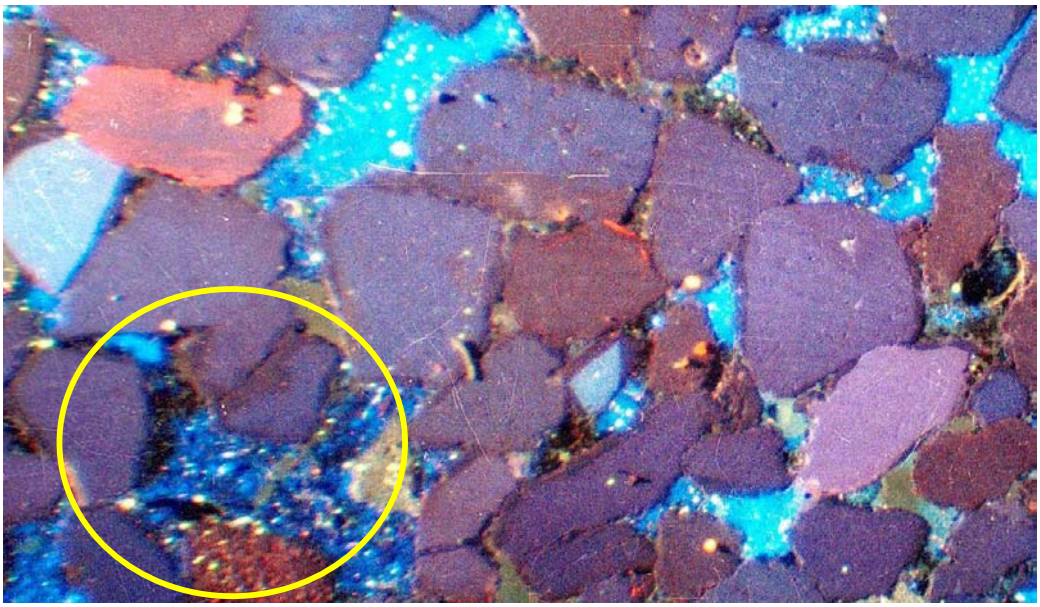

Figure 8.15b Cathodoluminescence image

Figure 8.16 Cormorant-1, 2640.2 m. Photomicrographs showing extensive siderite micrite rims that etch the framework grains. A feldspar grain (yellow circle) has been completed altered to a dense mat of kaolin. The ends of the feldspar are shown by minor siderite. Beyond the original grain, slightly coarser kaolin grows into primary porosity (red circle).

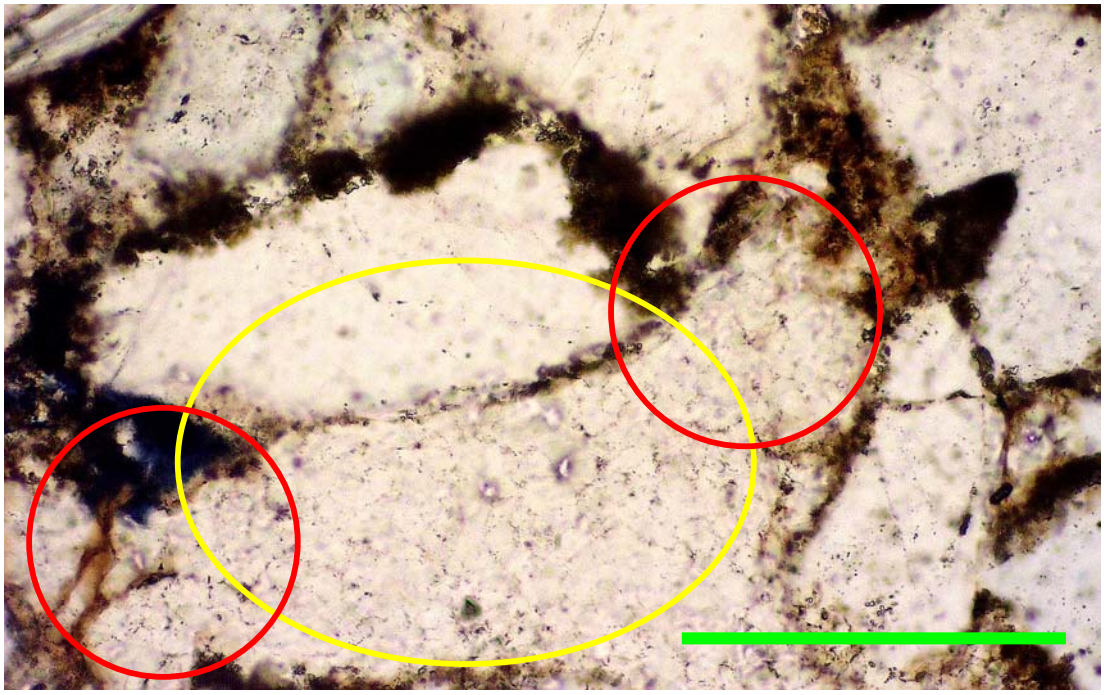

Figure 8.16a Plane polarised light (Scale bar 0.2 mm)

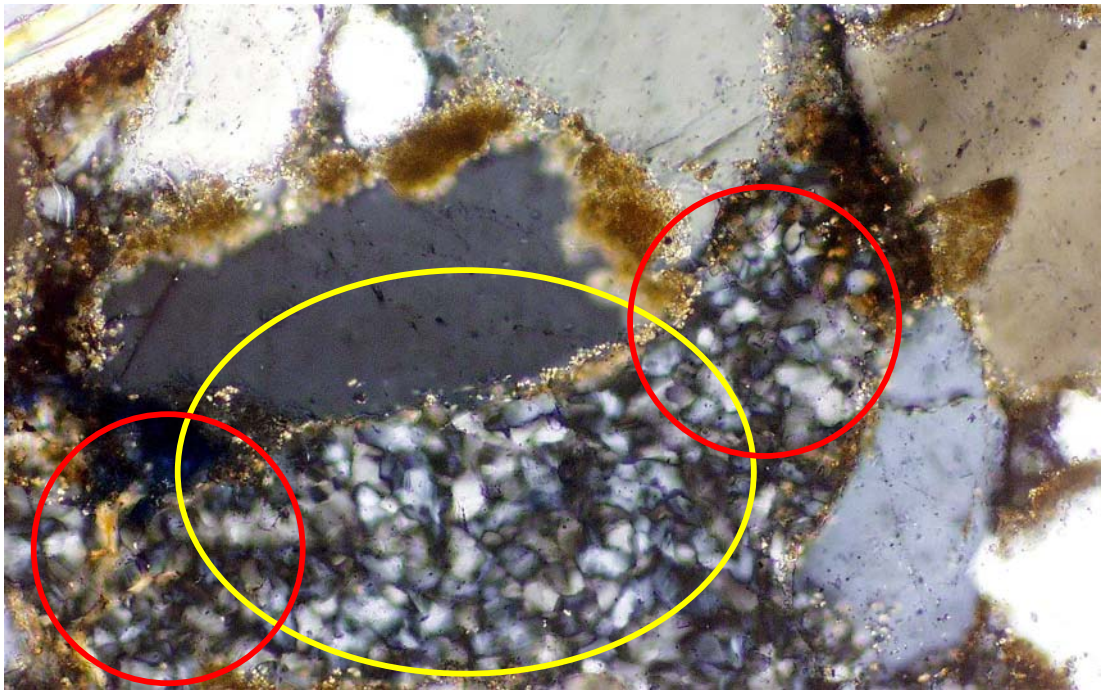

Figure 8.16b Crossed polars.

Figure 8.17 Dondu-1, 2349 m. Photomicrographs of a coarse sand to gravel in a channel. A shoreline connection, probably lacustrine, is suggested by the coarsening up, flaser bedded to flat bedded interval above. Euhedral quartz overgrowths (yellow circle) occur against open pore spaces. Where there is extensive kaolin growth (mottled grey tones), either as alteration of a feldspar or neoformed in the pore space adjacent, the authigenic quartz is intergrown with the kaolin. Dolomite (red cicle) shows dissolution prior to kaolin cement emplacement. The dolomite crystals in Figure 8.17b show zoned growth.

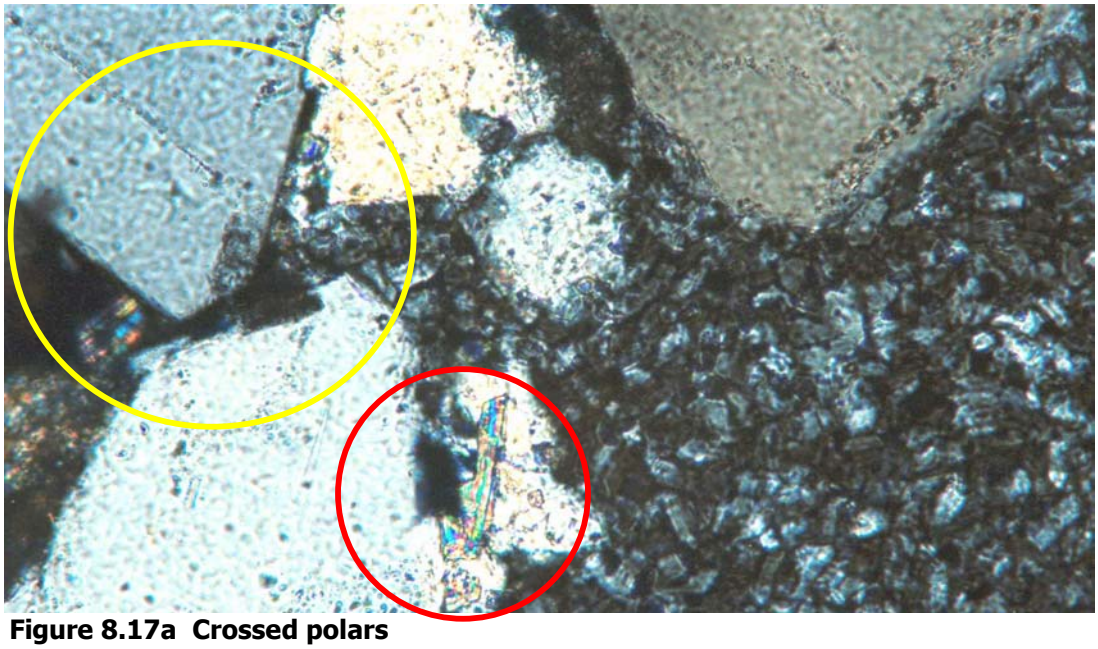

Figure 8.17a Crossed polars

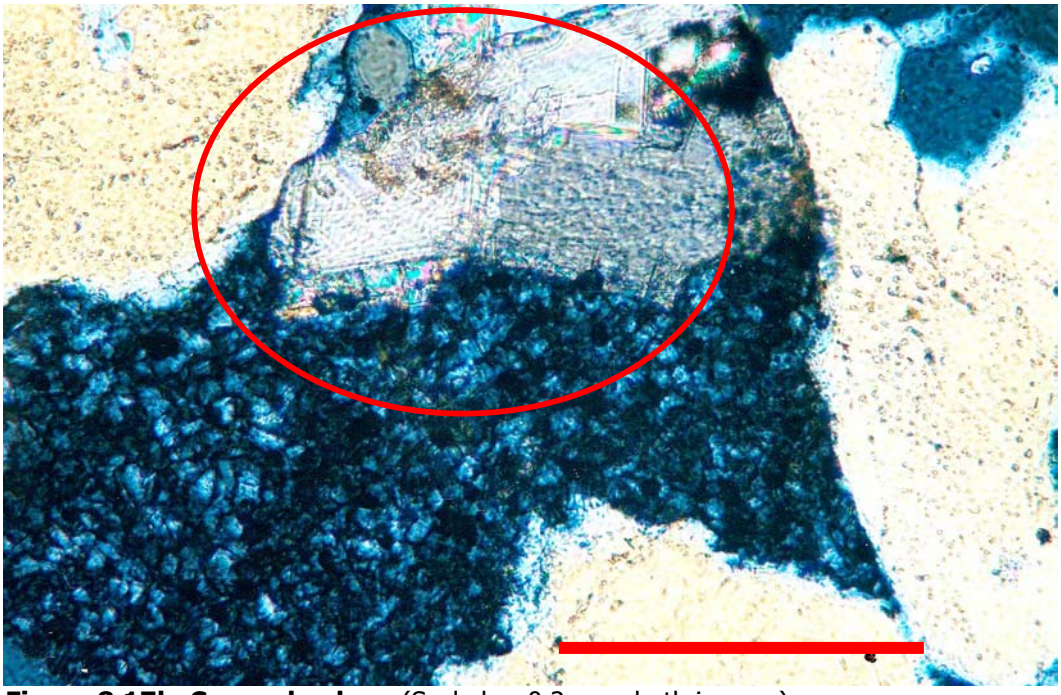

Figure 8.17b Crossed polars (Scale bar 0.2 mm, both images)

Figure 8.18 Pelican-1, 2896.15 m. Photomicrographs of a mud rip-up clast conglomerate in medium to coarse-grained sandstone. Thin siderite rims on framework grains predate extensive alteration of feldspars and rock fragments. The areas in these altered grains are then subject to considerable compaction which removes all porosity. Quartz-rich areas retain porosity. Thick quartz overgrowths (yellow circle) predate extensive compaction.

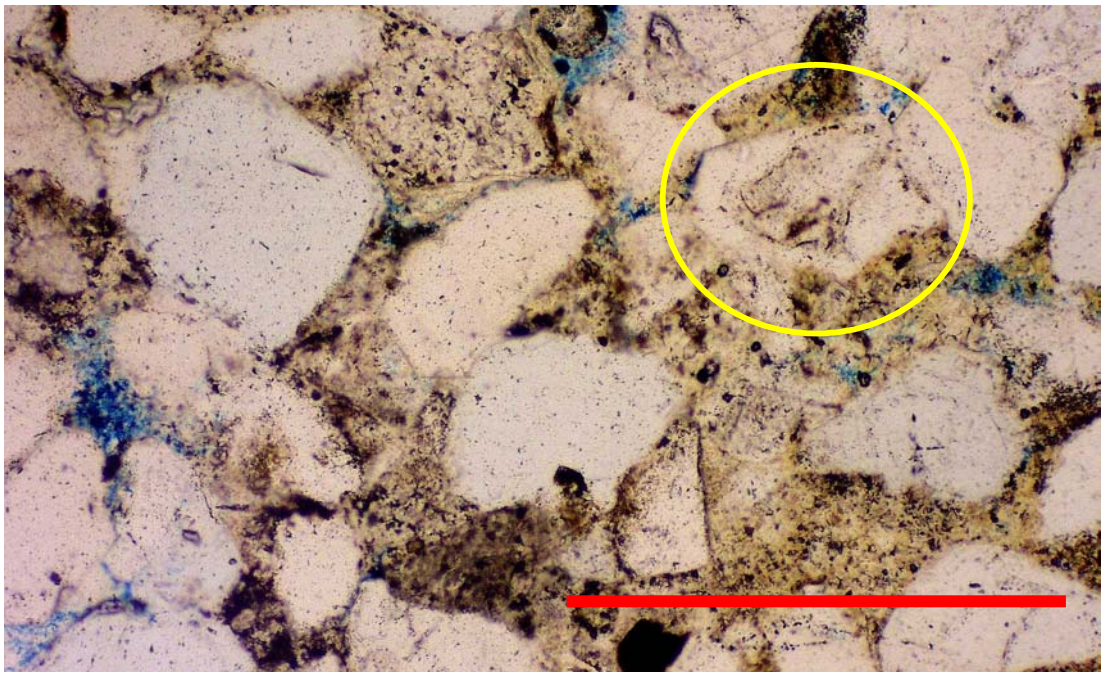

Figure 8.18a Plane polarised light (Scale bar 0.5 mm)

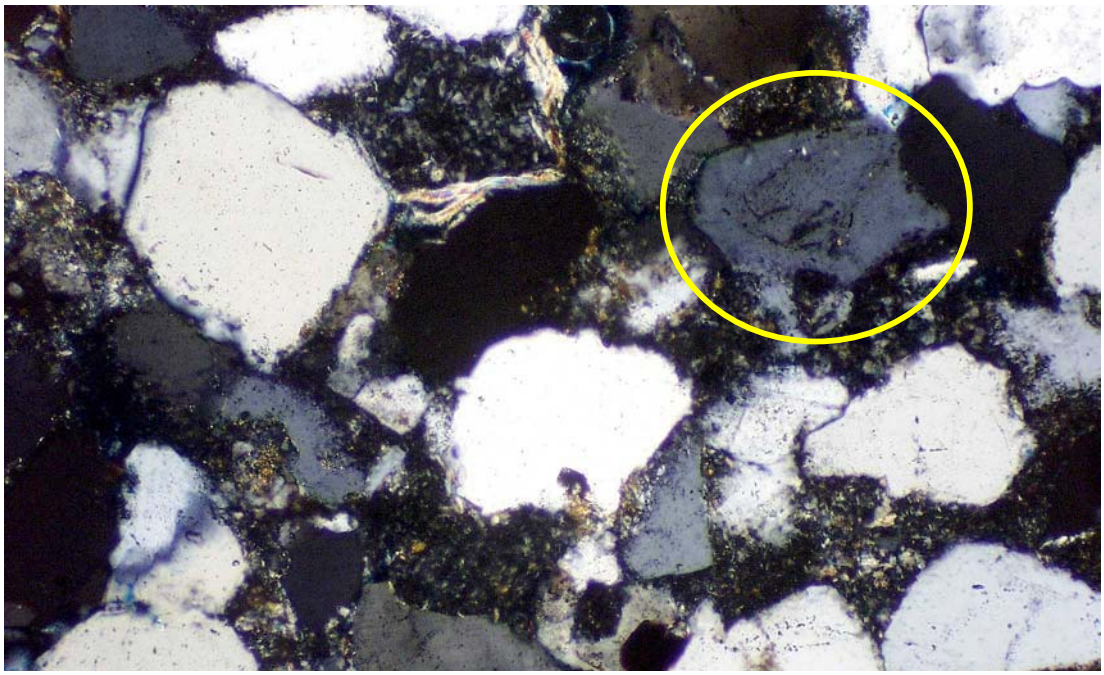

Figure 8.18b, Crossed polars

Figure 8.19 Pelican-1, 2896.15 m. Photomicrographs of a mud rip-up clast conglomerate in medium to coarse-grained sandstone. Detail of this image shows that some compaction has occurred after the quartz overgrowths formed. Plane light shows micritic siderite rimming and etching the framework grains. The porosity appears all secondary, created by the dissolution of a carbonate phase, probably dolomite, as siderite is still present.

Figure 8.19a Plane polarised light (scale bar, 0.5 mm)

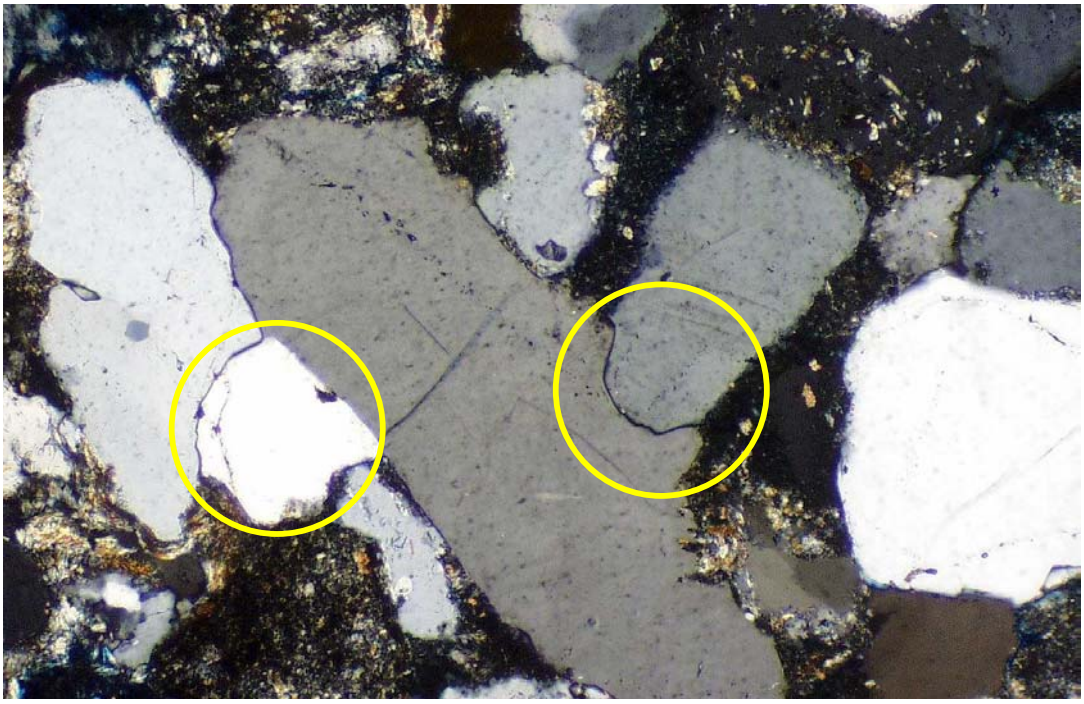

Figure 8.19b Crossed polars

Figure 8.20 Pelican-1, 2896.15 m. Photomicrographs of a mud rip-up clast conglomerate in medium to coarse-grained sandstone. Detail around the end of a quartz grain with thick overgrowth shows that some compaction occurred after the overgrowth was precipitated. A line of siderite micrite indicates the original edge of the grain.

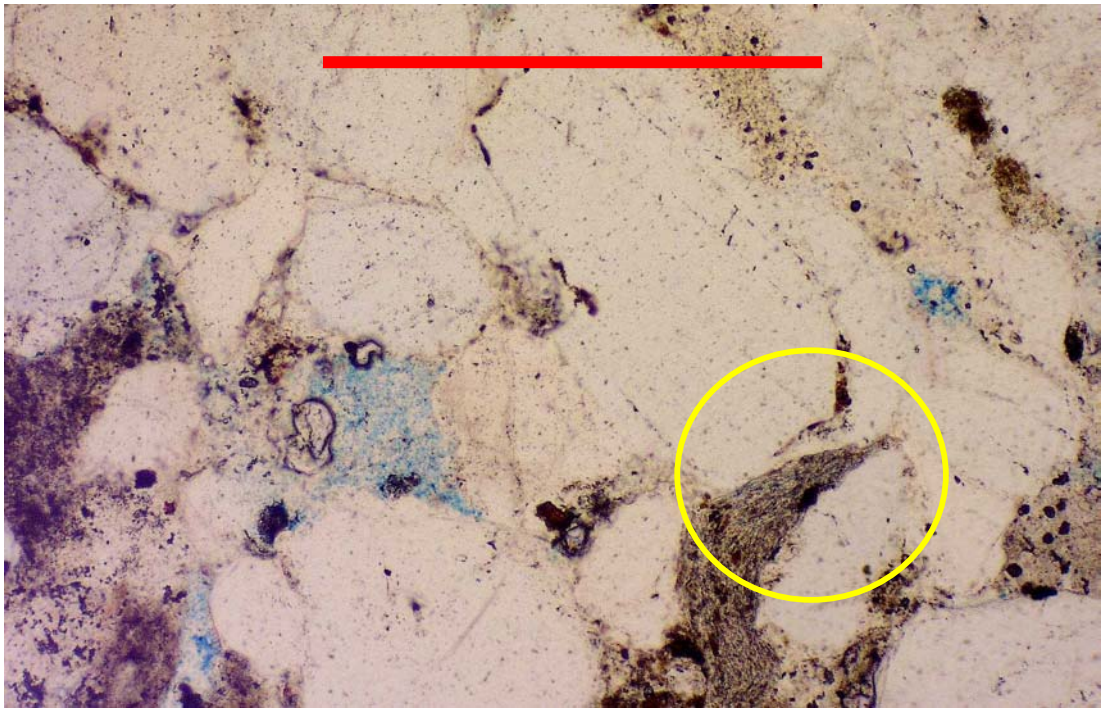

Figure 8.20a Plane polarised light (Scale bar 0.5 mm**)**

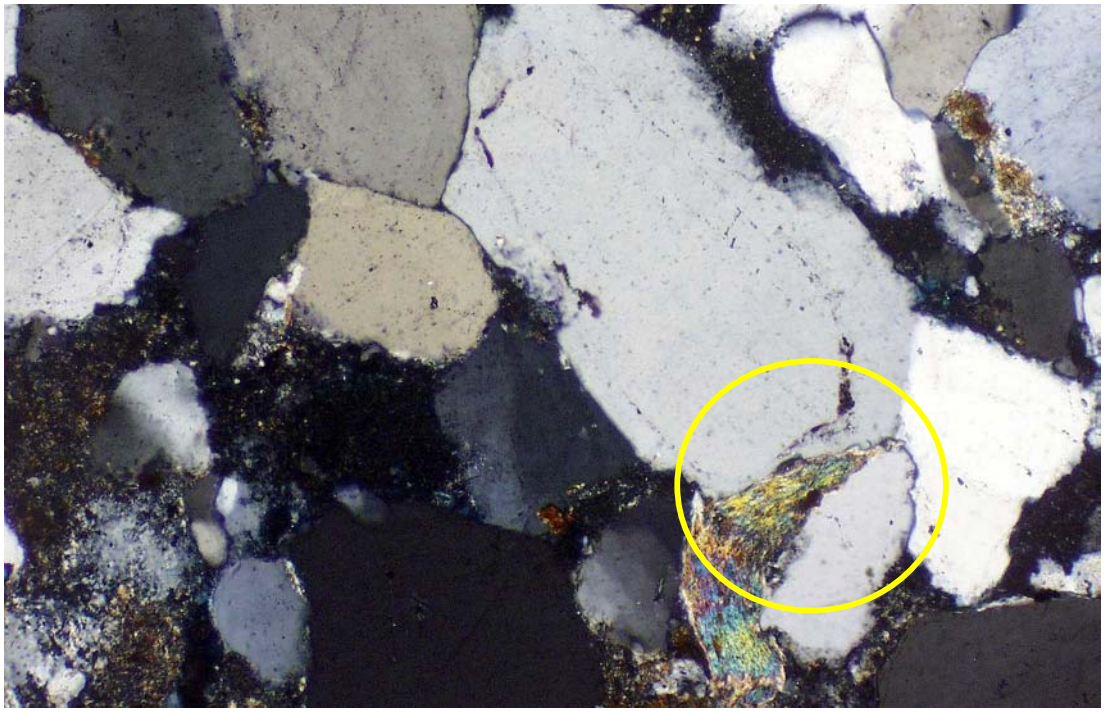

Figure 8.20b Crossed polars

Figure 8.21 Geothermal gradient as measured from the present day bottom hole temperatures. Contours are in degrees Celsius per kilometre (adapted from Cubitt, 1992).

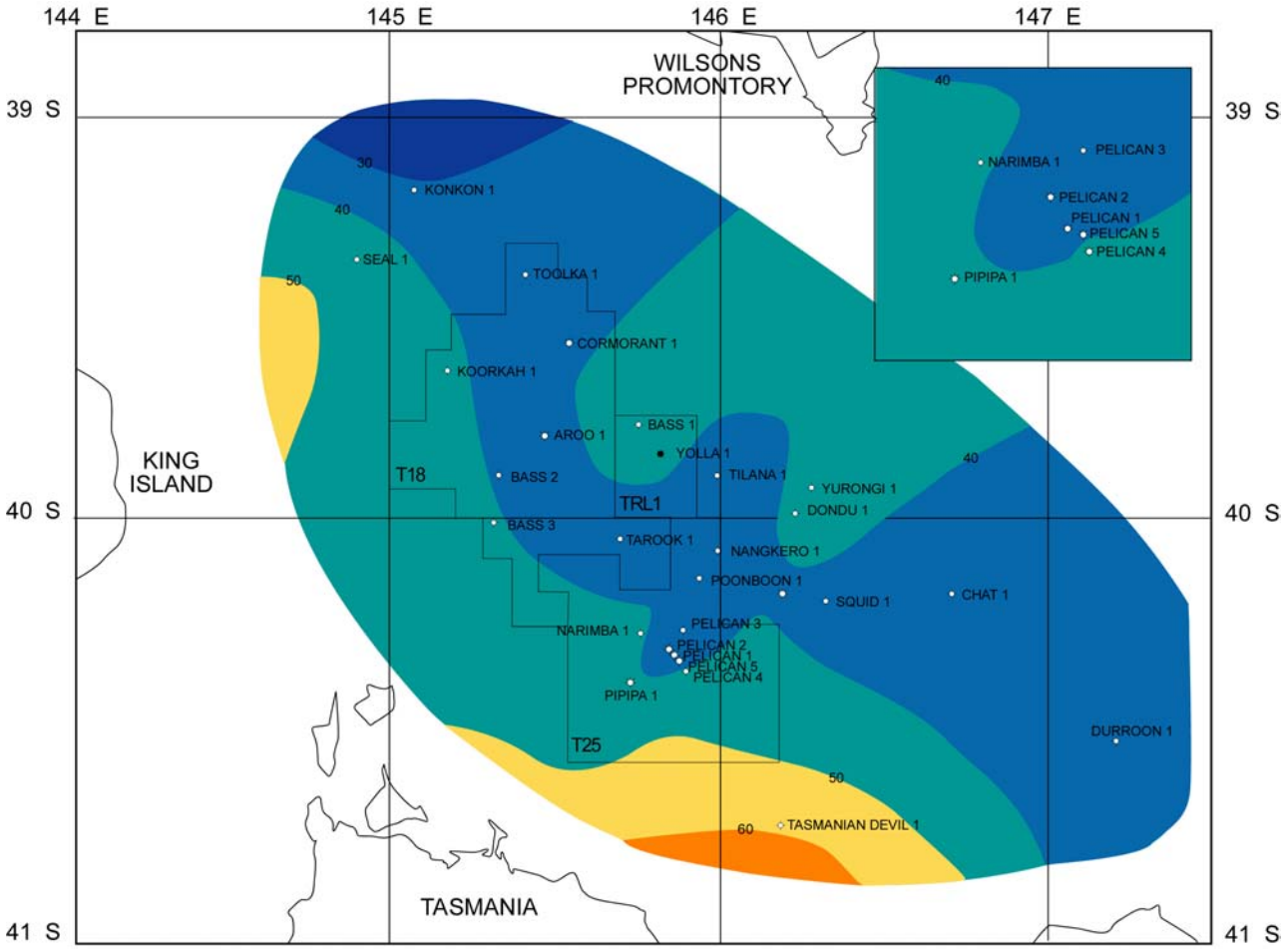

Figure 8.22 Isothermal map at a depth of 1000 m subsea. Contours are in degrees Celsius (adapted from Cubitt, 1992).

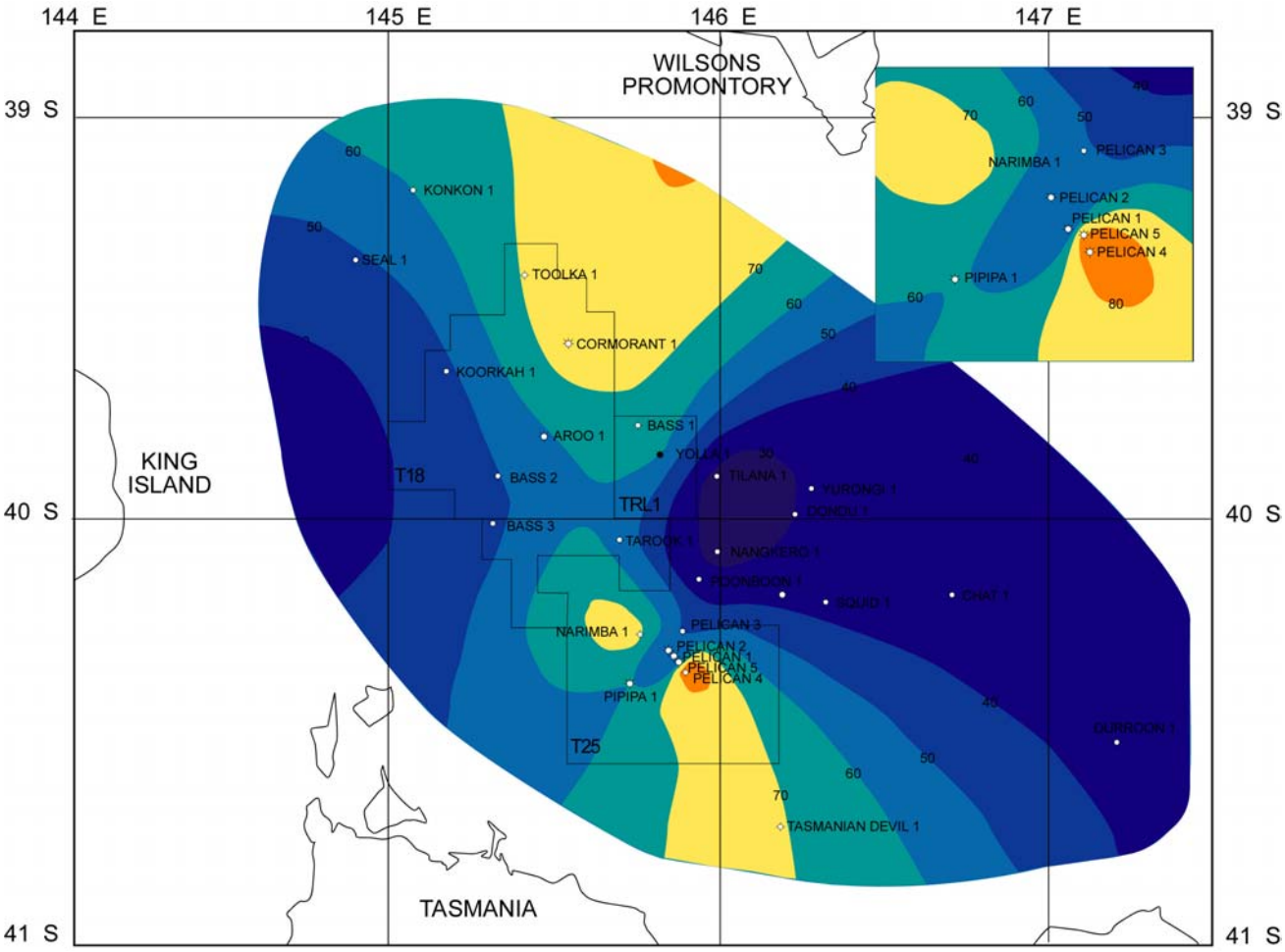

Figure 8.23 Isothermal map at the top of the *P. asperopolus* zone. Contours in degrees Celsius (adapted from Cubitt, 1992).

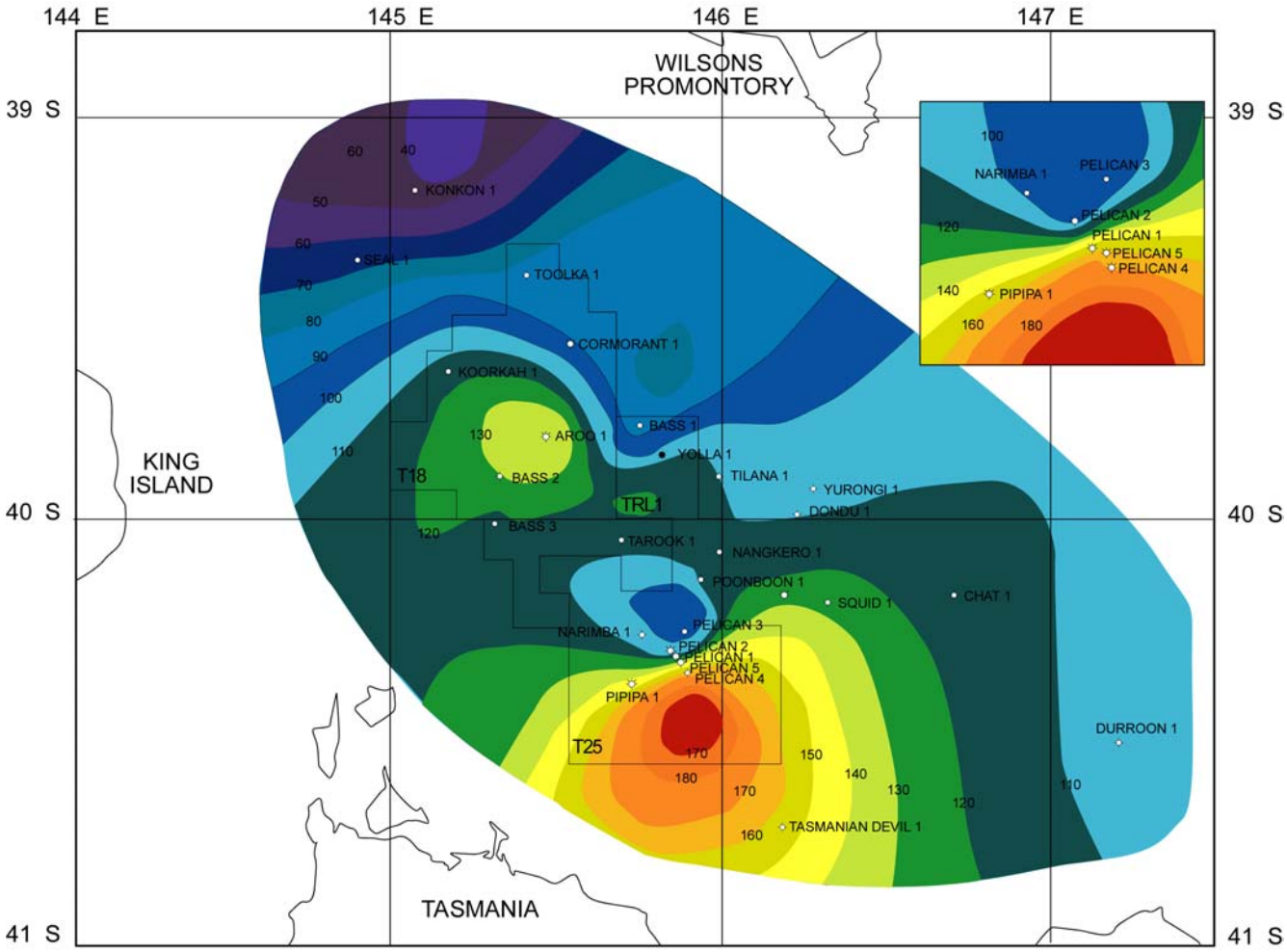

9. DEPOSITIONAL ENVIRONMENTS AND FACIES ANALYSIS

S. Lang and R. Root, National Centre for Petroleum Geology and Geophysics
J. McEachern, Simon Fraser University, British Columbia

9.1 KEY POINTS

- Based on new descriptions of 21 cores selected from nine wells, depositional environments in the Bass Basin ranged from fluvial channel belt and floodplain, to lacustrine and lacustrine delta. Lagoonal or interdistributary bay conditions, associated with a back-barrier marsh occur at several intervals, and foreshore, shoreface and shelf facies are also recognised. The overall setting is that of a land-locked alluvial and lacustrine basin, with an opening to the sea probably to the north or west that progressively became more important through time.
- Integration with palynological data supports the notion that the basin was well vegetated and dominated by peats that fringed extensive lakes and lagoons.
- Discrete channel belts were probably focused sub-parallel to basin-forming structures along fault relay zones.
- Several major lacustrine events associated with flooding surfaces can be recognised in the Upper Cretaceous to Eocene succession based on distinct stacking patterns and palynology. Freshwater lakes occurred within the Durroon (*P. mawsonii – T. apoxyexinus* zone), Tilana (Upper *F. longus* – Lower *L. balmei* zones*),* and Narimba sequences (Upper *L. balmei* – Middle *M. diversus* zones). Coastal lagoons and associated interdistributary bays (analogous with Lake Maracaibo, Venezuela) developed increasingly during the Middle to Late Eocene, associated with local flooding surfaces in the Aroo Sequence and the lower part of the Demons Bluff Sequence (Lower *N. asperus* zone).
- Wireline logs indicate alternating aggradational, retrogradational and progradational stacking patterns suggestive of cyclical variation in the balance between accommodation and sediment supply. Aggradational coaly intervals indicate a delicate balance between peat production and accommodation (especially during *P. asperopolus* zone).
- The highest ranking reservoir facies developed in coarse-grained sandstones within fluvial channels (meandering fluvial channel belt or distributary channels), possibly improved during low accommodation intervals associated with incised valley fill. Second ranking reservoir facies include the fine to medium-grained lacustrine shoreface and foreshore facies. The best reservoir potential exists within the *L. balmei* zone (Tilana and lower Narimba sequences).
- Deposition of the regional seal was associated with a regional transgressive bay/shallow marine event in the upper Demons Bluff Sequence (Anglesea Formation), however intra-formational seals within *L. balmei – N. asperus* zones offer excellent seal capacity, particularly in mudstones of the lower shoreface, lacustrine/lagoonal facies. Fine-grained abandoned channel fills, floodplain and coastal plain facies are moderate to poor seals.

- Optimum play conditions exist within coarse-grained fluvial channel belts or lacustrine shoreline/deltas sealed by lacustrine deposits within the *L. balmei* zone (Tilana and lower Narimba sequences). Higher risk plays occur within facies of fine-grained lacustrine or coastal lagoon shoreface sandstones, or in compositionally immature coarse-grained alluvial fan and proximal fluvial facies.

9.2 DEPOSITIONAL SETTING

The interpretation of depositional environments in the Bass Basin is based on a facies analysis of key wells (Figure 9.1), integrated with well log interpretations and the palynological results of Partridge (2002; Appendix C). In general, the Bass and Aroo megasequences (Late Cretaceous to Middle Eocene) are fluvial-lacustrine successions associated with peat-forming environments during the syn-tectonic and early thermal subsidence phases of basin development. From the Late Paleocene (Lower *M. diversus* zone) onwards, an increasing marine influence resulted in the formation of freshwater lakes and coastal lagoons within low-lying deltaic and coastal plain environments. Widespread thick coals developed from the early Middle Eocene onward (*P. asperopolus* to Lower *N. asperus* zones), as a result of steady slow subsidence (accommodation) across the basin. From the Middle to Late Eocene (Middle *N. asperus* zone) after widespread fluvial incision ('Boonah Sandstone'), the basin evolved into a protected estuarine and shallow marine embayment (Demons Bluff Sequence). Marine transgression continued through the Oligocene and Miocene, changing to cool-temperate shallow marine marl and limestone sedimentation (Torquay Sequence). Bioclastic carbonate sedimentation dominates through to the present day.

9.3 FACIES INTERPRETATIONS AND DESCRIPTIONS

The facies analysis is based on an interpretation of wireline log character from all available Bass Basin wells, with particular emphasis on new descriptions of 21 selected cores from nine key wells held at the Petroleum Data Repository, Geoscience Australia (Figure 9.1). The cores selected for logging are representative of both depositional facies and age range (Figure 9.2). Ichnofacies interpretations were determined from core photographs collected during the logging phase. The key for the graphic logs is shown in Figure 9.3, with graphic core log descriptions shown in Figures 9.13 to 9.21. A selection of core photos are included in Appendix M.

The following depositional environments were determined from the facies analysis:

- Alluvial fan and proximal fluvial system
- Alluvial plain (including fluvial channel belts and floodplain)
- Incised valley
- Peat mire
- Lacustrine delta/delta plain
- Lacustrine shoreface

- Freshwater lake
- Coastal lagoon/back barrier/interdistributary bay
- Barrier foreshore/shoreface
- Shallow marine/offshore bay

Alluvial Fan and Proximal Fluvial System

Although no cores intersected this facies, it is inferred based on the wedge-like progradational geometries observed in the seismic data across the Durroon Sub-basin (Figure 9.4, Durroon Sequence) and in the Cormorant Trough (Figure 9.5). The sediment composition is likely to reflect the local basement rock, along with mixing with sources farther inland. Coarse-grained sandstones and conglomerates are expected, and poor sorting associated with debris flows is also likely. The alluvial fan and proximal fluvial systems are located adjacent to fault scarps on the basin margin and in half graben within the depocentre.

Alluvial Plain (Fluvial Channel and Floodplain)

These facies are identified by medium to coarse-grained sandstone, ideally with evidence of fluvial channel fill (cross-bedded sandstones) and are not associated with marine fauna or micro-fossils. Good examples of these facies were observed at Durroon-1 (Figures 9.6 and 9.7), Yolla-2 (Figure 9.8), Poonboon-1 (Figures 9.9 to 9.11), Tilana-1 (Figure 9.12) and Pelican-5 (Figure 9.13), including local erosion surfaces, and fining-upward trends. Evidence of exposure (mudcracks, roots) in fine-grained overbank facies occurs in several cores and is interbedded with parallel-bedded and ripple-laminated crevasse splay sandstones. Some of the fluvial channel deposits may be distributary channels if associated with the top of a lacustrine deltaic succession (Poonboon-1, 2468-2470.6 m, Figure 9.11) or interbedded with lagoonal facies (Poonboon-1, 2684-2687 m, Figure 9.10). Fluvial channel deposits are common throughout the basin and appear to be the most optimum reservoir facies, especially within the *L. balmei* zone (Tilana and lower Narimba sequences). Porosity range up to 20%, and permeability typically between 10 and 300 mD, in some cases over 1000 mD based on core plug measurements.

Incised Valley Fill

Incised valley fill facies are more complex and the lowermost fluvial part was not intersected in the cores. However, based on the wireline log interpretation, the base of the "Boonah Sandstone" (Middle *N. asperus*, Demons Bluff Sequence) is a significant likely example of an incised valley fill. The "Boonah Sandstone" represents stacked sandy facies of variable thickness, that overlies a regional seismic-scale erosional unconformity. There is palynological evidence of estuarine conditions in Poonboon-1 (Core 1, 1953.8 and 1958.9 m) overlain by restricted marine to bay conditions (Partridge, 2002; Appendix C). The wireline log motif is typical of wave-dominated or mixed wave – tide-dominated incised valley fills, which have a sharp base (fluvial) fining-upward into shale (estuarine to central embayment) overlain by coarsening-upward, progradational motifs (marine transgressive foreshore and shoreface deposits) (Poonboon-1, Core 1, 1953-1960 m; Figure 9.11).

Peat Mire (Coal)

Peat, now coal, is common within the syn-rift and early post-rift successions, but is especially abundant in the *L. balmei* to *P. asperopolus* zones (Tilana, Narimba and Aroo sequences), where it forms thick extensive coals or thin localised coals. The most extensive coal-prone interval is an intra-Lower *N. asperus* package, lying within the uppermost part of the Aroo Sequence. Coal occurs less frequently in the "Boonah Sandstone" facies (Demons Bluff Sequence), within the confines of incised valleys. There is probably significant lateral variation in the peat systems, from forest peats to bogs or back-barrier marsh, to abandoned channel fill, all with specific geochemical character and hence different source potential (Boreham et al., 2003). Coals with relatively high hydrogen indices (HI) include coals in Poonboon-1 (3040.39-3040.54 m: HI 306) and Pelican-5 (2791.87-2792.00 m: HI 406.5). The sulphur content of the coals is generally very low (0.28 – 0.72%), although an anomalous coal with 2.46% sulphur, possibly indicative of marine influence, occurs in Pelican-5 (2034.00-2037.00m). Coal was also cored in Bass-1 (2261.4-2268.4 m; Figure 9.20).

Lacustrine Delta/Delta Plain

Lacustrine deltas are inferred from wireline log character (upward-cleaning progradational or aggradational cycles a few metres thick, often capped by emergent coals). In some cases distributary channels (Figure 9.10) can be interpreted within these cycles, identified by blocky, or fining-upward successions several metres thick. The main difficulty with the recognition of lacustrine deltas lies in distinguishing them from laterally extensive progradational lacustrine shorelines, which are typically cleaner, and lack distributary channels. A significant part of the succession represents upper or lower delta plain/coastal plain, especially in the western and southern parts of the basin. Lacustrine delta successions occur throughout the basin including the Durroon, Bass and Aroo sequences**.**

Lacustrine Shoreface

This facies is identified by clean, very fine to medium-grained, well-sorted sandstone, with a slight degree of coarsening-upward (e.g., Dondu-1, 2339-2356.5 m, Upper *L. balmei* to Lower *M. diversus* zones, Figure 9.16; Cormorant-1, 2222-2230.2 m, Upper *M. diversus* zone and 2773-2781.5 m, Lower *M. diversus* zone, Figure 9.17). The main sedimentary structures include parallel laminations, ripples, and small cross-beds. The lack of definitive marine palynomorphs suggests lacustrine shorelines or shorelines around coastal lagoons. Examples occur in both the Tilana, Narimba and Aroo sequences.

Freshwater Lake

Stacked fine-grained mudstones with high gamma log motifs are interpreted to be significant, but relatively shallow, lake successions, predominantly in the Narimba and Tilana sequences. Although rarely intersected in the cores (Poonboon-1, 3259-3255 m, Figure 9.9; Cormorant-1, 1994.2-1999.5 m, Figure 9.18), they range from massive to laminated mudstones, and represent periods of relatively high accommodation rates in the various half graben. Typically these are overlain by progradational log motifs. Lake successions are likely to occur throughout the basin especially within the Durroon, Bass and Aroo sequences.

Coastal Lagoon/Back Barrier/Interdistributary Bay

Weakly bioturbated very fine-grained sandstone interbedded with mudstone containing a marine-influenced microplankton (acritarchs including *Micrhystridium* spp., and dinocysts; see Partridge, 2002; Appendix C), and intercalated with back-barrier coal represent this facies (Figures 9.10, 9.14 and 9.15). Marine influence of these coastal lagoons (*Lower M. diversus* zone, Narimba Sequence) is thought to have been via restricted estuarine embayments that connected the shallow lakes to the sea. For further detail see Partridge (2002; Appendix C) who compares this facies with coastal lagoons similar to Lake Maracaibo in Venezuela. These facies are expected to merge into the lacustrine shorelines in a landward direction, and be difficult to distinguish in a seaward direction until full marine facies are confirmed. Ichnofauna identified are typical of a stressed, brackish coastal lagoon or interdistributary bay. For example in Pelican-5 (2864.9 m, *M. diversus* zone), heterolithic fine-grained sandstones and siltstones include *Planolites*, *Thalassinoides, Skolithos* and *fugichnia.* In Poonboon-1 (2688-2688.2 m; Lower *M. diversus* zone), heterolithic mudstone and fine-grained sandstone includes *Ophiomorpha, Paleophycus, Planolites, Teichichnus, Cylindrichnus,* and *Thallasinoides.* In Cormorant-1 (1998 m, Upper *M. diversus* zone), laminated siltstones includes *Planolites, Cylindrichnus, Paleophycus,* and *fugichnia.*

Barrier Foreshore/Shoreface

These include clean, marine influenced fine- to medium-grained sandstone in cleaning-upward cycles a few metres thick. These are most obvious in the upper part of the "Boonah Sandstone" (Demons Bluff Sequence) where the incised valley(s) was initially filled with estuarine, then shoreface sediments resulting from rising relative sea level. For examples, see Poonboon-1 (2683-2683.8 m, Figure 9.10; 1953-1960 m, Figure 9.11), and Cormorant-1 (1504-1512.5 m, Figure 9.19) which show transgressive barrier foreshore and shoreface deposits. Ichnofauna identified in Poonboon-1 (2683-2683.8 m, Lower *M. diversus* zone*,* Narimba Sequence) include *Ophiomorpha* and *Planolites.* A more abundant ichnofauna was identified in Cormorant-1 between 1054 and 1513.3 m (Lower *N. asperus,* Aroo Sequence). Ichnofossils include evidence of both rootlets and restricted marine bioturbation such as *Planolites, Cylindrichnus, Skolithos, Thallasinoides, Paleophycus, Lockeia,* and *fugichnia.*

Shallow Marine/Offshore Bay

This facies includes fine sandstone, siltstone and mudstone with marine microfauna, merging landward into glauconitic fine-sandstones. These facies represent the final stages of widespread marine flooding of the basin (Anglesea Formation; upper Demons Bluff Sequence), that lead to widespread transgressive embayment sedimentation (Bass-2, 1159-1165 m, Figure 9.21). Ichnofauna include an intensely bioturbated assemblage of *Arenicolites, Helminthopsis, Planolites,* and *Chondrites*, distinctly different from the more restricted assemblage of the coastal lagoon or interdistributary bay facies.

9.4 RELATIONSHIP BETWEEN FACIES AND RESERVOIR QUALITY

Reviews of the diagenesis of hydrocarbon reservoirs in the Bass Basin (Chapter 8) provides an overall summary of the diagenetic events in the basin. The primary relationship noted between reservoir quality and depositional facies is linked to the coarse grain size associated with specific facies, with a secondary link to dissolution of early-formed siderite associated with organic-rich facies.

Coarse-grained facies in the Bass Basin include the fluvial channels, some crevasse-splays and coarser-grained elements of the lacustrine/lagoonal shoreface or foreshore facies. The coarser-grained, arkosic or more quartzose rocks, particularly where the rock is clean with moderate to good sorting, have the best chance of retaining good reservoir quality even where deeply buried. Of these reservoirs, channels are the highest ranking, followed by the shoreface and foreshore facies.

Coarse-grained lithic rocks from Lower Cretaceous (Otway Megasequence) fluvial facies in Durroon-1 (3020-3024 m and 2552-2567 m; Figure 9.6) have generally poor reservoir permeability due to early compaction around lithic grains and diagenetic alteration of labile constituents. However, some good reservoir properties based on core-plug results occur in fluvial facies in Durroon-1 (1693.5-1696 m, Early Cretaceous; Figure 9.7). It is likely that undrilled alluvial fan or proximal fluvial coarse-grained or conglomeratic facies in the Upper Cretaceous Durroon Megasequence are also likely to have poor reservoir quality.

Within the Cainozoic succession, reservoir properties (>12% and up to 20% plug porosity and typically >10 mD to 300 mD based on core plugs) are preferentially developed within medium to coarse-grained fluvial channel, splay or distributary channel facies, as well as some fine- to medium-grained shoreface to foreshore facies. These facies were observed in the following core intervals examined for this study (listed from oldest to youngest):

***N. asperus* (Aroo and Demons Bluff sequences)**

Poonboon-1 (1953-1958 m, Middle *N. asperus* zone, shoreface; Figure 9.11)

Cormorant-1 (~1512 m, Lower *N. asperus* zone, shoreface; Figure 9.19)

***M. diversus* (Narimba and lower Aroo sequences)**

Poonboon-1 (2467-2472.5 m, Middle *M. diversus* zone, channels; Figure 9.11)

Pelican-5 (2871-2880.2 m, Lower *M. diversus* zone, channels; Figure 9.13)

Poonboon-1 (2684-2686.8 m, Lower *M. diversus* zone, channels; Figure 9.10)

***L. balmei* (Tilana and lower Narimba sequences)**

Yolla-2 (3033.5 – 3050.3 m, Lower *L. balmei*, zone, channels; Figure 9.8)

Poonboon-1 (3036 –3040 m, Lower *L. balmei* zone, channels; Figure 9.9)

Dondu-1 (2343.3-2356.4 m, Upper *L. balmei* zone, shoreface; Figure 9.16)*****

Tilana-1 (2789-2807.4 m, Upper *L. balmei* zone, channels; Figure 9.12)

** Dondu 1, 2349 m illustrated in Chapter 8 (Figures 8.15 and 8.17).*

Dissolution of early-formed micritic siderite (i.e., pre-compaction siderite) associated with slightly organic-rich facies is a secondary process linked to facies type that is associated with some improved reservoir properties (Chapter 8). The micritic siderite is formed by early reducing conditions in organic-rich, fine- or coarse-grained sandstone and siltstone (e.g., crevasse splays on the floodplain or lacustrine shoreface facies). An example is Cormorant-1 (2773 m, Lower *M. diversus* zone; Figure 9.17) (Chapter 8; Figures 9.6 to 9.8). Later dissolution of the siderite can lead to late compaction effects but modest secondary porosity can still be retained. Other diagenetic processes not directly related to facies type involve sediment composition (provenance), burial history and fluid interaction (Chapter 8).

A key observation by Cubitt (1992) is that the *L. balmei* zone interval (Tilana and Narimba sequences) has a predisposition to good reservoir quality even though it is represented mainly in deeper parts of the basin. From a facies perspective, this may be due to the relatively high-energy of the depositional systems when compared to the overlying succession. The intra-*L. balmei* unconformity event signals continued tectonic activity in the basin leading to increased depositional gradients. A combination of sediment composition, grain-size, early diagenetic history and subsequent burial history combine to maintain moderate to good reservoir quality despite deeper burial when compared with the overlying succession.

9.5 RELATIONSHIP BETWEEN FACIES AND SEAL CAPACITY

The relationship between depositional facies and seal capacity is mainly a function of grain-size, with fine-grained rocks from the lower and upper shoreface, lagoon, lacustrine or interdistributary bay, and stacked crevasse channel/floodplain having the most significant seal capacities (Chapter 7, Appendix L).

Of the MICP samples selected from cores examined for this study, the highest ranking sealing capacity was reported from mudstones of the lower shoreface facies (Dondu-1, 2342 m, Upper *L. balmei* zone, average oil column >1400 m). The other two lower shoreface samples from younger successions were siltstones with a predictably lower, but still good sealing capacity (Pelican-5, 2890.8 m, Lower *M. diversus* zone, average oil column 853 m; Poonboon-1, 1954.2 m, Middle *N. asperus* zone, average oil column 350 m).

The second highest ranking seal capacity was reported from finely laminated lagoonal or interdistributary bay mudstones (Cormorant-1, 1999.3 m, *P. asperopolus* - Upper *M. diversus* zones, average oil column ~1140 m). Other interdistributary bay or lacustrine facies also have good sealing capacities (Cormorant-1, 2231.6 m, Upper *M. diversus* zones, average oil column 797 m; Pelican-5, 2863.8 m, Lower *M. diversus* zones, average oil column 698 m; Poonboon-1 3259.8 m, Lower *L. balmei* zone, average oil column 568 m).

Other important sealing facies include fine-grained fluvial channel fills from Durroon-1 (3021.88 m, Early Cretaceous, 988m) and Tilana-1 (2800 m, Upper *L. balmei* zone, 898 m), both able to support an oil column

greater than 700 m. Coastal plain, fluvial overbank and back barrier berm deposits are the least significant sealing lithologies reported in the study, supporting <200 m oil columns. The only sample available from the regional seal, a shallow shelf or bay mudstone, had a modest to good sealing capacity (Bass-2, 1164.49 m, Upper *N. asperus* zone, 400 m).

A comparison of width/length aspect ratios for a variety of seal types suggest that lower lacustrine shoreface and lacustrine/lagoonal facies with high sealing capacity are also laterally extensive. Given that most of these samples were from intraformational units within the Tilana, Narimba or Aroo sequences (Eastern View Group), the potential to trap significant oil columns well below the regional seal is clear, provided other leakage pathways (faults, lateral seal failure) did not operate.

The *L. balmei* zone interval (Tilana and Narimba sequences) has both a predisposition for better reservoir quality for a given depth than the overlying succession, and contains good intraformational seals. Therefore the opportunity exists for significant stratigraphic and combined structural/stratigraphic traps in the deeper parts of the Bass Basin. Further work incorporating seal thickness, integrity and capacity is required to advance the evaluation of seals in the basin.

Figure 9.1 Map showing the location of wells with cores described and interpreted for this study.

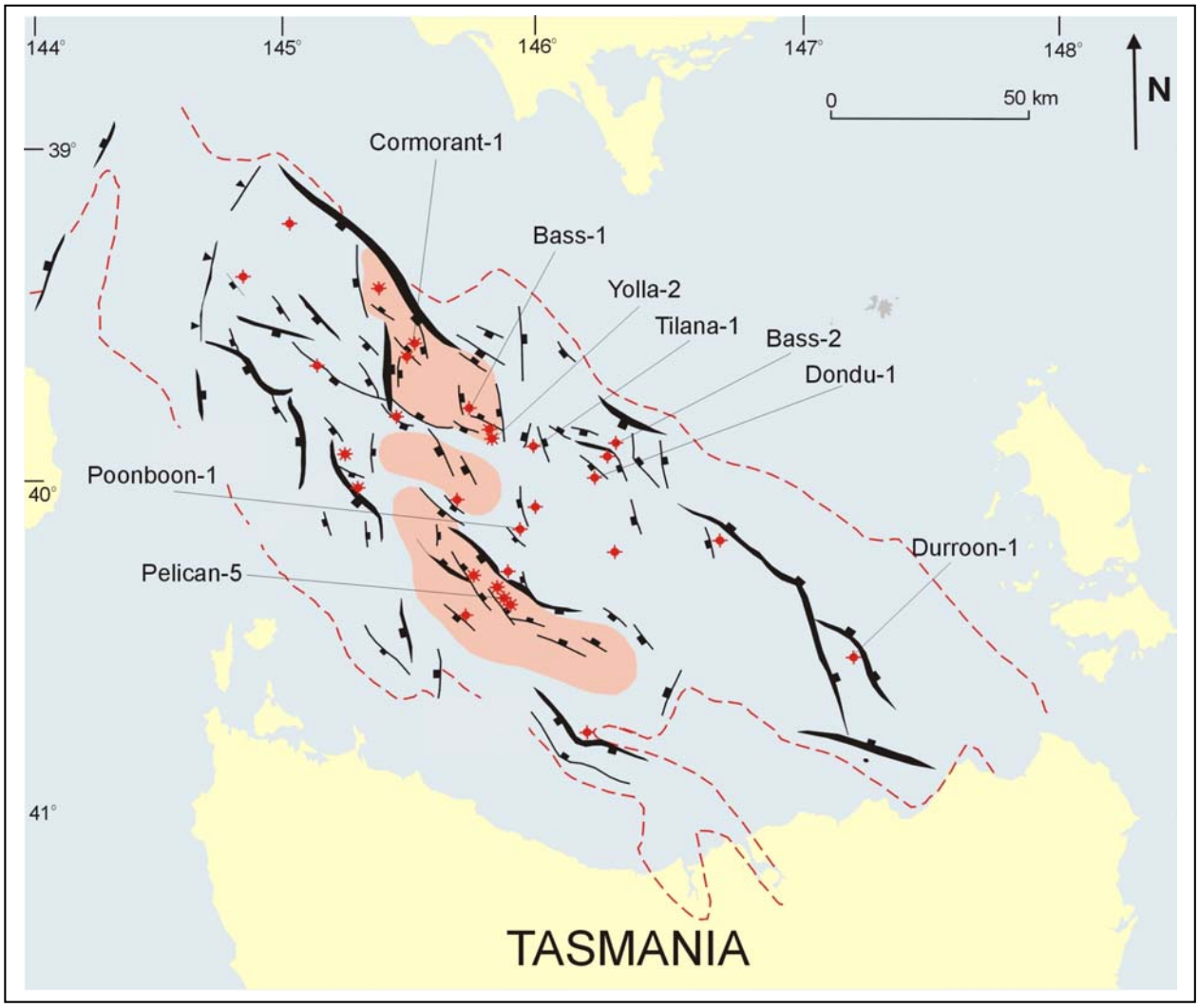

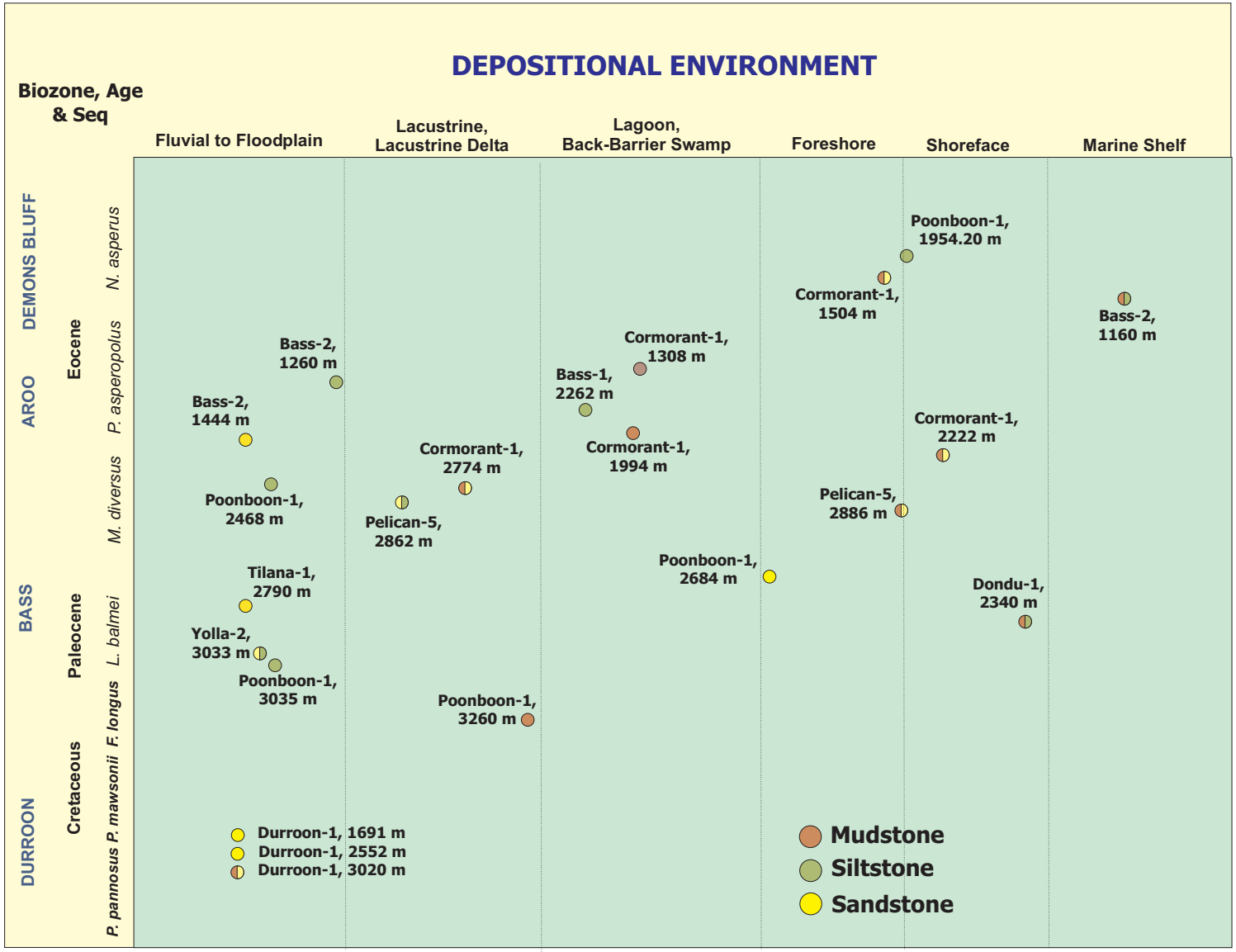

Figure 9.2 Depositional facies and spore/pollen biozones represented in selected cores in the Bass Basin.

Figure 9.3 Key for graphic logs showing the Figures 9.6 to 9.21.

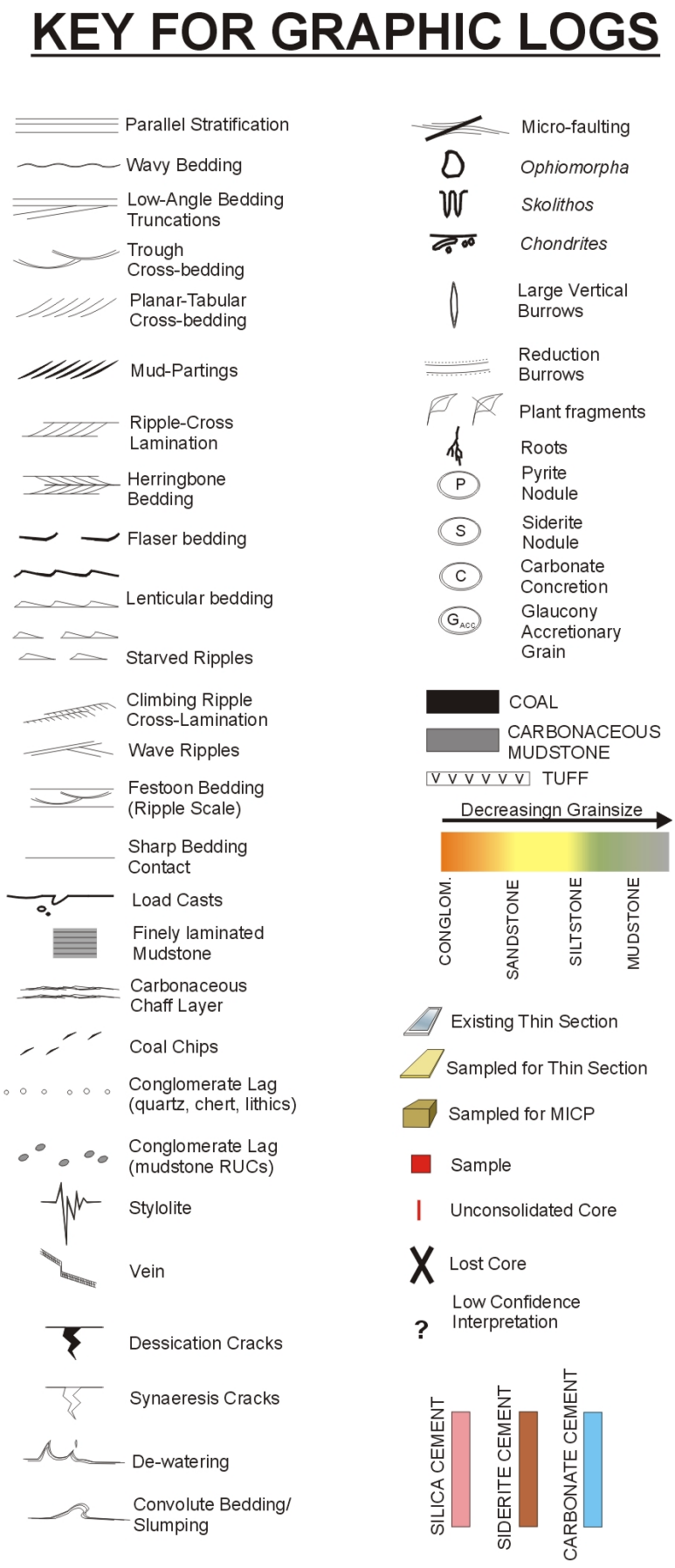

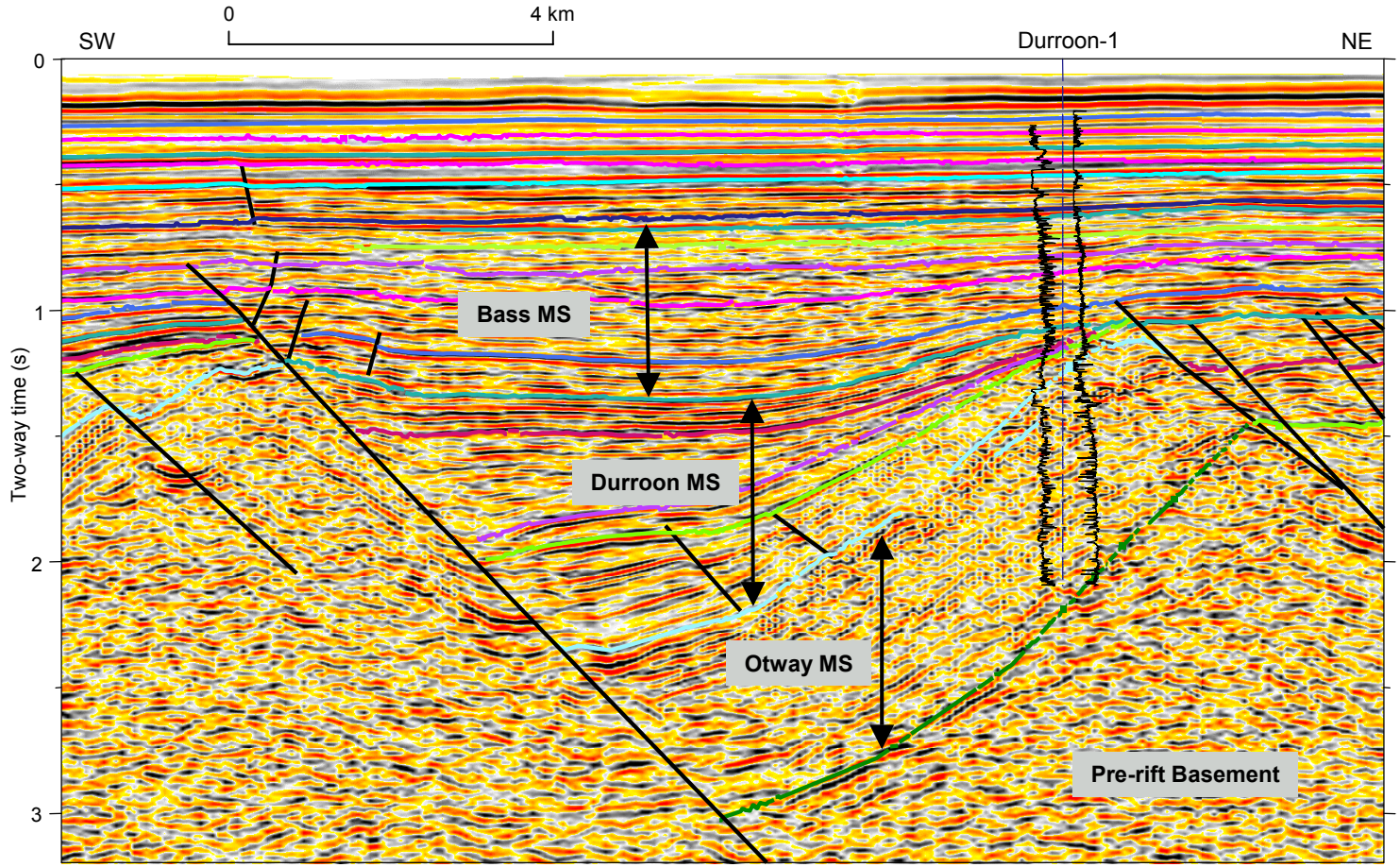

Figure 9.4 Geoscience Australia seismic line across part of the Durroon Sub-basin. This section shows in more detail the syn-tectonic successions intersected at the Durroon-1 well: the Early Cretaceous Otway Megasequence (Rift Phase 1) and the overlying early Late Cretaceous Durroon Megasequence (Rift Phase 2). Strata within the syn-rift succession has a wedge-like progradational geometry that is interpreted to contain fans. This seismic image is published with the permission of Fugro MCS.

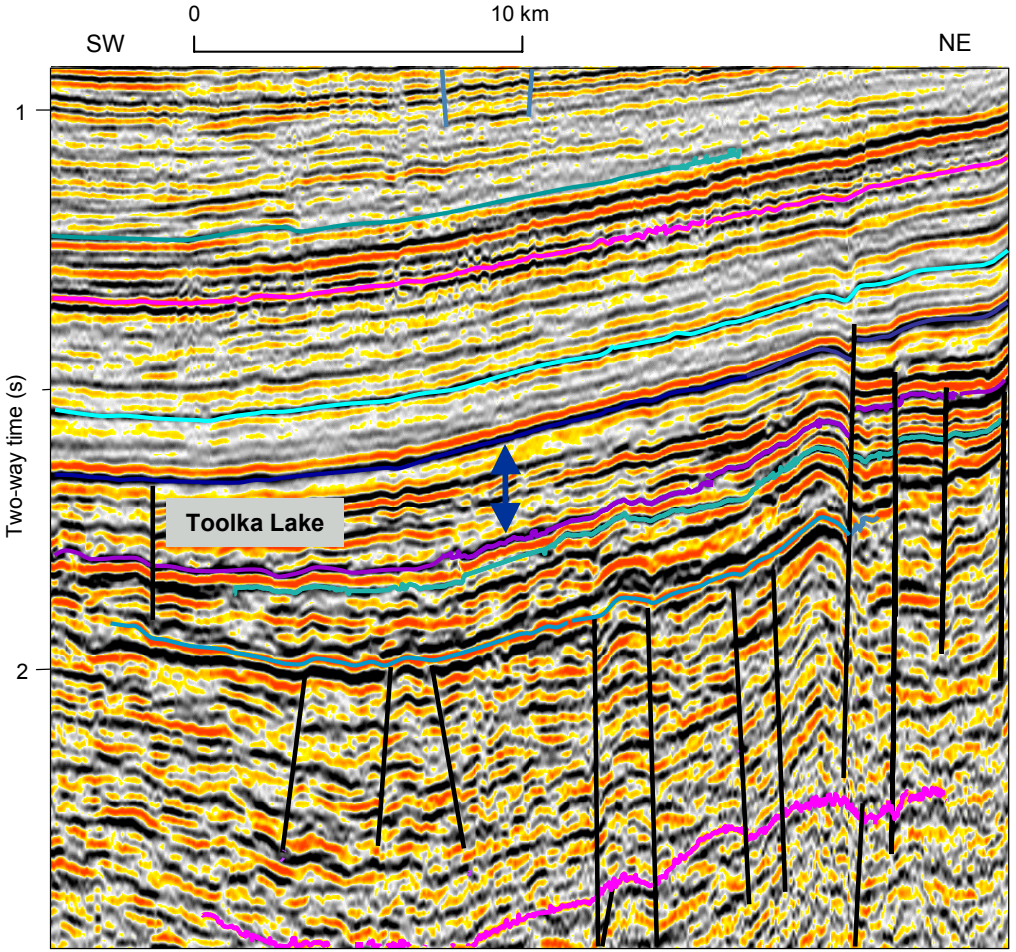

Figure 9.5 Geoscience Australia seismic line across the central Bass Basin showing the geometry and stratal character of sediments of Early to Middle Eocene age in the Cormorant Trough. The dark blue horizon marks the "Base of the Boonah Sand". This figure is published with the permission of Fugro MCS.

Figure 9.6 Fluvial channel deposits in Durroon-1 (3020-3024 m, 2552-2568 m) from the Lower Cretaceous Otway Megasequence (*P. pannosus* zone).

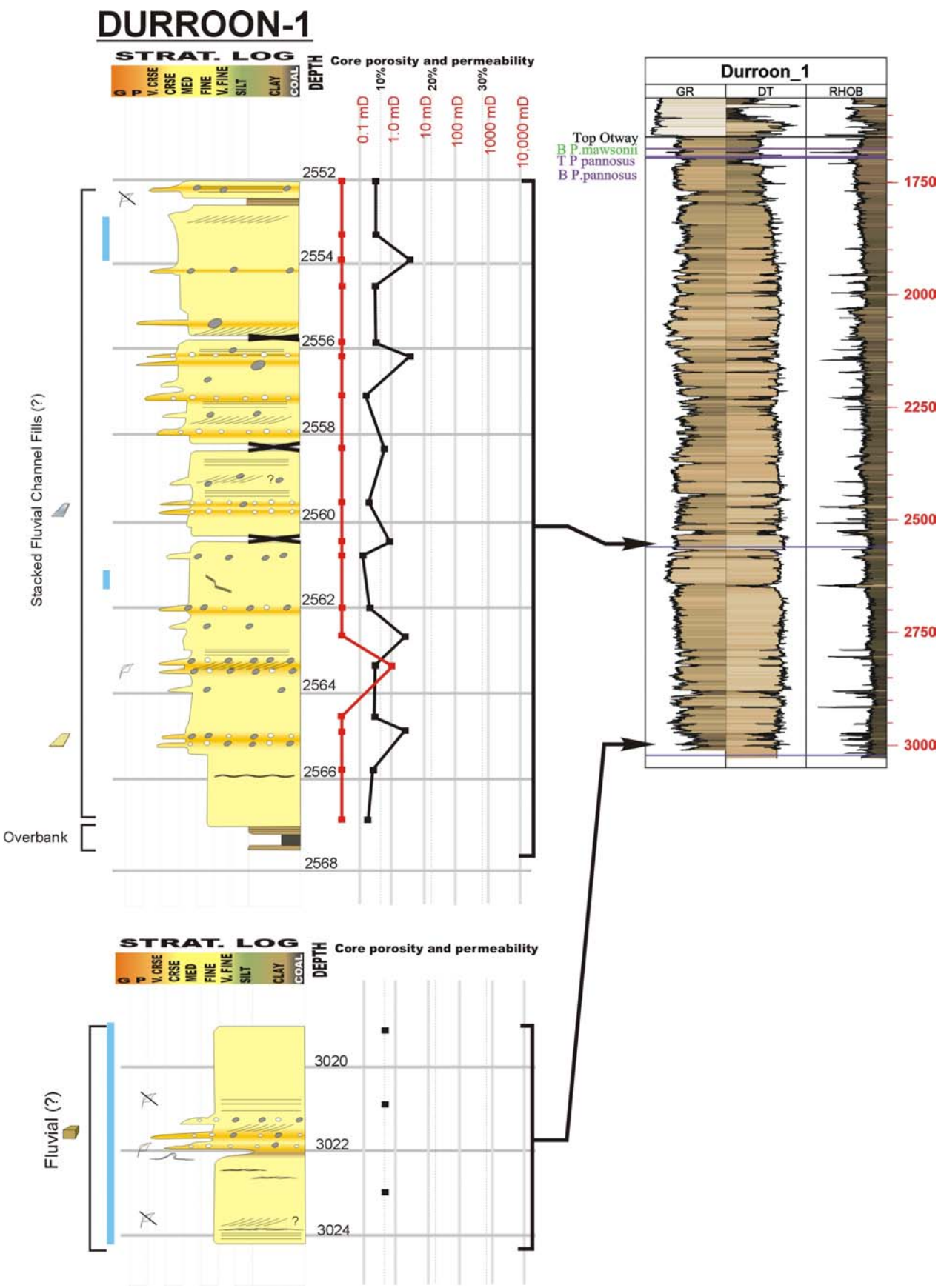

Figure 9.7 Fluvial channel and floodplain deposits in Durroon-1 (1691.3-1696.2 m) from the Lower Cretaceous Otway Megasequence (*P. pannosus* zone). Moderate porosity (>20%) and permeability (10-100 mD) occur in the fluvial channel-fill sandstones.

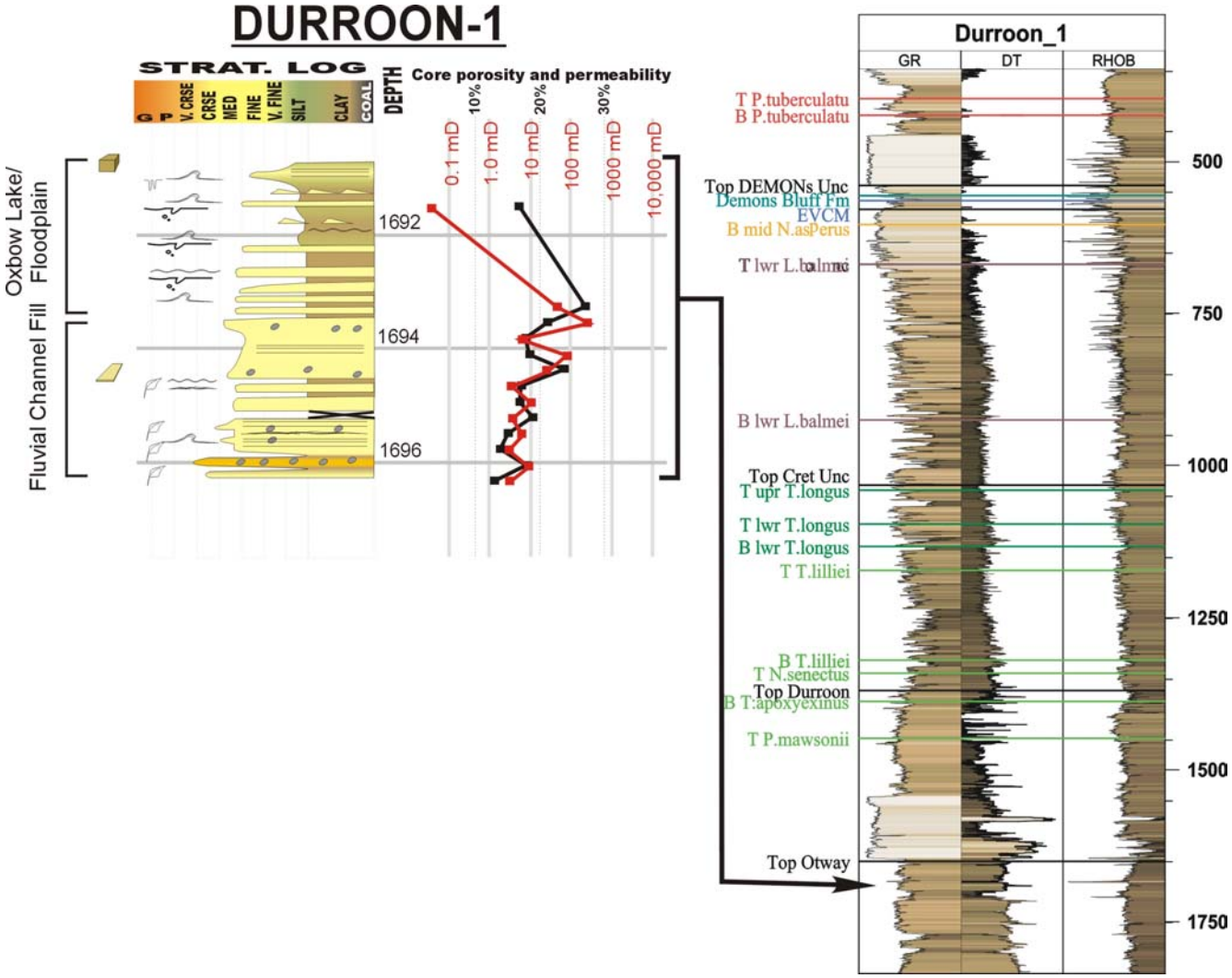

Figure 9.8 Example of stacked fluvial channels and overbank deposits in Yolla-1 (3033-3051 m) in the Tilana Sequence (Lower *L. balmei* zone).

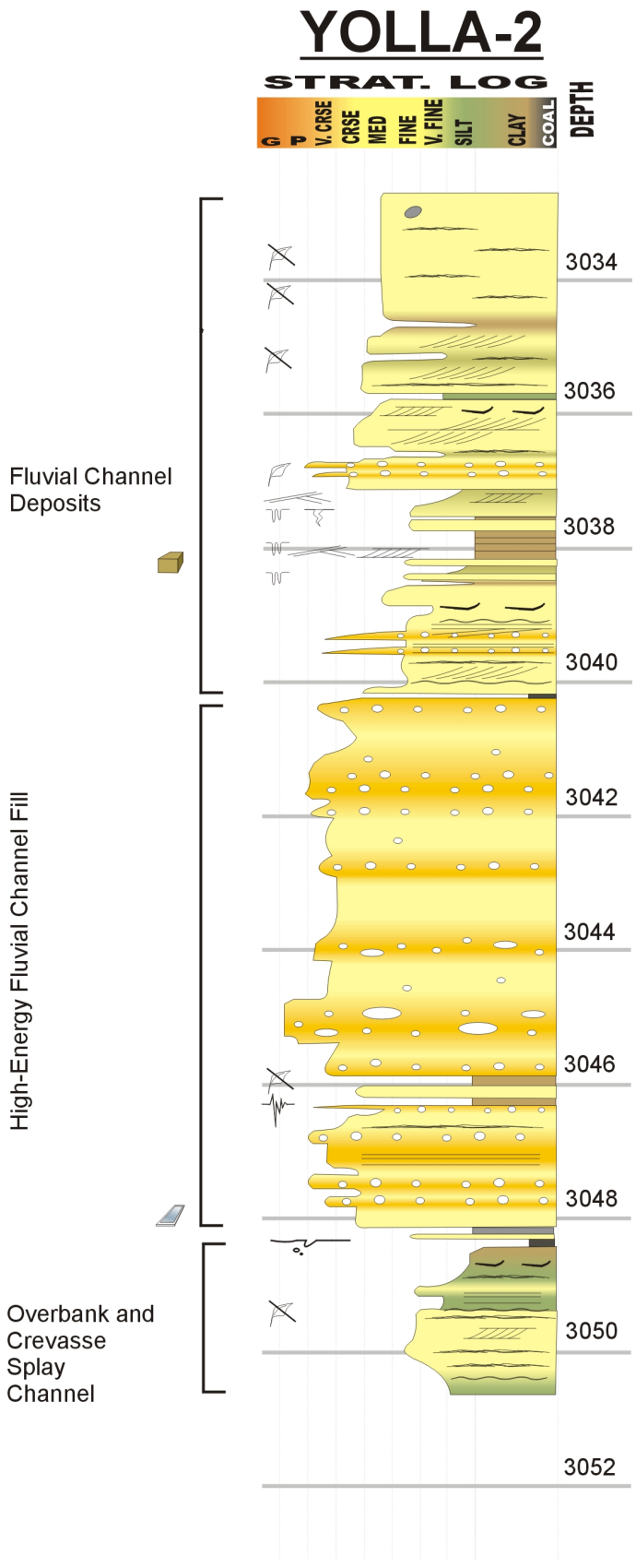

Figure 9.9 Poonboon-1 lacustrine (3259-3266 m; Upper *F. longus* zone) in the lowermost Tilana Sequence, and stacked fluvial channels or splays interbedded with overbank deposits and coal (3034-3042.6 m; Lower *L. balmei* zone) within the Tilana Sequence.

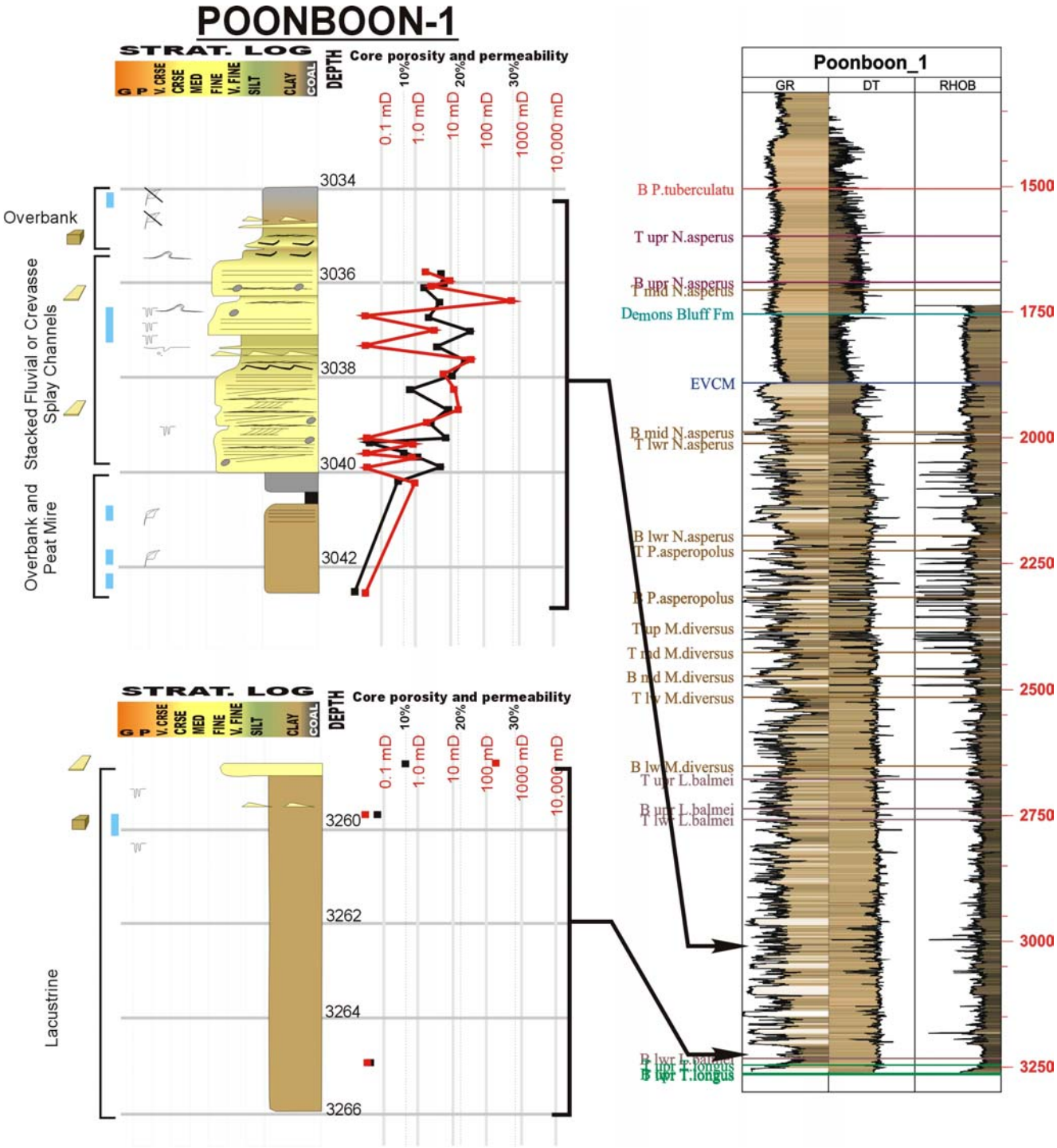

Figure 9.10 Poonboon-1 cores showing back-barrier berm and lagoon with crevasse splay deltas, distributary channels and foreshore lacustrine deltas forming part of an overall lower lacustrine delta plain succession (Core 3, 2683-2690.8 m). Palynology (Partridge, 2002; Appendix C) from core samples at 2688 and 2689.3 m record 33% and 50%, respectively, of the acritarch *Michystridium* spp., and the non-marine dinocyst *Morkallacysta* spp. Undifferentiated marine dinocysts (33%) are recorded at 2689.3 m supporting the interpretation of a coastal lagoon partially connected to the sea. This interval lies beneath a retrogradational fining-upward succession interpreted as a transgressive systems tract where a reliable marine dinocyst, *Apectodinium reburrus* is recorded (50%) in a sidewall core sample from 2678.6 m. The core lies within the Lower *M. diversus* zone, associated with the expansion of the "Koorkah" coastal lagoon to lake system identified by Partridge (2002; Appendix C), within the Narimba Sequence. Notice the moderate to good porosity and permeability of the fluvial succession (20-30% porosity, 100-1000 mD permeability). Also see Figure 9.14 and 9.15.

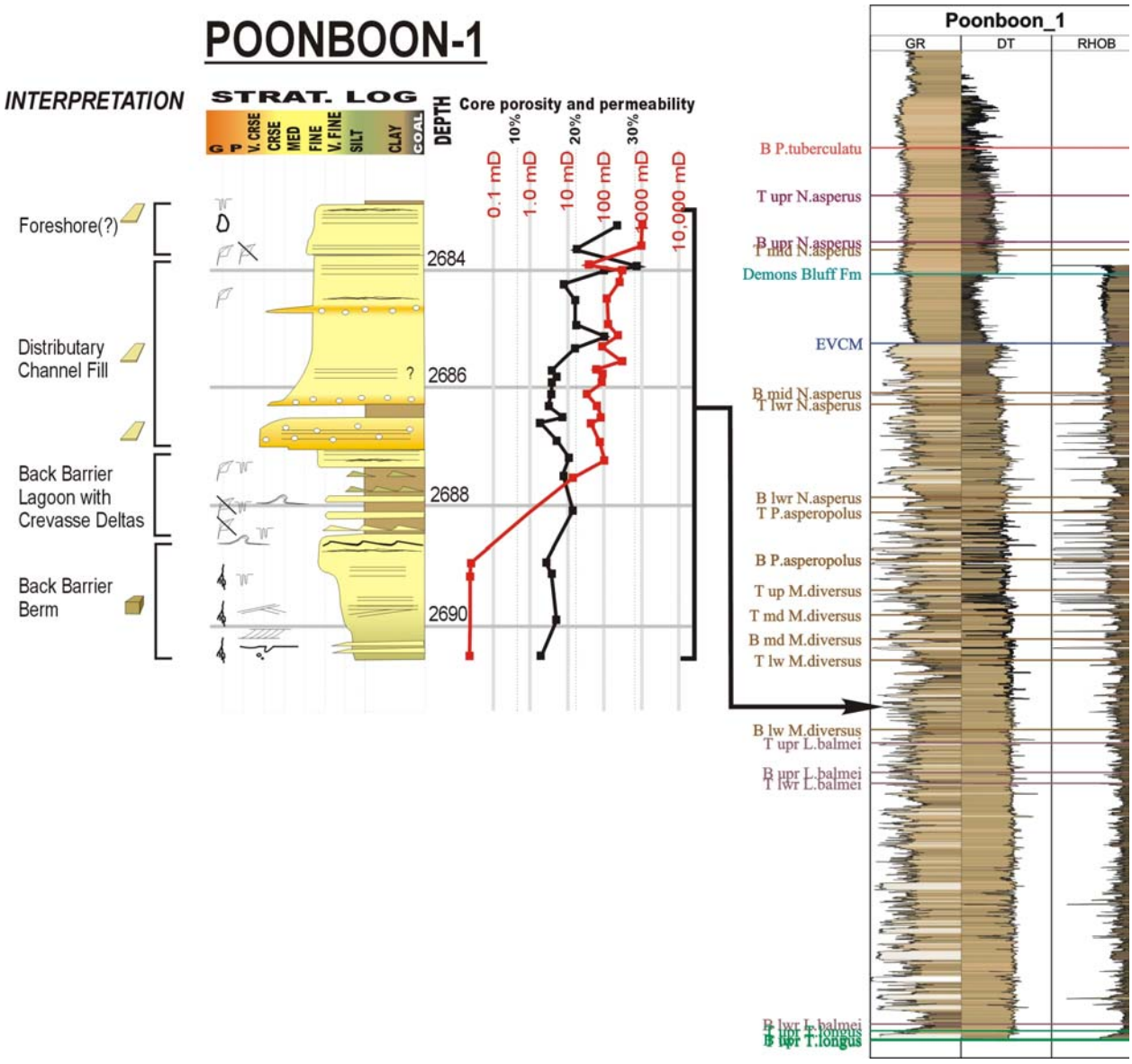

Figure 9.11 Poonboon-1 cores showing lacustrine foreshore to mid-shoreface (1953-1960.2 m) from the Demons Bluff Sequence (Middle *N. asperus* zone) and fluvial distributary channel-fill, splays and overbank deposits (2467-2474 m) from the Narimba Sequence (Middle *M. diversus* zone). Notice the development of moderate to good porosity and permeability of the fluvial succession (20-30% porosity, 100-1000 mD permeability).

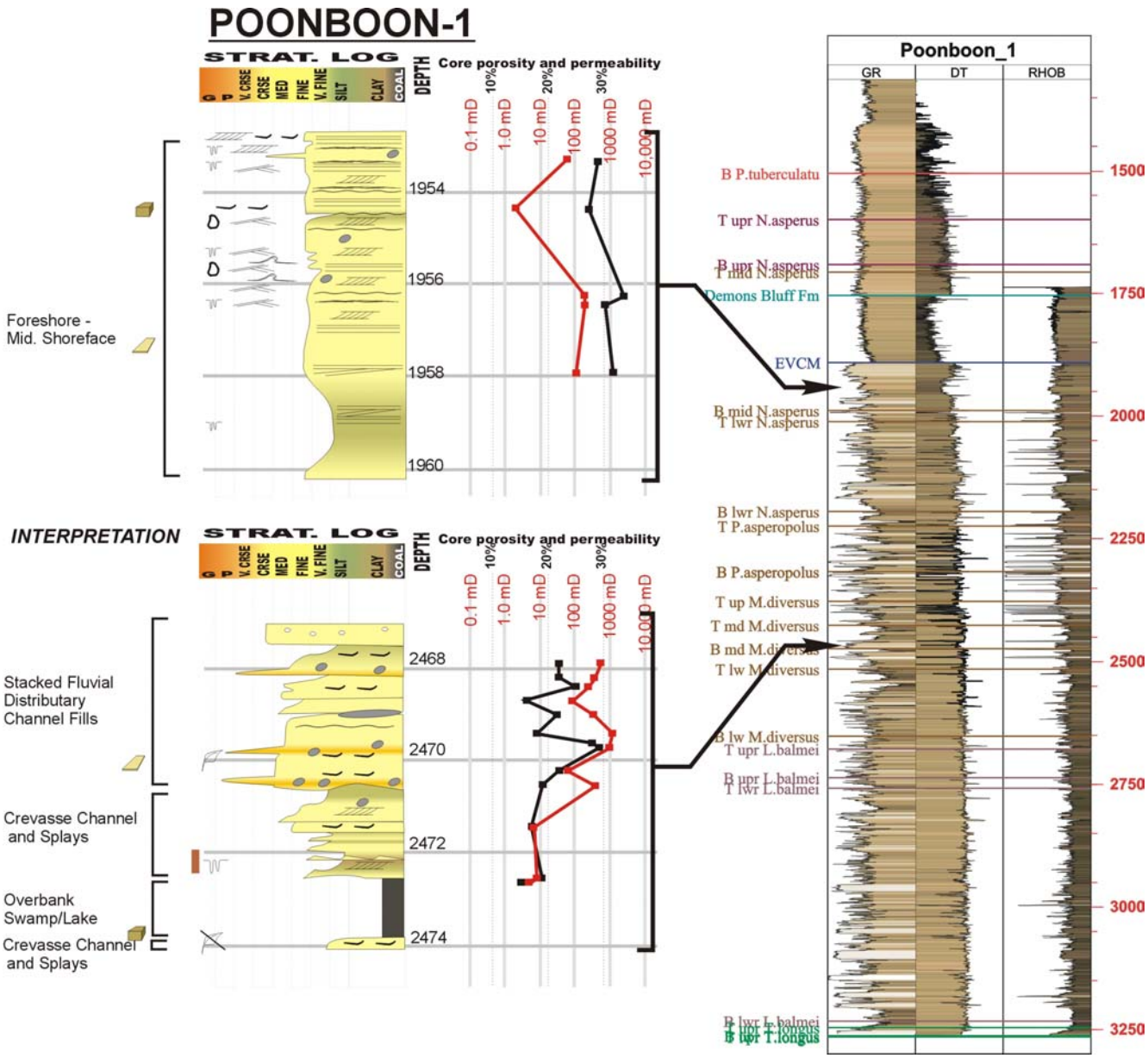

Figure 9.12 Tilana-1 core from 2789-2807.4 m showing fluvial distributary channels interbedded with lacustrine shoreface in the Narimba Sequence (Upper *L. balmei* to Lower *M. diversus* zones).

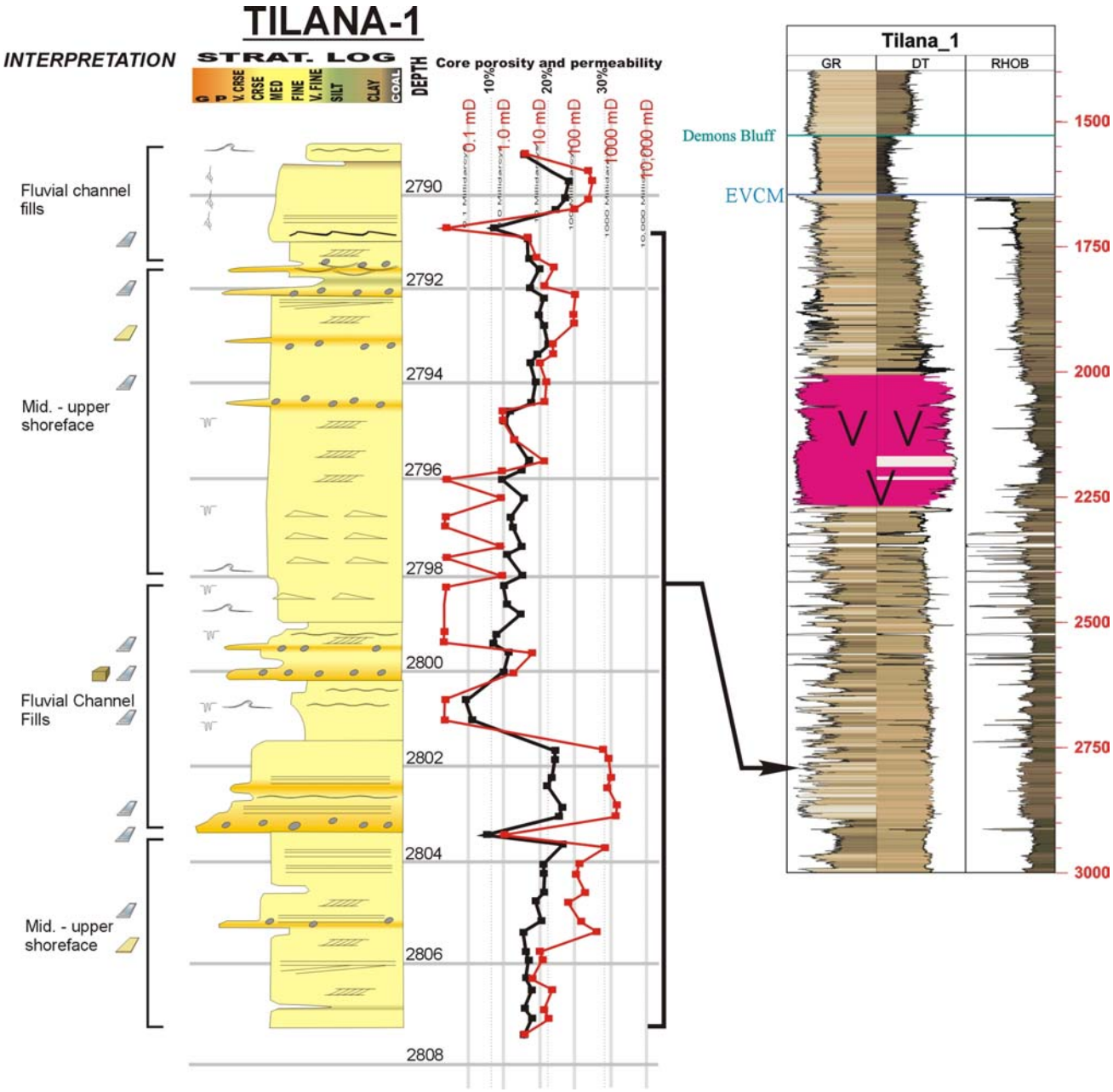

Figure 9.13 Pelican-5 core from 2862.2-2890.7 m showing lacustrine foreshore to shoreface overlain by stacked fluvial distributary channels topped by interdistributary bay facies. Porosity in the fluvial facies ranges from 10 to 20%, with pemeability from 5 to 12 mD, locally up to 300 mD. Good porosity (15-20%), but variable permeability (<0.1 to 200 mD) occurs in the lacustrine foreshore to shoreface. Part of a transgressive systems tract with increasingly isolated sandstone up section (Narimba Sequence; Middle *M. diversus* zone).

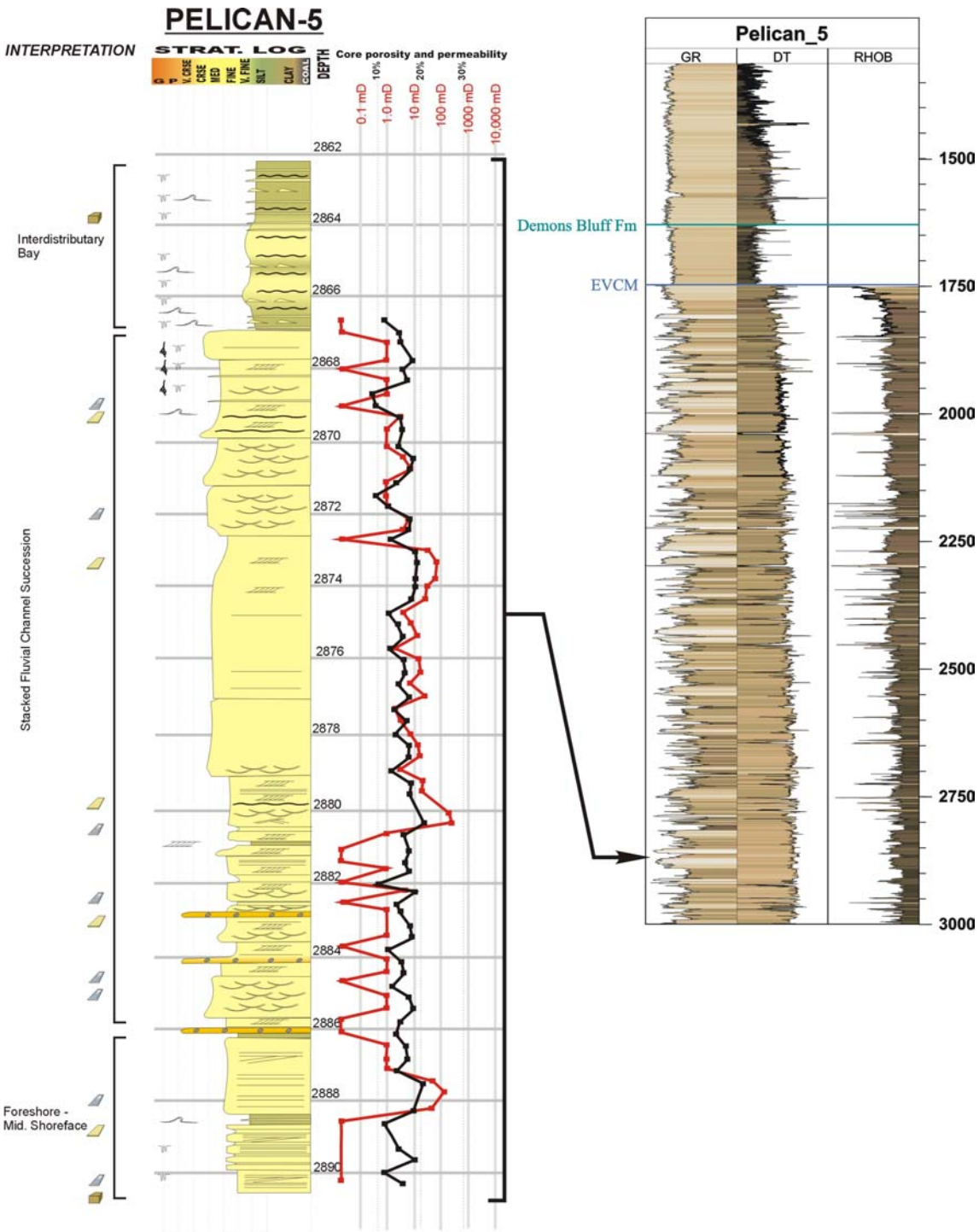

Figure 9.14 Lower part of Poonboon-1, Core 4, showing slightly bioturbated, tight, fine-grained sandstone with wave-influenced parallel lamination and rootlets (left) interpreted as back-barrier berm, overlain by coarsening-upward mudstones to fine-grained sandstones interpreted as back-barrier coastal lagoonal to lacustrine delta deposits (right). Acritarchs (*Micrhystridium* spp.) and dinocysts (*Morkallacysta* spp.) recorded from 2689.3 and 2688 m indicate a possible connection to the sea, supported by undifferentiated marine dinocysts recorded at 2689.3 m (Partridge 2002, Appendix C) (Lower *M. diversus* zone, Narimba Sequence).

Figure 9.15 Upper part of Poonboon-1, Core 4, showing reservoir facies interpreted as coarse-grained distributary channel sandstones with approximately 15-20% porosity and 100 mD permeability, overlying coarsening-upward mudstones to fine-grained sandstones interpreted as back-barrier coastal lagoonal deposits (left) at approximately 2686.8 m. Acritarchs and dinocysts recorded from 2688 m (blue dot) indicate a possible connection to the sea (Partridge, 2000, Appendix C) (Lower *M. diversus* zone, Narimba Sequence).

Figure 9.16 Example of lacustrine shoreface from Dondu-1 showing classic upward-coarsening, progradational log motif, with thinner backstepping parasequences at the top (2340-2356 m). Optimum reservoir conditions occur in the upper part of the cycle, with porosity ranging from 13-28% and permeability ranging from 1.0 to 500 mD (Upper *L. balmei* zone, lower Narimba Sequence).

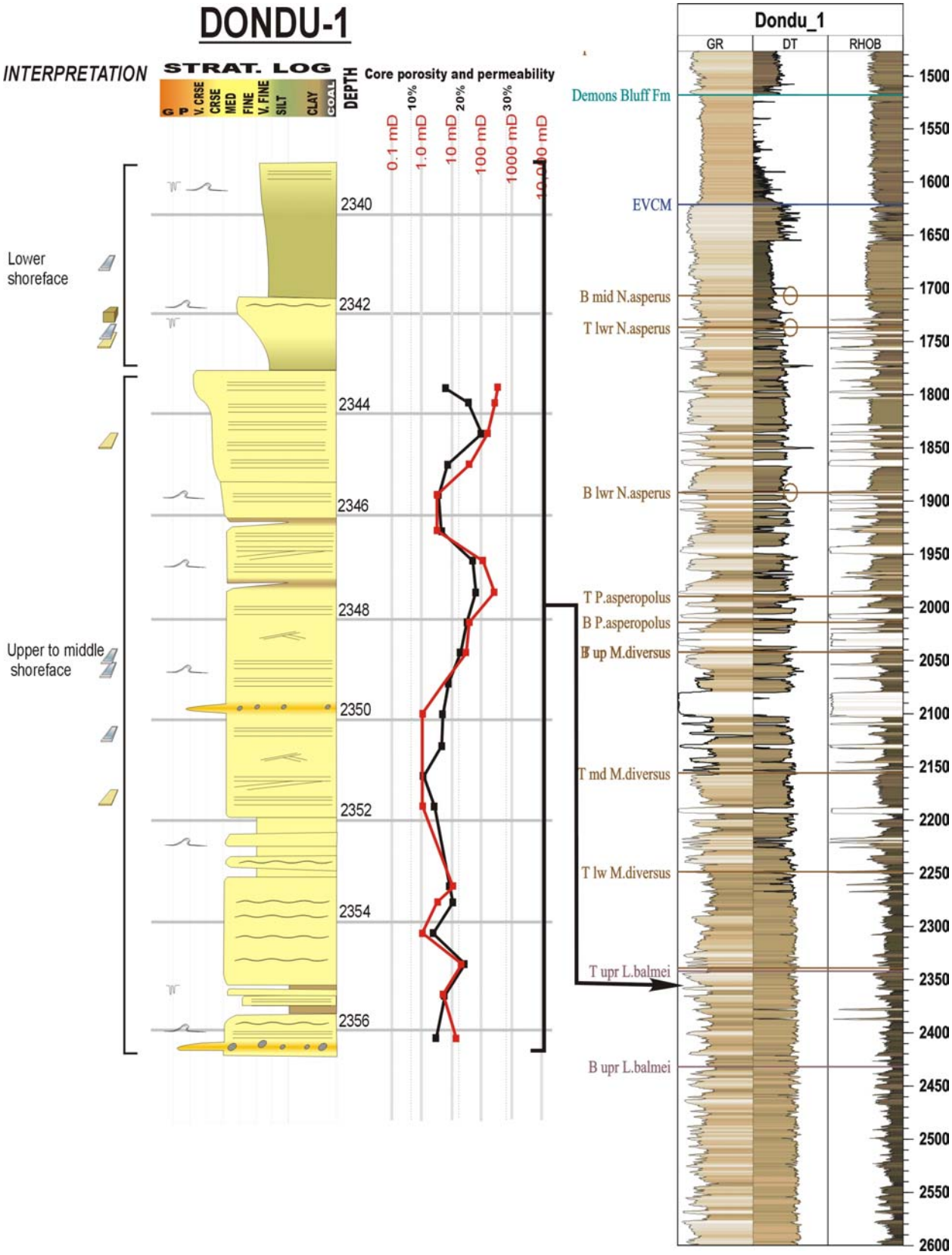

Figure 9.17 Cormorant-1 cores at 2222-2231.5 m, interpreted as peat mire and overlying lower shoreface (Upper *M. diversus* zone, lowermost Aroo Sequence), and 2773.2-2781.6 m interpreted as wave and tidally influenced lower delta plain, respectively (Lower *M. diversus* zone, Narimba Sequence).

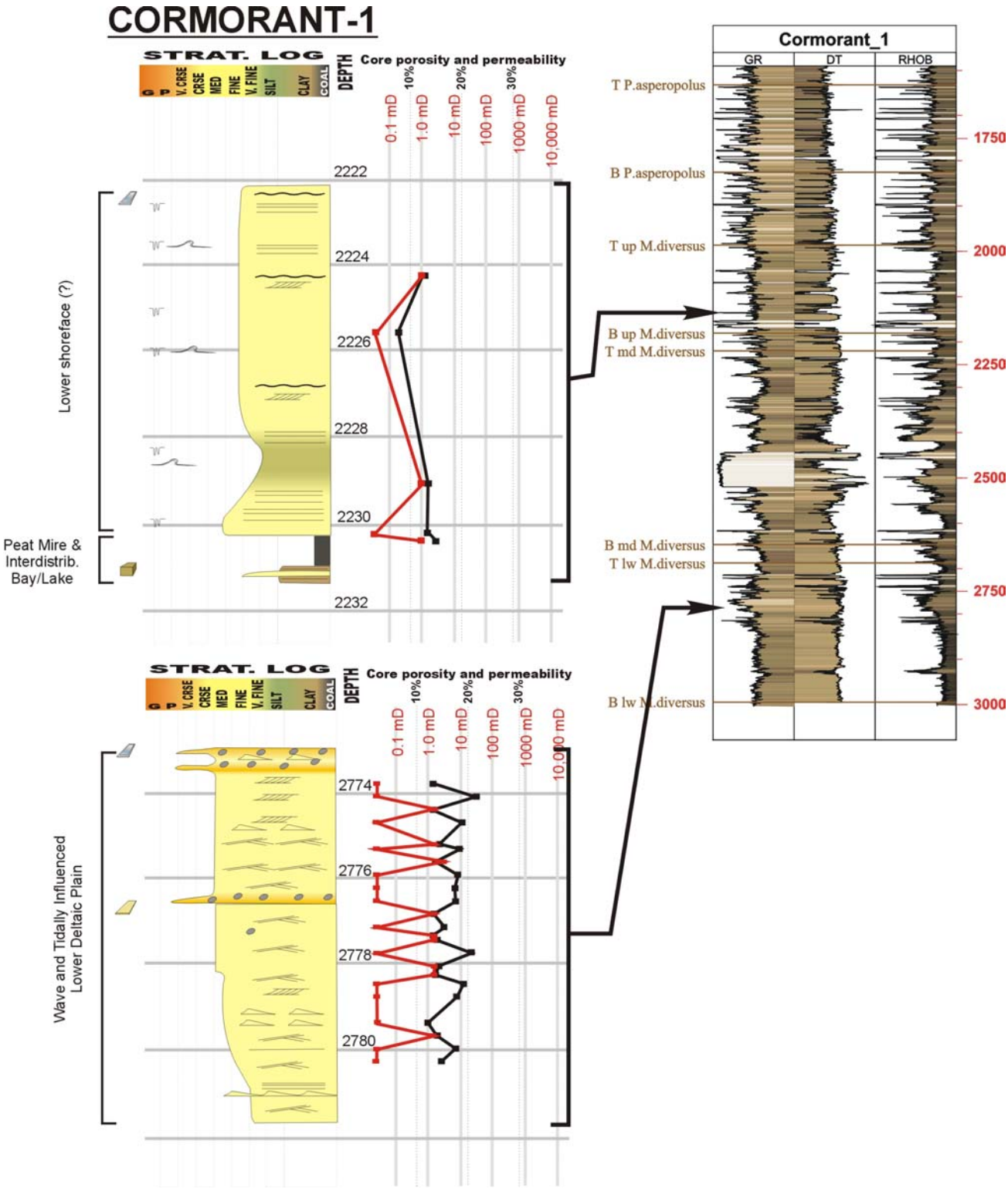

Figure 9.18 Cormorant-1 core 1994.2-2000.2 m interpreted as a lake or restricted coastal back barrier lagoon (Upper *M. diversus* zone, lowermost Aroo Sequence).

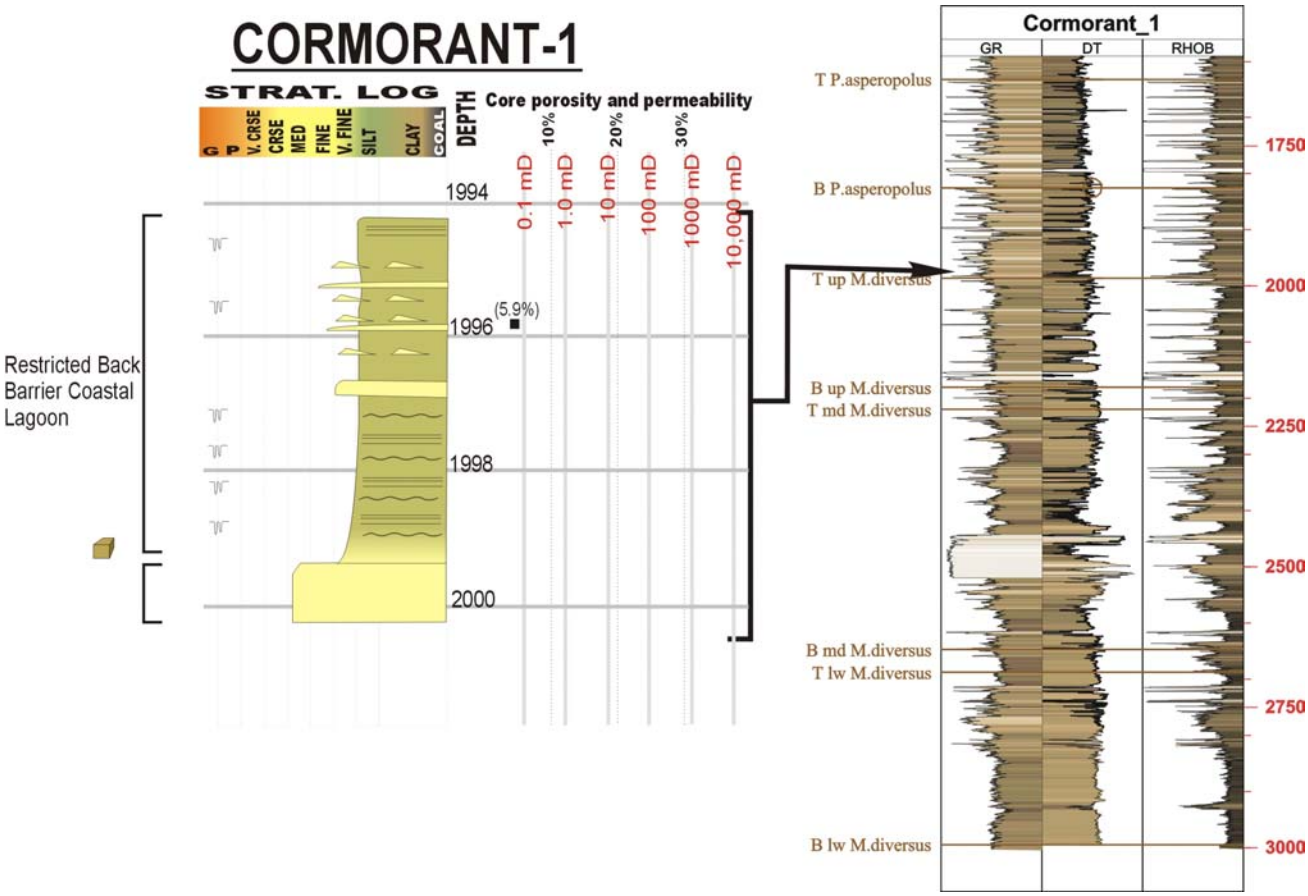

Figure 9.19 Cormorant-1 cores at 1307.2-1312.8 m interpreted as restricted coastal lagoon (Middle *N. asperus* zone, Demons Bluff Sequence) and 1503.8-1512.4 m interpreted as lacustrine shoreface and foreshore (Lower *N. asperus* zone, upper Aroo to lowermost Demons Bluff sequences).

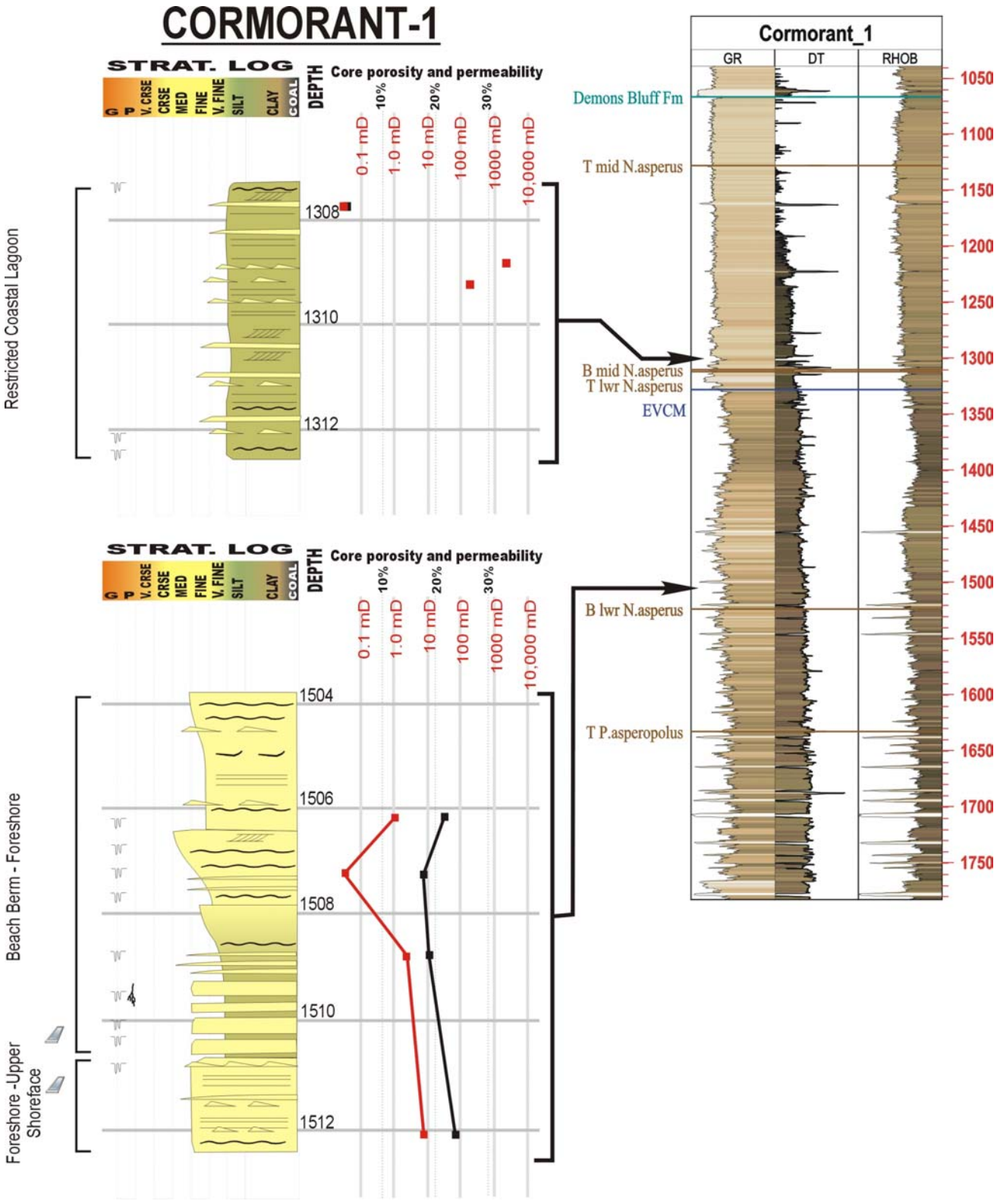

Figure 9.20 Bass-1 core at 2261.4-2268.5 m showing fine-grained shallow floodplain lake or inter-distributary bay deposits between peat mires (coals) (*P. asperopolus* zone; Aroo Sequence).

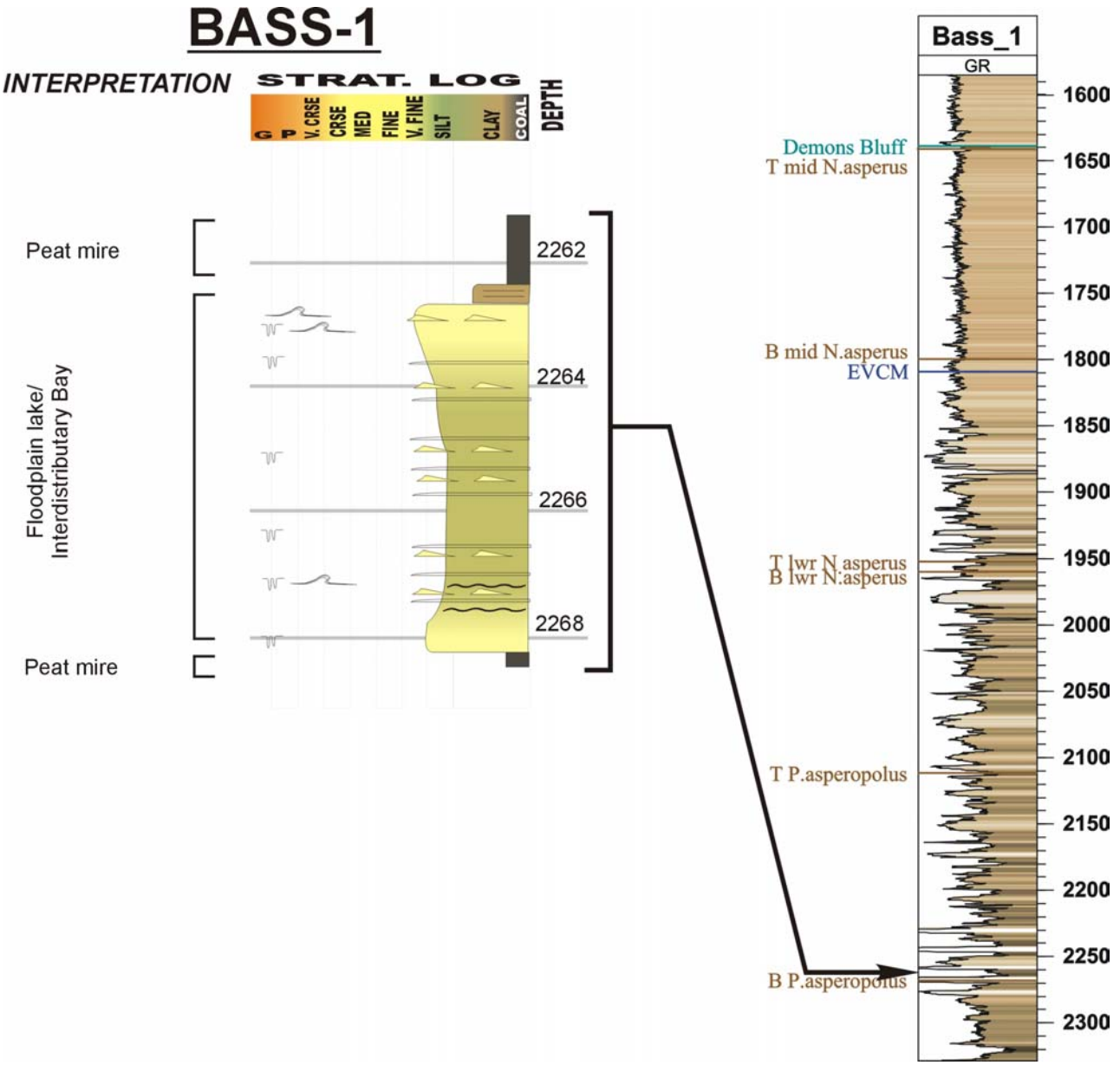

Figure 9.21 Bass-2 cores. Upper core (1159-1165 m) is glacuonitic siltstone forming part of the regional seal, interpreted as a transgressive shallow marine offshore deposit (Demons Bluff Sequence). Middle core (1259-1262.6 m) is coastal plain or overbank siltstones and very-fined grained sandstones (Aroo Sequence). Lower core (1444.4-1448.2 m) fine-grained sandstones, pebbly in places interpreted as crevasse splay deposits (Aroo to uppermost Narimba sequences).

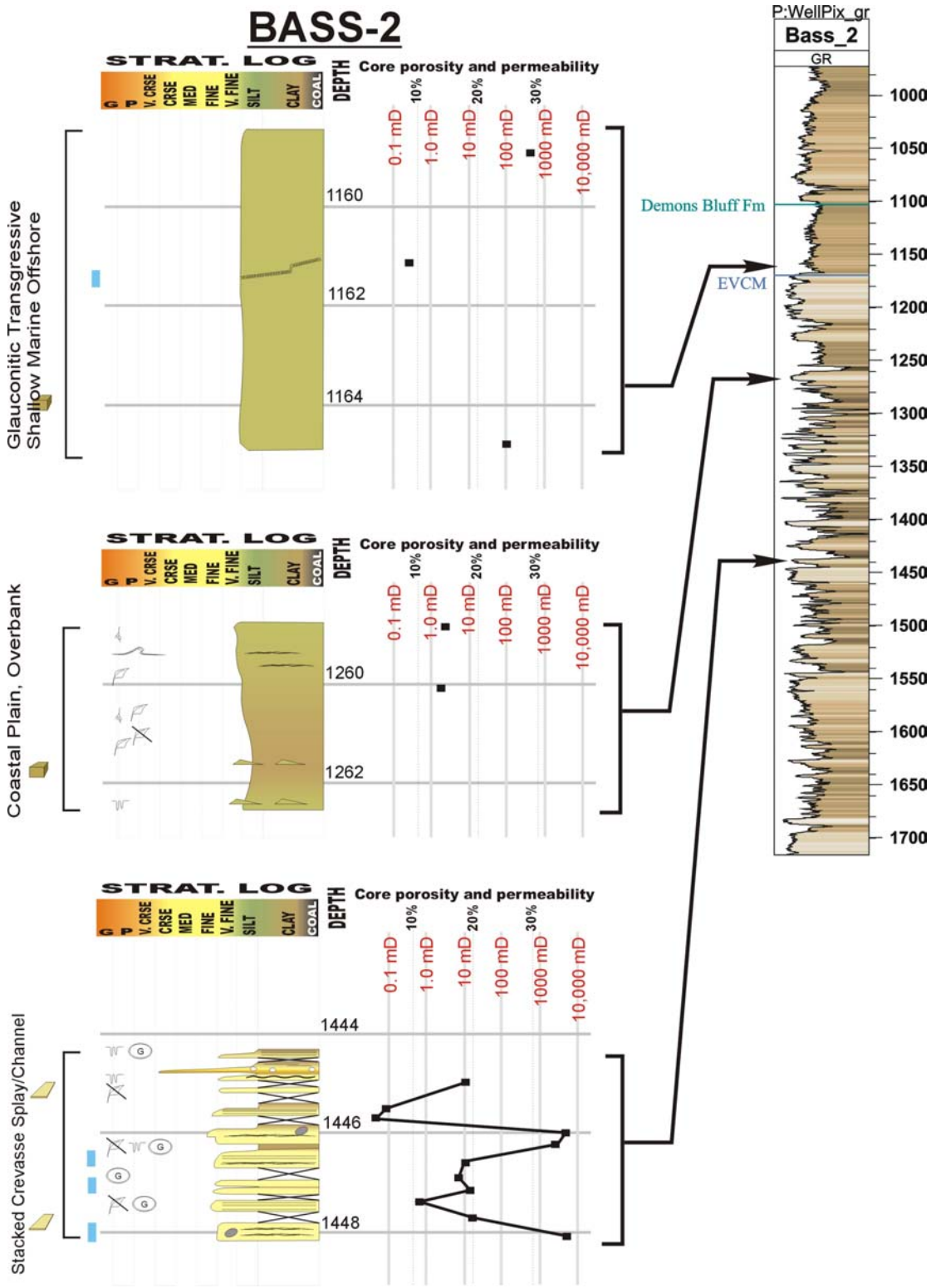

10. PETROLEUM SYSTEMS AND PLAY ANALYSIS

10.1 KEY POINTS

- A geochemical correlation between recovered hydrocarbons and potential source rocks has shown that the Bass Basin hosts an effective, terrestrial-based petroleum system (coals and fluvio-deltaic facies). Lacustrine shales are likely to be more important as seal facies, rather than as potential source rocks. The Middle Eocene and younger marine succession shows low source potential and does not lie within the oil window. Prospective areas of the Bass Basin are included in the 2002 and 2003 Offshore Acreage Release Areas (Figure 10.1).
- Geohistory modelling has shown that the onset of the main oil generation phase (Paleocene to Early Eocene coals and shales) occurred from the Late Eocene to Early Miocene, post-dating the main periods of seal deposition and trap formation. The Miocene inversion occurred after the onset of generation in the basin, and has resulted in large structures along the northern basin margin.
- The critical factor in sourcing accumulations from the coaly succession appears to be effective primary and secondary expulsion from the source rock and the volume of charge. The accumulations at Cormorant, Yolla and Pelican confirm that generation and migration have occurred within the deeper depocentres. Recent fluid inclusion studies suggest a migration phase onto the flankings of these structures (e.g., Aroo-1 and Tilana-1; Kempton et al., 2002), possibly driven by late gas charge.
- Other areas of potential prospectivity include the "Tertiary Platform" (Lennon et al., 1999) in the vicinity of Poonboon-1 and Nangkero-1, sourced locally by hydrogen-rich coals of Late Paleocene to Early Eocene age (Chapter 5). In addition, plays along the flanks of the "Tertiary Platform" (e.g., Yurongi-1 and Chat-1) have yielded some evidence of migration or potential oil zones (Kempton et al., 2002).
- Untested plays include reservoir/seal pairs associated with times of maximum flooding events in the western Bass Basin (e.g., Lower *M. diversus* and "top" *P. asperopolus* MFS).
- The petroleum systems elements of the Durroon Sub-basin differ significantly from the Cape Wickham Sub-basin owing to the cessation of tectonically-driven subsidence in the eastern Bass Basin (Durroon Sub-basin) from the mid-Campanian onward.

10.2 EXPLORATION RISKS

The main exploration risks in the Bass Basin are reservoir quality, seal properties, trap integrity (trap and seal breach) and access to mature source rocks (hydrocarbon charge) (Trigg et al., 2003; Trigg and Blevin, 2003). In the early years of exploration in the Bass Basin, poor data quality was also considered a significant exploration risk due to poor imaging below the regional seal, and the prolific occurrence of coals and volcanic rocks in the basin succession. However, advances in technology and increased knowledge of the basin's geology have minimised this aspect of risk. The use of geophysical evidence, such as AVOs, as a proxy for detecting hydrocarbon accumulations/contacts should be used with caution because of the widespread occurrence of coals, sills/flows and the intrusion of volcanic fluids into porous/fractured strata.

Recent commercial reprocessing of the existing industry seismic dataset has upgraded much of the open-file seismic dataset (Fugro Multi Client Services).

An audit of all open-file exploration wells in the Bass Basin has been compiled as part of the WTRMP (Trigg et al., 2003). This report summarises information on exploration targets, drilling results and associated technical data. The report also presents "snapshots" of composite logs (gamma and sonic) and seismic data to show the structures drilled and general well lithology. A summary of well results from the audit is presented in Figures 10.2 and 10.3 (Trigg et al., 2003). Of the 32 wells drilled in the basin, six have been determined to be invalid tests as a result of being drilled off-structure, or the absence of structural closure at the target horizons (primarily due to the presence of volcanics and associated velocity problems).

In combination with data on shows and accumulations, the drilling results clearly show that mature source rocks have generated and expelled hydrocarbons in the Cormorant, Pelican, Yolla and White Ibis troughs. However, trap breach is a significant exploration risk along much of northern basin margin, particularly in the northwest, as confirmed by the breached accumulations detected at Cormorant-1 (Kempton et al., 2002). In addition, several oil and gas zones were recorded between 1500 and 2800 m (*P. asperpolous* to Lower *M. diversus* zones) at Cormorant-1, well below the crest of the anticlinal structure and the regional "Demons Bluff" sealing facies. This suggests that Miocene inversion resulted in fault reactivation and partial breaching of traps and intra-formational seals that were in place prior to the deformational event. Biodegradation of the Cormorant oil was detected during the geochemical analyses (Chapter 5). Failure to trap hydrocarbons at Koorkah-1 and Konkon-1 has also been attributed (in part) to seal breach, with Koorkah-1 recording shows from 2400 m to TD. Hydrocarbon charge may also be a factor in the failures at Koorkah-1 and Konkon-1.

The absence of commercial accumulations in the Pelican Trough has been attributed to poor reservoir quality, primarily low permeability. Although sediment deposition in the Pelican Trough was dominated by sand-rich facies from the Late Paleocene to Middle Eocene (*M. diversus* to Middle *N. asperus* zones), subsequent diagenetic events have hindered preservation of the initial reservoir quality. This may be due to a combination of factors, including lack of an early marine cementation phase, sediment compaction, structural deformation, and elevated palaeoheatflow in the Pelican Trough and surrounding areas (e.g., Flinders-1, Pelican-3) (Chapters 5, 6 and 8). These factors may have been less pronounced along the margins of the trough.

In the southwestern part of the basin, the accumulation at White Ibis-1 was probably sourced through updip migration from the flanking trough (Yolla/White Ibis Trough). This is supported by the high maturity of the hydrocarbons as detected during the geochemical analyses (Chapter 5). Some late stage reactivation associated with uplift of the ramp margin has enhanced structural closure over the fault block at higher stratigraphic levels, but has also probably partly breached the fault seal of the in-place White Ibis accumulation. Similar to White Ibis-1, the Tilana-1, Aroo-1 and Tarook-1 wells were also positioned to have

received hydrocarbon charge from flanking depocentres. A palaeo-hydrocarbon charge is supported by the results of recent fluid inclusion studies (Kempton et al., 2002). The deeper successions at Tilana-1 and Aroo-1 penetrated basaltic flows (3100 m to TD) which may act as seals. Migration above the volcanic succession will depend on faults to provided conduits to mature source rocks in the flanking depocentres. Failure of wells drilled on the "Tertiary Platform" (Lennon et al., 1999) may be due to lack of hydrocarbon charge (Dondu-1, Nangkero-1, Poonboon-1 and Yurongi-1).

10.3 SOURCE ROCKS

The principal potential source rocks in the Bass Basin are interbedded coals (ranging from 5 to 25 m thick), fluvio-deltaic and lacustrine shales of early Palaeogene age. Geochemical analyses (Chapter 5) show these source rocks have generated liquid and gaseous hydrocarbons, with the coals being the dominant source for the liquids (Boreham et al., 2003). The lacustrine shales have a low source potential, and geochemical analyses do not support a correlation of the potential source rock to recovered hydrocarbons. The largely terrestrial setting of the basin has meant that coals and fluvio-deltaic shales are present thoughout the pre-Oligocene succession. There were two peak periods of coal deposition as indicated by plots of source-richness (TOC) versus age (Chapter 5, Figures 5.1 to 5.8). These periods were Early to Late Eocene (54 to 35 Ma, Lower *M. diversus* to Middle *N. asperus* zones) and Maastrichtian to mid-Late Paleocene (70 to 59 Ma, mid-Lower *F. longus* to Lower *L. balmei* zones). The single well to penetrate the pre-Campanian succession (Durroon-1) indicates only minor occurrences of coal within the early rift section, although thin coaly intervals within the Aptian to Albian succession show good source potential (Chapter 5). The latest Eocene and younger succession (upper Demons Bluff and Torquay sequences) show poor source potential and are immature across the basin.

The older period of increased coal deposition (Maastrichtian to mid-Late Paleocene (70 to 59 Ma, mid-Lower *F. longus* to Lower *L. balmei* zone), coincided with the occurrence of deep lakes across the central and northwestern parts of the Bass Basin (Chapter 4; Partridge, 2002; Appendix C). These lakes began to form during the Maastrichtian, and persisted until the Early Eocene (Middle *M. diversus* zone). Coals deposited during this time probably accumulated in peat mires and lower delta plain environments that fringed the lakes and basin margin. Geochemical analyses have shown that the lacustrine shales have poor source potential (Chapter 5; Boreham et al., in press), and thus are probably more important as an intra-formational seal facies, rather than as a potential source rocks. The overall distribution of coals through time reflects the expansion and contraction of the lake systems and related environments. In general, areas of higher subsidence such as the Cormorant and Yolla troughs, recorded the deepening and shallowing of the lakes, while the fringing areas recorded the shifts between lacustrine and non-lacustrine environments.

The observed decrease in the frequence of coals during the ensuing Late Paleocene to earliest Eocene time (59 to 54 Ma; Chapter 5) does not appear to be an artefact of sampling or drilled section. Where penetrated, this succession consists of mostly sandstone with minor coal (e.g., Yurongi-1, Nangkero-1, Pelican-3), or thick lacustine shales with minor sandstone and very thin coal (e.g, Koorkah-1, Toolka-1A, Yolla-1, Aroo-1).

The lack of coals may be related to an overall expansion of the lake system and a related transgressive cycle that peaked during the Early Eocene (intra-Lower *M. diversus* MFS; Chapter 4). The only wells to penetrate coal-rich intervals of this age (mid-Lower *L. balmei* to Lower *M. diversus* zones) were Poonboon-1 and Bass-3. Analyses of the coal at Poonboon-1 (3042 m) show it to be one of the most hydrogen-rich coals in the basin (Chapter 5).

The younger period of increased coal deposition (54 to 35 Ma, Lower *M. diversus* to Middle *N. asperus* zones) coincided with a time of decreased accommodation across the Bass Basin due to a waning of tectonic-driven subsidence and sediment supply (Subsidence Phase 1). The increased frequency in coal deposition can be observed in almost every well in the basin (e.g., Toolka-1A, Dondu-1, Konkon-1, Cormorant-1), even those in the Pelican Trough, where deposition of sand-rich facies continued to be high. Within this younger period of increase coal deposition, coals younger than 39 Ma (Middle *N. asperus* zone and younger) show significantly less source potential than those within the underlying succession (see Figure 5.1). The younger coals were deposited during the time of overall marine flooding of the basin from the northwest, while the underlying coals (Middle *M. diversus* to Lower *N. asperus* zones) were associated with lagoonal environments and the shallower Lake Toolka lacustrine system (Chapter 4; Partridge, 2002; Appendix C). A hydrogen-rich coal analysed at Pelican-5 (2800 m; Middle M. diversus zone) was deposited following a time of peak transgression in the Early Eocene (intra-Lower *M. diversus* MFS; Chapter 4) and at the onset of a period of slower subsidence.

Oils in the Bass Basin are a single oil population sourced mainly from Early Eocene to Paleocene coals. Biodegradation of the Cormorant oil has resulted in a statistically separate oil family when compared to the Pelican and Yolla crudes. Much better oil-to-source correlations are found between the oils and the coals, than the claystones. Gases in the Bass Basin are wet and high in CO_2 content. The CO_2 is sourced from igneous intrusions. Gaseous hydrocarbons have a similar source to oils, but are generated over a wider maturity range. Analyses show that the White Ibis-1 gas is of higher maturity than Yolla-2 gas.

Geochemical analysis and modelling undertaken for this study has detemined that the basin-wide onset of oil generation and expulsion occurs at a depth of between 2450 to 3200 m (Chapters 5 and 6), with wireline data suggesting the occurrence of overpressure below a depth of approximately 2800 m (Miyazaki, 1995). The SANS results (Appendix H; Perlican-5 and Cormorant-1) show that the scattering intensity within samples decreases with depth, and is followed by a matrix reorganization and stabilization below 2800 to 2900 m depth. There is a permeability barrier below 2900 m which relates to a decrease in pore space, probably the result of oil moving from smaller to larger pore spaces. This depth correlates to approximately 0.7% VR, or the onset of primary migration (Appendix H). Igneous intrusions, mainly within Paleocene, Oligocene and Miocene sediments, have produced localised elevated maturity up to 5% VR. This study has determined that key events in the process of petroleum generation and migration from effective source rocks are:

- onset of oil generation occurred at a VR of 0.65% (2450 m in Pelican-5);

- onset of expulsion (primary migration) occurred at a VR of 0.75% (2700 to 3200 m in Bass Basin; 2850 m in Pelican-5);
- main oil window occurred between VR of 0.75% and 0.95% (2850 to 3300 m in Pelican-5); and
- main gas window occurred at VR>1.2% (>3650 m in Pelican-5).

The defined source rocks linked to hydrocarbon accumulations within the Bass Basin (Paleocene to Early Eocene coals) entered the oil generation window just prior to and following deposition of regional shaley facies of the Demons Bluff Sequence, and after the major trap forming structural events of the Late Cretaceous and Early Eocene. Paleocene to Early Eocene units continued to pass into the oil expulsion window during and after Miocene structural reactivation events. The base of the Pelican-5 well (~ 67 Ma, Maastrichtian) entered the main gas generation window (1.15 – 2.6 %Ro) around the start of the Miocene (~23 Ma). Paleocene to Early Eocene source rock intervals have not entered the main gas generation window. However, deeper undrilled sediments of the Durroon Megasequence (Tasman Rift Phase) may have entered the main gas generation window as early as the Paleocene. Migration from mature source rocks into available traps may have occurred via local fault-related conduits and intra-stratal fairways.

10.4 RESERVOIR ROCKS

Proven petroleum-bearing reservoirs in the Bass Basin occur mainly within the Paleocene (Upper and Lower *L. balmei* zones) and Lower Eocene (Lower M*. diversus* zone) succession (see Figure 2.2), and are predominantly fluvio-deltaic sandstones with net thicknesses of between 20 to 50 m. Some degraded oil was recovered at Cormorant-1 (1500 m depth) reservoired in much younger strata (*P. asperopolus* and Lower *N. asperus* zones), while an oil columnn at Yolla-1 was intersected within a Middle *N. asperus* age succession. The occurrence of oil in the younger succession at Cormorant-1 can possibly be attributed to upward migration from a deeper accumulation(s) that was breached during the Miocene inversion. Facies analysis and correlation of cores with wireline logs suggests that reservoir sandstones were deposited in a range of terrestrial, paralic and shallow marine environments (Baillie et al., 1991; Chapters 8 and 9). The lateral continuity of these facies is expected to vary widely. Porosity analyses on cores and sidewall cores at Cormorant-1 and Yolla-1 recorded average values of 15 to 25 percent.

At a field scale, the quality of the reservoir facies has been attributed to the textural maturity and grainsize, as well as diagenesis, depth of burial and heat flow within the basin (Chapter 8). Coarse-grained facies in the Bass Basin include fluvial channels, crevasse-splays, and coarser-grained facies deposited in lacustrine/lagoonal shoreface and foreshore environments (Chapters 8 and 9; Appendix L). The primary relationship between reservoir quality and depositional facies is linked to coarse grain size associated with specific facies, with a secondary link to dissolution of early siderite cementation phase associated with organic-rich facies. Early cementation by siderite served to preserve porosity and permeability during subsequent periods of compaction and deformation. The cement was later removed leaving behind good secondary intergranular porosity. Cubitt (1992) observed that the *L. balmei* interval has a predisposition to good reservoir quality even though it is represented mainly in deeper parts of the basin. The first "marine

influence" observed in the Bass Basin succession occurred in the Early Paleocene and coincided with deposition of the Lower *L. balmei* facies (Partridge, 2002; Appendix C). It was likely that the marine influence during sedimentation of *L. balmei* facies served to remove silt and provide some carbonate to act as an early cement. This maybe particularly true for wells formerly situated in more fluvial environments during the time of the lower Koorkah Lake succession (e.g., Yurong-1, Nangkero-1, Pelican-5, Chat-3, and Bass-3), along with the relatively high-energy of these depositional systems.

A study of the nature and distribution of porosity suggests that present-day reservoir quality is highest between 1900 and 2700 m subsea over the extent of the basin (Meszoly et al., 1986). In general, porosity declines fairly moderately with increasing depth (approximately 5.7 porosity units per 1000 meters; Meszoly et al., 1986), while permeabilities range from 16 to 308 mD. Two depth-related diagenetic zones have been recognised within the quartz-rich siliciclastics – an upper zone characterised by carbonate authigenesis from 1950 m to the base of the Demons Bluff shale facies; and, a lower zone lying below 2000 m, characterised by dissolution, compaction, quartz overgrowth cementation and authigenic illite and kaolinite (Meszoly et al., 1986).

10.5 SEALS

The MICP analysis of 15 selected samples from cores undertaken for this study has shown a wide variation in seal capacity (Chapter 7, Appendix L). It should be stressed that many of the cores taken during exploration drilling have focused on the recovery of reservoir facies, rather than seal facies. As such, the samples that were selected for seal analysis represent fine-grained intervals within the cores examined, but they are considered only a subset of all potential seal facies in the Bass Basin.

The highest capacity seal identified in this study occurred within a lower shoreface, carbonaceous mudstone in Dondu-1 (2342 m; average oil column >1400 m; Upper *L. balmei* zone). Other high capacity seal facies analysed (average oil column of 700 to 1150 m) were detected in lacustrine, lagoonal and interdistributary bay mudstones of latest Paleocene to Early Eocene age (Upper *L. balmei* to Middle *M. diversus* zones; Appendix L). The Late Paleocene to earliest Eocene was a period of low coal production (Section 10.3), and has been interpreted to coincide with an overall expansion of the Koorkah Lake system. A comparison of width/length ratios for a variety of seal types suggest that lower lacustrine shoreface and lacustrine/ lagoonal facies with high sealing capacity are also laterally extensive. The single sample to be analysed from the shaley facies of the "Demons Bluff" regional seal (Bass-2, 1164.69m, Upper *N. asperus* zone) yielded only modest to good sealing capacity (average oil column of 400 m). However, the low seal capacity result determined from the "Demons Bluff" regional seal may reflect secondary fracturing due to trap breaching or the influence of late volcanics, rather than primary seal properties. Further MICP analysis are required from potentially less-affected samples to determine a valid result for the "Demons Bluff" regional sealing facies.

10.6 PLAY CONCEPTS

Wells drilled to date in the western Bass Basin have tested a range of plays, including: 1) onlap onto or structural closure (drape) over the crest of intra-basin fault blocks located updip from deep flanking half-graben (White Ibis-1, Aroo-1 and Tilana-1); 2) Miocene and younger inversion structures and fault blocks associated the crestal collapse (Cormorant-1, Toolka-1A); 3) Eocene anticlines within the hanging wall of half graben and associated crestal collapse fault blocks (Pelican wells); 4) low-relief fault blocks within the basin associated with late-stage growth faults (Poonboon-1, Tarook-1), and, 5) footwall fault blocks along the basin margin with stratigraphic onlap (Tasmanian Devil-1; Flinders-1). Many of these plays have experienced late stage enhancement of structural closure (Eocene, Oligocene and Miocene) that may have partially breached in-place accumulations (White Ibis-1, Cormorant-1). The most successful plays have been those located updip or along the flanks of Cretaceous half graben where growth faulting continued until the Early Eocene. Prospective parts of the Bass Basin are offered in the 2002 and 2003 Release of Offshore Petroleum Exploration Areas – including areas overlying the Cormorant, White Ibis and Pelican troughs, as well as the prospective coal-rich areas around Poonboon-1 in the central basin.

The occurrence of the petroleum systems elements within the stratigraphic succession has been summarised in Figure 10.4. The main reservoirs within the basin that presently lie at drilling depths of 2800 to 3200 m are Paleocene or younger in age (Upper and Lower *L. balmei* zones). Within the deeper areas of the Cormorant, Yolla, Pelican and White Ibis troughs, where late stages of extension resulted in thicker Paleocene and Eocene sections, the target reservoirs are earliest Eocene and younger (Lower *M. diversus* and younger zones). Although deeper sections have been drilled (e.g., Pelican Trough), reservoir quality appears to be degraded below 3500 m. On the basin margins and shallower flanks of the troughs, Late Cretaceous reservoirs are also viable targets (Upper *F. longus* zone). The deposition of laterally extensive, intraformational and regional seal facies occurred during the Early to Late Paleocene ("Koorkah Lake" shales), Late Paleocene to Early Eocene (lower shoreface, carbonaceous mudstones; Dondu-1, 2342 m; Upper *L. balmei* zone; average oil column >1400 m), early Middle Eocene (associated with top *P. asperopolus* MFS), mid-Middle Eocene ("Toolka Lake" facies), and Late Eocene ("Demons Bluff" shale facies). The Maastrichtian to late Early Eocene was the main period of trap development across the basin (fault blocks; Upper *F. longus* to Middle *M. diversus* zones), with some traps developing locally during the late Early Eocene (growth faults and sediment loading) to mid-Middle Eocene (contraction deformation).

A geochemical correlation between recovered hydrocarbons and potential source rocks has shown that the Bass Basin hosts an effective, terrestrial-based petroleum system. The Middle Eocene and younger marine succession shows low source potential and does not lie within the oil window. A minor, intermittent marine influence in older rocks has been detected through biostratigraphic analyses, and is thought the be reflected in Eocene and Paleocene coals with locally high sulphur content (Poonboon-1). Geohistory modelling has shown that the onset of the main oil generation phase (Paleocene to Early Eocene coals and shales) occurred from the Late Eocene to Early Miocene, post-dating the main periods of seal deposition and trap formation. The Miocene inversion occurred after the onset of generation in the basin, and has resulted in

large structures along the northern basin margin. The critical factor in sourcing accumulations from the coaly succession appears to be effective primary and secondary expulsion from the source rock and the volume of charge. The accumulations at Cormorant, Yolla and Pelican confirm that generation and migration have occurred within the deeper depocentres. Recent fluid inclusion studies suggest a migration phase onto the flankings of these structures (e.g., Aroo-1 and Tilana-1; Kempton et al., 2002), possibly driven by late gas charge. Other areas of potential prospectivity include the "Tertiary Platform" (Lennon et al., 1999) in the vicinity of Poonboon-1 and Nangkero-1, sourced locally by hydrogen-rich coals of Late Paleocene to Early Eocene age (Chapter 5). In addition, plays along the flanks of the "Tertiary Platform" (e.g., Yurongi-1 and Chat-1) have yielded some evidence of potential oil zones (Kempton et al., 2002). A generalised map showing potential migration from mature source rocks is shown in Figure 10.5. Untested plays include reservoir/seal pairs associated with times of maximum flooding events in the western Bass Basin (e.g., Lower *M. diversus* and "top" *P. asperopolus* MFS). The petroleum systems elements of the Durroon Sub-basin differ significantly from the Cape Wickham Sub-basin owing to the cessation of tectonically-driven subsidence in the eastern Bass Basin (Durroon Sub-basin) from the mid-Campanian onward.

Figure 10.1 Location map of the Bass Basin and adjacent region, southeastern Australia. The basin outline, permits, well and field locations, including the 2002 (black) and 2003 (red) Acreage Release areas, are also shown.

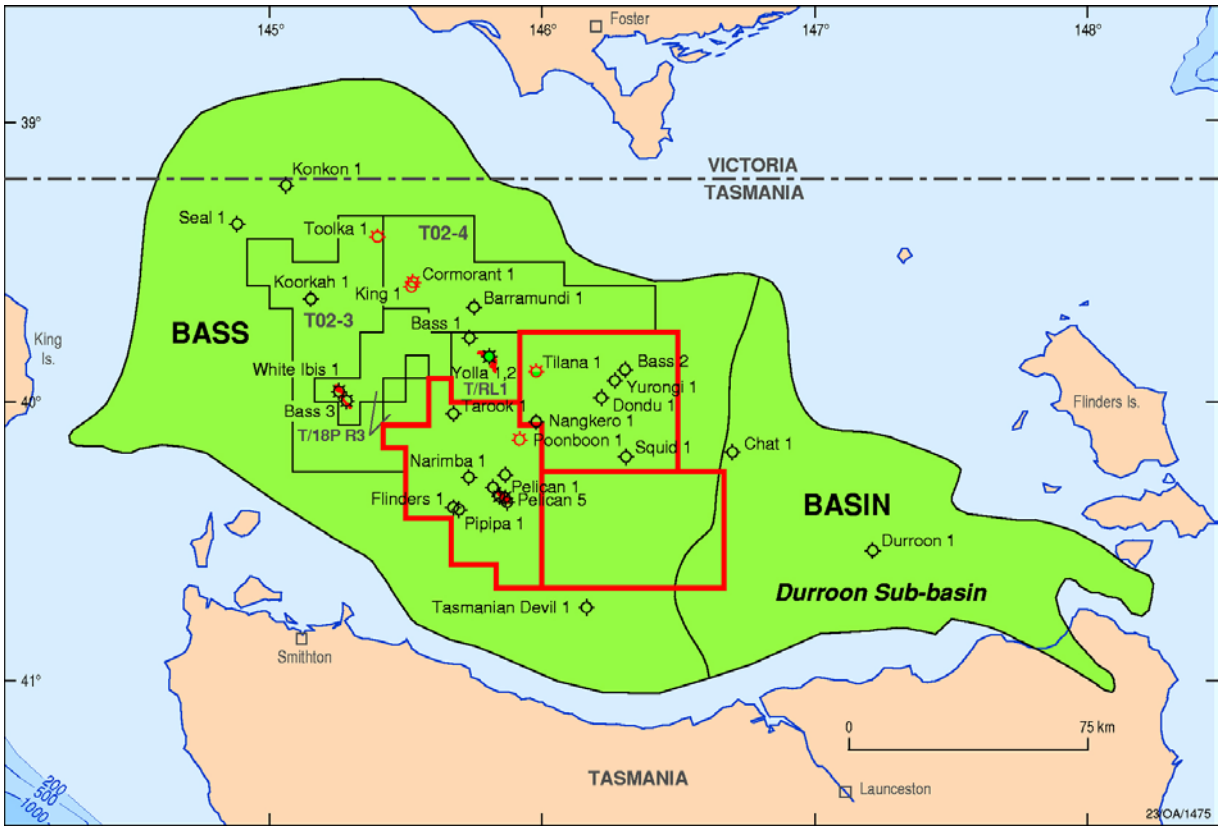

Figure 10.2 Chart summarising drilling results in the Bass Basin, and interpreted reasons for success and failures (from Trigg et al., 2003; Trigg and Blevin, 2003). A map showing the geographic distribution of these results is shown in Figure 10.3.

	Well	Operatror & year	Hydrocarbon Show	TD (m)	Rock Age at TD	Source Rock oil & gas potential	Invalid Structural Test	Reservoir Risk	Seal Risk	Charge Risk	Hydrocarbon Accumulation
Durroon Sub-basin	Chat 1	Bridge Oil Ltd, 1986	No significant	3104	Volcanic rock (*N. senctus*)	Immature to TD				Charge	
	Durroon 1	Esso E & P, 1972	No shows	3024	*P. notensis*	Generation & expulsion Below 3000m			No seal		
Cormorant Trough	Barramundi 1	Globex Far East, 1999	Carbon dioxide	2100	No data available	No data available			Seal Breach		
	Bass 1	Esso E & P, 1965	No shows	2352	Upper *M. diversus*	Immature to TD	Volcanic rock as primary objective				
	Cormorant 1	Esso E & P, 1970	Minor gas, trace oil	3001	Lower *M. diversus*	Generation: 1500-2250m Expulsion below 2500m			Seal Breach		
	King 1	SAGASCO, 1992	Fluroescence, gas, trace oil	2223	*M. diversus*	No data available			Seal Breach		
	Toolka 1	Esso E & P, 1974		2715	Volcanic rock Lower *M. diversus*	Generation below 2500m, but poor source richness/quality				Charge	
Pelican Trough	Flinders 1	SAGASCO, 1992	Minor gas	2723	Lower *L. balmei*	Localised high maturity due to igneous intrusion. Immature below 2400m	Volcanic rock as primary objective				
	Narimba 1	Esso E & P, 1973	Dry	3354	Lower *M. diversus*	Generation: below 2800m. Expulsion close to TD but poor source richness/quality				Charge	
	Pelican 1	Esso E & P, 1970	Condensate, gas	3178	Lower *M. diversus* Upper *L. balmei*	Elevated maturity. Poor sampling limits interpretation		Poor Permeability			
	Pelican 2	Esso E & P, 1970	Condensate, gas	3068	Lower *M. diversus*	Generation below 2700m		Poor Permeability			
	Pelican 3	Esso E & P, 1972	Minor gas	2907	Lower *L. balmei*	Elevated maturity. Poor sampling limits interpretation		Poor Permeability			
	Pelican 4	Hematite Petroleum, 1979	Condensate, gas	3051	No data available	Generation below 2700m. No expulsion to TD		Poor Permeability			
	Pelican 5	Amoco, 1985	Condensate, gas	4267	*T. lillei*	Generation: below 2450m Expulsion: 2850-3300m, >3650m (gas)		Poor Permeability			
	Pipipa 1	Hematite Petroleum, 1982	Fluorescence, trace gas	2115	Lower *N. asperus*	Localised high maturity due to igneous intrusion. Poor source richness/quality to TD				Charge	
	Tasmanian Devil 1	Weaver Oil & Gas, 1984	Dry	864	Volcanic rock (*P. tuberculatus*)	Limited data. Poor source richness/ quality and immature to TD	Volcanic rock as primary objective				
Western Bass	Konkon 1	Esso E & P, 1973		1537	Intra - *T. longus*	Immature to TD			Seal Breach		
	Koorkah 1	Amoco, 1985	Dry	3149	*T. lillei*	Generation: below 2800m. Expulsion: below 3000m			Seal Breach		
	Seal 1	Bridge Oil, 1986	No significant	1670	Volcanic rock Lower *L. balmei*	Limited data. Localised high maturity				Charge	
Central-western Bass	Bass 3	Esso E & P, 1967	Minor gas	2432	Lower *T. longus*	Immature to TD	Off structure				
	White Ibis 1	Premier Oil, 1998	Gas	2220	Volcanic rock	No data available			Partial Fault Seal Breach		Hydrocarbon Accumulation
Central-eastern Bass	Bass 2	Esso E & P, 1966	No shows	1801	Lower *L. balmei*	Immature to TD			No Seal		
	Dondu 1	Esso E & P, 1973	Dry	2927	Lower *L. balmei*	Generation & expulsion at 2784m				Charge	
	Nangkero 1	Hematite Petroleum, 1974	Dry	2877	Upper *L. balmei*	Generation: below 2300m. No expulsion to TD				Charge	
	Poonboon 1	Esso E & P, 1972	Trace gas	3266	Lower *T. longus*	Generation: below 2800m. Expulsion close to TD.				Charge	
	Squid 1	Weaver Oil & Gas, 1984	Dry	2922	Intra - *L. balmei*	Immature to TD			Trap integrity		
	Tilana 1	Amoco, 1985	Minor gas	3900	Volcanic rock (*T. longus*)	Generation: below 2500m. Expulsion: below 3000m (oil), >3900m (gas)	No structural closure			Charge	
	Yurongi 1	Esso E & P, 1973	No shows	2438	Lower *L. balmei*	Immature to TD				Charge	
Central Bass	Aroo 1	Hematite Petroleum, 1974	Fluorescence, minor gas	3692	Volcanic rock Lower *L. balmei*	Mature for liquids below 2900m	Volcanic rock as primary objective				
	Tarook 1	Esso E & P, 1972	No shows	2774	Volcanic rock (Middle *M. diversus*)	Generation at TD, but poor source richness/quality				Charge	
	Yolla 1	Amoco, 1985	Condensate, gas, oil	3347	Volcanic rock Lower *L. balmei*	Generation:1980-2580m. Expulsion: below 2500m					Hydrocarbon Accumulation
	Yolla 2	Premier Oil, 1998	Gas	3165	Volcanic rock	No data available					Hydrocarbon Accumulation

14-1/379

Figure 10.3 Map showing the geographic distribution of drilling results in the Bass Basin, and interpreted reasons for success and failures (from Trigg et al., 2003; Trigg and Blevin, 2003). A chart summarising this information is shown in Figure 10.2.

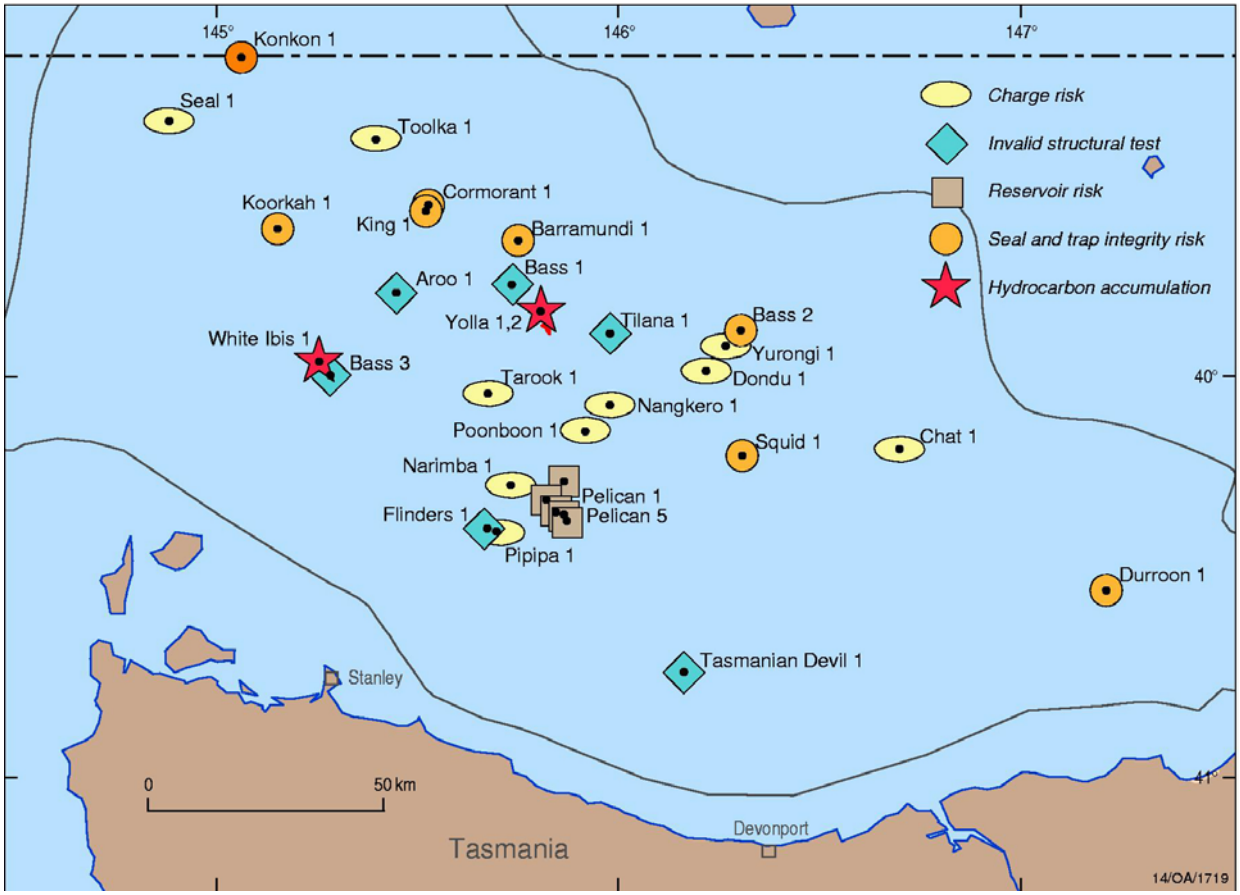

Figure 10.4 Stratigraphic column for the western Bass Basin showing the distribution of petroleum systems elements (reservoir, source, seal) and the overall timing of trap development. The terrestrial nature of the basin until the mid-Eocene (Middle N. asperus zone) means that elements of reservoir, source and seal occur mainly as interbedded (intra-formational) facies. Sealing shales deposited as part of the Koorkah and Toolka Lake cycles are thicker and more regional in nature. These shales are important as fault-seals (juxtaposition). Coals deposition increased across the basin from the late Early Eocene (Upper M. diversus) onward due to a decrease in the rate of tectonic-driven subsidence.

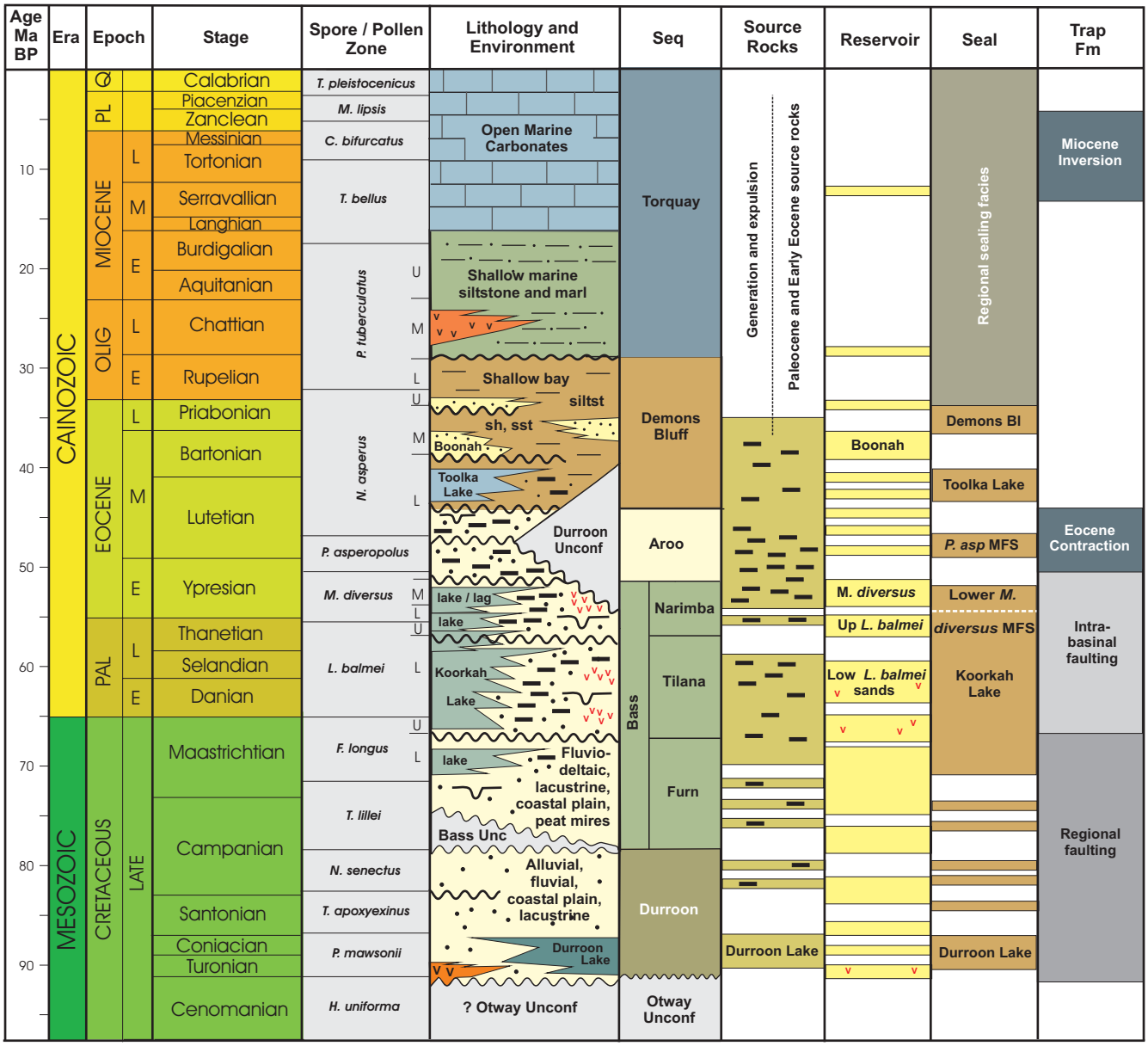

Figure 10.5 Generalised map showing the distribution of mature potential source rocks and areas of potential hydrocarbon charge in the Bass Basin. This map is based on the modelling of potential source rocks of Late Cretaceous to Early Eocene age, and evidence from fluid inclusion studies (Kempton et al., 2002).

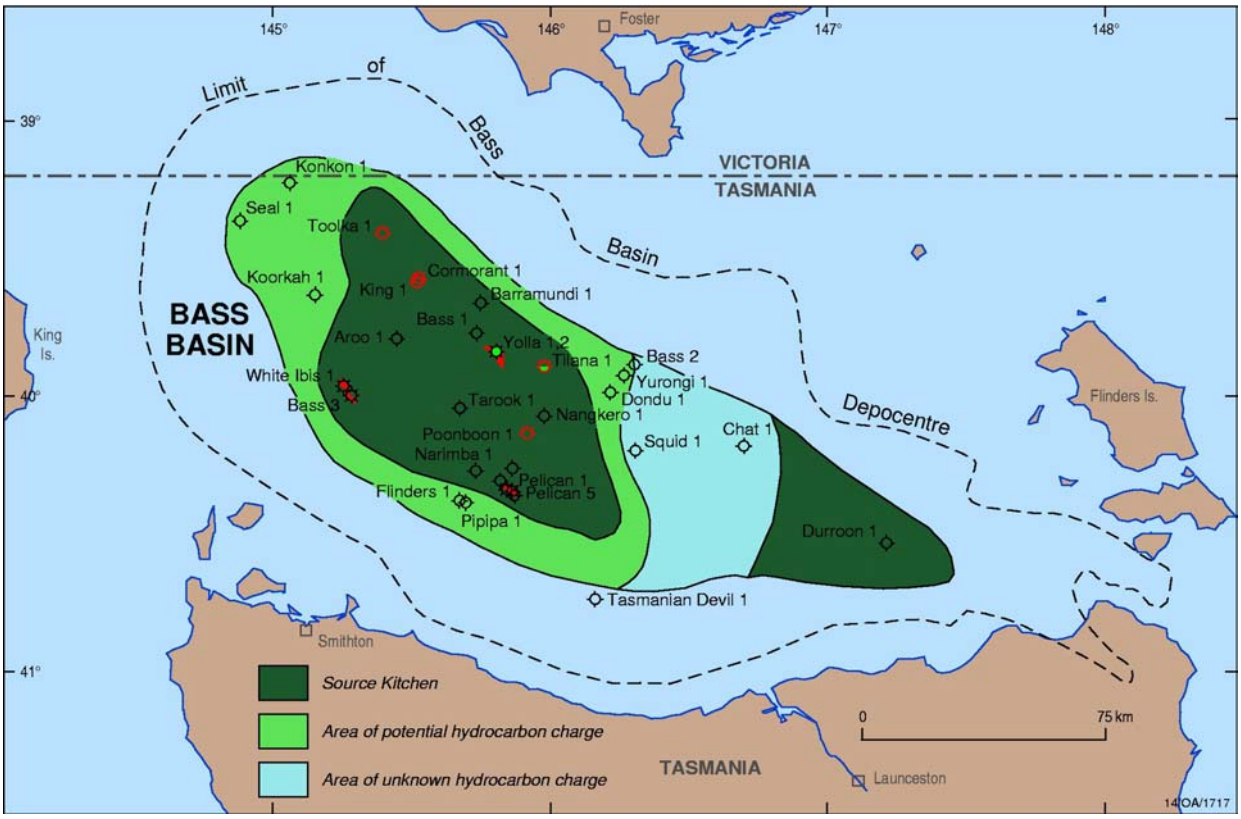

11. ACKNOWLEDGEMENTS

Geoscience Australia and the National Centre for Petroleum Geology and Geophysics acknowledge the financial support provided by Mineral Resources Tasmania to undertake studies to enhance the understanding of the petroleum geology of the Bass Basin. The study was undertaken under the auspices of the Western Tasmanian Regional Minerals Program. Carol Bacon and Clive Calver are gratefully acknowledged for their support and coordination of the project. Fugro Multi Client Services are acknowledged for permission to use seismic images in numerous figures in this Record.

The MRT-funded Bass Basin project was undertaken as a collaborative effort by Geoscience Australia and the National Centre for Petroleum Geology and Geophysics (University of Adelaide). This project would not have been possible without the contributions of many others from both organisations who provided scientific input and a wide range technical support and expertise. The NCPGG acknowledges Igor Filipi, Nathan Ceglar and Catherine Gibson-Poole who assisted with drafting and computer support. Schlumberger is also thanked for access to GeoFrame training suite software at the NCPGG. Those from Geoscience Australia who are thanked for their scientific input over the course of this project include Chris Nicholson, Rosalie Pollock, and Barry West. In particular, Jennie Totterdell and Tony Stephenson are gratefully acknowledged for their editorial undertakings. Technical support for the Bass Basin Project was provided by Anne Fleming, Cameron Mitchell, Neville Montgomerie, Carmine Moscaritolo, Mark Webster, David Rowland and Alison Hancock - their professional contributions are gratefully acknowledged.

Murray Woods, Brian Pashley, Karin Weiss, Leanne McMahon, Silvio Mezzomo, Lindell Emerton and Terry Brown from Geoscience Australia are also acknowledged for the provision of cartography, graphic and report production services. Processing and preparation of biostratigraphic and SANS samples was undertaken at Geoscience Australia by Christian Thun, Andrew Kelman, Tony Watson and Richard Brown. Drs. Clinton Foster, Eric Monteil (Geoscience Australia) and Mike Macphail (Australian National University) provided additional input to the biostratigraphy. Organic geochemistry sample preparation and analyses were undertaken at the laboratories at Geoscience Australia by Janet Davenport, Paul Greenwood, Natalie Johns and Janet Hope. A sub-set of samples were analysed under contract for maturity properties by Dr. Jane Newman (Newman and Associates, New Zealand) and Dr. Alan Cook (Keiraville Konsultants). Access to all samples analysed for the Bass Basin Project was provided by the Petroleum Data Repositories at Geoscience Australia (Canberra) – Paula Cronin, Ben Miller, Eddie Resiak, Danny Britten are thanked for their assistance.

Reports commissioned from external companies on behalf of MRT, as well as all data generated from analyses carried out at Geoscience Australia and the National Centre for Petroleum Geology, are available through the Geoscience Australia website (www.ga.gov.au). Geochemical and biostratigraphic analysis are can be downloaded free-of-charge through the internet, while other reports have been lodged with the Petroleum Data Repositories at Geoscience Australia as Destructive Analysis Report. These reports can be ordered on the internet and are available at the cost-of-transfer.

12. REFERENCES

AGSO AND Geomark Research, 1996. The Oils of Western Australia. Proprietary Report, Canberra and Houston (unpublished).

Australian Financial Review, 2002. Gas competition on the boil (Corporate Focus Section). Friday, 6 December 2002, 62.

Baillie, P.W., 1992. Relationship of coal facies with sea level in the Bass Basin. Geological Society of Australia, Abstracts, 32, 116-117.

Baillie, P.W., 1993. Regional Geology. In: Maung, T.U, Miyazaki, S., Baillie, P.W., Lavering, I.H., Vuckovic, V., Stephenson, A.E., Williamson, P.E., Staunton, J., Radke, S.G., West, B.W., Gippespie, R.G., Resiak, E., and Temple, P.R., Eastern Bass Basin Petroleum Prospectivity Bulletin. Bureau of Resource Sciences, Petroleum Prospectivity Bulletin, 1993/2.

Baillie, P.W. and Bacon, C.A., 1989. Integrated sedimentological analysis, the Eocene of the Bass Basin. APEA Journal, 29 (1), 312-327.

Baillie, P.W. and Pickering, R., 1991. Tectonic evolution of the Durroon Basin, Tasmania. Exploration Geophysics, 22, 13-18.

Baillie, P.W., Tingate, P.R. and Stuart, W.J., 1991. Reservoir development and diagenesis in the Bass Basin, Tasmania. The APEA Journal, 33(1), 85-100.

Baillie, P.W. and Brown, A.V., 1984. Igneous rocks from Tasmanian Devil-1. Tasmanian Department of Mines, Unpublished Report 1984/74.

Blevin, J., 2001. Hydrocarbon prospectivity of Australia's remote frontier areas in offshore east and south-east Australia – examples from the basins of Lord Howe Rise. In: Hill, K.C. and Bernecker, T. (editors), Eastern Australasian Basins Symposium, A Refocused Energy Perspective for the Future, Petroleum Exploration Society of Australia, Special Publication, 25-35.

Blom, W.M. and Alsop, D.B., 1988. Carbonate mud sedimentation on a temperate shelf, Bass Basin, southeast Australia. Sedimentary Geology, 60, 269-280.

Boreham, C.J. and Powell, T.G., 1994. Petroleum source rock assessment of coal and associated sediments: qualitative and quantitative aspects. In: Law, B. and Rice, D. (editors), Hydrocarbons from Coal, AAPG Special Publication, 133-157.

Boreham, C.J. and DeBoer, R.A., 1998. Origin of Gilmore gas and oil, Adavale Basin, central Queensland. APPEA Journal, 38(1), 399-420.

Boreham, C.J. and Summons, R.E., 1999. New insights into the active petroleum systems in the Cooper and Eromanga basins, Australia. APPEA Journal 39(1), 263-96.

Boreham, C.J., Horsfield, B. and Schenk, H.J., 1999. Predicting the quantities of oil and gas generated from Australian Permian coals using pyrolytic methods. Marine and Petroleum Geology, 16, 165-188.

Boreham, C.J., Hope J.M. and Hartung-Kagi, B., 2001. Understanding source, distribution and preservation of Australian natural gas: a geochemical perspective. APPEA Journal, 41(1), 523-547.

Boreham, C.J., Blevin, J.E., Duddy, I., Newman, J., Liu, K., Middleton, H., Macphail, M.K. and Cook, A.C., 2002. Exploring the potential for oil generation, migration and accumulation in Cape Sorell-1, Sorell Basin, offshore west Tasmania. APPEA Journal 2002, 42(1), 405-435.

Boreham, C.J., Blevin, J.E., Radlinski, A.P. and Trigg, K.T., 2003. Coal as a source of oil and gas, a case study from the Bass Basin, Australia. APPEA Journal 2003, 43(1), 117-148.

Brown, B.R., 1976. Bass Basin, some aspects of the petroleum geology. In: Leslie, R.B., Evans, H.J. and Knight, C.L. (editors), Economic Geology of Australia and Papua New Guinea, 3. Petroleum, Monograph Series No. 7. The Australasian Institute of Mining and Metallurgy, 67-82.

Bryan, S.E., Constantine, A.E., Stephens, C.J., Ewart, A., Schon, R.W., and Parianos, J., 1997. Early Cretaceous volcano-sedimentary successions along the eastern Australian continental margin, implications for the break-up of eastern Gondwana. Earth and Planetary Science Letters 153, 85-102.

Burnham, A.K. and Sweeney, J.J., 1989. A chemical kinetic model of vitrinite maturation and reflectance. Geochimica et Cosmochimica Acta, 53, 2649-2657.

Cartwright, J.A. and Dewhurst, D.N., 1998. Layer-bound compaction faults in fine-grained sediments. GSA Bulletin (October 1998), 110, 1241-1257.

Chung, H.M., Gormly, J.R. and Squires, R.M., 1988. Origin of gaseous hydrocarbons in subsurface environments: theoretical considerations of carbon isotope distribution. Chemical Geology 71, 97-103.

Cook, C., 2002. Organic petrology of suites of samples from a number of petroleum exploration boreholes drilled in the Bass Basin, Australia. Keiraville Konsultants, Client report prepared for the National Centre for Petroleum Geology and Geophysics (unpublished) (included as Appendix I in this Geoscience Australia Record).

Core Laboratories, Inc., 1985. Core analysis report for Amoco Australia Petroleum Company, Durroon-1, Bass Basin, Victoria. Amoco Australia, Durroon-1, Well Completion Report.

Crist, R.P., Conolly, J.R. and Robinson, L.D., 2001. Barrimundi-1, A case history in fracture analysis and seal integrity in the Bass Basin. APPEA Journal, 41(1), 71-90.

Cubitt, C.J., 1992. Diagenetic controls and reservoir evaluation of the Eastern View Group, Bass Basin, Tasmania, Australia. Honours Thesis, National Centre for Petroleum Geology and Geophysics, University of Adelaide (unpublished).

Cummings, A.M., Hillis, R.R. and Tingate, P.R., 2002. Structural evolution and thermal maturation modeling of the Bass Basin. APPEA Journal 2002, 42(2), 175-191.

Das, P.K., 2001. Extensional subsidence, inversion and volumetric contraction in the Bass Basin of Australia, a seismic study. PhD Thesis, National Centre for Petroleum Geology and Geophysics, University of Adelaide (unpublished).

Das, P.K. and Lemon, N., 2000a. Flat spot anomaly; possible gas sands in the NW Bass Basin. PESA Journal, 28, 51-57.

Das, P.K. and Lemon, N., 2000b. A new model for the tectonic evolution of the southeastern Bass Basin, Australia (Poster Abstract). APPEA Journal, 40(1), 775-776.

Davidson, J.K. and Morrison, K.C., 1986. A comparison of hydrocarbon plays in the Bass, Gippsland, Otway and Taranaki Basins. In: Glenie, R.C. (editor), Second South-Eastern Australia Oil Exploration Symposium, PESA Symposium, Melbourne, 365-374.

Deighton, I.R., 1981. Burial and thermal geohistory analysis of the Bass Basin. Paltech Pty Ltd., Client report prepared for Cue Minerals N.L. (unpublished).

Duddy, I.R., 1992. Assessment of thermal history data from the Durroon-1 well, Bass Basin. Geotrack International Pty Ltd., Client report prepared for Bridge Oil (unpublished).

Duddy, I.R. and Erout, B., 2001. AFTA calibrated 2-D modeling of hydrocarbon generation and migration using Temispack, preliminary results from the Otway Basin. In: Hill, K.C. and Bernecker, T. (editors), Eastern Australasian Basins Symposium, A refocused energy perspective for the future, PESA Special Publication, 485-498.

Eadington, P. J., Lisk, M. and Kridger, F. W., 1996. Identifying oil well sites. United States Patent No. 5, 543-616.

Edwards, D.S., Struckmeyer, H.I.M., Bradshaw, M.T. and Skinner, J.E., 1999. Geochemical characteristics of Australia's southern margin petroleum systems. APPEA Journal 39(1), 297-321.

Edgerly, D.W. and Taylor, J., 1990. Seismic interpretation and basin analysis, Bass Basin T/15P. Petroconsultants Australasia Pty. Ltd. Report for Bridge Oil Ltd., (unpublished).

Etheridge, M.A., Branson, J.C. and Stuart-Smith, P.G., 1984. Structural interpretation of extensional sedimentary basins and its relevance to hydrocarbon exploration, examples from the Bass Strait region. Bureau of Mineral Resources, Canberra. Geological Society of Australia, Abstracts, 163-164.

Etheridge, M.A., Branson, J.C. and Stuart-Smith, P.G., 1985. Extensional basin-forming structures in Bass Strait and their importance for hydrocarbon exploration. The APEA Journal, 25(1), 344-361.

Etheridge, M.A., McQueen, H. and Lambeck, K., 1991. The role of intraplate stress in Tertiary (and Mesozoic) deformation of the Australian continent and its margins, a key factor in petroleum trap formation. Exploration Geophysics, 22, 123-128.

Exon, N.F., White, T.S., Malone, M.J., Kennett, J.P. and Hill, P.J., 2001. Petroleum potential of deepwater basins around Tasmania, insights from Ocean Drilling Program Leg 189. In: Hill, K.C. and Bernecker, T. (editors), Eastern Australasian Basins Symposium, A refocused energy perspective for the future, PESA Special Publication, 49-60.

Fardon, R., 2000. Western Tasmania Regional Minerals Program, Project 2, Digitisation of Tasmanian geological data. Ross Fardon and Associated Pty. Ltd., Consultants Report, Prepared for Mineral Resources Tasmania, 6 Sept 2000 (unpublished).

Faustmann, C., 1995. The seismic expression of volcanism in the Bass Basin referring to western Victorian analogues. Honours Thesis, The University of Adelaide (unpublished).

Fleming, A. and Blevin, J.E., 2003. Western Tasmania regional seismic data, selected reprocessed lines from seismic surveys T69A and T70A. An output of the Western Tasmanian Regional Minerals Program, Geoscience Australia Record 2003/6.

Geoscience Australia and Geomark Research, 2002. The oils of eastern Australia. Proprietary Report, Canberra and Houston (unpublished).

Gleadow, A.J.W. and Duddy, I.R., 1980. Early Cretaceous volcanism and the early breakup history of southeastern Australia, evidence from fission track dating of volcanoclastic sediments. In: Creswell, M.M. and Vellay, P. (editors), Gondwana V, Balkema Press, Rotterdam, 295-300.

Gretner, P.E., 1992. Geothermics, using temperature in hydrocarbon exploration. AAPG Education Course Notes Series 17, 170 p.

Gunn, P.J., Mitchell, J.N. and Meixner, T.J., 1996. The structure and evolution of the Bass and Durroon basins as delineated by aeromagnetic data. AGSO Record 1996/14.

Haq, B.U., Hardenbol, J. and Vail, P.R., 1988. Mesozoic and Cenozoic chronostratigraphy and eustatic cycles. In: Wilgus, C.K., Hastings, B.S., Kendall, C.G.St.C., Posamentier, H.W., Ross, C.A. and Van Wagoner, J.C. (editors), Sea-level changes, an integrated approach. Society of Economic Paleontologists and Mineralogists, Special Publication 42, 71-108.

Hayes, D.E. and Ringis, J., 1973. Seafloor spreading in the Tasman Sea. Nature, 243, 454-458.

Helby, R., Morgan, R. and Partridge, A.D., 1987. A palynological zonation of the Australian Mesozoic. Association of Australasian Palaeontologists, Memoir 4, 1-94.

Hill, K.A., Cooper, G.T., Richardson, M.J. and Lavin, C.J., 1994. Structural framework of the Eastern Otway Basin, inversion and interaction between two major structural provinces. Exploration Geophysics, 25, 79-87.

Hill, K.C., Hill, K.A., Cooper, G.T., O'Sullivan, A.J., O'Sullivan, P.B., and Richardson, M.J., 1995. Inversion around the Bass Basin, SE Australia. In: Buchanan, J.G. and Buchanan, P.G. (editors), Basin Inversion, Geological Society Special Publication 88, 525-547.

Hill, P.J., Moore, A.M.G. and Exon, N.F., 2001. Sedimentary basins and structural framework of the South Tasman Rise and East Tasman Plateau. In: Hill, K.C. and Bernecker, T. (editors), Eastern Australasian Basins Symposium, A refocused energy perspective for the future, PESA Special Publication, 37-48.

Holdgate, G.R., Smith, T.A.G., Gallagher, S.J. and Wallace, M.W., 2001. Geology of coal-bearing Palaeogene sediments, onshore Torquay Basin, Victoria. Australian Journal of Earth Sciences, 48, 657-679.

James, A.T., 1983. Correlation of natural gas by use of carbon isotopic distribution between hydrocarbon components. AAPG Bulletin, 67, 1176-1191.

James, A.T., 1990. Correlation of reservoired gases using the carbon isotopic compositions of wet gas components. AAPG Bulletin 74, 1441-1458.

Kaiko, A.R., 1998. Thermal history analysis of the Barrow and Dampier sub-basins, North West Shelf, Western Australia. PhD Thesis, The University of Adelaide (unpublished).

Kaldi, J.G., O'Brien, G.W. and Kivior, T., 1999. Seal capacity and hydrocarbon accumulation history in dynamic petroleum systems: the East Java Sea, Indonesia, and the Timor Sea, Australia. APPEA Journal, 39(1), 73-86.

Kempton, R.H., Liu, K., Boreham, C.J., Blevin, J.E. and Eadington, P.J., 2002. Hydrocarbon migration and accumulation in the Middle to Upper Eastern View Coal Measures of the Bass Basin, Tasmania, evidence from GOI™, QGF and QGF-E. CSIRO, Division of Petroleum Resources, Confidential Report 02-089 (unpublished).

Knowles, D.J., Suttill, R.J., and Migliucci, A.C., 1994. T/25P permit assessment project. SAGASCO Resources Ltd, (July 1994) (unpublished).

Lennon, R.G., Suttill, R.J., Guthrie D.A. and Waldron, A.R., 1999. The renewed search for oil and gas in the Bass Basin – results of Yolla-2 and White Ibis-1. APPEA Journal 39(1), 248-262.

Liu K., Kurusingal, J., Eadington, P.J. and Coghlan, D., 2001. Identify oil reservoirs. Australian Provisional Patent No. 16404/01.

Maung, T.U, Miyazaki, S., Baillie, P.W., Lavering, I.H., Vuckovic, V., Stephenson, A.E., Williamson, P.E., Staunton, J., Radke, S.G., West, B.W., Gippespie, R.G., Resiak, E., and Temple, P.R., 1993. Eastern Bass Basin Petroleum Prospectivity Bulletin. Bureau of Resource Sciences, Petroleum Prospectivity Bulletin, 1993/2.

Meszoly, G.F.J., Bodard, J.M., and Wall, V.J., 1986. Diagenesis and porosity in the Eastern View Group, Bass Basin. In: Glenie, R.C. (editor), Second South-Eastern Australia Oil Exploration Symposium, PESA Symposium, Melbourne, 303-315.

Middleton, M.F., 1982. The subsidence and thermal history of the Bass Basin, southeastern Australia. Tectonophysics, 87, 383-397.

Miyazaki, S., 1993. Source Rocks. In: Maung, T.U, Miyazaki, S., Baillie, P.W., Lavering, I.H., Vuckovic, V., Stephenson, A.E., Williamson, P.E., Staunton, J., Radke, S.G., West, B.W., Gippespie, R.G., Resiak, E., and Temple, P.R., Eastern Bass Basin Petroleum Prospectivity Bulletin. Bureau of Resource Sciences, Petroleum Prospectivity Bulletin, 1993/2.

Miyazaki, S., 1995. Oil generation from coals and carbonaceous claystones in the Bass Basin. PESA Journal, 23, 91-100.

Moore, W.R., Baillie, P.W., Forsyth, S.M., Hudspeth, J.W., Richardson, R.G. and Turner, N.J., 1984. Boobyalla Sub-basin, a Cretaceous onshore extension of the southern edge of the Bass Basin. APEA Journal, 24(1), 110-117.

Moore, A.M.G., Willcox, J.B., Exon, N.F. and O'Brien, G.W., 1992. Continental shelf basins on the west Tasmania margin. APEA Journal, 32(1), 231-250.

Mutter, J.C., Hegarty, K.A., Cande, S.C. and Weissel, J.K., 1985. Breakup between Australia and Antarctica, a brief review in light of new data. Tectonophysics, 114, 255-279.

Newman, J., 1997. New approaches to detection and correction of suppressed vitrinite reflectance. APPEA Journal, 37(1), 524-35.

Ozimic, S., Nicholas, E. and Pain, L., 1987. Bass Basin, Tasmania and Victoria. Bureau of Mineral Resources, Australian Petroleum Accumulations, Report 2.

Newman, J., Eckersley, K.M., Francis, D.A., and Moore, N.A., 2000. Application of vitrinite-inertinite reflectance and fluorescence to maturity assessment in the East Coast and Canterbury Basins of New Zealand. New Zealand Petroleum Conference, Proceedings, 314-333.

Nicholas, E., Lockwood, K.L., Martin, A.R., and Jackson, K.S., 1981. Petroleum potential of the Bass Basin. BMR Journal of Australian Geology and Geophysics, 6, 199-212.

Norvick, M.S. and Smith, M.A., 2001. Mapping the plate tectonic reconstruction of southern and southeastern Australia and implications for petroleum systems. APPEA Journal, 41(1), 15-35.

O'Sullivan, P.D. and Kohn, B.P., 1997. Apatite fission track thermochronology of Tasmania. AGSO Record 1997/35.

Partridge, A.D., 1999. Late Cretaceous to Tertiary geological evolution of the Gippsland Basin, Victoria. PhD thesis, La Trobe University, Victoria, 439 pp.

Partridge, A.D., 2001. Revised stratigraphy of the Sherbrook Group, Otway Basin. In: Hill, K.C. and Bernecker, T. (editors), Eastern Australasian Basins Symposium, A refocused energy perspective for the future, PESA Special Publication, 455-464.

Partridge, A.D., 2002. Bass Basin palynology project, unraveling a Late Cretaceous to Eocene geological history of large palaeolakes, coastal lagoons and marine bays. Biostrata Pty. Ltd, Biostrata Report 2002/13 (included as Appendix C in this Geoscience Australia Record).

Pittman, E. D. 1992. Relationship of porosity and permeability to various parameters derived from mercury injection, capillary pressure curves for sandstones. AAPG, Bulletin, 51, 191-198.

Purcell, W.R., 1949. Capillary pressures, their measurement using mercury and the calculation of permeability there from. Petroleum Transactions, American Institute of Mining, Metallurgical and Petroleum Engineers, 186, 39-48.

Powell, T.G. and Boreham, C.J., 1994. Terrestrially sourced oils, Where do they exist and what are our limits of knowledge? a geochemical perspective. In: Scott, A.C. and Fleet, A.J. (editors), Coal and coal-bearing strata as oil-prone source rocks? Geological Society Special Publication 77, 11-29.

Raggatt, H.G. and Crespin, I., 1952. Geology of Tertiary rocks between Torquay and Eastern View, Victoria. Australian Journal of Science, 14, 143-147.

Raggatt, H.G. and Crespin, I., 1955. Stratigraphy of Tertiary rocks between Torquay and Eastern View, Victoria. Proceedings of the Royal Society of Victoria, 67, 75-142.

Rezaee, M.R., Lemon, N.M. and Seggie, R.J., 1997. Tectonic fingerprints in siderite cement, Tirrawarra Sandstone, southern Cooper Basin, Australia. Geological Magazine, 134 (1), 99-112.

Robinson, V.A., 1974. Geologic history of the Bass Basin. APPEA Journal, 14(1), 45-49.

Royer, J-Y. and Rollet, N., 1997. Plate-tectonic setting of the Tasmanian region. Australian Journal of Earth Sciences, 44, 543-560.

Russell, N.J. and Baillie, P.W., 1989. Vitrinite palaeothermometry of offshore exploration wells, Tasmania. APPEA Journal, 29(1), 130-156.

Sayers, J., Symonds, P.A., Direen, N.G., and Bernardel, G., 2001. Nature of the continent-ocean transition on the non-volcanic rifted margin of the central Great Australian Bight. In, Wilson, R.C.L., Whitmarsh, R.B., Taylor, B., and Froitzheim, N., (editors), Non-Volcanic Rifting of Continental Margins; A Comparison of Evidence from Land and Sea. Geological Society, London, Special Publications, 187, 51-77.

Schowalter, T.T., 1979. Mechanics of secondary hydrocarbon migration and entrapment. AAPG Bulletin, 63, 723-760.

Schulz-Rojahn, J.P. and Phillips, S.E., 1989. Diagenetic alteration of Permian sandstone reservoirs in the Nappamerri Trough and adjacent areas, southern Cooper Basin. In: O'Neill, B.J. (editor), The Cooper and Eromanga Basins, Australia. Proceedings of Petroleum Exploration Society of Australia, Society of Petroleum Engineers, Australian Society of Exploration Geophysicists (SA Branches), Adelaide, 629-645.

Shaw, R. D., 1978. Sea-floor spreading in the Tasman Sea, a Lord Howe Rise-eastern Australia reconstruction. Bulletin Australian Society of Exploration Geophysics, 9(3), 75-81.

Siebert, R.M., Moncure, G.K. and Lahann, R.W., 1984. A theory of framework grain dissolution in sandstones. In: McDonald, D.A. and Surdam, R.C. (editors), Clastic Diagenesis, AAPG Memoir 37, 163-176.

Smit, R., 1988. A new tectonic model for the Bass Basin. Exploration Geophysics, 19, 163-168.

Smith, G.C., 1986. Bass Basin geology and petroleum exploration. In: Glenie, R.C. (editor), Second South-Eastern Australia Oil Exploration Symposium, PESA Symposium, Melbourne, 257-284.

Smith, J.W. and Pallasser, R.J., 1996. Microbiological origin of Australian coalbed methane. AAPG Bulletin, 80, 891-897.

Sneider, R.M., 1987. Practical petrophysics for exploration and development. AAPG Continuing Education Short Course Notes.

Stagg, H.M.J., Cockshell, C.D., Willcox, J.B., Hill, A., Needham, D.J.L., Thomas, B., O'Brien, G.W. and Hough, P., 1990. Basins of the Great Australian Bight region, geology and petroleum potential. Bureau of Mineral Resources, Australia, Continental Margins Program Folio 5.

Streit, J.E., 1994. Effects of fluid-rock interaction on shear zone evolution in Proterozoic granites on King Island, Tasmania. Honours Thesis, The Australian National University (unpublished).

Summons, R.E., 1996. Origin of petroleum from the Bass Basin. AGSO Professional Opinion with data from Oils of Australia, GeoMark Research Inc and the Australian Geological Survey Organisation (AGSO) (unpublished).

Surdam, R.C., Bosse, S.W. and Crossey, L.J., 1984. The chemistry of Secondary Porosity. In: McDonald, D.A. and Surdam, R.C., (editors) Clastic Diagenesis, AAPG Memoir 37, 127-150.

Sykes, R., 2001. Depositional and rank controls on the petroleum potential of coaly source rocks. In: Hill, K.C. and Bernecker, T., Editors, Eastern Australasian Basins Symposium: A Refocused Energy Perspective for the Future, Petroleum Exploration Society of Australia, Special Publication, 591-602.

Symonds, P.A., Colwell, J.B., Struckmeyer, H.I.M., Willcox, J.B. and Hill, P.J., 1996. Mesozoic rift basin development off eastern Australia. Mesozoic Geology of the Eastern Australia Plate Conference, Geological Society of Australia Inc., Extended Abstracts 43, 528-542.

Taylor, R., 2001. Horizon velocity analysis for depth conversion – A case study. ASEG 15th Geophysical Conference and Exhibition, August 2001, Brisbane, Extended Abstracts.

Teasdale, J.P., Pryer, L.L., Etheridge, M.A., Stuart-Smith, P.G., Loutit, T.S., Shi, Z., Vizy, J., and Henley, P., 2001. Regional potential field interpretation report, Bass and Durroon Basins. SRK Consulting (Energy Services), Report AG701, Non-exclusive client report commissioned by Geoscience Australia (now available as Geoscience Australia Record 2003/4).

Teasdale, J.P., Pryer, L.L., Stuart-Smith, P.G., Romine, K.K., Etheridge, M.A., Loutit, T.S. and Kyan, D.M., 2003. Structural framework and basin evolution of Australia's southern margin. APPEA Journal 2003, 43(1), 13-37.

The Australian Financial Review, 2002. Gas competition on the boil (Corporate Focus Section). Friday, 6 December 2002, 62.

Totterdell, J.T., Bradshaw, B.E. and Willcox, J.B., in press. Chapter 4: Structural and tectonic setting. In: O'Brien, G.W., Paraschivoiu, E. and Hibburt, J.E., Editors, Petroleum Geology of South Australia, Volume 5 – Great Australian Bight. Primary Industries and Resources South Australia.

Ting, F.T.C., 1978. Petrographic techniques in coal analysis. In: Karr, C. (editor), Analytical Methods for Coal and Coal Products, Volume I, Academic Press, New York, 3-26.

Trigg, K.T. and Blevin, J.E., 2003. Evaluation of exploration risk in the Bass Basin, results of a well audit study (Poster Abstract). APPEA Journal 2003, 43(1), 829-830.

Trigg, K.T., Blevin, J.E. and Boreham, C.J., 2003. An audit of exploration wells in the Bass Basin, 1965-1999. An output of the Western Tasmanian Regional Minerals Program, Geoscience Australia Record 2003/11.

Vavra, C.L., Kaldi, J.G. and Sneider, R.M. 1992. Geological applications of capillary pressure, a review. AAPG, Bulletin, 76, 840-850.

Veevers, J.J. and Ettreim, S.L., 1988. Reconstruction of Australia and Antarctica at breakup (95 ± 5 Ma) from magnetic and seismic data at the continental margin. Australian Journal of Earth Sciences, 35, 355-362.

Veevers, J.J., Powell, C.McA., and Roots, S.R., 1991. Review of seafloor spreading around Australia, I. Synthesis of the patterns of spreading. Australian Journal of Earth Sciences, 38, 373-389.

Waples, D.W., 1998. Basin modelling, how well have we done? In: Duppenbecker, S.J. and Iliffe, J.E. (editors), Basin Modelling; Practice and Progress. Geological Society of London, Special Publication 141, 1-14.

Waples, D.W. and Ramly, M., 2001. A statistical method for correcting log-derived temperatures. Petroleum Geoscience, 7, 231-240.

Waples, D.W., Kamata, H. and Suizu, M., 1992. The art of maturity modeling, Part 1, finding a satisfactory geological model. AAPG Bulletin, 76, 31-46.

Waples, D., Green, P., Hegarty, K. Duddy, I., 1996. Quantified thermal history reconstruction and basin modelling; essential aspects of basin modelling for oil and gas exploration. Geotrack International Pty Ltd., Workshop Course Notes, November 1996 (unpublished).

Wardlaw, N.C., 1980. The effects of pore structure on displacement efficiency in reservoir rocks and in glass micromodels. In: 1st Joint SPE/DOE Symposium on Enhanced Oil Recovery, SPE No. 8843, 345-352.

Wardlaw, N.C. and McKellar, M., 1981. Mercury porosimetry and the interpretation of pore geometry in sedimentary rocks and artificial models. Powder Technology, 29, 127-143.

Weissel, J.K. and Hayes, D.E., 1977. Evolution of the Tasman Sea reappraised. Earth and Planetary Science Letters, 36, 77-84.

Wilkins, R.W.T. and George, S.C., 2002. Coal as a source rock for oil, a review. International Journal of Coal Geology, 50, 317-361.

Willcox, J.B. and Stagg, H.M.J., 1990. Australia's southern margin, a product of oblique extension. Tectonophysics, 173, 269-281.

Williamson, P.E., Pigram, C.J., Colwell, J.B., Sherl, A.S., Lockwood, K.L. and Branson, J.C., 1985. Pre-Eocene stratigraphy, structure, and petroleum potential of the Bass Basin. APEA Journal, 25 (1), 362-381.

Williamson, P.E. and Pigram, C.J., 1986. Subsidence and maturation history of the Bass Basin from geohistory calculations. In: Glenie, R.C. (editor), Second South-Eastern Australia Oil Exploration Symposium, PESA Symposium, Melbourne, 285-299.

Williamson, P.E., Pigram, C.J., Colwell, J.B., Scherl A.S., Lockwood, K.L., and Branson, J.C., 1987. Review of stratigraphy, structure, and hydrocarbon potential of Bass Basin, Australia. AAPG. Bulletin, 71, 253-280.

Wood, T., 2003. BassGas project underway. Discovery, Victoria's Earth Resources Journal (February 2003). State Government Victoria, Department of Primary Industries, Minerals and Petroleum Division, 4.

Woodward-Clyde, 1999. Western Tasmanian Regional Minerals Program, Final Regional Development Plan. Report prepared for Department of Industry Science Resources, Mineral Resources Tasmania and Tasmanian Minerals Council. AGC Woodward-Clyde Pty Limited (unpublished).

Young, G.A. and Laurie, J.R. (Editors), 1996. An Australian Phanerozoic Timescale. Oxford University Press, Melbourne, 279 p.

Young, I.M., Trupp, M.A. and Gidding, M.J., 1991. Tectonic evolution of Bass Strait, origins of Tertiary inversion. Exploration Geophysics, 22, 465-468.

Zampatti, D., 1991. Diagenesis of the Eastern View Group sediments, Bass Basin, Tasmania. Honours Thesis, National Centre for Petroleum Geology and Geophysics, University of Adelaide (unpublished).